Aveiroko eta Zamorako zeramika ekoizpenen azterketa arkeometrikoa eta jalkitze-osteko kutsadura- eta eraldaketa-prozesuen identifikazioa

2022

DOKTOREGO TESIA

UXUE SANCHEZ-GARMENDIA

eman ta zabal zazu

Universidad del País Vasco
Euskal Herriko Unibertsitatea

2022

Doktorego Tesia – *Doctoral Thesis*

Aveiroko eta Zamorako zeramika ekoizpenen azterketa arkeometrikoa eta jalkitze-osteko kutsadura- eta eraldaketa-prozesuen identifikazioa

An archeometric approach to Aveiro and Zamoran pottery productions and the identification of post-depositional contaminations and alterations

Uxue Sanchez-Garmendia

Zuzendariak – *Supervisors*: Javier García Iñañez, Gorka Arana Momoitio

Diziplinarteko Estrategia Zientifikoak Ondarean eta Paisaian Doktorego Programa (DEZOP)

Doctoral Programme in Scientific Cross-Disciplinary Approaches to Heritage and Landscape (SCAHL)

Hitzaurrea / *Preface*

Doktorego Tesi honen bidez Erdi Aroko eta Erdi Aro osteko Iberiar Penintsulako ipar-mendebaldeko buztingintza-jardueraren inguruko ezagutza arkeologikoan sakondu nahi da. Ahalegin berarekin, laborategiko zahartze-prozesu esperimental bat aurkezten da, ur-inguruneetan jalkitako zeramikek jasaten dituzten eraldaketa- eta kutsadura-prozesuak biltzen dituena. Gainera, teknika analitiko ez-suntsitzaile baten erabilera ere aurkezten da. Teknika hau ikerketa honetan aztertutako kasu-azterketa batean ebaluatu da.

Lan hau egiteko hautagaiak doktorego-beka bat lortu zuen Euskal Herriko Unibertsitatearen (UPV/EHU) eskutik (PIF2017/153). Gainera, ikerketa hau *"Arqueología y Arqueometria de la producción y distribución cerámica en el Centro-Norte Peninsular del siglo XVI al XVIII"* CERANOR-2 (HAR2017-84219-P) eta *"Arqueología y Arqueometría del expansionismo atlántico Ibérico en el Norte de África y las Islas de la Macaronesia (siglos XV-XVI): cerámica, poblamiento y comercio" CERIBAM (PID2020-113198GB-I00)* ikerketa-proiektuen esparruan egin da, eta Espainiako Ekonomia, Industria eta Lehiakortasun Ministerioak eta Zientzia eta Berrikuntza Ministerioak, Estatuko Ikerketa Bulegoak eta Eskualde Garapeneko Europako Funtsak (MINECO/AEI/FEDER, EB) finantzatu dituzte. Proiektu hauek ipar-zentro eta -mendebaldeko Iberiar penintsulako eta Atlantikoko XVI-XX. mendeetako zeramiken ekoizpenaren eta banaketaren ikerketa arkeometrikoa eta arkeologikoa dituzte ardatz.

Doktorego Tesi honetan jasotako lanaren zati bat nazioarteko aldizkari entzutetsuetan (ikus. Iñañez et al., 2020; Sanchez-Garmendia et al., 2020a, 2020b, 2021a), liburuetan eta akta-liburuetan (ikus. Sanchez-Garmendia et al., 2018, 2021b) argitaratu da, edo argitaratzeko prozesuan dago. Era berean, emaitzak nazioarteko hainbat kongresu zientifikotan aurkeztu dira. Gainera, hautagaiak Doktorego Tesi honen esparrutik kanpoko hainbat lanetan ere parte hartu du, bere lankideekin batera (ikus. Calparsoro eta Sanchez-Garmendia, 2021; Calparsoro et al., 2019b, 2021, Iñañez et al., 2021).

Ikerketa-lanak Geografia, Historiaurrea eta Arkeologia Sailan eta Kimika Analitikoa Sailan egin dira nagusiki. Gainera, hautagaiak eta haren lankideek lankidetza estuan lan egin dute SGIkerreko Geokronologia eta Geokimika

Isotopikoa Zerbitzuarekin (EHU, MICINN, EJ, FEDER eta ESF), SGIkerreko X-Izpien Zerbitzu Orokorrarekin eta SGIkerreko Multiespektroskopia akoplatuen laborategi bereziarekin (Raman-MAKLAB), denak Euskal Herriko Unibertsitatekoak.

Lan esperimentala osatzeko hautagaiak hiru hilabeteko egonaldia egin zuen atzerrian Estokolmoko Suediako Historia Naturaleko Museoan (*Naturhistoriska riksmuseet*), Euskal Herriko Unibertsitateak emandako MOV19/55 bekarekin. Bertan, beiraduren berun isotopoen analisiak egin zituen, Dr. Kjell Billström, Dr. Ellen Kooijman, Melanie Kielman eta Dr. Jeremy Bellucciren zuzendaritzapean.

Azkenik, Doktorego Tesi hau euskaraz aurkeztua eta, aldi berean, Doktorego Tesi internazionala izan dadin, lanaren % 50 euskaraz idatzita dago eta beste % 50 ingeleraz, 47/2012 Dekretuak arautzen duen moduan. Gainera, eranskinetan eskuragarri dago euskaraz idatzita dauden atalen ingelerarako itzulpena (atal honetan agertzen diren irudiek tamaina txikiagoa dute; irakurleak jatorrizko euskarazko bertsiora jo dezala irudien benetako tamaina ikusteko).

—

With this Doctoral Thesis it is intended to advance in the archaeological knowledge about the pottery activity of the north-west of the Iberian Peninsula of Medieval and Post-Medieval times. With the same effort, an aging experimental approach is presented, which incorporates different alteration and contamination ways in ceramics deposited in water environments. Besides, the usage of a non-destructive analytical technique is presented, whose performance is evaluated in a case study addressed in the course of this research.

To carry out this work the candidate obtained a doctoral grant (PIF2017/153) from the University of the Basque Country (UPV/EHU). Besides, this research has been carried out under "Arqueología y Arqueometria de la producción y distribución cerámica en el Centro-Norte Peninsular del siglo XVI al XVIII" CERANOR-2 (HAR2017-84219-P) and "Arqueología y Arqueometría del expansionismo atlántico Ibérico en el Norte de África y las Islas de la Macaronesia (siglos XV-XVI): cerámica, poblamiento y comercio" CERIBAM (PID2020-113198GB-I00) research projects, funded by the Spanish Ministry of Economy, Industry and Competitiveness and the Ministry of Science and Innovation, the State Bureau of Investigation, and the European Regional Development Fund (MINECO/AEI/ERDF, UE). These projects focus on the archeology and archeometry of ceramic production and distribution in the north-central and -west Iberian Peninsula and the Atlantic expansion (16th to

20th centuries).

Part of the work included in this Doctoral Thesis has been published or is in the process of being published in prestigious international journals (see Iñañez et al., 2020; Sanchez-Garmendia et al., 2020a, 2020b, 2021a) book chapters and proceedings (Sanchez-Garmendia et al., 2018, 2021b). Likewise, the results have been presented at various scientific conferences, also internationally. Besides, the candidate has also collaborated in several works out of the framework of this Doctoral Thesis, together with her colleagues (see Calparsoro and Sanchez-Garmendia, 2021; Calparsoro et al., 2019b, 2021, Iñañez et al., 2021).

The research tasks have been developed mainly at the Department of Geography, Prehistory and Archeology and at the Department of Analytical Chemistry. Besides, the candidate and colleagues have been working in close collaboration with the SGIker-Geochronology and Isotope Geochemistry Facility (UPV/EHU, MICINN, GV/EJ, ERDF and ESF), the General X-Ray Service from SGIker and the Coupled Multispectroscopy Singular Laboratory (LASPEA) from SGIker, all of them belonging to the University of the Basque Country (UPV/EHU).

In order to complement the experimental work the candidate made a three-month stay abroad at the Swedish Museum of Natural History of Stockholm (Naturhistoriska riksmuseet), with a grant received by the University of the Basque Country (MOV19/55). Here, lead isotope analyses in glazes have been carried out, under the direction of Dr. Kjell Billström, Dr. Ellen Kooijman, Melanie Kielman and Dr. Jeremy Bellucci.

Finally, in order to present this Doctoral Thesis in Euskara and, at the same time, as an International Doctoral Thesis, 50 % of the work is written in Euskara and the other 50 % in English, as regulated by Decree 47/2012. In addition, the appendices provide an English translation of the sections written in Euskara (note that the figures are smaller in the translated part; readers are referred to the original text for the actual size figures).

Esker onak / *Acknowledgements*

Esker formalekin hasiz, eskerrak nire zuzendariei, Gorka Arana Momoitiori eta Javier García Iñañezi hain zuzen, gidaritzagatik, pazientziagatik eta prozesuan beti laguntzeko prestutasuna erakutsi izanagatik. Gainera, esker bereziak eman nahi dizkiot Estokolmoko Historia Naturaleko Museoko Geologia Departamentuari, nire doktoregoko egonaldi internazionala bertan egitea baimentzeagatik. También me gustaría agradecer al Museo de Zamora por habernos cedido las cerámicas para su estudio y a Víctor Redondo y a Paco Pascual y su familia por todos los conocimientos que nos transmitieron sobre la producción cerámica de Zamora. Del mismo modo, mis agradecimientos a los y las compañeras de Portugal, J. Bettencourt, P. Carvalho, R. Silva, A. Teixeira, J. Torres, I. Pinto, por habernos cedido las cerámicas de Aveiro y Angra y por habernos trasmitido también sus conocimientos sobre la producción cerámica portuguesa. Para finalizar, también quisiera agradecer a las compañeras del ARQUB de la Universidad de Barcelona, especialmente a Marisol Madrid, Cristina Fernández de Marcos, Judit Peix y Marta Valls, así como a Maite Maguregui, por las charlas y consejos que han tenido lugar en espacios informales de congresos, en los pasillos y en comidas compartidas, ya que me motivaban para seguir adelante con mi trabajo.

Jarraitzeko, tesi hau egin bitartean lau urte hauetan zehar nire ondoan egon zareten horiei guztiei eskerrak eman nahi dizkizuet, funtsezkoa izan baita niretzat zuen eguneroko babesa. Tesi bat prozesu luze eta potentea da eta nire burua askotan jarri dut zalantzan prozesu honetan zehar, batzuetan era konstruktibo batean, baina beste batzuetan, neure buruari harrika ematen. Horregatik, momentu zail horietan guztietan zuen zaintza eta maitasuna eskaintzeagatik, ondorengo guztiei eskerrak. A ti Dani, por quererme tan bien y por apoyarme en todo siempre y nunca juzgarme, por haber estado ahí en cada momento difícil en el proceso de esta tesis y por estar siempre presente en mi día a día, celebrando conmigo los logros y ofreciéndome tu hombro en cada caída. Aunque la tesis me haya dado muchos dolores de cabeza, ha sido un proceso que me ha permitido conocerme mucho más, y lo veo como un claro ejemplo de autosuperación en el que tú has sido pieza clave, porque me has acompañado en todo momento, reforzando el hilo que un día creamos. Por todo ello y por mucho más, por siempre transmitirme paz y hacerme reír en todos esos momentos en los que sentía que me ahogaba, esta tesis te la dedico a ti. Bestalde, familia osoari, maitasunagatik eta ni zuen etxeetan pozik jasotzeagatik behar izan dudanetan, eta bereziki aita, ama eta Itxasori, beti hor egoteagatik, salbuespenik gabe. Ainhoari, Aneri, Iratiri, Eneritzi eta Iratiri ere esker berezi eta beroak, oinarrizko euskarri izateagatik, kezka eta egonezinekin nentorrenean entzuteagatik, beti besarkada bat eta babesa eskaintzeagatik eta erokeri, asteburupasa, plan aktibo, dantza, barre, mozkor eta desmelene guztiengatik. Oihanari, noski, bidelagun izateagatik, y a la familia gallega, por recibirme siempre con los brazos abiertos y por cuidarme siempre tanto y tan bien. A Vecis, mi familia de Gasteiz, por haber hecho de esta ciudad fría y un poco gris, un lugar divertido y activo, en el que me he sentido apoyada, querida y libre siempre, algo que ha sido crucial para poder llevar a cabo este proceso. Gasteizen azken urtean egin ditudan lagunei ere eskerrak, zuen ertzetako bizi-ereduak inspirazio-iturri izan baitira nire bidean eta arnasgune bat eskaini didazuelako nire zurrunbiloetan. GPAC-ekoei (pasa zinetenoi eta zaudetenoi), kafeetakoei eta Julen, Andrea eta Aitorri ere eskerrak, lan-orduak beti umore onez arintzeagatik kafe eta bazkari ordutan.

Estefaniari, txarla eta babes guztiagatik, beti nire ondoan lankide eta bereziki lagun bezala egoteagatik, eta, noski, Juleni, Aidari, Jaiori eta Larari ere, azken denboraldi honetan ni animatzeagatik, beti laguntzeko prest egoteagatik, barre guztiengatik eta konplizidadeagatik. Julen, plazerra izan da gotorlekua elkarrekin defendatzea! Zure hurrengo memearen zain geratzen naiz! Por supuesto, también a Javi: sinceramente, me siento afortunada por haberte tenido como director, porque más allá de la relación director-doctoranda, he sentido un gran apoyo en las decisiones y problemas que he tenido que superar en el camino, y en momentos que hemos compartido. ¡Nunca olvidaré esa expedición tan divertida que hicimos a Zamora! Gracias por haber sabido cumplir tu papel de director tan bien y tan enrolladamente a la vez. I also would like to thank Bogdana, Kjell, Melanie and Ellen, from the Geology Department of the *Naturhistoriska riksmuseet* from Stockholm, for having received me with open arms and for always helpping me. I have been really happy in those three months with you. Ezin eskertu gabe utzi Joxean Mujika. Zuri esker ezagutu nuen kimika eta arkeologiaren arteko lotura eta lehen pausuetan asko lagundu zenidan, eta beti egon zara prest horretarako. Miren Ostrari eta zuri, eskerrik asko Aizkoltxoko lurrontziei buruzko GRAL hori aurrera eramateko posibilitatea eskaini zenidatelako. Eta animo hitz bat falta izan ez zaizuen eta entzuteko eta laguntzeko prest agertu zareten horiei ere eskerrak: Garaziri, Raqueli, Andreari, Elenari, Ioritzi, Laiari, Enraizadasekoei, Andoaingoei, Arnedillokoei, Estokolmokoei, kimikakoei, pisukideei, Erasmusekoei, eszenatokietakoei, Luberrikoei, unibertsitatekoei, kuadrillakoei, parrandetakoei eta azken momentuan agertu zaretenoi. Azkenik, nire buruari ere eskerrak eman nahi dizkiot, indarrak ateratzeagatik, zaurgarri izaten uzteagatik, bizitzeko gogoagatik eta amore ez emateagatik.

Aurkibidea / *Index*

“Ontziak ez dira simetrikoak bizitza ez delako simetrikoa. Gizakia inperfektua da eta ondorioz artea ere bai.”

“Las vasijas no son simétricas porque la vida no es simétrica. El ser humano es imperfecto y, por lo tanto, el arte también lo es.”

“Vessels are not symmetrical because life is not symmetrical. The human being is imperfect, and so is art.”

- Kirmen Uribe -

1. KAPITULUA: SARRERA

1.1. Zer dira zeramikak?

Zeramika, geografikoki zein kronologikoki indusketetan aurkitzen diren material ugarien artean dago, bere izaera iraunkorrari esker, Neolitotik gizakiok erabilitako tresna nagusietako bat izan delako (Gliozzo, 2020a). "Zeramika" hitza *keramos* hitz grekotik dator, "material erre" edo "loza" bezala itzulita. Suarekin tratatutako produktu bati egiten dio erreferentzia, buztinezko lehengaiari baino (Rice, 1987).

Gorputz zeramikoa ("pasta zeramikoa" ere esaten zaiona) plastikotasun handiko eta plastikotasun txikiko osagaiz (koipegabetzaileak) osatuta dago eta buztina manipulatzearen ondorioz lortzen dena izango litzateke. Plastikotasun handiko osagaiak lehengaietan aurkitzen diren filosilikatoak dira (mika eta kaolinita, illita edo montmorillonita, etab. bezalako buztinak, besteak beste); koipegabetzaileak, berriz, arroka naturalak edota mineral zatiak izan daitezke (feldespatoak, kuartzoa, harea, arroka birrindua, etab., esaterako), baita jatorri biologikoa duten materialak ere (landare-zuntzak, maskorrak edo simaurra, adibidez) edo material ez-organiko artifizialak (adibidez, zeramika hautsia– "txamota"[1] ere deiturikoa-, errautsak, etab.) (Shepard, 1956). Koipegabetzaileak zeramikak erretzean[2] gertatu daitekeen uzkurdura neutralizatzeko eta piezak pitzatu ez daitezen buztinei edo buztin-nahasteei gehitzen zaizkien materialak dira, plastikotasuna eta koipe-edukia murrizteko (Astarloa et al., 2016). Horrela, plastikotasun handiko eta plastikotasun txikiko osagaien nahasteak berariazko ezaugarriak ematen dizkio zeramikari, hala nola testura, kolorea, egoera koloidala, plastikotasuna eta partikulen tamaina (Rice, 1987).

Erdi Aroko eta Erdi Aro osteko zeramikak hainbat kategoriatan multzokatzen diren arren (konposizioaren, erreketaren eta gainazal-tratamenduen arabera, adib. terrakotak, lozak, gresak eta portzelanak), bi talde nagusitan banatzen dira: sinpleak eta konplexuak (1.1. irudia) (Buxeda i Garrigós eta Madrid i Fernández, 2017). Alde batetik, zeramika sinpleek ez dute inolako estaldurarik, hau da, soilik pastaz osatuta daude eta dekorazio-teknika sinpleekin (leunketa edo ebakidura, adibidez) apainduta egon daitezke. Bestalde, zeramika konplexuek material exogenoz egindako dekorazioak (pigmentuak), beiradurak[3] edo buztin-

[1] Ingeleraz, *grog*; frantsesez, *chamotte*; eta gazteleraz, *chamota*.
[2] Euskaraz, erreketa-prozesua; gazteleraz, *cocción*; ingeleraz, *firing.*
[3] Ingeleraz, *glaze*; gazteleraz, *vidriado*.

lohiak[4] dituzte, pastaz gain. Buztin-lohia uretan esekiduran dagoen buztinaz osatuta dago, eta erreketa-prozesuaren aurretik aplikatzen zaio gorputz zeramikoari, estaldura mehe bat eratzeko. Buztin-lohiei ere "engobe" deitzen zaie, baina termino hori nagusiki tenperatura altuko erreketa izan duen zeramikari dagokio. Bestalde, beiradura beira-mota berezi bat da, urtu ondoren berehala hozten den eta zeramika baten gainazalarekin fusionatzen den substantzia ez-kristalinoa. Beiradurak buztin-lohien arrazoi beragatik aplikatzen dira, hau da, kolorea edo testura gehitzeko eta iragazkortasuna murrizteko. Hala ere, buztin-lohiekiko oso desberdinak dira, konposatu konplexuak eta tenperatura altuan erretakoak direlako eta gainazala guztiz iragazgaitza egiten dutelako (Rice, 1987). Zeramikak beiratzearen teknologia islamiarrek ekarri zuen Iberiar penintsulara (Salinas eta Pradell, 2018; Tite et al., 1998). Beiradurak opakuak edo zeharrargiak, distiratsuak edo mateak, koloreztatuak edo kolorerik gabekoak edota lodiak edo meheak izan daitezke eta, batzuetan, kristal-egitura bat gara dezakete. Gainera, hainbat modutan aplikatzen ziren antzinan: 1) artefaktua lehen aldiz erre baino lehen (erreketa bakarraren metodoa deiturikoa); 2) aurretik erretako gorputz zeramikoan, "bizkotxo" ere esaten zaiona (bi urratseko erreketa-metodoa deiturikoa); edo 3) hirugarren erreketa batean, lustrezko zeramikarako edo *copperta* maiolika teknikarako erabili zena, besteak beste. Beiradura eta gorputz zeramikoaren arteko itsaspena beiraduraren konposatuen egonkortasun termikoak, horien uzkurdurak eta hedapen-koefizienteak baldintzatzen dute, besteak beste (Molera et al., 1997). Antzinako beiraduretan erabilitako osagai nagusia silizea zen (silizio dioxidoa, SiO_2, naturan kuartzo gisa aurkitu ohi dena), eta bere urtze-puntua murrizteko urgarri gisa jarduten duen osagai bat gehitzen zitzaion silizeari. Osagai horiek, errautsak edo berun (II) oxidoa (PbO) izan zitezkeen, esaterako. Errautsek errauts-beiratu bat edo beiradura alkalino garden bat osatzen zuten, zeinetan potasioa eta sodioa ziren urgarri nagusiak. Beruna, ordea, asko erabili zen beiraduretan, gorputz zeramikoan dauden buztinen antzeko hedapen-koefizientea duelako. Aldiz, koefiziente horiek antzekoak ez direnean, beiradurak altxatu edo hautsi daitezke (Tite et al., 1998). Gainera, Cu, Co eta Mn konposatuak pigmentu gisa gehitzen ziren batzuetan, beiradurak kolore berdez, urdinez edota marroi/beltzez apaintzeko, hurrenez hurren. Cu kobrezko metalen hondakinetatik edo malakita eta azurita bezalako mineraletatik, Co kobaltita, eskuterudita eta eritrita bezalako mineraletatik eta Mn braunita eta hausmannita bezalako

[4] Ingeleraz, *slip*.

mineraletatik lor zitezkeen. Pigmentu horiek beiraduraren gainean edo beiraduraren azpian aplikatzen ziren (Molera et al., 1997; Rice, 1987). Beiraduraren gaineko aplikaziorako, bizkotxoari lehenengo beiradura aplikatzen zitzaion eta pigmentuak horren gainean aplikatzen ziren. Beiraduraren azpiko aplikaziorako, ordea, pigmentuak bizkotxoaren gainean aplikatzen ziren eta gainean beiradura ezartzen zen. Azken teknika hau zeramika islamikoaren beiradura gardenetan jada dokumentatu zen (Coentro et al., 2020), hau da, IX. mendeko zeramiketan, Raqqadan (Ben Amara et al., 2011) eta Palermon (Arcifa eta Bagnera, 2018), adibidez. Gero, XIV. mendean, teknika hau zeramika zuri opakuetan garatzen hasi zen. Ebidentzia arkeologikoen arabera, Valentziako beiradura zuri opakuetan pigmentu urdina bizkotxoaren gainean aplikatzen zuten eta gero dena batera erretzen zuten lehenengo aldiz (Coentro et al., 2020). Gero, fritakina gehitzen zioten eta bigarren aldiz erretzen zuten pieza (Coll Conesa, 2009). Teknologia hau, adibidez, Granadako XIV. mendeko zeramiketan dokumentatu da (García-Porras, 2012).

1.1. irudia. Zamora probintziako indusketa batzuetan ateratako zeramika sinple eta konplexuak, ezkerretik eskuinera: bizkotxo beixa (sinplea), bizkotxo gorria (sinplea), beiradura zeharrargidun zeramika (konplexua), beiradura opaku zuria duen zeramika (konplexua) eta beiradura opaku apaindua duen zeramika (konplexua). Eskala-barra: 8 cm

Zeramikagintza tradizionalean berunezko beiradurak asko erabili izan dira X-XI. mendeetatik gaur egun arte (Molera et al., 2001; Rice, 1987; Tite et al., 1998). Erdi Arotik, berunezko beiradura zeharrargiak (ikus. 1.1. irudia) bi modutan ekoizten ziren: esekidura gordin gisa eta fritakin gisa. Lehenengoa berun konposatuen (berun(II) oxidoa (PbO), berun gorria (Pb_3O_4), berun zuria ($2PbCO_3{\cdot}Pb(OH)_2$) edo galena (PbS)) eta silizearen hauts-nahaste bat egitean zetzan, ur-esekidura gisa. Berun oxidoak berun metalikoa labe batean edo etxe baten sutondoan urtzean eta gero oxido-geruza kentzean lortzen ziren. Beiradurentzat zuzenean galena erabil zitekeen arren, ohikoa zen galena erretzea, horren oxidoa lortzeko (Tite et al., 1998). Hala ere, metodo honek zikinkeria sortzen zuen beiraduran bere erreketa bitartean, eta, gainera, beiraduretan disolbatu gabeko zatiak agertzen ziren, nahaste heterogeneo bat erakutsiz (Paynter, 2001). Bigarren modua (fritakinaren metodoa),

aldiz, berun konposatuak eta silizea elkarrekin urtzean zetzan, horrela, nahaste homogeneo bat lortzeko, fritakin[5] izenez deitua. Fritakin hori gero ehotu egiten zen hauts bihurtzeko, eta, ondoren, ur-esekidura prestatzen zen (Tite et al., 1998). Azkenik, aipatutako bi ekoizpen-moduetatik lortutako ur-esekidura erre gabeko zeramika lehortu batean edo bizkotxo batean (gorria, normalean) aplikatzen zen, 700 °C eta 1000 °C bitarteko tenperaturan urtuz, konposizioaren arabera. Lan honetan "beiradura zeharrargi" terminoa erabiltzean, berunezko beiradura zeharrargiei buruz ari naiz.

Beiradura zeharrargiaz gain, eztainu-berunezko beiradurak (beiradura zuri opakuak) ere oso erabiliak izan dira zeramikagintza tradizionalean (ikus. 1.1. irudia), baina hauen ekoizpen-sekuentzia konplexuagoa zen. Beiradura hauek ingeleraz "majolica" edo "faience" izenez ezagutzen dira ere. Maiolika eta faiantza izenek eskualde desberdinetako merkataritza sareetan dute jatorria: Mallorca uhartetik Italiara eztainu-berunez beiraztatutako zeramikak itsasontziratzen zituzten bertan saltzeko, eta italiarrek zeramika mota horri *maiolica* izena jarri zioten (italieraz), uhartearen izena zela eta. Faenza, aldiz, Italiako hiri bat da eta bertatik Frantziara eztainu-berunez beiraztatutako zeramikak esportatzen ziren, eta frantsesek *faïence* (frantsesez) izenez ezagutzen zituzten (Rice, 1987). Beiradura hauen ekoizpen-sekuentzian lehenengo, silizeaz, berun konposatuez, kasiteritaz (eztainu dioxidoa, SnO_2, beiratu zuri opakoa lortzeko) eta alkali batez osatutako nahastea egin behar zen, fritakin modura, hau da, elkarrekin urtuz. Ondoren, ehotu egiten zen hauts bihurtzeko, eta, gero, ur-esekidura prestatzen zen, berunezko beiradura zeharrargiekin egiten zen bezala (Tite et al., 1998). Ur-esekidura hori, normalean, bizkotxo bati aplikatzen zitzaion (jada erretako zeramikari), horrela, pieza ez zelako hedatzen edo uzkurtzen hezetzearen eta horren ostean lehortzearen eraginez. Gero, zeramika erre egiten zen. Gainera, batzuetan koloredun apaingarriak gehitzen zitzaizkion beiradurari, lehen aipatu bezala, beiraduraren gainean edo beiraduraren azpian.

1.1.1. Zeramikaren azterketa, zertarako?

Arkeologia gizartea bere hondakin materialen bitartez aztertzean datza (González-Ruibal eta Ayán Vila, 2018), eta lan honetan aztertzen diren materialak zeramikak dira. Zeramikak aztertzearen arrazoietako bat gehien erabili izan diren

[5] Gaztelaraz, *frita*; ingeleraz, *frit*.

materialak direla da, bai maila kronologikoan eta baita banaketa geografikoan ere; gainera, kontserbazio-baldintza ezin hobeak dituzte (Fantuzzi, 2010).

Gainera, zeramikak berezko dualtasuna du: dimentsio kulturala eta naturala (Neustupný, 1971, 1993). Zeramikak aztertzeko motibazio nagusia beren dimentsio kulturalari dagokio: zeramikek adierazle teknologiko, sozioekonomiko, soziokultural eta kronologiko gisa jarduten baitute (Buxeda i Garrigós eta Madrid i Fernández, 2017; Buxeda i Garrigós et al., 2010; Schiffer, 2011; Skibo, 2013; Skibo eta Schiffer, 2008). Esate baterako, alderdi sozioekonomikoari dagokionez, zeramikak aztertuz gero, egunero erabiltzen diren objektuak (seguruenik kostu ertainekoak) eta objektu preziatuak (familia aberatsetakoak) identifika daitezke. Hala, ikertzaileek populazio jakin baten ezaugarri kulturalei eta elikadura-ohiturei buruz gehiago jakin dezakete (Colombini et al., 2005; Evershed, 2008; Pecci, 2014; Roffet-Salque et al., 2017). Gainera, zeramika ekoizpen-zentroen kokapen geografikoa identifikatzean, merkataritza-sareak berreraiki daitezke (adibidez, epe laburreko edo epe luzeko trukea, tokiko kontsumoa edo esportazioa, etab.) eta salgaiak garraiatzeko erabiltzen zen ibilbide-mota (lurrekoa, ibaikoa, aintzirakoa edo itsasokoa) ere ezagutu daiteke (Blomster et al., 2005; Glascock, 2002; Knappett, 2013; Remesal et al., 2019).

Zeramikaren alderdi kronologikoari dagokionez, material hauek adierazle kronologiko gisa jardun dezakete indusketa arkeologikoan sekuentzia estratigrafikoa periodikatzeko. Hala, geruza batean aurkitutako objektu zeramiko berrienak geruza datatzeko *post quem* terminoa ematen du (Harris, 1979; Renfrew eta Bahn, 1993).

Azkenik, alderdi teknologikoari dagokionez, zeramika ekoizpena aztertzeak aukera ematen du buztinlariek erabiltzen zuten fabrikazio-teknikari buruzko ezagutza eskuratzeko; fabrikazio-teknika hori buztinlariak bizi ziren gizartearen trebetasun teknikoek, tradizioek eta kultura-esparruak zehazten dute. Adibidez, erreketa-egitura berrien esperimentazioa (adib. sua, ganbera bakarreko labea, ganbera bikoitzeko labea, etab.) zeramiken formen eta dekorazioen garapenari lotuta zetorren (estaldura funtzionalen aplikazioa, esate baterako). Alde horretatik, lehengaiak zeramika artefaktu bihurtzeak, baldintza jakin batzuk bilatzea eskatzen zuen. Baldintza hauek, gero, azken objektuaren propietate desiragarriak lortzea ahalbidetzen zuten (malgutasuna eta galdagarritasuna, diseinua, etab.), azken produktuak nahi zen funtzioa bete ahal izan zezan (Buxeda i Garrigós eta Madrid i Fernández, 2017; Gliozzo, 2020a; Heimann, 1989; Roux, 2019; Schiffer, 2011).

Zeramika aztertzen hasi aurretik, edo bitartean, sortzen diren galdera garrantzitsu batzuk ondorengoak dira: zein lehengai erabili ziren? Zeramikaren erabileraren arabera lehengai mota desberdinak erabiltzen al ziren (adibidez, baxerarako, garraio-ontzietarako, likidoak gordetzeko etab.)? Nola prestatu ziren lehengaiak? Koipegabetzailea gehitu al zen? Zergatik? Zer atmosfera mota lortu zen erreketan (oxidatzailea ala erreduzitzailea)? Zein izan ziren erreketa-tenperaturak zeramikentzat? Lortutako atmosferak eta lortutako tenperaturak nahita izan al ziren? Zeramiken gainazalak beiraztatuta al zeuden? Eta apainduta? Nola? Zergatik? Zer lehengai erabili ziren gainazal-akaberarako? Eskuragarri al zeuden ekoizpen-zentrotik gertu ala inportatu egin behar al ziren? Ba al dago korrelaziorik formaren, konposizioaren eta funtzioaren artean? Zeramika bertako erabilerarako edo esportatzeko zen, ala biak? Biztanleria pobre edo/eta aberatsek kontsumitzen al zuten zeramika mota hori? Zein da zeramika horren jatorria? Ba al zegoen zeramika horren esportaziorik? Merkataritza sarerik? Zein? Zer elikadura-ohitura edo eguneroko beste jarduera ondoriozta daiteke ebidentzia zeramikotik? Ikus daitekeenez, arazo horiek guztiek alderdi teknologikoei, sozioekonomikoei, soziokulturalei, jatorriari eta zeramikaren kronologiari dagozkie.

1.2. Azterketa arkeologikoaren ezaugarri nagusiak

Arkeometria zientzia esperimentaletatik hartutako teknika analitikoak aplikatzean datza. Hauek zeramiken dimentsio kulturala bere dimentsio naturaletik abiatuz aztertzeko aukera ematen dute. Arkeometriak galdera arkeologikoak erantzuten ditu, ikergai den gaiari buruz dagoen jakintza arkeologiko guztia kontuan hartuz.

Arkeologian, zeramika arkeologikoaren azterketa materialen ezaugarri morfologikoetan, pastaren kolorean eta apainduren ezaugarrietan oinarritutako sailkapenean oinarritu izan da. Zeramika-ekoizpena aztertzeko sailkapen hori balio handikoa dela onartuz, kasu batzuetan ez dela nahikoa aipatu behar da, batez ere zati txikiak direnean, askotan dekorazio edo tipologia argirik gabeak, edo material ezezagunak edo jatorri ezezagunekoak direnean. Alde horretatik, zeramikaren jatorriari, alderdi teknologikoei, sozioekonomikoei, soziokulturalei eta kronologikoei buruzko galderei, zeramikek duten dimentsio naturala aztertuz erantzun behar zaie (eredu arkeometrikoa erabiliz), objektu materialak baitira (Buxeda i Garrigós et al., 1995). Eredu horri buruz argitaratutako artikulu

garrantzitsu batzuk Boulanger et al. (2013), Buxeda i Garrigós (1999) eta Buxeda i Garrigós eta Madrid i Fernández (2017)-enak dira. Hurrengo lerroetan azaltzen da Doktorego Tesi honetan erabilitako hurbilketa arkeometrikoaren funtsa. Jarraitutako ikuspegia bi zati osagarritan banatzen da nagusiki: jatorria eta teknologiaren azterketa. Horien bidez, alderdi sozioekonomikoak, soziokulturalak eta kronologikoak ere aztertzen dira. Nabarmentzekoa da zeramikaren azterketak ikuspegi zabalagoa izan dezakeela; lan honetan, beste material zeramiko batzuk baztertu dira, hala nola eraikinekin zerikusia dutenak (azulejuak, adibidez) edo zeramikaren hondakinetan dagoen materia organikoa, iraganeko giza portaerari buruzko informazio baliotsua eman dezakeena (adibidez, Blanco-Zubiaguirre et al., 2018; Pecci, 2014).

Lan honetan jarraitutako eredu arkeometrikoa Buxeda i Garrigós eta Madrid i Fernández (2017)-ek planteatutakoa da, eta zeramiken *chaîne opératoire*-a (Roux, 2019) du oinarri. Katea jasotako zeramikatik hasten da (leku arkeologikoan egindako berreskurapenetik, alegia) eta zeramikagileak lehengaiak erauzi zituen eremuraino doa, seguruenik lantegitik gertu zegoen eremu bat izan zena. Horrez gain, garrantzitsua da adieraztea arkeologian, zeramika kaltziodun edo kaltzio eduki baxuko zeramika bezala sailkatzen dela. Lan honetan, zeramiken banaketa kaltziodun zeramika (% 6 ≥ CaO) eta kaltzio eduki baxukoa (% 6 < CaO) bezala egin da.

1.2.1. Jatorriaren azterketa

Lehenik eta behin, argitu behar da zeramika baten jatorria ez dela nahitaez artefaktua berreskuratu zen tokia. Jatorria da zeramika ekoitzi zen tokia, buztinaren jatorria eta ekoizpenarena bera zela suposatzen baita. Suposizio hori egiazkoa izan ohi da antzinatean, garraioak ekarriko lituzkeen kostuak direla eta, edo lehengai kopuru handiak ezin izango liratekeelako merkaturatu. Hori dela eta, lehengaietara iristeko erraztasunak ekoizpen-jarduerarako kokapena ezarri zuen kasu gehienetan (Buxeda i Garrigós, 2010). Jatorriari buruz hitz egitean, batez ere pasta zeramikoen jatorriari buruz ari naiz, baina jatorriaren azterketak ere berun beiraduratan egin daitezke. Horrela, aurrerantzean jatorriari buruzko aipamen guztiak pasta zeramikoei buruz egingo dira, bestelakorik adierazi ezean.

Erdi Aroko eta Erdi Aro osteko zeramika arkeologikoen jatorria identifikatzeko lehen urratsa, zeramika talde esanguratsuetan sailkatzea da.

Taldeak zeramikaren dimentsio materialaren bidez definitzen dira, hau da, pasta zeramikoen konposizio kimikoa aztertuz edo analisi petrografikoak eginez (Buxeda i Garrigós eta Madrid i Fernández, 2017) (1.2. irudia). Edozein materialen jatorria analisi kimikoen bidez zehazteko, *Jatorriaren Postulatua* hartzen da oinarri gisa; horrek esan nahi du material-iturri bakar baten barruko desberdintasun kimikoak hainbat iturriren arteko desberdintasun kimikoak baino txikiagoak direla (Weigand et al., 1977). Beraz, lantegi zehatz batean eta errezeta zehatz batekin ekoitzi edo eraldatu den zeramikak, ziur aski, beste leku batean ekoitzitakoaren konposizio kimiko desberdina izango du, erabilitako lehengai eta/edo fabrikazio-metodo desberdinengatik (Hein eta Kilikoglou, 2017). Zeramika-talde esanguratsuak oinarri kimikoko sailkapen baten unitate txikiena dira, hau da, Pasta Konposiziozko Erreferentzia-unitatea (PCRU)[6] (Buxeda i Garrigós eta Madrid i Fernández, 2017). Gainera, nahiz eta erlaziozko edota ustekabeko beste propietate batzuk, hala nola apaingarriak edo zigiluak, ez diren erabiltzen zeramika-taldeak definitzeko, hauek informazio garrantzitsua eman dezakete zeramiken testuingurua ezagutzeko eta datu arkeometrikoak ebaluatzeko (Buxeda i Garrigós eta Madrid i Fernández, 2017). PCRU-ak definitu ondoren, hauek konparatu egiten dira erreferentzia-taldeekin (RG)[7], datu-baseak erabiliz. RG-ak kimikoki finkatutako zeramika-taldeak dira, jatorri ezaguna edo ustezkoa dutenak, eta ekoizpen-eremu edo lantegi jakin bateko zeramika-moten adierazgarriak dira (Hein et al., 2002). PCRU baten eta RG baten artean antzekotasun kimikoa badago, erreferentzia-talde berekotzat hartzen dira. Aitzitik, PCRU bat ezagutzen diren RG-en antzekoa ez bada, PCRU horri ezin zaio esleitu ez tokiko jatorria, ez jatorri exogenoa, eta bere jatorria zehaztugabea izango da RG berri baten antza izan arte. Gainera, kontuan hartu behar da lantegi berean erreferentzia-talde bat baino gehiago egon daitekeela; izan ere, litekeena da zeramikariak buztin desberdineko pastak prestatu izana hainbat zeramika-mota egiteko, adibidez, buztin bat baxerarako eta beste bat sukaldaritzarako. Esate baterako, Logroñoko (Errioxa) XIII-XV. mendeetako zeramiken kasua da hori, zeinak RG desberdinak erakusten baititu ekoizpen-zentro berean, denboran zehar (Calparsoro et al., 2021). Gainera, baliteke eremu berean dauden lantegiek lehengai berberak erabili izana eta pastak antzeko moduan prestatu izana. Kasu horietan, lantegi horietan ekoitzitako zeramikek antzeko konposizio kimikoak izango dituzte, eta, beraz, lantegi bakoitzean zaila edo

[6] Ingeleraz, *Paste Compositional Reference Unit.*
[7] Ingeleraz, *reference groups*.

ezinezkoa izango da RG desberdinak identifikatzea. Zona horri ziurgabetasun-eremu edo bereizmenik gabeko eremu deritzo (Buxeda i Garrigós eta Madrid i Fernández, 2017), hau da, eremu horretan ezin dira analitikoki bereizi lantegietan zeramikagileek erabiltzen zituzten lehengaiak, ezaugarri komunak baitituzte, eremu geologiko berean baitaude.

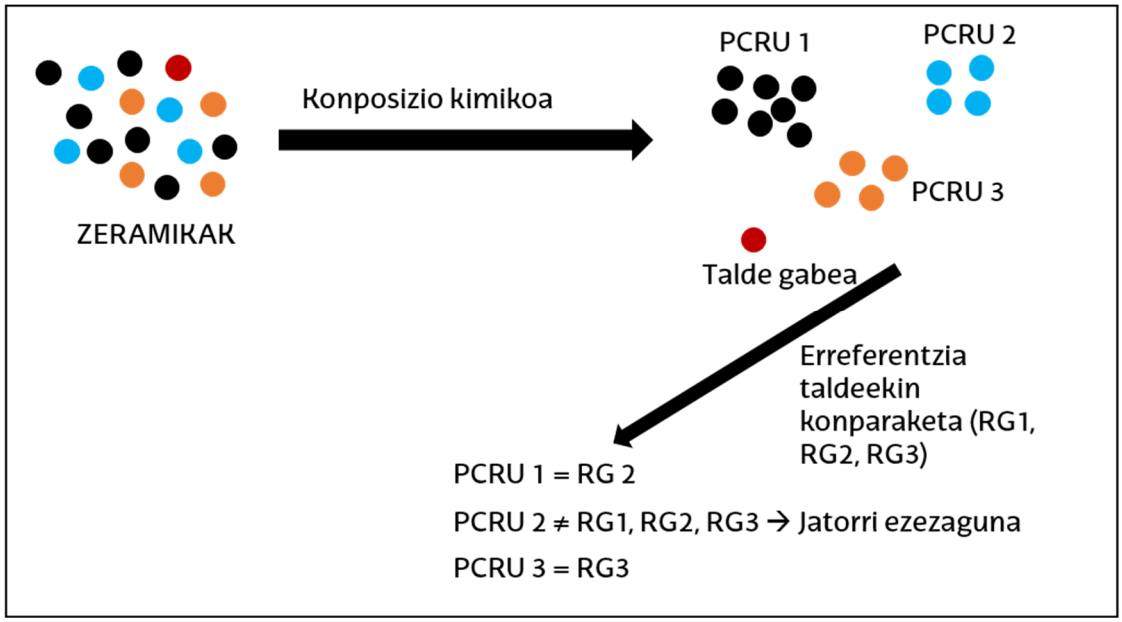

1.2. irudia.Jatorriaren ebaluazioaren azalpen grafikoa

Baina, nola definitzen dira RG-ak? Bada, leku arkeologikoan, zeramikazko ekoizpen-zentro zahar bat zegoen tokian (lantegi gisa ere ezaguna), artisau-tresnak berreskuratu ohi direlako. Denboran zehar gorde daitezkeen ebidentzia zuzenenak zeramika-labeen ebidentziak dira, zeramikak erretzen ziren egitura iraunkorrak. Gainera, ekoizpen-tresna gehiago ere aurki daitezke, hala nola, labe-hodietako treberak -pieza labetik bereizteko (beiren teknologia sartu ondoren hasi ziren erabiltzen, eta, normalean, kontsumorako zeramikarako erabilitako buztin berekin fabrikatu ziren)-, zeramika lantzeko tornuak eta fritakinak ehotzeko tornuak (1.3. irudia). Bestalde, pasta zeramikoak, gaizki erretako edo erre gabeko zeramikak, zeramiken hondakindegiak (baztertu egingo liratekeen zeramikaz beteak, zeramikagintzaren zuzeneko ebidentzia adierazten dutenak) eta erabilitako lehengaiak ere aurki daitezke, batzuk aipatzearren (Calparsoro, 2019). Egoera horri esker, zeramika lantegiak geografikoki koka daitezke edo, behintzat kokapen bat iradoki daiteke. Gainera, gaizki erretako zeramiken, treberen edota

hondakindegietan dauden zeramiken analisi kimikoa egitean, ekoizpen-zentro jakin bat karakteriza daiteke (Buxeda i Garrigós eta Madrid i Fernández, 2017). Zenbait faktorek, hala nola, lehengaien fintzeak, nahasteak edo koipegabetzaileak gehitzeak, zaildu egiten dute lehengaien konposizioaren eta zeramikaren arteko konparazio zuzena, eta, horregatik, jatorriaren azterketarako nahiago da zeramika buztina baino (Hein et al., 2002). Buxeda et al. (2003)-k egindako azterketa etnoarkeometrikoan frogatu zen hori: lau zeramikagileen pasta zeramikoak eta pasta horiek egiteko erabili zituzten lehengaiak kimikoki karakterizatu zituzten eta emaitzek erakusten dute pastek eta lehengaiek ez dutela zerikusirik. Hala ere, arreta jarri behar zaio hondakindegietan berreskuratutako zeramikak aztertzeko ekintzari (adibidez, gehiegi erretako zeramikak edo labe-hondakinak). Akastuntzat jotzen direnez, oso erabilgarriak dira jatorria aztertzeko, baina zailagoa izan liteke zeramikentzat aurreikusten ziren edo nahi ziren errendimendu-ezaugarriak edota funtzionalitatea ulertzea. Beraz, azken alderdi hauetarako, komenigarria da kontsumo-zentroetako (egoitzak, hiriak, biltegiratze-instalazioak, etab.) zeramika aztertzea beren jatorria esleitu ondoren, hondakinak aztertu ordez (Buxeda i Garrigós eta Madrid i Fernández, 2017). Kontsumo-zentroetako zeramika aztertzeak aukera ematen du zeramikaren aldaketa teknikoa/teknologikoa, aurreikusitako errendimendu-ezaugarriak eta erabilera-katean zeramikek gauzekin eta pertsonekin izan duten elkarrekintza ezagutzeko. Gainera, lantegiak askotarikoak izan daitezke, labe bat edo gehiagorekin (Zamorako Olivareseko lantegien kasua, Sanz et al., 2005) eta/edo gremiotan antolatzen direnak, dagokion denboraldiaren arabera (Solaun, 2005). Doktorego Tesi honen esparruak Zamora eta Aveiro eskualdeetako Erdi Aroko eta Erdi Aro osteko zeramikaren (XV. mende bukaera - XX. mende hasiera) jarduera tradizionala hartzen du. Horrela, hemendik aurrera, aipamen guztiak hertsiki aplikatzen zaizkie aipatutako aldiari, kontrakorik esaten ez bada behintzat.

1.3. irudia. Olivareseko lantegietan (Zamora hirian) berreskuratutako bi trebera (laberako tresnak). Eskala-barra: 8 cm

Berun beiraduren jatorriari buruzko azterketei dagokienez, hori posible da “berunezko mineral arrunt” gisa ezagutzen diren galena (PbS), zerusita ($PbCO_3$) edo

anglesita ($PbSO_4$) bezalako mineralen berunaren arrazoi-isotopikoak denboran zehar konstante mantentzen direlako (Hunt, 2003). Berunak isotopo ez-erradiogeniko bat (^{204}Pb) eta hiru isotopo erradiogeniko (^{206}Pb, ^{207}Pb eta ^{208}Pb) ditu, uranioaren eta torioaren azken desintegrazio produktuak direnak; ^{206}Pb ^{238}U-tik deskonposatzen da, ^{207}Pb ^{235}U-tik eta ^{208}Pb ^{232}Th-tik. Berunezko mineral arruntek U/Pb erlazio txikia dutenez, Pb-ren konposizio isotopikoa gutxi aldatzen da edo ez da aldatzen denborarekin. Honek berunezko mineral arrunt horren iturriaren adina neurtzeko aukera ematen du (Dickin, 2018). Beraz, beiradurak egiteko erabilitako galenaren (erabiltzen zen mineral ohikoena) arrazoi-isotopikoak bere iturriaren berdinak izango lirateke (1.4. irudia). Horregatik, iturri ezberdinetako galenen berunaren arrazoi-isotopikoen datu-basea eta gure zeramiken beiraduren berunaren arrazoi-isotopikoak konparatuz, berun mineralaren iturri geologikoa identifika daiteke, eta, kasurik onenean, beruna erauzi zen meatze zehatza.

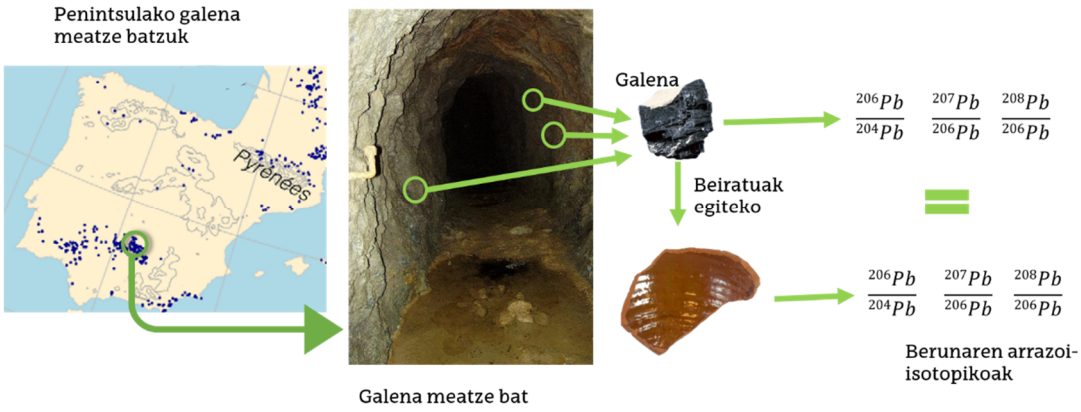

1.4. irudia. Berun isotopoen analisien funtsaren azalpen grafikoa

Tradizionalki, Pb, U eta Th isotopoen analisiak geokronologian eta Lurraren eta planeten zientzietan erabili izan dira nagusiki, arroken sorreraren adina, eta Lurraren eta meteoritoen adina aztertzeko, besteak beste (Albarède et al., 2012, Faure, 2004). Gai geologikoetan oinarritutako ikerketez gain, berun isotopoen analisiak asko erabili izan dira arkeometalurgian (Artoli et al., 2020; García de Madinabeitia eta Gil Ibarguchi, 2019; Montero-Ruiz, 2018 lanetan laburbilduta), lehengaien jatorri geologikoa arakatzeko eta metal-fluxua historiaurreko garaietan edo garai berriagoetan aztertzeko (ikus, adibidez, Ponting et al., 2003; Shortland 2006; Stos-Gale eta Gale 2009; Stos-Gale et al. 1997; Thibodeau et al. 2007; Yener et al. 1991-en lanak). Aitzitik, azken urteetan berun beiradurak gero eta gehiago

aztertzen dira, berunaren balizko jatorria arakatzeko eta, ondoren, merkataritza bide posibleak proposatzeko. Horrelako lehen lanen artean daude Brill et al. (Brill eta Wampler 1967; Brill et al., 1987) eta Joel et al. (1988)-en lanak. Azken lana Ameriketan aurkitu den Espainiako zeramika maiolikoaren arrazoi-isotopikoetan zentratzen da. Hasierako argitalpen horietatik aurrera, Pb isotopoen bitartez beiraduradun zeramiken berunaren jatorria aztertzeko beste proiektu batzuk egin dira. Adibide batzuk dira Mason et al. (1992)-ek egindako beiradura islamiarren analisiak, Resano et al. (2008)-ek aztertutako zeramika hispaniar-moriskoa eta zeramika islamiarra, Pingitore et al. (1997)-k aztertutako El Paso eremuko zeramikak, Habicht-Mauche et al. (2000, 2002)-ek aztertutako Rio Grandeko zeramika beiraztatua eta Reslewic eta Burton (2002)-ek aztertutako XVIII. mendeko Espainia Berriko espetxeetako maiolika (azken hiru lanetan aipatzen diren lekuak AEBko hegoaldeko eskualdean daude). Gainera, Wolf et al. (2003)-k eta Marzo et al. (2007)-k argitaratutako lanak garrantzitsuak dira. Lehenengo ikerketan, egileek Fustateko (Egipto) eztainu-berunez beiraztatutako 48 zeramika islamiar aztertu zituzten eta ondorioztatu zuten Fustateko buztinlari islamiarrek beirak ekoizteko erabilitako beruna urruneko mineral-iturrietatik lortu zutela. Bestalde, bigarren lanean, egileek Aragoiko XI-XVI. mendeetako beiraztatutako 12 zeramika aztertu zituzten. Lan honek frogatzen du Induktiboki Akoplatutako Plasmaren Masa Espektrometrirekin (ICP-MS) beiraduren berun isotopoen arrazoien datu fidagarriak lor daitezkeela. Gainera, Iñañez et al. (2010)-ek Romita zeramika motaren beiradurak aztertu zituzten, baita Espainiako eta Mexikoko ekoizpen-zentroetako maiolika eta beiraztatutako zeramika batzuk ere. Gero, emaitza hauek Erdi- eta Hego-Ameriketako eta Europako datuekin alderatu zituzten, berun mineralen jatorri geologikoa argitzeko. Datu horiek erakusten dutenez, Purépecha artisauek ekoitzi zuten Romita zeramika. Purépecha hauek arrakastaz konbinatu zituzten zeramika tradizioak, Espainiako maiolika bezalako Europako zeramikak erreplikatzeko. Honez gain, Iñañez et al. (2016)-ek Panamako eztainu-berunezko zeramika beiraztatuak egiteko erabilitako berunaren jatorria ikertu zuten. Emaitzek erakusten dutenez, XVI-XVII. mendeetako maiolikaren ekoizpenerako Andeetatik lortutako beruna erabili zen. Hala ere, XVII. mendetik aurrera, Panaman maiolika ekoizteko erabilitako berunaren jatorria espainiarra zen. Bestalde, beiraduren berun isotopoen analisiei buruzko lan berriagoekin jarraituz, Schurr et al.(2018)-en lana aipatu daiteke. Egile hauek XIX. mendeko zeramika amerikarra eta euroamerikarra aztertu zituzten eta beruna Ingalaterratik ekartzen zutela ondorioztatu zuten. Gainera, Santarelli et al. (2019)-ek Amerikako hego-

mendebaldeko K.o. 750-850-ko beiraduren berun isotopoak aztertu zituzten eta ondorioztatu zuten zeramikagileek erabilitako beruna Lake Cityko (Utah) Galena Distritutik eta Coloradoko mendietatik ekarri zutela. Honez gain, Medeghini et al. (2020)-ek, beiraztatutako zeramika erromatarren berun isotopoak aztertu zituzten eta beruna Britainiar uharteetatik ekartzen zutela ondorioztatu zuten. Azkenik, Métreau et al. (2021)-ek Brittany eta Anjouko Erdi Aroko azuleju apainduen jatorria aztertu zuten berun isotopoen bidez eta beruna Derbyshiretik (Britainiar Uharteak) ekartzen zutela ondorioztatu zuten.

Gainera, buztinen jatorriari dagokionez, iturri ez-materialak ere badaude (adibidez: toponimia), zeramika ekoizten zuten zentroak identifikatzeko. Kontuan izan, Espainia eta Portugalen, herri askotan oraindik ere badirela *Ollerías* izeneko kaleak (buztingintza lantegiak), adibidez, *Barrio das Olarias* (Aveiro, Portugal). Zamoran horren adibide den Alfaraz de Sayago izeneko herri bat dago, inguruko buztin gorriei erreferentzia egiten diena (Fuentes Guerra, 1964). Etnografia-lanen dokumentazio idatzia ere oso erabilgarria da. Adibidez, Enrike Ibabe eta Emili Sempere etnografistek zeramikaren ekoizpen tradizionalari buruzko ikuspegi orokorra eman zuten Euskal Herrian (Ibabe, 1995a) eta Espainian eta Portugalen (Sempere, 1982). Alde batetik, Ibabek Euskal Herriko zazpi probintzietako herrietan zeuden buztingintzako jarduerak jasotzen ditu. Gainera, autoreak lantegiei eta artisauei buruzko informazioa ematen du, beren izenak eta bizitzen xehetasunak barne, eta erabiltzen zuten buztin-mota, teknologia (adibidez, nolakoak ziren tornuak eta labeak, nola erretzen zuten zeramika, beiradura nola aplikatzen zuten, etab.), non saltzen zuten zeramika, etab. deskribatzen du, eta herri bakoitzean ekoitzitako zeramika-bilduma handia ere erakusten du. Bestalde, Semperek Espainian eta Portugalen 1982an sakabanatuta zeuden 280 zeramika-zentroen errealitatea erakusten du. Gainera, autoreak agerian uzten ditu beren arteko antzekotasunak eta material, teknika eta labeei dagokienez beren arteko desberdintasun nabarmenenak.

1.2.2. Teknologiaren azterketa

Zeramiken teknologia konposizio-taldeak identifikatu ondoren aztertzen da, analisi mineralogiko eta mikroestrukturalen bidez. Zeramikaren ikerketa teknologikoaren bidez, ekoizpen-ziklo osoa berreraiki daiteke, lehengaiak manipulatzetik objektuaren akaberaraino. Alderdi teknologikoak zeramika konplexuaren atal bakoitza hartzen du, hala nola, beiradurak, inklusioak, porositatea eta pigmentuak. Gainera, ekoizpenarekin lotutako tresnen eta azpiegituren azterketa ere ikertu daiteke (Buxeda i Garrigós eta Madrid i Fernández, 2017).

Zeramiken teknologiari buruzko lehen idatzia 1301. urtean egin zen; Abu'l-Qasim-Kashani buztinlari persiarrak zeramikaren fabrikazioari buruzko tratatu bat idatzi zuen (Allan, 1973). Gainera, 1556an, Cipriano Piccolpassok buztinlarien artisautzaren arteari buruzko tratatu bat argitaratu zuen, lehengaiak eta fabrikazio-prozesuak barne, Italiako zeramika maiolikoari buruzko tratatuan (Lightbown eta Caiger-Smith, 1980). Tratatuak *Le Tre Libri dell'Arte del Vasaio* du izena (ingeleraz *The Three Books of the Potter's Art* bezala itzulia). Bilduma hori zeramika maiolikoari buruzko idatzizko lehen dokumentua da. Gainera, Montelupon berriki egindako *Codice Calabranci*-ren aurkikuntza izan liteke mendebaldeko Erdi Aroko tradizio zeramikoari buruzko lehen idatzia (Chiarantini et al., 2014). Hauez gain, badaude ekoizpen teknologiari buruzkoak diren beste dokumentu garrantzitsu batzuk ere, berriagoak direnak, hala nola hiri desberdinetako buztinlarien gremioen ordenantzak (adib. Bartzelonakoak (Cerdà, 2021; García-Oses, 2018) eta Sevillakoak (Fernández de Marcos, 2018; Sánchez-Cortegana, 1994)).

Pasta buztina manipulatzearen ondorioz lortzen dena da. Manipulazio horietan sartzen dira, besteak beste, buztinari koipegabetzaileak gehitzea, buztin bat beste buztin batzuekin nahastea edo ekintza horiek konbinatzea. Ekintza horiek, azaldu den bezala, zeramikak erretzean gertatu daitekeen uzkurdura neutralizatzeko, piezak pitzatu ez daitezen eta nahi den plastikotasuna lortzeko egiten dira (Rice, 1987). Ondoren, pasta modelatzeko, erretzeko, etab. erabiltzen diren baldintzen arabera, fabrika desberdinak lortuko dira. Lerro horietan, fabrika bat zeramika fabrikatzeko prozesu teknologikoa osatu ondoren pastaren azken emaitza izango litzateke (Buxeda i Garrigós eta Cau, 1995; Buxeda i Garrigós eta Madrid i Fernández, 2017). Fabrika hori konposizio mineralogikoaren eta pastaren testuraren arabera identifika daiteke. Hau da, pasta fabrikara bihurtzeko, aldaketak

gertatu behar dira pastaren konposizio kimikoan (Hein eta Kilikoglou, 2017), mineralogian (Maggetti, 1981) eta mikroegituran (Maniatis eta Tite, 1981).

Zeramika sortzeko erabili zen teknologia aztertuz gero, populazio jakin baten faktore sozioekonomikoetan sakondu daiteke, ekoizpen-zikloak aldatu eta egokitu egiten baitira noizean behin, hainbat premia sozial, tekniko eta ekonomiko asetzeko. Ildo horietan, zeramikaren fabrikazioan konplexutasun handiagoa izateak, garapen teknologikoaz gain, konplexutasun sozial handiagoa ere ekar lezake (Buxeda i Garrigós eta Madrid i Fernández, 2017). Horrez gain, koipegabetzaileen identifikazioa, adibidez, garrantzitsutzat jotzen da azterketa arkeometrikoetan, gehitutako materialak kultura-bereizgarri eta aro jakin batekoak izan daitezkeelako. Beraz, erabilgarriak izan daitezke materialak datatzeko garaian eta merkataritza-harremanen azterketan (Rice, 1987).

1.2.3. Zeramiken arkeometriaren arloko egoera

Zeramikaren azterketa arkeologikoaren gaiak duen interesa azken urteetan hazi egin da, eta argitalpen ugari eta aldizkari espezializatuak sortu dira, hala nola *Archaeometry, Journal of Archaeological Science, Journal of Archaeological Science: Reports* eta *Heritage Science* (1.5. irudia).

1.5. irudia. Web of Science datu-basearen emaitzak erakusten dituen grafikoa (2021/11/17an kontsultatua), ingeleraz "topic: archaeometr*", "AND topic: ceramic", "OR topic: pottery" batera sartzen direnean. y ardatzak termino horiek erabiltzen direnean aurkitutako argitalpenen kopurua adierazten du eta x ardatzak argitalpen horien urteak adierazten ditu (1950etik 2020ra)

Arkeometriaren garapenaren deskribapenari dagokionez, hiru fase ezarri ziren arkeometalurgiaren garapenean, eta fase horiek zeramiken arkeometrian ere aplika daitezke (Pernicka, 2011): *prestakuntza-fasea*, *garapen-fasea* eta *hedapen-fasea*. Prestakuntza-faseari dagokionez (XVIII. mendea-1930. urtea), arkeometriaren garapenaren lehen urratsak XVIII. mendekoak dira, nahiz eta XIX. mendearen hasiera arte ez ziren egin lehenengo azterketa sistematikoak. Hala, 1752an, Comte de Caylusek lan bat egin zuen, ziurrenik, lehenengo aplikazio arkeometrikoa izan zena, zeramika Atikoaren berniz beltzak eta terra sigillataren berniz gorrien konposatuak identifikatzeko asmoz (Maniatis et al., 1993). Gero, M. Faradayk (1791-1867) beiraztatutako zeramika erromatarretan berunaren erabilera identifikatu zuen (Trigger, 1988). Gainera, zeramikaren jatorria petrografiaren eta analisi kimikoren bidez ere aztertu zen; Mesa Verden (Colorado) bildutako zeramiken xafla finak analizatu zituen petrografiaz Nordenskiöldek eta emaitza horiek argitaratu zituen gero (Nordenskiöld, 1893). Richardsek, aldiz, Bostongo Arte Ederren Museoko Atenasko zeramika ikertu zuen analisi kimikoen bidez (Richards, 1895) Bestalde, garapen-fasean (1930-1970), X Izpien Fluoreszentzia (XRF) (adibidez,

Hall, 1960) eta Neutroien Aktibazio Bidezko Analisia (NAA) (adibidez, Sayre et al., 1957) areagotu egin ziren. Gainera, literatura arkeometrikoan funtsezko lanetako bat dena idatzi zuen Shepard-ek 1956an, *Ceramics for the Archaeologist* izeneko lana hain zuzen ere, eta zeramika aztertzeko printzipioak eta estrategiak adierazten ditu. Azkenik, hedapen-fasean (1970-oraina) neurketa teknika instrumentalen erabilera areagotzen da, Emisio Optikoko Espektrometrian (OES), ICP-MS, etab. (Pernicka 2011; Pollard eta Heron 1996; Pollard et al., 2007) eta lan gehiago publikatzen dira. Fase honetan, Rice (1987, 2015. urtean berrikusia)-ek liburu bat idatzi zuen, *Pottery Analysis: a source-book* liburua, alegia, buztinen propietateak, ekoizpen-teknologiak eta zeramikaren analisiak, besteak beste, sakonago azaltzen dituen erreferentzia-gida osoa ematen duena. Gainera, fase berri bat gehitu beharko litzateke, *analisi ez-suntsitzaileen fasea* (2000-gaurkotasuna), zeinetan material arkeologikoak aztertzeko metodo eta teknika ez-suntsitzaileak garatzen ari diren (adibidez, Calparsoro et al., 2019a; Liritzis eta Zacharias, 2011; Neff, 2000, 2003, 2012).

Gainera, ikuspegi arkeometrikoa barne hartzen duten zeramikari buruzko argitalpenak, nabarmen hazi ziren 1990eko hamarkadan. Lan zientifiko eta tesi ugariek frogatzen dute hori. Euskal Herrian eta Katalunian arreta handiagoa jarriz, pasta zeramikoetan egindako hurbilpen arkeometrikoei buruzko azterlan eta Doktorego Tesien adibideak ondorengo lerroetakoak dira: Buxeda i Garrigós-ek Cluniako terra sigillatari buruz egindako Doktore Tesi erreferentea (Buxeda i Garrigós, 1994) eta autore beraren eta lankideen lan batzuk (Buxeda i Garrigós, 2008; Buxeda i Garrigós eta Kilikoglou, 2003; Buxeda i Garrigós eta Madrid. 1995, 2003, 2015). Azken lan horietan gai hauek aztertzen dira, besteak beste: konposizio-datuak eta horien aldakortasuna, metodo arkeometrikoa, Erromatar Aroko zeramikari eta Sevilla eta Bartzelonako zeramikari buruzko azterketa tradizional eta arkeometrikoak, eta Pereruelako zeramikaren aldakortasun kimikoa. Gainera, Calparsororen Doktorego Tesia ere garrantzitsua da (Calparsoro, 2019), euskal eta Errioxako zeramika-ekoizpenen karakterizazio arkeologiko eta arkeometrikoari buruzkoa, autore beraren eta lankideen lanekin batera (Calparsoro et al., 2019b,c, 2021). Lan hauetan, Urduñako (Euskal Herria), Logroñoko eta Naiarako (Errioxa) Erdi Aro osteko zeramika aztertzen da arkeometrikoki. Lan hauez gain, Iñañezen Doktorego Tesia (Iñañez, 2007) eta autore beraren eta lankideen lanak (Iñañez et al., 2008, 2009, 2018, 2020, 2021) ere aipatu behar dira. Tesi horretan, Iberiar Penintsulako Behe Erdi Aroko zeramiken karakterizazio arkeometrikoa egin zen,

eta beste lanetan Erdi Aroko eta Erdi Aro osteko Iberiar Penintsulako, Kanariar Uharteetako, Ceutako, Marokoko, Zamorako eta Angra D ontzi-hondakineko zeramikak aztertu ziren arkeometrikoki. Bestalde, Madrid i Fernández-ek ere ekarpen garrantzitsuak egin ditu: bi, Erromatar Errepublikar Garaiko beira beltzeko zeramikari buruzkoa (Madrid i Fernández eta Sinner, 2019, 2021), eta, bestea, Augustoren garaian merkaturatutako terra sigillata ekoizpenen karakterizazio arkeometrikoari buruzkoa (Madrid i Fernández eta Buxeda i Garrigós, 2007). Gainera, K.o. I. mendeko sigillata hispanoa ere aztertu zuen lankideekin batera (Madrid i Fernández eta Buxeda i Garrigós, 2014), baita Galia hegoaldeko sigillata zeramika ere, Baetuloko (Badalona) herrixka erromatarrean dokumentatua (Madrid i Fernández et al., 2014). Lan hauek argitaratu baino lehen, gainera, Baetuloko terra sigillataren karakterizazio arkeometrikoari buruzko Doktorego Tesia argitaratu zuen Madrid i Fernández-ek (Madrid i Fernández, 2006). Hauez gain, berriki argitaratutako Puig Barrachina (2016)-ren, Fernández de Marcos (2018)-en eta Pinto-Monte (2021)-ren Doktorego Tesiak ere gehitu daitezke, lehenengoa euskal zeramikari buruzkoa, bigarrena Sevillako zeramikari buruzkoa eta azkena Valentziako zeramikari buruzkoa. Bestalde, pasta zeramikoei, beiradurei eta pasta eta beiraduren arteko elkarrekintzari buruzko ikerketen adibide bat Moleraren Doktorego Tesia da (Molera, 1997). Gainera, autorearen eta lankideen lanak ere aipatu behar dira (Molera et al., 1997, 1998, 1999, 2001). Lan hauetan, berun beirarekin beiraztatutako zeramika hispaniar-moriskoen teknologia eta kolore-garapena, kaltziodun pasta zeramikoen kolorea, eztainu-berunezko beiraduretan eztainu-oxidoa birkristalizatzearen ebidentzia eta gorputz zeramikoen eta berun beiraduren arteko elkarrekintzak aztertzen dira. Aipatzekoak dira ere antzinako beiraduren koloreari eta teknologiari buruzko Molina-ren Doktorego Tesia (Molina, 2014) eta zeramiken pigmentu horiei buruzko Ferrer-en Doktorego Tesia (Ferrer, 2014). Gainera, Peix Visiedo et al. (2021), Salinas eta Pradell (2018), Tite et al. (1998) eta Vendrell-Saz et al. (2000)-ek Bartzelonako XIII.-XIV. mendeetako eztainu berunezko (eta berdez eta beltzez apaindutako) zeramika beiraztatuari buruzko, Al-Andalusen beiradura erabiltzen hasteari buruzko, antzinateko ekoizpen-metodoei eta antzinatean berun beiradurak erabiltzeko arrazoiei buruzko eta berun beiraduren propietate optikoei buruzko azterlanak egin zituzten, hurrenez hurren. Lerro hauetan, pigmentuen azterketari buruzko lan batzuk Iñañez eta lankideenak (Iñañez et al., 2013) eta Pérez-Arantegui et al. (2008)-enak dira. Gainera, beiraduren berunaren jatorriari buruzko lanak ere badaude (Iñañez et al., 2010, 2016). Bestalde,

Grassi eta Quirósek Erdi Aroko zeramikaren azterketa arkeometrikoen berrikuspen bat argitaratu zuten (Grassi eta Quirós, 2018).

Honez gain, berriki argitaratu diren berrikuspenen artean, *Ceramics: Research questions and answers* izeneko bilduma dago eta ikertzaileak zeramika arkeologikoaren azterketan orientatzeko helburua du, indusketetatik hasi, zeramikak aztertu eta museoetan bildumak gordetzeraino. Hala, ikerketa-galderak eta laginketa-irizpideak Gliozzo (2020a)-an aztertzen dira. Gero, lan batzuk lehengaien ikerketaz arduratzen dira: hauen ikerketa kimikoak Hein eta Kilikoglou (2020)-k, eta mineralogiko-petrografikoak Montana (2020)-k jasotzen dituzte, eta Gualtieri (2020)-k lehengaien teknologia- eta egokitasun-izaerari buruz idazten du. Gainera, Eramo (2020)-k buztinen prozesaketari buruzko lan bat argitaratu du, eta lerro horietan, Thér (2020)-ek buztinen modelizazioaren gaia landu du. Honez gain, Gliozzo (2020b)-k eta Maritan (2020)-ek zeramikaren eraldaketaren gaiari heldu diote, hala nola, zeramika erretzeari eta jalkitze-osteko eraldaketak identifikatzeari. Gainera, zeramika zaharberritzearen eta musealizatzearen gaiari buruz argitaratu du Lapérouse (2020)-k. Bestalde, gainazalari eta estaldurari buruzko gaiak ere argitaratu dira. Ildo horietan, Ionescu eta Hoeck (2020)-ek gainazalaren akaberari buruz idatzi dute, eta hainbat estalduraren ikerketa, hala nola beira beltzena, terra sigillatarena eta beiradurena, Aloupi-Siotis (2020), Pradell eta Molera (2020) eta Sciau et al. (2020)-ek azaltzen dute, hurrenez hurren. Gainera, Hendersonek eta lankideek hainbat produktu-motaren azterketa isotopikoa aztertu dute, hala nola tenperatura altuetan erretako zeramika txinatarrarena (Henderson et al., 2020). Gero, zeramikaren datazioa Gallik eta lankideek azaltzen dute (Galli et al., 2020). Azkenik, bilduma hau datu estatistikoen prozesamenduari buruzko tutorial batekin amaitzen da (Papageorgiou, 2020).

Aipatu beharra dago lan honetan zehar atal ezberdinei buruzko arloko egoera atal zehatz horietan jaso dela (esate baterako, berun beiraduren analisien arloko egoera 1. kapituluko 1.2.1. atalean ematen da).

1.3. Gaur egungo erronkak ikerketa arkeologikoan

Ikerketa arkeometrikoaren egungo erronka nagusiak metodologia ez-suntsitzaileak garatzea eta jalkitze-osteko kutsadura- eta eraldaketa-prozesuen identifikazioa dira.

1.3.1. Metodologia ez-suntsitzaileak garatzea

Teknika analitiko suntsitzaileak, hala nola, Absortzio Atomikoaren Espektrometria (AAS) (adibidez, Tubb et al., 1980), Induktiboki Akoplatutako Plasmaren Emisio Atomikoaren Espektrometria (ICP-AES) (adibidez, Storey et al., 1988) eta Induktiboki Akoplatutako Plasmaren Masa espektrometria (ICP-MS) (Dussubieux, 2020) nagusi izan dira zeramiken analisi kimikoetarako (Glascock, 2016; Hunt, 2016; Pérez-Arantegui, 2018; Pollard et al., 2007). ICP-MS da erabiliena horretarako, eta lagina neurtu ahal izateko, lehenbizi ehotu egin behar da, eta gero disolbatu. Erabiltzen den beste teknika suntsitzaile bat Neutroien Aktibazio Bidezko Analisia da (NAA). Teknika hau oso eraginkorra da, eta, gainera, lagina ez da aurrez prestatu behar, baina gutxiago erabiltzen da, erreaktore nuklearra behar delako horretarako (ikus, adibidez, Speakman eta Glascock (2007)-en NAAri buruzko zenbaki berezia eta García-Heras et al., 2001; Glascock, 1992, 2014; Iñañez et al., 2008; Neff, 2000-en lanak). Beste teknika alternatibo batzuk X Izpien Fluoreszentzian (XRF) oinarritzen dira, eta hauek lagina prestatzeko kostu txikiagoa dute edo ez dute behar. XRF arrunterako, adibidez, laginaren pastilla prestatu behar da analisietarako. Ordea, beste XRF mota batzuekin analisi ez-suntsitzaileak egin daitezke. Hauen artean daude, adibidez, ED-XRF (Energia Sakabanatzailezko X Izpien Fluoreszentzia) screening metodologia, Calparsoro eta lankideek optimizatua (Calparsoro et al., 2019a), HH-ED-XRF (Eskuko Energia Sakabanatzailezko X Izpien Fluoreszentzia) (Maguregui et al., 2018), edo XRF eramangarria (pXRF) (Forster et al., 2011; Hunt, 2016; Hunt and Speakman, 2015; Kelloway et al., 2019; Liritzis et al., 2020; Millhauser et al., 2011; Speakman et al., 2011). Hala ere, teknika hauen emaitzen fidagarritasuna ez da ICP-MS-ek eman dezakeenarena bezain altua. Gainera, ICP-aren beste instrumentu analitiko alternatibo bat, ez-suntsitzailetzat jotzen dena, gero eta gehiago erabiltzen da, Laser Ablazioa-ICP-MS (LA-ICP-MS), alegia (Dussubieux et al., 2016; Giussani et al., 2009; Neff, 2012; Resano et al., 2005). Hala ere, lagina (zeramika) LA-ICP-MS edo ED-XRF-ren lagin-ganbera baino handiagoa bada, lagina moztea beharrezkoa izan daiteke, teknika suntsikorra bihurtuz. Nolanahi ere, zeramika mozteak suntsitzea badakar ere, urrats horrek inbasibitate-maila oso baxua du, laginak ehotzearekin alderatuta; izan ere, ebaketa-zatiak berriro erabil daitezke beste azterketa batzuk egiteko edo gordetzeko.

Zeramika arkeologikoaren analisi kimikoak batez ere teknika analitiko suntsitzaileen bidez egin izana arazo garrantzitsua da kultura-ondarea eta museo-

bildumak lantzeko orduan, kultura-ondarea zaintzea eta gordetzea baita kezka nagusietako bat. Gainera, kasu batzuetan ezin da lagina laborategira eraman; beraz, funtsezkoa da tresna eramangarri ez-suntsitzaileen metodoak optimizatzea kultura-ondarea aztertzeko. Lerro hauetan, adibidez, Maguregui et al. (2018)-ek lehen aldiz aurkeztu zuten HH-ED-XRF-rentzako metodologia *in situ* ez-inbaditzailea, Edo periodoko (1603–1869) armadura japoniarra sortzeko erabilitako metalen eta aleazioen eta laken konposizioa karakterizatzeko. Armadura in situ ikertu zen, laginik hartu behar izan gabe, ondoren, Arabako Zaharberrikuntza Zerbitzuan kontserbatzeko.

1.3.2. Jalkitze-osteko kutsadura- eta eraldaketa-prozesuak zeramika arkeologikoan

Lurpean denbora luze batez egon ondoren berreskuratutako antzinako zeramikak hainbat aldaketa eta kutsadura jasan ditu. Hauek aldakortasun kimiko bat eragiten dute, aldakortasun naturalari eragiten diona, hau da, pasta zeramikoaren konposizio kimikoa eta mineralogikoa ez dira jatorrian izan ziren berak izango (Buxeda i Garrigós, 1999). Beraz, funtsezkoa da lurperatutako zeramikan gertatzen diren kutsadura- eta eraldaketa-osteko prozesuak ezagutzea. Atal honek eraldaketa mota horiei buruzko oinarri orokor bat ematen du, eta Doktorego Tesi honen 5. kapitulurako sarreratzat har daiteke.

Zeramika arkeologikoen jalkitze-osteko kutsadura- eta eraldaketa-prozesuak kanpo-agenteen (jalkitzearen testuingurua edo ingurumena definitzen dutenak), agente intrintsekoen (objektuaren parte direnak, hala nola materialak edo teknologia) eta bien arteko elkarrekintzaren emaitza dira (Fantuzzi, 2010 eta bertako erreferentziak). Kanpo-agenteek gune naturalak eratzeko zenbait prozesu hartzen dituzte, hala nola bioturbazioa eta ibai-garraioa, baita kultura-prozesu batzuk ere (adibidez, goldatzea, arpilatzea). Gainera, eragile abiotikoak, hala nola haizeak eragindako abrasioa, gai dira zeramikan hainbat aldaketa mota eragiteko. Halaber, garrantzitsua da sedimentuak eta lurzoruak aztertzea, zeramikan gertatu ziren lurperatze-baldintzak eta jalkitze-osteko prozesuak ulertzeko, lurperatze-testuinguruen portaera lurzoruena bezalakoa baita (Cremaschi, 2000). Arroketan eta sedimentuetan jarduten duten prozesu fisiko, kimiko eta biologiko ugariren arteko interakzio konplexuaren emaitza da lurzorua, eta etengabe mugimendu kimikoak eta haien elementuen birbanaketa gertatzen diren sistema dinamikoa da

(Holliday, 1992). Materialaren kontserbazioari dagokionez, lurzoruen testura (granulometria, morfologia, etab.), pH-a (azidoa, neutroa edo basikoa), erredox potentziala (Eh) (ingurune erreduktorea edo oxidatzailea), hezetasuna, gatzak eta agente biologikoak (fauna eta flora) bezalako ezaugarriak dira materialaren kontserbazioari eragiten diotenak (Guevara, 2001; Magaña et al., 2001). Lurzoruen granulometriak eragina du airea eta ura garraiatzeko, eta, hala, eragina du oxidazio eta hidrolisi prozesu kimikoetan ere. Lurzoruen pH-ari dagokionez, material zeramikoak hobeto kontserbatzen dira lurzoru basikoetan, hau da, kaltzio, sodio eta magnesio ugari duten lurzoruetan. Eh da lurzoru batek elektroiak emateko edo hartzeko duen gaitasuna, ingurunea erreduzitzailea edo oxidatzailea den arabera, eta pH-arekin eta inguruneko oxigeno-edukiarekin lotuta dago. Bestalde, hezetasunak katalizatzaile gisa jarduten du erreakzio gehienetan, eta klimaren eta faktore edafokimikoen (hala nola iragazkortasuna, hedatzeko eta uzkurtzeko gaitasuna eta lixibiazioa) araberakoa izango da, besteak beste. Flora eta faunari dagokionez, sustraien ekintza da zeramika honda dezaketen faktore nagusietako bat. Tamaina jakin bateko faunak aldaketa fisiko batzuk ere eragin ditzake (adibidez, zatikatzea), ez bakarrik animalien zulaketen ondorioz, baita beste prozesu batzuen ondorioz ere, hala nola zapalketaren ondorioz. Lurperatzearen testuinguruaren alderdi horietatik haratago, garrantzitsua da aipatzea klima ere funtsezko faktorea dela, materialak lurperatzen diren lurzoruen barruan gertatzen diren zenbait mekanismo definitzen baititu. Adibidez, klima tropikalak bereziki kaltegarriak dira zeramikaren kontserbaziorako, lurzoru azidoak daudelako eta bereziki karedunak diren osagaiak disolbatzen laguntzen dutelako (Fantuzzi, 2010; Maritan, 2020).

Aitzitik, agente intrintsekoak material zeramikoaren ezaugarriak dira, alegia, erabilitako lehengaiak eta fabrikatzeko eta erretzeko teknikak. Agente hauek objektu baten erresistentzia, iraunkortasuna eta ahultasun-maila zehaztuko dituzte (Oakley eta Jain, 2002). Beraz, funtsezkoa izango da zeramikaren fabrikazioaren urratsak ezagutzea (lehengaien erauzketa eta prestaketa, fabrikatzea, lehortzea, erretzea eta erabilpena), hauek zeramikaren eraldapen prozesuan duten eragina ulertzeko (Buxeda i Garrigós eta Madrid i Fernández, 2017). Materialaren kontserbazioa definitzen duten ezaugarriak hauek dira, eta erlazionatuta daude: buztinak erreketan hartzen duen kohesio-maila, bitrifikazio-maila eta zeramikaren gogortasuna eta porositatea, besteak beste (Berducou, 1990).

Gainera, zeramikaren eta ingurumenaren arteko elkarrekintzaren mende ere badago materialaren kontserbazioa. Interakzio horietako bat, esate baterako, zeramika errehidratatzea da; erretzean, buztin-partikulek egiturazko ura galtzen dute, hala ere, lurperatutako zeramikak ingurunetik xurga dezake ura, eta materiala hedatu egin daiteke (Freestone, 2001; Rice, 1987). Beste interakzio bat gatzen kristalizazioa da; lurzoruan zirkulatzen duten disoluzioak zeramikan sar daitezke poroetatik kapilaritate bidez. Ondoren, disoluzio horiek lurrundu egin daitezke, eta sodio, potasio, kaltzio eta magnesio kloruroak, sodio, potasio eta magnesio sulfatoak, nitratoak, bikarbonatoak, azetatoak eta fosfatoak, kristaliza daitezke zeramikaren azalean eta poroetan (Maritan, 2020; Paterakis, 1987). Gainera, zeramikaren eta lurperatuta dagoen ingurunearen arteko interakzioak ioien adizioa, ioien eliminazioa edo ingurunearen eta zeramikaren arteko truke ionikoa ekar dezake. Elementu batzuen kontzentrazioan anomaliak egotea (metaletan, hala nola K, Na, Mn, Mg, Ca, Fe eta ez-metaletan, hala nola F eta P) elementuak finkatzearen ondoriozko kutsadurarekin lotuta egon daiteke (Buxeda et al., 2002a; Freestone et al., 1985, 2001; Lemoine eta Picon, 1982; Maritan eta Mazzoli, 2004; Maritan, 2020; Schwedt et al., 2004, 2006). Finkatze-fenomeno hori "U" itxurako difusio-profil baten bidez azter daiteke zeramikaren hormetan zehar, gainazalak nukleoak baino kutsatuago egongo baitira. Honez gain, zeramikaren eraldaketaren faktore nagusia uraren zirkulazioa da eta honek inguruko lurzoru-soluzioarekin katioiak trukatzea ahalbidetzen du, zeramikaren porositatearen arabera. Beste aldaketa batzuk (adib. gainazalaren abrasioa), pastaren gogortasunaren, porositatearen, eta koipegabetzaileen inklusioen banaketa eta orientazioaren araberakoak dira, esate baterako (Schiffer eta Skibo, 1989; Skibo eta Schiffer, 1987). Estalduraren eta pasta zeramikoaren osagaien heterogeneotasuna ere eraldaketa-iturri izan daiteke. Heterogeneotasun horrek zeramikari beste portaera termiko bat eman diezaioke, hura dilatatuz eta hedatuz, eta horrek zatiketa zeramikoa eragin dezake (Fantuzzi, 2010). Hala ere, estaldurak lurzoruko soluzioak sartzea eragozten du, korrosioa ekidinez (Freestone, 2001). Azkenik, zeramiken kontserbazioari eragin diezaiokeen beste alderdi bat ontzien funtzionaltasuna da; elikagaiak gordetzeko erabiltzen diren ontziak aldatu egin daitezke hainbat azido-motaren bidez (adibidez, zitrikoa, malikoa, sukzinikoa eta azetikoa) (de la Fuente, 2008; Skibo, 1992).

Jalkitze-osteko kutsadura- eta eraldaketa-prozesuen arloko egoerari dagokionez, zenbait autorek arazo horiek aztertu eta ebaluatu dituzte kasu errealak

aztertuz eta esperimentuak eginez. Alde batetik, kasu errealak aztertzeko lanen artean, adibidez, Amadori et al. (1998)-en lana dago, zeinetan Italiako azuleju maiolikoetan gertatutako eraldaketa-bideak aztertu zituzten, eta wairakita eta kaltzita dokumentatu zituzten alterazio-produktu gisa. Gainera, Buxeda i Garrigós eta lankideek (Buxeda i Garrigós, 1999; Buxeda i Garrigós eta Cau, 1994; Buxeda i Garrigós et al., 2001, 2002a,b) zeramika arkeologikoaren eraldaketak eta kutsadurak aztertu zituzten. Lan horietan, zeramiketan bigarren mailako kaltzita zegoela dokumentatu zuten (hau da, eraldaketa-prozesuen ondorioz agertutako kaltzita; Cau et al. (2002)-k eta Gilstrap et al. (2021)-ek ere aztertu zuten kasu hau). Gainera, Na, K eta Rb-ren kontzentrazioen aldaketak ere aztertu zituzten, analtzimaren kristalizazioarekin zerikusia dutenak (aldaketa-mota horiek sakonki azalduta daude 5. kapituluan), baita Iulia Felix ontzi-hondakinean aurkitutako anfora erromatarrean bigarren mailako piritaren kristalizazioa ere (eraldaketa-modu hau sakonki azaltzen da 6. kapituluan). Ontzi-hondakinetan berreskuratutako zeramikaren alterazioekin zerikusia duten beste ikerketa batzuk Iñañez et al. (2020)-ena, Renson eta Glascock (2021)-ena eta Mise et al. (2021)-enak dira. Lehenengoan, pirita identifikatu zen, bigarrenean, berun bidezko kutsadura identifikatu zen berun isotopoen analisiaren bidez eta hirugarrenean, ikertutako anforak elementu batzuetan aberasten zirela eta beste elementu batzuen edukia jaitsi egiten zela dokumentatu zen. Gainera, Freestone (2001)-ek lurperatutako zeramiketan eta beiraduretan gertatzen diren aldaketak aztertu zituen, eta Freestone et al. (1985)-ek lurperatutako zeramikan fosfatoaren atxikipena aztertu zuen. Ildo horietan, Lemoine eta Picon (1982)-ek ere fosforoaren finkapena aztertu zuten zeramikan, eta Lemoine et al. (1981)-ek itsas lur inguruneetan lurperatutako zeramiken aldaketak aztertu zituzten. Fosforoarekin lotutako alterazioa 6. kapituluan azaltzen da. Bestalde, Picon (1976)-en lana ere jalkitze-osteko eraldaketak aztertzen dituen beste adibide bat da. Autoreak itsasoko uretan dagoen magnesioaren fijazioa identifikatu zuen zeramiketan. Gainera, Pradell et al. (1996)-ek eta Secco et al. (2011)-ek itsas giroetan eta lakuen antzeko inguruneetan lurperatutako zeramiken aldaketa-prozesuak aztertu zituzten, hurrenez hurren, eta azken lanean pirita eta jarosita zegoela dokumentatu zuten. Gainera, Schwedt et al. (2004, 2006)-ek zeramikan gertatutako aldaketak aztertu zituzten, eta analtzimaren kristalizazioa dokumentatu zuten, hurrenez hurren, eta Tschegg (2009)-ek jalkitze-ostean gertatu izan den artefaktu zeramikoen azaleko zuritzea aztertu zuen. Azkenik, Stoner eta Shaulis (2021)-ek eta Golitko et al. (2021)-ek, beste gauzen artean, zenbait laginen pasten konposizio kimikoaren mapatze bat egin zuten,

elementu batzuek zeramiken barruan edo kanpoan izan zezaketen lixibiazioa identifikatzeko. Bestalde, lan esperimentalen artean, Béarat et al. (1992)-en lana aurkitzen da, zeinetan itsasoan jalkitako zeramiken alterazio fisiko-kimikoak aztertu zituzten. Autore horiek hiru esperimentu-talde egin zituzten, esperimentu bakoitza buztin mota batekin, guztiak ere tenperatura desberdinetan erreta. Lehen taldeko zeramikak hauts bihurtu zituzten eta 6 urtez berritu gabeko itsas uretan murgildu zituzten. Bigarren esperimentuko zeramikak ere hauts bihurtu zituzten eta bi hilabetez itsasoko uretan murgildu zituzten. Aitzitik, hirugarren esperimentuko zeramika batzuk hauts bihurtu zituzten, eta beste batzuk briketa gisa utzi zituzten eta 3, 5, 6 eta 10 hilabetez berritu gabeko eta berritutako itsas uretan murgildu zituzten. Heimann eta Maggetti (1981)-k ere esperimentuak egin zituzten klima heze batean zeramiken jalkitzea simulatuz. Horretarako, autoreek La Penicheko buztinak jaso eta erre zituzten eta gero Tefloiz estalitako autoklabeetan baldintza naturalak simulatzen zituzten soluzioetan murgildu zituzten. Autoreek autoklabeak lehortze-armairuan utzi zituzten bi astez 200 °C-tan erreakzioak azkartzeko eta, hartara, zeramikaren jalkitze-denbora erreala simulatzeko. Gainera, Montana et al. (2014a)-ek eta Belfiore et al. (2014)-ek ere esperimentu bat egin zuten itsas uretan jalkitako zeramikaren eraldaketak eta kutsadura aztertzeko. Autore hauek sei pasta ezberdin fabrikatu zituzten kaltziodun eta kaltzio baxuko buztinekin, eta bi harea mota gehitu zituzten koipegabetzaile gisa, guztiak Sizilian bilduak. Pasta horiek 150 briketa eta zilindro egiteko erabili zituzten. Zeramika horiek itsaso irekian finkatutako euskarrietan eta itsasoko urez betetako sistema konfinatu batean jarri zituzten eta sistema honen ura etengabe berritzen zuten. Gainera, astero parametro fisiko-kimikoak monitorizatzen zituzten, hala nola tenperatura, pH-a, eroankortasuna, gazitasuna, disolbatutako solido totalak (TDS) eta erredox potentziala. Azkenik, Franklin eta Vitali (1985)-k jalkitako zeramiken egonkortasuna aztertu zuten, giro-tenperaturan. Horretarako, konposizio ezaguneko kaltziodun briketa zeramikoak egin eta erre zituzten, eta hainbat ur-disoluzioren eraginpean jarri zituzten. Disoluzio horien pH-a eta tenperatura (25 °C-an eta 90 °C-an) kontrolatu zituzten.

Azterketa horiei esker (kasu errealak eta lan esperimentalak), jakina da zenbait elementuren alterazio- eta kutsadura-prozesuak eta zenbait elementuren bazterketa kontuan hartu behar direla zeramika aztertzerako garaian, hauen jatorriari, teknologiari eta artefaktuaren erabilerari buruzko interpretazio okerrak saihesteko, baita artefaktua behar bezala kontserbatu ahal izateko ere (Buxeda,

1999; Buxeda et al., 2001; Calparsoro, 2019; Franklin eta Vitali, 1985; Freestone, 2001; Maritan, 2020; Maritan eta Mazzoli, 2004). Beraz, hor jarri behar da arreta jatorriaren ebaluazioa bezalako azterketak egiteko garaian.

2. KAPITULUA: ZAMORAKO ETA AVEIROKO EKOIZPENAK

Doktorego Tesi honetan Zamora lurraldeko (Zamora hiria, Toro eta Benavente herriak, Espainian) eta Aveiroko (Portugalen) ekoizpenak aztertu dira. Kapitulu honetan, bi lekuak deskribatuko dira, beren zeramika ekoizpenari dagokionez.

2.1. Zamora probintziaren ekoizpena

Zamora hiria Iberiar Penintsularen ipar-mendebaldean kokatzen da, Duero ibaiaren arroan, eta Espainiako izen bereko probintziaren hiriburua da (2.1. irudia). Zamorak tradizio luzea du zeramikan eta bertako Erdi Aro osteko zeramikek lotura estua dute Gaztelako Berant Erdi Aroko zeramika tradizionalekin, bereziki tipologiei dagokienez. Hala, Zamorako zeramikak, maiz, tipologia irekiak erakusten ditu, hala nola platerak eta goporrak, baita itxiak ere, pitxerrak eta sukaldeko eltzeak bezalakoak (Larrén, 1991; Villanueva, 2011).

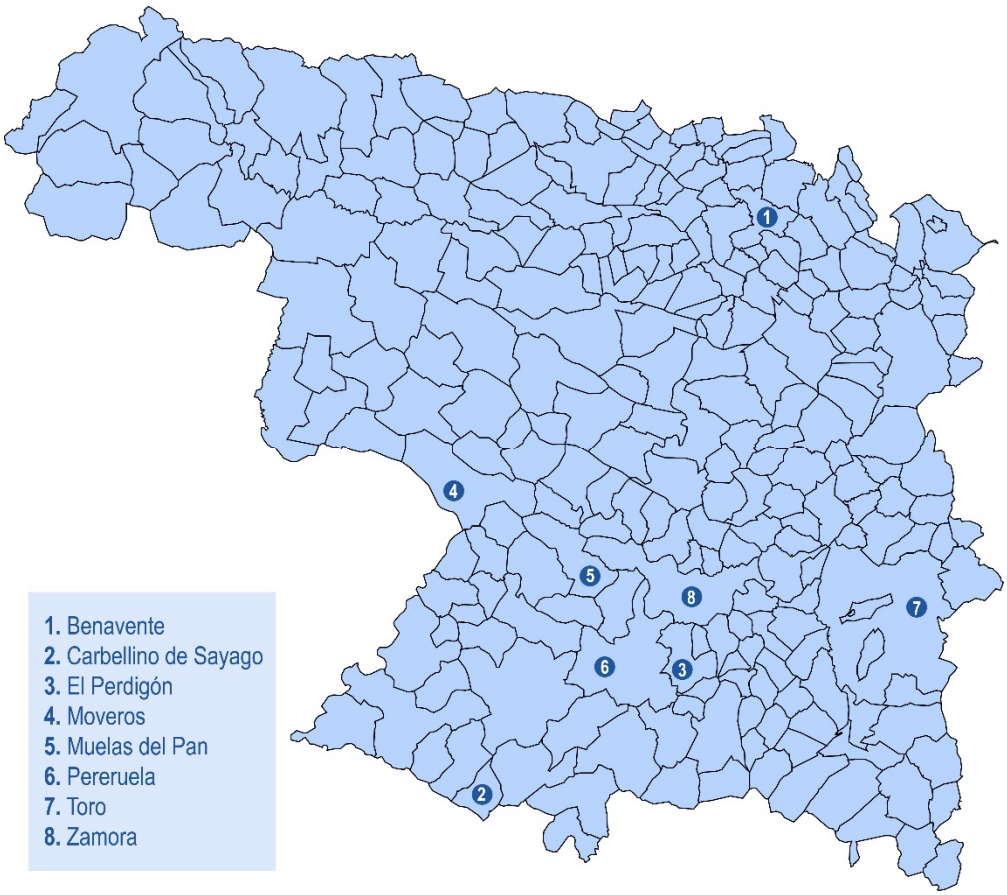

2.1. irudia. Zamora probintziaren mapa, non Zamora, Toro, Benavente, Pereruela, Muelas del Pan, Moveros, Carbellino de Sayago eta El Perdigón markatuta agertzen diren

Zamorako ia probintzia osoa Dueroko Arro Hidrografikoan kokatzen da. Gertaera tektoniko bat garatu zen Alpetar orogenian zehar: Afrika eta Europako plakek talka egin zuten, eta horrek mendikate handiak altxatzea ekarri zuen, hala nola Kantauriarra, Sistema Iberikoa, Pirineoak, Betikoak edota Sistema Zentrala. Erliebe hauen higadurak sortutako materialak Tertziarioan eratu ziren arroak (adibidez, Duerokoa) bete zituen. Sedimentazioak patroi honekin jarraitu du gaur egun arte, eta, horrela, Kuaternarioko metaketak sortu dira. Metaketa horiek probintziaren mapa geologikoa osatzen dute eta lurralde osoan zehar banatzen dira, batez ere gaur egungo ibaien haranetan. Zamora probintzian bi eskualde geologiko handi edo arroka-multzo aurki daitezke: Iberiar Mendigunea osatzen duen basamentua, mendebaldeko ertz osoa hartzen duena, eta Duero ibaiaren Arroko material sedimentarioak, ekialdeko erdialdean azaleratzen direnak. Beraz, basamentu hertzinikoa probintzia osoaren zokaloa da, mendebaldeko ertz osoan azaleratzen dena. Bertan, aurrekanbrikoko eta paleozoikoko arroka sedimentarioen segida batzuk aurki daitezke, eta orogenia hertziniarreko arroka igneo ugari (Fadón, 2011).

Buztingintzarako, Zamorako probintzian batez ere bi buztin mota ustiatu izan dira gaur egun arte: buztin gorriak eta buztin zuriak. Alde batetik, buztin gorrien ustiaketa batez ere Toro eta Benavente herrien inguruan zentratu da, baina buztin horiek antzinako zeramikagintzarako Pereruelan, Moverosen eta Zamora hirian ere ustiatzen ziren harrobi txikiagoetan. Bestalde, buztin zurien taldean kaolinita (aluminio silikato hidratatua) eta buztin kaolinitikoak sartzen dira. Kaolinita oso erabilia izan da (eta gaur egun ere erabiltzen da) material errefraktatzaileak egiteko (hau da, tenperatura altuak jasan ditzaketen materialak), granulometria lodiko ezpurutasunetan aberatsa (granitoan, alegia) baita. Buztin hauen ustiapena Tamame de Sayagon, Pereruelan, Peñausende edo Fresnon egin izan da (Fadón, 2011).

Buztinen banaketa geografiko horrek ekarri zuen Zamorako herri desberdinetan zeramika desberdinen ekoizpenen espezializazioa. Horrela, Erdi Arotik Pereruelan, Moverosen eta Muelas del Panen, esate baterako, sukalderako zeramikak egiten zituzten kaolinita erabiliz (eta, horretarako, askotan buztin gorriekin nahasten zuten kaolinita; Buxeda et al., 2003; Villanueva, 2011). Buztin hauek erabilita lortzen ziren zeramikei zeramika mikatsu ere deritze. Aipatutako hiru herriek eta Torok eta Benaventek (azken bi hauetan batik bat baxerarako zeramika gorri ez-mikatsua egiten zen) eratu zuten Zamorako zeramikagintzaren

hasiera-puntua, eta hauez geroztik, beste zeramika-zentro batzuk sortu eta garatu ziren Zamoran, esate baterako, Zamora hirian, Carbellino de Sayagon, Cibanalen, Fornillos de Fermosellen, Junquera eta Milla de Teran, El Perdigónen edo Venialbon. Hauek guztiek zeramika tradizionalaren ikuspegia osatu zuten Zamoran, XX. mende hasiera arte. Une horretan, gehienek beren lantokiak itxi behar izan zituzten modernitatearen aurrerapenen aurrean, baina beste batzuek bizirik diraute (Moratinos eta Villanueva, 2006) (2.2. irudia).

2.2. irudia. Paco zeramikagilea da eta *Alfarería Pascual* izeneko lantegian egiten du lan, Moverosen. Lantegi hau bere familiarena da eta haren emazteak eta alabek ere bertan egiten dute lan, zeramika ekoizten. Argazkia 2019an atera zuen Sanchez-Garmendiak

Muelas del Panen zeramikagintzaren historia (2.3. irudia) 1547ko erreferentzia zaharrenak hasten du. Erreferentzia horretan Muelas del Paneko zeramikagile batek Gaztelako Juana I erreginak Tordesillasen zuen jauregirako behar zituen konketak (*barreño*) egiten zituela aipatzen da (Villanueva, 2011). Berri

honek adierazten du, ezbairik gabe, Muelas del Panen bazegoela jada data honen aurretik zeramika ekoizpen finkatu bat. Bere lantegietan baxerarako eta sukalderako zeramika mikatsuak egiten ziren, hala nola eltzeak, pitxerrak, konketak, txongilak eta arragoak. Bestalde, Pereruelako zeramikagintza, miken eta kuartzoen intrusioetan aberatsagoak diren buztinekin egindakoa, Muelas del Paneko zeramikagintza baino lehenago hasi zen, 1410. urtean jada aipatzen baita (2.4. irudia) (Moratinos eta Villanueva, 2006; Villanueva, 2011).

2.3. irudia. Muelas del Paneko emakume zeramikagile bat (Iturria: Luis Cortés, Gaztela eta Leongo Museo Etnografikoa, Zamora, Moratinos eta Villanueva (2006)-tik berreskuratua)

2.4. irudia. Víctor Redondo Tamameren (Pereruelako zeramikagilea) *Alfarería de Pereruela* izeneko lantegian gordeta dauden zeramika mikatsuak. Argazkiak 2019an atera zituen Sanchez-Garmendiak

Gainera, Toro herrian ere bazegoen zeramikari eskainitako artisau-sektore garrantzitsu bat. Bertako *Cuesta del Negrillo 11* kaleko eraikina buztinlarien jardunari lotutako eraikina izan zen, eta hemen egindako indusketa arkeologikoek pieza akastunen hondakindegi bat aurkitu zuten; besteak beste, janaria prestatzeko eta gordetzeko ontziak eta baxerarako ontziak aurkitu ziren bertan (adibidez, eltzeak, kikarak, pitxerrak, bolak, txongilak eta platerak) (Larrén 1991, 1992). Bestalde, Benaventeko zeramikaren jarduera ere ezaguna izan zen Erdi Arotik Aro

Modernorako trantsizioan. XVIII. mendearen erdialdean, hamaika eltzegile agertu ziren posizioen eta lanbideen zerrendan. Benaventeren produkzioan, zenbait pitxer beren tipologia bereziagatik nabarmentzen dira eta "jarritas carenadas" bezala ezagutzen dira gaztelaniaz. Baxerarako ontzi bezala erabil zitezkeen: kirtena zutenak likidoak isurtzeko, eta kirtenik gabekoak edalontzi bat bezala. Baina, hiru tamainatan fabrikatzen zirenez, beste funtzio espezifiko bat ere izan zezaketen: 300 ml, 200 ml edo 100 ml neurtzea, hain zuzen (Villanueva, 2011).

Toro eta Benaventeko buztinlariek buztin burdintsuak erabiltzen zituzten, ez-mikatsuak, buztin gorri bezala ere ezagunak (*barro rojo o bermejo* bezala ezagutzen direnak gaztelaniaz) (2.5. irudia) (De La Mata, 1989). Buztinak batez ere Toro eta Benavente herrietatik gertu zeuden Los Toriles, Tagarabuena, Eras del Sepulcro, San Antón eta Valle la Zarza eremuetan erauzten ziren eta erauzketa zeramikariek edota beren laguntzaileek egiten zuten. Buztin hauek ezaugarri fisiko onak zituzten modelatzeko, beren plastikotasunagatik; hala ere, harearekin nahasten ziren sukalderako bideratu nahi bazituzten (zartaginak, eltzeak...) (De La Mata, 1989; Larren 1991).

2.5. irudia. Toro eta Benaventeko zeramikak (lehenengo biak Torokoak dira, eta azkeneko biak Benaventekoak). Eskala-barra: 8 cm

Zamora hiriko *Olivares*-eko lantegiei dagokienez, tradizionalki (Goi Erdi Arotik), hiria eta eskualdeko zati handi bat bertan ekoitzitako zeramikaz hornitzen zituzten tokitzat hartu dira (Villanueva, 2011). Zamora hiriko zeramikaren ekoizpenaren lehen ebidentzia idatzia 1279koa da, eta Erdi Aroko harresidun hiritik kanpo dagoen buztinlari-auzo bat aipatzen du. Gainera, XV. eta XVI. mendeetan zeramika ekoizteko jarduerari buruzko beste ebidentzia batzuk daude, hiriko errolda zaharrean erregistratutako enpleguen izenen arabera. XVIII. mendean sei buztinlariren izenak 1752ko katastro orokorrean agertu ziren (*Catastro de Marqués de la Ensenada*), eta horietako hiruk Olivares izeneko auzoan zeukaten bere lantegia. Gainera, handik urte gutxira, 1770ean, Olivaresen lan egiten zuten buztinlarien kopurua hamar izatera iritsi zen, eta haien ofizial eta ikasleak ere

agertzen ziren. 1807an buztinlariek gremio bat ezarri zuten beren interes eta hornidura kolektiboak babesteko, eta hamabi lantegi kontatu ziren aldi horretarako (Moratinos eta Villanueva, 2006). Gainera, XIX. mendearen azken hamarkadan, Pérez (1895)-ek Olivaresen lanean hamar buztingile zeudela aipatzen du. Hala ere, kopuru hori laster jaitsiko zen, bi zeramikari bakarrik geratuko baitziren 1930ean, eta erabat utziko zen, azken buztinlaria, Benito Toranzo, 1944an hil zenean (Moratinos eta Villanueva, 2006). Olivaresen, oro har, "Olivareseko zeramikak" deritzenak egiten ziren, beiradura zuri opakuak (eztainu-berunezko beiradurak) zituzten baxerarako zeramikak, kolore urdin, berde, beltz eta marroiz apainduak. Zeramika beiraztatua erabiltzeak aurrerapen handia ekarri zuen zeramikaren teknikan. Dokumentazio bibliografikoaren arabera, Olivaresen labe itxi bat behar zen beiradura urtzeko, baita beiradura hori ehotzeko errotak edo erretzean piezak babesteko moldeak ere. Baina, beste gauza askoren artean, beiraztatze-prozesuak labe bereziak behar zituen mineralen nahasketa prestatzeko (beruna eta eztainu-mineralak). Labe berezi horiei *padilla* deitzen zitzaien eta eztainu mineralak, berun mineralak, harea eta gatza urtzen ziren fritakina lortzeko. Ondoren, fritakina errotetan ehotzen zen eta gero uretan diluitzen zen, azkenean zeramika bizkotxoaren gainean aplikatzeko. Zeramikariek beruna kintaletan (1 kintal = 100 kg) edo arroaka (1 arroa = 25 libra) erosten zuten eta eztainua libratan (1 libra = 0.45 kg). XVIII. mendetik aurrera, Espainiako Estatuak, industria-garapenerako bere politikarekin, lehengai horiek estatuko tabako dendetan banatzen zituen, lehengaien prezioak igo ez zitezen eta eskasia izan ez zedin (Moratinos eta Villanueva, 2006). Denda hauek, normalean, hirietan edo zeramika ekoizpen-zentroetatik gertu zeuden. Bestalde, bibliografiaren arabera, sukalderako zeramikak (mikatsuak, Muelas del Pan eta Pereruelako lantegitan egiten zirenaren antzekoak), eta zeramika gorriak (Toron eta Benaventen ekoitzitako zeramiken antzekoak), Olivaresen ere ekoizten ziren (Moratinos eta Villanueva, 2006) (2.6. irudia).

2.6. irudia. Olivareseko lantegietako zeramikak. Eskala-barra: 8 cm

Zamorako zeramika mikatsuen (Muelas del Pan edo Pereruelakoak, esate baterako) salerosketak Zamorako probintzia gainditu zuen. Adibidez, Valladoliden oinarrizkotzat jotzen ziren zeramika horiek, eta, garai modernoetan, ekoizpen horiek Espainia erdialdera, Kantauriko kostaldera eta Galiziara iritsi ziren geroago. Gainera, baliteke Aro Modernotik aurrera, zeramika mikatsu horiek Olivareseko lantegietan, baita Euskal Herriko lantegietan ere (adibidez, Elosun, Durangon, Ametzagan, Zegaman) beiraztatu izana (Ibabe, 1995; Solaun, 2005). Eltzeak garraiatzen zituzten merkatariak euskal merkatuetara eta frantziarretara iritsi ziren, leku horietatik era guztietako produktuak ekartzeko, horrela, ibilbide interesgarriak sortuz. 1612ko dokumentazioaren arabera, Muelas del Paneko Bartolomé Casquerok eta Alonso Miguelek Gasteiztik ondasunak ekarri zituzten, batez ere burdina, bertan Muelas del Paneko zeramika ontziak saldu ondoren. Gero, XX. mendean, eta bereziki Gerra Zibila amaitu ondoren, zeramikaren erabilerak aldatu egin ziren pixkanaka, kaleko salmentak gutxituz eta denda egonkor gehiago sortuz, edo zeramikako herri azoken bidez (70eko hamarkadatik aurrera) (2.7. irudia) (Moratinos eta Villanueva, 2006; Villanueva, 2011).

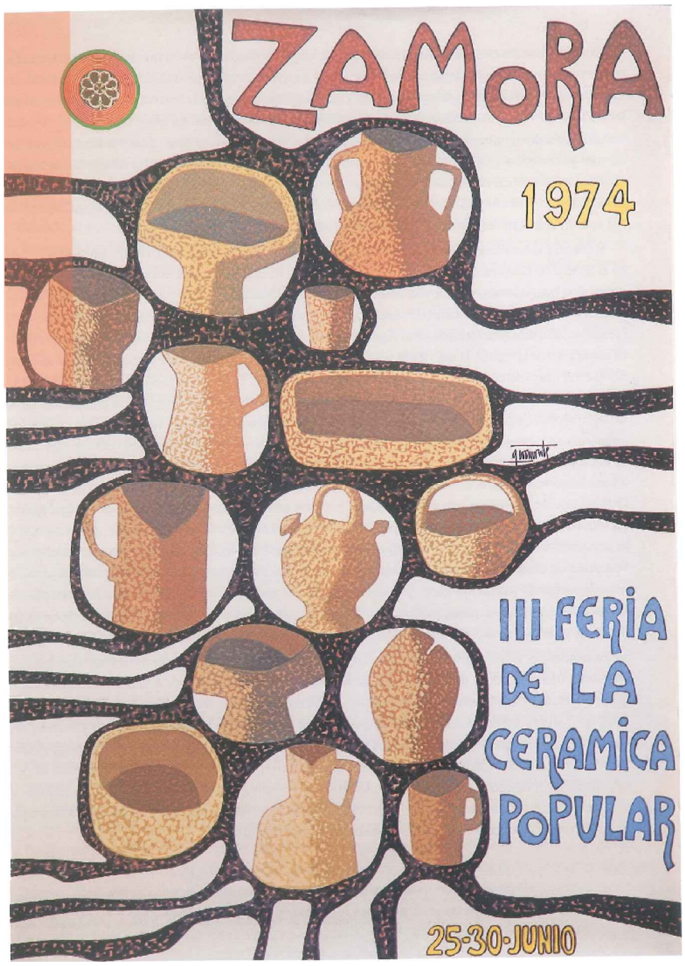

2.7. irudia. 1974ko Zamorako zeramika azokaren kartela (Moratinos eta Villanueva (2006)-tik berreskuratua)

Azken bi hamarkadetan, hainbat indusketa arkeologiko egin dira Zamoran, hiriaren hedapenari eta eraikin publiko berriak eraikitzeari buruzko hiri-garapenarekin batera. Adibidez, bi indusketa gaur egungo Artxibo Historiko Probintzialaren (Martín et al., 2002, 2003) eta Estatuko Liburutegi Publikoaren lekuetan egin ziren (Martín et al., 2003; Villanueva et al., 2000) (2.8. irudia), beste bat Gaztela eta Leongo Museo Etnografikoan (Misiego et al., 1997-1998) (2.9. irudia) eta azkena Olivaresen (Piñel, 1993; Sanz et al., 2005) (2.10., 2.11. eta 2.12. irudiak).

2.8. irudia. La Concepción elizan egindako esku-hartze arkeologikoa (ezkerreko argazkia, iturria: Martín et al. (2003)) eta eliza eta komentuaren gaur egungo eraikinak, hau da, artxiboa eta liburutegia (eskuineko argazkia, argazkia 2019an atera zuen Sanchez-Garmendiak)

2.9. irudia. Errege Kartzelaren atari nagusia, XVI. mendearen amaierakoa (ezkerrean), eta gaur egun Museo Etnografikoaren itxura (eskuinean). Iturria: Museo Etnográfico (2021)

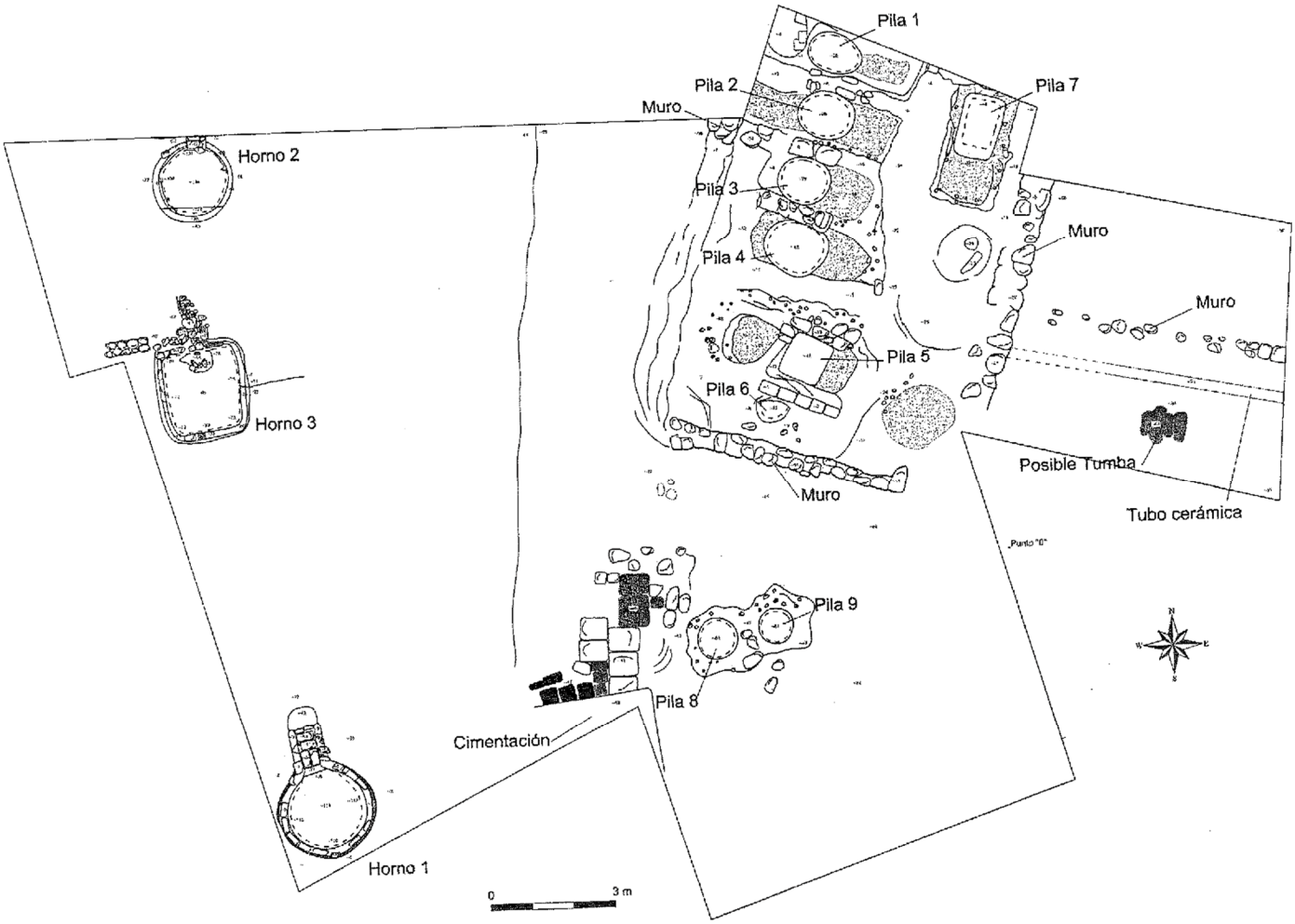

2.10. irudia. Esku-hartze arkeologikoko eremuaren mapa, non zeramika lantegien labeak eta zeramikazko lantegien ondoan dauden larrugintza lantegietako harraskak nabarmentzen baitira. *Horno = labea; pila = harraska; muro = horma; cimentación = zimendatzea; posible tumba = hilobi posiblea; tubo cerámica = zeramikazko hodia.* (Iturria: Sanz et al. (2005))

2.11. irudia. Labeak Santiago Viejo eta San Claudio Olivareseko kale eta plazaren inguruan. Iturria: Museo de Zamora (2018)

2.12. irudia. Zamora hiriaren planoa, testuan zehar aipatutako lekuekin: 1 = Museo Etnografikoa; 2 = Estatuko Liburutegi Publikoa; 3 = Artxibo Historiko Probintziala; 4 = San Claudio enparantza

Gaur egun Artxibo Historiko Probintziala dagoen lekuari dagokionez, bere garaian *Convento de Nuestra Señora de La Concepción* izeneko komentu zaharra izan zen, eta aldameneko eraikinean, Estatuko Liburutegi Publikoa eraiki zen tokian, *Iglesia de Nuestra Señora de La Concepción* izeneko eliza zegoen. Esku-hartze arkeologikoei esker, komentu zaharraren eta elizaren okupazio-fase ezberdinak aztertu ahal izan ziren (Martín et al., 2002, 2003; Villanueva et al., 2000): 1626an, Kontzepzionistak "Casas de Gonzalo de Valencia" izeneko eraikinetara aldatu ziren, Claudio Moyano plazan zeuden eraikinetara, alegia, La Concepción komentua eta beraien etxea izango zena hurrengo bi mendeetan. Geroago, eliza 1672an hasi zen eraikitzen eta 1676 arte iraun zuen (Martín et al., 2003). 1837an, Espainiako gobernuak agindutako Mendizabalen desamortizazioaren ondorioz Kontzepzionistek komentua utzi behar izan zuten eta bi eraikin horiek Estatuaren jabetzara pasatu ziren (Martín et al., 2003). Gainera, lan arkeologikoek argi uzten

dute badirela lehenagoko aztarnak elizaren azpian. Alde batetik, XIII. mendea baino lehenagoko zeramikaz betetako hainbat zulo dokumentatu ziren (Villanueva et al., 2000); eta, bestalde, XIII. eta XVI. mendeen artean aktibo zegoen urregintza-lantegi baten aztarnak ere aurkitu ziren (Martín et al., 2003) (2.8. irudia).

Gainera, Gaztela eta Leongo Museo Etnografikoko gune arkeologikoan bost okupazio-fase dokumentatu ahal izan ziren lan arkeologikoei esker (2.9. irudia). Ebidentziarik zaharrena 1583koa da, lursail horretan Errege Kartzela bat eraiki zenekoa (1583-XVIII. mendea), eta eraikinaren azken okupazioa XIX. mendearen amaieran egin zen, Zamora Industrial S.A. enpresaren biltegi bat izan zena (Herrero, 2016; Martín et al., 1997; Misiego et al., 1997-1998).

Azkenik, Olivareseko lantegiak buztinlarienak izan ziren batik bat, eta berreskurapen-lanek erakutsi zuten hiru labe zeudela San Claudio plazan buztingintzarako. Plaza hori Zamora hiriaren hego-mendebaldean dago, Duero ibaiaren ertzean (Sanz et al., 2005) (2.10. irudia). Materialen eta ebidentzia estratigrafikoen azterketari esker, arkeologoek labeen egiturak XIX. mendearen amaieran eta XX. mendearen hasieran kokatu zituzten. Lehen aldiz agertu dira Zamoran buztingintzaren jarduerarekin lotutako labe-egiturak, eta mugarri interesgarria eman dute Zamorako probintziaren eta Iberiar Penintsularen iparraldean zeramika-tradizio luzea eta haren merkataritza-sareak aztertzeko (2.11. irudia). Gainera, zurrategien arrastoak ere aurkitu dira leku honetan (Sanz et al., 2005). Arrasto horiek 2.10. irudian erakusten diren harraskak dira.

Bestalde, Benavente eta Toroko indusketetan ere zeramika lantegien aztarnak agertu ziren. Benavente hiriko eraikin enblematikoetako bat eraitsi egin zuten, *Casa del Tinte* eraikina, alegia, hiriko ondare historiko eta artistikoaren zati zena (De La Mata, 1989) eta Toron Cuesta del Negrillo 11n, *Patio del Siete*-n eta *Cuesta del Matadero*-n egin zituzten esku-hartzeak 1988tik 1989ea bitartean (Larrén, 1991).

Esku-hartze horietan guztietan, material arkeologiko ugari berreskuratu zen, zeramika-multzo handi bat barne (ikus zeramikaren argazkiak 4. kapituluko 4.1.1. atalean).

Alde batetik, La Concepción-en (zehazki urregintza-lantegiaren estratuetan, XIII.-XVI. mendeak) berreskuratutako zeramikazko ontziak bi taldetan bana daitezke: zeramika beiraztatua eta beiradurarik gabea. Azken horien artean, komunak eta mikatsuak bereizten dira (Villanueva et al., 2000). Horien artean

identifikatutako zeramikaren beste tipologia bat *Duque de la Victoria* izenekoa da. Izen hori Valladolideko izen bereko kaleari dagokio. Bertan, Erdi Aro amaierako zeramikagintzako lantegi batzuk aurkitu ziren. Mota horretako sei zeramika zati urregintza-lantegiaren estratuan berreskuratu ziren. Tipologia honetan sartzen dira baxerarako, elikagaiak biltegiratzeko eta elikagaiak garraiatzeko diren zeramikak, eta guztiek antzeko ezaugarri teknikoak dituzte: tornuz eginak daude, piezen barruan dauden arteka paraleloek eta zirkularrek erakusten duten bezala. Tipologia honetako zeramikak atmosfera oxidatzailean erretzen ziren (Erdi Aroan oso ohikoa zena), eta kolore laranjako zeramikak lortzen zituzten. (Fernández et al., 1991; Villanueva et al., 2000).

Bestalde, Museo Etnografikoaren gunean lurpetik ateratako zeramiken multzoak hainbat tipologia ditu: alde batetik, zeramika batzuk baxerarako zeramikak dira, besteak beste, platerak, goporrak edo bolak; bestetik, sukalderako edo janaria gordetzeko tipologiak ere ugariak dira, hala nola txongilak, lusuilak, eltzeak, zartaginak, sukaldeak eta olio-lanparak (Herrero, 2016; Martín et al., 1997). Gainera, zeramikazko ontzi horiek bi multzotan bana daitezke, beren estalduren arabera: beiraduradun baxera eta beiraztatu gabeko garraiorako, biltegiratzeko, sukaldatzeko edota baxerarako zeramika. Beiraztatu gabeen artean (berreskuratutako zeramikaren gehiengoa), zeramika komunak eta mikatsuak bereizten dira (Herrero, 2016; Martín et al., 1997; Misiego et al., 1997-1998).

Olivareseko lantegietako beiraduradun zeramiken artean baxerarako (platerak, bolak, pitxerrak) eztainu-berunezko zeramikak berreskuratu ziren, kolore urdin edota berdeekin eta motibo begetalekin edota geometrikoekin apainduta kasu batzuetan (Larrén, 1991; Villanueva, 2011). Hauez gain, ezti-koloreko berun beiradura zeharrargiak eta zeramika mikatsuak ere berreskuratu ziren Olivareseko lantegietan (Sanz et al., 2005). Beiradura zuri opakodun zeramiken pastek krema-beix edota arrosa kolorea (*beix/arrosa*[8] bezala deitua testuan zehar) erakusten dute (Turina, 1994); ezti-koloreko berun beiradura zeharrargidun zeramikek, berriz, pasta gorriskak dituzte. Hauek bat datoz Ramos (1980)-ek emandako informazio historikoarekin. Autoreak aipatutako zeramika mota horien manufakturari buruz hitz egiten du Olivareseko lantegietako azken hamarkadei dagokienez (XX. mende hasieran). Hauez gain, zeramika mikatsuak ere, batez ere sukaldeko eltzeak eta pitxer handiak, aurkitu ziren arkeologia-lanetan. Hala ere, ezin da ziur esan Olivares

[8] Ingeleraz, *buff-coloured*.

denik beraien jatorria, Pereruelan eta Muelas del Panen, adibidez, horrelako zeramikak egiteko tradizio luzea baitago. Kontuan hartu behar da, halaber, baztertzeko pieza asko ekoizpen-etapa desberdinetan dokumentatu zirela, adibidez, beiradurarik gabeko bizkotxo-zatiak, beiradura tantakinak beste piezetan, etab. Zeramikak labean bereizten lagunduko luketen treberak edo elementu osagarriak aurkitzea ere ohikoa da. Olivaresen aurkitutako batzuek beiradura-zipriztinak dituzte, Olivaresen beiraduren ekoizpena berretsiz (Sanz et al., 2005). Aipatutako zeramikez gain, tinak ere aurkitu ziren zurrategiak zeuden lekuan.

Benaventeko Casa del Tinteren indusketetan 1500 zeramika pieza inguru berreskuratu ziren. Horien artean, ondo definitutako bi talde daude: 1) XVII. mendetik XVIII. mendera bitarteko multzoa, likidoak gordetzeko zeramikarena (txongilak, lusuilak) eta baxerari dagokiona (Casa del Tinteko upategi posible bati lotua). Zeramika batzuk probintziako beste ekoizpen batzuetan, bereziki Toron, identifikatutako zeramiken antzekoak dira eta beste batzuk erreketa oxidatzailean erretako pasta mikatsuak eta beix/arrosa koloreko zeramikak dira, eztainu-berunezko beiradura zuri opakuekin eta hainbat dekoraziorekin (Arnau, 1997). 2) XV. mendeko jarritas carenadasen multzoa (Larrén, 1991, 1992, 1997-1998).

Halaber, 1988tik 1989ra bitartean Toron egindako esku-hartzeek, zehazki Cuesta del Negrillo 11n, XVII. mendeko zeramika-multzo bat berreskuratzea ahalbidetu zuten (Larrén, 1991). Gainera, zeramika-multzoak Toroko *Patio del Siete* eta *Cuesta del Matadero* lekuetan ere berreskuratu ziren; hala ere, aurkikuntza horiek ez ziren indusketa arkeologikoen emaitza izan, ustekabeko aurkikuntzak baizik (Larren, 1992). Zeramika hauek irekiak, itxiak eta eraikuntzarako zeramikak dira. Gainera, piezen akabera bi motatakoa da: berdindua eta beiraztatua (akabera marroi edo gorria), barruko azalerara eta objektuen ertzetara mugatua. Printzipioz, literaturaren arabera, badirudi lantegi hauek luxuzkoak ez ziren ekoizpenak eta landa-ingurunearekin lotutakoak egiten zituztela. Hau da, oinarrizko eta beharrezko formak ziren eguneroko bizitzan: ura garraiatu eta biltegiratzeko pitxerrak eta bolak, eltzeak eta zartaginak, elikagaiak prestatu eta kontsumitzeko platerak eta kikarak, norberaren garbitasunerako pixontziak eta eraikuntza-arazoak konpontzeko hodiak (Larrén, 1991).

Zoritxarrez, Zamora hiriko eta probintziako material zeramikoei buruzko gaur egungo ezagutza arkeometrikoa zatituta dago eta lan bilduma sakabanatu batek irudikatzen du. Horien artean, Pereruelako sukalderako zeramiken

ekoizpenari buruzko ikerketa etnoarkeometrikoa azpimarratu behar da. Lan honetan zeramika ekoizpena eta buztinen horniketa ikertzen dira testuinguru geologiko konplexu batean (Buxeda et al., 2003). Beste azterlan garrantzitsu bat Iñañez et al. (2018)-k egindakoa da, non autoreek Olivareseko lantegi zaharretan berreskuratutako zeramika karakterizatu baitzuten. Gainera, Calparsoro (2019)-k Zamorako jatorria iradokitzen du arkeometrikoki aztertutako zeramika batzuetarako, Logroñon eta Naiaran (Errioxa) berreskuratuak, bai eta Urduñan, Elosun eta Durangon (Euskal Herria) ere (Calparsoro, 2019; Calparsoro et al., 2019b,c, 2021). Berriki, Puig Barrachina (2016)-k Zamorar jatorria iradoki zuen (PB5 talde gisa etiketatua) zenbait euskal lekutan, hala nola Durangon, Munitibarren, Getarian eta Bilbon aurkitutako zeramiketarako, behaketa petrografikoen eta analisi kimikoen ondoren.

2.2. Aveiroko ekoizpena

Aveiro Portugalen kokatzen da, Iberiar Penintsularen mendebaldean, eta “Ria de Aveiro” izeneko urmaelaren eremu handi baten ondoan dago (2.13. irudia). Urmaela 50 km baino gehiagoko duna-lerro batek bereizten du Ozeano Atlantikotik, eta Erdi Arotik Aro Modernorako biztanleen bizitzan eragina izan zuen; kokalekuetako biztanleek itsas jarduerekin eta merkataritzarekin zerikusi handia zuten eta nekazaritza gatz-ekoizpenarekin eta arrantzarekin batera konbinatzen zuten. Ondorioz, itsas portu garrantzitsua bihurtu zen. Gainera, jarduera ekonomiko horiek —maiz urtarokoak eta osagarriak— urmaelaren paisaia markatu zuten (Alves et al., 2001; Amorim, 2011; Carvalho et al., 2014).

2.13. irudia. Aveiroren kokapena Portugalko mapan (ezkerreko mapa txikian dagoen zirkulu gorria) eta *Ria de Aveiro A (RAVA)* eta *Santo António* eliza mapa nagusian (zirkulu gorriak)

Hala ere, Aveiro ez zen itsas eta merkataritza-jarduerengatik bakarrik ospetsua izan; hiria, zeramika-ekoizpeneko eskualde tradizionala zen, eta gaur egun ere da, bere buztin-erreserba ugariengatik. Buztin horien propietate kimiko eta mineralogikoek zeramika egiteko lehengai gisa erabiltzera eraman zuten. Zeramikaren ekoizpena handitu egin zen XVI. mendearen hasieran, hiria hazi zelako eta itsas merkataritza hazi zelako eta hauek eskatzen zutelako zeramika, itsasontziak eta merkataritza hornitzeko (Barbosa et al., 2009; Bettencourt eta Carvalho, 2007-2008; Carvalho eta Bettencourt, 2012).

Aveiroko zeramikek pasta gorri eta beltza dute, antzeko ezaugarriekin. Giro oxidatzailean erretako baxera gorria kolore laranjatik gorrira bitarteko piezez osatuta dago, gainazal gris ilunagoekin. Zeramika askok tonu desberdinak dituzte, baita orban beltzak ere kanpoko gainazaletan, labearen erreketa-giroaren eta tenperaturaren aldaketen ondorioz. Zeramika bildumaren ehuneko txiki bat zeramika beltzek osatzen dute. Hauek giro erreduzitzailean erre ziren eta pasta grisak eta beltzak erakusten dituzte; batzuetan, distira metalikoko akabera erakutsiz. Zeramika gorri eta beltzen behaketa makro-bisualaz pastak meheak eta gogorrak direla ikusten da, eta bi taldeek inklusio berberak dituzte: kuartzoa eta mika, ale finetik ertainera, matrize osoan ondo banatuak. Mika ugariagoa da, eta oso ikusgarria da kanpoko gainazaletan. Ontzi gehienek gainazal-tratamendu

batzuk jaso zituzten seguruenik, batez ere gainazalak berdintzen zituztenak, kasu batzuetan, pastaren kolore bereko buztin-lohia aplikatu ondoren, baina zertxobait ilunagoa (Bettencourt eta Carvalho, 2007-2008; Carvalho eta Bettencourt, 2012).

Zeramika horiek hainbat multzotan sailka daitezke: a) etxean erabiltzeko zeramikak, adibidez, baxerarako (kikarak, bolak, pitxerrak), sukaldeko tresnak (sukaldeko eltzeak) eta norberaren higienerako zeramikak (pixontziak); b) distantzia luzeko biltegiratzerako eta garraiorako (adibidez: olio-pitxerrak[9]); eta azukrerako-zeramika[10] (2.14. irudia).

[9] Portugaleraz, *anforeta/botija*; ingeleraz, *olive-jar.*

[10] Portugaleraz, *forma de açucar;* ingeleraz, *sugar mould.*

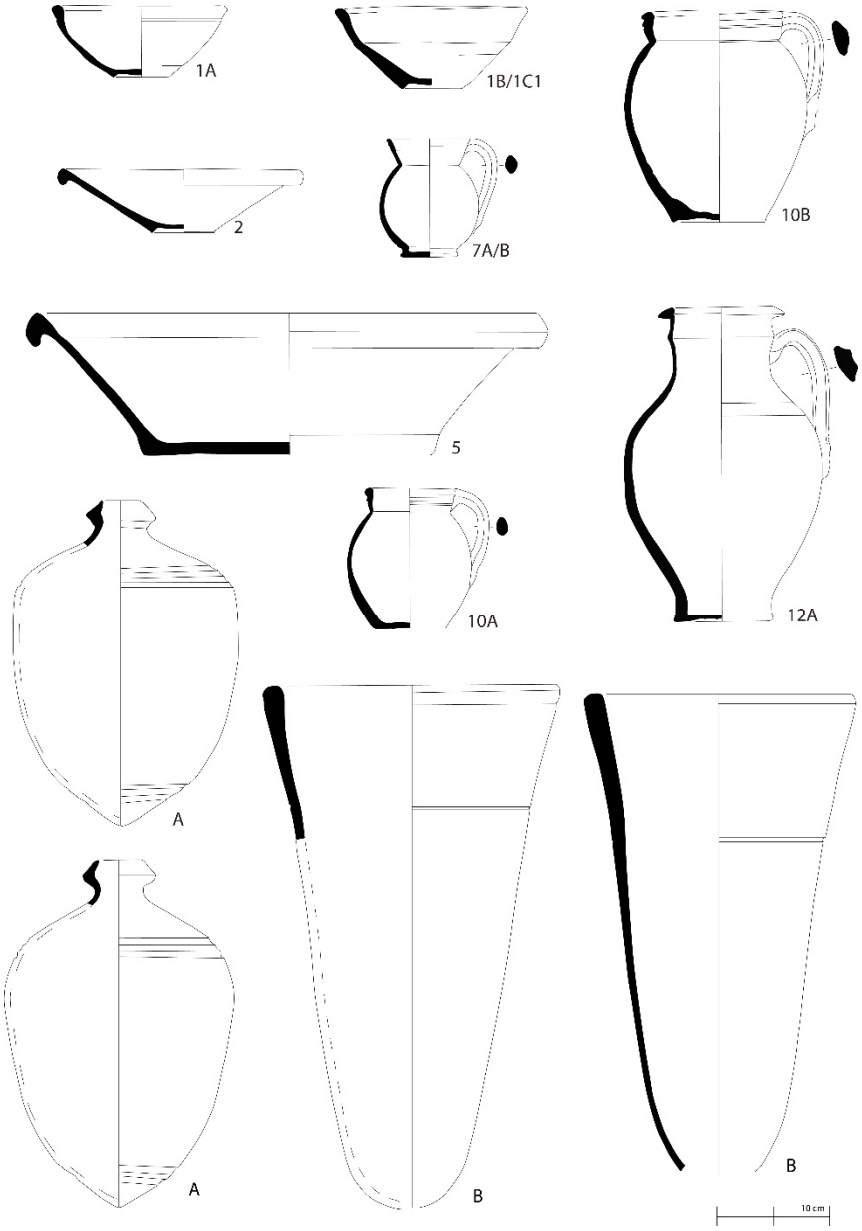

2.14. irudia. Zeramika mota nagusiak: A – olio-pitxerrak; B – azukrerako zeramikak; 1A/1B/1C – bolak; 2 – platera; 5 – askak; 7A/B – katiluak; 10A/B – sukaldeko eltzeak; 12A – pitxerra

Azukrerako zeramikak funtsezkoak ziren azukrea ekoizteko prozesuan. Forma konikoa dute eta goialdean zulo bat. Gaur egun, ohikoa da baztertutako piezak aurkitzea hiriko alde zaharreko eraikin zaharretako horma osatzeko elementu gisa (Bettencourt eta Carvalho, 2007-2008; Morgado et al., 2012). Azken urteotan, azukrerako zeramikak eta Aveiroko hainbat formatako zeramikak identifikatu dira nazioarteko lekuetan. Silva (2018)-k dioenez, Aveiro izan zen, seguruenik, XVI. mendetik aurrera, azukrerako zeramiken ekoizle eta hornitzaile nagusia Portugalko Erresumako azukre-ekoizpeneko eremuetan, hala nola Madeiran, Azoresen eta Cabo Verden, eta eragin handia izan zuen beste merkatu

batzuetan, hala nola Kanarietan. Aveiroko zeramikak ere aurkitu ziren Ingalaterran eta Ternuan. Gertaera horiek guztiak Erdi Aroan eta Erdi Aro ostean izandako merkataritza-fluxu atlantiko eta transatlantikoen froga dira. Ingelesek Ternuan harrapatutako bakailaoaren kontsumitzaile handia izan zen Portugal (Bettencourt eta Carvalho, 2007-2008; Carvalho eta Bettencourt, 2012; Newstead, 2014; Silva, 2018).

Bestalde, Aveiro eskualdeko gatz-ekoizpenaren tradizioa oso ezaguna da X. mendetik, eta produkzioa XIII. mendetik aurrera handitu zen, aintzirako uraren gazitasun-maila konstantearen eta paisaiaren eta ingurumenaren aldeko baldintzen ondorioz. Izan ere, zenbait mapari esker, aintziran gatz-ekoizpenaren kokapena ikus daiteke, Lucas Janszoon Waghenaer holandar kartografoak 1584an egindako mapan bezala (2.15. irudia). Hala, Aveirok ere zeregin garrantzitsua izan zuen gatzaren horniduran Erdi Arotik, ez bakarrik Europako ipar-mendebaldean (Ingalaterra, Finlandia eta Suedia), baita Galizian eta Asturiasen eta Herbeheretako merkatuan ere XVI. eta XVII. mendeetan (Amorim, 2019; Antunes, 2008a). Gatza elikagaiak eta larruak fabrikatu eta kontserbatzeko erabiltzen zen. Arrantza eta beste jarduera batzuk itsasoaren azpiprodukturen honen mende zeuden neurri handi batean (Antunes, 2008b).

2.15. irudia. Portugalko itsas mapa, Lucas Janszoon Waghenaer kartografo holandarrak 1584an egina. Aveiroko gatz-ekoizpeneko zentroak laugarren ibaian ikus daitezke ezkerretik hasita. [Izenburua: Gedaente en vodoeninge vant Landt van Portugal; iturria: Mariner's Mirror (T'eerste deel vande Spieghel der zeevaerdt, van de navigatie der Westersche zee, innehoudende alle de custen van Vranckrijck, Spaingen ende't principaelste deel van Engelandt, in diversche zee caerten begrepen", Leiden, Christoffel Plantijn, 1584). Iturria: University of Texas at Arlington Libraries]

Aveiroko zeramikaren banaketa atlantikoa dokumentatuta dago, baita Aveiroko zeramika beste herri batzuetan aurkitu izana ere, itsaspeko erregistro arkeologiko askori esker, ia dozena bat leku arkeologikorekin (Carvalho et al., 2014). Adibideetako batzuk "Ria de Aveiro A, B eta C" izeneko gune arkeologikoei dagozkie. Azken bi lekuetan, Aveiroko zeramika bilduma handia aurkitu zen, baita itsas jarduerekin lotutako zenbait tresna ere. Horrek adierazten du Aveiro Erdi Arotik Europako iparraldearekin eta hegoaldearekin lotuta egon zela (Bettencourt, 2009; Carvalho et al., 2014). Gainera, lehenengo kasua itsaspean hondoratuta zegoen ontzi-hondakin bati dagokio eta *Ria de Aveiro A (RAVA)* bezala ezagutzen da (ikus. 2.13. irudiko mapa). RAVA Aveiroko urmaelean aurkitu zen (Ílhavon) 1992an (2.16. irudia). Lekuak egurrezko Ibero-Atlantiko tradizioko itsasontzi txiki baten (18 metroko luzera zuena, gutxi gora behera) atzealdea gordetzen zuen eta itsasontziak zeramika kargamentu bat garraiatzen zuen. Kargamentua ontziaren sotoan zegoen, eta zeramika 200 mm inguruko lodierako bilgarri batek babesten zuen; elkarren artean gurutzatutako makilek, arbaztek, lastoak eta pinu-hostoek osatzen zuten bilgarria (Alves et al., 2001). Hasierako ikerketa-fasean egindako karbono-14 analisiek XV. mendearen erdialdeko kronologia bati esleitu zioten testuingurua (Alves et al., 2001), baina indusketek eta zeramiken azterketek data berriago bat adierazten dute, modernitatearen hasierari dagokiona, XVI. edo XVII. mendearen hasierari (Carvalho eta Bettencourt, 2012). RAVAk garraiatzen zituen zeramikak Ria de Aveirotik kanpoko merkatuetan saltzeko zela pentsatzen da, baina ezin izan da azken helmuga definitu. Kargaren tamainak eta testuinguru arkeologikoak, ordea, helmugatzat seguruenik Portugalen kokaturiko portua iradokitzen dute (Bettencourt eta Carvalho, 2007-2008).

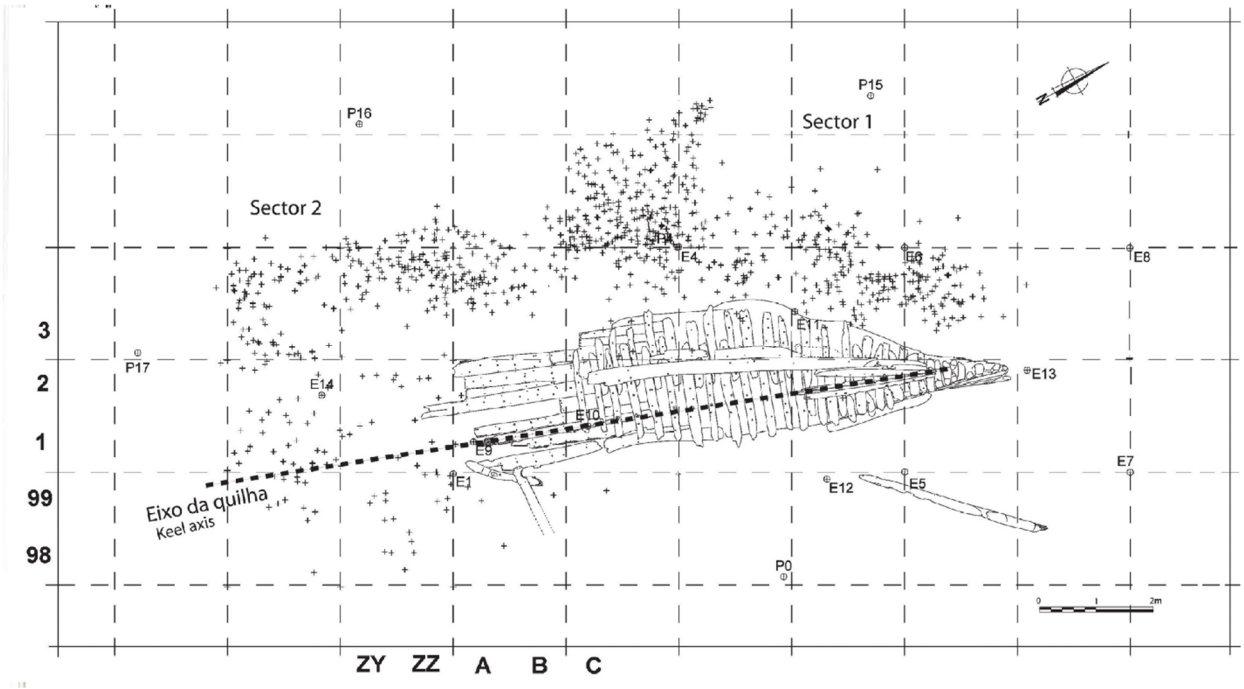

2.16. irudia. RAVA aztarnategi arkeologikoa. Bertan ontziak garraiatzen zituen materialak (gurutzeak) eta hondoratutako ontzia erakusten dira. Iturria: Carvalho eta Bettencourt (2012)

Berreskuratutako zeramika-piezak eguneroko bizitzan erabiltzen ziren formekin lotu ziren. Zeramika handi batzuek, hala nola eltze handiek, barruan zeramika txikiagoak garraiatzen zituzten. Antzeko zeramikak aurkitu ziren Portugalen, bereziki iparraldean (Viana do Castelon, Porton, Coimbran), baina baita Atlantikoan ere, Azoreetan, Madeiran eta Ternuan, hau da, arrantzarekin zerikusia duten lekuetan, edota Ingalaterran (Alves et al., 2001; Bettencourt eta Carvalho, 2007-2008; Carvalho eta Bettencourt, 2012). Azpimarratu behar da, halaber, ontzian sute bat gertatu zela adierazten duten zenbait proba dokumentatu zirela. Froga hauek kiskalitako, deformatutako eta bitrifikatutako zeramika multzo batean ikus daitezke (Carvalho eta Bettencourt, 2012) (frogak erakusten dituzten zeramika horiek 4. kapituluko 4.1.1. atalean ageri dira). Zeramikak ontziaren sotoan zeudenez eta bilduta zeudenez, zeramikaren inguruko erreketa-giroa giro erreduktorea izan zitekeela ondorioztatzen da, sutearen ondorioz.

Bestalde, beste arkeologia-lan batzuk egin ziren Aveiroko *Santo António* elizan (Ikus. 2.13. irudiko mapa). Elizako goi-koruko kupulan betekin bezala erabili ziren hainbat tipologiatako 90 zeramika inguru berreskuratu ziren (2.17. irudia). Santo António-ko frantziskotar komentu zaharra, eliza eta klaustroaren zati bat besterik ez duena, 1524an sortu zen eta Monumentu Nazional gisa sailkatu zen.

Kupulak eraikitzeko zeramikaren erabilera antzinako teknika berezia da, segur aski erromatarra, eta Erdi Aroan garatu zen. Koruko gainazaleko hondakinak garbitu ondoren, zeramikak lurzoru buztintsu oso fin eta solteaz inguratuta zeudela ikusi zen. Indusketaren eta zeramiken aurkikuntzaren testuinguruek aukera eman zuten lote hori kronologia zehatz bati esleitzeko (1524). Horietako askok fabrikazio-akatsak zituztenez, oro har onartzen da testuinguru horietan berrerabilitako zeramika tokiko ekoizpenekoa zela. Gehien bat zeramika gorri eta beiradura gabea aurkitu zen, baina sukaldeko eltze beltz batzuk ere berreskuratu ziren. Elizan, Aveiron oso ezagunak ziren etxeko zeramikez eta azukrerako zeramikez gain, hainbat olio-pitxer aurkitu zituzten, berreskuratutako bildumaren zati nagusia izanik. Olio-pitxerren ezaugarri bereizgarrienetako bat kanpo-gainazala buztin-lohi zuriaren bidez tratatzen zutela da. Buztin-lohi hori ez da uniformea eta ez ditu piezak osorik estaltzen (Silva, 2018).

2.17. irudia. Goiko argazkian Santo António elizaren goi-koruko kupula eta behean Santo António eliza. Iturria: Silva (2018) (goiko argazkia Andreia Lourençok atera zuen (Silva, 2018))

Aveiroko eta inguruetako material zeramikoen azterketa arkeometrikoei dagokienez, ikerketa gutxi egin dira. Horien artean, nabarmentzekoa da Alves et al.

(1988)-ren ikerketa arkeometrikoa, Ria de Aveiro A ontzi-hondakinean berreskuratutako zeramikari buruzkoa. Ikerketan, Alvesek eta kolaboratzaileek tokiko produktu gisa katalogatu zituzten zeramika horiek, Bairro das Olariasen (Aveiro) eta Casa do Infanten (Oporto) berreskuratutako zeramikekin X Izpien Fluoreszentzia (FRX) bidez alderatu ondoren. Egileek, XRD bidez, burdin oxidoa ere identifikatu zuten koloratzaile komun gisa, kolore desberdinak emanez (gorria, marroia, grisa eta beltza), burdinaren oxidazio-egoeraren arabera. Beste azterlan garrantzitsu bat Sousa et al. (2005)-ek egindakoa da. Sousak eta lankideek Machicotik (Madeira uhartea) ateratako azukrerako zeramikak karakterizatu zituzten, eta ondorioztatu zuten zeramika horiek Aveiron ekoitziak izan zitezkeela. Gainera, Vieira et al. (2013)-k Mata da Machadako (Lisboako hegoaldea) faenza ekoizpenaren eta Aveiroko Erdi Aroko etxe batean aurkitutako eztainu-berunezko zeramika beiraztatuen datu espektroskopikoak konparatu zituzten. Lortutako emaitzek espektroen antzekotasuna erakusten dute beren beiradura eta pastetan.

3. KAPITULUA: HELBURUAK

Lan honen helburu orokorrak ondorengo puntuetan azaltzen dira (1-3):

1. Zeramikaren analisi kimikoetarako gure metodo analitikoa optimizatzea, kalibrazio-zuzenak hobetuz eta emaitza fidagarriak lortzeko modu egokia proposatuz. Atal honen azalpena eta emaitzak 4. kapituluan azaltzen dira.

2. Ur-inguruneetan urperatutako zeramiketan gerta daitezkeen jalkitze-osteko eraldaketa eta kutsadurak karakterizatzea, laborategiko zahartze-esperimentu baten bidez. Atal honetako emaitzak 5. kapituluan azaltzen dira.

3. Zamora eta Aveiro eskualdeetako zeramikaren fabrikazio-, erabilera- eta merkataritza-prozesuak berreraikitzeko eta interpretatzeko ezagutza garrantzitsuak eskuratzea. Emaitzak 6. kapituluan aurkezten dira, eta Zamorako zeramikarako sei azterketa-kasu eta Aveiroko zeramikarako bi azterketa-kasu jaso dira.

Helburu horiek lortzeko, Doktorego Tesi honek ikerketa arkeometrikoaren arazoen azterketa eta ondo ezarritako errutina arkeometrikoaren aplikazioa biltzen ditu. Bi alderdiek modu sinergikoan lagundu dute ikerketa honetan. Batetik, ikerketa arkeometrikoko arazoak aztertuta, zeramikaren karakterizaziorako errutina arkeometrikoa hobetu daiteke, metodo analitikoa optimizatuz (1. helburua) eta zeramikan gertatzen diren jalkitze-osteko eraldaketa- eta kutsadura-prozesuak aztertuz (2. helburua). Metodo analitikoaren optimizazioa proposatu da gero metodo hau aztertutako laginetara egokitzeko. Horrez gain, zeramiketan gertatzen diren jalkitze-osteko eraldaketa- eta kutsadura- prozesuak aztertzea proposatzen da, hauek kontuan hartu behar baitira zeramikekin zerikusia duten alderdien interpretazio okerrak saihesteko. Bestalde, ongi ezarritako errutina arkeometrikoa aplikatuz, Zamora eta Aveiroko lantegietan ekoitzitako zeramiken karakterizazio arkeometrikoa egin daiteke (3. helburua). Horrela, Zamoran eta Aveiron Erdi Aroko eta Erdi Aro osteko zeramikaren ekoizpenari buruz dagoen informazio falta beteko da, eta zeramikaren tokiko edo eskualdeko jatorria ebaluatuko da, eskualdeko edo eskualdez gaindiko merkataritzari eta tokiko kontsumoari buruzko informazioa jasoz.

4. KAPITULUA: METODOLOGIA

Kapitulu honetan, lan honekin lotutako metodologiaren alderdi guztiak deskribatzen dira. Lehenik, laginketa-estrategia orokorra eta aukeratutako zeramika-laginak (4.1. atala), eta, ondoren, laborategiko zahartze-esperimentuaren prozesu metodologikoa (4.2. atala) azaltzen dira. Gero, lan honetan erabilitako teknika guztiak deskribatzen dira, baita neurketak egiteko erabilitako errutina analitikoa ere (4.3. atala). Gainera, kontuan hartu diren kontsiderazio analitikoak (4.4. atala) eta, azkenik, analisi kimikoen emaitzak tratatzeko erabilitako estatistika-eredua zehazten dira (4.5 atala).

4.1. Zeramiken laginketa-estrategia

Zeramiken laginketaren aurretik komeni da zenbait alderdi kontuan hartzea, laginketa-irizpideen egokitasuna bermatzeko. Kontuan hartzekoa da lurraldearen eta/edo lekuaren azterketa arkeologikoa eta, bereziki, zeramika-bildumaren analisi morfologiko-estilistikoa amaitu diren edo ez jakitea. Gogoan izateko beste kontsiderazio batzuk, aurrez ikerketa-galderak egitea eta prozedura esperimentala zehaztea dira (Gliozzo, 2020a).

Laginketa-irizpideen egokitasunari dagokionez, laginketak bilduma osoaren adierazgarri, funtzionala eta egokia izan behar du. Adierazgarritasunari dagokionez, fase eta periodo estratigrafiko desberdinetako indibiduoak lagindu beharko lirateke. Horrela, hauen arteko konposizio-desberdintasunak identifika daitezke. Bigarren baldintzak laginketa-estrategiaren funtzionaltasuna bermatuko du, ikerketaren helburu orokorrekiko. Esate baterako, ikerketa-galdera bat leku batean aurkitutako zeramika gorri eta beltzari buruzkoa bada, lehenik eta behin, zeramika gorri eta beltzen bilduma adierazgarri bat beharko da. Azken baldintza hartutako lagin-moten eta erabilitako teknika analitikoen arteko egokitasunari dagokio. Objektua preziatua den edo zeramika mota horren pieza ugari dauden jakitea beharrezkoa da, material mota eta kantitatea egokiak direla bermatzeko (Gliozzo, 2020a).

4.1.1. Hautatutako laginak

Arestian azaldutako guztia kontuan hartuta, aztarnategi arkeologiko bakoitzean hautatutako materialak 4.1. taulan eta ondorengo lerroetan deskribatzen dira.

4.1. Taula. Laginak, lurraldea, herria, gune arkeologikoa, zeramika aurkitu zen testuingurua, tipologia, beiraduren apaingarrien kolorea, zeramiken forma eta kronologia (mendeak). (e/e= ez ezaguna)

Laginak	Lurraldea	Herria	Gune arkeologikoa	Testuingurua	Tipologia	Apaingarrien kolorea	Forma	Kronologia
ZMR001	Zamora	Zamora hiria	Olivares	01 labea	beiraztatu gabea	-	bola	XIX.bukaera-XX.hasiera
ZMR002	Zamora	Zamora hiria	Olivares	01 labea	eztainu-berunez beiraztatua	zuria eta urdina	platera	XIX.bukaera-XX.hasiera
ZMR003	Zamora	Zamora hiria	Olivares	01 labea	eztainu-berunez beiraztatua	zuria eta berdea	platera	XIX.bukaera-XX.hasiera
ZMR004	Zamora	Zamora hiria	Olivares	01 labea	beiraztatu gabea	-	platera	XIX.bukaera-XX.hasiera
ZMR005	Zamora	Zamora hiria	Olivares	01 labea	eztainu-berunez beiraztatua	zuria eta urdina	platera	XIX.bukaera-XX.hasiera
ZMR006	Zamora	Zamora hiria	Olivares	01 labea	eztainu-berunez beiraztatua	zuria eta berdea	platera	XIX.bukaera-XX.hasiera
ZMR007	Zamora	Zamora hiria	Olivares	01 labea	beiraztatu gabea	-	bola	XIX.bukaera-XX.hasiera
ZMR008	Zamora	Zamora hiria	Olivares	01 labea	eztainu-berunez beiraztatua	zuria	goporra	XIX.bukaera-XX.hasiera
ZMR009	Zamora	Zamora hiria	Olivares	01 labea	beiraztatu gabea	-	tina	XIX.bukaera-XX.hasiera
ZMR010	Zamora	Zamora hiria	Olivares	01 labea	beiraztatu gabea	-	kopa	XIX.bukaera-XX.hasiera
ZMR011	Zamora	Zamora hiria	Olivares	01 labea	mikatsua beiraztatu gabea	-	tina	XIX.bukaera-XX.hasiera

ZMR012	Zamora	Zamora hiria	Olivares	01 labea	beiradura zeharrargidun zeramika mikatsua	beixa (beiradura gordina)	tina	XIX.bukaera-XX.hasiera
ZMR013	Zamora	Zamora hiria	Olivares	01 labea	mikatsua beiraztatu gabea	-	tina	XIX.bukaera-XX.hasiera
ZMR014	Zamora	Zamora hiria	Olivares	01 labea	beiradura zeharrargiduna	beixa (beiradura gordina)	pitxerra	XIX.bukaera-XX.hasiera
ZMR015	Zamora	Zamora hiria	Olivares	01 labea	beiradura zeharrargidun zeramika mikatsua	beixa (beiradura gordina)	pitxerra	XIX.bukaera-XX.hasiera
ZMR016	Zamora	Zamora hiria	Olivares	01 labea	beiradura zeharrargiduna	beixa (beiradura gordina)	pitxerra	XIX.bukaera-XX.hasiera
ZMR017	Zamora	Zamora hiria	Olivares	01 labea	beiraztatu gabea	-	trebera (laberako tresna)	XIX.bukaera-XX.hasiera
ZMR018	Zamora	Zamora hiria	Olivares	01 labea	beiraztatu gabea	-	trebera (laberako tresna)	XIX.bukaera-XX.hasiera
ZMR019	Zamora	Zamora hiria	Olivares	01 labea	beiradura zeharrargiduna	beixa (beiradura gordina)	platera	XIX.bukaera-XX.hasiera
ZMR020	Zamora	Zamora hiria	Olivares	01 labea	eztainu-berunez beiraztatua	zuria eta berdea	platera	XIX.bukaera-XX.hasiera
ZMR021	Zamora	Zamora hiria	Olivares	01 labea	eztainu-berunez beiraztatua	zuria eta urdina	platera	XIX.bukaera-XX.hasiera
ZMR022	Zamora	Zamora hiria	Olivares	02 labea	beiradura zeharrargiduna	marroia	eltzea	XIX.bukaera-XX.hasiera
ZMR023	Zamora	Zamora hiria	Olivares	02 labea	beiradura zeharrargiduna	marroia	eltzea	XIX.bukaera-XX.hasiera

ZMR024	Zamora	Zamora hiria	Olivares	02 labea	beiradura zeharrargiduna	berdea	eltzea	XIX.bukaera-XX.hasiera
ZMR025	Zamora	Zamora hiria	Olivares	02 labea	beiradura zeharrargiduna	marroia	eltzea	XIX.bukaera-XX.hasiera
ZMR026	Zamora	Zamora hiria	Olivares	02 labea	beiraztatu gabea	-	trebera (laberako tresna)	XIX.bukaera-XX.hasiera
ZMR027	Zamora	Zamora hiria	Olivares	02 labea	beiraztatu gabea	-	bola	XIX.bukaera-XX.hasiera
ZMR028	Zamora	Zamora hiria	Olivares	02 labea	beiradura zeharrargidun zeramika mikatsua	marroia	estalkia	XIX.bukaera-XX.hasiera
ZMR029	Zamora	Zamora hiria	Olivares	03 labea	beiradura zeharrargiduna	beixa (beiradura gordina)	pitxerra	XIX.bukaera-XX.hasiera
ZMR030	Zamora	Zamora hiria	Olivares	03 labea	beiradura zeharrargiduna	beltza (kiskalia)	heldulekua	XIX.bukaera-XX.hasiera
ZMR031	Zamora	Zamora hiria	Olivares	03 labea	beiraztatu gabea	-	bola	XIX.bukaera-XX.hasiera
ZMR032	Zamora	Zamora hiria	Olivares	03 labea	beiradura zeharrargidun zeramika mikatsua	marroia	tina	XIX.bukaera-XX.hasiera
ZMR033	Zamora	Zamora hiria	Olivares	03 labea	beiradura zeharrargidun zeramika mikatsua	zuria (kiskalia)	e/e	XIX.bukaera-XX.hasiera
ZMR034	Zamora	Zamora hiria	Olivares	03 labea	beiraztatu gabea	-	trebera (laberako tresna)	XIX.bukaera-XX.hasiera

ZMR035	Zamora	Zamora hiria	Olivares	03 labea	beiradura zeharrargidun zeramika mikatsua	beltzaska (kiskalia)	heldulekua	XIX.bukaera-XX.hasiera
ZMR036	Zamora	Zamora hiria	Olivares	01 labea	beiraztatu gabea	-	kopa	XIX.bukaera-XX.hasiera
ZMR065	Zamora	Zamora hiria	Olivares	03 labea	eztainu-berunez beiraztatua	beltza eta zuria (kiskalia)	e/e	XIX.bukaera-XX.hasiera
ZMR037	Zamora	Zamora hiria	La Concepción eliza	urregintza-lantegia	mikatsua beiraztatu gabea	-	eltzea	XV-XVI
ZMR038	Zamora	Zamora hiria	La Concepción eliza	urregintza-lantegia	mikatsua beiraztatu gabea	-	bola	XV-XVI
ZMR039	Zamora	Zamora hiria	La Concepción eliza	urregintza-lantegia	mikatsua beiraztatu gabea	-	tina	XV-XVI
ZMR040	Zamora	Zamora hiria	La Concepción eliza	urregintza-lantegia	eztainu-berunez beiraztatua	zuria	bola	XV-XVI
ZMR041	Zamora	Zamora hiria	La Concepción eliza	urregintza-lantegia	eztainu-berunez beiraztatua	zuria	bola	XV-XVI
ZMR042	Zamora	Zamora hiria	La Concepción eliza	urregintza-lantegia	mikatsua beiraztatu gabea	-	lusuila	XV-XVI
ZMR043	Zamora	Zamora hiria	La Concepción eliza	urregintza-lantegia	mikatsua beiraztatu gabea	-	eltzea	XV-XVI
ZMR044	Zamora	Zamora hiria	La Concepción eliza	urregintza-lantegia	mikatsua beiraztatu gabea	-	lusuila	XV-XVI
ZMR045	Zamora	Zamora hiria	La Concepción eliza	urregintza-lantegia	eztainu-berunez beiraztatua	berdea, beltza eta zuria	bola	XV-XVI
ZMR046	Zamora	Zamora hiria	La Concepción eliza	urregintza-lantegia	eztainu-berunez beiraztatua	zuria eta urdina	bola	XV-XVI

ZMR047	Zamora	Zamora hiria	La Concepción eliza	urregintza-lantegia	eztainu-berunez beiraztatua	zuria eta urdina	bola	XV-XVI
ZMR048	Zamora	Zamora hiria	La Concepción eliza	urregintza-lantegia	eztainu-berunez beiraztatua	berdea,marroia eta zuria	platera	XV-XVI
ZMR049	Zamora	Zamora hiria	La Concepción eliza	urregintza-lantegia	eztainu-berunez beiraztatua	zuria	bola	XV-XVI
ZMR050	Zamora	Zamora hiria	La Concepción eliza	urregintza-lantegia	beiraztatu gabea - Duque de la Victoria motakoa	-	e/e	XV-XVI
ZMR051	Zamora	Zamora hiria	Museo Etnografikoa	e/e	eztainu-berunez beiraztatua	zuria, berdea eta beltza	bola	XVII-XVIII
ZMR052	Zamora	Zamora hiria	Museo Etnografikoa	e/e	eztainu-berunez beiraztatua	zuria, berdea eta beltza	bola	XVI
ZMR053	Zamora	Zamora hiria	Museo Etnografikoa	e/e	eztainu-berunez beiraztatua	zuria eta berdea	bola	XVII-XVIII
ZMR054	Zamora	Zamora hiria	Museo Etnografikoa	e/e	eztainu-berunez beiraztatua	zuria eta urdina	goporra	XVII-XVIII
ZMR055	Zamora	Zamora hiria	Museo Etnografikoa	e/e	eztainu-berunez beiraztatua	zuria eta urdina	platera	XVII-XVIII
ZMR056	Zamora	Zamora hiria	Museo Etnografikoa	e/e	eztainu-berunez beiraztatua	zuria	platera	XVII-XVIII
ZMR057	Zamora	Zamora hiria	Museo Etnografikoa	e/e	eztainu-berunez beiraztatua	zuria	bola	XVII-XVIII
ZMR058	Zamora	Zamora hiria	Museo Etnografikoa	e/e	eztainu-berunez beiraztatua	zuria	platera	XVII-XVIII
ZMR059	Zamora	Zamora hiria	Museo Etnografikoa	e/e	eztainu-berunez beiraztatua	zuria	platera	XVII-XVIII

ZMR060	Zamora	Zamora hiria	Museo Etnografikoa	e/e	eztainu-berunez beiraztatua	zuria	bola	XVII-XVIII
ZMR061	Zamora	Zamora hiria	Museo Etnografikoa	e/e	eztainu-berunez beiraztatua	zuria	bola	XVII-XVIII
ZMR062	Zamora	Zamora hiria	Mengue Etorbidea	zurrategia	mikatsua beiraztatu gabea	-	tina	e/e
ZMR063	Zamora	Zamora hiria	Mengue Etorbidea	zurrategia	mikatsua beiraztatu gabea	-	tina	e/e
TOR001	Zamora	Toro	Cuesta del Negrillo 11	zabor-multzoa	beiradura zeharrargiduna	marroia	katilua	XVII
TOR002	Zamora	Toro	Cuesta del Negrillo 11	zabor-multzoa	beiradura zeharrargiduna	marroia	pitxerra	XVII
TOR003	Zamora	Toro	Cuesta del Negrillo 11	zabor-multzoa	beiraztatu gabea	-	pitxerra	XVII
TOR004	Zamora	Toro	Cuesta del Negrillo 11	zabor-multzoa	beiraztatu gabea	-	pixontzia	XVII
TOR005	Zamora	Toro	Cuesta del Negrillo 11	zabor-multzoa	beiradura zeharrargiduna	marroia	pitxerra	XVII
TOR006	Zamora	Toro	Patio del Siete	zabor-multzoa	beiraztatu gabea	-	pitxerra	XVII
TOR007	Zamora	Toro	Patio del Siete	zabor-multzoa	beiraztatu gabea	-	pitxerra	XVII
TOR008	Zamora	Toro	Patio del Siete	zabor-multzoa	beiraztatu gabea	-	pitxer handia	XVII
TOR009	Zamora	Toro	Cuesta del Matadero	labe-hondakinak	beiraztatu gabea	-	lusuila	XVII
TOR010	Zamora	Toro	Cuesta del Matadero	labe-hondakinak	beiradura zeharrargiduna	marroia	lusuila	XVII
TOR011	Zamora	Toro	Cuesta del Matadero	labe-hondakinak	beiradura zeharrargiduna	marroia	estalkia	XVII
TOR012	Zamora	Toro	Cuesta del Matadero	labe-hondakinak	beiradura zeharrargiduna	marroia	kikara	XVII

TOR013	Zamora	Toro	Cuesta del Matadero	labe-hondakinak	beiraztatu gabea	-	hodia	XVII
TOR014	Zamora	Toro	Cuesta del Matadero	labe-hondakinak	beiraztatu gabea	-	hodia	XVII
BNV001	Zamora	Benavente	Casa del Tinte	ospitalea	eztainu-berunez beiraztatua	zuria eta urdina	bola	XVII-XVIII
BNV002	Zamora	Benavente	Casa del Tinte	ospitalea	eztainu-berunez beiraztatua	zuria	platera	XVII
BNV003	Zamora	Benavente	Casa del Tinte	ospitalea	eztainu-berunez beiraztatua	zuria	bola	XVII-XVIII
BNV004	Zamora	Benavente	Casa del Tinte	ospitalea	eztainu-berunez beiraztatua	zuria eta berdea	pixontzia	XVII-XVIII
BNV005	Zamora	Benavente	Casa del Tinte	zabor-multzoa (ospitalea baino lehenagokoa)	beiraztatu gabea	-	lusuila	XVI-XVIII
BNV006	Zamora	Benavente	Casa del Tinte	zabor-multzoa (ospitalea baino lehenagokoa)	beiraztatu gabea	-	lusuila	XVI-XVIII
BNV007	Zamora	Benavente	Casa del Tinte	zabor-multzoa (ospitalea baino lehenagokoa)	beiraztatu gabea	-	lusuila	XVI-XVIII
BNV008	Zamora	Benavente	Casa del Tinte	zabor-multzoa (ospitalea baino lehenagokoa)	beiraztatu gabea	-	pitxerra	XVI-XVIII
BNV009	Zamora	Benavente	Casa del Tinte	zabor-multzoa (ospitalea baino lehenagokoa)	beiraztatu gabea	-	pitxerra	XVI-XVIII
BNV010	Zamora	Benavente	Casa del Tinte	zabor-multzoa (ospitalea baino lehenagokoa)	beiraztatu gabea	-	pitxerra	XVI-XVIII

BNV011	Zamora	Benavente	Casa del Tinte	zabor-multzoa (ospitalea baino lehenagokoa)	beiraztatu gabea	-	pitxerra	XVI-XVIII
BNV012	Zamora	Benavente	Casa del Tinte	zabor-multzoa (ospitalea baino lehenagokoa)	beiraztatu gabea	-	pitxerra	XVI-XVIII
BNV013	Zamora	Benavente	Casa del Tinte	zabor-multzoa (ospitalea baino lehenagokoa)	beiraztatu gabea	-	txongila	XVI-XVIII
BNV014	Zamora	Benavente	Casa del Tinte	zabor-multzoa (ospitalea baino lehenagokoa)	beiraztatu gabea	-	txongila	XVI-XVIII
BNV015	Zamora	Benavente	Casa del Tinte	zabor-multzoa (ospitalea baino lehenagokoa)	beiraztatu gabea	-	txongila	XVI-XVIII
BNV016	Zamora	Benavente	Casa del Tinte	zabor-multzoa (ospitalea baino lehenagokoa)	beiraztatu gabea	-	txongila	XVI-XVIII
AVR001	Aveiro	Aveiro hiria	Ria de Aveiro A	RAVA	beiraztatu gabea	-	aska	XVI-XVII
AVR002	Aveiro	Aveiro hiria	Ria de Aveiro A	RAVA	beiraztatu gabea	-	aska	XVI-XVII
AVR003	Aveiro	Aveiro hiria	Ria de Aveiro A	RAVA	beiraztatu gabea	-	platera	XVI-XVII
AVR004	Aveiro	Aveiro hiria	Ria de Aveiro A	RAVA	beiraztatu gabea	-	katilua	XVI-XVII

AVR005	Aveiro	Aveiro hiria	Ria de Aveiro A	RAVA	beiraztatu gabea	-	pitxerra	XVI-XVII
AVR006	Aveiro	Aveiro hiria	Ria de Aveiro A	RAVA	beiraztatu gabea	-	bola	XVI-XVII
AVR007	Aveiro	Aveiro hiria	Ria de Aveiro A	RAVA	beiraztatu gabea	-	bola	XVI-XVII
AVR008	Aveiro	Aveiro hiria	Ria de Aveiro A	RAVA	beiraztatu gabea	-	aska	XVI-XVII
AVR009	Aveiro	Aveiro hiria	Ria de Aveiro A	RAVA	beiraztatu gabea	-	bola	XVI-XVII
AVR010	Aveiro	Aveiro hiria	Ria de Aveiro A	RAVA	beiraztatu gabea	-	katilua	XVI-XVII
AVR011	Aveiro	Aveiro hiria	Ria de Aveiro A	RAVA	beiraztatu gabea	-	katilua	XVI-XVII
AVR012	Aveiro	Aveiro hiria	Ria de Aveiro A	RAVA	beiraztatu gabea	-	lusuila	XVI-XVII
AVR013	Aveiro	Aveiro hiria	Ria de Aveiro A	RAVA	beiraztatu gabea	-	aska	XVI-XVII
AVR014	Aveiro	Aveiro hiria	Ria de Aveiro A	RAVA	beiraztatu gabea	-	aska	XVI-XVII
AVR015	Aveiro	Aveiro hiria	Ria de Aveiro A	RAVA	beiraztatu gabea	-	platera	XVI-XVII
AVR016	Aveiro	Aveiro hiria	Ria de Aveiro A	RAVA	beiraztatu gabea	-	platera	XVI-XVII
AVR017	Aveiro	Aveiro hiria	Santo António eliza	goi-koruko kupula	beiraztatu gabea	-	olio-pitxerra	XVI
AVR018	Aveiro	Aveiro hiria	Santo António eliza	goi-koruko kupula	beiraztatu gabea	-	azukrerako zeramika	XVI

AVR019	Aveiro	Aveiro hiria	Santo António eliza	goi-koruko kupula	beiraztatu gabea	-	azukrerako zeramika	XVI
AVR020	Aveiro	Aveiro hiria	Santo António eliza	goi-koruko kupula	beiraztatu gabea	-	azukrerako zeramika	XVI
AVR021	Aveiro	Aveiro hiria	Santo António eliza	goi-koruko kupula	beiraztatu gabea	-	eltzea	XVI
AVR022	Aveiro	Aveiro hiria	Santo António eliza	goi-koruko kupula	beiraztatu gabea	-	eltzea	XVI
AVR023	Aveiro	Aveiro hiria	Santo António eliza	goi-koruko kupula	beiraztatu gabea	-	bola	XVI
AVR024	Aveiro	Aveiro hiria	Santo António eliza	goi-koruko kupula	beiraztatu gabea	-	lusuila	XVI
AVR025	Aveiro	Aveiro hiria	Santo António eliza	goi-koruko kupula	beiraztatu gabea	-	lusuila	XVI
AVR026	Aveiro	Aveiro hiria	Santo António eliza	goi-koruko kupula	beiraztatu gabea	-	katilua	XVI
AVR027	Aveiro	Aveiro hiria	hondakindegia	zabor-multzoa	beiradura zeharrargiduna	horia	bola	XVI-XVII
AVR028	Aveiro	Aveiro hiria	hondakindegia	zabor-multzoa	eztainu-berunez beiraztatua	zuria eta urdina	platera	XVI-XVII

Batetik, Zamora hirian, Olivareseko lantegietan berreskuratutako bildumatik 37 zeramika hautatu dira (XIX. mende amaiera eta XX. mende hasiera bitartekoak) (4.1. irudia). Aukeratutako 37 horien artean, 22 lehenengo labean berreskuratu ziren, 7 bigarren labean eta 8 hirugarrenean eta, horietatik 4 treberak (laberako tresnak) dira. Lagin ezezagunak tokian tokiko ekoizpenekin konparatzeko aukerak handitzeko aukeratu dira treberak. Gainera, 37 zeramiketatik lauk kiskalketaren eta beiradura akatsen ebidentziak dituzte, eta seik beiradura gordina dute; ezaugarri horiei esker, zeramika hauen ekoizpena Olivareseko labeekin lot daiteke.

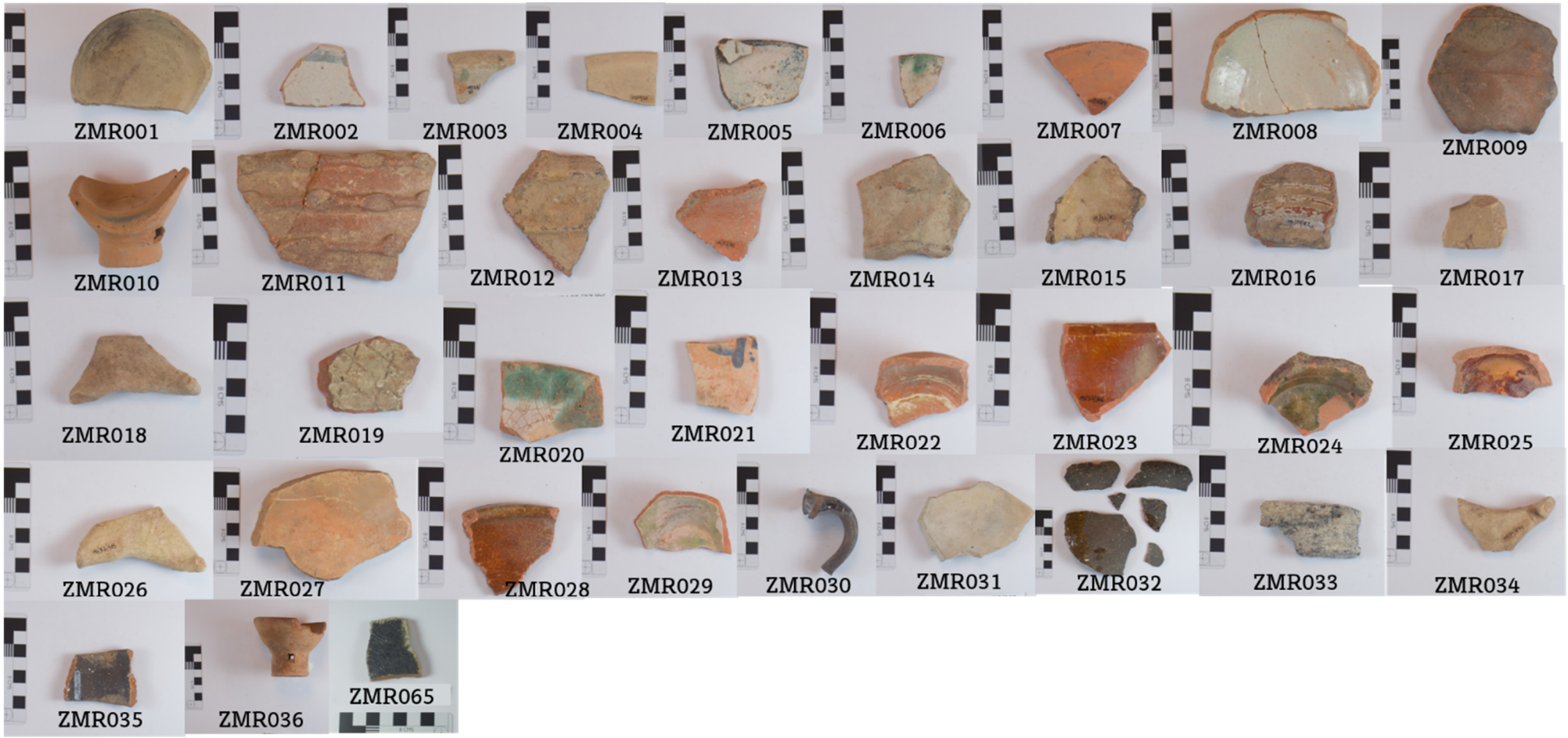

4.1. irudia. Olivareseko lantegietan berreskuratutako 37 zeramika, ezkerretik eskuinera. Eskala-barra: 8 cm

La Concepción-en berreskuratutako XV-XVI. mendeetako zeramiketatik 14 ere hautatu dira (4.2. irudia). Zeramika hauek zehazki XIII-XVI. mendeetan jardunean egon zen urregintza-lantegiaren estratuetan aurkitu ziren. Zeramika hauek baxerarako, sukalderako eta elikagaiak gordetzeko zeramikak dira, besteak beste. *Duque de la Victoria* motako zeramika bat ere badago horien artean (ZMR050 zeramika).

4.2. irudia. La Concepcionen berreskuratutako 14 zeramika, eskala-barra: 8 cm

Gainera, Museo Etnografikoko aztarnategi arkeologikoan berreskuratutako bildumatik XVI-XVIII. mendeetako eztainu-berunez beiraztatutako 11 zeramika ere aukeratu dira. (4.3. irudia). Garai honek bat egiten du Zamorako antzinako espetxea jardunean zegoen garaiarekin (1583-XVIII. mendea), gaur egun Museo Etnografikoa kokatzen den leku berean zegoena, beraz, zeramika horiek espetxearen jardunari lotuta egongo lirateke.

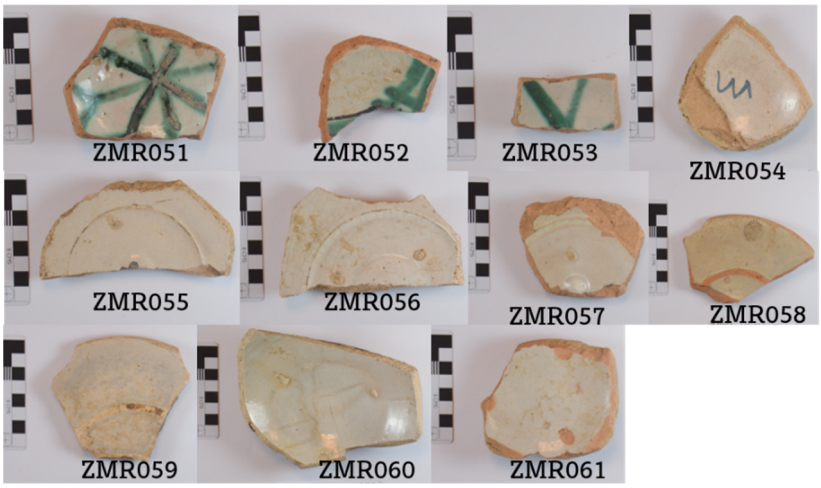

4.3. irudia. Kolore zuri opakuko zeramika beiraztatuak (eztainu-berunezkoak), Zamorako Museo Etnografikoko aztarnategian ateratakoak, eskala-barra: 8 cm

Gainera, bi tinen zatiak ere gehitu dira. Hauek Zamora hiriko Mengue etorbidean kokatzen ziren zurrategietan berreskuratu ziren, Olivareseko zeramika lantegietatik oso gertu (4.4. irudia).

4.4. irudia. Zamorako Mengue etorbidean erreskatatutako bi tina mikatsu, eskala-barra: 8 cm

Hauez gain, Toro herrian, Cuesta del Negrillo 11 kalean zegoen zeramika lantegiko zabor-multzoan berreskuratutako XVII. mendeko zeramika bildumatik bost aukeratu dira. Gainera, Patio del Sieteko zabor-multzoan berreskuratutako XVII. mendeko beste hiru zeramika ere aukeratu dira. Azkenik, Cuesta del Matadero kalean aurkitutako XVII. mendeko sei zeramika ere hartu dira (4.5. irudia). Horiek guztiak (bi izan ezik, hodi zatiei baitagozkie) baxerarako eta sukalderako zeramikak dira, beiraztatu gabekoak edota beiradura zeharrargia dutenak.

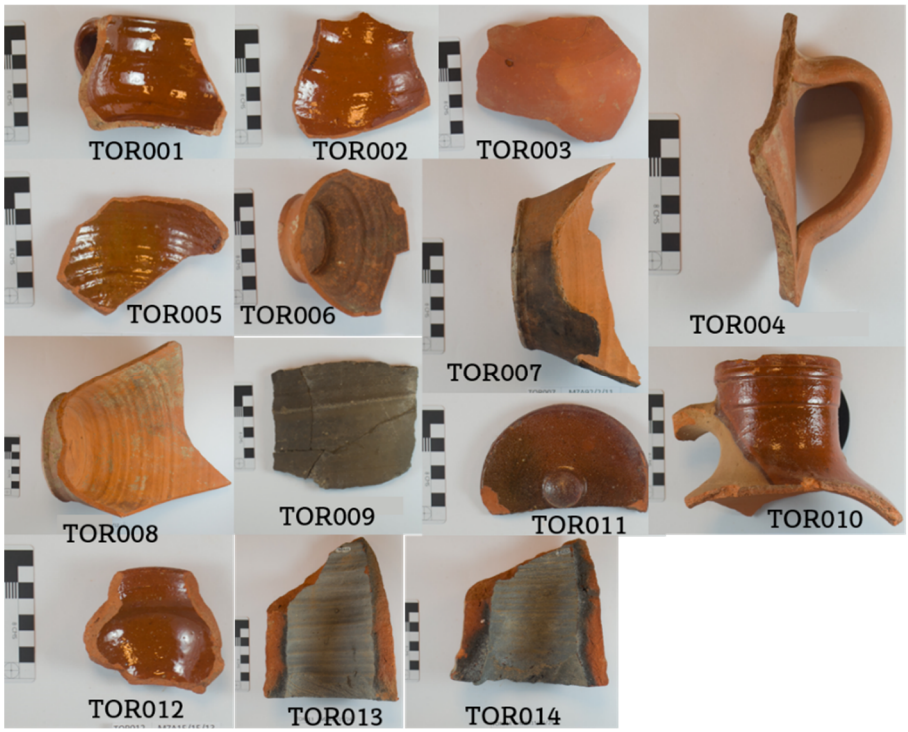

4.5. Irudia. Toroko leku desberdinetan (Cuesta del Negrillo 11, Patio del Siete eta Cuesta del Matadero) berreskuratutako 14 zeramika gorri, beiradura zeharrargiarekin eta gabe. Eskala-barra: 8 cm

Amaitzeko, Benavente hiriko Casa del Tinten berreskuratutako 16 zeramika aukeratu dira. Horien artean, XVII-XVIII. mendeetako eztainu-berunez beiraztatutako 4 zeramika ospitaleari dagokion estratuan aurkitu ziren eta beiradurarik gabeko XVI-XVII. mendeetako 12 zeramika, berriz, ospitalea baino lehen zegoen zabor-multzo batean (4.6. irudia).

4.6. Irudia. Benaventeko Casa del Tinten berreskuratutako 16 zeramika, batzuk eztainu-berunez beiraztatuak eta besteak beiradurarik gabeak. Eskala-barra: 8 cm

Bestalde, Aveiron, RAVAn berreskuratutako zeramiketatik 16 zeramika hautatu dira, eta Santo António elizako goi-koruko kupulan erreskatatutako bildumatik 10, guztiak XVI-XVII. mendeetakoak. Etxerako zeramiken taldearen barruan (AVR001, AVR002, AVR003, AVR004, AVR005, AVR006, AVR007, AVR008, AVR009, AVR010, AVR011, AVRR012, AVR013, AVR014, AVR015, AVR016, AVR021 eta AVR022) beiradurarik gabeko zeramika gorri eta beltzak agertzen dira eta zeramika guztiak tornuaz eginak izan ziren, gainazaletan dituzten marka eta lerroek erakusten duten bezala (4.7. Irudia). Hauez gain, Aveiron berreskuratutako zeramikatik hondakindegietan berreskuratutako bi zeramika beiraztatu (bat zeharrargia eta bestea opakua) ere aukeratu dira. 28 zeramiken artean loza gorria da nagusi, eta pasten kolorea aldatu egiten da gorri-laranja eta beix artean. Loza gorri honetako pastak trinkoak dira, gogorrak, ertainak eta itxura laminarrekoak, purifikatuak edo plastizitaterik ez duten osagai txiki eta ertainak (funtsean kuartzoa eta kaltzita) eta mika dituztenak, matrize osoan ondo banatuak. Pasta beltzak aurrekoen antzekoak dira, eta erreketan atmosfera erreduzitzailea erabili izanak bakarrik bereizten ditu. Zeramika horien artean, AVR003 eta AVR005 dira zeramikarik bitxienak. Lehenak bi koloretako gainazal bat eta pasta beltz bat ditu;

bigarrenak, berriz, itsatsitako bi zeramika zati ditu (4.7. irudia). Gainera, azukrerako hiru zeramika daude (AVR018, AVR019 eta AVR020) (4.7. irudia). Zeramika hauek pasta trinkoak, testura hareatsua, kolore laranja argia eta purifikazio gutxi dute, eta plastizitaterik gabeko eta heterogeneoki banatutako osagai txiki ugari (kuartzo pikorrak eta kolore iluneko burdin-partikula txikiak) eta mikak dituzte, eta hauen gainazalak mate beltzak dira. Azkenik, olio-pitxerra da bilduma honetara gehitu den distantzia luzeetako garraiorako eta elikagaiak gordetzeko erabilitako edukiontzia (AVR017) (4.7. irudia). Pasta laranja fin eta purifikatuak bereizten du olio-pitxer honen fabrikazioa. Bere gainazala ez dago beiraduraz hornitua; hala ere, kanpoko gainazalaren tratamendu bereizgarria erakusten du, buztin-lohi zuriarena.

4.7. irudia. Aveiron RAVAn, Santo António elizan eta hondakingietan berreskuratutako 28 zeramika. Eskala-barra: 8 cm

Bildumako zeramika beltz batzuen akabera ere aipagarria da: lau zeramikek gainazal metaliko distiratsu beltza dute (AVR003, AVR005, AVR015 eta AVR016), eta bederatzik, berriz, mate beltza (AVR001, AVR002, AVR012, AVR018, AVR019, AVR020, AVR021, AVR022 eta AVR025) (4.7. Irudia). Itsasontzian gertatutako sutearen ebidentziei dagokienez, badirudi AVR005 guztiz kiskalita dagoela, pasta beltzak eta gainazal bitrifikatuak erakusten dituelako. Gainazalean kiskalketa

ebidentziak erakusten dituen beste zeramika bat AVR013 da. Pastei eta gainazalei buruzko informazioa 4.2. taulan laburtzen da.

4.2. taula. Aveiron berreskuratutako 28 zeramika, gune arkeologikoa, pasten forma eta pasten eta gainazalen kolorea

Laginak	Gune arkeologikoa	Forma	Pasta	Gainazala
AVR001	Ria de Aveiro A	aska	beixa	beltz matea
AVR002	Ria de Aveiro A	aska	beltza	beltz matea
AVR003	Ria de Aveiro A	platera	beltza	beltz eta beix distiratsua
AVR004	Ria de Aveiro A	katilua	beixa	beixa
AVR005	Ria de Aveiro A	pitxerra	beltza	beltz distiratsua
AVR006	Ria de Aveiro A	bola	gorria	gorria
AVR007	Ria de Aveiro A	bola	gorria	gorria
AVR008	Ria de Aveiro A	aska	beixa	beixa
AVR009	Ria de Aveiro A	bola	beixa	beixa
AVR010	Ria de Aveiro A	katilua	gorria	gorria
AVR011	Ria de Aveiro A	katilua	gorria	gorria
AVR012	Ria de Aveiro A	lusuila	gorria	beltz matea
AVR013	Ria de Aveiro A	aska	gorria	gorri eta beltz matea
AVR014	Ria de Aveiro A	aska	gorria	gorria
AVR015	Ria de Aveiro A	platera	beltza	beltz distiratsua
AVR016	Ria de Aveiro A	platera	gorri iluna	beltz distiratsua
AVR017	Santo António eliza	olio-pitxerra	gorria	zuria
AVR018	Santo António eliza	azukrerako zeramika	gorria	beltz matea
AVR019	Santo António eliza	azukrerako zeramika	gorria	beltz matea

AVR020	Santo António eliza	azukrerako zeramika	gorria	beltz matea
AVR021	Santo António eliza	eltzea	beltza	beltz matea
AVR022	Santo António eliza	eltzea	gorria	beltz matea
AVR023	Santo António eliza	bola	gorria	gorria
AVR024	Santo António eliza	lusuila	gorria	gorria
AVR025	Santo António eliza	lusuila	gorria	beltz matea
AVR026	Santo António eliza	katilua	gorria	gorria
AVR027	Hondakindegia	bola	beixa	beiradura zeharrargiduna (horia)
AVR028	Hondakindegia	platera	beixa	eztainu-berunezko beiradura (zuria eta urdina)

4.2. Laborategiko zahartze-esperimentua, jalkitze-osteko kutsadura- eta eraldaketa-prozesuak ebaluatzeko

Urpeko bi ingurunetan (itsasokoa eta iturrikoa) murgildutako 60 zilindro zeramikotan gertatzen diren aldaketak eta kutsadurak aztertzeko egin da laborategiko zahartze-esperimentua. Horretarako, 69 zilindro prestatu ziren 30 mm-ko diametroko eta 15 mm-ko altuerako zilindro-moldeekin. Horietatik hirurogei zilindro uretan murgildu ziren (probetak), baina bederatzi ez (kontrol-piezak), azken hauek erreferentzia gisa erabili baitira murgildutako piezekin konparaketa kimikoak eta mineralogikoak egiteko. Hiru buztin komertzial mota erabili ziren 69 pieza horiek prestatzeko. Piezak giro-tenperaturan lehortu ziren, eta gero 100 °C-an, laborategiko labe elektriko batean. Ondoren, laborategiko labe batean erre ziren 850, 950 edo 1100 °C-ko giro oxidatzaile batean, eta ordubetez utzi ziren tenperatura maximoan erretzen. Hala, 3 pasta desberdin eta 9 fabrika (3 fabrika pasta bakoitzeko) sortu ziren buztin komertzialetatik abiatuta (4.8. irudia, 4.3. taula). Garrantzitsua zen fabrika mota desberdinak produzitzea, inguruneak nola eragiten dien ikusteko. Bestalde, esperimentuaren errepikakortasuna ere

kalkulatu da. Horretarako, pasta bakoitzeko 3 pieza erabili dira, guztiak 850 °C-an erreak eta itsasoko uretan murgilduak, baldintza horiek muturrekoenak direla uste baita. Hala, 9 zeramika horietarako kalkulatutako errepikakortasunek esperimentu osoaren adierazgarri izan behar lukete.

4.8. irudia. Probeten eta kontrol-piezen manufaktura prozesua: **(a)** buztina; **(b)** piezak erre aurretik; **(c)** probetak itsasoko uretan murgilduta ontzi baten barruan; **(d)** ur bainu elektrikoa, barruan ingurumen desberdinekin betetako (iturriko ura eta itsasoko ura) bi edukiontzi dituena

4.3. taula. Manufakturatutako 9 fabriken zerrenda, buztin eta erreketa-tenperatura desberdinak konbinatzen dituztenak, probeten eta kontrol-piezen kopurua eta urpeko ingurune bakoitzari dagozkion piezak. PF, PT eta AP buztin-mota bakoitzerako erabiltzen diren laburdurak dira. (*) duten piezak errepikakortasuna kalkulatzeko erabilitakoak dira. Piezak jalkitze-denboraren arabera ordenatuta daude (001, 006, 009, 012, 015 eta 018 piezak 3 hilabetez, 002, 007, 010, 013, 016 eta 019 piezak 10 hilabetez eta 003, 004, 005, 008, 011, 014, 017 eta 020 piezak 18 hilabetez murgildu dira)

Fabrikak	Buztina	Erreketa-tenperatura (°C)	Probetak	Itsasoko ura	Iturriko ura	Kontrol-piezak
1	Kaltzio baxukoa (~5% CaO) (PF)	850	8	PF001-PF003*; PF004*; PF005*	PF006-PF008	1 (PF-01)
2	Kaltzio baxukoa (~5% CaO) (PF)	950	6	PF009-PF011	PF012-PF014	1 (PF-05)
3	Kaltzio baxukoa (~5% CaO) (PF)	1100	6	PF015-PF017	PF018-PF020	1 (PF-09)
4	Kaltzioduna (~14% CaO) (PT)	850	8	PT001-PT003*; PT004*; PT005*	PT006-PT008	1 (PT-01)
5	Kaltzioduna (~14% CaO) (PT)	950	6	PT009-PT011	PT012-PT014	1 (PT-05)
6	Kaltzioduna (~14% CaO) (PT)	1100	6	PT015-PT017	PT018-PT020	1 (PT-09)
7	Mikatsua (~1% CaO) (AP)	850	8	AP001-AP003*; AP004*; AP005*	AP006-AP008	1 (AP-01)
8	Mikatsua (~1% CaO) (AP)	950	6	AP009-AP011	AP012-AP014	1 (AP-05)
9	Mikatsua (~1% CaO) (AP)	1100	6	AP015-AP017	AP018-AP020	1 (AP-09)

Piezak erre ondoren, probetak 4,7 L-ko polipropilenozko bi edukiontzitan sortutako bi ur-ingurunetan murgildu ziren 3 periodo desberdinez (3, 10 eta 18 hilabetez). Hala, fabrika bakoitzeko 3 pieza De Stefano eta lankideen (De Stefano et al., 1994) errezetari jarraituz prestatu zen itsasoko ur simulatuan murgildu ziren, eta fabrika bakoitzeko beste 3 pieza iturriko-uretan (4.8.c irudia). Periodoak 3, 10 eta 18

hilabetekoak zirenez, fabrika bakoitzeko bi probeta (bat itsasoko uretatik eta beste bat iturriko uretatik) hirugarren hilabetean hartu ziren, beste bi hamargarren hilabetean eta beste laurak (3 itsasoko uretatik errepikakortasuna kalkulatzeko eta bat iturriko uretatik) hemezortzigarren hilabetean (ikus 4.3. taula). Bi edukiontziak ur bainu elektriko batean murgildu ziren 50 °C-tan, hau da, itsasoko uraren giro-tenperaturaren balio bikoitzaren gainetik, jalkitze-aldi erreala simulatzeko eta eraldaketa-erreakzioak bizkortzeko (ikus. 4.8.d irudia). Horrez gain, esperimentuaren zenbait parametro, hala nola pHa, eroankortasuna, TDS, gazitasuna eta tenperatura, bi astean behin monitorizatu ziren hasieran, aldaketak ikusteko, eta, ondoren, hilero, nahiko egonkorrak zirelako. pH-ak prozesu eta erreakzio biologiko eta kimiko asko erregulatzen dituenez, garrantzitsua zen esperimentuan zehar neurtzea (García-Castrillo et al., 2003). pH-aren aldaketa bat ingurumenak zeramikari egindako eraso baten adierazle izan daiteke (mineralen disoluzioa, adibidez) (Franklin eta Vitali, 1985). Gainera, eroankortasuna soluzio batek korronte elektrikoa eroateko duen ahalmena denez, TDS-arekin (disolbatutako solido totalak) eta gazitasunarekin lotuta dago, eta ioi-kopuru totala adierazten du. Gainera, gazitasuna itsasoko uraren kilogramo batean disolbatutako solidoen kantitatea da, eta horrek, besteak beste, oxidazio-erredukzio ahalmena zehaztu dezake (García-Castrillo et al., 2003).

4.3. Techniques used for the archaeometric approach

The techniques used for the archaeometric approach are the following ones:

- Inductively Coupled Plasma-Mass Spectrometry (ICP-MS), carried out at the University of the Basque Country (UPV/EHU) and at the Vegacenter (a microanalytical facility at the Swedish Museum of Natural History of Stockholm)
- Multi Collector-Inductively Coupled Plasma-Mass Spectrometry (MC-ICP-MS) carried out at the Vegacenter
- Laser Ablation-Multi Collector-Inductively Coupled Plasma-Mass Spectrometry (LA-MC-ICP-MS) and Laser Ablation-High Resolution-Inductively Coupled Plasma-Mass Spectrometry (LA-HR-ICP-MS) carried out at the Vegacenter
- X-Ray Diffraction (XRD) carried out at UPV/EHU

- Scanning Electron Microscopy-Energy Dispersive Spectrometry (SEM-EDS) carried out at UPV/EHU
- Raman microscopy carried out at UPV/EHU

In the following lines, a description about each instrument and their usage in Archaeometry, and specifically in this Doctoral Thesis, will be explained.

4.3.1. The family of ICP-MS

ICP-MS, LA-HR-ICP-MS, MC-ICP-MS and LA-MC-ICP-MS are instruments for compositional analyses. These analyses have been carried out in ceramic pastes and glazes.

On the one hand, the results of chemical analyses in the ceramic pastes, treated by a statistical approach (see section 4.5. in this chapter), are used mainly for provenance purposes. Remembering what has been explained in Chapter 1, section 1.2.1., the first step for the identification of the provenance of archaeological ceramics of Medieval and Post-Medieval Eras, is to classify them into meaningful ceramic groups (that is, PCRUs), analysing the chemical composition of the pastes, by the solution mode ICP-MS (UPV/EHU) in this case. Besides, the chemical analyses of some glazes have been carried out by LA-HR-ICP-MS (Vegacenter). On the other hand, LA-MC-ICP-MS and solution mode MC-ICP-MS (both at Swedish Museum of Natural History) have been used for lead isotope analyses in glazes. These approaches have been used in this work for lead provenancing of Zamoran glazes, because common lead minerals (such as galena) have a very low, or insignificant, U/Pb ratio and that is why their Pb isotopic composition change little, or not at all, with time, giving the opportunity to constrain the origin and age of their source (Dickin, 2018). Therefore, the isotopic ratio of e.g. galena lead used for manufacturing the glazes, would be the same as its source (see Chapter 1, section 1.2.1.). The ICP-MS in Archaeometry not only has been carried out in ceramics pastes (e.g. Golitko and Dussubieux, 2016), but also in other materials (Hill, 2007; Nelms, 2005; Speakman et al., 2002) such as metals and slags (e.g. García de Madinabeitia et al., 2017; Heimann et al., 2002; Wang et al., 2021a; Young et al., 1997), obsidians (e.g. Chan Kim and Chang, 2021; Lucarini et al., 2020; Suda et al., 2021) or glazes (e.g. Beauvoit et al., 2021; Blet-Lemarquand and Gratuze, 1997).

The ICP-MS allows analysing most of the elements (except H, He, C, N, O, F, Ne, Cl, Ar and some actinides) and it offers multielement detection limits below ng/g. There are a number of different ICP-MS modes of operation, such as the instruments presented above: laser ablation (LA-MC-ICP-MS; LA-HR-ICP-MS), solution analysis (MC-ICP-MS; ICP-MS), multi collector (MC) and high resolution (HR). On the one hand, the primary difference between the use of laser ablation and solution analysis is the way in which the sample is introduced for its analysis: while for laser ablation analyses the sample is analyzed in the solid state and it needs a minimal preparation (e.g. subsampling for fitting within the sample chamber), in solution mode, as the name indicates, the sample should be previously prepared (solubilized). On the other hand, the multi collector (that is, the use of more than one detector simultaneously measuring different masses) enables greater precision and accuracy for the analysis of isotope ratios (Pollard et al., 2007).

4.3.2. XRD

Every sample subjected to chemical analysis has also been analysed by XRD in order to obtain information about the spatial disposition of the elements quantified by ICP-MS. XRD is useful for determining the crystallographic structure of the material, and specifically for the case of ceramics, because it identifies the mineralogical phases present in the ceramic body. Since these minerals occur only at certain conditions (such as temperatures and oxidation or reduction firing), it is possible to estimate the Equivalent Firing Temperature (EFT), which is the maximum firing temperature reached in the ceramic kiln, and the type of firing. The variations in the mineralogical phases and their subsequent EFT determine the fabric type. In these lines, a fabric is the final result that reaches the paste, after completing the technological process of the fabrication of the ceramics (Buxeda i Garrigós and Cau, 1995; Buxeda i Garrigós and Madrid i Fernández, 2017), which can be observed by the array of mineralogical composition and paste textures. Thus, within the same compositional group, different fabrics can be found. Therefore, as explained in Chapter 1, section 1.2.2., the study of the minerals will help us to have more information about production technology, since these minerals occur only at certain conditions. XRD technique has been mainly used in Archaeometry for the identification of minerals in ceramic pastes with a view to characterizing pottery types and to investigating sources for raw materials and for the examination of firing temperatures (e.g. Buxeda i Garrigós, 2001; Calparsoro, et al., 2021; Gliozzo,

2020b; Iñañez et al., 2021; Maniatis and Tite, 1981; Pinto Monte et al., 2021; Tite, 1995). In addition, among many other applications, pigments have also been studied by XRD (e.g. Centeno et al., 2012; De Benedetto et al., 1998; Sabbatini et al., 2000).

XRD uses X-rays of known wavelengths to determine the spacing in crystalline structures, so in ceramics analyses, it is used to determine the crystal phases of the ceramic body, that is, provides information about the minerals (such as quartz, calcite, hematite) present in the clay. For that, ceramic paste powder (in our case less than 1 g) is irradiated by a collimated beam of monochromatic X-rays of a certain wavelength, which will be diffracted at different angles, depending on the crystal structures and the X-rays are reflected at determined angles for each crystal, providing a characteristic diffraction pattern. These patterns are used to identify the minerals (Pollard et al., 2007).

4.3.3. SEM-EDS

In pottery, this technique is used to characterize the microstructure and pigments of the glaze coatings that are embedded in epoxy resin, in addition to the microstructure, extent of vitrification, alterations and contaminations of the ceramic body (through the study of freshly fractured surfaces). For example, Maniatis and Tite (1978) studied Aegean pottery sherds by SEM to obtain information on the ceramic technologies employed during the Bronze Age, showing the extent of vitrification of the ceramics. Besides, aggregates occurring in ceramics due to post-depositional contaminations have also been documented, for example, in the works of Iñañez et al. (2020) who show pyrite aggregates by SEM-BSD (Backscattered Electron images) and in the work of Maritan and Mazzoli (2004), who show phosphate aggregates by SEM-BSD.

In SEM-EDS, the area to be studied is irradiated with a finely focused electron beam. This beam can be static to obtain a chemical analysis (by the EDS) at one position, or it can be swept in a raster across the surface of the material to form images (by the SEM). The interaction between the electron beam and the material produce different signals such as secondary electrons (SEM-SED), backscattered electrons (SEM-BSD) and characteristic x-rays (SEM-EDS), obtained from specific emission volumes within the sample. The signals of backscattered electrons vary depending on the surface composition. Thus, backscattering increases with increasing atomic number and in the obtained image different grey tones between

white and black will be seen. For example, glazes are shown in almost white, due to the high atomic number of lead. Moreover, the analysis of the characteristic x-rays provides both qualitative identification and quantitative elemental information from the studied regions (Goldstein et al., 2003).

4.3.4. Raman microscopy

Raman microscopy is used for molecular analyses and, in this work, it has been used for the identification of some inclusions and components present in glazes and ceramic surfaces. Raman is widely used to characterize pigments and compounds present in samples belonging to the arts and archaeological fields (Edwards and Vandenabeele, 2016; Lydzba-Kopczynska and Madariaga, 2016). For example, regarding archaeological samples, Colomban (2003, 2008), Colomban and Trepozz (2001) and Colomban et al. (2004) carried out Raman works on porcelain and ancient glasses for studying their molecular composition. Besides, Colomban et al. (2021) studied the glazes and pastes of blue-and-white Ming porcelain by coupling Raman analysis with SEM-EDS analysis, and Wang et al. (2021b) studied rusty oil spotted glaze from Linfen kilns (Shanxi province). In addition, Marcaida et al. (2018) used Raman microscopy supported by XRD to study the ochre pigments rescued in the burial of Pompeii.

Raman microscopy is a non-invasive spectroscopic technique, which can detect compounds that are present in the samples at minor or trace levels, thanks to the precise focusing on particles of interest. In the instrument, a laser beam is focused on the material and the response is recorded on a sensor in the visible range, providing a spectrum characteristic of each molecule, since it is characteristic of the bonds present in the sample, but the detection will depend on the Raman scattering of the measured compound (Marcaida et al., 2018; Pollard et al., 2007).

4.3.5. Sample preparation

For the ICP-MS, MC-ICP-MS, XRD and SEM-EDS techniques, the sample should be previously prepared in order to meet the requirements of each analytical technique.

Sample preparation for ICP-MS and XRD (both at UPV/EHU) and MC-ICP-MS (at the Vegacenter)

At UPV/EHU, the laboratory of Archaeometry at Micaela Portilla (UPV/EHU) as well as the SGIker-Geochronology and Isotope Geochemistry facilities were used to perform the sample preparation for ICP-MS and XRD. For these instruments, prior to the analyses, glazed and exterior surfaces of a 10-12 g piece of each ceramic were mechanically removed by means of a tungsten carbide abrading tool, to minimize contamination of the ceramic matrix by glaze and soil. Then, those clean pieces were powdered in a planetary mill for 4 min at 300 rpm, using tungsten carbide balls and jar. In this way, the sample is homogenized, that is, the sample after this step is representative of the bulk chemical composition of the ceramic. At this point, samples for XRD technique were ready for their analysis. Besides, and only for the samples that were going to be analysed by ICP-MS, powdered ceramic pastes were calcined up to 950 ºC to remove organic materials and other gasses like CO_2 and H_2O. Those calcined pastes, along with standards from the Geological Survey of Japan used for the external calibration of ICP-MS (basalt JB-3, andesite JA-2, granodiorite JG-1a, granite JG-2) were melted by means of an alkaline fusion using a Fluxy automatic gas fluxer (Corporation Scientifique Claisse, Canada), based on the method optimized by García de Madinabeitia et al. (2008). It involved the melting of approximately 250 mg of sample into a Pt-Au crucible together with 500 mg of a flux at more than 1100 ºC for several minutes. The flux agent was $LiBO_2$ (anhydrous, for analysis grade pure) of Corporation Scientifique Claisse, with solution of 50 % LiBr (Merck Suprapur) in deionized water used as anti-adherent. The melted pearls were poured into a polypropylene beaker with a solution of HNO_3 with several drops of HF to ensure the stability of the High Field Strength Elements (HFSE). Those primary solutions were then treated inside a class 100 clean room. The solutions were diluted gravimetrically 200 times in a 1 % HNO_3 solution. 10 g of dilution were prepared for each primary solution; using an analytical balance with the readability of ± 0.00001 g and the resulting solutions were analysed by ICP-MS. The internal standard solution (In) was prepared from 1000 g/ml stock solution for its dilution. The commercial reagents (Merck Pro Analysi hydrofluoric acid 50.2 % and nitric acid 69.8 %) were purified in the clean room by sub-boiling quartz-distillation (HNO_3) and Teflon bottle-distillation (HF). Ultrapure water (resistivity ≥ 18.2 MΩ) was obtained by a MilliQ water purification system (Millipore) after a previous step by reverse osmosis (Nanopure Barnstead).

Besides, at the Vegacenter, for the MC-ICP-MS analyses of the glazes, samples were dissolved. For this process, fragments were chipped off the sample using a scalpel. Following a leaching step using a diluted nitric acid and subsequent dissolution with a HF-HNO_3 acid mixture, the lead was purified by electrodeposition.

Sample preparation for SEM-EDS at EHU

Prior to the analyses, on the one hand, cross-sections of the sherds (approximately 1 cm long) were prepared in epoxy resin moulds and polished (down to below 1 μm) and gold coated. On the other hand, freshly fractured surfaces were cut perpendicularly to the outer/inner surfaces of the ceramic bodies and gold coated.

4.3.6. Measurements

Procedure for ICP-MS at UPV/EHU and MC-ICP-MS at the Vegacenter

First, the procedure of ICP-MS analyses carried out at the laboratory of the Analytical Chemistry Department of UPV/EHU will be explained:

The chemical analyses of the ceramics were performed with a NexION 300 ICP-MS (Perkin Elmer, Ontario, Canada) provided with an OneNeb pneumatic concentric nebulizer (Agilent, Santa Clara, USA), cyclonic spray chamber and standard nickel cones. Besides, argon (99.999 %) was used as carrier gas in the ICP-MS measurements. 42 elements and compounds were measured for each sample: Al_2O_3, Ba, CaO, Ce, Co, Cr, Cs, Cu, Dy, Er, Eu, Fe_2O_3, Gd, Hf, Ho, K_2O, La, Lu, MgO, MnO, Na_2O, Nb, Nd, Ni, P_2O_5, Pb, Pr, Rb, SiO_2, Sm, Sn, Sr, Ta, Tb, Th, TiO_2, Tm, U, V, Yb, Zn and Zr. The concentrations of ^{27}Al, ^{31}P, ^{85}Rb, ^{88}Sr, ^{120}Sn, ^{90}Zr, ^{93}Nb, ^{133}Cs, ^{137}Ba, ^{139}La, ^{140}Ce, ^{141}Pr, ^{142}Nd, ^{147}Sm, ^{153}Eu, ^{158}Gd, ^{159}Tb, ^{164}Dy, ^{165}Ho, ^{166}Er, ^{169}Tm, ^{174}Yb, ^{175}Lu, ^{180}Hf, ^{181}Ta, $^{206+207+208}Pb$, ^{232}Th and ^{238}U were analysed in standard mode. ^{23}Na, ^{24}Mg, ^{28}Si, ^{39}K, ^{44}Ca, ^{47}Ti, ^{51}V, ^{52}Cr, ^{55}Mn, ^{56}Fe, ^{59}Co, ^{60}Ni, ^{63}Cu and ^{66}Zn, however, were analysed in collision mode with He as cell gas. The plasma operating conditions such as the nebulizer flow rate, the position of the torch and the ion lens voltages of the instrument were optimized every day prior to any experiment with a 10 ng/mL standard solution of Mg, Rh, In, Ba, Pb and U. The nebulizer gas-flow rate was optimized to obtain a good compromise between high sensitivity and low oxide levels (lower than 2.5 % for

CeO/Ce). Sample introduction and experimental conditions for the data acquisition of the ICP-MS are collected in Table 4.4.

Table 4.4. Sample introduction and experimental conditions for the data acquisition of the ICP-MS

Sample introduction and experimental conditions	
Nebulizer gas flow	0.90-1.00 L/min
Plasma gas flow	18 L/min
Auxiliar gas flow	1.2 L/min
RF power	1600 W
Cell gas flow (He)	4.0 mL/min
Dwell time	50 ms
Integration time	1000 ms
Sweeps	20
Readings	1
Replicates	3

In addition, the procedure of solution MC-ICP-MS analyses for lead isotope analyses carried out at the Vegacenter, will be explained:

A similar set-up as applied for LA-MC-ICP-MS analyses (see the section below) has been used for analyses in solution mode. For the latter, Tl was added to the sample solutions to enable an internal mass bias correction, and the isobaric ^{204}Hg interference was managed in the same way as for the laser analyses. Moreover, NBS981, NBS982 and BCR-2 Pb standard solutions were run in between the analyses. This approach allowed the assessment of the LA-MC-ICP-MS results obtained on potentially heterogeneous glaze materials. Given the absence of matrix-matched reference materials for ceramic glazes analysed by LA-MC-ICP-MS, the solution data was used to verify the accuracy of the laser ablation results (see Chapter 6, section 6.3.). Thus, the solution isotopic data was compared with laser ablation isotopic data corrected in two different ways; 1) corrected only for mass bias (Tl correction) or 2) corrected both for mass bias and to compensate for the deviation between Tl-corrected NIST 610 data and corresponding published data.

Procedure for X-Ray Diffraction (XRD)

The XRD analyses performed in this Doctoral Thesis were carried out by SGIker general services at the UPV/EHU.

The mineralogical analyses were performed with a PANalytical X'pert PRO (Malvern Panalytical, Malvern, UK) powder diffractometer equipped with a copper tube ($\lambda CuK_{\alpha mean}$ = 1.5418 A) and Ni filter for removing the K_β wavelength, vertical goniometer (Bragg-Brentano geometry) programmable divergence aperture, automatic sample changer, secondary graphite monochromator and PixCel detector (Malvern Panalytical, Malvern, UK). For the measurements, small amounts of powdered ceramic pastes obtained following the procedure explained above were irradiated (less than 1 g) by a collimated beam of monochromatic X-rays of a certain wavelength. These rays would be diffracted at different angles, depending on the crystal structures. The operating conditions for the Cu tube were 40 kV and 40 mA. The angular range (2 Θ) was scanned between 5 º and 70 º. The treatment of the diffractogram data was carried out using X'pert HighScore (PANalytical, Malvern Panalytical, Malvern, UK) software in combination with the Powder Diffraction File (PDF-2) database (International Centre for Diffraction Data – ICDD, Newtown Square, PA, USA).

Procedure for Scanning Electron Microscopy-Electron Dispersive Spectroscopy (SEM-EDS)

SEM-EDS analyses were conducted in the SGIKER general services from the UPV/EHU.

All of them were analysed using the EVO 40 Carl-Zeiss Scanning Electron Microscope (SEM) (Zeiss, White Plains, NY, USA) coupled to an energy dispersive X-ray analyser (EDS) X-Max (Oxford Instruments). The working conditions for this instrument for the studied glazes and ceramic bodies were the following: 20 kV, 100 mA, full vacuum conditions and 7.5-10.5 mm working distance. Then, for EDS the intensity was increased to 500 mA to improve the signal. The elemental composition of decorative coatings was determined by an Energy Dispersive Spectrometry (EDS) analysis of areas corresponding to each colour; the EDS spectra were acquired and treated using the INCA software (Oxford Instruments, Abingdon, UK). Cobalt was used as internal standard for adjusting the internal calibration of the instrument, acquiring a standardless semiquantitative analysis.

Procedure for Laser Ablation-Multi Collector-Inductively Coupled Plasma-Mass Spectrometry (LA-MC-ICP-MS)

LA-MC-ICP-MS analyses were conducted at the Vegacenter. For the analyses of Pb isotope ratios of the glazes (see Chapter 6, section 6.3.), a NWR ESI193 excimer laser ablation system was coupled to a Nu plasma (II) MC-ICP-MS. Helium gas was flushed through the ablation cell and used to entrain the ablated particles. Before the plasma torch, the He sample gas from the laser ablation cell was combined with Ar gas (see Table 4.5. for typical gas-flow settings). Parallel Faraday cups outfitted with $10^{12}\ \Omega$ resistors were used to collect the simultaneous ion currents from masses 208, 207, 206, 205, 204, 203 and 202. Laser ablation analyses were conducted during a single continuous analytical session on the exterior surface of the glaze of each sample. Before each sample analysis, the sample was pre-ablated to remove potential surface contamination (see Table 4.5. for laser parameters). Then, an on-peak background was taken for 50 seconds before the sample was ablated for 25 seconds (generating data scans along 100 μm long lines with a spot size of 12 μm). Data reduction was done using the Iolite software package (Paton et al., 2011) establishing an average background signal for each analysis and to calculate the background-corrected signals from each time-resolved increment (0.5 seconds integration) of the main ablation. The potential isobaric interference of ^{204}Hg on ^{204}Pb was corrected using the background-corrected ^{202}Hg signal and the natural isotope abundances of each Hg isotope (^{202}Hg/^{204}Hg = 0.2299, De Laeter et al., 2003). To correct for mass bias, a Tl solution was introduced into the sample stream using an Aridus II desolvating system. The known stable ratio of ^{205}Tl/^{203}Tl (2.3871; Dunstan et al., 1980) was used to determine a bias factor, which was applied to Pb isotope ratios, using the exponential law. The laser spots were directed towards white areas of glazes in the cases of tin-lead glazed ceramics, with exception of ZMR045 and ZMR048, in which a region with green and white colour has been ablated. As referred, the laser ablation data was corrected in two different ways (Tl correction and Tl+NIST correction).

Table 4.5. LA-MC-ICP-MS analytical conditions for Pb isotope analysis at the Vegacenter of the Swedish Museum of Natural History, Stockholm

Instrument Settings	
Mass spectrometer	**Nu plasma (II) MC-ICP-MS**
Cooling gas flow rate	13 L/min
Aux gas flow rate	0.9 L/min
Mass resolution	low
Cones	common Ni cones
Torch	glass
Aridus II (for Tl injection)	**Nu plasma (II) MC-ICP-MS**
Sweep gas (Ar)	1.9 L/min
Nebuliser pressure	30 psi
Tl solution	10 ppb (run 1 and 2), 20 ppb (run3 and 4) in 0.3M HNO3
Laser ablation	**NWR ESI193 laser ablation system**
Ar flow rate (Mix Gas)	0.50 L/min
He flow rate	0.30 L/min
Preablation (on glazes)	
Burst count	3
Fluence	3 J/cm^2
Ablation (linescan)	
length of linescan	~100 um
Frequency	15 Hz
Translation rate	5 um/second
Spot size	12 um (glazes)
	150 um (NIST612 and NIST610)
Fluence	3 J/cm^2
Data collection	

washout time	50 seconds
ablation time	~25 seconds
Integration	0.5 seconds

Procedure for Laser Ablation-High Resolution-Inductively Coupled Plasma-Mass Spectrometry (LA-HR-ICP-MS)

Apart from obtaining lead isotope ratios, elemental data was gathered for selected artefacts using an Attom single-collector high-resolution ICP-MS instrument, manufactured by Nu Instruments, connected to the NWR ESI193 laser system (LA-HR-ICP-MS). All concentrations (in ppm) are semi-quantitative and normalized to values of the certified NIST 610 glass. NIST 612 was analysed as an external standard to monitor accuracy and precision. Trace elements (n=29) and major elements (n=20) in artefacts were measured separately in translucent-glazed parts and in white-coloured parts of tin-lead glazed sherds in adjoining, separate spots of different sizes (30 and 60 microns for the major elements and trace elements, respectively). Each element was measured three times and the laser conditions for the pre-ablation, ablation and data collections steps were similar to the settings used for isotope ratio measurements (see Table 4.5.).

Procedure for Raman microscopy

The Raman analyses were performed with two different Raman spectrometers, one from the SGIker general services from the University of the Basque Country (UPV/EHU) and the other from the department of Analytical Chemistry of the University of the Basque Country (UPV/EHU).

For the Raman analyses performed at the department of Analytical Chemistry, the inVia Renishaw confocal Raman spectrometer coupled to a DMLM Leica microscope with 5×, 20× and 50× long working distance lenses was used. A 532 nm excitation laser was used. The spectrometer was daily calibrated by using the 520.5 cm^{-1} Raman band of a silicon chip. Lasers were set at low power (<1 mW at the sample) to avoid sample decomposition. Data acquisition was carried out using the Wire 4.2 software package (Renishaw). Spectra were acquired between 100 and 3000 cm^{-1} spectral region. Measurements were acquired between 5 and 30 s and several

scans (between 5 and 40 scans) were accumulated for each spectrum to improve the signal-to-noise ratio.

Besides, for the Raman analyses performed at the SGIker general services from UPV/EHU, a Renishaw InVia Raman spectrometer, joined to a Leica DMLM microscope was used. The spectra were acquired with the Leica 50x N Plan (0.75 aperture) objective. Besides, for the visualization and focusing, another Leica 5x N Plan (0.12 aperture) and a 20x N Plan EPI (0.40 aperture) objectives were used. The spatial resolution for the 50x objectives is 2 microns. For the focusing and searching of the points of interest, the microscope implements a Prior scientific motorised stage (XYZ) with a joystick. A 785 nm excitation laser was used (diode laser, Toptica). The power at the source of this laser is 300 mW, being the maximum power at the sample 150 mW. In all the measurements, the power of the laser was reduced in order to avoid the photo-decomposition of the samples (burning) using neutral density filters. For each spectrum, 20 seconds were employed and 5 scans were accumulated with the 10 % of the maximum power of the laser in the spectral window from 150 cm^{-1} to 1200 cm^{-1}. The spectrometer was daily calibrated using the 520.5 cm^{-1} Raman band of a silicon chip. Data acquisition was carried out using the Wire 4.2 software package (Renishaw).

To interpret all the Raman results, the acquired Raman spectra were compared with Raman spectra of pure standard compounds collected in the e-VISNICH dispersive Raman database (Castro et al., 2005; Maguregui et al., 2010) and with free Raman databases (e.g., RRUFF, Downs and Hall-Wallace, 2002) for the assignation of Raman bands. For spectral treatment and analysis, Wire 2.0 (Renishaw) and OMNIC® Version 7.2 software Thermo Nicolet (Madison, WI, USA) were used.

4.4. Analytical considerations for the archaeometric approach

As explained in Chapter 1, the questions about the provenance, technological, socio-economical, socio-cultural, and chronological aspects of ceramics require to be answered by means of their natural aspect, since they are material objects (Buxeda i Garrigós et al., 1995). For that, an archaeometric model is used, and in this work, it is divided mainly in two complementary parts: the provenance and the technological studies. The analytical considerations that

should be taken into account for obtaining reliable results will be explained in this section.

4.4.1. Optimization of the calibration curves

Since the chemical fingerprint of the ceramics is decisive for provenancing, analytical techniques with low uncertainty are required, as they will provide results able to distinguish between different but compositionally similar populations (Hein et al., 2002). The ICP-MS is the most appropriate instrument for that, because it provides simultaneous multi-elemental analysis of numerous matrices, with high sensitivity and precision (Bulska and Wagner, 2016; Eggins et al., 1997). However, the disadvantage of this technique is that it requires a complex sample treatment and, in addition, is a destructive technique. Therefore, as explained in Chapter 1, section 1.3.1., the main problem could be the availability of hundreds of milligrams of sample, which often is limited. The ICP-MS needs an accurate calibration, which enables the relation between the signal and the concentration of the unknown sample. Hence, reference materials and/or well-defined standards are required to provide the mathematical relationship between the selected signal intensities and the concentration of the analytes within the concentration range involved in the analysis. The Certified Reference Materials (CRMs) are certified solutions or solid materials, which are generally used to verify the accuracy of the results obtained by the analytical measurement, as well as to demonstrate their traceability. The calibration strategies for the quantitative analyses are several: external calibration with pure standard solution or matrix-matched standards and with or without Internal Standard (IS); standard addition; and Isotope Dilution (ID) (Bulska and Wagner, 2016).

In the following lines, the calibration strategy followed in this work will be explained. The common calibration strategy for ceramic composition analyses and geological analyses is the external calibration, using calibration solutions prepared by alkaline fusion of multielemental geological CRMs with an internal standard, as explained in the Chapter 3, section 4.3.5. (e.g. Amosova et al., 2016; Bulska and Wagner, 2016; Calparsoro et al., 2019b, 2019c, 2021; Igea et al., 2013; Iñañez et al., 2020, 2021; García de Madinabeitia et al., 2008; Murillo-Barroso et al., 2019; Nelms, 2005). The relative intensities of the CRM solutions (relative intensity= $CRM_{intentsity}/IS_{intensity}$) are plotted versus their concentrations to calculate the linear

regressions with their corresponding linear equations y=*a*x+*b*, in which *a* are the slopes and *b* the intercepts. Then, the unknown sample is analysed and its concentrations can be calculated isolating x (the concentration) from these equations, as y (the relative intensities) is known (Figure 4.9.). The use of geological CRMs and not pure standard solutions prepared in the laboratory is justified because in this way, the matrix of the CRMs and of the samples are similar (Bulska and Wagner, 2016; García de Madinabeitia et al., 2008). In addition, internal standards are used to correct variations in the instrument response. The best internal standard for the calibration would be an element, which is similar to the analyte in mass, ionization potential and chemical behaviour. (Bulska and Wagner, 2016; Nelms, 2005).

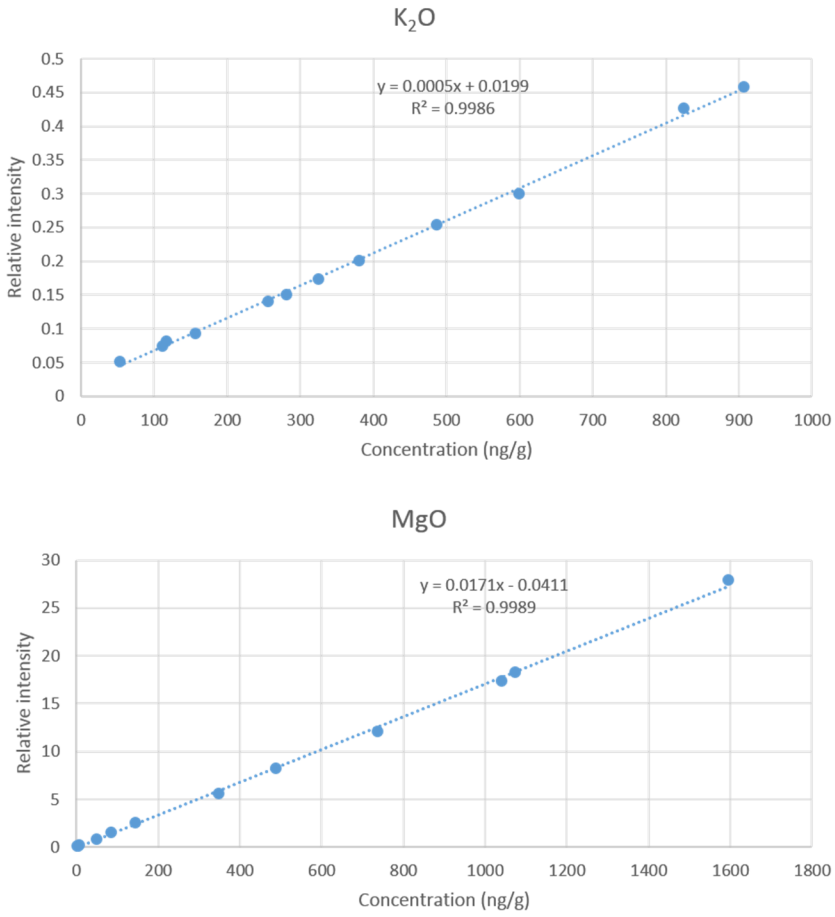

Figure 4.9. External calibrations, equations and coefficient of determination (R^2) of K_2O and MgO, made with 12 solutions obtained with different concentrations of CRMs

In the works of the present Doctoral Thesis the same methodology as García de Madinabeitia et al. (2008) was followed, that is, the CRM solutions were obtained from the Geological Survey of Japan (JB-3, JA-2, JG-1A, JG-2) and Indium (In) was the internal standard. These CRM solutions were prepared for ICP-MS analysis in the same way as samples are prepared, that is, using an alkaline fusion with $LiBO_2$ in Pt–Au crucibles. In addition, the internal standard was a solution of In prepared in the laboratory and this dilution was mixed with the solutions (CRM solutions, samples and blanks) to be analysed in the ICP-MS before entering the nebulizer in order to have a constant flow throughout the measurements. Finally, the drift correction of the signal was applied on the data, calculated using a drift correction solution (a reference solution with the same matrix as the samples that is analysed every specific amount of solutions), as explained in Calparsoro (2019) and García de Madinabeitia and collaborators (2008). However, there have been some changes in the procedure of making the calibration curves. At the beginning of the Doctoral Thesis, calibration curves were obtained with 4 calibration solutions (one for each CRM, taking 0.25 g samples). Nevertheless, after several observations of the calibrations and the sample concentration, the decision of obtaining an external calibration with wider concentration range was taken. For that, 2 different weights (0.125 g and 0.25 g) of the CRMs were fused. After that, 2 different dilutions were made from the solution coming from the 0.25 g sample and one dilution from the solution coming from 0.125 g sample, obtaining 3 solutions of different concentrations from each CRM, and to get, in total, 12 different calibration solutions. In this sense, if any concentration point turned out to be an outlier (e.g. because of instrument drift or analytical error), it was more appropriate to dispose of that concentration point from a more extensive calibration, than from a reduced calibration of four points. Additionally, in this case there is a higher probability for the sample concentrations to fall inside the calibration curve range (Figure 4.10. and Figure 4.11.).

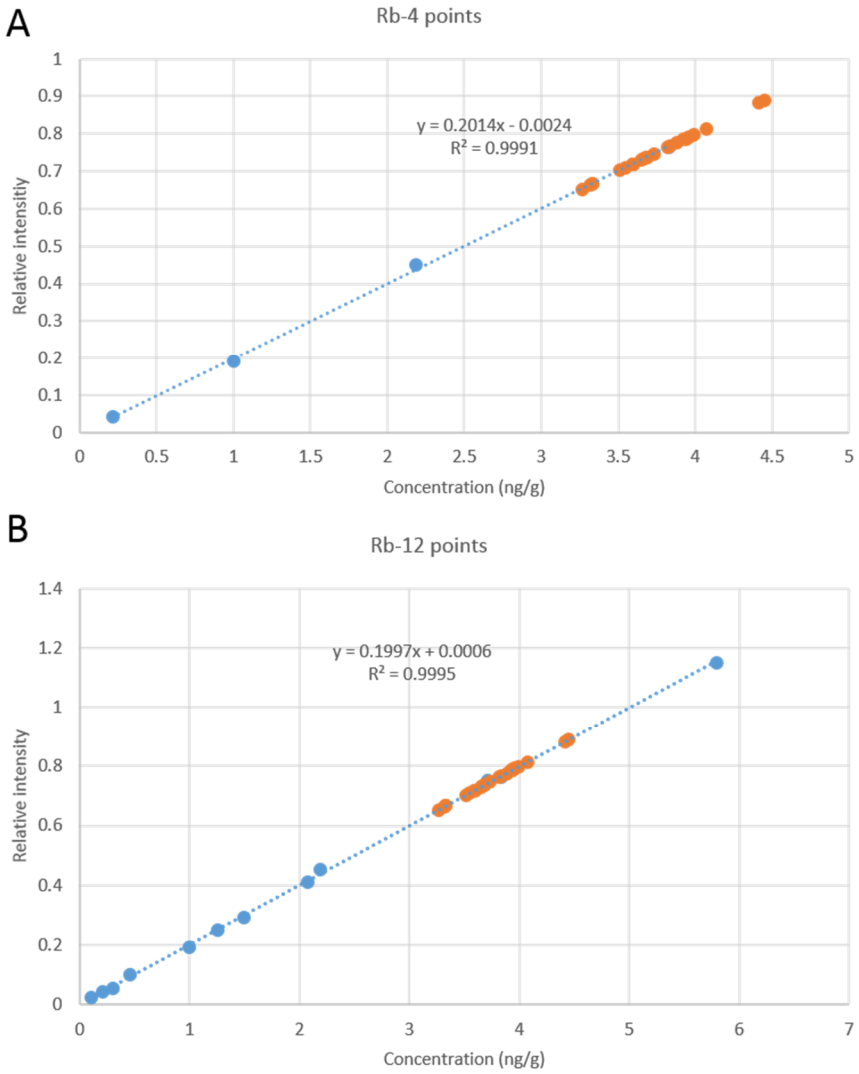

Figure 4.10. Comparison between two calibrations and their equations for the same element. Blue points: CRMs; orange points: real samples. **(a)** Calibration made with 4 CRM concentration solutions. Sample values are out of the calibration range; **(b)** calibration made with 12 CRM concentration solutions. Sample values are within the calibration range

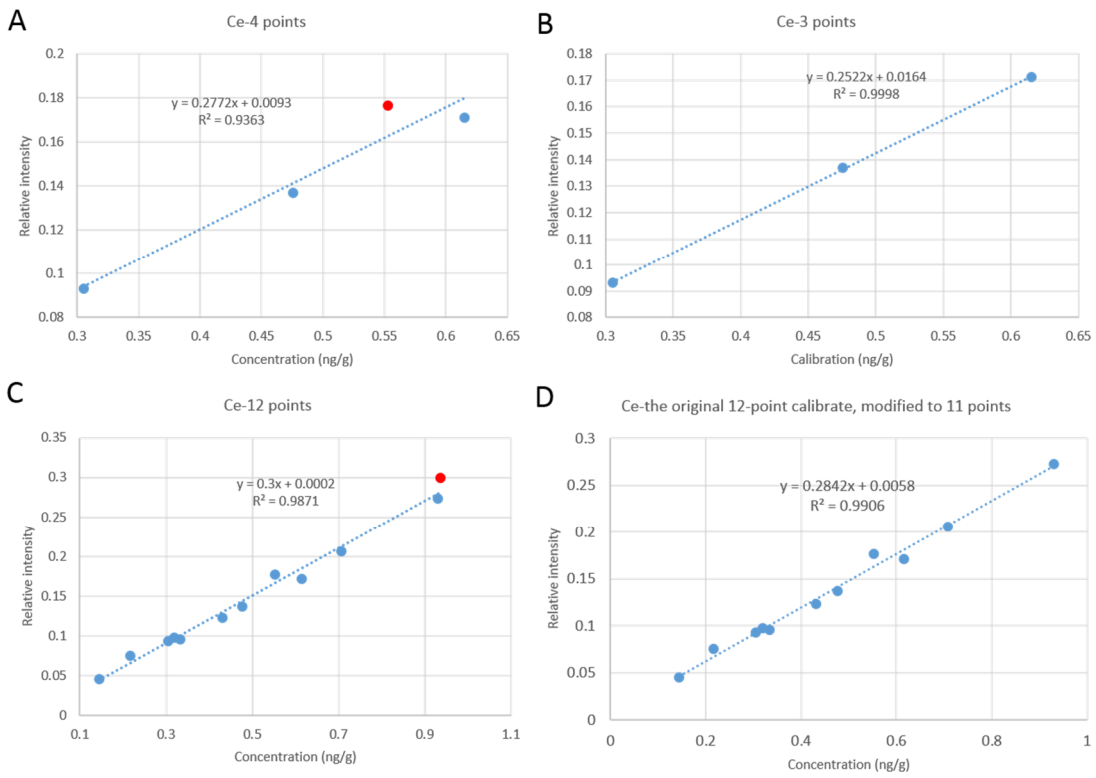

Figure 4.11. Comparison between a calibration with 4 CRM concentration solutions and 12 CRM concentration solutions. **(a)** One CRM concentration solution is an outlier; **(b)** a calibration without this outlier; **(c)** one CRM concentration solution is an outlier; **(d)** a calibration without this outlier

4.4.2. Alterations due to sample preparation and sample nature

The analytical variance should be minimized in such a way that is originated by natural sources and not because of sample preparation process, sample nature, experimental errors and/or alterations arising from post-depositional processes. All of these alterations will introduce a chemical variability that is not representative of the original chemical composition of the paste. For this reason, several components are not taken into account for the statistical analyses; some, which will be explained in this section, are related to the sample preparation as well as sample nature and others to post-depositional alterations and contaminations, which are explained in Chapter 1, section 1.3.2. and in Chapter 5.

The sample preparation process is one of the sources of chemical variability. On the one hand, the potential contamination by the tungsten carbide cell used to mill the ceramics was regarded: as Co is a known binder of tungsten alloys and usually occurs along with Ta traces (Boulanger et al., 2013), they were removed from the statistical analyses. Furthermore, as explained, prior to ICP-MS analyses the

milled pastes were mixed with the fluxer $LiBO_2$ and fused in Pt-Au crucibles. In consequence, Li, Pt and Au are not determined.

Regarding the sample nature, Pb and Sn are the major components of the glaze composition for tin-lead glazed wares. Since they are prone to diffuse from the glaze into the clay body during firing process (Molera et al., 2001), they are not used in the statistical treatment (Calparsoro, 2019; Molera et al., 2001).

4.4.3. Uncertainty

The purpose of this section is to explain the importance and the way to present reliable chemical results, where their uncertainty plays an important role. The uncertainty is a "parameter associated with the result of a measurement that characterizes the dispersion of the values that could reasonably be attributed to the measurand" (Ellison and Williams, 2012). A measurand is, therefore, the quantity intended to be measured, usually the concentration or mass fraction, total or not, of an analyte in a certain matrix obtained following a certain analytical procedure. This is directly related to the methodology that has been followed from sample preparation to its measurement, as each step can be a source of variability, which affects the final results. It is generally agreed that the usefulness of measurement results is largely determined by the quality of the statements of uncertainty that accompany them (Possolo, 2016). Thus, the corresponding uncertainty of each measurand should be expressed when giving the results, because only in this way the results will be comparable to other results either from the literature or obtained in the laboratory, since it sets the limits for considering a result as accurate, that is, precise and true.

The sources of the uncertainty in an analytical procedure are several: the sampling, the homogeneity of the sample, or even the temperature and pressure effects, among others, contribute to the uncertainty. All of the steps of the sample treatment such as homogenization, milling and dissolution, to name but a few, can also contribute. Similarly, different facts like the uncertainty of the standards, the sample matching to calibration, or the instrument precision, need to be taken into account. Finally, many other factors involved in the analysis and data processing steps, like the operator effects, the reagents purity, the interferences from the matrix, statistics, or even the processing algorithms, do also contribute to the uncertainty (Ellison and Williams, 2012).

A guide for beginners in calculating the uncertainty was published by Bell (2001), and further developed by Ellison and Williams (2012). However, these latter works provide a more general guide for the evaluation of the uncertainty in analytical measurements. In the following lines, the GUM methodology (Guide to the Expression of Uncertainty in Measurement) to estimate the expanded uncertainty associated with a measurement result is described and explained step-by-step for the ceramic compositional analyses. GUM methodology follows the propagation of errors approach for the calculation of the uncertainty. It identifies and quantifies all the sources of uncertainty associated with the measurement process (Possolo, 2015). The authors who follow GUM method are several. García de Madinabeitia et al. (2008), for example, developed a method to determine chemical elements simultaneously in geological samples by ICP-MS and estimated the uncertainty <10 % of the result. Likewise, Frackiewicz et al. (2012) proposed an extraction of uranium from low-grade Polish ores and reported the uncertainty as an expanded uncertainty with a coverage factor k = 2, obtaining an expanded uncertainty of 5.0-20 % depending on the element. Similarly, Mas et al. (2012) calculated the uncertainties within the ranges 0.60-8.0 % for the development of the method to determine trace element concentrations and Pb, U and Th isotope ratios by quadrupole-ICP-MS. Likewise, Calparsoro (2019) followed this methodology on her comprehensive provenance study of Medieval and Post-Medieval pottery from northern Spain reporting an expanded uncertainty, with the coverage factor of k=2, within the range of 1.0-34 %.

Besides, it is also important to distinguish between the error and uncertainty. The error, or bias, is defined as the difference between an individual result and the true value of the measurand and can be corrected, if it is known (Ellison and Williams, 2012). However, uncertainty takes the form of a range or interval and cannot be used to correct a measurement result (Ellison and Williams, 2012). In this sense, the repeatability is not the same as uncertainty; although the results are repeatable, it does not mean that the uncertainty is low.

With regard to the calculation of uncertainty following GUM method, first (step 1), the measurand should be specified and the definition of the relationship between the measurand and the input quantities should be given, that is, the equation for the calculation of the concentration with respect of the variables like mass of the sample, instrumental signal, volumes taken, etc. Secondly (step 2), the sources of uncertainty of those variables should be identified and listed. These

sources of uncertainty could be of Type A, which involve the calculation of the standard deviation of replicate measurements of that variable carried out in the laboratory, and of Type B, which involve the use of uncertainties that have not been measured in the laboratory, such as concentration of CRMs or calibration certificates, among others (Possolo, 2015). This list will include the value and uncertainty of the parameters needed in the calculation of the measurand. It could be useful to split the analytical procedure into a set of generic steps with a view to identifying the possible sources of uncertainty. These general steps are sampling, sample preparation, preparation of the CRMs, calibration of the instrument, data acquisition, etc. Then (step 3), the quantity of the uncertainty component corresponding to the concentration of the measurand could be estimated. It will consist of a number of quantified contributions to overall uncertainty and they must be expressed as standard uncertainty (s) before the next step. It should be taken into account that not all of the components will make a significant contribution to the uncertainty. After that (step 4), the combined standard uncertainty (u_c) should be calculated following the law of the Propagation of the Uncertainty, which involves the propagation of the uncertainties associated with each of the parameters used in the calculation of the final concentration. The general relationship between the combined standard uncertainty of a value y ($u_c(y)$) and the uncertainty of the independent parameters (x_1, x_2,...x_n) is shown by the next equation when there is no correlation between the parameters (Ellison and Williams, 2012):

$$u_c\big(y(x_1, x_2, \dots)\big) = \sqrt{\sum_{i=1,n}\left(\frac{\partial y}{\partial x_i}\right)^2 \cdot \big(u(x_i)\big)^2} \quad \text{Eq.4.1.}$$

Where $y(x_1, x_2, \dots)$ is a function of several parameters, for example: $y = \frac{a \cdot b}{c \cdot d}$. Therefore, in this specific case, for the calculation of the combined standard uncertainty, Eq.4.1. would be transformed to:

$$u_c(y) = y \cdot \sqrt{\left(\frac{u_a}{a}\right)^2 + \left(\frac{u_b}{b}\right)^2 + \left(\frac{u_c}{c}\right)^2 + \left(\frac{u_d}{d}\right)^2} \quad \text{Eq.4.2.}$$

Where u_a, u_b, u_c and u_d are the standard uncertainties of the variables a, b, c and d, respectively.

The general procedure for the calculation of the combined standard uncertainty requires the generation of partial differentials of the measurement model with respect to the variables involved in the model. In many cases, the model is simple and consists on combinations of additions, subtractions, multiplications

and divisions. In that case, the addition of variances (standard uncertainties squared) or relative variances of the variables may be enough. However, in more complicated models, partial differentials would be needed. Alternatively, two numerical methods are used for the expressions for combining uncertainties: Kragten method and Monte Carlo simulation (Ellison and Williams, 2012). On the one hand, the method suggested by Kragten, makes effective use of spreadsheet software (such as Microsoft Excel). This method provides a combined standard uncertainty from input standard uncertainties and a known measurement model. On the other hand, the Monte Carlo simulation calculates the result corresponding to one value of each input quantity drawn at random depending on its uncertainty and its uncertainty distribution, and repeats this calculation thousands of times to calculate the average value and standard deviation of the measurand. The latter is, thus, considered equivalent to its uncertainty. Finally (step 5), the appropriate coverage factor (k) should be applied to give the expanded uncertainty (U) or the relative expanded uncertainty (U %). This coverage factor is a numerical factor that produces a range of values around the measurement result (y), corresponding to a specified confidence level. In this way, the interval (y – U) to (y + U) is defined, within which an important fraction of the distribution of values, which could reasonably be attributed to the measurand, is included. When a normal (Gaussian) distribution can be attributed to the measurand the use of the coverage factor k = 2 is generally accepted. In this case, the associated expanded uncertainty corresponds to a coverage probability of 95 %, that is, the confidence level of 95 %.

A specific example will be detailed in the next lines in order to understand better these 5 steps. For this, the estimation of the uncertainty of the total concentration of Fe_2O_3 in AVR001 ceramic from Aveiro, Portugal will be explained, step by step:

(step 1: the measurand should be specified and the definition of the relationship between the measurand and the input quantities should be given). In this specific case, the measurand is the total concentration of Fe_2O_3 in AVR001 ceramic from Aveiro. Other inputs:

- The mass taken from the calcined ceramic for its fusion (later it will be called “mass x1”): 0.2521 g

- The mass of the solution after the fusion (later it will be called “mass x2”): 96.09 g
- The mass taken from this last solution for the dilution (later it will be called “mass x3”): 0.05157 g
- The mass of the last dilution (later it will be called “mass x4”): 10.00 g
- The concentration of Fe_2O_3 obtained directly from the calibration curve for each ceramic: c_c= 601.2 ng/g
- The concentration of the reference dilution measured 3 times through the analyses (used for the drift correction of ICP-MS) obtained directly from the calibration: reference concentration 1 = 910.5; ref. conc. 2 = 899.6; ref. conc. 3 = 862.0 ng/g
- The Fe_2O_3 corrected concentration of the ceramic: 4.545 wt %. In this case, the way that the corrected concentration values were obtained was composed of several steps that are summarized in the next equations (Eq.4.3. is for minor compounds, such as Cu, and Eq.4.4. for major compounds, such as Fe_2O_3):

$$\frac{c_c \cdot m_2 \cdot conc.ref._1}{\frac{m_1 \cdot m_3 \cdot 10^3}{m_4} \cdot \left[conc.ref._2 + (conc.ref._3 - conc.ref._2) \cdot \frac{x}{y}\right]} \quad Eq.\,4.3.$$

$$\frac{c_c \cdot m_2 \cdot conc.ref._1}{\frac{m_1 \cdot m_3 \cdot 10^7}{m_4} \cdot \left[conc.ref._2 + (conc.ref._3 - conc.ref._2) \cdot \frac{x}{y}\right]} \quad Eq.\,4.4.$$

Where m_1, m_2, m_3 and m_4 are the values corresponding to mass x_1, mass x_2, mass x_3 and mass x_4, respectively, and (x/y) corresponds to the way the concentrations were corrected. In this case, one reference sample for every eight samples was analysed. Thus, the ref. conc. 1 would be the concentration of the reference sample measured the first time before the samples, and the ref. conc. 2 and 3 would be the values of the reference sample that were measured before and after the sample AVR001 in this case. Then, x would be the position of AVR001 in the block of 8 samples (x = 2) and y would be the number of samples in the block (y = 8) (Table 4.6.).

Table 4.6. An example of the results obtained directly from the calibration, showing the values of the reference samples and some ceramics. The reference concentrations 1, 2 and 3 are marked in pink and AVR001 sample in blue

Samples	Fe_2O_3 ng/g
JA-2 = ref. conc. 1	910.5
8 samples	
JA-2	839.1
8 samples	
JA-2	939.4
8 samples	
JA-2	868.8
8 samples	
JA-2 = ref. conc. 2	899.6
CTA078	714.1
AVR001	601.2
AVR002	466.9
AVR003	614.0
AVR004	563.0
AVR005	624.4
AVR006	501.0
AVR007	590.3
JA-2 = ref. conc. 3	862.0

(steps 2,3: sources of uncertainty and quantity of the uncertainty component):

1. Source: weighing all the mases → calculation: the uncertainty of the linearity of the analytical balance (Type B).
2. Source: calculating the concentration of Fe_2O_3 obtained directly from the calibration for each ceramic (c_c) → calculation: calibration uncertainty ($u(c_c)$) (Type A):
3. Source: calculating the concentration of the reference solution measured 3 times through the analyses (used for the drift correction of ICP-MS) obtained directly from the calibration → calculation: uncertainty derived from the calibration uncertainty (Type A).
4. Source: calculating the Fe_2O_3 corrected concentration of the ceramic → calculation: combined standard uncertainty (Type A).

Calculations:

1. Uncertainty of the linearity of the analytical balance: in this case, the standard uncertainty cannot be calculated through the measurements because this type of uncertainty is of type B. However, the linearity of the analytical balance is known (0.0002 g). This uncertainty is calculated dividing the value by the squared root of three, because it follows a rectangular distribution and it is multiplied by two because the weighing is carried out as a difference:

   $s = \sqrt{2 \times \left(\frac{0.0002}{\sqrt{3}}\right)^2} = 1.63 \cdot 10^{-4}\ g$ Eq.4.5.

2. For the calculation of the uncertainty of the calibration, the next sequence is followed:

   2.1. The calibration used for Fe_2O_3 needs to be annotated (Table 4.7. and Figure 4.12.):

Table 4.7. The concentration solutions of each CRM and their relative intensities, for Fe_2O_3

CRMs	Concentration Fe_2O_3 (ng/g)	Relative intensity
GSJ JA-2 0.5	399.2	42.27
GSJ JB-3 0.5	793.4	78.80
GSJ JG-1a 0.5	141.6	14.30
GSJ JG-2 0.5	66.92	7.306
GSJ JA-2	876.7	91.21
GSJ JB-3	1678	169.3
GSJ JG-1a	245.8	25.54
GSJ JG-2	123.5	13.27
GSJ JA-2 1.5	1303	139.4
GSJ JB-3 1.5	2370	241.3
GSJ JG-1a 1.5	416.7	43.20
GSJ JG-2 1.5	186.7	19.62

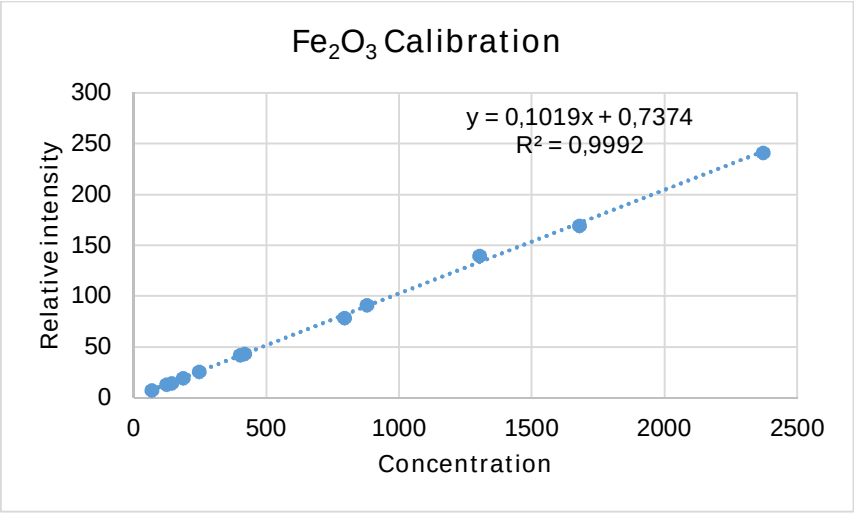

Figure 4.12. The calibration, equation and coefficient of determination (R^2) for Fe_2O_3 using 12 CRM concentration solutions

2.2. Calibration uncertainty should be calculated based on Ellison and Williams (2012) guide reference equations. The equations are the following ones:

$$u(c_c) = \frac{S_y}{m}\sqrt{\frac{1}{p}+\frac{1}{n}+\frac{(c_c-\bar{c})^2}{S_{xx}}}$$ Eq.4.6.

$$s_y = \sqrt{\frac{\sum(y_i-(m\cdot c_i+b))^2}{n-2}}$$ Eq.4.7.

$$s_{xx} = \sum(c_i-\bar{c})^2$$ Eq.4.8.

Inputs of these equations: s_y, s_{xx}, m, p, n, c_c, c_i and $\bar{c}$.

c_i: the concentrations of each calibration solution.

m: the slope of the calibration.

p: the measurement replicates of each dissolution.

n: the number of points used for the calibration (number of CRMs).

c_c: Fe_2O_3 concentration (before the drift correction) of AVR001.

$\bar{c}$: the average concentration of the 12 points of the calibration.

s_y: the standard error of estimate y.

s_{xx}: sum of squared differences.

In this case, p=3, n=12, c_c=601.2 ng/g.

There is a function in Microsoft Excel called “LINEST”, which calculates the value of m and s_y, among others. In this case, the response of excel for the “LINEST” function is showed in Table 4.8.:

Table 4.8. The response of excel for the "LINEST" function

m = 0.1019	0.7374
0.0009386	0.9385
0.9992	**s_y = 2.267**
1.179E+04	10.00
6.056E+04	51.38

The next step would be the calculation of s_{xx}. For this, the average concentration of the calibration solutions is needed (Table 4.9.).

Table 4.9. Table showing the calculation of S_{xx}

CRMs	Concentration Fe_2O_3 (ng/g)	Relative intensity	c_i-$\bar{c}$
GSJ JA-2 0.5	399.2	42.27	-317.6
GSJ JB-3 0.5	793.4	78.80	76.63
GSJ JG-1a 0.5	141.6	14.30	-575.2
GSJ JG-2 0.5	66.92	7.306	-649.9
GSJ JA-2	876.7	91.21	159.9
GSJ JB-3	1678	169.3	960.9
GSJ JG-1a	245.8	25.54	-471.1
GSJ JG-2	123.5	13.27	-593.3
GSJ JA-2 1.5	1303	139.4	586.6
GSJ JB-3 1.5	2370	241.3	1653
GSJ JG-1a 1.5	416.69	43.20	-300.1
GSJ JG-2 1.5	186.7	19.62	-530.1
AVERAGE→	716.8	SUMSQ→	s_{xx} = 5.832E+06

2.3. Once all these parameters are calculated, the uncertainty of the calibration, $u(c_c)$, is calculated using the Eq.4.6. In this case, the $u(c_c) = 14.4$.

2.4. A table, which gathers these values, is designed in Microsoft Excel and the relative standard uncertainties are calculated dividing the standard uncertainty by the value (Table 4.10.).

Table 4.10. A table gathering the values of the inputs, their standard uncertainties and the relative standard uncertainties

Fe_2O_3			
Inputs	**Value**	**Standard uncertainty**	**Relative standard uncertainty**
mass x1	0.2521	1.63E-04	0.06 %
mass x2	96.09	1.63E-04	0.00 %
mass x3	0.05157	1.63E-04	0.32 %
mass x4	10.00	1.63E-04	0.00 %
c_c	601.2	14.39	2.39 %

2.5. To calculate the uncertainty of the measured concentrations of the reference solution, an approximation is made, assuming it would be similar to the uncertainty found for the sample solution AVR001 ($u(c_c)$) (2.39 %). Therefore, this value was multiplied with the value of the concentration of each reference solution, obtaining the values of the standard uncertainties of the concentrations of the reference solution. (Table 4.11.).

Table 4.11. Table showing the calculation of the standard uncertainty of the reference concentrations 1, 2 and 3

Fe_2O_3			
Inputs	**Value**	**Standard uncertainty**	**Relative standard uncertainty**
mass x1	0.2521	1.63E-04	0.06 %
mass x2	96.09	1.63E-04	0.00 %
mass x3	0.05157	1.63E-04	0.32 %
mass x4	10.00	1.63E-04	0.00 %
c_c	601.2	14.39	2.39 %
Ref. conc. 1	910.5	21.80	2.39 %
Ref. conc. 2	899.6	21.54	2.39 %
Ref. conc. 3	862.0	20.64	2.39 %

(step 4: calculation of the combined standard uncertainty (u_c)):

4.1. To calculate the combined standard uncertainty (u_c), the law of the Propagation of the Uncertainty will be followed using the Kragten numerical method. To do that, first, the whole equation for obtaining the AVR001 last concentration, that is, taking into account the drift correction, should be written (this equation is Eq.4.3. and 4.4.). Then, the procedure for obtaining the combined standard uncertainty will be shown in detail. The general way for calculating it could be consulted in the Ellison and Williams (2012) guide. The procedure is the next:

4.1.1. Write down the equation (in this case Eq.4.3. and 4.4.) linking all the values of the column B of the Table 4.12. in the cell B10 of the Table 4.12., so that the equation will calculate the last concentration of AVR001. This equation will be the same equation for Table 4.14. as well.

Table 4.12. An excel table showing the calculation process of the combined standard uncertainty. First step

Fe_2O_3	A	B	C	D
1	**Inputs**	**Value**	**Standard uncertainty**	**Relative standard uncertainty**
2	mass x1	0.2521	1.63E-04	0.06 %
3	mass x2	96.09	1.63E-04	0.00 %
4	mass x3	0.05157	1.63E-04	0.32 %
5	mass x4	10.00	1.63E-04	0.00 %
6	c_c	601.2	14.3964	2.39 %
7	Ref. conc. 1	910.5	21.80	2.39 %
8	Ref. conc. 2	899.6	21.54	2.39 %
9	Ref. conc. 3	862.0	20.64	2.39 %
10	Concentration	Eq.4.3. or 4.4.	u_c?	u_c %?

In this case, the final concentration of Fe_2O_3 for AVR001 using the values above is 4.545 wt %, and it will appear in the cell B10.

4.1.2. Create another table next to Table 4.12., so that it has the next form (copy and paste the “value” column of Table 4.12. in all the columns of Table 4.13.):

Table 4.13. A table showing the calculation process of the combined standard uncertainty. Second step

mass x1	mass x2	mass x3	mass x4	c_c	Ref. conc. 1	Ref. conc. 2	Ref. conc. 3
0.2521	0.2521	0.2521	0.2521	0.2521	0.2521	0.2521	0.2521
96.09	96.09	96.09	96.09	96.09	96.09	96.09	96.09
0.05157	0.05157	0.05157	0.05157	0.05157	0.05157	0.05157	0.05157
10.00	10.00	10.00	10.00	10.00	10.00	10.00	10.00
601.2	601.2	601.2	601.2	601.2	601.2	601.2	601.2
910.5	910.5	910.5	910.5	910.5	910.5	910.5	910.5
899.6	899.6	899.6	899.6	899.6	899.6	899.6	899.6
862.0	862.0	862.0	862.0	862.0	862.0	862.0	862.0

4.1.3. Create a diagonal in which the value of the variable (mass x1, mass x2, etc.) and its standard uncertainty are (from column C in Table 4.12.) added up. Then, add a line copying the cell B10 of Table 4.12. (Table 4.14.):

Table 4.14. An excel table showing the calculation process of the combined standard uncertainty. Third step

	A	B	C	D	E	F	G	H
1	**mass x1**	**mass x2**	**mass x3**	**mass x4**	**c_c**	**Ref. conc. 1**	**Ref. conc. 2**	**Ref. conc. 3**
2	Value+ std.unc.	0.2521	0.2521	0.2521	0.2521	0.2521	0.2521	0.2521
3	96.09	Value+ std.unc.	96.09	96.09	96.09	96.09	96.09	96.09
4	0.05157	0.05157	Value+ std.unc.	0.05157	0.05157	0.05157	0.05157	0.05157
5	10.00	10.00	10.00	Value+ std.unc.	10.00	10.00	10.00	10.00
6	601.2	601.2	601.2	601.2	Value+ std.unc.	601.2	601.2	601.2
7	910.5	910.5	910.5	910.5	910.5	Value+ std.unc.	910.5	910.5
8	899.6	899.6	899.6	899.6	899.6	899.6	Value+ std.unc.	899.6
9	96.09	862.0	862.0	862.0	862.0	862.0	862.0	Value+ std.unc.
10	Eq.4.3. or 4.4.	Eq.4.3. or 4.4.	Eq.4.3. or 4.4.	Eq.4.3. or 4.4.	Eq.4.3. or 4.4.	Eq.4.3. or 4.4.	Eq.4.3. or 4.4.	Eq.4.3. or 4.4.

When the equation is added, the Fe_2O_3 concentration of AVR001 in wt % will be calculated automatically for each column and it will be different in all the cells of line 10, due to the different uncertainties occurring to each variable (Table 4.15.).

Table 4.15. An excel table showing the calculation process of the combined standard uncertainty. Fourth step

	A	B	C	D	E	F	G	H
1	**mass x1**	**mass x2**	**mass x3**	**mass x4**	**c_c**	**Ref. conc. 1**	**Ref. conc. 2**	**Ref. conc. 3**
2	2.52E-01	0.2521	0.2521	0.2521	0.2521	0.2521	0.2521	0.2521
3	96.09	9.61E+01	96.09	96.09	96.09	96.09	96.09	96.09
4	0.05157	0.05157	5.17E-02	0.05157	0.05157	0.05157	0.05157	0.05157
5	10.00	10.00	10.00	1.00E+01	10.00	10.00	10.00	10.00
6	601.2	601.2	601.2	601.2	6.16E+02	601.2	601.2	601.2
7	910.5	910.5	910.5	910.5	910.5	9.32E+02	910.5	910.5
8	899.6	899.6	899.6	899.6	899.6	899.6	9.21E+02	899.6
9	96.09	862.0	862.0	862.0	862.0	862.0	862.0	8.83E+02
10	4.542	4.545	4.531	4.545	4.654	4.654	4.464	4.519

4.1.4. The final concentration of Table 4.12. (cell B10) should be subtracted to the concentrations of line 10 of Table 4.15. in a new line (line 11) (Table 4.16.). After that, the square of each difference should be calculated in line 12. Finally, all the values of line 12 should be summed up in a new cell I12 to calculate the combined variance (U^2) (cell I12) and its square root would be calculated in cell C10 of Table 4.12., so that this value would be the combined standard uncertainty, u_c, of the analytical procedure (Table 4.16. and Table 4.17.).

Table 4.16. An excel table showing the calculation process of the combined standard uncertainty. Fifth step

	A	B	C	D	E	F	G	H	I
1	**mass x1**	**mass x2**	**mass x3**	**mass x4**	**c_c**	**Ref. conc. 1**	**Ref. conc. 2**	**Ref. conc. 3**	
2	2.52E-01	0.2521	0.2521	0.2521	0.2521	0.2521	0.2521	0.2521	
3	96.09	9.61E+01	96.09	96.09	96.09	96.09	96.09	96.09	
4	0.05157	0.05157	5.17E-02	0.05157	0.05157	0.05157	0.05157	0.05157	
5	10.00	10.00	10.00	1.00E+01	10.00	10.00	10.00	10.00	
6	601.2	601.2	601.2	601.2	6.16E+02	601.2	601.2	601.2	
7	910.5	910.5	910.5	910.5	910.5	9.32E+02	910.5	910.5	
8	899.6	899.6	899.6	899.6	899.6	899.6	9.21E+02	899.6	
9	96.09	862.0	862.0	862.0	862.0	862.0	862.0	8.83E+02	
10	4.542	4.545	4.531	4.545	4.654	4.654	4.464	4.519	
11	-0.00294	0.00001	-0.01435	0.00007	0.10883	0.10883	-0.08102	-0.02619	
12	0.000009	0.000000	0.000206	0.000000	0.01184	0.01184	0.006563	0.000686	0.03115

Table 4.17. An excel table showing the values of the standard uncertainties, relative standard uncertainties and the combined standard uncertainty (cells C10 and D10)

Fe_2O_3	**A**	**B**	**C**	**D**
1	**Inputs**	**Value**	**Standard uncertainty**	**Relative standard uncertainty**
2	mass x1	0.2521	1.63E-04	0.06 %
3	mass x2	96.09	1.63E-04	0.00 %
4	mass x3	0.05157	1.63E-04	0.32 %
5	mass x4	10.00	1.63E-04	0.00 %
6	c_c	601.2	14.3964	2.39 %
7	Ref. conc. 1	910.5	21.80	2.39 %
8	Ref. conc. 2	899.6	21.54	2.39 %
9	Ref. conc. 3	862.0	20.64	2.39 %
10	Concentration	4.545	0.177	3.88 %

4.1.5. Then the contribution of each input to the combined variance (U^2) could be evaluated in a pie chart, dividing the values of line 12 by cell I12 of Table 4.16. and multiplying by 100 to get a percentage. As can be seen in Figure 4.13., the uncertainty of the calibration and the uncertainty of the first reference concentration are the highest contributors to the uncertainty Fe_2O_3 in AVR001.

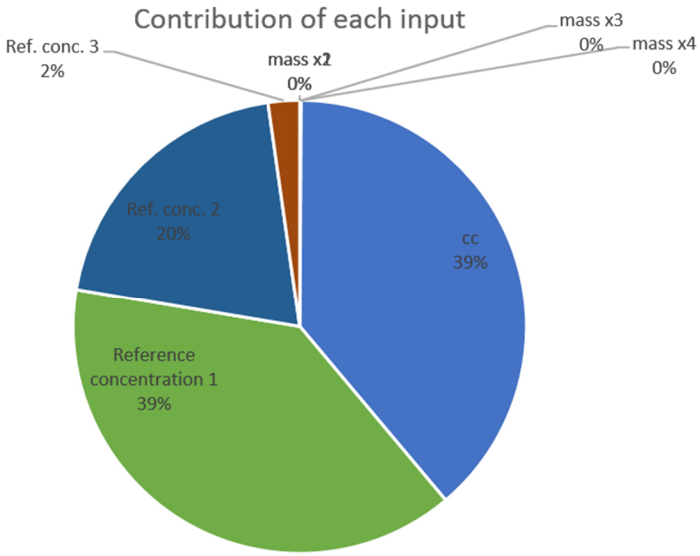

Figure 4.13. A pie chart showing the contribution of each input to the combined variance (U^2) in the form of percentages.

(Step 5: calculation of the expanded uncertainty):

Finally, the appropriate coverage factor (k) should be applied to give the expanded uncertainty (U).

In this case, the coverage factor is 2, so the expanded uncertainty would be the standard uncertainty multiplied by 2: U = 0.177 x 2 = 0.354 = 0.35. In these lines, the relative expanded uncertainty would be the relative standard uncertainty multiplied by 2: U (%) = 3.88 x 2 = 7.76 % = 7.8 %. Thus, in this case, the reported uncertainty of Fe_2O_3 for AVR001 is based on a standard uncertainty multiplied by a coverage factor k=2, providing a level of confidence of approximately 95 %. The final result of the Fe_2O_3 concentration is 4.54 ± 0.35 wt %.

Once the sources of the uncertainty are evaluated and the uncertainty calculated, the pie chart of Figure 4.13. could be useful to identify the major

contributors for improving the analytical procedure. Frackiewicz et al. (2012), for example, published that the major contributor to the uncertainty in their research was the dilution of samples and standards. In our particular case, the source of uncertainty in which special attention could be paid, is the calibration curve. The nearer the concentrations of the sample are to the centroid of the calibration curve, the lower should be the calibration uncertainty. Therefore, the calibration curves could be checked and modified (e.g. adding more concentration points) after having analysed the CRMs, for reducing the uncertainty. Besides, the fact of making calibration curves with more calibration solutions gives a higher and more reliable possibility to modify the curves in order to obtain more appropriate concentration intervals (see Figure 4.10.) depending on the concentration of the samples.

4.5. Statistical model

As explained in Chapter 1, section 1.2.1., after analysing the chemical composition of ceramic pastes, ceramics should be classified into meaningful ceramic groups called PCRUs (Buxeda i Garrigós and Madrid i Fernández, 2017), and in this work, this procedure was done through a statistical model. Thus, the interpretation of the chemical results of ceramic pastes obtained is in accordance with Aitchison's approach and Buxeda's observations on compositional data (Aitchison, 1982, 2008; Buxeda i Garrigós, 1999; Buxeda i Garrigós and Kilikoglou, 2003). In this way, it is possible to search for the variabilities of the data in order to identify the PCRUs according to different chemical patterns, as well as to identify the elements responsible for the variabilities among the samples, by means of multivariate statistical techniques (Buxeda i Garrigós, 2008; Buxeda i Garrigós et al., 2003).

The model and routines followed for that are based on the works on statistical modelling by Calparsoro (2019) and are published with the name "arch_flow" (Calparsoro, 2021) through a repository on the GitHub website, the largest worldwide platform dedicated to collaborative software development. This repository contains all the code necessary to execute the archeometric routines concerning compositional analysis and allows its complete reproduction in the R software (Core Team, 2013), an open source programming language.

The raw compositional data consists of vectors whose components sum a constant (Aitchison, 1982). These kinds of data are constrained, they are not absolute

values since they have a dependency from each other (Buxeda i Garrigós and Kilikoglou, 2003). Since applying standard multivariate analyses could lead to spurious results (Pearson, 1897), log-ratio transformations (Aitchison, 1982) are applied:

Logarithmic transformations act as "quasi-standardization" of the data (Martín-Fernández et al., 2015; Neff, 2000; Sayre et al., 1976). They compensate the differences in magnitudes between major elements (e.g. Al or Fe) and trace elements (e.g. the lanthanides or rare earth elements) and make the distributions of geochemical data more nearly normal, that is, to place the elements onto more or less the same scale (Glascock, 2016).

In the first approximation, the examination of the degree of compositional variability is carried out. This is done analysing the variability introduced by each component into the dataset (compositional evenness), by means of the matrix of compositional variability (MCV). In the model that is followed in this work, first, a graphical representation of the MCV is obtained. The graph displays the individual contribution of the variability from each element to the whole dataset, from the highest to the lowest (y-axis (τ.i)). Moreover, other values such as vt = Total variation, n = number of specimens, H_2 = information entropy and H_2 % = percentage of information entropy over the maximum possible, are displayed. The value of total variation describes the extent of variability of the set of ceramics. Generally speaking, a large value of the total variation (vt) indicates greater variability and suggests that the dataset is polygenic (i.e. presence of several compositional groups). In contrast, a small value for vt indicates a possible monogenic nature of the dataset (Buxeda i Garrigós and Kilikoglou, 2003).

In the present study, similarity of individuals, and subsequently their hypothetical provenance, according to the provenance postulate (Weigand et al., 1977) (see Chapter 1, section 1.2.1.), was tested using Hierarchical Cluster Analysis (HCA) and Principal Component Analysis (PCA). Firstly, for HCA, the clr transformation was used, that is, log-ratio transformations were applied, dividing all the chemical components by the geometric mean. In this model, the centroid algorithm and squared Euclidean distances were used (Aitchison, 1982). Thus, from all the initial individuals that are in their base, a hierarchical process of agglomeration is established. This is the union of an individual with another individual, of an individual with another group, or of one group with another group. In this way, groups formed by some of the individuals analysed is obtained. Thus,

the farther away from the base the union occurs, the less similar are the individuals that come together in its chemical composition. While HCA provides information about the possible groupings between ceramics according to their similarities, PCA provides similar information and points out the elements that are the responsible for the similarities or dissimilarities. For PCA, all the chemical components were divided by the component that introduces the lowest chemical variability to the entire set of specimens (additive log-ratio transformation, alr) (Aitchison, 1982).

Additionally, the log-ratio transformation also highlights possible perturbations in the chemical data because of diagenesis, contamination, or other alteration processes that may occur (Buxeda i Garrigós and Kilikoglou, 2003; see Martín-Fernández et al., 2015 for a thorough discussion on the use of log-ratio principles).

5. KAPITULUA: LABORATEGIKO ZAHARTZE-ESPERIMENTUA, KUTSADURA- ETA ERALDAKETA-PROZESUAK EBALUATZEKO

Atal honetan, laborategiko zahartze-esperimentuan lortutako emaitzak azaltzen dira. Esperimentu honen metodologiaren xehetasunak 4. kapituluko 4.2 atalean ageri dira.

Behin piezak ur-inguruneetatik atera eta lehortu ondoren, instrumentu ezberdinen bidez analizatu dira. Aipatu beharra dago, piezak ez direla garbitu ez uretatik ateratzean ezta beren analisietarako ere. Alde batetik, ICP-MS eta XRD probeten eta kontrol-piezen analisi kimiko eta mineralogikoetarako erabili dira. Gainera, XRD ere buztin gordinen analisi mineralogikoa egiteko erabili da. ICP-MS baliagarria da zeramiketan gertatzen diren aldaketa kimikoak eta elementuen aberastasun- edo lixibiazio-kasuak identifikatzeko, eta XRD, aldiz, lehengaietan (hau da, buztin gordinetan) dauden mineralak (hauek lehen mailakoak izango lirateke) eta zeramikak erretzean kristalizatutako mineral berriak edota jalkitze-aldian kristalizatutakoak (bigarren mailakoak) identifikatu eta kuantifikatzeko. Bestalde, karakterizazio mikroestrukturala, bitrifikazio-mailaren ebaluazioa eta alterazioen eta kutsaduren presentzia ere aztertu dira SEM–EDS-ren eta Raman espektrometriaren bidez (metodologiaren xehetasun orokorretarako, ikus 4. kapitulua, 4.3. atala). Beraz, guztira, 69 probeta eta kontrol-pieza eta 3 buztin gordin aztertu dira (ikus 4. kapituluko 4.3. taula). Azkenik, 60 probetak kolorimetroaz ere aztertu dira bai uretan murgildu aurretik eta baita uretatik atera ondoren ere; izan ere, kolore-aldaketak zeramikaren erabileraren eta jalkitze-osteko eraldaketen adierazle makroskopikoak izan daitezke (Maritan, 2020). Kolorimetroa PCE-CSM 5 PCE Instruments (Meschede, Alemania) kolorimetroa da, eta neurketetarako CIELAB kolore-espazioa 10º-ko behatzailearekin, D65 argitzailearekin eta 8º/d-ko geometriarekin erabili da. Horrela, L, a eta b parametroak neurtu dira. L argitasunaren parametroa da, 0-tik (beltza) 100-era (zuria) bitarteko balioak erregistratzen dituena, eta a eta b parametro kromatiko kartesiarrak dira. Lehenengoa berdetik gorrira da, eta bigarrena, berriz, urdinetik horira. Neurketak ur-inguruneekin kontaktuan egon den gainazal berberean egin dira.

5.1. Ur-inguruneen parametroak

5.1. taulan, bi ur-inguruneetan periodo bakoitzean (3, 10 eta 18 hilabete) neurtutako parametroen batezbesteko balioak laburtzen dira. pH-a nahiko egonkorra izan da bi inguruneetan, 8.02 balio minimotik 9.7 balio maximora (itsasoko uretan) eta iturriko uretan, aldiz, 10.26 balio minimotik 10.71 balio maximora. Gainerako parametroak periodoetan zehar nahiko egonkorrak izan

diren arren, 18 hilabeteko periodoan beherakada nabaritu da parametro guztietan. Hala ere, ez da aurkitu parametro horien eta konposizio kimikoaren arteko loturarik.

5.1. taula. Esperimentuan neurtutako parametroen batezbesteko balioak (pH-a, eroankortasuna, TDS, gazitasuna eta tenperatura)

	pH		Eroankortasuna (ms/cm)		TDS (g/L)		Gazitasuna		T(°C)	
Periodoa (hilabeteak)	**Itsasoko ura**	**Iturriko ura**	**Itsasoko ura**	**Iturriko ura**	**Itsasoko ura**	**Iturriko ura**	**Itsasoko ura**	**Iturriko ura**	**Itsasoko ura**	**Iturriko ura**
3	8.02	10.26	43.60	1.49	25.24	0.66	28.15	0.61	49.97	49.39
10	8.68	10.71	43.86	1.06	25.16	0.56	27.94	0.5	49.7	49.55
18	9.07	10.71	40.87	0.97	23.49	0.51	25.83	0.48	43.48	43.54

5.2. Kolorimetroaren emaitzak

5.1. irudian ageri dira murgildu aurreko eta ondorengo kolorimetroaren emaitzak. Emaitzek erakusten dute tenperatura maximoan (1100 °C) erretako laginen koloreak gainerako laginen koloretik aldentzen direla, murgilduak izan baino lehen. Aldiz, tenperatura baxuan (850 °C) eta ertainean (950 °C) erretako laginen koloreak elkarren antzekoagoak ziren murgildu aurretik, uretatik atera ondoren baino. Hala ere, urperatuta egon ondoren, badirudi laginen gainazalean hauspeatutako gatzek murriztu egin dituztela aipatutako desberdintasunak, baina laginen kolorea orokorrean heterogeneoago bihurtzen dutela. Honek erakusten du garrantzitsua dela laginak garbitzea aztertu aurretik.

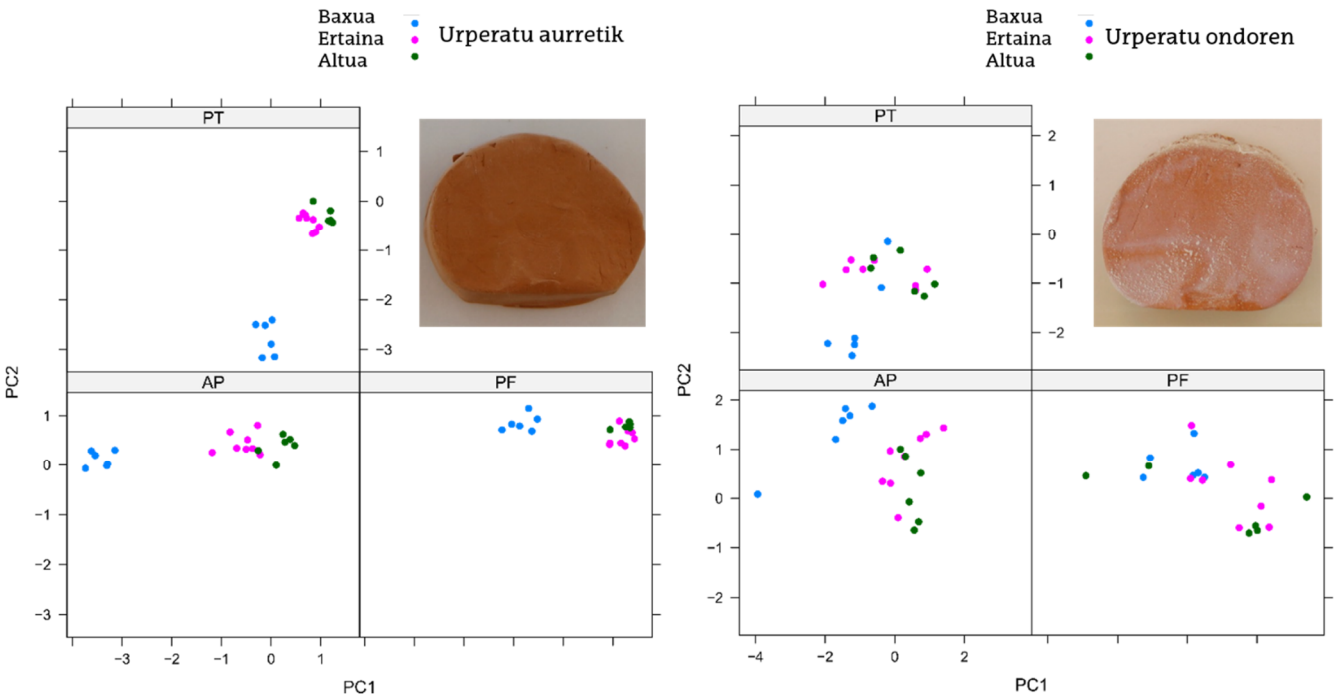

5.1. irudia. Kolorimetroaren bidez lortutako hiru pastetako laginen emaitzak, dagokien urringurunean murgildu aurretik eta ondoren; eta PT taldeko pieza baten itxura 18 hilabete murgilduta igaro eta gero eta urperatu aurretik

5.3. ICP-MS emaitzak

5.2. taulan jaso dira analisi kimikoen emaitzak eta hauen batezbesteko ziurgabetasun hedatu erlatiboak[11] (U %). Pasta mota bakoitzerako (PT, PF, AP) errepikakortasuna (RSD %), berriz, 5.3. taulan jaso da. Ziurgabetasuna kalkulatzeko hurbilketa bat egin da, esperimentuko zeramikentzat erabilitako kalibrazio mota Aveiroko zeramikentzat erabilitako berdina izan baita: horrela, Aveiroko 25 zeramikentzat kalkulatutako ziurgabetasuna esperimentuko laginetara estrapolatu da (ikus. 6. kapitulua, 6.2. atala). Bestalde, errepikakortasuna ekuazio hau erabiliz kalkulatu da:

$$\text{RSD}(\%) = \frac{100s}{\bar{x}} \qquad Eq.\,5.1.$$

s hiru probeten (850 °C, itsasoko ura, 18 hilabete) emaitzen desbideratze estandarra da pasta mota bakoitzerako (PF, PT, AP); x, berriz, emaitzen batezbestekoa da. Kasu gehienetan errepikakortasuna ona izan da (% 20tik beherako balioekin). Hala ere, kasu batzuetan, konposatu baten errepikakortasuna ona izan da pasta mota batentzat, baina okerragoa beste pasta batentzat, adibidez, CaO, Cu eta Pb-rentzat.

[11] Ingeleraz, *Average Expanded Uncertainty.*

% 20-tik gorako errepikakortasuna duten osagaiak hauek izan dira: CaO (AP), Co (PF), Cu (PF, AP), Ni (PT, PF, AP), P_2O_5 (PT), Pb (PF) eta Zn (PT, PF, AP). Zenbaki hauek pentsaraz lezakete zeramika bakoitzean gertatu diren jalkitze-osteko alterazioak zenbait faktoreren mende zeudela, hala nola zeramikak ingurunean zuen kokapenaren eta ingurunearen baldintzen mende. Halaber, iradoki lezake errepikakortasun okerrena duten konposatuek joera handiagoa dutela jalkitze-giro batean eraldaketak jasateko.

5.2. taula. 69 laginen konposizio kimikoa. Laginak; taldea= itsasoko uretan edo iturriko uretan murgildua izan den; tenperatura= erreketa-tenperatura; periodoa= 3, 10 edo 18 hilabete; pieza= probeta edo kontrol-pieza; U (%)=batezbesteko ziurgabetasun hedatu erlatiboa, GUM erabiliz kalkulatua, k=2 izanik (ikus 4. kapitulua, 4.4.3. atala)

Laginak	Taldea	Tenperatura	Periodoa	Pieza	Al_2O_3	Ba	CaO	Ce	Co	Cr	Cs	Cu	Dy	Er	Eu	Fe_2O_3	Gd	Hf	Ho	K_2O	La	Lu
PT001	Itsasoko a	850	3	Probeta	15.4	3.79E+03	12.2	73.3	23.0	59.6	6.86	47.4	4.27	2.06	1.66	3.52	5.23	3.54	0.594	2.51	37.3	0.373
PT002	Itsasoko a	850	10	Probeta	15.2	3.46E+03	12.1	70.5	14.0	56.8	7.62	40.4	4.21	2.11	1.58	3.44	5.11	3.41	0.575	2.42	35.6	0.367
PT003	Itsasoko a	850	18	Probeta	14.9	3.29E+03	11.6	72.0	17.7	56.0	6.51	49.5	4.02	2.02	1.61	3.49	5.26	3.20	0.571	2.52	35.8	0.374
PT004	Itsasoko a	850	18	Probeta	15.2	3.51E+03	11.9	69.8	19.7	62.9	7.04	45.1	3.91	2.02	1.57	3.49	5.12	3.49	0.544	2.38	34.8	0.358
PT005	Itsasoko a	850	18	Probeta	15.3	3.32E+03	12.8	69.4	14.4	60.7	6.07	49.2	3.81	2.00	1.52	3.58	4.94	2.98	0.547	2.36	34.5	0.346
PT006	Iturriko a	850	3	Probeta	14.3	2.99E+03	12.5	64.5	16.3	61.1	7.52	158	3.61	2.00	1.42	3.41	4.69	2.72	0.543	2.52	32.2	0.345
PT007	Iturriko a	850	10	Probeta	15.0	3.30E+03	11.7	68.7	37.3	64.0	6.99	36.3	3.62	2.03	1.56	3.47	4.97	2.77	0.543	2.53	34.4	0.350
PT008	Iturriko a	850	18	Probeta	15.0	3.24E+03	12.1	69.2	15.4	61.0	7.89	37.5	3.87	2.09	1.52	3.53	4.91	2.93	0.572	2.48	34.6	0.352
PT009	Itsasoko a	950	3	Probeta	14.9	3.36E+03	12.1	69.6	24.1	76.8	6.49	37.4	3.93	2.09	1.55	3.54	5.07	3.11	0.550	2.46	34.7	0.356
PT010	Itsasoko a	950	10	Probeta	15.0	3.46E+03	11.5	68.5	18.8	53.2	7.20	35.7	3.75	2.01	1.57	3.41	4.97	3.11	0.564	2.29	33.9	0.367
PT011	Itsasoko a	950	18	Probeta	14.9	3.47E+03	11.7	68.5	17.2	53.9	6.35	39.6	3.82	1.96	1.57	3.46	5.05	3.22	0.554	2.28	34.1	0.346
PT012	Iturriko a	950	3	Probeta	14.9	3.57E+03	13.1	68.0	26.3	78.2	8.14	36.2	3.79	2.06	1.63	3.55	5.16	3.13	0.560	2.55	33.8	0.370
PT013	Iturriko a	950	10	Probeta	15.0	3.44E+03	12.8	69.3	53.2	70.4	6.72	110	3.86	1.98	1.58	3.61	5.06	3.03	0.559	2.45	34.6	0.357
PT014	Iturriko a	950	18	Probeta	15.0	3.63E+03	13.0	70.5	17.8	71.6	8.20	55.9	3.86	1.96	1.64	3.44	5.31	3.60	0.548	2.47	35.0	0.353
PT015	Itsasoko a	1100	3	Probeta	14.8	3.61E+03	12.0	68.7	26.4	60.2	7.92	28.1	3.75	1.93	1.57	3.47	5.05	3.02	0.521	2.37	34.0	0.350
PT016	Itsasoko a	1100	10	Probeta	15.0	3.63E+03	11.3	70.4	25.7	56.2	9.38	29.8	3.97	2.07	1.69	3.47	5.23	3.20	0.557	2.34	34.8	0.348

Laginak	Taldea	Tenperatura	Perioda	Pieza	Al_2O_3	Ba	CaO	Ce	Co	Cr	Cs	Cu	Dy	Er	Eu	Fe_2O_3	Gd	Hf	Ho	K_2O	La	Lu
PT017	Itsasoko a	1100	18	Probeta	14.6	3.63E+03	11.2	69.4	25.4	67.9	8.47	23.2	3.75	1.90	1.56	3.32	5.27	3.26	0.521	2.11	34.6	0.319
PT018	Iturriko a	1100	3	Probeta	15.1	3.74E+03	14.0	70.7	24.2	58.9	9.76	21.2	3.95	1.99	1.66	3.43	5.44	3.37	0.538	2.75	35.1	0.349
PT019	Iturriko a	1100	10	Probeta	15.2	3.95E+03	13.8	71.9	38.3	84.8	8.76	44.6	4.06	2.10	1.65	3.46	5.47	3.45	0.566	2.77	36.1	0.373
PT020	Iturriko a	1100	18	Probeta	15.1	3.58E+03	12.2	69.9	33.1	79.9	9.63	24.5	3.92	1.98	1.61	3.48	5.23	3.11	0.551	2.61	34.7	0.365
PT-01	Kontrol a	850	-	Kontrol-pieza	15.1	3.59E+03	12.6	68.5	19.5	61.7	7.88	19.7	4.08	2.06	1.56	3.48	4.97	2.24	0.599	2.59	33.6	0.335
PT-05	Kontrol a	950	-	Kontrol-pieza	14.2	3.62E+03	13.2	67.0	29.8	60.3	7.97	39.3	3.98	2.12	1.52	3.40	4.97	2.27	0.581	2.57	33.1	0.335
PT-09	Kontrol a	1100	-	Kontrol-pieza	15.8	3.92E+03	15.4	75.1	28.1	70.3	9.65	68.1	4.26	2.33	1.67	3.89	5.62	2.41	0.637	2.97	37.1	0.369
PF001	Itsasoko a	850	3	Probeta	16.6	9.06E+02	3.85	73.8	20.8	68.0	11.4	47.3	4.01	2.05	1.32	6.14	5.14	3.02	0.568	3.30	36.3	0.355
PF002	Itsasoko a	850	10	Probeta	17.8	9.66E+02	3.91	78.1	22.8	73.1	12.5	50.7	4.20	2.17	1.37	6.65	5.58	3.06	0.591	3.48	38.6	0.377
PF003	Itsasoko a	850	18	Probeta	16.9	9.22E+02	3.74	74.3	27.8	70.9	11.6	44.5	4.13	2.06	1.31	6.42	5.40	2.93	0.583	3.41	37.1	0.379
PF004	Itsasoko a	850	18	Probeta	17.3	9.33E+02	4.24	76.1	20.1	71.7	10.4	843	4.19	2.14	1.32	6.58	5.33	2.62	0.599	3.39	37.8	0.380
PF005	Itsasoko a	850	18	Probeta	17.3	9.20E+02	4.51	75.2	18.6	74.7	9.14	49.9	4.03	2.12	1.25	6.32	5.27	2.53	0.597	3.18	37.5	0.381
PF006	Iturriko a	850	3	Probeta	17.6	9.50E+02	4.68	77.4	25.0	79.8	9.48	53.4	4.34	2.16	1.33	6.54	5.43	2.75	0.605	3.32	39.2	0.392
PF007	Iturriko a	850	10	Probeta	17.6	9.43E+02	4.29	77.5	26.2	74.2	10.7	61.8	4.22	2.17	1.31	6.57	5.38	2.64	0.590	3.36	38.7	0.384
PF008	Iturriko a	850	18	Probeta	17.6	9.59E+02	4.23	77.8	21.9	87.9	9.79	68.3	4.33	2.15	1.34	6.49	5.57	3.15	0.620	3.32	39.3	0.411
PF009	Itsasoko a	950	3	Probeta	17.7	9.32E+02	3.51	76.9	22.3	73.3	11.1	60.6	4.22	2.20	1.34	6.43	5.31	2.71	0.597	3.25	38.7	0.418
PF010	Itsasoko a	950	10	Probeta	16.0	8.71E+02	3.16	71.0	26.4	69.0	9.75	48.7	3.98	2.06	1.23	5.96	5.11	2.50	0.571	3.07	36.1	0.391
PF011	Itsasoko a	950	18	Probeta	17.5	9.31E+02	3.83	77.0	22.6	70.4	11.8	55.9	4.20	2.23	1.34	6.47	5.39	2.47	0.589	3.28	38.9	0.414
PF012	Iturriko a	950	3	Probeta	16.9	8.93E+02	3.50	73.7	34.4	71.2	9.66	39.7	4.06	2.23	1.30	6.41	5.30	2.59	0.579	3.20	36.7	0.389
PF013	Iturriko a	950	10	Probeta	17.7	9.35E+02	3.70	76.2	29.6	89.9	12.1	49.9	4.16	2.26	1.40	6.55	5.44	2.97	0.597	3.44	38.3	0.377

Laginak	Taldea	Tenperatura	Perioda	Pieza	Al_2O_3	Ba	CaO	Ce	Co	Cr	Cs	Cu	Dy	Er	Eu	Fe_2O_3	Gd	Hf	Ho	K_2O	La	Lu
PF014	Iturrikoa	950	18	Probeta	16.5	8.74E+02	3.66	69.5	21.1	71.1	10.4	57.5	4.00	2.08	1.27	6.12	5.07	2.91	0.547	3.32	34.7	0.369
PF015	Itsasoko a	1100	3	Probeta	17.3	9.02E+02	4.65	75.2	84.5	77.6	12.0	64.2	4.18	2.24	1.38	6.55	5.36	2.96	0.567	3.42	37.4	0.392
PF016	Itsasoko a	1100	10	Probeta	16.0	8.37E+02	4.15	68.3	47.4	68.5	10.7	53.7	3.84	2.06	1.21	6.14	5.01	2.85	0.549	3.31	33.4	0.342
PF017	Itsasoko a	1100	18	Probeta	15.6	8.52E+02	3.63	68.1	31.9	65.0	11.3	55.4	3.88	2.02	1.22	5.77	4.93	2.33	0.550	3.24	34.1	0.351
PF018	Iturrikoa	1100	3	Probeta	17.5	9.21E+02	4.80	76.1	42.7	83.4	11.6	55.0	4.27	2.25	1.40	6.99	5.60	2.96	0.601	3.67	37.9	0.406
PF019	Iturrikoa	1100	10	Probeta	17.4	9.25E+02	5.40	75.2	80.1	75.3	13.0	47.8	4.23	2.22	1.36	6.68	5.58	3.02	0.625	3.54	37.4	0.392
PF020	Iturrikoa	1100	18	Probeta	17.7	9.34E+02	4.84	76.0	35.9	74.9	13.1	52.1	4.27	2.26	1.39	6.61	5.62	2.95	0.639	3.51	38.1	0.394
PF-01	Kontrola	850	-	Kontrol-pieza	15.9	8.89E+02	4.45	71.1	25.1	72.1	13.0	66.2	4.07	2.05	1.22	6.16	5.21	2.21	0.588	3.49	35.0	0.346
PF-05	Kontrola	950	-	Kontrol-pieza	16.7	8.99E+02	4.64	73.5	25.7	74.7	12.1	57.9	4.12	2.05	1.32	6.12	5.38	2.35	0.597	3.33	36.0	0.351
PF-09	Kontrola	1100	-	Kontrol-pieza	15.7	8.52E+02	5.18	70.2	32.8	68.9	12.6	72.7	3.86	1.97	1.26	5.70	5.20	2.10	0.560	3.52	34.1	0.333
AP001	Itsasoko a	850	3	Probeta	22.3	1.70E+03	0.947	125	43.5	75.7	16.9	18.3	15.0	7.86	4.15	10.7	18.0	3.22	2.34	3.55	64.1	1.22
AP002	Itsasoko a	850	10	Probeta	22.0	1.72E+03	1.48	125	41.3	78.2	18.8	20.1	15.0	7.45	4.09	10.7	18.0	3.19	2.35	3.61	64.5	1.23
AP003	Itsasoko a	850	18	Probeta	21.1	1.63E+03	0.874	120	34.9	72.0	17.4	13.2	14.2	7.35	3.93	9.83	17.6	2.55	2.19	3.42	61.7	1.15
AP004	Itsasoko a	850	18	Probeta	19.6	1.55E+03	1.18	112	29.6	68.4	18.6	28.6	13.2	6.82	3.61	9.36	16.2	2.56	2.02	3.48	57.4	1.02
AP005	Itsasoko a	850	18	Probeta	20.9	1.59E+03	1.40	119	29.5	77.8	17.6	13.6	14.0	7.20	3.87	9.55	16.9	2.55	2.12	3.38	61.0	1.06
AP006	Iturrikoa	850	3	Probeta	20.5	1.62E+03	1.69	115	29.3	102	19.9	17.3	13.7	6.91	3.69	9.55	16.8	2.45	2.03	3.54	59.5	1.00
AP007	Iturrikoa	850	10	Probeta	21.5	1.65E+03	1.44	120	30.5	89.8	18.8	13.7	13.9	7.20	3.77	9.75	17.5	2.55	2.08	3.49	61.2	1.02
AP008	Iturrikoa	850	18	Probeta	20.4	1.61E+03	1.56	115	28.4	73.9	20.3	12.7	13.6	6.99	3.64	9.65	16.6	2.32	2.00	3.58	59.5	0.971
AP009	Itsasoko a	950	3	Probeta	20.5	1.56E+03	0.612	115	49.1	89.0	15.8	18.2	13.7	6.92	3.65	9.41	16.6	2.07	1.98	3.19	59.2	0.989
AP010	Itsasoko a	950	10	Probeta	22.8	1.73E+03	1.30	127	55.8	86.8	15.2	9.71	15.0	7.75	4.19	10.6	18.1	2.47	2.20	3.25	65.4	1.09

Laginak	Taldea	Tenperatura	Perioda	Pieza	Al_2O_3	Ba	CaO	Ce	Co	Cr	Cs	Cu	Dy	Er	Eu	Fe_2O_3	Gd	Hf	Ho	K_2O	La	Lu
AP011	Itsasoko a	950	18	Probeta	20.5	1.60E+03	1.48	116	37.5	87.8	13.0	15.7	13.7	7.03	3.84	9.80	16.8	2.25	2.05	3.16	59.9	1.04
AP012	Iturriko a	950	3	Probeta	22.2	1.73E+03	1.23	125	43.6	83.2	15.9	20.3	14.9	7.61	4.20	10.3	17.8	2.42	2.19	3.39	64.3	1.15
AP013	Iturriko a	950	10	Probeta	22.0	1.67E+03	2.53	123	46.6	81.8	13.9	23.3	14.5	7.46	4.09	10.1	17.7	2.46	2.13	3.28	62.4	1.14
AP014	Iturriko a	950	18	Probeta	22.3	1.68E+03	1.17	124	36.1	77.7	16.3	12.2	14.6	7.53	4.35	10.2	17.8	2.49	2.22	3.33	63.3	1.24
AP015	Itsasoko a	1100	3	Probeta	20.6	1.64E+03	1.44	119	60.4	92.3	14.0	3.45	13.9	7.05	4.09	9.58	16.6	2.15	2.07	3.21	60.5	1.16
AP016	Itsasoko a	1100	10	Probeta	22.1	1.71E+03	1.07	128	79.5	90.5	17.1	18.6	14.8	7.66	4.29	10.4	17.8	2.56	2.30	3.44	64.6	1.19
AP017	Itsasoko a	1100	18	Probeta	20.5	1.59E+03	0.461	117	68.8	84.9	14.8	16.6	13.6	7.09	3.97	10.1	16.1	2.29	2.12	3.35	58.9	1.10
AP018	Iturriko a	1100	3	Probeta	21.7	1.64E+03	2.19	124	57.1	83.2	16.8	19.0	14.5	7.72	4.25	10.5	17.1	2.70	2.25	3.44	62.0	1.14
AP019	Iturriko a	1100	10	Probeta	21.9	1.66E+03	0.949	125	60.4	82.4	15.9	19.7	14.5	7.74	4.19	10.4	16.7	2.72	2.26	3.41	62.9	1.12
AP020	Iturriko a	1100	18	Probeta	14.7	1.18E+03	0.460	85.0	33.8	52.2	15.5	0.264	10.1	5.35	2.88	7.17	11.8	1.92	1.57	2.96	42.7	0.745
AP-01	Kontrol a	850	-	Kontrol-pieza	19.8	1.59E+03	1.01	116	41.2	77.8	16.6	26.0	13.4	6.83	3.74	9.64	16.4	2.10	1.97	3.44	57.8	0.991
AP-05	Kontrol a	950	-	Kontrol-pieza	19.0	1.48E+03	0.859	108	43.8	66.5	16.9	6.33	12.7	6.52	3.56	9.13	15.4	2.10	1.86	3.34	54.1	0.958
AP-09	Kontrol a	1100	-	Kontrol-pieza	19.9	1.55E+03	0.972	115	66.2	76.1	15.8	15.8	13.5	6.96	3.71	9.83	16.6	2.19	1.97	3.39	57.6	0.993
U (%)					6	5	84	6	26	38	4	24	13	22	11	8	10	6	20	4	5	17

5.2. taula *(jarraipena).* 69 laginen oinarrizko konposizioa. T = taldea; T °C = erreketa-tenperatura; S = itsasoko ura; T = iturriko ura; C = kontrola; L = baxua (850 °C); M = ertaina (950 °C); H = altua (1100 °C)

Laginak	T	T ºC	MgO	MnO	Na_2O	Nb	Nd	Ni	P_2O_5	Pb	Pr	Rb	SiO_2	Sm	Sr	Ta	Tb	Th	TiO_2	Tm	U	V	Yb	Zn	Zr
PT001	S	L	2.08	0.0420	0.488	14.9	34.2	28.3	0.0913	20.0	8.97	121	46.4	6.45	242	1.52	0.767	11.6	0.667	0.365	3.95	96.9	2.09	15.8	165
PT002	S	L	2.11	0.0412	0.491	14.3	33.2	22.7	0.0857	29.9	8.73	119	46.6	6.44	230	1.46	0.775	11.7	0.661	0.394	3.82	96.6	2.19	14.0	151
PT003	S	L	2.49	0.0507	0.517	14.0	34.0	35.1	0.107	21.2	8.92	117	47.0	6.53	231	1.46	0.754	11.7	0.653	0.390	3.80	99.6	2.13	24.5	152
PT004	S	L	2.10	0.0422	0.552	12.1	33.5	105	0.0705	21.1	8.71	112	45.9	6.18	226	1.40	0.745	11.3	0.659	0.382	3.80	97.7	1.99	16.1	155
PT005	S	L	2.15	0.0439	0.521	14.2	33.4	26.6	0.0689	28.9	8.74	110	48.2	6.29	226	1.44	0.751	10.8	0.667	0.382	3.68	97.5	2.02	17.9	139
PT006	T	L	1.89	0.0422	0.366	13.4	31.0	207	0.0666	24.0	8.17	119	45.2	5.72	216	1.32	0.683	10.0	0.630	0.393	3.46	99.0	2.01	26.8	126
PT007	T	L	1.86	0.0422	0.249	12.9	31.9	29.1	0.0714	23.9	8.61	120	45.7	6.03	222	1.41	0.715	10.5	0.656	0.382	3.69	103	1.95	14.1	128
PT008	T	L	1.88	0.0423	0.317	12.7	32.3	26.0	0.0750	24.4	8.68	122	46.4	6.21	224	1.41	0.735	10.9	0.659	0.406	3.69	101	2.04	21.6	135
PT009	S	M	2.10	0.0421	0.494	10.6	32.5	29.1	0.0612	21.2	8.57	112	44.9	5.98	226	1.31	0.754	11.4	0.666	0.390	3.62	99.9	1.99	15.3	137
PT010	S	M	2.12	0.0403	0.514	11.2	31.9	24.7	0.0721	23.5	8.57	116	43.7	5.91	230	1.33	0.728	11.1	0.655	0.401	3.55	92.6	2.01	12.4	142
PT011	S	M	2.10	0.0401	0.482	10.5	32.3	25.1	0.0559	21.9	8.50	109	44.3	5.96	228	1.31	0.703	11.3	0.666	0.394	3.50	93.9	2.03	15.5	144
PT012	T	M	1.89	0.0451	0.241	10.3	31.8	23.8	0.0648	26.2	8.38	122	45.0	5.71	227	1.35	0.758	11.2	0.659	0.413	3.53	97.3	1.90	13.4	138
PT013	T	M	1.94	0.0433	0.338	10.4	32.5	28.2	0.0773	24.5	8.46	114	44.3	6.09	234	1.33	0.764	11.2	0.660	0.412	3.66	100	1.94	1.29E+03	144
PT014	T	M	1.92	0.0407	0.505	10.5	33.0	29.1	0.0799	88.7	8.75	123	44.1	6.17	244	1.38	0.742	11.5	0.662	0.425	3.63	97.4	1.91	30.2	156
PT015	S	H	2.49	0.0440	0.688	10.1	31.7	20.0	0.0754	32.0	8.48	123	43.8	6.09	223	1.30	0.724	11.3	0.656	0.399	3.53	91.0	1.94	3.10	144
PT016	S	H	2.93	0.0411	0.772	9.90	32.3	26.5	0.0765	23.0	8.76	133	42.8	6.58	231	1.38	0.793	11.7	0.644	0.429	3.71	93.3	2.06	2.87	151
PT017	S	H	2.73	0.0396	0.799	9.82	31.4	23.3	0.0823	23.1	8.39	127	41.6	6.35	229	1.33	0.758	11.6	0.630	0.406	3.63	92.5	1.98	4.41	148
PT018	T	H	1.87	0.0415	0.323	10.2	32.4	21.2	0.0964	24.8	8.54	152	42.6	6.53	246	1.39	0.812	12.0	0.643	0.410	3.80	80.6	2.02	3.12	155
PT019	T	H	1.95	0.0437	0.713	9.89	33.3	28.4	0.0948	88.9	8.88	154	41.4	6.90	265	1.35	0.836	11.9	0.662	0.425	3.89	86.8	2.14	36.1	155
PT020	T	H	1.94	0.0428	0.308	9.81	32.4	20.7	0.0652	23.0	8.52	161	44.3	6.47	235	1.35	0.763	11.6	0.665	0.417	3.63	89.6	2.07	1.38	147
PT-01	C	L	1.91	0.0418	0.261	8.32	31.5	22.6	0.0744	23.8	8.29	129	47.7	5.97	230	1.40	0.747	10.8	0.654	0.374	3.57	94.0	2.06	7.20	114
PT-05	C	M	1.82	0.0425	0.277	8.14	30.9	44.5	0.0563	22.7	8.02	125	45.8	5.99	218	1.39	0.734	10.8	0.622	0.391	3.46	90.1	2.12	4.87	111

Lagina k	T	T °C	Mg O	MnO	Na_2O	Nb	Nd	Ni	P_2O_5	Pb	Pr	Rb	SiO_2	Sm	Sr	Ta	Tb	Th	TiO_2	Tm	U	V	Yb	Zn	Zr
PT-09	C	H	2.04	0.0456	0.295	8.87	34.1	42.6	0.0430	31.0	9.10	141	53.3	6.75	242	1.55	0.808	12.0	0.716	0.410	3.79	102	2.35	11.1	119
PF001	S	L	3.01	0.101	0.518	10.6	32.5	33.8	0.105	25.6	8.88	144	42.0	6.22	118	1.38	0.780	11.9	0.766	0.407	2.86	110	2.07	4.51	142
PF002	S	L	3.52	0.110	0.554	12.0	34.6	33.6	0.119	21.5	9.54	155	47.1	6.62	125	1.57	0.818	12.9	0.826	0.425	2.98	117	2.29	11.3	149
PF003	S	L	3.12	0.105	0.474	11.1	33.1	30.9	0.116	34.6	8.97	149	44.4	6.70	118	1.41	0.772	12.3	0.788	0.407	2.88	109	2.23	10.2	140
PF004	S	L	3.35	0.108	0.502	11.3	33.1	51.9	0.105	48.8	9.26	141	49.9	6.48	117	1.57	0.775	12.1	0.822	0.415	2.98	115	2.24	43.7	128
PF005	S	L	3.29	0.104	0.529	10.4	33.1	40.9	0.121	20.6	9.01	133	46.8	6.47	119	1.44	0.775	11.9	0.809	0.412	2.89	112	2.19	5.62	126
PF006	T	L	2.80	0.107	0.213	11.4	34.9	40.9	0.113	26.9	9.56	137	49.4	6.79	131	1.57	0.772	12.6	0.836	0.405	2.99	112	2.25	4.16	139
PF007	T	L	2.76	0.107	0.211	11.4	34.3	37.0	0.107	23.4	9.46	144	48.8	6.79	129	1.55	0.780	12.4	0.832	0.416	2.94	110	2.21	7.00	134
PF008	T	L	2.82	0.108	0.412	11.8	34.8	40.8	0.116	105	9.53	136	49.3	6.84	132	1.55	0.776	12.6	0.834	0.400	3.02	109	2.29	31.2	143
PF009	S	M	3.21	0.106	0.525	11.3	34.9	34.4	0.112	22.6	9.49	143	48.8	6.64	123	1.52	0.774	12.5	0.812	0.416	3.00	112	2.17	1.98	135
PF010	S	M	3.24	0.098	0.526	10.3	32.4	36.3	0.105	19.9	8.85	135	42.6	6.29	112	1.29	0.698	11.4	0.760	0.390	2.75	105	2.12	2.49	122
PF011	S	M	3.31	0.106	0.558	11.0	34.8	36.4	0.127	21.0	9.33	148	48.6	6.62	124	1.45	0.767	12.3	0.807	0.404	3.09	111	2.19	6.03	128
PF012	T	M	2.72	0.105	0.223	11.0	33.1	29.7	0.114	46.8	8.99	134	47.3	6.44	124	1.41	0.749	11.8	0.798	0.394	2.86	100	2.11	5.78	128
PF013	T	M	2.80	0.107	0.274	11.6	34.6	32.1	0.133	26.8	9.10	150	48.4	6.42	130	1.41	0.758	12.6	0.824	0.410	3.02	105	2.17	27.2	138
PF014	T	M	2.65	0.100	0.221	10.3	31.8	34.1	0.128	20.9	8.36	141	42.3	6.11	122	1.24	0.721	11.5	0.758	0.379	2.74	97.7	1.95	3.98	136
PF015	S	H	2.95	0.106	0.487	11.8	33.6	36.1	0.123	24.4	8.94	151	48.0	6.32	132	1.55	0.790	12.4	0.831	0.414	2.94	117	2.17	5.56	140
PF016	S	H	2.85	0.101	0.466	9.93	30.6	30.5	0.127	20.1	7.95	142	41.3	5.90	123	1.23	0.716	11.1	0.775	0.373	2.66	109	1.96	7.75	135
PF017	S	H	2.77	0.0988	0.464	8.14	30.3	33.2	0.129	22.0	8.06	145	38.0	5.79	120	1.16	0.718	10.6	0.754	0.366	2.66	104	1.98	5.85	116
PF018	T	H	3.01	0.114	0.298	10.5	34.3	36.9	0.110	26.9	8.91	148	49.7	6.65	126	1.44	0.808	12.8	0.899	0.418	2.97	121	2.21	15.0	141
PF019	T	H	2.75	0.107	0.256	10.8	32.9	32.2	0.123	22.7	8.72	157	47.3	6.22	130	1.58	0.807	12.7	0.850	0.427	3.00	111	2.31	3.81	145
PF020	T	H	2.76	0.107	0.278	10.7	34.5	32.6	0.123	21.3	9.04	159	47.7	6.65	131	1.52	0.790	13.1	0.831	0.422	2.98	112	2.26	3.21	145
PF-01	C	L	2.62	0.100	0.256	9.41	30.9	33.4	0.089	22.2	8.28	153	46.9	6.05	117	1.41	0.789	11.2	0.783	0.389	2.72	114	2.20	8.38	111
PF-05	C	M	2.63	0.100	0.221	9.90	31.9	28.9	0.119	20.5	8.62	151	46.7	6.07	121	1.51	0.733	11.7	0.772	0.408	2.85	110	2.18	7.05	118
PF-09	C	H	2.51	0.0956	0.269	9.54	30.1	30.3	0.107	31.4	8.12	153	44.4	6.06	120	1.42	0.719	10.7	0.741	0.389	2.65	105	2.06	9.34	108
AP001	S	L	1.17	0.0654	0.591	14.4	82.8	61.9	0.0548	36.6	18.5	232	45.2	19.1	68.8	2.66	2.80	14.2	0.827	1.44	4.24	117	7.00	6.30	158
AP002	S	L	1.23	0.0659	0.628	14.3	83.8	61.9	0.0327	25.4	18.4	234	45.2	19.1	68.8	2.75	2.82	14.2	0.824	1.40	4.22	116	6.93	5.43	150

Lagina k	T	T °C	Mg O	MnO	Na_2O	Nb	Nd	Ni	P_2O_5	Pb	Pr	Rb	SiO_2	Sm	Sr	Ta	Tb	Th	TiO_2	Tm	U	V	Yb	Zn	Zr
AP003	S	L	1.13	0.0594	0.548	12.4	79.8	58.1	0.0409	22.2	17.7	228	41.8	18.3	64.7	2.52	2.67	13.2	0.785	1.34	4.03	111	6.56	6.69	131
AP004	S	L	1.05	0.0567	0.524	11.8	75.6	618	0.0485	20.9	16.5	229	38.8	17.5	59.2	2.29	2.47	12.1	0.721	1.25	3.78	101	6.12	3.66	123
AP005	S	L	1.09	0.0590	0.613	12.8	80.1	55.7	0.0411	24.2	17.6	229	40.2	18.2	65.3	2.51	2.59	13.0	0.745	1.32	4.06	107	6.38	13.3	130
AP006	T	L	0.992	0.0596	0.221	12.6	78.8	57.8	0.0379	46.1	17.0	234	41.1	17.8	74.5	2.42	2.53	12.4	0.763	1.25	3.99	102	6.19	11.5	121
AP007	T	L	1.02	0.0598	0.225	13.1	79.5	58.0	0.0422	22.0	17.6	226	42.8	18.4	79.0	2.59	2.60	12.7	0.789	1.31	4.05	100	6.55	11.4	127
AP008	T	L	0.99	0.0594	0.226	12.4	78.5	55.9	0.0321	23.2	17.0	225	41.6	17.9	69.7	2.50	2.43	12.0	0.752	1.23	3.92	94.2	6.12	7.91	115
AP009	S	M	1.18	0.0598	0.496	11.6	79.7	57.8	0.0295	31.0	16.9	217	41.2	17.4	66.3	2.44	2.50	11.7	0.752	1.25	3.90	111	6.15	8.89	111
AP010	S	M	1.42	0.0648	0.493	13.5	86.5	61.8	0.0495	22.7	18.8	220	46.6	19.4	72.1	2.79	2.72	13.2	0.826	1.39	4.36	121	6.92	15.4	123
AP011	S	M	1.35	0.0620	0.551	12.3	79.5	62.1	0.0582	27.5	17.0	206	42.5	17.6	71.5	2.41	2.49	11.8	0.764	1.27	3.91	111	6.33	29.5	116
AP012	T	M	1.08	0.0645	0.201	13.1	85.8	90.9	0.0362	23.2	18.4	223	46.7	18.1	74.5	2.69	2.70	12.9	0.835	1.37	4.22	116	6.84	14.1	122
AP013	T	M	1.06	0.0629	0.212	12.9	84.6	68.9	0.0487	20.7	17.8	213	45.2	17.9	77.8	2.58	2.63	12.7	0.809	1.35	4.28	113	6.58	18.2	125
AP014	T	M	1.04	0.0634	0.179	13.0	84.9	62.3	0.0489	24.9	18.1	227	45.1	17.7	74.0	2.54	2.68	12.5	0.802	1.34	4.22	109	6.85	6.50	125
AP015	S	H	1.04	0.0601	0.261	11.4	79.9	59.1	0.0360	25.6	17.3	212	42.7	17.3	68.2	2.53	2.52	12.0	0.780	1.27	4.01	117	6.44	7.21	109
AP016	S	H	1.14	0.0647	0.304	13.1	85.2	64.3	0.0386	23.9	18.7	231	46.5	18.5	73.4	2.69	2.70	13.1	0.835	1.38	4.23	131	7.00	10.7	126
AP017	S	H	1.11	0.0629	0.287	12.4	78.9	63.5	0.0262	21.8	17.2	214	44.9	17.0	66.8	2.46	2.55	12.0	0.792	1.22	3.93	124	6.36	8.39	115
AP018	T	H	1.07	0.0654	0.229	13.6	82.8	68.0	0.0401	27.6	18.1	229	46.6	18.6	75.3	2.62	2.73	13.0	0.818	1.30	4.15	127	6.79	44.2	127
AP019	T	H	1.02	0.0643	0.201	14.1	82.3	64.2	0.0432	26.5	18.4	229	44.7	18.8	74.1	2.55	2.74	13.2	0.785	1.34	4.12	119	7.01	27.3	130
AP020	T	H	0.728	0.0447	0.214	10.1	56.7	42.9	0.0349	16.4	12.5	202	29.6	13.5	50.5	1.57	1.87	8.8	0.544	0.876	2.73	83.3	4.70	3.31	89
AP-01	C	L	0.973	0.0588	0.219	12.3	74.1	62.1	0.0202	34.8	16.4	222	41.8	18.1	66.4	2.46	2.49	11.3	0.741	1.25	3.70	114	6.26	16.6	105
AP-05	C	M	0.898	0.0549	0.170	12.5	69.6	52.6	0.0415	20.8	15.4	222	38.9	16.6	63.9	2.34	2.33	10.7	0.686	1.18	3.50	103	5.84	4.07	104
AP-09	C	H	0.974	0.0594	0.189	13.2	73.7	59.7	0.0263	21.0	16.3	214	41.4	17.7	65.8	2.50	2.52	11.4	0.765	1.30	3.70	116	6.38	5.15	112
U (%)			18	28	34	4	6	82	-	63	5	3	5	6	19	8	8	13	9	22	17	16	19	-	6

5.3. taula. Pasta mota bakoitzaren konposatuen errepikakortasuna (RSD %) (PT, PF, AP)

Konposatuak	RSD (%)		
	PT	PF	AP
Al_2O_3	1.5	1.2	3.9
Ba	3.5	0.8	2.7
CaO	5.0	9.3	23
Ce	2.0	1.2	4.0
Co	15	22	10
Cr	5.9	2.8	6.6
Cs	7.4	12	3.7
Cu	5.2	147	47
Dy	2.8	1.9	3.8
Er	0.43	2.0	3.9
Eu	2.9	2.8	4.5
Fe_2O_3	1.5	2.0	2.5
Gd	3.1	1.2	4.1
Hf	7.9	7.7	0.18
Ho	2.7	1.5	4.0
K_2O	3.6	3.8	1.5
La	2.0	0.92	3.8
Lu	3.9	0.23	6.2
MgO	9.3	3.7	3.7
MnO	9.8	1.7	2.6
Na_2O	3.7	5.4	8.2
Nb	8.7	4.2	4.0
Nd	0.91	0.13	3.2
Ni	77	25	1.3
P_2O_5	26	7.3	10
Pb	19	41	7.5
Pr	1.3	1.7	3.6

Rb	3.2	5.8	0.25
SiO_2	2.5	6.0	3.8
Sm	2.9	1.9	2.4
Sr	1.2	0.77	5.3
Ta	2.0	5.8	5.5
Tb	0.59	0.21	4.0
Th	3.8	1.6	4.6
TiO_2	1.1	2.1	4.4
Tm	1.2	1.0	3.6
U	1.8	1.8	3.9
V	1.2	2.7	5.0
Yb	3.6	1.3	3.4
Zn	23	105	62
Zr	5.8	5.8	3.5

ICP-MS bidez lortutako emaitzen interpretazioak 4. kapituluko 4.5. atalean azaldutako estatistika-prozedurari jarraitu dio. Gainera, zeramika ehotzeko erabili den tungsteno-karburoaren zelda kutsatzaile potentziala denez (ikus. 4. kapituluko 4.4.2. atala), Co eta Ta estatistika-prozeduratik kendu dira. Gainera, Sn, Ni, Cu eta Zn ere kendu dira; lehena, bere balioak kuantifikazio-mugaren azpitik daudelako eta gainerakoak, errepikakortasun txikia dutelako. Errepikakortasun hau ezin izan da inolako aldaketa espezifikorekin erlazionatu, beraz, akats analitikoren bat gertatu dela pentsa daiteke.

5.2. irudian ageri da 69 zeramiken Konposizioaren Aldakortasunaren Matrizea (MCV), konposatu bakoitzak aldakuntza totalari egiten dion ekarpenaren zenbatespena ematen duena (ikus 4. kapitulua, 4.5 atala). 5.2.a irudiak erakusten duenez, CaO izan da 69 zeramika datuen multzoan aldakortasun handiena gehitu duen konposatua, eta hori espero zen buztinak CaO kantitatearen arabera hautatu zirelako. Gainera, irudiak erakusten du Sr, P_2O_5 eta Ba aldagaiek aldakortasun handia gehitzen dutela. Bestalde, 5.2.b,c irudietan 23 PT eta PF laginen (hogei probeta eta hiru kontrol-pieza) Konposizioaren Aldakortasunaren Matrizea ageri da. Irudi hauek erakusten dute aldakortasun handiena gehitzen duten konposatuak

Pb, Na_2O, P_2O_5 eta Nb izan direla. Gainera, 5.2.d irudian 23 AP laginen MCV ageri da, eta, kasu honetan, Na_2O, CaO, P_2O_5 eta Pb izan dira aldakortasun handiena gehitu duten konposatuak. Konposatu hauen aldakortasunaren azalpena beherago ematen da.

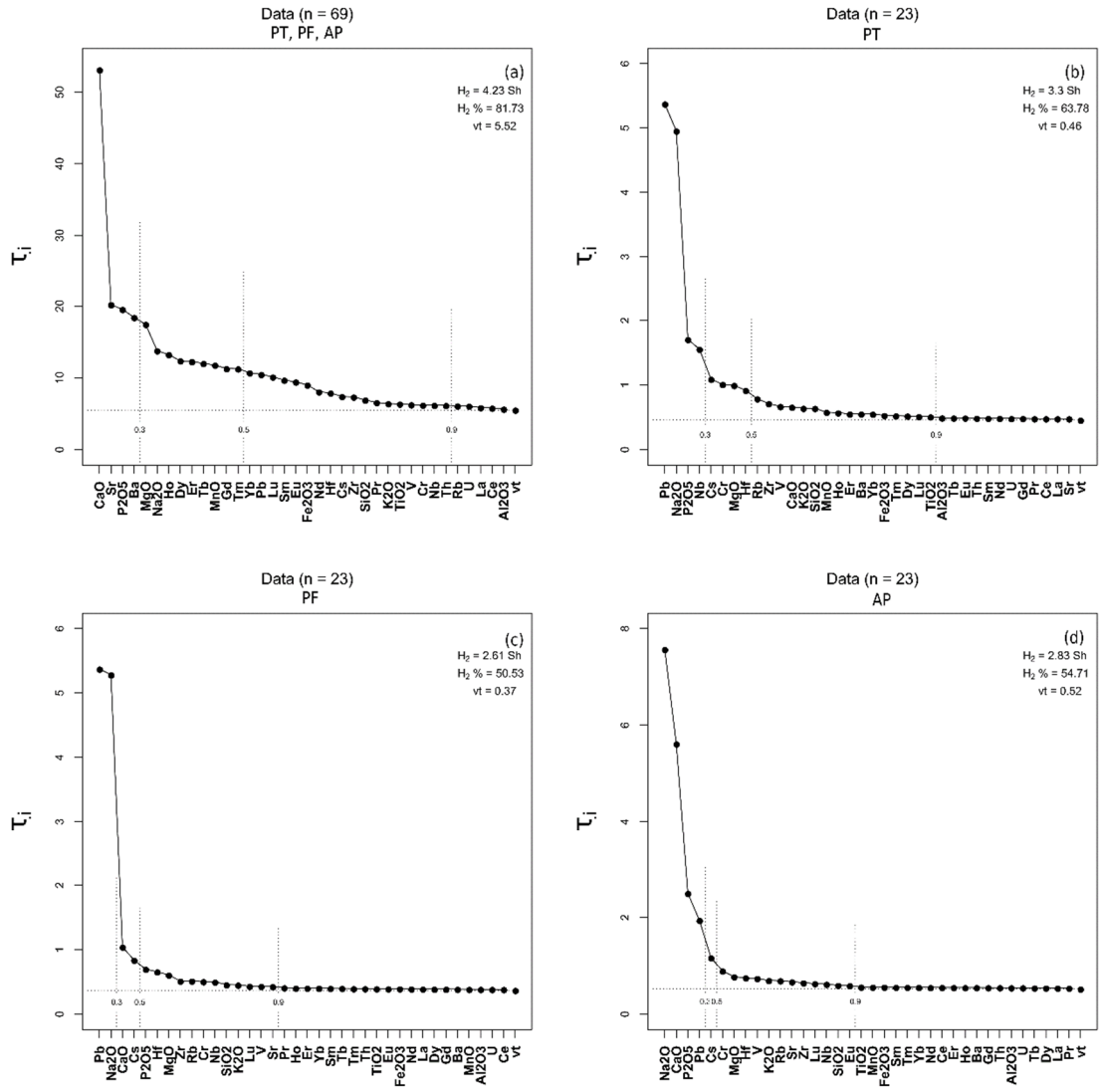

5.2. irudia. **(a)** ICP-MS bidez aztertutako 69 laginen Konposizioaren Aldakortasunaren Matrizearen uniformetasunaren irudikapen grafikoa; **(b)** Aztertutako 23 PT laginen MCV-ren uniformetasunaren adierazpen grafikoa; **(c)** Aztertutako 23 PF laginen MCV-ren uniformetasunaren adierazpen grafikoa; **(d)** Aztertutako 23 AP laginen MCV-ren uniformetasunaren adierazpen grafikoa. Co, Ta, Sn, Cu, Zn eta Ni kendu egin dira grafiko guztietatik. (y ardatza (τ.i) = elementu bakoitzak datu-multzo osoari egiten dion ekarpen indibiduala, handienetik txikienera; vt = aldakortasun totala; H_2 = informazioaren entropia; H_2% = informazioaren entropiaren ehunekoa, ahal den gehienekoari dagokionez; n = lagin-kopurua)

Gainera, 5.3. irudian lau PCA (Osagai Nagusien Analisia) ageri dira (ikus 4. kapitulua, 4.5. atala), L, M eta H bezala etiketatutako laginekin. L horrek esan nahi du lagin horiek tenperatura baxuetan erre zirela (850 °C), M-k tenperatura ertainetan (950 °C) eta H-k tenperatura altuetan (1100 °C). 5.3.a irudian 69 laginen PCA ageri da eta bertan hiru pastak nabarmen bereizten dira. Alde batetik, PT kontrol-laginek gainerako laginek baino CaO eduki handiagoa dute (% 14 inguru, 5.2. taulan ageri den bezala); beraz, PT laginak horrela orientatzea espero zen. Gainera, PT laginek Sr, Ba eta Na_2O gehiago dutela dirudi. Gertaera horiek batez ere lehengaien izaerari lotuta egon arren, jalkitzeak zeramikaren kontzentrazio elementalari ere eragiten dio. Hala, zeramika sodioz aberastu daiteke, elementu hori lurreko nahiz itsasoko inguruneetan dagoelako (Maritan, 2020) edota analtzimaren eraketaren eta halita hauspeatzearen ondorioz (Buxeda i Garrigós et al., 2002a; Secco et al., 2011). Gainera, gainazalak barioa eta estrontzioa ere xurga ditzake, edo barioa barita ($BaSO_4$) eta estrontzioa karbonato, sulfato, borato, fosfato edo haluro gisa hauspeatu daitezke (Maritan, 2020). PF laginei dagokienez, hauek gainerako laginek baino MgO, MnO eta P_2O_5 gehiago dute; AP laginek, berriz, Cs, Rb, Fe_2O_3 eta traza elementu gehiago dituzte, beren pasta mikatsuarekin erlazionatzen direnak. Ohikoa da itsas inguruneetan lurperatutako zeramikak magnesioan aberastea (Lemoine et al., 1981; Maritan, 2020). Manganesoa lurperatutako zeramikan ere metatzen da, eta oxido gisa hauspeatzeko joera du (Maritan, 2020). Hauez gain, fosforoa eta kobrea oro har identifikatzen dira lurpean nahiz urpean aurkitzen diren zeramiketan, sedimentuen, zirkulazioan dauden uren eta lur horietan gizakiak izan duen eraginaren ondorioz (Buxeda i Garrigós, 1999; Buxeda i Garrigós and Kilikoglou, 2003; Freestone et al., 1985; Lemoine eta Picon, 1982; Maritan eta Mazzoli, 2004; Molera et al., 1993; Pradell et al., 1996). Bestalde, 5.3.b irudiak PT laginen PCA erakusten du, eta, horretarako, Pb ez da kontuan izan, ez baitago arrazoi berezirik 5.2.b,c irudietan berunak erakusten duen aldakortasuna justifikatzen duenik. 5.3.b irudiko PCA-n, tenperatura altuetan (1100 °C) erretako itsasoko hiru lagin eta iturriko bat izan dira Na_2O gehien duten laginak. Horrez gain, Nb gehien erakusten duten laginak tenperatura baxuenean erretako laginak dira, eta hain bitrifikatuak ez dauden lagin horiek Nb gehiago xurgatzen dutela iradokitzen dute. Gainera, kontrol-piezak iturriko laginetatik gertuago daude itsasoko laginetatik baino, eta horrek adierazten du aldaketa gehiago gertatu direla itsasoko laginetan. 5.3.c,d irudiek PF eta AP laginen PCA-k erakusten dituzte (Pb ez da 5.3.c irudian erabili). Bi PCA-tan iturriko laginek CaO gehiago dutela dirudi, eta PF-ren kasuan, CaO eduki handiagoa duten laginak tenperatura altuetan erreak

izan ziren. Eztabaida sakonagoa XRD eta SEM–EDS analisiak azaltzen direnean emango da (hurrengo lerroetan).

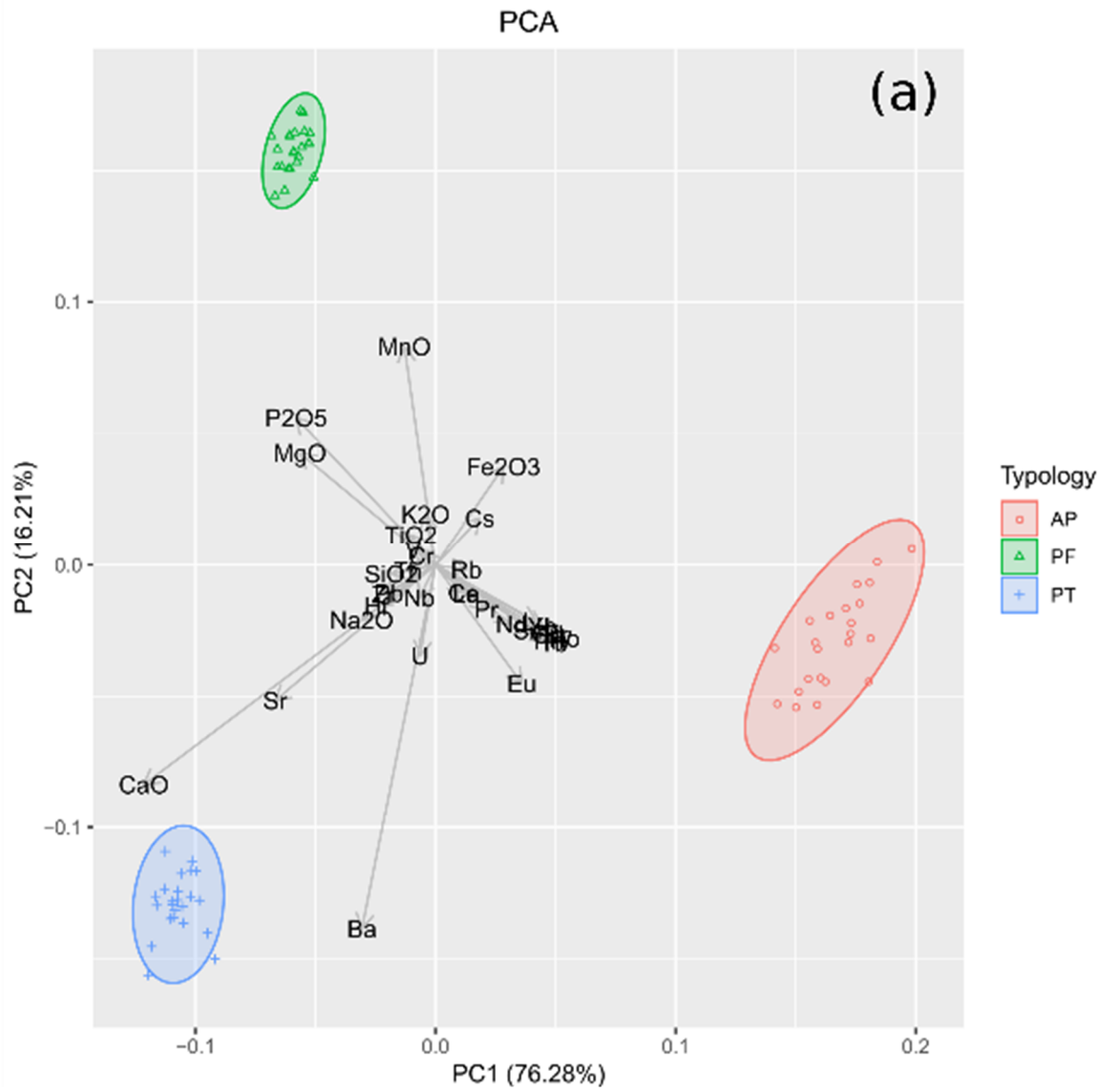

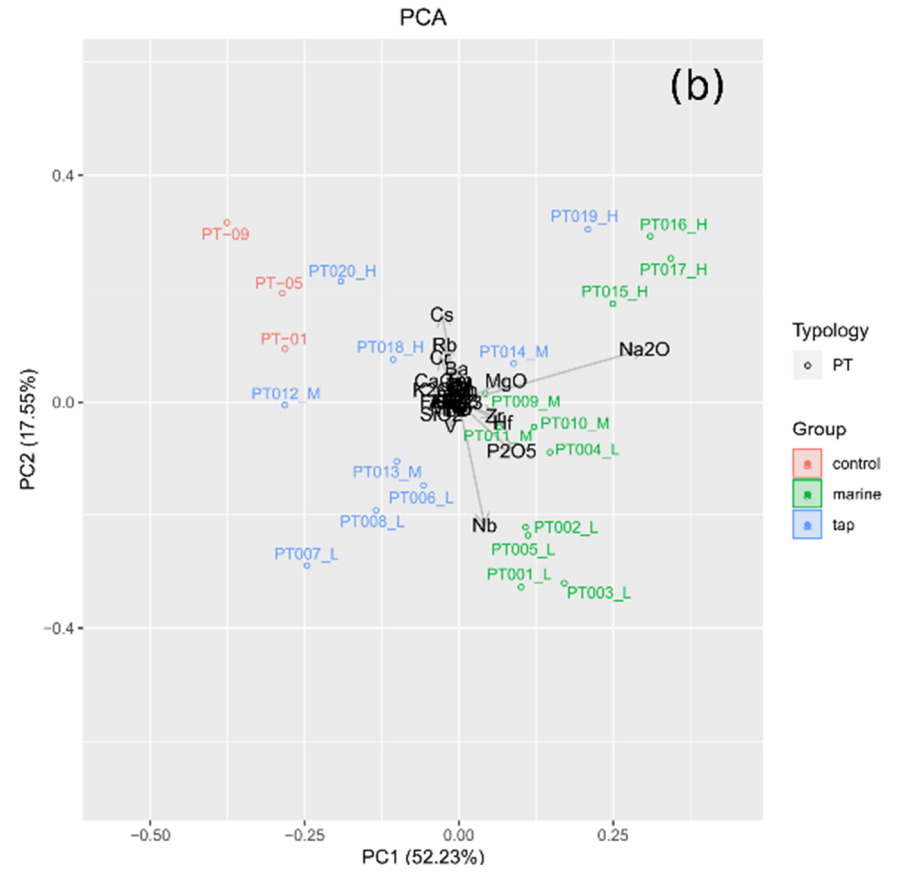
PCA
(b)
PC2 (17.55%)
PC1 (52.23%)
0.4
0.0
−0.4
−0.50
−0.25
0.00
0.25
PT-09
PT-05
PT-01
PT020_H
PT019_H
PT016_H
PT017_H
PT015_H
PT018_H
PT014_M
PT012_M
PT009_M
PT010_M
PT011_M
PT004_L
PT013_M
PT006_L
PT008_L
PT002_L
PT005_L
PT007_L
PT001_L
PT003_L
Cs
Rb
Ba
MgO
Na2O
P2O5
Nb
Typology
PT
Group
control
marine
tap

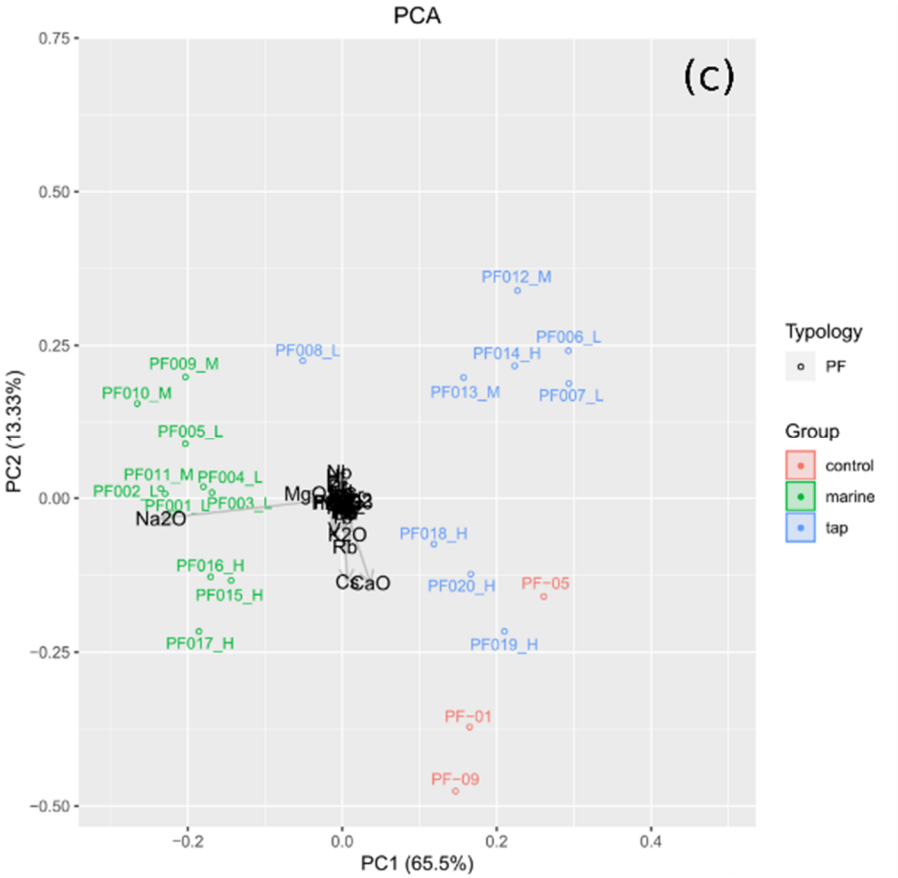
PCA
(c)
PC2 (13.33%)
PC1 (65.5%)
0.75
0.50
0.25
0.00
−0.25
−0.50
−0.2
0.0
0.2
0.4
PF012_M
PF008_L
PF006_L
PF014_H
PF009_M
PF010_M
PF013_M
PF007_L
PF005_L
PF011_M
PF004_L
PF002_L
PF001_L
PF003_L
Na2O
MgO
K2O
Rb
CaO
Nb
PF018_H
PF016_H
PF015_H
PF020_H
PF-05
PF017_H
PF019_H
PF-01
PF-09
Typology
PF
Group
control
marine
tap

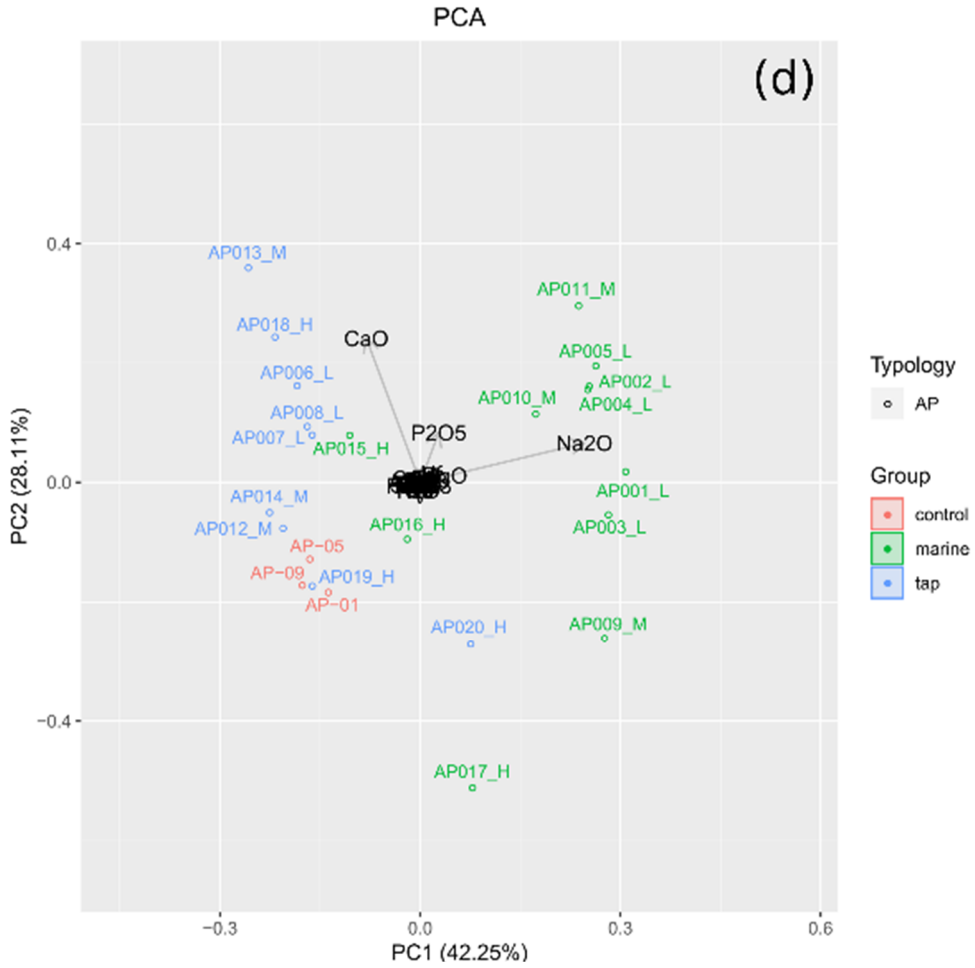

5.3. irudia. (a) 69 laginen Osagai Nagusien Analisia; **(b)** 23 PT laginen Osagai Nagusien Analisia; **(c)** 23 PF laginen Osagai Nagusien Analisia; **(d)** 23 AP laginen Osagai Nagusien Analisia. Lau PCA-k Al_2O_3, Ba, CaO, Ce, Cr, Cs, Dy, Er, Eu, Fe_2O_3, Gd, Hf, Ho, K_2O, La, Lu, MgO, MnO, Na_2O, Nb, Nd, P_2O_5, Pb, Pr, Rb, SiO_2, Sm, Sn, Sr, Tb, Th, TiO_2, Tm, U, V, Yb eta Zr erabiliz kalkulatu dira baina (b) eta (c)-n Pb kendu da

Analisi kimikoen eta kolore-neurketen ondoren, 69 pieza aztertu dira XRD eta SEM–EDS tekniken bidez. SEM-EDS-rentzat epoxian sartu gabeko 69 zeramika zati prestatu dira. Emaitzak pasta mota bakoitzerako probetak eta kontrol-piezak konparatuz interpretatu dira. Alde batetik, XRD emaitzek zeramikaren konposizio mineralogikoa erakusten dute, eta SEM–EDS emaitzekin batera aztertu dira. Bestalde, SEM azterketek informazioa ematen dute erreketan garatutako barne-morfologiari, bitrifikazio-mailari eta poroen egiturari buruz (ikus 4. kapitulua, 4.3.3. atala). SEM-ek aukera ematen du, halaber, jalkitze aldiaren osteko edozein eraldaketaren itxura aztertzeko. Gainera, EDS analisien bidez, pasten mikroanalisi elementala egin daiteke.

5.4. XRD emaitzak

Atal honetan jalkitze-osteko eta erreketa prozesuko eraldaketak deskribatzen dira, beraien erreakzio bideekin batera.

Lehenik eta behin, buztin gordinak XRD bidez aztertu dira konparazioetarako (5.4. taula). Horien arteko desberdintasun nagusia kaltzitaren, dolomitaren eta hematitaren agerpena da. Hauen agerpenak lehengaien kolorean eragiten du (kolore beix/arrosa PT-rentzat eta kolore gorria PF eta AP-rentzat). Gainera, erreta ez daudenez, filosilikato ugari agertzen dira.

5.4. taula. Pasta zeramikoak egiteko erabilitako buztinen fase mineralogikoen laburpena. Qz = kuartzoa; Cal = kaltzita; Dol = dolomita; Hem = hematita; Kfs = feldespato potasikoa; X = mineral bakoitzaren presentzia buztin gordinean, laburdurak Whitney eta Evans (2010)-en arabera

Buztin gordina	**Mineralogia**					
	Qz	Cal	Dol	Hem	Kfs	Filosilikatoak
Kaltzio eduki altuko buztina (≈14 % CaO) (PT)	X	X			X	X
Kaltzio eduki baxuko buztina (≈5 % CaO) (PF)	X	X	X	X	X	X
Buztin mikatsua (≈1 % CaO) (AP)	X			X		X

Hurrengo lerroetan, PT (5.5. taula), PF (5.6. taula) eta AP (5.7. taula) kontrol-piezen eta probeten konposizio mineralogikoa erakutsiko da, eta erreketa prozesuko eta jalkitze-osteko eraldaketa bideak azalduko dira.

5.5. taulan ikus daitekeenez, badira erreketa prozesuen ondorioz sortutako desberdintasun mineralogiko batzuk PT kontrol-piezen artean, tenperatura desberdinetan erre zirelako. Lehenengo desberdintasun argia da illita (buztin-minerala) desagertu egiten dela erreketa tenperatura igo ahala. Fenomeno hori gertatzen da buztin-mineralek duten ura galtzen dutelako, eta, ondorioz, haien egitura kristalinoa desegiten delako, buztin-mineralak deskonposatuz eta silikato berriak sortuz (Rice, 1987). Bestalde, kaolinak zeramikan ez zeuden arren, segur aski buztin gordinean bazeuden. Kaolinitaren dihidroxilazioa 400 eta 500 °C bitartean gertatzen da, eta metakaolinita sortzen da. Gero, 900 °C-an, aluminioan aberatsa den espinela ($MgAl_2O_4$) metakaolinita horretatik sortzen hasten da, eta 1000–1100 °C-an, berriz, mullitan kristalizatzen da ($3Al_2O_3{\cdot}2SiO_2$). Mullita orratz edo hagatxo

moduko kristaletan existitzen da, erretako pieza indartuz (Abubakar et al., 2020; Aras, 2004; Rice, 1987). Testuinguru honetan, mullita egotea interesgarria da; izan ere, oro har, kaltzio kontzentrazio altuko buztinetan karbonato kopuru txikiak daudenean (< 10 %), mullitaren eraketa inhibitu egiten da eta Ca-silikatoak sortzen dira. Hala ere, laginetan dagoen Al_2O_3 kontzentrazioaren arabera, eta karbonato kopurua % 10etik gorakoa bada, mullita sor daiteke. El Ouahabi et al. (2015)-ek mullita kaltzio kontzentrazio altuko eta Al_2O_3 % 15 inguru zuen zeramika batean identifikatu zuen. Kasu honetan, PT zeramikek % 14-16 inguruko Al_2O_3 dute eta horrek justifikatzen du zeramika horietan mullita egotea. 5.4. irudian erakusten da PT-09 kontrol-piezaren difraktograma, mullita duena.

5.5. taula. PT kontrolen eta probeten (itsasoko uretan eta iturriko uretan murgilduak) fase mineralogikoen laburpena. Qz = kuartzoa; Cal = kaltzita; Gh = gehlenita; Hem = hematita; Kfs = feldespato potasikoa; Pl = plagioklasa; Di = diopsidoa; Ilt = illita; Gp = igeltsua; Anl = analtzima; Mul = mullita, laburdurak Whitney eta Evans (2010)-en arabera

		Mineralogia											
		Qz	**Cal**	**Gh**	**Hem**	**Kfs**	**Pl**	**Di**	**Ilt**	**Mul**	**Gp**	**Anl**	**Wo**
	PT-01 (850 °C)	X	X	X	X	X			X				
	PT-05 (950 °C)	X		X	X	X	X	X	X				
	PT-09 (1100 °C)	X		X	X	X	X	X		X			
Itsasokoa	**PT001 (850 °C, 3 hilabete)**	X	X	X	X	X			X				
	PT002 (850 °C, 10 hilabete)	X	X	X	X	X			X		X		
	PT003 (850 °C, 18 hilabete)	X	X	X	X	X			X		X		
	PT009 (950 °C, 3 hilabete)	X	X	X	X	X	X	X	X				
	PT010 (950 °C, 10 hilabete)	X		X	X	X	X	X	X				
	PT011 (950 °C, 18 hilabete)	X		X	X	X	X	X	X				
	PT015 (1100 °C, 3 hilabete)	X		X	X	X	X	X		X		X	
	PT016 (1100 °C, 10 hilabete)	X		X	X	X	X	X		X		X	
	PT017 (1100 °C, 18 hilabete)	X		X	X	X	X	X				X	
Iturrikoa	**PT006 (850 °C, 3 hilabete)**	X	X	X	X	X			X				
	PT007 (850 °C, 10 hilabete)	X	X	X	X	X			X				

		Qz	Cal	Gh	Hem	Kfs	Pl	Di	Ilt	Mul	Gp	Anl	Wo
	PT008 (850 °C, 18 hilabete)	X	X	X	X	X			X				
	PT012 (950 °C, 3 hilabete)	X		X	X	X	X	X	X				
	PT013 (950 °C, 10 hilabete)	X		X	X	X	X	X	X				
	PT014 (950 °C, 18 hilabete)	X		X	X	X	X	X	X				
	PT018 (1100 °C, 3 hilabete)	X		X	X	X	X	X		X			
	PT019 (1100 °C, 10 hilabete)	X		X	X	X	X	X		X			X
	PT020 (1100 °C, 18 hilabete)	X		X	X	X	X	X		X			

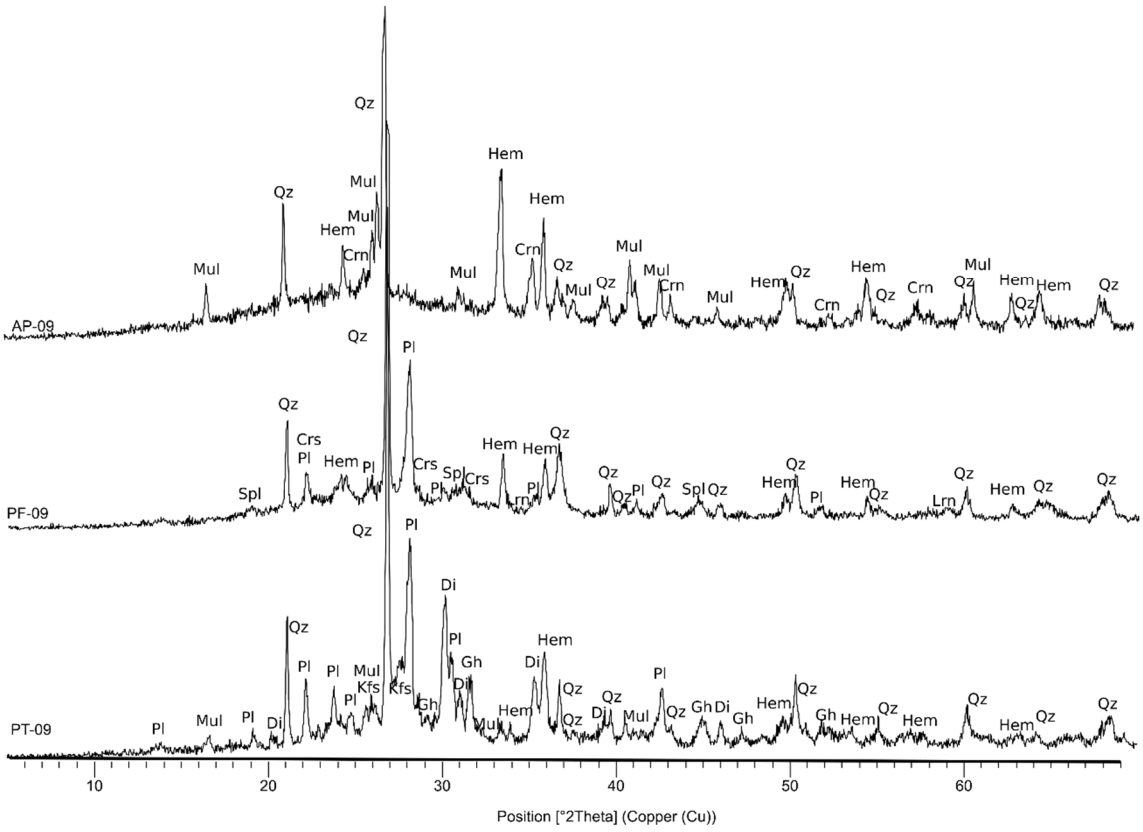

5.4. irudia. AP-09, PF-09 eta PT-09 kontrol-piezen difraktogramak. Qz = kuartzoa; Cal = kaltzita; Gh = gehlenita; Hem = hematita; Kfs = feldespato potasikoa; Pl = plagioklasa; Di = diopsidoa; Ilt = illita; Gp = igeltsua; Anl = analtzima; Mul = mullita; Crs = Cristobalita; Spl = spinela; Lrn = larnita, Crn = korindoia, laburdurak Whitney and Evans (2010)-en arabera

Gainera, kaltzita tenperatura baxuenean erretako laginean agertzen da, baina ez dago beste laginetan. Aldiz, gehlenita ($Ca_2Al_2SiO_7$) eta diopsidoa ($Ca(Mg,Fe)Si_2O_6$) lagin horietan agertzen dira. Kaltzitaren desagerpena kaltzita 600–900 °C-an gutxi gorabehera deskonposatu egiten delako gertatzen da, eta karea

(CaO) eta karbono dioxidoa (CO_2) sortzen dira, hurrengo erreakzioaren arabera (Buxeda i Garrigós eta Cau, 1994; Cau et al., 2002; Fabbri et al., 2014; Rice, 1987):

$$CaCO_3 \xrightarrow{650-900\ °C} CaO + CO_2 \uparrow \quad \text{Eq. 5.2.}$$

Ondoren, CaO-ak, erreketa tenperaturaren, iraupenaren, karbonato zatien granulometriaren edota beren kristal-egituraren arabera, zeramika gorputzean dauden buztin-mineralekin erreakzionatzen du. Horrela, Ca-silikatoak eta aluminosilikatoak eratzen dira, hala nola gehlenita, anortita ($CaAl_2Si_2O_8$, honen kontzentrazioa erreketa tenperaturarekin handitzen da), eta diopsidoa (Cau et al., 2002). Horregatik agertzen dira diopsidoa, plagioklasa (adibidez, anortita, albita) eta gehlenita tenperatura altuagoetan erretako kontrol-piezetan.

Gainera, Heimann eta Maggetti (1981)-k 1000 °C-tan eta hortik gorako tenperaturetan gehlenitatik abiatuz anortita sortzeko erreakzioak deskribatu zituzten.

$$Al_2SiO_7 + 2\,SiO_2 \rightarrow CaAl_2Si_2O_8 + CaSiO_3 \quad \text{Eq. 5.3.}$$

$$Ca_2Al_2SiO_7 + 3\,SiO_2 + Al_2O_3 \rightarrow 2\,CaAl_2Si_2O_8 \quad \text{Eq. 5.4.}$$

Erreakzio-bide horiek anortitaren gehitzea eta gehlenitaren gutxitzea azaldu dezakete PT-09-an (1100 °C-an erretakoa). Horrez gain, hematita kantitatea ere handitu egin da tenperaturarekin. Horren arrazoia izan liteke hematita kristaliza daitekeela kaltzita deskonposatzen delako kuartzoaren eta burdina daramaten buztin-mineralen presentzian (Nodari et al., 2007). Karbonatoak deskonposatu egiten dira fase amorfoarekin erreakzionatzean, kaltzio silikatoak sortzeko. Hala, hematitak nukleatu eta hazi egin daitezke.

PT-ren itsasoko laginen DRX emaitzei dagokienez (5.5. taula), 850 °C-an erretako laginetatik (PT001, PT002, PT003) kaltzita eta gehlenita kopuru handiagoa dago PT001 laginean (3 hilabeteko murgilaldia). Jalkitze-osteko periodoaren ondoriozko kaltzitaren eta gehlenitaren deskonposizio-erreakzioek zerikusia izan dezakete mineral horien gutxitzean, murgilaldi luzeagoa pasa duten piezetan (Buxeda i Garrigós eta Cau, 1994; Fabbri et al., 2014; Heimann eta Maggetti, 1981). Qz, Pl, Kfs eta Ilt kantitateak antzekoak dira lagin guztietan, baina PT002 eta PT003 laginetan igeltsua egoteak ($CaSO_4{\cdot}2H_2O$) markatzen du lagin horien arteko desberdintasun nagusia. Igeltsuaren agerpena itsas ingurune erreduzitzailean eratutako piritarekin edota kaltzitaren disoluzioarekin eta ingurune azidoan sulfatoarekin erreakzionatzearekin lotuta egon ohi da (Secco et al., 2011); hala ere,

ez da hala gertatu lagin hauetan, esperimentuko itsas ingurunea oxidatzailea zelako eta bi inguruneak basikoak zirelako. Igeltsua lehengaiarekin lotuta egon daiteke ere, baina kontrol-piezen difraktogrametan ez da identifikatu. Beraz, litekeena da itsasoko uraren sulfatoa hauspeatu izana probetetan. Gainera, 950 °C-tan erretako laginetatik (PT009, PT010, PT011) kaltzita PT009-an identifikatu da eta Qz, Pl, Gh, Hem, Kfs eta Ilt kopurua antzekoa da lagin guztietan. Kaltzita ez litzakete PT009 laginean azaldu behar, PT-05 kontrol-laginean ez baitago. Hala ere, erreakzionatu ez duen CaO-a $CaCO_3$-ra birkarbonatatu daiteke (Buxeda i Garrigós eta Cau, 1994; Fabbri et al., 2014; Freestone, 2001; Freeth, 1967) eta pH basikoan (7-8 baino altuagoa) hauspeatu egiten da (Maritan, 2020). Lehenengo, CaO-k urarekin erreakzionatzen du kaltzio hidroxidoa ($Ca(OH)_2$, portlandita) emateko, eta, ondoren, portlanditak CO_2-rekin erreakzionatzen du eta kaltzita sortzen da, hurrengo erreakzio-bidearen arabera (Fabbri et al., 2014).

$$CaO + H_2O \rightarrow Ca(OH)_2 \quad \text{Eq. 5.5.}$$

$$Ca(OH)_2 + CO_2 \rightarrow CaCO_3 + H_2O\uparrow \quad \text{Eq. 5.6.}$$

Gehlenita dagokion kontrol-piezan (PT-09) baino kantitate txikiagoan agertu da, ziurrenik anortita eratzeko gehlenita eraldatu delako. Gainera, mullita ez dago PT017 laginean, eta horrek, ziur aski agerian uzten du erreketa garaian erreakzio batzuk desberdin gerta daitezkeela laginetan. Baliteke karbonatoen kopurua lagin honetan baxuagoa izatea beste laginetan baino gertaera horien ondorioz, eta orduan mullita ez sortzea (El Ouahabi et al., 2015).

Azkenik, 1100 °C-an erretako lagin guztietan (PT015–017) analtzima ($NaAlSi_2O_6 \cdot H_2O$) agertu da. Buxeda i Garrigós et al. (2002a)-ek 1000 °C-tik gorako tenperaturan erretako kaltziodun zeramiketan Na eta batzuetan Mg eta Sr-ren edukian gorakada nabaritu zuten, K eta Rb-ren edukiaren beherakadarekin batera, lurperatze baldintza zehatzetan. Gainera, zenbait azterlanek (Buxeda i Garrigós, 1999; Buxeda i Garrigós et al., 2001, 2002a; Heimann eta Maggetti, 1981; Schwedt et al., 2006) analtzimaren (analtzita bezala ezagutua ere) formakuntza dokumentatu dute, aipatutako gertaeraren kausa bezala. Buxeda i Garrigós et al. (2002a)-ek Picon (1976)-en behaketetatik abiatuta, adierazi zuten zeramiken erreketa-tenperaturaren arabera bitrifikatutako fase bat agertzen dela zeramiketan (normalean, gainazaletik gertu dagoen zatian). Bitrifikatutako zati honek zeramikaren potasio eduki handi bat bereganatzen du, Rb-rekin batera lixibiatu egiten dena jalkitze-aldian zehar, bitrifikatutako fase hori ezegonkorra delako.

Gero, analtzima kristalizatzen da, silikatoetan inguruneko Na finkatzen delako. Hori guztia itsasoko uretan murgildutako probetetan ikus daiteke: hauen Na kontzentrazioa altua da eta horrek justifikatzen du analtzimaren agerpena zeramika horietan eta ez iturriko uretan murgildutako probetetan. Gainera, gertaera hau bat dator 5.3.b irudian erakusten den PCA-rekin; bertan, 1100 °C-tan erretako eta itsasoko uretan murgildutako laginek dute Na_2O eduki altuena.

Iturriko uretan murgildutako PT-ren XRD emaitzei dagokienez (5.5. taula), ez da aldaketarik hauteman murgilaldi desberdinetako laginen faseetan, ziurrenik iturriko ura ez delako itsas ura bezain agresiboa. Wollastonita izan da PT piezetan agertu den fase berria, bereziki PT019 piezan. Mineral hori tenperatura altuko fase sekundarioa da, eta kaltzioan aberatsak diren buztinetatik kristalizatzen da (Gliozzo, 2020b).

Bestalde, 5.6. taulan ikus daitekeenez, PF kontrol-piezetan gertatutako aldaketa mineralogikoak PT kontrol-piezetan gertatutako aldaketen oso antzekoak dira. Desberdintasunak PT laginetan mullitaren agerpena eta PF laginetan mullita ez dagoela eta PF laginetan kristobalita, espinela eta larnita agertu direla da. Kaltzita, gehlenita, hematita, plagioklasa eta diopsidoaren eraldatze erreakzioak PT kontrol-piezetan azaldutakoen berdinak dira. Hauez gain, kristobalita, kuartzoaren polimorfoa, PF-09-an agertzen da, tenperatura altuetan kuartzoan gertatzen diren inbertsioen ondorioz. Gainera, larnita, kaltzio silikato bat (Ca_2SiO_4) eta aluminioz aberatsa den espinela ($MgAl_2O_4$) agertu dira buztin mineralen tenperatura altuko aldaketen ondorioz (Rice, 1987). Larnita, kristobalita eta espinela dituen PF-09 kontrol-piezaren difraktograma 5.4. irudian ageri da.

5.6. taula. PF kontrolen eta probeten (itsasoko uretan eta iturriko uretan murgilduak) fase mineralogikoen laburpena. Qz = kuartzoa; Cal = kaltzita; Gh = gehlenita; Hem = hematita; Kfs = feldespato potasikoa; Pl = plagioklasa; Di = diopsidoa; Ilt = illita; Crs = kristobalita; Spl = espinela; Lrn = larnita, laburdurak Whitney eta Evans (2010)-en arabera

		Mineralogia										
		Qz	Cal	Gh	Hem	Kfs	Pl	Di	Ilt	Crs	Spl	Lrn
	PF-01 (850 °C)	X	X	X	X	X	X		X			
	PF-05 (950 °C)	X		X	X	X	X		X			
	PF-09 (1100 °C)	X			X		X	X		X	X	X
Itsasokoa	**PF001 (850 °C, 3 hilabete)**	X	X	X	X	X	X		X			
	PF002 (850 °C, 10 hilabete)	X	X	X	X	X	X		X			
	PF003 (850 °C, 18 hilabete)	X	X	X	X	X	X		X			
	PF009 (950 °C, 3 hilabete)	X	X	X	X	X	X		X			
	PF010 (950 °C, 10 hilabete)	X	X	X	X	X	X		X			
	PF011 (950 °C, 18 hilabete)	X		X	X	X	X		X			
	PF015 (1100 °C, 3 hilabete)	X			X		X	X			X	X
	PF016 (1100 °C, 10 hilabete)	X			X		X	X			X	
	PF017 (1100 °C, 18 hilabete)	X			X		X	X			X	X
Iturrikoa	**PF006 (850 °C, 3 hilabete)**	X	X	X	X	X	X		X			
	PF007 (850 °C, 10 hilabete)	X	X	X	X	X	X		X			
	PF008 (850 °C, 18 hilabete)	X	X	X	X	X	X		X			
	PF012 (950 °C, 3 hilabete)	X	X	X	X	X	X		X			
	PF013 (950 °C, 10 hilabete)	X	X	X	X	X	X		X			
	PF014 (950 °C, 18 hilabete)	X	X	X	X	X	X		X			
	PF018 (1100 °C, 3 hilabete)	X			X		X	X			X	
	PF019 (1100 °C, 10 hilabete)	X			X		X	X			X	X
	PF020 (1100 °C, 18 hilabete)	X			X		X	X			X	

850 °C-tan erretako eta itsasoko uretan murgildutako PF probeten (PF001–003) XRD emaitzei dagokienez (5.6. taula), kaltzita- eta gehlenita-kantitatea handiagoa da PF001-ean (3 hilabete urperatuta), PT atalean azaldutako arrazoi berberengatik. Gainera, 950 °C-an erretako laginen kasuan (PF009–011), kaltzita

PF009-an agertzen da CaO-ren birkarbonatazioagatik, PT009 laginean bezala, eta Qz, Pl, Gh, Hem, Di, Kfs eta Ilt kantitateak antzekoak izan dira lagin guztietan. Azkenik, 1100 °C-an erretako laginen kasuan, plagioklasa eta hematita edukiak altuagoak dira PF017-an (18 hilabeteko murgilaldia). Esan bezala, anortita eratzeko gehlenitaren alterazioak eragin lezake plagioklasa kopuru handiagoa. Qz, Spl eta Di gainerako laginetan antzekoak dira, eta Ilt desagertu egin da. Crs ez da lagin hauetan hauteman, erretzen ari zirela garatu ez zelako, eta larnita PF015 eta PF017 probetetan agertu da, PF016-an ez bezala.

Gainera, iturriko uretan murgildutako PF probeten emaitzak PT probeten oso antzekoak izan dira; beraz, oso aldaketa gutxi hauteman da murgilaldi desberdinetan iturriko uretan (5.6. taula).

Bestalde, AP zeramika mikatsuko kontrol-piezei dagokienez, 5.7. taulak erakusten du zenbait desberdintasun mineralogiko daudela beraien artean, erreketa prozesuko eraldaketen ondorioz. Lehenengo desberdintasun argia da mullita dagoela erreketa-tenperatura altuko zeramikan, PT piezetan bezala. Gainera, hematita kantitatea handitu egin da tenperaturarekin. Fenomeno hau PT eta PF laginekin ere gertatu da. Era berean, korindoia (Al_2O_3) AP-09an agertu da, erreketa-tenperatura altuengatik.

5.7. taula. AP kontrol-piezen fase mineralogikoen laburpena. Qz = kuartzoa; Ilt = illita; mul = mullita; Hem = hematita; Kfs = feldespato potasikoa; Crn = korindoia; Pl = plagioklasa, laburdurak Whitney eta Evans (2010)-en arabera

	Mineralogia					
	Qz	**Illt**	**Mul**	**Hem**	**Kfs**	**Crn**
AP-01 (850 ºC)	X	X		X	X	
AP-05 (950 ºC)	X	X	X	X	X	
AP-09 (1100 ºC)	X		X	X		X

Itsasoko eta iturriko AP probeten XRD emaitzei dagokienez, ez da alde nabarmenik hauteman ez faseetan (hau da, lagin guztiek beren kontrol-piezen fase berak dituzte), ez urperatze-aldi desberdinak dituzten laginen artean. Laginen arteko aldeak 5.7. taulan ageri diren erreketa-tenperaturei dagozkienak dira.

5.5. SEM-EDS emaitzak

Hiru pasta moten kontrol-piezen SEM–EDS analisiei dagokienez, lehenik eta behin, 850 °C-tan erretako kontrol-piezek (PT-01, PF-01 eta AP-01) bitrifikazio-maila baxua erakusten dute, gainazal lauko eremu isolatuak agertzen baitira (5.5.a–c irudia). PT-05, PF-05 eta AP-05-ek (950 °C-tan erretakoak), aldiz, bitrifikazio-maila ertaina erakusten dute (5.5.d–f irudia), eta 1100 °C-tan erretakoek (PT-09, PF-09 eta AP-09) bitrifikazio jarraia (5.5.g–i irudia), gainazal guztian zehar eremu lauak erakusten dituztelako (Maniatis eta Tite, 1978). PF laginetan tamaina desberdinetako fase mineralak identifikatu dira. EDS analisien arabera, fase mineral hauek batez ere Si, O, Ca, Fe, Mg, Al, K eta, batzuetan, Ti-z osatuta daudela ikus daiteke, eta, XRD emaitzen arabera, kuartzoa, feldespato potasikoa, illita, kaltzita, hematita, gehlenita, plagioklasa, kristobalita eta diopsidoa direla ondoriozta daiteke, besteen artean. Gainera, PT kontrol-piezen EDS analisiek erakusten dute hiru kontrol-piezetan kaltzio eta magnesio ugari dagoela. Elementu horiek karbonato, oxido eta silikato gisa ager daitezke, besteak beste. Gainera, S eta Cl PT-05 laginean agertzen dira, eta gertaera honek elementu horiek lehengaian zeudela erakusten du. Kasu honetan, S igeltsuarekin lotuta egon daiteke, eta horrek PT002 eta PT003 probetetan XRD bidez igeltsuaren agerpena sostengatu dezake. Azkenik, ikusi da AP kontrol-piezek fase mineral luze eta lauak dituztela, eta fase horiek egitura laminarra osatzen dutela zeramikaren pastaren barruan, segur aski mika taldekoak. 850 °C-tan erretako probetek egitura laminar hori agertzen dute; 1100 °C-tan erretakoek, berriz, geruza bitrifikatu jarrai eta leuna erakusten dute. EDS analisiek erakusten dute fase mineral horiek batez ere Si, O, Fe, K, Al, Mg, Ca eta, batzuetan, Ti-z osatuta daudela, eta, XRD emaitzen arabera, kuartzoa, potasio feldespatoa, illita eta hematita, besteak beste, izan daitezke fase horiek. Halaber, Ca eta Mg-ren agerpena erlazionatuta dagoela dirudi. Gainera, AP-05 laginaren EDS analisietan ikusten da, AP-01 laginean bezala, fase horiek Fe, Ca, K, Mg, C, Al, Ca, O, Si, Ti eta, zenbait kasutan, S eta Mn-z osatuta daudela eta XRD emaitzek iradokitzen dutela fase horiek kuartzo, feldespato potasiko, illita eta mullita izan daitezkeela. Kaltzio karbonatoak eta silikatoak DRX bidez identifikatu ez diren arren, ziur aski eduki txikiagoa dutelako, agregatu batzuk SEM–EDS bidez identifikatu dira, baina PT eta PF laginetan baino kantitate txikiagoetan.

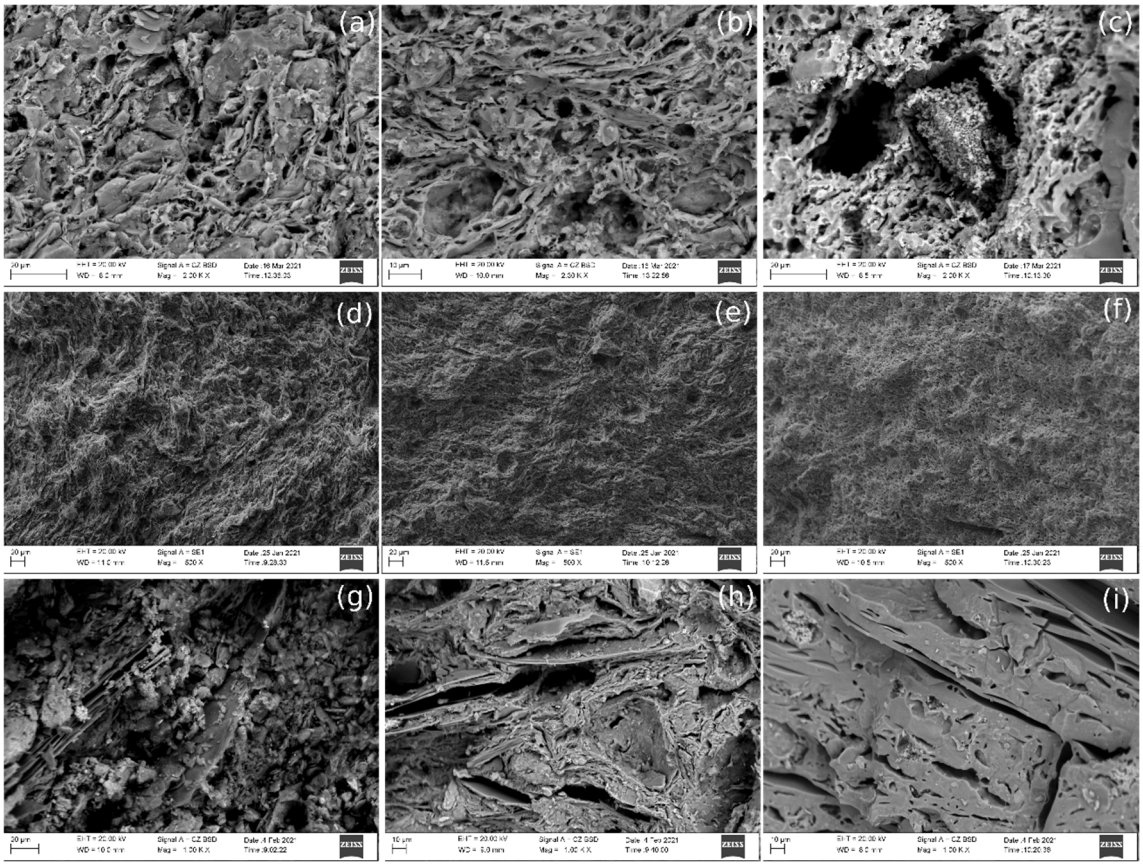

5.5. irudia. PT, PF eta AP kontrol-piezen zatien SEM-SED (d,e,f,) eta SEM-BSD (a,b,c,g,h,i) irudiak: **(a–c)** PT-01, PT-05, PT-09; **(d-f)** PF-01, PF-05, PF-09; **(g–i)** AP-01, AP-05, AP-09

Probeten SEM eta EDS analisien emaitzak askotarikoak dira, eta forma desberdinak aurkitu dira, hala nola orratzak, malutak, esponja modukoak, hagatxo modukoak eta prisma luze eta laburrak, batez ere PT eta PF laginetan. Itsas eta iturriko uretako AP probeten SEM-EDS analisiei dagokienez, ikusi da, PT eta PF piezekin alderatuta, AP piezek askoz agregatu gutxiago erakusten dituztela beren pastetan. Espero ez bezala, tenperatura altuan erretako AP laginetan bigarren mailako fase gehiago hauteman dira tenperatura baxuetan erretakoetan baino, nahiz eta tenperatura baxuetan erretako pastak porotsuagoak izan. Beharbada, horren arrazoia da pastek duten egitura laminarrak zaildu egiten duela inguruneko soluzioak sartzea, eta, beraz, fase sekundarioen eraketa ekidin dezakeela. Aitzitik, litekeena da AP laginen tenperatura altuetako egitura bitrifikatuan kanal moduko batzuk sortu izana eta beraietatik inguruneko soluzioak sartu izana.

Hiru pastetako itsasoko laginek Na, Cl eta S duten zenbait kristalizazio erakutsi dituzte (5.6. irudia). Kristalizazio horiek NaCl-arenak (halita) eta kaltzio sulfatoarenak izan daitezke, kasu gehienetan, itsasoko uretik hauspeatuta. Hala

ere, litekeena da igeltsua PT eta AP lagin batzuetan lehengaitik etortzea, S-a EDS-ren bidez identifikatu baita kontrol-piezetan. PT eta PF laginetan, badirudi aipatutako agregatuak zuloetan eratu direla; AP laginetan, aldiz, fase mineral handien gainean kokatzen direla dirudi, eta horrek iradokitzen du lagin hauetan uraren mugimendua fluxu laminarrekoa izan litekeela perkolazioaren ordez, AP-ren egituraren berezitasunagatik. Hala ere, salbuespen gisa, 1100 °C-tan erretako eta itsasoko uretan murgildutako AP laginek NaCl agregatuak erakusten dituzte pasta bitrifikatuetan eratutako zuloetan. Bestalde, iturriko uretan murgildutako eta 850 °C-an eta 950 °C-tan erretako AP laginek ez dute eratu berri den agregaturik erakusten eta AP kontrol-piezen antzeko faseak erakusten dituzte.

5.7. irudian, PF eta PT laginetan identifikatutako kristalizazioetako bat ageri da, itsas eta iturriko giroetan murgildu direnetan. Kristalizazio horiek batez ere PF-ko iturriko uretako laginetan agertu dira, baina itsas eta iturriko PT laginetan ere agertu dira. Esponjen antzekoak dira eta zuloetan agertu ohi dira, eta batez ere Ca eta F-z osatuta daude. Gainera, agregatu hauen muturretan Mn identifikatu da, baita Ca, O, C, Al eta Si elementuak ere zulo horien inguruan (ziur aski kaltzio silikatoekin erlazionatuta).

Thomas et al. (1977)-en arabera, fluorra lehengaietan egon daitekeen elementua da. García-Ten et al. (2006)-ek azaltzen dute, zeramika erretzean, fluor ioiak mikaren eta beste buztin mineral batzuen (adibidez, illita edo montmorillonita) kristal-egituran dauden OH^- taldeak ordezkatzen dituela. Erreakzio horren ondorioz, besteak beste, azido fluorhidrikoa (HF) eta silizio tetrafluoruroa (SiF_4) sortzen dira. Konposatu horiek 500 °C eta 700 °C bitartean askatzen dira erreketan. Hala ere, kaltzio eduki altuko zeramiketan, HF-ak kaltzitarekin erreakziona dezake fluorita sortzeko (CaF_2). Gainera, De Bonis et al. (2014)-ek silikatoen (feldespatoak eta kuartzoa, esaterako) ertzetan sortutako kuspidina [$Ca_4Si_2O_7(F,OH)_2$] identifikatu zuten fluoritadun karbonatoekin kontaktuan, 850 °C-tik 1100 °C-ra bitarteko tenperaturatan erretako zeramikan. Egileek honako erreakzio-bide hau proposatu zuten kuspidina sortzeko.

$$3CaO + 2SiO_2 + CaF_2 \rightarrow Ca_4Si_2O_7F_2 \quad \text{Eq. 5.7.}$$

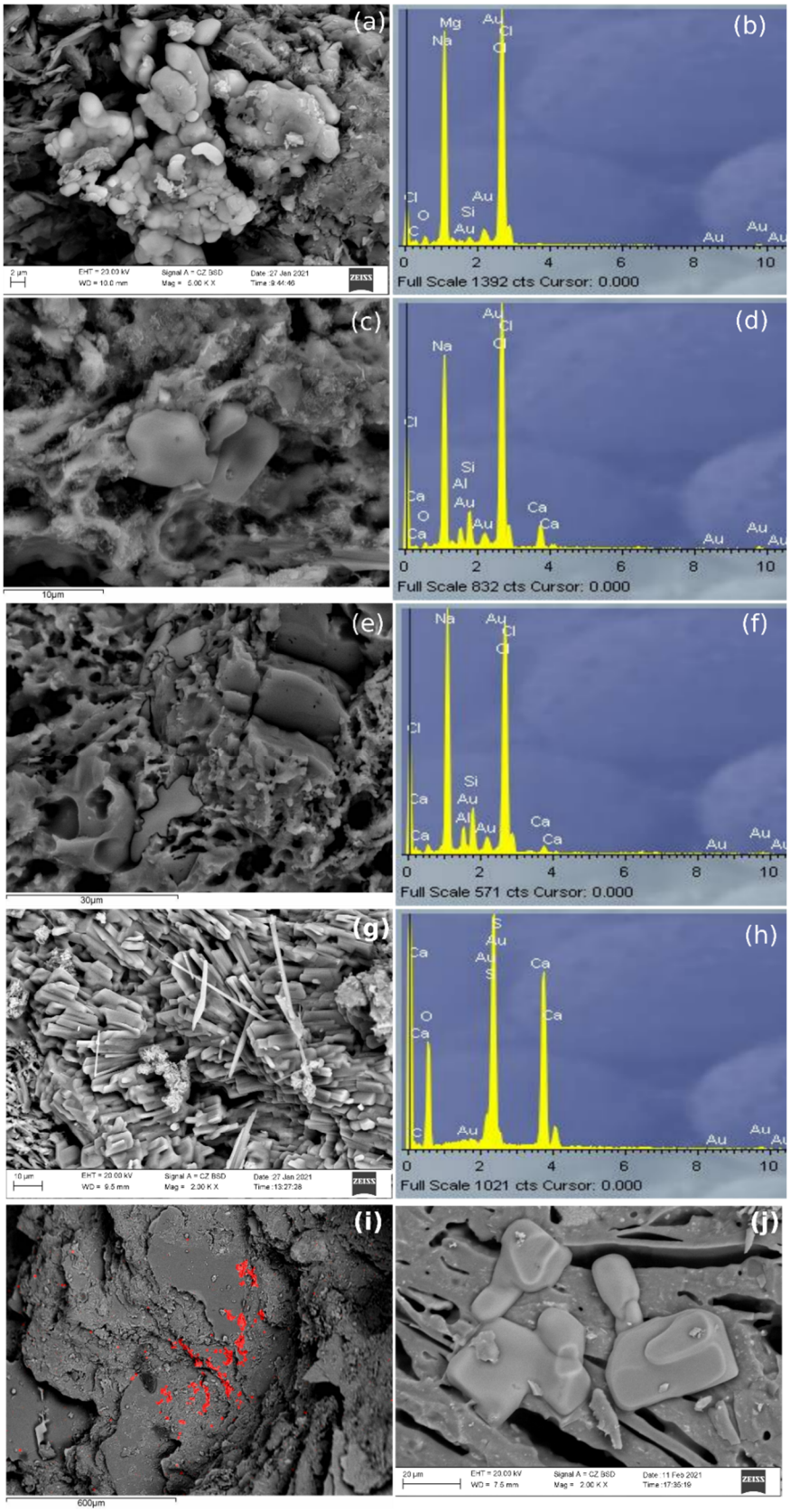

5.6. irudia. PT eta PF-ren itsasoko laginen SEM-BSD irudiak eta hauen analisi elementalak EDS bidez: **(a–f)** Na eta Cl-z osatutako agregatuak, NaCl gisa iradokitakoak. Hainbat modutan agertzen dira; **(g,h)** kaltzio sulfato gisa iradokitako Ca, S, O orratz formako kristalak; **(i)** NaCl (gorriz markatua) AP002 piezaren fase mineral handien gainean; **(j)** NaCl AP015-en zuloetan

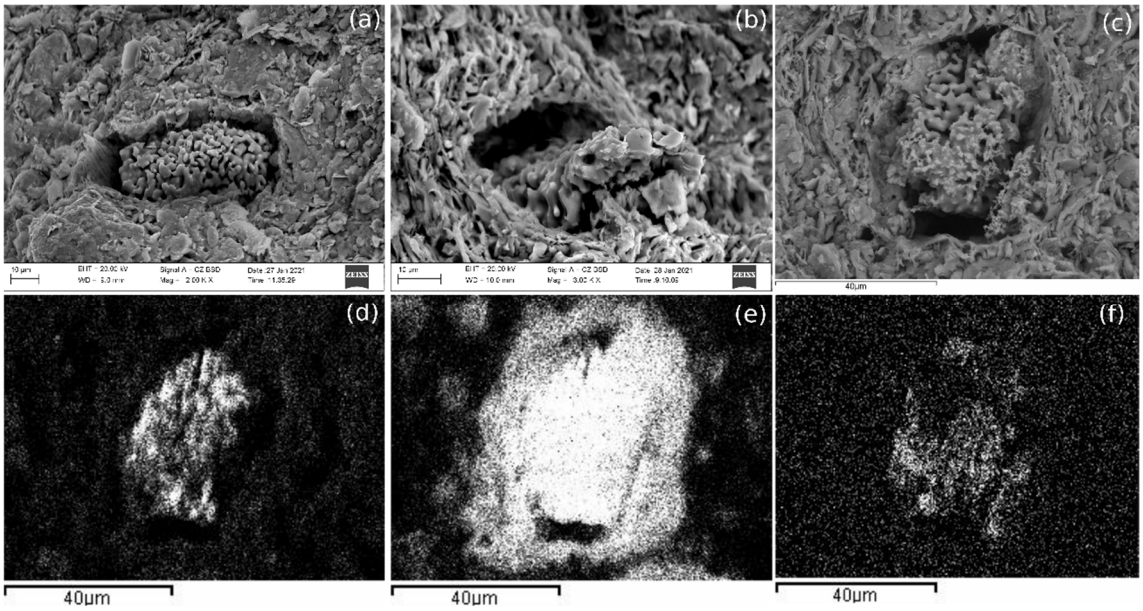

5.7. irudia. PT eta PF laginetan identifikatutako ohiko kristalizazioak SEM-BSD irudien bidez: **(a)** Ca-F agregatua PF008-ren zulo batean (iturriko uretan sartuta dagoen lagina); **(b)** Ca-F agregatua PF012-ren zulo batean (iturriko uretan sartuta dagoen lagina); **(c)** Ca-F agregatua PF013-ren zulo batean (iturriko uretan sartuta dagoen lagina); **(d)** mapa elementala: F-ren banaketa (c)-ren Ca-F agregatuan; **(e)** mapa elementala: Ca-ren banaketa (c)-ren Ca-F agregatuan; **(f)** mapa elementala: Mn-ren banaketa (c)-ren Ca-F agregatuan

Beraz, lagin horien esponja moduko egitura horiek kuspidina izan daitezke. Ca-F agregatuaren muturretan Mn agertzeak iradoki lezake kasu horietan mineral sortu berria Mn duen kuspidina taldeko mineral bat izan daitekeela, hala nola normandita [$NaCa(Mn,Fe)(Ti,Nb,Zr)(Si_2O_7)OF$]. Sortu berri diren egitura horiek kaltzitan eduki dezakete jatorria. Kaltzita CaO-ra deskonposatu daiteke zuloak utziz; orduan, kuspidina edo normandita sor daitezke zulo horietan. Gainera, iturriko uretan murgildutako laginetan itsasoko uretan baino zulo gehiago daudela dirudi. Baliteke iturriko uretan fluor gehiago egotea; beraz, agian kaltzita gehiagok erreakzionatu du fluorrarekin, CaF_2 sortzeko, lagin horietan. Gainera, kasu batzuetan, agregatu horiek ez dute egitura bera; arrazoia izan liteke kristalizazio-maila desberdina izatea. Azkenik, AP probeten EDS analisietan F agertu bada ere, esponja moduko egitura hauek ez dira ageri. AP, PT eta PF laginen SEM–EDS analisi kualitatiboak alderatuta, PF eta PT laginek kaltzioa duten askoz mineral gehiago dituzte, eta agian, horregatik dira PF eta PT pasten alterazioak nabarmenago. AP piezen kasuan, hauek kaltzio eduki handirik ez dutenez, segur aski lehengaiaren edo uraren fluorrak ezin izan du kaltzitarekin erreakzionatu.

Gainera, NaCl eta $MgCl_2$ gatzak (ingurunean daude), kaltzio karbonatoen agregatuak eta bario sulfatoaren agregatuak (seguruenik barita, 5.3.a irudian adierazten den bezala) PT010 laginean ere identifikatu dira (5.8. irudia), baita Mg eta kaltzio hidroxidoa edo karbonatoa dituen egitura bat ere, PT016 laginean. Honez gain, kaltzioa duten faseak AP laginetan egon litezke, baina segur aski kantitate txikitan, eta horregatik ez dira ia identifikatu. Salbuespenak AP011 eta AP014 laginetan agertu dira, zeintzuetan kaltzio-silikatoa eta Mg-rekin lotutako kaltzioa identifikatu baitziren, ziur aski hauen jatorria kaltzitan eta filosofikatoetan egonik. Azkenik, itsas ingurunean murgildutako eta 1100 °C-an erretako AP laginek kaltzio karbonato edo silikato agregatuak erakutsi dituzte. 5.9. irudian, 1100 °C-an erretako AP lagin baten pasta-aldaketa ageri da; Mg eta O homogeneoki eta leku berean banatuta agertzen dira, eta NaCl-z osatutako zati batzuk ere identifikatu dira (itsasoko uretatik etorriak). Gainera, Ca identifikatu da agregatu horren inguruan (agian dolomita edo kaltzitan du jatorria). Iturriko uretan murgildutako eta 1100 °C-an erretako AP laginek ere kaltzio karbonatoaren edo silikatoen agregatu mota bera erakusten dute.

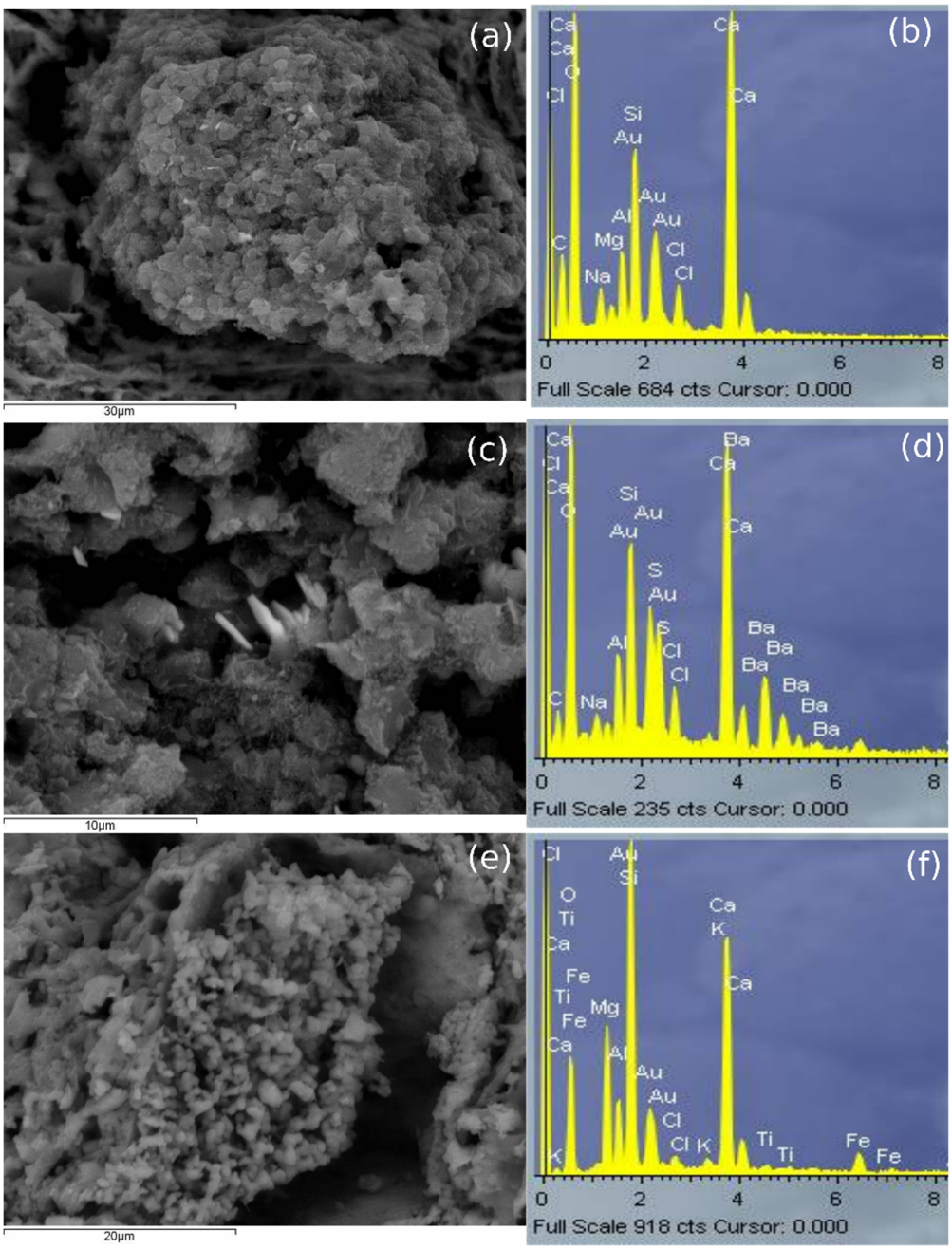

5.8. irudia. (a,b) batez ere Ca, Mg, O, C, Na eta Cl-z osatutako PT010eko agregatu baten SEM-BSD eta EDS analisien irudiak, ziur aski kaltzio karbonatoa eta gatzak; **(c,d)** PT010 agregatu baten SEM-BSD eta EDS analisien irudia, ziurrenik barita; **(e,f)** PT016 agregatu baten SEM-BSD eta EDS analisien irudia, segur aski magnesio eta kaltzio hidroxidoa edo karbonatoa

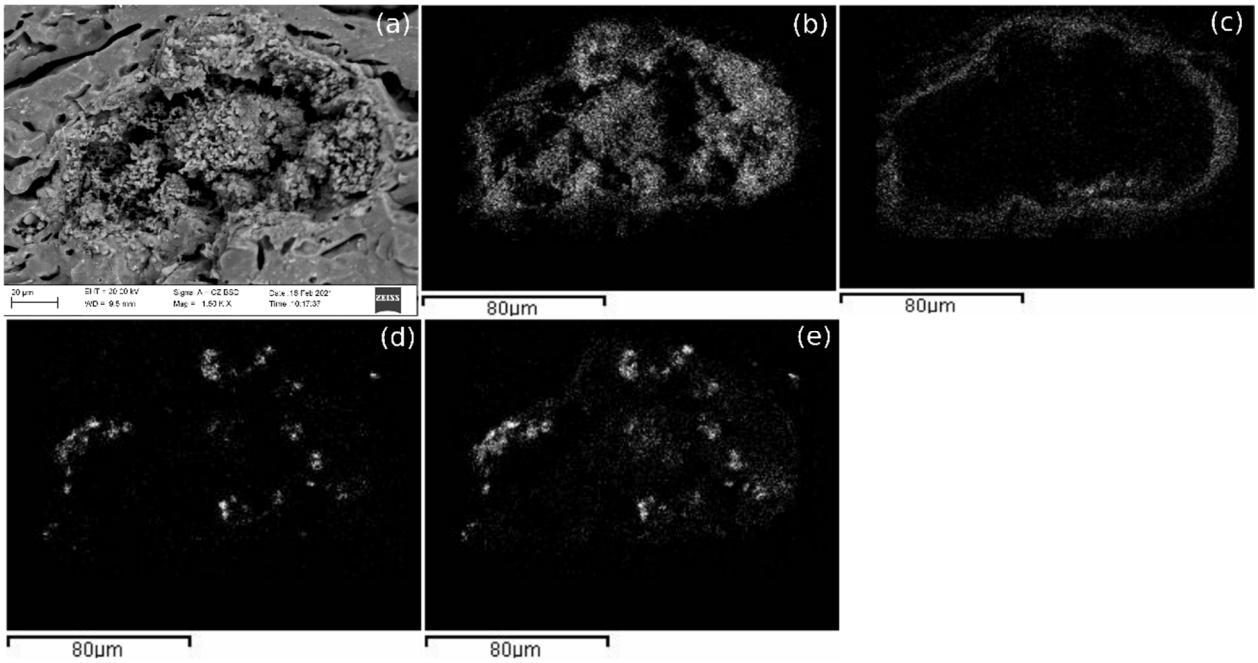

5.9. irudia. (a) AP016-an dagoen agregatu baten SEM-BSD irudia; **(b)** mapa elementala: Mg-aren banaketa (a) agregatuan; **(c)** mapa elementala: Ca-ren banaketa (a) agregatuan; **(d)** mapa elementala: Na-ren banaketa (a) agregatuan; **(e)** mapa elementala: Cl-aren banaketa (a) agregatuan

Pasten analisiez gain, PF010 eta PF014 laginen gainazalak Raman espektroskopia bidez aztertu dira (5.10. irudia). Emaitzek erakusten dute NaCl eta kaltzio sulfato mota desberdinak itsasoko uretik zeramikaren gainazalean hauspeatzen direla. Gainera, ondorioztatu da zenbait formatako orratz formako kristalak kaltzio sulfatoa direla; lehenengoa (a) anhidrita da ($CaSO_4$), eta (c) kaltzio sulfato hemihidratoa (bassanita) [$CaSO_4 \cdot \frac{1}{2}(H_2O)$]. Segur aski, $CaSO_4$-H_2O sistemaren hainbat faseren nahastea dago, Prieto-Taboada et al. (2014)-k azaltzen duten bezala. Gainera, kaltzita identifikatu da PF014 laginaren pastan, Raman bidez (e). Honek 950 °C-an eta 1100 °C-an erretako laginetan gertatu den kaltzitaren birkarbonatazioa berresten du.

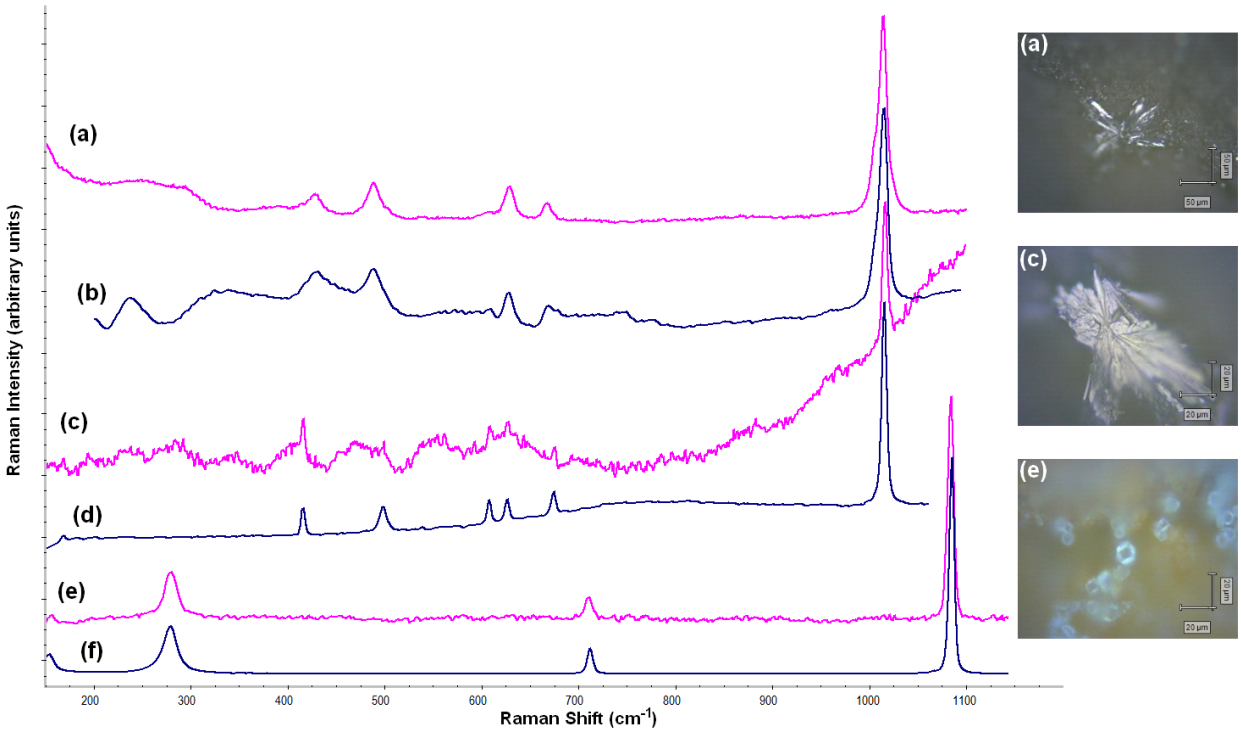

5.10. irudia. PF010 gainazalean eta PF014 pastan egindako Raman analisien emaitzak: **(a)** anhidritaren (CaSO4) espektroa PF010 gainazalean; **(b)** anhidritaren espektroa datu-basean; **(c)** bassanitaren [$CaSO_4 \cdot \frac{1}{2}(H_2O)$] espektroa PF010 gainazalean; **(d)** bassanitaren espektroa datu-basean; **(e)** kaltzitaren ($CaCO_3$) espektroa PF014 pastan; **(f)** kaltzitaren espektroa ($CaCO_3$) datu-basean

6. KAPITULUA: AZTERKETA KASUAK

4. kapituluko 4.1.1 atalean aurkeztutako zeramiken emaitzak eta eztabaida bi zatitan azaltzen dira: Zamora eta Aveiro. Alde batetik, Olivares, La Concepción, Museo Etnografikoa, Benavente eta Toroko aztarnategi arkeologikoetako zeramiken emaitzak Zamorako atalean aurkezten dira (6. kapitulua, 6.1. atala). Bestetik, RAVA, Santo António eliza, hondakindegiak eta Angra D aztarnategi arkeologikoetako (geroago azalduko den ontzi-hondakin bat) zeramiken emaitzak, berriz, Aveiro atalean daude (6. kapitulua, 6.2. atala). Azkenik, 6. kapituluko 6.3. atalean, Zamorako beiraduretan egindako berun isotopoen azterketa sakon deskribatzen da.

6.1. Zamora

ICP-MS-ren bidez aztertutako 94 zeramikentzako konposatu bakoitzaren kontzentrazioak eta haien batezbesteko ziurgabetasun hedatu erlatiboak (U %) 6.1. taulan ageri dira. Emaitzen batezbesteko ziurgabetasun hedatu erlatiboak Museo Etnografikoko 11 zeramikentzat kalkulatu dira, Neurketen Ziurgabetasuna Adierazteko Gidari (GUM) jarraiki, k = 2 izanik (hau da, % 95eko konfiantza-mailaren baliokidea, prozedura analitiko osoa kontuan hartuta) (ikus 4. kapituluko 4.4.3. atala). 4. kapituluko 4.13. irudian ageri denez, kalibrazioaren ziurgabetasuna eta lehen erreferentzia-kontzentrazioaren ziurgabetasuna (kalibrazioarekin lotuta dagoena ere) dira ziurgabetasunean ekarpen handiena egiten dutenak AVR001eko Fe_2O_3 kontzentrazioaren kasuan, eta material zeramikoaren ekarpena oso txikia izanik. Beraz, kalibraketa mota berdina erabili zenez Zamorako zeramikaren multzo osorako, hurbilketa bat egin da: Museo Etnografikoko 11 zeramikentzat kalkulatutako ziurgabetasunak gainerako zeramiketara estrapolatzen dira (ikus 6.1. taula). Hala ere, azpimarratu behar da Tb eta U-ren ziurgabetasunak ezin izan direla kalkulatu, Museo Etnografikoko zeramiketarako beraien kontzentrazioak kuantifikazio-mugaren azpitik daudelako.

6.1. taula. ICP-MS-ren bidez aztertutako 94 zeramikentzat beraien konposatuen kontzentrazioak eta hauen batezbesteko ziurgabetasun hedatu erlatiboa (U %). Marratxoa kuantifikazio-mugatik beherako balioei dagokie. Tb eta U-ren ziurgabetasunak ezin izan dira kalkulatu, Museo Etnografikoko zeramiketarako beraien kontzentrazioak kuantifikazio-mugaren azpitik zeudelako. Elementuen kontzentrazioak ng/g-tan adierazita daude, eta oxidoenak masa %-tan. Kaltziodun zeramika edo kaltzio kontzentrazio altuko zeramika letra lodiz markatuta dago (CaO ≥ % 6)

Laginak	Al_2O_3	Ba	CaO	Ce	Co	Cr	Cs	Cu	Dy	Er	Eu	Fe_2O_3	Gd	Hf	Ho	K_2O	La	Lu	MgO	MnO	Na_2O
ZMR001	12.5	423	**10.1**	66.9	17.0	49.2	6.46	-	4.58	2.52	1.16	3.94	5.36	5.39	0.783	3.88	32.4	0.363	2.42	0.0639	1.27
ZMR002	11.7	417	**9.56**	63.8	29.6	45.4	5.83	-	4.51	2.45	1.05	4.01	5.17	5.78	0.761	3.94	30.5	0.339	2.32	0.0661	1.37
ZMR003	13.4	458	**9.19**	72.7	37.7	44.6	6.12	-	5.07	2.66	1.19	3.84	5.97	6.44	0.823	3.76	34.8	0.392	1.91	0.0617	1.35
ZMR004	13.3	458	**10.4**	71.4	27.0	52.8	6.83	-	4.70	2.50	1.25	4.27	5.66	5.61	0.816	4.01	34.4	0.362	2.45	0.0703	1.31
ZMR005	12.1	419	**12.1**	61.5	23.3	55.1	5.74	-	4.25	2.27	1.10	4.62	5.08	4.85	0.752	3.57	29.9	0.310	2.67	0.0715	1.31
ZMR006	11.6	403	**10.5**	59.3	50.3	55.9	6.69	-	4.22	2.42	1.02	4.50	4.89	5.17	0.763	3.75	28.8	0.362	2.50	0.0710	1.36
ZMR007	12.6	289	1.03	76.4	20.9	63.2	9.67	-	4.81	2.58	1.16	4.30	5.56	7.68	0.816	1.70	39.4	0.418	0.483	0.0195	0.739
ZMR008	11.2	390	**9.81**	59.9	12.6	44.0	6.30	-	4.15	2.36	1.08	3.93	4.82	4.80	0.737	3.37	29.0	0.324	2.60	0.0604	1.17
ZMR009	12.7	266	1.13	66.5	10.8	62.5	9.51	-	5.00	2.76	1.18	4.02	5.49	7.91	0.823	1.67	33.2	0.425	0.462	0.0224	0.723
ZMR010	17.9	538	**6.67**	90.9	19.0	84.3	8.73	-	5.46	2.82	1.66	6.47	6.94	4.56	0.876	4.22	44.6	0.410	1.84	0.104	1.05
ZMR011	19.1	392	1.09	50.3	14.8	56.6	11.3	-	3.61	1.86	1.31	5.21	4.91	2.65	0.641	3.14	23.6	0.202	1.00	0.0298	0.899
ZMR012	17.9	416	1.49	74.8	19.2	48.8	11.6	-	4.35	2.08	1.54	4.04	6.48	3.40	0.714	3.15	33.8	0.224	0.730	0.0233	0.922
ZMR013	18.8	400	1.28	97.9	11.3	45.8	7.63	-	3.60	1.72	1.55	3.61	6.56	3.35	0.610	2.57	43.8	0.185	0.570	0.0193	0.856
ZMR014	12.8	295	1.40	69.5	24.0	65.3	10.7	-	4.60	2.64	1.05	4.21	5.24	6.83	0.803	1.89	35.3	0.368	0.482	0.0205	0.744
ZMR015	16.0	379	1.14	65.1	37.5	46.2	13.1	-	5.60	2.58	1.71	4.70	7.41	3.02	0.867	2.64	33.7	0.288	0.711	0.0262	0.786
ZMR016	12.2	290	0.332	67.9	39.5	66.1	7.71	-	4.79	2.85	1.13	5.14	5.38	8.15	0.861	1.79	35.0	0.408	0.466	0.0391	0.818
ZMR017	12.7	433	**10.6**	66.7	34.3	47.7	6.10	-	4.45	2.56	1.21	4.02	5.38	4.92	0.777	2.98	32.5	0.328	2.36	0.0606	1.18
ZMR018	11.9	409	**12.1**	66.4	26.3	53.2	6.00	-	4.39	2.43	1.10	4.34	5.15	5.02	0.766	3.79	32.3	0.322	2.51	0.0729	1.33
ZMR019	12.8	292	0.869	73.1	31.3	63.4	9.63	-	5.07	2.86	1.26	4.01	5.89	7.62	0.870	1.80	37.3	0.433	0.421	0.0290	0.784

	Al_2O_3	Ba	CaO	Ce	Co	Cr	Cs	Cu	Dy	Er	Eu	Fe_2O_3	Gd	Hf	Ho	K_2O	La	Lu	MgO	MnO	Na_2O
ZMR020	13.0	442	**11.2**	67.7	25.0	45.2	7.73	-	4.69	2.65	1.16	3.86	5.41	5.39	0.818	3.18	33.4	0.405	2.20	0.0630	1.26
ZMR021	12.9	433	**11.4**	68.8	36.6	53.2	6.29	-	4.70	2.61	1.15	4.12	5.38	5.55	0.800	3.22	33.6	0.374	2.32	0.0642	1.34
ZMR022	13.2	297	1.01	80.8	20.4	56.2	7.82	-	4.71	2.57	1.13	3.34	5.39	7.36	0.795	1.58	41.2	0.364	0.450	0.0171	0.731
ZMR023	14.3	317	1.51	74.7	24.9	61.2	11.1	-	4.79	2.76	1.13	4.43	5.63	7.41	0.831	1.69	38.3	0.415	0.483	0.0177	0.759
ZMR024	11.5	298	0.398	72.9	30.8	58.0	6.99	-	4.45	2.56	1.16	4.18	5.29	7.50	0.786	1.37	37.6	0.377	0.422	0.0345	0.730
ZMR025	13.2	285	0.561	66.1	36.1	54.5	11.2	-	5.23	2.92	1.08	4.15	5.29	7.98	0.866	1.54	33.9	0.443	0.429	0.0150	0.720
ZMR026	12.4	424	**9.88**	66.8	30.7	45.5	6.07	-	4.56	2.49	1.15	3.75	5.37	5.56	0.776	3.12	32.4	0.339	2.24	0.0589	1.34
ZMR027	11.7	409	**13.0**	63.8	21.4	50.9	5.64	-	4.54	2.46	1.13	4.22	5.05	5.25	0.755	3.54	31.1	0.341	2.31	0.0684	1.37
ZMR028	20.1	351	3.75	70.9	20.3	36.0	9.38	-	4.10	1.96	1.51	3.21	6.19	3.07	0.650	2.18	34.7	0.200	0.558	0.0164	0.809
ZMR029	16.0	357	1.18	105	29.0	85.6	13.0	-	4.83	2.69	1.41	5.20	6.45	8.41	0.818	2.92	50.6	0.379	0.559	0.0215	0.947
ZMR030	12.2	277	1.46	72.3	60.2	61.9	7.25	-	5.09	2.80	1.16	4.47	5.54	8.87	0.820	1.48	36.3	0.433	0.468	0.0290	0.699
ZMR031	12.4	409	**11.1**	63.7	21.0	48.8	4.48	-	4.16	2.27	1.18	4.00	4.96	4.57	0.715	3.30	31.1	0.326	2.66	0.0608	1.16
ZMR032	21.5	482	1.75	111	27.6	57.7	15.8	-	5.20	2.33	2.05	4.86	8.03	3.78	0.784	2.26	56.0	0.279	0.720	0.0194	0.808
ZMR033	19.4	389	0.733	76.0	53.4	42.9	11.3	-	7.07	3.18	2.30	3.60	9.05	3.35	1.00	3.14	36.5	0.395	0.552	0.0204	0.837
ZMR034	13.8	461	**10.4**	68.1	27.2	58.0	6.20	-	4.56	2.50	1.32	4.49	5.39	4.59	0.815	3.54	33.2	0.350	2.91	0.0703	1.22
ZMR035	21.3	418	0.455	64.7	30.7	51.8	17.5	-	6.59	2.92	1.99	4.93	7.95	3.78	0.961	3.92	32.5	0.399	0.734	0.0231	0.894
ZMR036	17.4	506	**7.48**	89.2	20.2	79.2	7.92	-	5.29	2.77	1.67	5.95	6.65	4.46	0.878	3.65	43.7	0.415	1.88	0.0919	0.963
ZMR037	22.5	291	0.473	92.4	20.1	14.3	10.8	1.74	4.14	1.81	1.95	2.12	7.46	2.85	0.592	2.12	39.7	0.128	0.769	0.0101	0.348
ZMR038	26.5	334	3.80	44.3	27.9	20.9	33.4	15.6	6.76	3.52	1.13	2.58	6.54	5.19	1.12	3.35	21.2	0.499	0.949	0.0383	0.670
ZMR039	23.2	459	2.63	82.2	7.44	29.9	10.9	6.33	4.99	2.10	1.93	2.85	8.01	3.19	0.718	2.80	35.4	0.137	0.746	0.00933	0.484
ZMR040	11.9	377	**18.5**	67.1	22.6	50.4	2.58	14.1	4.59	2.57	1.35	3.81	5.79	5.91	0.768	2.85	33.6	0.322	1.94	0.0711	0.711
ZMR041	8.7	276	**15.1**	50.3	9.40	32.9	3.34	4.71	3.37	1.99	0.924	2.95	4.35	4.87	0.614	2.52	24.9	0.227	1.54	0.0489	0.651
ZMR042	21.7	277	2.34	54.6	15.6	22.7	25.3	4.65	5.29	2.77	0.969	2.30	5.76	4.54	0.845	2.97	27.1	0.311	0.758	0.0367	0.566
ZMR043	25.6	314	4.02	45.4	10.5	21.1	29.5	1.67	5.43	2.98	0.876	2.52	5.43	4.80	0.871	3.84	21.5	0.336	1.02	0.0437	0.583
ZMR044	24.9	294	4.03	46.3	9.38	22.5	34.4	2.39	5.24	3.00	0.787	2.51	4.98	4.92	0.890	3.73	21.1	0.355	0.853	0.0422	0.653

	Al_2O_3	Ba	CaO	Ce	Co	Cr	Cs	Cu	Dy	Er	Eu	Fe_2O_3	Gd	Hf	Ho	K_2O	La	Lu	MgO	MnO	Na_2O
ZMR045	13.6	385	**7.09**	72.0	16.9	64.3	5.62	18.4	4.56	2.56	1.42	4.54	5.98	4.58	0.759	3.36	36.4	0.336	1.86	0.0591	0.597
ZMR046	16.2	425	**19.2**	79.2	29.3	73.7	7.32	49.3	5.27	2.93	1.47	5.30	6.78	4.95	0.875	3.84	42.2	0.425	3.02	0.0803	0.523
ZMR047	10.6	307	**13.8**	55.4	14.2	44.0	5.87	74.4	3.74	2.11	1.06	3.31	4.89	3.42	0.671	2.73	28.5	0.233	1.97	0.0347	0.462
ZMR048	17.0	469	**9.09**	90.2	18.1	74.5	7.61	64.1	5.70	3.02	1.74	5.82	7.59	5.33	0.931	3.51	45.9	0.416	2.44	0.0929	0.606
ZMR049	11.3	376	**19.3**	67.5	12.7	43.1	3.21	115	4.44	2.60	1.22	3.70	5.69	5.55	0.742	2.89	33.5	0.290	2.15	0.0560	0.764
ZMR050	22.3	606	5.04	94.8	17.4	93.0	9.87	74.0	5.89	3.28	1.91	7.47	7.80	4.46	0.972	5.38	47.8	0.380	2.40	0.0488	0.624
ZMR051	11.8	408	**10.3**	70.7	11.4	40.7	5.46	75.3	5.06	2.85	1.39	3.62	6.20	5.94	0.833	3.01	35.4	0.346	1.77	0.0554	0.693
ZMR052	13.6	427	**16.5**	75.1	12.6	44.7	6.42	58.4	5.15	2.79	1.42	4.21	6.39	5.52	0.826	3.40	37.4	0.363	2.17	0.0645	0.669
ZMR053	9.1	337	**12.0**	59.7	12.5	29.3	4.05	105	4.11	2.32	1.12	2.95	5.17	5.15	0.697	2.51	29.4	0.298	1.59	0.0424	0.553
ZMR054	10.7	392	**18.6**	63.9	10.7	41.5	4.14	50.8	4.49	2.36	1.24	3.57	5.48	5.72	0.729	2.45	31.7	0.269	1.74	0.0484	0.473
ZMR055	10.1	304	**16.7**	59.8	9.58	38.4	2.85	107	4.19	2.31	1.08	3.34	5.14	5.68	0.697	2.52	29.4	0.305	1.94	0.0439	0.578
ZMR056	12.1	437	**20.7**	67.7	11.7	44.9	3.11	45.8	4.61	2.53	1.28	3.92	5.51	5.48	0.778	2.83	33.6	0.310	2.07	0.0620	0.773
ZMR057	11.2	415	**15.8**	69.0	23.2	40.7	4.69	18.9	4.95	2.63	1.36	3.59	5.86	5.72	0.772	2.89	34.7	0.353	2.16	0.0591	0.611
ZMR058	12.8	421	**17.1**	74.3	33.1	49.1	5.50	18.7	5.47	2.77	1.44	3.86	6.45	6.00	0.839	3.33	37.3	0.425	2.46	0.0559	0.645
ZMR059	9.3	316	**13.8**	53.4	12.0	33.6	2.91	10.6	3.48	1.98	1.05	3.24	4.54	4.78	0.657	2.43	26.8	0.242	1.86	0.0451	0.498
ZMR060	9.6	341	**13.6**	58.3	9.69	33.0	4.93	7.64	4.24	2.32	1.09	3.00	5.16	4.54	0.718	2.58	29.4	0.293	2.15	0.0480	0.550
ZMR061	10.4	376	**14.8**	63.7	11.7	42.6	4.55	6.69	4.29	2.52	1.27	3.44	5.62	5.37	0.769	2.98	31.9	0.337	2.35	0.0524	0.724
ZMR062	18.0	246	4.10	71.7	4.59	13.5	6.36	-	2.94	1.50	1.08	1.70	5.35	2.71	0.499	2.35	33.3	0.048	0.584	0.00476	0.546
ZMR063	22.7	343	**8.30**	89.8	7.29	18.9	7.58	-	3.56	1.70	1.54	2.10	6.59	3.00	0.563	2.24	43.3	0.092	0.538	0.00564	0.484
ZMR065	13.6	458	**10.5**	69.4	35.0	50.4	5.83	-	4.74	2.62	1.24	3.96	5.50	5.16	0.796	2.99	33.5	0.359	2.29	0.0640	1.18
BNV001	13.5	457	**14.3**	73.7	20.8	64.4	3.98	38.2	4.63	2.47	1.35	5.18	5.84	5.66	0.759	3.14	37.6	0.383	1.81	0.0561	0.565
BNV002	8.5	282	**11.9**	50.7	12.2	41.2	3.07	33.0	3.23	1.85	0.955	3.55	4.24	3.98	0.585	1.95	25.2	0.216	1.73	0.0493	0.507
BNV003	14.7	413	**13.5**	78.8	13.4	72.7	4.92	84.7	5.00	2.66	1.59	5.69	6.56	5.38	0.808	3.74	39.4	0.410	1.55	0.0610	0.518
BNV004	10.2	337	**9.31**	55.4	23.2	50.0	3.57	59.7	3.54	2.02	1.09	4.28	4.80	3.41	0.613	2.54	27.3	0.257	1.66	0.0424	0.506
BNV005	21.7	616	1.90	95.6	34.0	109	7.88	43.4	6.31	3.13	2.10	8.03	8.09	5.56	0.939	3.36	47.3	0.567	1.21	0.0487	0.634

	Al_2O_3	Ba	CaO	Ce	Co	Cr	Cs	Cu	Dy	Er	Eu	Fe_2O_3	Gd	Hf	Ho	K_2O	La	Lu	MgO	MnO	Na_2O
BNV006	20.3	655	0.599	80.1	24.2	96.4	7.03	55.7	5.22	2.70	1.82	6.88	6.92	4.43	0.809	3.23	40.7	0.458	1.10	0.0342	0.591
BNV007	24.7	657	1.54	84.5	30.8	122	8.84	54.6	5.51	2.80	1.90	8.73	7.16	4.64	0.806	3.72	43.4	0.457	1.38	0.0444	0.587
BNV008	21.2	583	1.18	72.3	20.3	109	7.44	48.4	4.60	2.38	1.64	7.09	6.18	4.04	0.737	3.33	36.9	0.398	1.24	0.0320	0.566
BNV009	22.9	668	1.73	89.9	35.4	122	8.71	27.8	6.00	3.18	2.06	8.31	8.01	5.24	0.943	3.73	45.2	0.527	1.33	0.0438	0.633
BNV010	22.1	576	1.79	85.3	35.9	120	7.21	15.2	5.42	2.78	1.91	7.92	7.06	5.29	0.820	3.36	43.7	0.429	1.30	0.0384	0.628
BNV011	23.8	673	1.44	85.7	31.5	122	9.05	12.8	5.43	2.90	1.91	8.00	7.24	4.94	0.870	3.59	44.3	0.481	1.31	0.0360	0.612
BNV012	25.9	713	1.90	86.0	29.5	141	8.41	10.1	5.60	2.98	2.01	9.53	7.50	4.66	0.853	3.99	44.6	0.458	1.59	0.0529	0.621
BNV013	25.1	696	1.90	89.8	25.6	135	8.94	6.40	6.13	3.10	2.09	8.93	7.92	4.51	0.927	4.05	46.1	0.496	1.59	0.0515	0.628
BNV014	25.0	672	1.82	84.5	21.6	131	8.01	5.72	5.54	2.93	1.86	8.49	7.27	5.32	0.874	3.91	44.4	0.440	1.54	0.0420	0.637
BNV015	26.0	679	4.29	90.5	27.5	134	9.12	5.69	5.82	3.07	1.89	8.89	7.73	4.96	0.892	4.00	47.0	0.443	1.49	0.0426	0.615
BNV016	25.0	731	1.91	92.5	31.2	132	8.36	5.81	5.89	3.00	1.94	9.41	7.87	5.38	0.899	3.89	47.9	0.475	1.45	0.0577	0.612
TOR001	21.0	596	2.16	103	25.5	89.7	8.23	16.7	6.32	3.35	2.21	6.71	8.56	5.41	0.982	3.83	52.7	0.535	1.17	0.0251	0.501
TOR002	14.9	464	0.689	74.0	16.9	68.3	8.26	19.4	4.66	2.43	1.47	4.84	6.23	4.03	0.729	3.32	37.6	0.338	0.859	0.0192	0.449
TOR003	21.3	623	1.86	101	16.2	91.5	8.66	71.2	6.80	3.36	2.14	6.50	8.31	4.92	0.977	3.77	51.3	0.498	1.16	0.0251	0.485
TOR004	15.0	458	0.872	71.1	10.8	61.8	7.50	105	4.63	2.43	1.53	4.62	6.03	3.75	0.751	3.40	35.2	0.343	0.863	0.0160	0.455
TOR005	20.4	583	1.68	99.1	19.4	85.7	10.5	24.6	6.32	3.29	1.95	6.08	7.97	5.01	0.982	3.77	51.2	0.492	1.04	0.0234	0.507
TOR006	16.1	547	0.871	82.9	16.5	69.9	8.47	7.72	5.62	2.87	1.61	5.48	6.78	4.84	0.814	3.46	42.2	0.439	1.11	0.0404	0.453
TOR007	21.7	613	1.26	96.9	17.2	94.0	11.0	8.87	6.19	3.02	2.04	6.43	7.63	4.94	0.886	4.04	49.8	0.480	1.11	0.0234	0.475
TOR008	22.7	657	1.82	105	20.7	110	9.95	7.04	7.00	3.28	2.13	7.21	8.36	5.19	0.960	4.33	53.3	0.511	1.34	0.0316	0.524
TOR009	15.4	397	1.43	84.4	13.4	47.6	10.7	3.74	5.12	2.56	1.19	4.34	6.65	6.03	0.768	3.70	40.7	0.335	1.55	0.0512	1.07
TOR010	20.0	638	1.76	105	25.9	92.2	8.81	4.84	6.53	3.35	2.11	7.05	8.43	6.42	0.969	3.85	52.8	0.515	1.19	0.0648	0.518
TOR011	20.9	664	1.56	104	20.1	96.9	10.1	4.27	7.00	3.47	2.16	6.92	8.33	6.17	1.01	4.16	53.0	0.557	1.45	0.0503	0.521
TOR012	19.9	630	2.08	101	25.2	85.3	8.63	6.16	6.60	3.25	2.21	6.35	8.23	6.23	0.981	3.73	51.5	0.533	1.18	0.0451	0.459
TOR013	13.3	475	0.211	69.4	24.4	57.9	7.92	4.40	4.62	2.33	1.35	4.49	5.76	4.14	0.754	3.10	35.0	0.296	0.927	0.0403	0.401
TOR014	20.3	624	0.786	102	32.2	86.9	8.67	10.6	6.69	3.28	2.10	6.32	8.46	6.26	0.951	3.61	51.6	0.554	1.17	0.0535	0.428

	Al_2O_3	Ba	CaO	Ce	Co	Cr	Cs	Cu	Dy	Er	Eu	Fe_2O_3	Gd	Hf	Ho	K_2O	La	Lu	MgO	MnO	Na_2O
U (%)	53	6	12	31	19	30	28	26	30	15	10	32	16	22	21	30	31	57	14	53	172

(jarraipena)

Laginak	Nb	Nd	Ni	P_2O_5	Pb	Pr	Rb	SiO_2	Sm	Sn	Sr	Ta	Tb	Th	TiO_2	Tm	U	V	Yb	Zn	Zr
ZMR001	13.0	33.2	-	-	9.50E+02	8.04	126	63.7	6.23	15.5	186	1.26	0.807	12.4	0.645	0.380	2.87	58.3	2.50	-	238
ZMR002	12.4	31.7	-	-	8.99E+02	7.64	121	74.3	6.13	15.6	184	1.27	0.773	12.5	0.661	0.365	2.77	59.7	2.32	-	248
ZMR003	14.1	36.1	-	-	6.82E+02	8.73	131	67.4	6.76	46.3	189	1.45	0.860	14.5	0.640	0.397	3.22	55.7	2.69	-	270
ZMR004	13.5	35.2	-	-	7.98E+02	8.53	129	73.4	6.67	28.7	194	1.36	0.843	14.1	0.679	0.382	3.09	57.2	2.47	-	243
ZMR005	12.6	30.5	-	-	2.74E+03	7.41	116	70.3	5.64	27.4	206	1.14	0.741	11.8	0.728	0.330	2.95	72.0	2.23	-	194
ZMR006	11.9	29.2	-	-	2.06E+03	7.12	120	75.4	5.87	8.67	188	1.25	0.729	11.7	0.730	0.343	2.84	67.0	2.35	-	214
ZMR007	17.1	35.7	-	-	4.40E+02	8.68	96.1	82.8	6.58	8.09	103	1.97	0.833	14.7	0.972	0.386	3.01	58.4	2.68	-	359
ZMR008	11.8	29.4	-	-	5.99E+02	7.27	118	64.2	5.64	17.6	191	1.16	0.724	11.6	0.626	0.334	2.67	55.0	2.27	-	198
ZMR009	17.8	32.4	-	-	6.68E+02	7.74	94.1	83.8	6.52	7.99	69.7	2.00	0.854	14.6	1.01	0.427	3.24	54.5	2.88	-	361
ZMR010	17.1	45.2	-	-	1.52E+02	10.9	148	63.2	7.97	7.90	203	1.72	1.04	15.9	0.946	0.436	3.67	116	2.85	-	181
ZMR011	12.5	31.1	-	-	4.44E+01	7.15	136	72.6	6.61	16.9	163	2.08	0.708	7.46	0.495	0.235	2.87	68.0	1.71	-	93.8
ZMR012	12.0	42.1	-	-	1.15E+04	10.0	135	67.3	8.18	20.9	197	1.88	0.902	9.88	0.493	0.249	2.80	57.2	1.93	-	126
ZMR013	12.2	49.1	-	-	3.23E+01	12.0	105	79.3	8.90	19.0	109	2.04	0.807	9.76	0.419	0.210	2.02	48.4	1.55	-	129
ZMR014	16.9	32.2	-	-	4.47E+02	7.97	107	81.7	6.32	8.48	77.2	1.91	0.826	14.2	0.998	0.375	3.15	66.1	2.63	-	318
ZMR015	11.2	41.6	-	-	5.01E+04	9.44	126	58.8	8.55	16.5	92.8	1.57	1.11	9.08	0.441	0.342	2.26	59.6	2.29	-	103
ZMR016	15.9	32.8	-	-	4.86E+02	7.73	91.9	81.5	6.45	7.58	66.5	1.78	0.809	13.8	0.945	0.422	3.54	59.7	2.85	-	394
ZMR017	12.9	33.1	-	-	4.10E+03	8.02	119	54.4	6.56	60.1	226	1.28	0.789	12.5	0.595	0.352	3.14	60.5	2.40	-	205
ZMR018	12.5	33.2	-	-	4.32E+03	8.04	117	73.8	6.39	49.4	200	1.26	0.787	12.5	0.702	0.356	3.06	68.9	2.38	-	219
ZMR019	15.6	36.6	-	-	1.05E+03	8.58	99.6	70.1	7.40	7.88	77.1	1.81	0.925	14.4	0.946	0.410	3.31	55.1	2.81	-	348
ZMR020	13.1	34.1	-	-	1.97E+03	8.09	135	60.5	6.69	70.0	225	1.28	0.849	13.1	0.604	0.400	3.25	56.4	2.57	-	228
ZMR021	13.1	34.3	-	-	4.44E+03	8.29	118	66.2	6.79	69.2	220	1.26	0.822	13.0	0.651	0.371	3.30	71.3	2.52	-	243

	Nb	Nd	Ni	P_2O_5	Pb	Pr	Rb	SiO_2	Sm	Sn	Sr	Ta	Tb	Th	TiO_2	Tm	U	V	Yb	Zn	Zr
ZMR022	16.1	37.0	-	-	7.44E+02	9.00	96.6	74.9	7.02	7.75	94.8	1.74	0.825	14.6	0.832	0.412	3.13	55.1	2.67	-	356
ZMR023	17.5	34.5	-	-	5.27E+02	8.31	112	70.9	6.74	9.92	95.7	1.97	0.861	15.6	0.890	0.408	3.27	58.5	2.81	-	356
ZMR024	14.7	35.5	-	-	3.07E+02	8.41	81.2	67.8	6.95	6.93	109	1.73	0.828	13.5	0.819	0.380	3.28	45.0	2.62	-	359
ZMR025	19.4	30.2	-	-	9.43E+02	7.39	95.5	76.1	6.07	9.73	71.1	2.23	0.910	14.9	0.941	0.462	3.34	52.0	2.95	-	384
ZMR026	12.9	33.4	-	-	6.05E+03	8.01	123	61.5	6.50	95.6	195	1.31	0.813	12.9	0.623	0.377	3.15	58.5	2.48	-	240
ZMR027	12.6	32.5	-	-	4.05E+03	7.59	115	71.3	5.96	53.4	201	1.20	0.797	12.1	0.680	0.395	3.07	64.8	2.43	-	219
ZMR028	12.9	39.7	-	-	1.46E+03	9.31	127	67.2	8.10	25.2	241	2.63	0.862	8.58	0.355	0.260	2.80	43.8	1.66	-	109
ZMR029	18.0	46.4	-	-	7.79E+02	11.4	124	74.2	7.98	10.3	95.4	1.94	0.921	15.5	0.930	0.422	3.93	81.9	2.77	-	375
ZMR030	15.3	35.1	-	-	1.57E+02	8.31	88.7	86.8	6.67	7.27	78.7	1.82	0.894	13.5	0.896	0.483	3.51	69.8	2.91	-	430
ZMR031	12.5	31.5	-	-	6.78E+02	7.56	105	50.2	5.83	11.0	261	1.15	0.752	11.9	0.554	0.394	3.12	64.7	2.34	-	195
ZMR032	14.0	60.7	-	-	6.06E+02	14.8	128	67.0	10.3	19.1	193	2.05	1.03	11.7	0.472	0.336	3.05	68.7	2.17	-	146
ZMR033	11.9	51.9	-	-	1.63E+04	11.1	148	60.6	10.9	24.7	129	2.13	1.39	11.2	0.435	0.474	2.47	54.7	2.73	-	130
ZMR034	13.7	33.5	-	-	8.57E+03	7.97	123	55.7	6.33	79.6	229	1.53	0.822	12.9	0.665	0.398	3.15	74.9	2.50	-	185
ZMR035	14.2	42.4	-	-	1.21E+02	9.49	185	69.5	9.17	25.2	112	2.86	1.26	10.4	0.469	0.447	2.88	59.4	2.77	-	141
ZMR036	17.4	43.8	-	-	1.87E+02	10.5	140	59.6	7.85	6.61	207	1.52	0.965	15.6	0.833	0.448	3.66	105	2.74	-	175
ZMR037	14.5	51.7	6.62	0.1	5.28E+01	12.4	147	76.7	9.61	16.3	248	3.56	0.421	7.79	0.218	0.250	-	22.1	1.65	13.4	96
ZMR038	26.1	21.5	12.1	1.1	4.38E+01	5.44	478	71.3	5.15	35.4	126	8.30	0.460	7.83	0.275	0.597	-	25.9	3.51	90.7	209
ZMR039	15.3	46.2	9.80	1.3	8.88E+01	11.1	155	77.0	9.29	46.8	275	3.56	0.435	9.00	0.337	0.278	-	30.5	1.76	66.2	117
ZMR040	13.9	31.4	30.5	2.2	9.22E+03	8.04	91.8	58.6	6.28	31.9	328	1.43	0.424	12.5	0.556	0.427	-	46.7	2.40	54.6	337
ZMR041	10.0	23.4	14.8	0.6	3.85E+03	6.05	89.1	47.7	4.57	22.6	233	0.88	0.402	9.58	0.417	0.329	-	38.3	1.98	25.3	264
ZMR042	22.7	26.6	11.4	0.4	9.87E+01	6.67	375	57.9	5.44	32.3	141	6.90	0.444	8.59	0.272	0.438	-	25.1	2.60	39.2	196
ZMR043	25.5	21.5	9.40	0.2	4.68E+01	5.40	451	69.9	5.12	32.7	102	7.95	0.426	8.65	0.276	0.478	-	22.5	2.78	46.4	212
ZMR044	24.1	19.4	6.75	0.1	5.47E+01	5.16	455	71.5	4.57	34.8	57.9	7.73	0.452	8.57	0.312	0.498	-	23.3	2.97	75.3	227
ZMR045	14.7	33.1	25.6	0.5	2.86E+03	8.60	121	55.9	6.47	67.5	217	1.40	0.402	12.4	0.584	0.417	-	70.3	2.70	57.8	254
ZMR046	17.4	39.2	35.6	0.9	8.35E+03	9.84	149	54.6	7.19	22.5	314	1.92	0.434	14.4	0.655	0.460	-	71.1	2.95	49.6	257

	Nb	Nd	Ni	P_2O_5	Pb	Pr	Rb	SiO_2	Sm	Sn	Sr	Ta	Tb	Th	TiO_2	Tm	U	V	Yb	Zn	Zr
ZMR047	12.1	26.0	20.3	0.9	1.11E+04	6.60	111	37.0	5.07	13.5	224	1.28	0.414	9.78	0.471	0.329	-	48.2	2.16	62.1	160
ZMR048	18.7	43.0	31.9	0.6	2.19E+03	10.9	148	66.9	7.91	34.5	258	1.85	0.437	15.8	0.747	0.480	-	74.0	3.00	70.3	292
ZMR049	12.9	32.0	18.0	0.4	3.76E+03	8.05	101	61.7	5.80	10.2	346	1.33	0.414	12.4	0.548	0.375	-	46.2	2.59	45.6	318
ZMR050	21.6	45.3	40.7	0.4	6.39E+01	11.5	205	63.0	8.36	5.51	241	2.37	0.478	18.0	0.818	0.516	-	99.1	3.22	98.1	212
ZMR051	14.5	33.2	16.4	1.3	1.01E+03	8.45	129	56.6	6.43	7.55	235	1.50	0.418	13.4	0.567	0.455	-	42.4	2.85	58.5	338
ZMR052	15.3	35.4	21.9	3.6	9.69E+02	8.84	141	58.5	6.58	6.22	327	1.59	0.420	14.2	0.577	0.450	-	51.3	2.75	100	293
ZMR053	12.0	28.1	14.7	3.9	1.47E+03	7.21	105	44.4	5.50	4.26	243	1.21	0.421	11.6	0.448	0.386	-	34.2	2.42	77.1	281
ZMR054	13.2	29.1	24.5	1.7	2.92E+03	7.59	104	59.7	5.67	6.99	282	1.20	0.431	11.5	0.493	0.405	-	35.9	2.40	47.7	308
ZMR055	11.9	26.9	17.3	1.2	5.01E+03	7.09	94.0	51.0	5.32	16.2	279	1.14	0.412	11.0	0.445	0.395	-	35.7	2.37	32.8	319
ZMR056	13.3	31.1	21.1	1.3	1.36E+04	8.05	97.9	58.4	6.19	12.6	388	1.35	0.448	12.4	0.496	0.388	-	46.9	2.59	34.0	307
ZMR057	13.9	32.7	17.1	3.3	9.01E+02	8.31	115	53.8	6.40	5.02	278	1.51	0.417	12.8	0.537	0.419	-	41.5	2.67	65.7	310
ZMR058	14.9	35.5	19.6	2.4	1.07E+03	8.84	131	57.3	6.98	7.10	300	1.54	0.415	14.4	0.577	0.467	-	50.9	2.82	65.8	337
ZMR059	10.8	25.4	8.42	3.6	5.22E+03	6.22	90.0	49.3	4.90	5.62	326	1.06	0.404	9.55	0.432	0.311	-	38.4	2.02	35.9	252
ZMR060	12.0	27.6	11.1	2.0	3.48E+03	6.87	114	41.8	5.54	5.95	261	1.11	0.421	10.7	0.460	0.358	-	37.0	2.37	29.9	230
ZMR061	13.1	29.7	11.2	1.6	1.53E+03	7.65	113	54.1	6.16	6.33	273	1.30	0.450	11.8	0.562	0.401	-	44.0	2.61	56.7	295
ZMR062	12.2	32.9	0.431	0.1	5.12E+01	8.49	102	52.2	6.14	11.2	375	2.67	0.426	6.61	0.215	0.190	-	19.8	1.34	4.04	93.9
ZMR063	15.0	44.2	3.13	0.1	8.31E+01	11.2	119	70.1	8.47	14.4	1.02E+03	3.32	0.463	9.21	0.261	0.230	-	23.9	1.56	18.9	104
ZMR065	13.8	34.2	-	-	1.07E+03	8.22	124	60.5	6.35	72.6	232	1.38	0.850	12.9	0.612	0.411	3.28	65.1	2.59	-	217
BNV001	14.3	34.0	27.8	0.9	4.94E+04	8.78	103	63.6	6.31	551	422	1.34	0.410	12.7	0.565	0.432	-	81.8	2.67	34.4	310
BNV002	9.7	23.0	14.6	0.3	6.48E+03	5.97	82.6	39.3	4.32	8.14	370	0.76	0.400	8.47	0.390	0.307	-	47.9	1.88	13.1	200
BNV003	15.2	35.4	30.3	1.0	1.49E+04	9.28	122	61.8	6.68	7.35	454	1.44	0.456	13.6	0.568	0.444	-	83.0	2.74	33.9	293
BNV004	10.2	24.8	18.7	0.5	7.97E+03	6.43	89.8	47.6	5.02	11.5	321	0.77	0.413	9.43	0.382	0.335	-	57.5	2.03	23.4	154
BNV005	19.7	45.4	35.8	0.2	8.07E+01	11.3	164	68.9	8.10	3.01	120	1.89	0.429	18.9	0.835	0.553	-	107	3.37	49.2	320
BNV006	18.5	37.5	28.9	0.1	9.43E+01	9.49	159	53.0	6.90	3.09	109	1.68	0.418	16.2	0.744	0.451	-	102	2.77	55.5	237
BNV007	20.4	40.1	32.0	0.1	8.11E+01	10.1	182	64.7	7.36	3.27	132	1.92	0.409	18.9	0.828	0.491	-	122	2.84	54.7	246

	Nb	Nd	Ni	P_2O_5	Pb	Pr	Rb	SiO_2	Sm	Sn	Sr	Ta	Tb	Th	TiO_2	Tm	U	V	Yb	Zn	Zr
BNV008	18.0	34.2	26.8	0.1	5.62E+01	8.67	158	54.6	6.23	3.24	116	1.55	0.410	15.5	0.745	0.434	-	110	2.60	54.8	207
BNV009	20.8	41.7	30.7	0.2	2.80E+01	10.7	180	64.5	8.10	3.11	122	2.06	0.482	18.5	0.844	0.547	-	111	3.27	71.4	278
BNV010	19.3	40.4	32.9	0.1	4.14E+01	10.3	153	71.9	7.32	2.88	117	1.89	0.412	17.5	0.853	0.470	-	118	2.93	43.4	297
BNV011	20.4	40.9	33.7	0.1	4.63E+01	10.2	180	66.6	7.65	3.00	124	1.90	0.430	18.6	0.817	0.495	-	123	2.92	60.8	269
BNV012	20.9	41.2	43.7	0.1	7.97E+01	10.4	181	68.8	7.86	3.31	140	2.00	0.421	19.1	0.843	0.489	-	121	3.00	59.1	234
BNV013	21.4	43.6	42.9	0.1	3.97E+01	10.7	186	67.3	8.13	3.57	137	1.93	0.429	18.6	0.822	0.525	-	121	3.13	48.9	237
BNV014	22.1	40.7	39.4	0.1	4.59E+01	10.1	173	69.1	7.46	3.15	137	1.93	0.400	19.0	0.913	0.490	-	118	3.07	42.6	286
BNV015	21.4	43.1	45.7	0.1	5.01E+01	10.8	187	68.3	8.23	3.49	141	1.99	0.430	20.0	0.815	0.513	-	123	3.21	55.7	253
BNV016	21.5	44.5	44.8	0.1	8.53E+01	10.9	175	72.0	8.03	3.95	134	1.92	0.427	20.0	0.840	0.497	-	123	3.11	75.9	293
TOR001	19.4	49.5	32.4	0.1	4.35E+02	12.3	175	72.2	8.73	4.12	202	2.04	0.445	19.0	0.752	0.568	-	104	3.29	44.3	288
TOR002	14.0	34.9	21.7	0.0	1.80E+03	8.77	155	46.6	6.51	3.46	149	1.41	0.414	13.6	0.588	0.407	-	76.6	2.59	52.2	199
TOR003	19.5	49.3	35.7	0.1	8.68E+02	12.3	178	69.4	8.74	4.06	211	2.07	0.413	19.0	0.766	0.552	-	88.0	3.51	50.4	272
TOR004	13.9	32.5	20.2	0.0	1.09E+03	8.51	142	44.5	6.06	3.26	142	1.30	0.412	13.5	0.519	0.422	-	75.9	2.47	43.6	189
TOR005	18.8	48.5	28.5	0.1	7.05E+03	12.0	186	66.0	8.56	4.31	185	1.99	0.462	18.6	0.731	0.540	-	88.8	3.39	52.7	281
TOR006	16.2	38.9	26.3	0.1	1.94E+02	10.0	155	57.8	7.19	3.61	153	1.66	0.431	15.4	0.630	0.495	-	86.2	2.94	51.2	257
TOR007	19.0	47.0	35.2	0.1	5.92E+01	11.9	194	62.8	8.28	4.34	190	1.86	0.387	18.9	0.734	0.517	-	87.6	3.09	67.3	259
TOR008	20.4	50.0	42.1	0.2	6.19E+02	12.7	193	70.7	9.09	8.17	219	2.12	0.448	20.2	0.834	0.535	-	105	3.40	64.4	270
TOR009	15.7	40.8	15.1	0.1	4.18E+01	10.5	181	54.9	7.71	5.28	78.1	2.00	0.418	19.2	0.572	0.398	-	51.3	2.61	46.6	332
TOR010	19.8	48.6	43.7	0.2	4.29E+02	12.6	167	73.1	9.13	4.32	181	2.00	0.445	20.0	0.788	0.551	-	104	3.47	54.9	340
TOR011	19.9	48.6	43.5	0.1	2.34E+02	12.8	183	75.7	9.00	4.24	194	2.01	0.451	19.6	0.821	0.565	-	107	3.55	60.1	327
TOR012	19.1	48.8	33.5	0.2	3.05E+02	12.3	170	70.4	8.73	4.14	176	1.99	0.432	18.8	0.744	0.555	-	92.9	3.33	40.8	328
TOR013	13.0	31.5	25.4	0.0	1.69E+02	8.37	140	44.7	5.80	2.55	126	1.23	0.405	13.1	0.522	0.383	-	76.0	2.48	50.4	199
TOR014	19.3	49.2	38.0	0.2	1.10E+02	12.5	169	72.5	8.97	3.62	181	2.05	0.398	19.4	0.716	0.560	-	101	3.50	48.6	349
U (%)	4	18	27	16	44	2	21	39	19	149	21	4	-	11	1	25	63	-	27	33	623

ICP-MS-ren bidez lortutako emaitza kimikoak interpretatzeko eta zeramika talde esanguratsuak identifikatzeko, 4. kapituluko 4.5. atalean azaldutako estatistika-prozedurari jarraitu zaio. Prozedura estatistiko horretan, bariantza analitikoa murriztu egin behar da iturri naturalek sor dezaten, eta ez akats esperimentalek eta/edo jalkitze-osteko prozesuetatik datozen aldaketek. Horregatik, estatistika-analisietarako zenbait konposatu ez dira erabili (ikus 4. kapitulua, 4.4.2. atala). Alde batetik, zeramika ehotzeko erabiltzen den tungsteno-karburoaren zelulak zeramika Co eta Ta trazekin kutsa dezakeenez (Boulanger et al., 2013), estatistika-analisietatik ezabatu dira Co eta Ta. Bestalde, Pb beiraduren konposizioaren osagai nagusia denez eta Sn eztainu-berunezko zeramika beiraztatuena ere badenez, tratamendu estatistikoan ez dira erabili, hauek beiraduratik pastara migratzean sor dezaketen kutsadura saihesteko (Molera et al., 2001). Gainera, kuantifikazio-mugatik beherako balioak dituzten osagaiak ere alde batera utzi dira, kasu honetan Cu, Ni, P_2O_5 eta Zn, Olivaresen berreskuratutako zeramikentzat; Cu eta U ZMR062 eta ZMR065 zeramikentzat; eta U, gainerakoentzat. Ohikoa da ere P_2O_5 eta Cu estatistika-errutinetan baztertzea, lurpeko eta itsaspeko inguruneetan agertzen direlako (Buxeda i Garrigós, 1999; Buxeda i Garrigós eta Kilikoglou, 2003; Freestone et al.,1985; Lemoine eta Picon, 1982; Maritan eta Mazzoli, 2004; Molera et al., 1993; Pradell et al., 1996). Gainera, laginen ziurgabetasunari buruzko ohar batzuk eman behar dira. Izan ere, Zamorako zeramikentzat konposatu batzuen ziurgabetasuna handia denez (% 53 Al_2O_3-rentzat, % 57 Lu-rentzat, % 53 MnO-rentzat, % 172 Na_2O-rentzat, % 63 U-rentzat eta % 623 Zr-rentzat), hauek kentzeko aukera aztertu zen. Hala ere, alde batetik, kasu honetan ziurgabetasun altua duten konposatu batzuk garrantzitsuak dira zeramikaren teknologia aztertzeko garaian (adib. Al_2O_3 eta Na_2O, zeintzuek koipegabetzaile edo lehengai motari buruzko informazioa eman baitezakete). Bestalde, konposatuak ezabatzen direnean, laginaren aldakortasunaren ikuspegi osoa baztertzen da. Egia da jalkitze-osteko kutsadurarekin (adibidez, Cu, P_2O_5), laginaren prestaketarekin (adibidez, Co, Ta) eta laginaren izaerarekin (adibidez, Pb, Sn) zerikusia duten konposatuak ezabatu egin direla, eta horrek ere laginaren aldakortasun osoa kontuan ez hartzea dakarrela, baina kasu honetan, aldakortasunari egiten dioten ekarpenak iturri ezagun bat du. Aitzitik, ez da jakina zein den ziurgabetasun altuko konposatuen aldakortasunaren iturria, baina ziur aski materialaren izaerarekin lotuta egongo da (ikus, adibidez, 6.1. irudia, non MnO-k eta Zr-k 64 zeramikazko multzoaren aldakortasunean eragiten dutela erakusten

baita). Aipatutako guztiagatik, konposatu horiek tratamendu estatistikorako mantentzea erabaki da.

4. kapituluan deskribatzen den bezala, aztertutako 94 zeramikak ekoizpen- eta kontsumo-zentroei dagozkie. Hurrengo lerroetan, erreferentzia-taldeak eta zeramika-talde esanguratsuak (PCRU-ak) definitzeko 94 zeramiken azterketa hiru zatitan egingo da: lehenik, Zamora hiriari dagozkion 64 zeramika aztertuko dira (6.1.1. atala). Ondoren, Benaventeri dagozkion 16 zeramika (6.1.2. atala) eta, azkenik, Torori dagozkion 14 zeramika (6.1.3. atala). Erreferentzia-taldeak eta PCRU-ak, definitu ondoren, 6.1.4. atalean deskribatzen dira.

6.1.1. Zamora hirian berreskuratutako zeramikak

Kasu honetan, Zamora hiriko 64 zeramika heterogeneoen (tipologiari dagokionez) multzoak (Olivareseko ZMR001-ZMR036 eta ZMR065; La Concepción-eko ZMR037-ZMR050; Museo Etnografikoko ZMR051-ZMR061 eta Mengue etorbideko ZMR062-ZMR063) vt altua erakusten du (8.46). vt honek Pb, CaO eta Sn-ren ekarpen handia agertzen du (6.1.a irudia), eta datuen multzoa poligenikoa dela iradokitzen du, hau da, zenbait zeramika talde esanguratsu egon daitezkeela (Buxeda i Garrigós eta Kilikoglou, 2003). Alde batetik, Pb eta Sn-ren ekarpena espero zen, eztainu-berunezko beiraduren osagai nagusiak baitira, eta, esan bezala, beiraduratik pastara migratu dezaketelako, pasten Pb eta Sn kontzentrazio globalean eraginez. 64 zeramikak hainbat motatakoak dira, hala nola kaltziodun eta kaltzio baxuko zeramika beiraztatuak (opakuak eta zeharrargiak) eta mikatsuak (beiradura zeharrargiarekin eta gabe), eta hau da elementu horien aldakortasun handiaren arrazoietako bat. Bestalde, CaO-aren aldakortasun handiaren arrazoi bat izan daiteke zeramika batzuk kaltziodunak izatea (≥ % 6), eta beste batzuk kaltzio baxukoak edo mikatsuak izatea (ikus 6.1. taula). eta hori, ziur aski, lehengaien jatorri desberdinari lotuta dago. Gainera, Pb, Sn eta alterazioekin lotutako elementuak (Co eta Ta) errutina estatistikotik kanpo daudenean, vt 4,4-ra jaisten da, oraindik ere balio altua, multzo poligeniko baten izaera iradokitzen duena (6.1.b irudia).

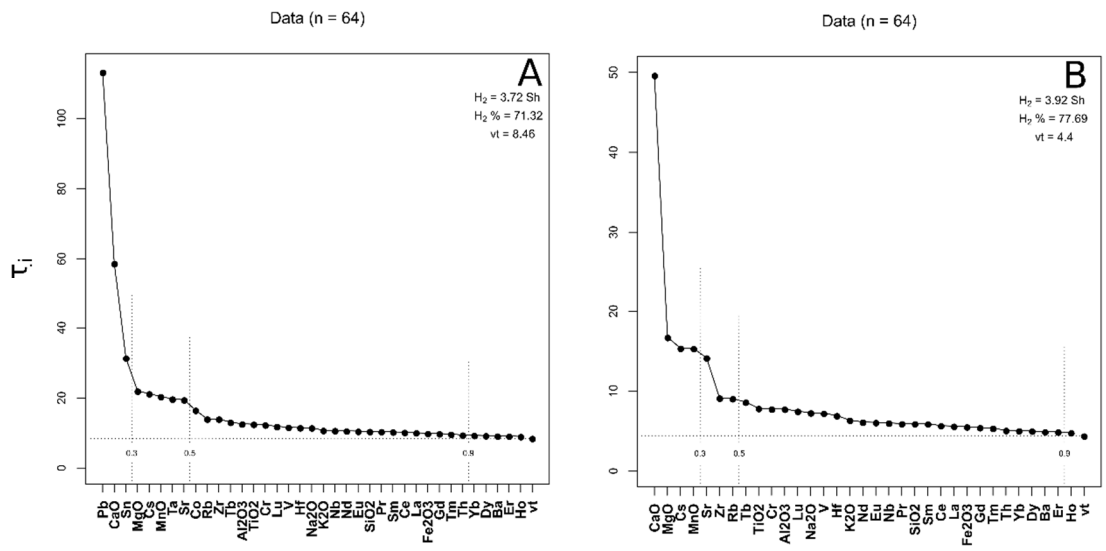

6.1. irudia. ICP-MS bidez aztertutako Zamora hirian berreskuratutako 64 zeramiken Konposizioaren Aldakortasunaren Matrizearen uniformetasunaren irudikapen grafikoa: **(a)** Ni, Cu, P_2O_5, U eta Zn ez dira kontuan hartu, hauen balioak kuantifikazio-mugaren azpitik daudelako; **(b)** Co, Pb, Sn eta Ta ez dira kontuan hartu aipatutakoez gain, kutsaduran eragina izan dezaketelako (y ardatza (τ.i) = elementu bakoitzak datu-multzo osoari egiten dion ekarpen indibiduala, handienetik txikienera; vt = aldakortasun totala; H_2 = informazioaren entropia; H_2% = informazioaren entropiaren ehunekoa, ahal den gehienekoari dagokionez; n = lagin-kopurua)

Olivares produkzio-zentroa zenez, lehenik eta behin, Olivaresen berreskuratutako 37 zeramikak ebaluatu dira, eta Multzokatze Hierarkikoaren Analisia[12] (HCA) egin da, ekoizpen-zentro horretarako egon daitezkeen erreferentzia-taldeak (RG) identifikatzeko (6.2. irudia). Horrela, 6.2. irudiko dendrogramak erakusten du Olivareseko zeramikak 3 PCRU-tan banatzen direla, Z-1, Z-2 eta Z-3 deituak (6.2. taula). PCRU horiek identifikatzea aurrerapauso handia da Zamora eskualdeko zeramika-ekoizpena aztertzeko; izan ere, talde horiek erreferentzia-talde gisa har daitezke, berreskuratu eta analizatu diren akastun-zeramikak eta laberako tresnak talde horien barruan baitaude. Labeko tresnak Z-3 kaltziodun zeramiken taldekoak dira (ikus 6.3. taula); aldiz, akastun zeramikak beiraztatuak dira eta Z-1 (zeramika gorriak) eta Z-2 (mikatsuak) taldeetakoak dira. Literaturaren arabera, Pereruelan eta Muelas del Panen (Zamorako probintziako herrietan) ekoitzi ziren sukalderako zeramika mikatsuen beiraztatzea ez zen bertako lantegietan egin, beste leku batzuetan baizik (Escribano, 2014). Beraz, Olivares lantegi garrantzitsua izan liteke jarduera horri dagokionez, non ekoizpen

[12] Ingeleraz, *Hierarchical Cluster Analysis.*

exogenoen beirak ekoitzi baitziren, literaturan iradokitzen den bezala (Villanueva, 2011). Beraz, kontuan hartu behar da Zamora hiritik kanpo ekoitzitako zeramika mikatsuak beiraztatzeko ekoizpen-taldea izan daitekeela Z-2 taldea; berriz, Z-1 eta Z-3 erreferentzia-taldeak Olivaresekoak dira: lehenengoa, kaltzio eduki baxuko zeramika gorrixketarako, beiradura zeharrargidunak edo beiradurarik gabeak, eta bigarrena, berriz, kaltziodun zeramikarentzat, gehienetan, eztainu-berunez beiraztatuak.

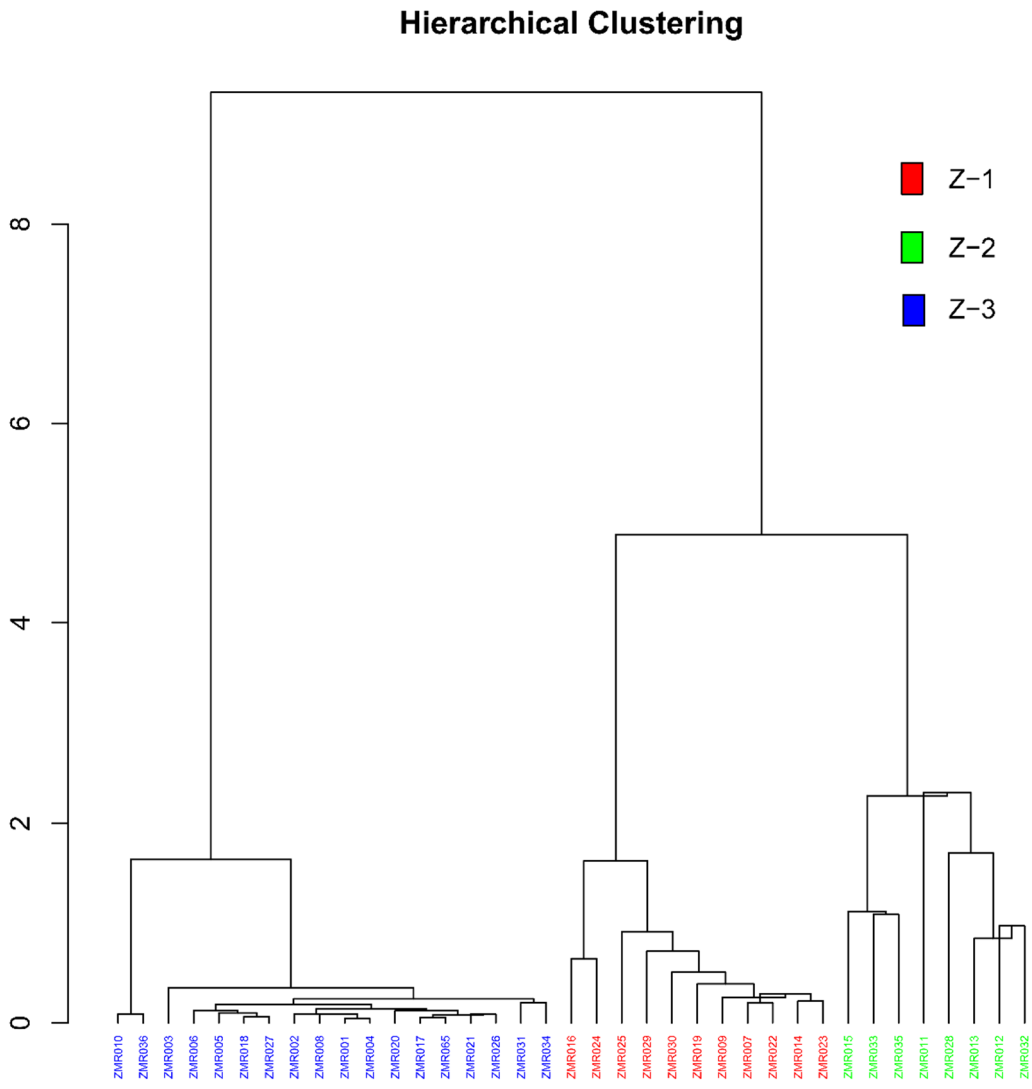

6.2. irudia. Euklidear distantzia karratua eta zentroidearen algoritmoa erabiliz lortutako Olivareseko 37 zeramiken dendrograma, hurrengo azpi-konposiziorako: neurtutako konposatu guztiak (42) Co, Cu, Ni, P_2O_5, Pb, Ta, Sn eta Zn izan ezik, batezbesteko geometrikoaz zatituz. Z-1, Z-2 eta Z-3 = Olivareseko ekoizpenaren erreferentzia-taldeak

6.2. taula. Laginak, gune arkeologikoa, zeramika zein testuingurutan erreskatatu zen, tipologia, beiraduren apaingarrien kolorea, forma, kronologia, erreferentzia-taldea edo PCRU-a eta pastaren kolorea. Taula taldeka ordenatuta dago. ZMR = Zamora hirian berreskuratutako zeramikak; BNV = Benaventen berreskuratutako zeramikak; TOR = Toron berreskuratutako zeramikak; unk = PCRU jakinik gabeko edota jatorri ezezaguneko zeramikak eta erreferentzia-taldea. Kolore beix/arrosak ingelerazko "buff-colour" esan nahi du eta "gorriska"-k kolore gorria baino kolore pixka bat argiagoa esan nahi du

Laginak	Gune arkeologikoa	Testuingurua	Tipologia	Apaingarrien kolorea	Forma	Kronologia	Taldea	Pastaren kolorea
ZMR007	Olivares	01 labea	beiraztatu gabea	-	bola	XIX.bukaera-XX.hasiera	Z-1	gorria
ZMR009	Olivares	01 labea	beiraztatu gabea	-	tina	XIX.bukaera-XX.hasiera	Z-1	gorria
ZMR014	Olivares	01 labea	beiradura zeharrargiduna	beixa (beiradura gordina)	pitxerra	XIX.bukaera-XX.hasiera	Z-1	gorria
ZMR016	Olivares	01 labea	beiradura zeharrargiduna	beixa (beiradura gordina)	pitxerra	XIX.bukaera-XX.hasiera	Z-1	gorria
ZMR019	Olivares	01 labea	beiradura zeharrargiduna	beixa (beiradura gordina)	platera	XIX.bukaera-XX.hasiera	Z-1	gorria
ZMR022	Olivares	02 labea	beiradura zeharrargiduna	marroia	eltzea	XIX.bukaera-XX.hasiera	Z-1	gorria
ZMR023	Olivares	02 labea	beiradura zeharrargiduna	marroia	eltzea	XIX.bukaera-XX.hasiera	Z-1	gorria
ZMR024	Olivares	02 labea	beiradura zeharrargiduna	berdea	eltzea	XIX.bukaera-XX.hasiera	Z-1	gorria
ZMR025	Olivares	02 labea	beiradura zeharrargiduna	marroia	eltzea	XIX.bukaera-XX.hasiera	Z-1	gorria
ZMR029	Olivares	03 labea	beiradura zeharrargiduna	beixa (beiradura gordina)	pitxerra	XIX.bukaera-XX.hasiera	Z-1	gorria
ZMR030	Olivares	03 labea	beiradura zeharrargiduna	beltza (kiskalia)	heldulekua	XIX.bukaera-XX.hasiera	Z-1	beltza
ZMR011	Olivares	01 labea	mikatsua beiraztatu gabea	-	tina	XIX.bukaera-XX.hasiera	Z-2	gorria
ZMR012	Olivares	01 labea	beiradura zeharrargidun zeramika mikatsua	beixa (beiradura gordina)	tina	XIX.bukaera-XX.hasiera	Z-2	gorria
ZMR013	Olivares	01 labea	mikatsua beiraztatu gabea	-	tina	XIX.bukaera-XX.hasiera	Z-2	gorria eta grisa
ZMR015	Olivares	01 labea	beiradura zeharrargidun zeramika mikatsua	beixa (beiradura gordina)	pitxerra	XIX.bukaera-XX.hasiera	Z-2	gorria
ZMR028	Olivares	02 labea	beiradura zeharrargidun zeramika mikatsua	marroia	estalkia	XIX.bukaera-XX.hasiera	Z-2	gorria
ZMR032	Olivares	03 labea	beiradura zeharrargidun zeramika mikatsua	marroia	tina	XIX.bukaera-XX.hasiera	Z-2	gorria

ZMR033	Olivares	03 labea	beiradura zeharrargidun zeramika mikatsua	zuria (kiskalia)	e/e	XIX.bukaera-XX.hasiera	Z-2	beltza
ZMR035	Olivares	03 labea	beiradura zeharrargidun zeramika mikatsua	beltzaska (kiskalia)	heldulekua	XIX.bukaera-XX.hasiera	Z-2	gorria
ZMR001	Olivares	01 labea	beiraztatu gabea	-	bola	XIX.bukaera-XX.hasiera	Z-3	beixa
ZMR002	Olivares	01 labea	eztainu-berunez beiraztatua	zuria eta urdina	platera	XIX.bukaera-XX.hasiera	Z-3	beixa/arrosa
ZMR003	Olivares	01 labea	eztainu-berunez beiraztatua	zuria eta berdea	platera	XIX.bukaera-XX.hasiera	Z-3	beixa/arrosa
ZMR004	Olivares	01 labea	beiraztatu gabea	-	platera	XIX.bukaera-XX.hasiera	Z-3	beixa/arrosa
ZMR005	Olivares	01 labea	eztainu-berunez beiraztatua	zuria eta urdina	platera	XIX.bukaera-XX.hasiera	Z-3	beixa/arrosa
ZMR006	Olivares	01 labea	eztainu-berunez beiraztatua	zuria eta berdea	platera	XIX.bukaera-XX.hasiera	Z-3	beixa/arrosa
ZMR008	Olivares	01 labea	eztainu-berunez beiraztatua	zuria	goporra	XIX.bukaera-XX.hasiera	Z-3	beixa/arrosa
ZMR010	Olivares	01 labea	beiraztatu gabea	-	kopa	XIX.bukaera-XX.hasiera	Z-3	gorriska eta grisa
ZMR017	Olivares	01 labea	beiraztatu gabea	-	trebera (laberako tresna)	XIX.bukaera-XX.hasiera	Z-3	beixa/arrosa
ZMR018	Olivares	01 labea	beiraztatu gabea	-	trebera (laberako tresna)	XIX.bukaera-XX.hasiera	Z-3	beixa/arrosa
ZMR020	Olivares	01 labea	eztainu-berunez beiraztatua	zuria eta berdea	platera	XIX.bukaera-XX.hasiera	Z-3	beixa/arrosa
ZMR021	Olivares	01 labea	eztainu-berunez beiraztatua	zuria eta urdina	platera	XIX.bukaera-XX.hasiera	Z-3	beixa/arrosa
ZMR026	Olivares	02 labea	beiraztatu gabea	-	trebera (laberako tresna)	XIX.bukaera-XX.hasiera	Z-3	beixa/arrosa
ZMR027	Olivares	02 labea	beiraztatu gabea	-	bola	XIX.bukaera-XX.hasiera	Z-3	beixa/arrosa
ZMR031	Olivares	03 labea	beiraztatu gabea	-	bola	XIX.bukaera-XX.hasiera	Z-3	beixa
ZMR034	Olivares	03 labea	beiraztatu gabea	-	trebera (laberako tresna)	XIX.bukaera-XX.hasiera	Z-3	beixa
ZMR036	Olivares	01 labea	beiraztatu gabea	-	kopa	XIX.bukaera-XX.hasiera	Z-3	gorriska eta grisa
ZMR040	La Concepción eliza	urregintza-lantegia	eztainu-berunez beiraztatua	zuria	bola	XV-XVI	Z-3	beixa/arrosa

ZMR041	La Concepción eliza	urregintza-lantegia	eztainu-berunez beiraztatua	zuria	bola	XV-XVI	Z-3	beixa/arrosa
ZMR045	La Concepción eliza	urregintza-lantegia	eztainu-berunez beiraztatua	berdea, beltza eta zuria	bola	XV-XVI	Z-3	gorriska
ZMR046	La Concepción eliza	urregintza-lantegia	eztainu-berunez beiraztatua	zuria eta urdina	bola	XV-XVI	Z-3	beixa/arrosa
ZMR047	La Concepción eliza	urregintza-lantegia	eztainu-berunez beiraztatua	zuria eta urdina	bola	XV-XVI	Z-3	beixa/arrosa
ZMR048	La Concepción eliza	urregintza-lantegia	eztainu-berunez beiraztatua	berdea, marroia eta zuria	platera	XV-XVI	Z-3	gorriska
ZMR049	La Concepción eliza	urregintza-lantegia	eztainu-berunez beiraztatua	zuria	bola	XV-XVI	Z-3	beixa/arrosa
ZMR051	Museo Etnografikoa	e/e	eztainu-berunez beiraztatua	zuria, berdea eta beltza	bola	XVII-XVIII	Z-3	beixa/arrosa
ZMR052	Museo Etnografikoa	e/e	eztainu-berunez beiraztatua	zuria, berdea eta beltza	bola	XVI	Z-3	beixa/arrosa
ZMR053	Museo Etnografikoa	e/e	eztainu-berunez beiraztatua	zuria eta berdea	bola	XVII-XVIII	Z-3	beixa/arrosa
ZMR054	Museo Etnografikoa	e/e	eztainu-berunez beiraztatua	zuria eta urdina	goporra	XVII-XVIII	Z-3	beixa/arrosa
ZMR055	Museo Etnografikoa	e/e	eztainu-berunez beiraztatua	zuria eta urdina	platera	XVII-XVIII	Z-3	beixa/arrosa
ZMR056	Museo Etnografikoa	e/e	eztainu-berunez beiraztatua	zuria	platera	XVII-XVIII	Z-3	beixa/arrosa
ZMR057	Museo Etnografikoa	e/e	eztainu-berunez beiraztatua	zuria	bola	XVII-XVIII	Z-3	beixa/arrosa
ZMR058	Museo Etnografikoa	e/e	eztainu-berunez beiraztatua	zuria	platera	XVII-XVIII	Z-3	beixa/arrosa
ZMR059	Museo Etnografikoa	e/e	eztainu-berunez beiraztatua	zuria	platera	XVII-XVIII	Z-3	beixa/arrosa
ZMR065	Olivares	03 labea	eztainu-berunez beiraztatua	beltza eta zuria (kiskalia)	e/e	e/e	Z-3	beixa
ZMR060	Museo Etnografikoa	e/e	eztainu-berunez beiraztatua	zuria	bola	XVII-XVIII	Z-3	beixa
ZMR061	Museo Etnografikoa	e/e	eztainu-berunez beiraztatua	zuria	bola	XVII-XVIII	Z-3	beixa/arrosa
BNV001	Casa del Tinte	ospitalea	eztainu-berunez beiraztatua	zuria eta urdina	bola	XVII-XVIII	Z-3	gorriska
BNV002	Casa del Tinte	ospitalea	eztainu-berunez beiraztatua	zuria	platera	XVII	Z-3	beixa

BNV003	Casa del Tinte	ospitalea	eztainu-berunez beiraztatua	zuria	bola	XVII-XVIII	Z-3	gorriska
BNV004	Casa del Tinte	ospitalea	eztainu-berunez beiraztatua	zuria eta berdea	pixontzia	XVII-XVIII	Z-3	beixa/arrosa
ZMR038	La Concepción eliza	urregintza-lantegia	mikatsua beiraztatu gabea	-	bola	XV-XVI	Z-4	beixa
ZMR042	La Concepción eliza	urregintza-lantegia	mikatsua beiraztatu gabea	-	lusuila	XV-XVI	Z-4	grisa eta beixa
ZMR043	La Concepción eliza	urregintza-lantegia	mikatsua beiraztatu gabea	-	eltzea	XV-XVI	Z-4	grisa eta beixa
ZMR044	La Concepción eliza	urregintza-lantegia	mikatsua beiraztatu gabea	-	lusuila	XV-XVI	Z-4	grisa eta beixa
BNV005	Casa del Tinte	zabor-multzoa (ospitalea baino lehenagokoa)	beiraztatu gabea	-	lusuila	XVI-XVIII	B-1	gorria
BNV006	Casa del Tinte	zabor-multzoa (ospitalea baino lehenagokoa)	beiraztatu gabea	-	lusuila	XVI-XVIII	B-1	gorriska
BNV007	Casa del Tinte	zabor-multzoa (ospitalea baino lehenagokoa)	beiraztatu gabea	-	lusuila	XVI-XVIII	B-1	gorria
BNV008	Casa del Tinte	zabor-multzoa (ospitalea baino lehenagokoa)	beiraztatu gabea	-	pitxerra	XVI-XVIII	B-1	gorria
BNV009	Casa del Tinte	zabor-multzoa (ospitalea baino lehenagokoa)	beiraztatu gabea	-	pitxerra	XVI-XVIII	B-1	gorria
BNV010	Casa del Tinte	zabor-multzoa (ospitalea baino lehenagokoa)	beiraztatu gabea	-	pitxerra	XVI-XVIII	B-1	gorria
BNV011	Casa del Tinte	zabor-multzoa (ospitalea baino lehenagokoa)	beiraztatu gabea	-	pitxerra	XVI-XVIII	B-1	gorria
BNV012	Casa del Tinte	zabor-multzoa (ospitalea baino lehenagokoa)	beiraztatu gabea	-	pitxerra	XVI-XVIII	B-1	gorria
BNV013	Casa del Tinte	zabor-multzoa (ospitalea baino lehenagokoa)	beiraztatu gabea	-	txongila	XVI-XVIII	B-1	gorria
BNV014	Casa del Tinte	zabor-multzoa (ospitalea baino lehenagokoa)	beiraztatu gabea	-	txongila	XVI-XVIII	B-1	gorria
BNV015	Casa del Tinte	zabor-multzoa (ospitalea baino lehenagokoa)	beiraztatu gabea	-	txongila	XVI-XVIII	B-1	gorria

BNV016	Casa del Tinte	zabor-multzoa (ospitalea baino lehenagokoa)	beiraztatu gabea	-	txongila	XVI-XVIII	B-1	gorria
TOR001	Cuesta del Negrillo 11	zabor-multzoa	beiradura zeharrargiduna	marroia	katilua	XVII	T-1	gorria
TOR002	Cuesta del Negrillo 11	zabor-multzoa	beiradura zeharrargiduna	marroia	pitxerra	XVII	T-1	gorria
TOR003	Cuesta del Negrillo 11	zabor-multzoa	beiraztatu gabea	-	pitxerra	XVII	T-1	gorria
TOR004	Cuesta del Negrillo 11	zabor-multzoa	beiraztatu gabea	-	pixontzia	XVII	T-1	gorria
TOR005	Cuesta del Negrillo 11	zabor-multzoa	beiradura zeharrargiduna	marroia	pitxerra	XVII	T-1	gorria
TOR006	Patio del Siete	zabor-multzoa	beiraztatu gabea	-	pitxerra	XVII	T-1	gorria
TOR007	Patio del Siete	zabor-multzoa	beiraztatu gabea	-	pitxerra	XVII	T-1	gorria
TOR008	Patio del Siete	zabor-multzoa	beiraztatu gabea	-	tina	XVII	T-1	gorria
TOR010	Cuesta del Matadero	labe-hondakinak	beiradura zeharrargiduna	marroia	lusuila	XVII	T-1	gorria
TOR011	Cuesta del Matadero	labe-hondakinak	beiradura zeharrargiduna	marroia	estalkia	XVII	T-1	gorria
TOR012	Cuesta del Matadero	labe-hondakinak	beiradura zeharrargiduna	marroia	kopa	XVII	T-1	gorria
TOR014	Cuesta del Matadero	labe-hondakinak	beiraztatu gabea	-	hodia	XVII	T-1	gorria
ZMR037	La Concepción eliza	urregintza-lantegia	mikatsua beiraztatu gabea	-	eltzea	XV-XVI	unk	beixa
ZMR039	La Concepción eliza	urregintza-lantegia	mikatsua beiraztatu gabea	-	tina	XV-XVI	unk	beixa
ZMR050	La Concepción eliza	urregintza-lantegia	beiraztatu gabea - Duque de la Victoria motakoa	-	e/e	XV-XVI	unk	gorria
ZMR062	Mengue Etorbidea	zurrategia	mikatsua beiraztatu gabea	-	tina	e/e	unk	zuria
ZMR063	Mengue Etorbidea	zurrategia	mikatsua beiraztatu gabea	-	tina	e/e	unk	zuria
TOR009	Cuesta del Matadero	labe-hondakinak	beiraztatu gabea	-	lusuila	XVII	unk	beltza
TOR013	Cuesta del Matadero	labe-hondakinak	beiraztatu gabea	-	hodia	XVII	unk	gorria

Ondoren, Multzokatze Hierarkikoaren Analisia (HCA) egin da Zamorako 64 zeramiken taldekatzea ebaluatzeko, erreferentzia gisa Z-1, Z-2 eta Z-3 erreferentzia-taldeak hartuta (6.3. irudia). Dendrogramaren azterketak 4 multzoko egitura argia erakusten du, La Concepción, Museo Etnografikoa eta dagoeneko ezarrita dauden

Olivareseko ekoizpenei dagokiena. Talde gehienek ebaketa argiak eta zehatzak dituzte. Gainera, multzo jakin bateko lagin gehienek beren konposizio kimikoaren homogeneotasuna erakusten dute, beraien elkarketa puntuetan ikus daitekeenez. Alde batetik, La Concepción eta Museo Etnografikoan berreskuratutako zeramika opakuek bat egiten dute Olivareseko lantegietako Z-3 taldearekin. Museo Etnografikoko zeramikak Z-3 multzokoak izatea bat dator Martín et al. (1997)-ek argitaratutako artikuluarekin, non autoreek iradokitzen baitute aztarnategi arkeologiko horretan bildutako zeramika mota Olivaresen garai horietan ekoitzitako zeramika mota berari dagokiola. Gainera, beste zeramika-multzo bat identifikatu da, Z-4 (ZMR038, ZMR042, ZMR043 eta ZMR044), guztiak ere La Concepción-ekoak. Beiradurarik gabeko zeramika mikatsuak dira guztiak, eta, funtsean, sukaldeko eltzeak eta zerbitzu-ontziak dira. Bestalde, 6.3. irudiak erakusten du, halaber, bost zeramikek ez dutela aipatutako erreferentzia taldeekin bat egiten (La Concepción-en berreskuratutako ZMR037, ZMR039 eta ZMR050, eta Mengue etorbidean berreskuratutako ZMR062 eta ZMR063). ZMR037 eta ZMR039 mikatsuak dira, baina ez dute Z-2 eta Z-4 taldeekin bat egiten (hauek ere mikatsuak dira). Gertaera hori agerian geratzen da CaO edukia txikiagoa delako eta Sr edukia handiagoa delako ZMR037 eta ZMR039-an (6.1. taula). Hauez gain, ZMR062 eta ZMR063 tina mikatsuek ere ez dute erreferentzia taldeekin bat egiten. Honek zerikusia izan dezake zeramika horien Sr eta Al_2O_3-ren eduki altuarekin. Litekeena da zeramika mikatsu hauek guztiak eskualdeko zeramikagintzako herri ezagunen zeramika-ekoizpenekoak izatea, hala nola Moveros, Pereruela edo Muelas del Panekoak. Ildo honetan, garrantzitsua da Pereruelako Víctor Redondo artisauak emandako informazioa helaraztea (2019, pers. comm.). Pereruelako buztingileek sukaldeko zeramika mikatsua egiteko bi lehengai nahasten zituztela (% 50:50) aipatu zuen. Material horiek Pereruelako buztin gorriak eta Pereruelako edo inguruetako kaolinak ziren (gaur egun, berak Pereruelatik 12 km-ra dagoen Tamame herriko kaolina erabiltzen du). Informazio hori bat dator Buxeda et al. (2003)-k egindako Pereruelako zeramikaren azterketa etnoarkeometrikoarekin. Lan honetan, autoreek ondorioztatu zuten Pereruelan hainbat alfarerok ekoiztutako zeramika mikatsuek, bai teknologia bera eta tokiko buztinak erabilita ere, aldakortasun handia erakusten zutela. Gainera, eltze bereko hainbat laginetan aldakortasun kimiko handia hauteman zuten ere. Aldagarritasun hori, batez ere, lehengai desberdinen nahasketarekin eta buztin gorrietan dauden monazita-inklusioekin lotu zuten autoreek. Mineral hori lur arraroen elementuak dituen fosfatoa da. Beraz, autoreek azaldu zuten gertaera horiek Pereruelako produkzioak

(edo antzeko produkzioak) edota zeramika baten lagin desberdinak jatorri desberdinekoak balira bezala sailkatzeko arriskua dagoela. Autoreek ere adierazi zuten zeramika batzuen aldakortasunaren ekarpena Th eta Y ematen zutela nagusiki. Gainera, eltze beraren hainbat lagin aztertu zituzten, eta aldakortasun handia dokumentatu zuten, Sm, Lu, Yb, La, Ce, Th, Eu eta Y lur arraroen elementuek emandakoa. Hori guztia kontuan hartuta, eta monazita Pereruelako eta inguruko arroka igneo granitikoetan buztin gorriei erlazionatuta kantitate txikitan agertzen denez (Buxeda et al., 2003), garrantzitsua da Z-2, Z-4 eta ZMR037, ZMR039, ZMR062 eta ZMR063 zeramika mikatsuen arteko konparaketa egitea, aipatutako lur arraroen elementuak kenduz, taldekatzeak berresteko. Garrantzitsua da azpimarratzea horrek zentzua izango lukeela zeramika mikatsu horiek buztin gorriak kaolinarekin nahastuz egiten bazituzten, Pereruelaren kasuan bezala. Horrela, 6.3.a irudiak vt balio altua (4.5) erakusten du lur arraroen elementuak kontuan hartzen direnean, eta oraindik vt balio altua erakusten du hauek kentzen direnean (3.75) (6.3.b irudia), kasu horretan, elementu horiek ez baitiote ekarpen garrantzitsurik egiten aldakortasunari. Zenbaki horiek adierazten dute zeramika horien izaera poligenikoa dela.

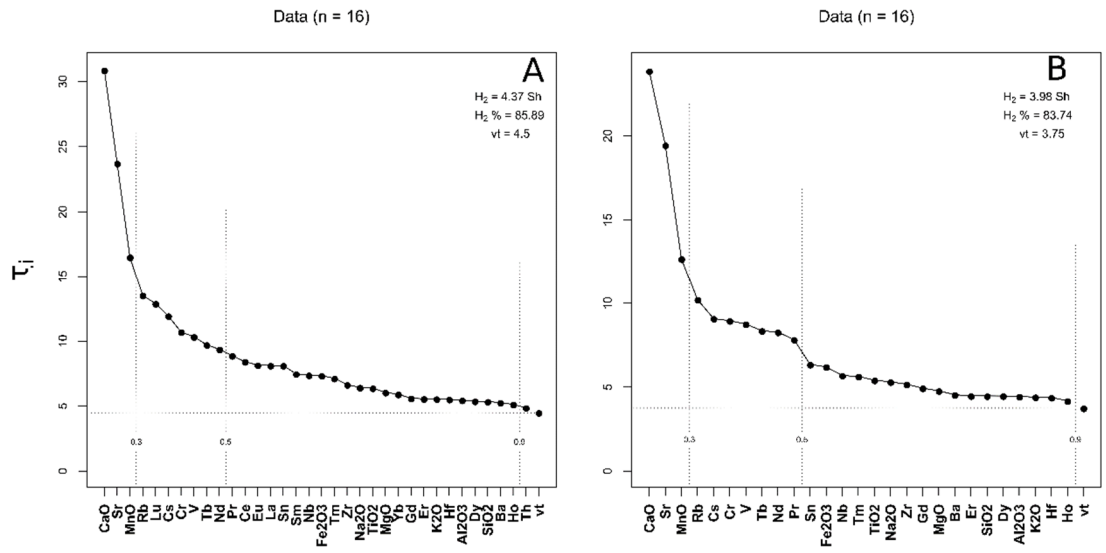

6.3. irudia. ICP-MS bidez aztertutako Z-2, Z-4 eta jatorri ezezaguneko 16 zeramika mikatsuen Konposizioaren Aldakortasunaren Matrizearen uniformetasunaren irudikapen grafikoa: **(a)** Co, Cu, Ni, P_2O_5, Pb, Ta eta U ez dira kontuan hartu, hauen balioak kuantifikazio-mugaren azpitik daudelako; **(b)** Co, Cu, Ni, P_2O_5, Pb, Ta eta U ez dira kontuan hartu aipatutakoez gain, kutsaduran eragina izan dezaketelako eta Sm, Lu, Yb, La, Ce, Th eta Eu lur arraroen elementuak ere ez (y ardatza (τ.i) = elementu bakoitzak datu-multzo osoari egiten dion ekarpen indibiduala, handienetik txikienera; vt = aldakortasun totala; H_2 = informazioaren entropia; H_2% = informazioaren entropiaren ehunekoa, ahal den gehienekoari dagokionez; n = lagin-kopurua)

Gainera, 6.4.a irudiak erakusten du ZMR037 eta ZMR039 zeramikak Z-2 taldeko zeramiken antzekoak direla lur arraroen elementuak kontuan hartzen direnean, eta, aldiz, talde berekotzat har daitezkeela elementu horiek kentzen direnean (6.4.b irudia). Baina hala ere, badirudi Z-2-k eta bi zeramikek jatorri desberdina erakusten jarraitzen dutela. Buxeda et al. (2003)-k frogatu zuten Pereruelako zeramikek jatorri desberdineko zeramikatzat hartuak izateko arriskua dutela, aldakortasun handia erakusten dutelako. Beraz, Z-2, Z-4, ZMR037, ZMR039, ZMR062 eta ZMR063 zeramiken kasua berdina izan daiteke, hau da, agian jatorri berdina dute baina desberdin ikusten dira. Zeramika hauei buruzko informazio gehiago ez dagoenez (adibidez, buztin gorriak eta kaolina nahasiz egin ote ziren) eta hauen aldagarritasun handia ez dagoenez bereziki lur arraroen elementuekin erlazionatuta, zeramika hauek jatorri ezberdinekoak eta ezezagunekoak izango balira bezala tratatuko dira. Hala ere, salbuespen batzuk egin dira: Z-2-ren jatorriaren hipotesia mantentzen da, hau da, a) Pereruela edo Muelas del Paneko ekoizpen bat izan daitekeela eta Olivaresera eramaten zela beiraztatzera edo b)

Olivaresen bertan ekoizten zirela zeramikak. Gainera, ZMR062 eta ZMR063 zeramikak segur aski jatorri berekoak eta ezezagunekoak dira, baina ez dira PCRU gisa tratatuko, oraindik ez baitago oso argi, eta ez daudelako zeramika gehiago konparaketetarako. Azkenik, ZMR037 eta ZMR039 zeramikek jatorri desberdina izan dezakete, elkarketa puntua altua baitute (ikus 6.5. irudia).

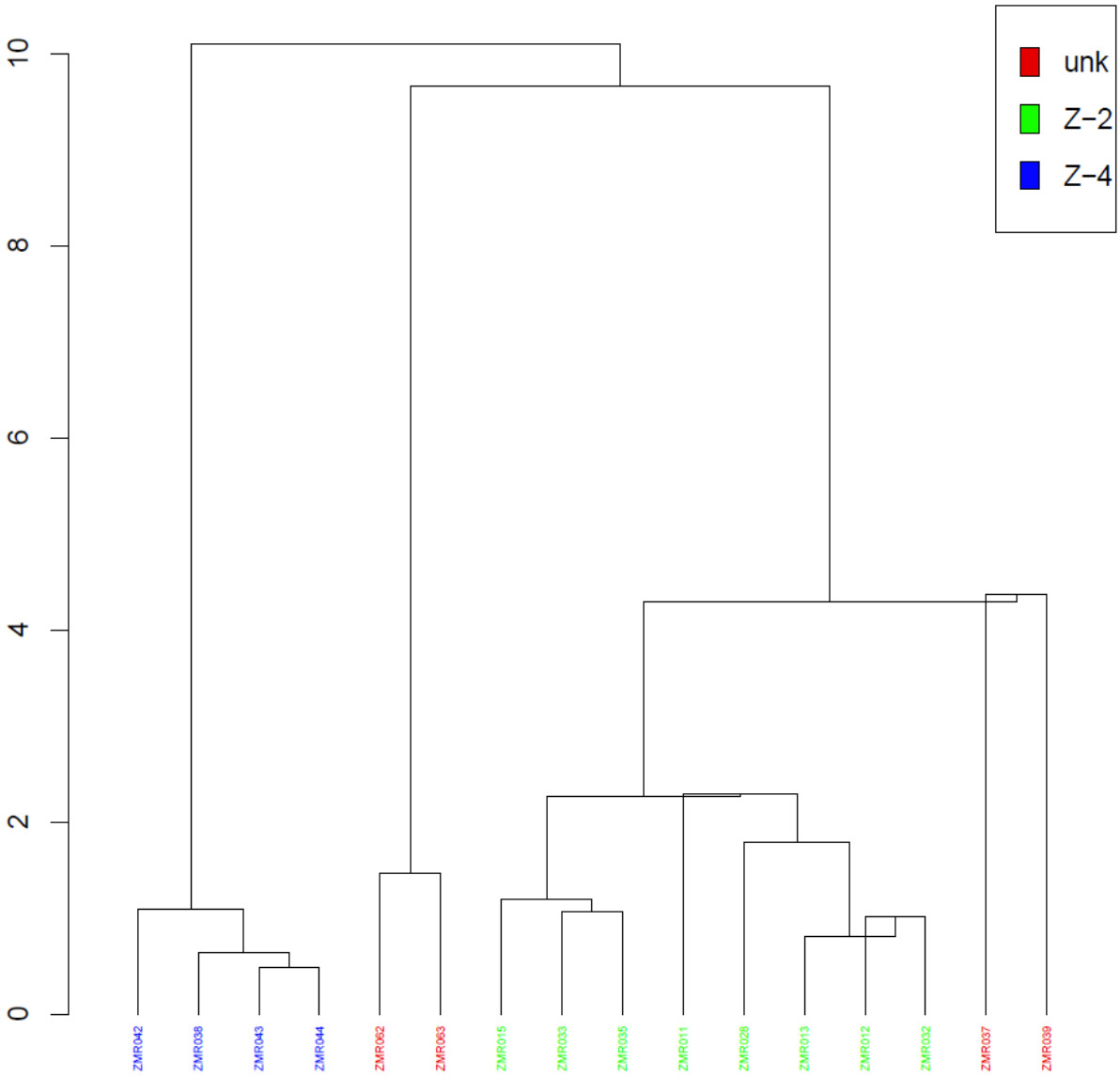

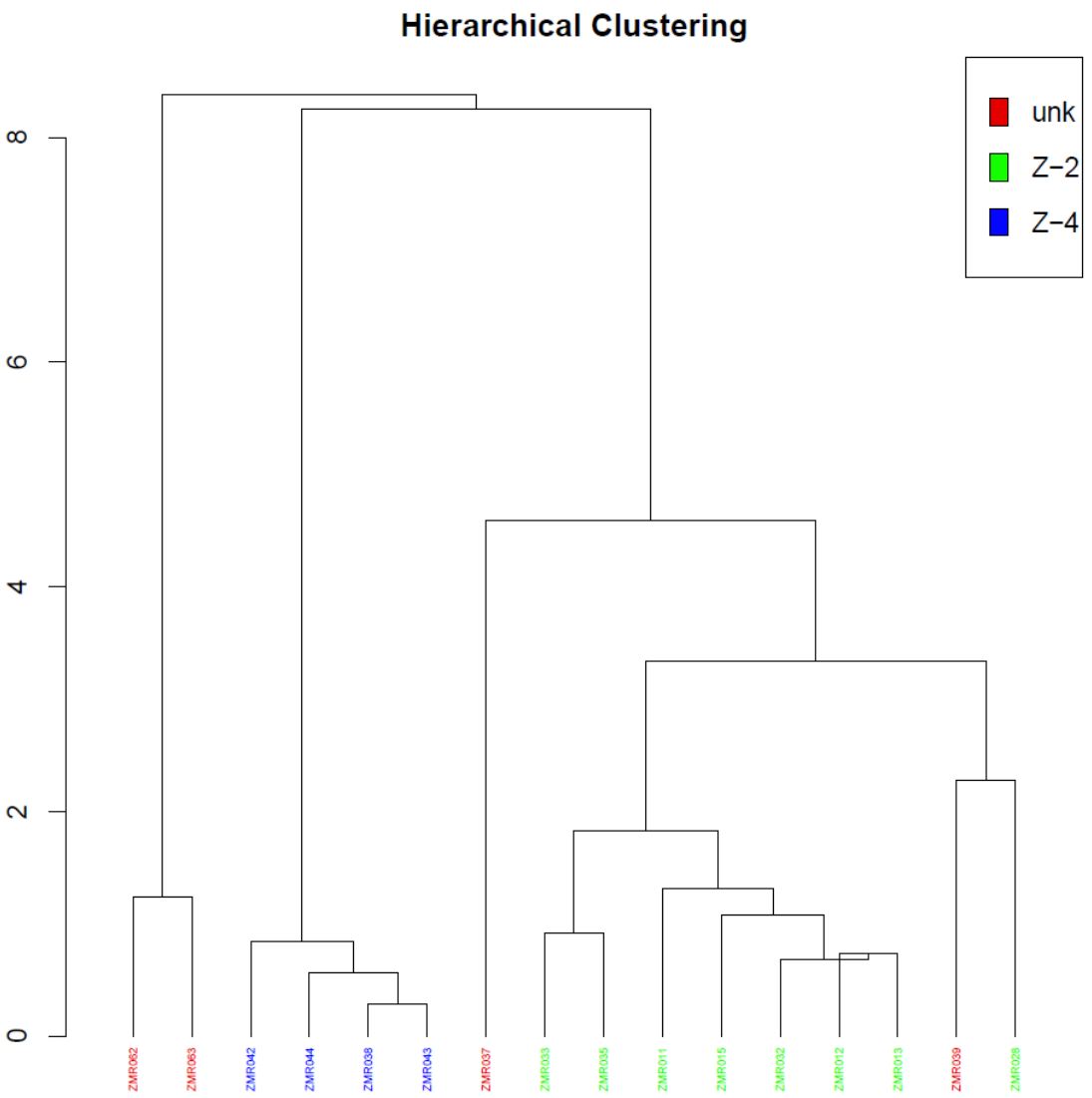

6.4 irudia. Euklidear distantzia karratua eta zentroidearen algoritmoa erabiliz lortutako Z-2-ko, Z-4-ko eta taldekatu gabeko 16 zeramika mikatsuen dendrograma: **(a, goian)** hurrengo azpi-konposiziorako dendrograma: neurtutako 42 konposatuak Co, Cu, Ni, P_2O_5, Pb, Ta eta U izan ezik, batezbesteko geometrikoaz zatituz; **(b, azpian)** hurrengo azpi-konposiziorako dendrograma: neurtutako 42 konposatuak Co, Cu, Ni, P_2O_5, Pb, Ta, U, Sm, Lu, Yb, La, Ce, Th eta Eu izan ezik, batezbesteko geometrikoaz zatituz

Azkenik, 6.5. irudian ZMR050 Z-3-ren parte dela dirudien arren, kontuz ibili behar da zeramika horrekin. Z-3-rekin duen elkarketa puntua nahiko altua da Z-3-ko gainerako zeramikekin alderatuta. Gainera, 6.6. irudiak erakusten du ZMR050 ez dela Z-3-koa. Seguruenik, zeramika hori Valladolideko ekoizpen batekoa da; izan ere, 2. kapituluan esan bezala, izen hori Valladolideko izen bereko kaleari dagokio, non Erdi Aro amaierari dagozkion zenbait buztingintza-tailer aurkitu baitziren

(Fernández et al., 1991; Villanueva et al., 2000). Taldeei buruzko informazio guztia 6.2. taulan laburtu da.

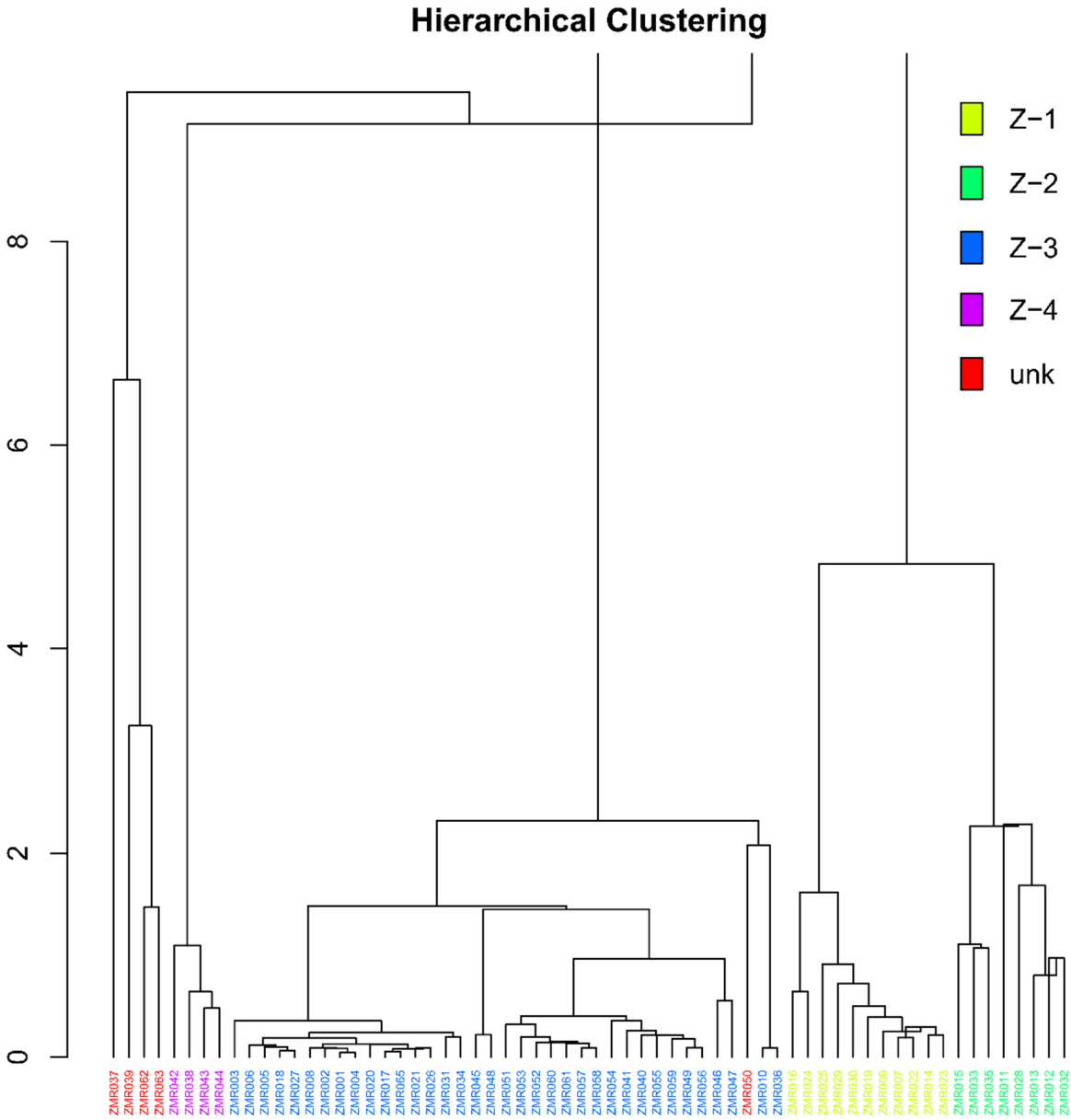

6.5. irudia. Euklidear distantzia karratua eta zentroidearen algoritmoa erabiliz lortutako Zamorako hainbat lekutako (Olivares, Museo Etnografikoa, La Concepción eta Mengue etorbidea) 64 zeramiken dendrograma, PCRU-ekin eta dagozkien erreferentzia-taldeekin adierazita, hurrengo azpi-konposiziorako: neurtutako 42 konposatuak Co, Cu, Ni, P_2O_5, Pb, Sn, Ta, U eta Zn izan ezik, batezbesteko geometrikoaz zatituz. Z-1, Z-2, Z-3 = Olivareseko ekoizpeneko erreferentzia-taldeak; Z-4 = eskualdeko jatorriko PCRU bat; unk = jatorri ezezaguneko zeramikak

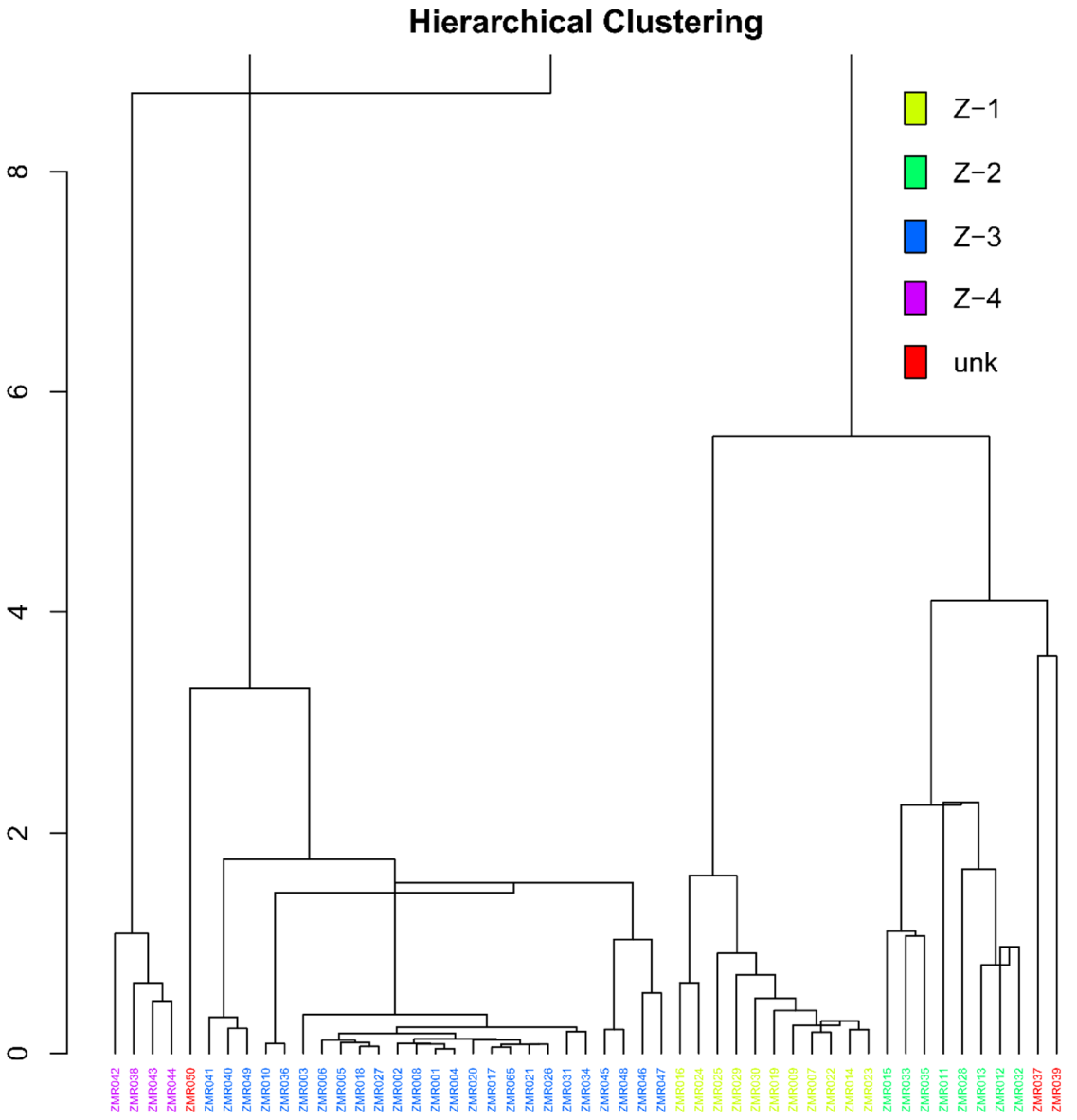

6.6. irudia. Euklidear distantzia karratua eta zentroidearen algoritmoa erabiliz lortutako Zamorako hainbat lekutako (Olivares eta La Concepción) 51 zeramiken dendrograma, PCRU-ekin eta dagozkien erreferentzia-taldeekin adierazita, hurrengo azpi-konposiziorako: neurtutako 42 konposatuak Co, Cu, Ni, P_2O_5, Pb, Sn, Ta, U eta Zn izan ezik, batezbesteko geometrikoaz zatituz. Z-1, Z-2, Z-3 = Olivareseko ekoizpeneko erreferentzia-taldeak; Z-4 = eskualdeko jatorriko PCRU bat; unk = jatorri ezezaguneko zeramikak

6.1.2. Benaventen berreskuratutako zeramikak

2. kapituluan adierazten den bezala, Benavente herria zeramikako ekoizpen zentro bat zen, Erdi Arotik Aro Modernoraino aktibo egon zena, non batez ere zeramika gorri ez-mikatsua ekoizten baitzen (De La Mata, 1989).

Kasu honetan, Benaventeko (Casa del Tinte) 16 zeramiken (BNV001-BNV016) multzo heterogeneoak (tipologiari dagokionez) vt altua (12.31) erakusten du, eta adierazten du Pb, CaO, Sn eta Cu-ren ekarpena handia dela (6.7.a irudia). Zeramika batzuk kaltzio baxukoak direnez, beiradurarik gabe, eta beste batzuk kaltziodunak beiradurekin, Pb, CaO eta Sn-ren aldakortasun handia espero zen zerbait da. Gainera, zeramika multzo honen vt 2,15-era jaisten da, Co, Cu, P_2O_5, Pb, Sn eta Ta konposatuak kentzen direnean, eta balio horrek multzoaren izaera poligenikoa iradokitzen du oraindik (6.7.b irudia).

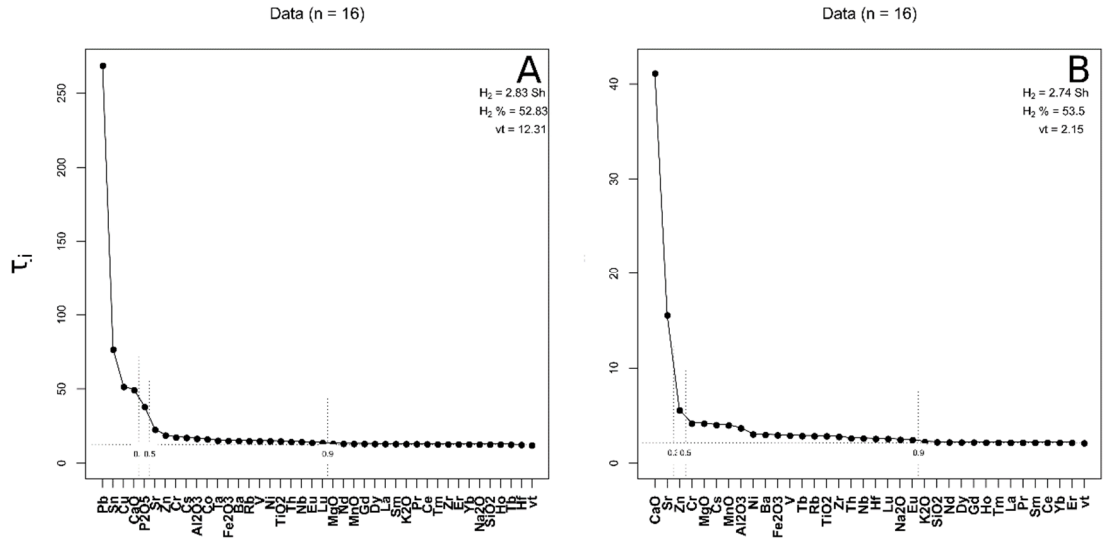

6.7. irudia. ICP-MS bidez aztertutako Benaventen berreskuratutako 16 zeramiken Konposizioaren Aldakortasunaren Matrizearen uniformetasunaren irudikapen grafikoa: **(a)** U ez da erabili, haren balioak kuantifikazio-mugaren azpitik daudelako; **(b)** Co, Cu, P_2O_5, Pb, Sn eta Ta ez dira erabili, U-z gain, kutsaduran eragina izan dezaketelako. (y ardatza (τ.i) = elementu bakoitzak datu-multzo osoari egiten dion ekarpen indibiduala, handienetik txikienera; vt = aldakortasun totala; H_2 = informazioaren entropia; H_2% = informazioaren entropiaren ehunekoa, ahal den gehienekoari dagokionez; n = lagin-kopurua)

6.8. irudiko dendrogramak Benaventen berreskuratutako16 zeramikek bi PCRU eratzen dituztela erakusten du. Honez gain, 6.9. irudiko dendrogramak erakusten du eztainu-berunez beiraztatutako 4 kaltziodun zeramika (BNV001-BNV004) Z-3 Olivareseko ekoizpen-taldekoak direla, eta gainerakoek Benaventeko zeramika gorrien ekoizpenaren erreferentzia-talde berri bat osatzen duela, B-1 izenekoa.

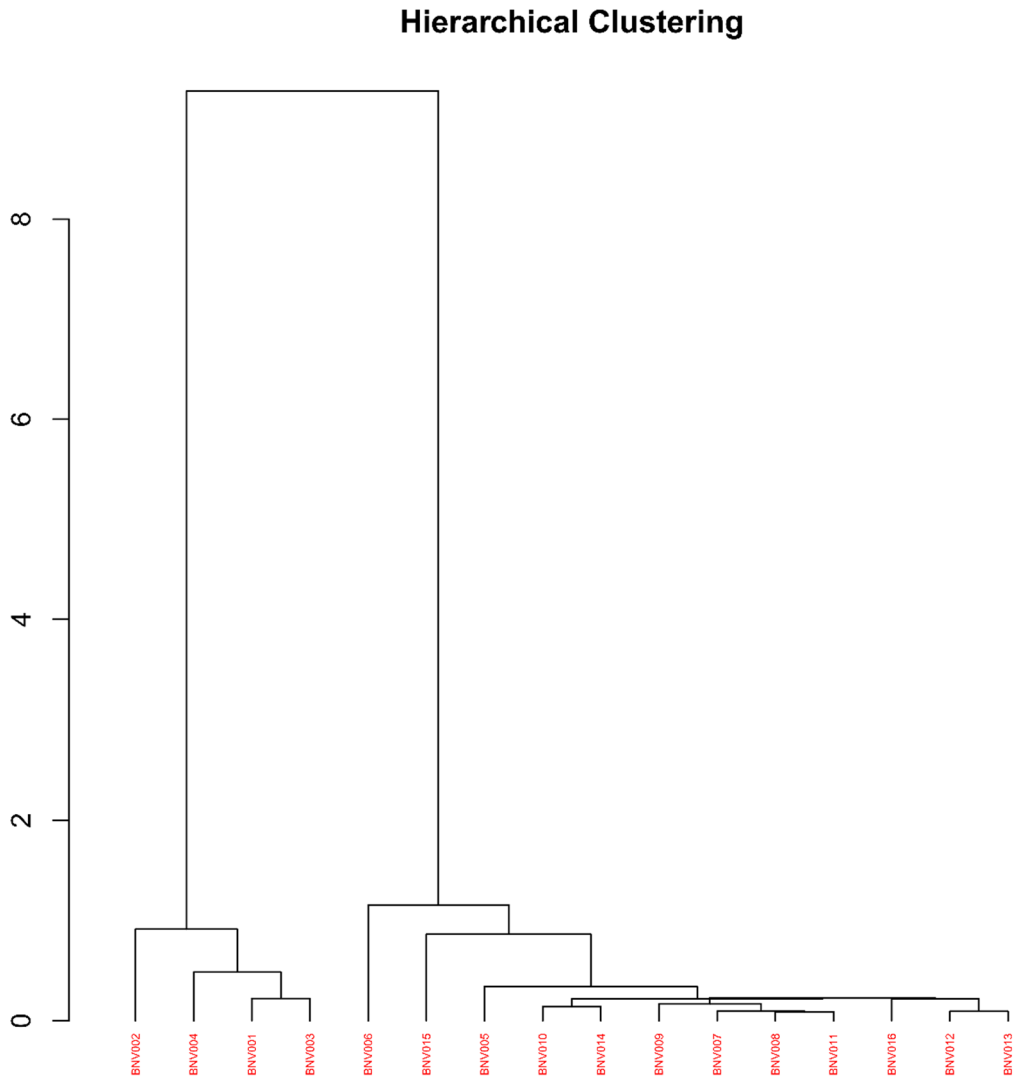

6.8. irudia. Euklidear distantzia karratua eta zentroidearen algoritmoa erabiliz lortutako Benaventeko 16 zeramiken dentrograma, hurrengo azpi-konposiziorako: neurtutako 42 konposatuak Co, Cu, P_2O_5, Pb, Ta, Sn eta U izan ezik, batezbesteko geometrikoaz zatituz

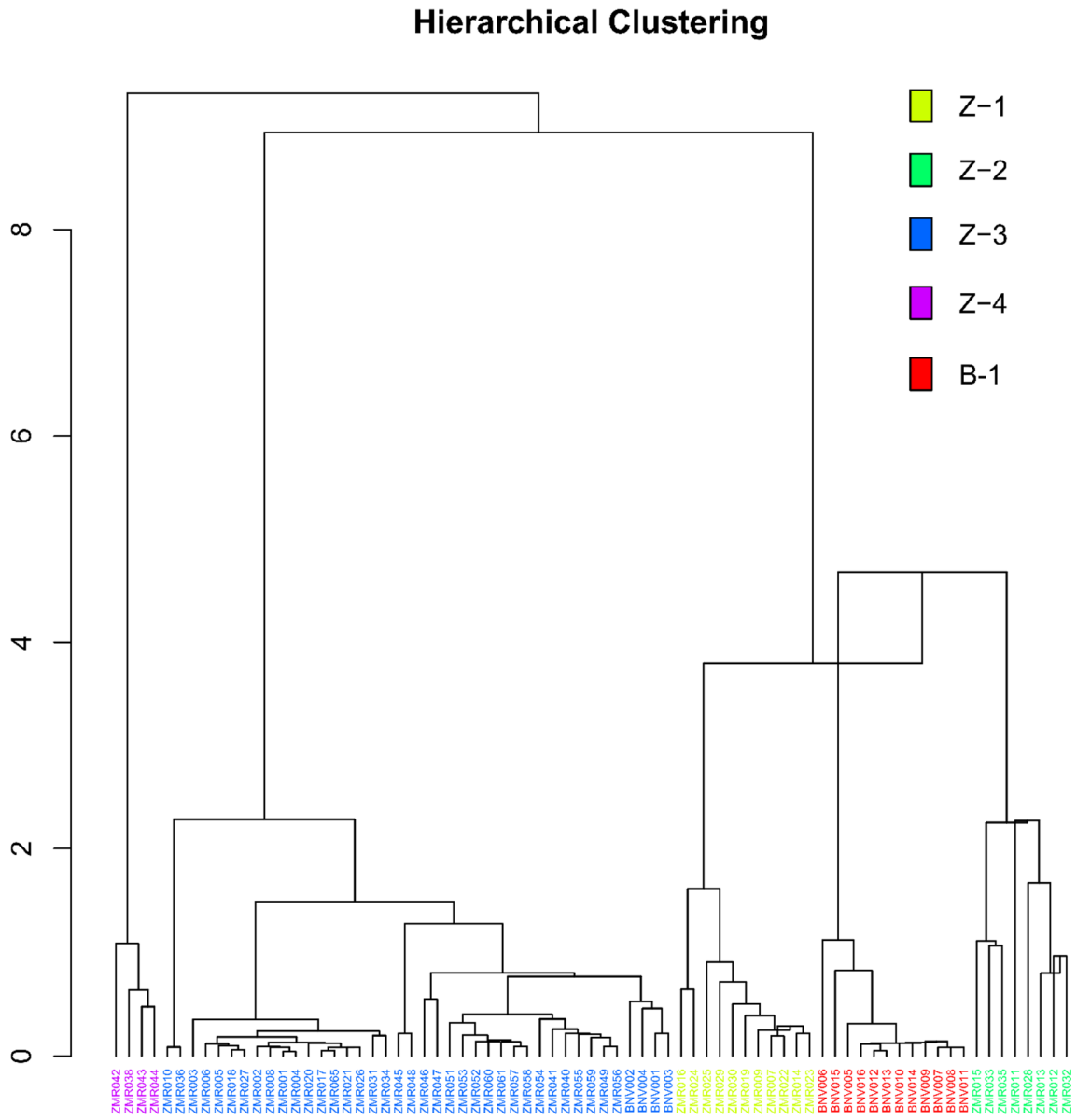

6.9. irudia. Euklidear distantzia karratua eta zentroidearen algoritmoa erabiliz lortutako Zamorako hainbat lekutako (Olivares, Museo Etnografikoa eta La Concepción) eta Benaventeko 75 zeramiken dendrograma, hurrengo azpi-konposiziorako: neurtutako 42 konposatuak Co, Cu, Ni, P_2O_5, Pb, Sn, Ta, U eta Zn izan ezik, batezbesteko geometrikoaz zatituz. Z-1, Z-2 eta Z-3= Olivareseko ekoizpenen erreferentzia-taldeak; B-1= Benaventeko ekoizpenaren erreferentzia-taldea; Z-4= Eskualdeko jatorriko PCRU-a

6.1.3. Toron berreskuratutako zeramikak

Benavente bezala, Toro ere ekoizpen-zentro aktiboa zen Erdi Arotik Aro Modernoraino, eta batez ere zeramika gorri ez-mikatsua ekoizten zen (ikus 2. kapitulua).

Kasu honetan, Toroko 14 zeramikaz osatutako multzoak (Cuesta del Negrilloko TOR001-TOR005; Patio del Sieteko TOR006-TOR008 eta Cuesta del Mataderoko TOR009-TOR014) nahiko vt altua erakusten du (3.97), konposatu batzuen ekarpen handia agertuz (bereziki Pb, Cu, CaO, MnO eta P_2O_5 konposatuena) (6.10.a irudia). Beruna oso aldakorra da, zeramika horietako batzuk zeharrargiak direlako eta beste batzuek ez dutelako beiradurarik. Gainera, Cu eta P_2O_5, sedimentuen, ur zirkulatzaileen eta inguruko lurzoruari eragiten dioten giza jardueraren ondoriozko kutsadurekin erlazionatuta egon ohi dira (Buxeda i Garrigós, 1999; Buxeda i Garrigós eta Kilikoglou, 2003; Freestone et al., 1985; Lemoine eta Picon, 1982; Maritan eta Mazzoli, 2004; Molera et al., 1993; Pradell et al., 1996). Aldiz, Pb, Co, Ta, Cu eta P_2O_5 ez badira kontuan hartzen, vt 0.85-era jaisten da, eta horrek zeramika multzoaren izaera monogenikoa iradokitzen du (6.10.b irudia).

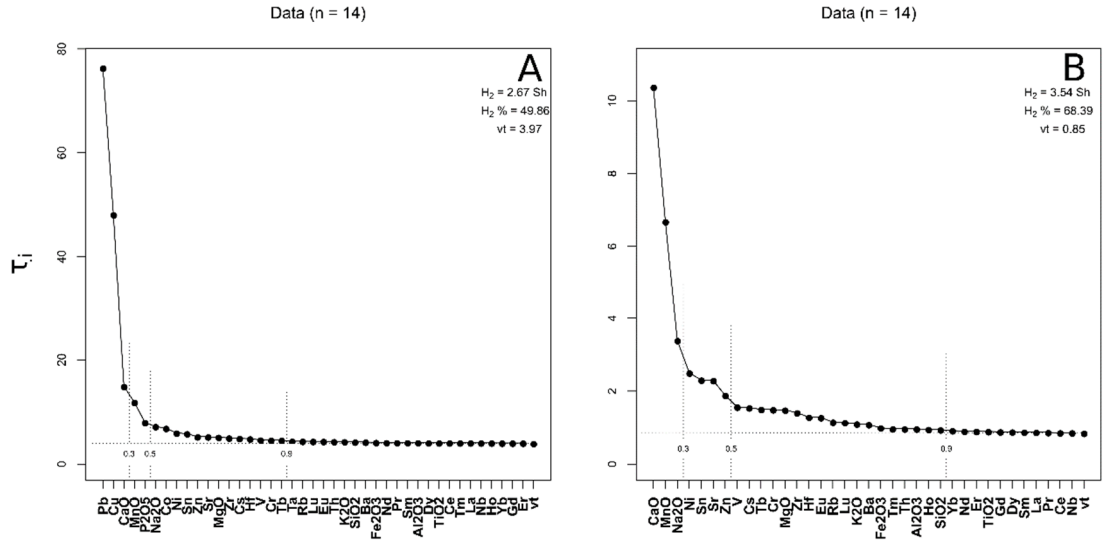

6.10. irudia. ICP-MS bidez aztertutako Toron berreskuratutako 14 zeramiken Konposizioaren Aldakortasunaren Matrizearen uniformetasunaren irudikapen grafikoa: **(a)** U ez da erabili, haren balioak kuantifikazio-mugaren azpitik daudelako; **(b)** Co, Cu, P_2O_5, Pb eta Ta ez dira erabili, U-z gain, kutsaduran eragina izan dezaketelako. (y ardatza (τ.i) = elementu bakoitzak datu-multzo osoari egiten dion ekarpen indibiduala, handienetik txikienera; vt = aldakortasun totala; H_2 = informazioaren entropia; H_2% = informazioaren entropiaren ehunekoa, ahal den gehienekoari dagokionez; n = lagin-kopurua)

6.11. irudiak erakusten du Toron jasotako 14 zeramiketatik 12-k (salbuespenak TOR009 eta TOR013 dira) Tororen ekoizpen gorriaren erreferentzia-taldea osatzen dutela. Gainera, 6.12. irudian agertzen denez, TOR009 eta TOR013 oraindik ezagutzen ez den talde bati dagozkio, beraz, beraien jatorria ezezaguna da.

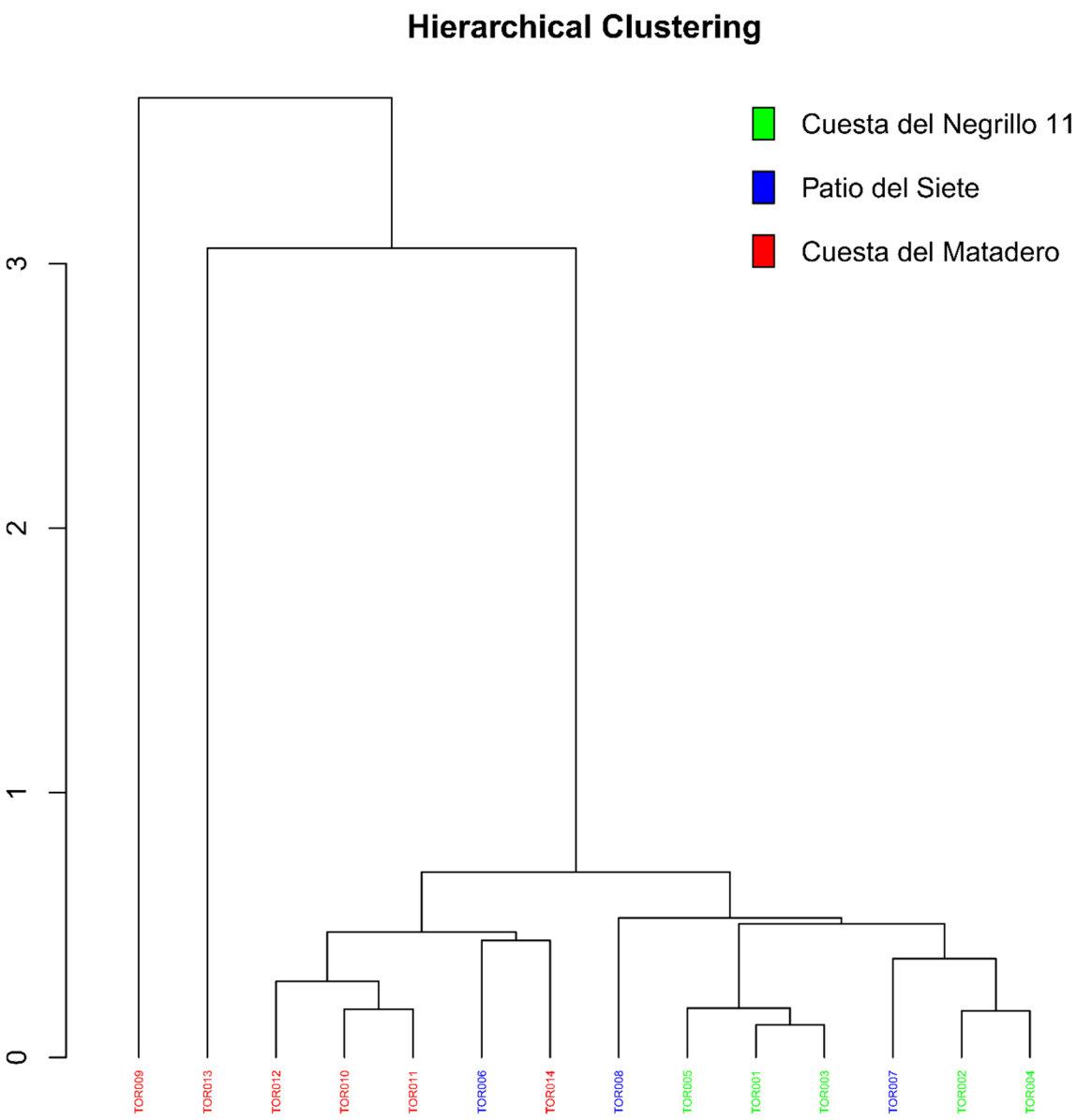

6.11. irudia. Euklidear distantzia karratua eta zentroidearen algoritmoa erabiliz lortutako Toroko hainbat lekutako (Cuesta del Negrillo, Patio del Siete eta Cuesta del Matadero) 14 zeramiken dendrograma, hurrengo azpi-konposiziorako: neurtutako 42 konposatuak Co, Cu, P_2O_5, Pb, Ta eta U izan ezik, batezbesteko geometrikoaz zatituz

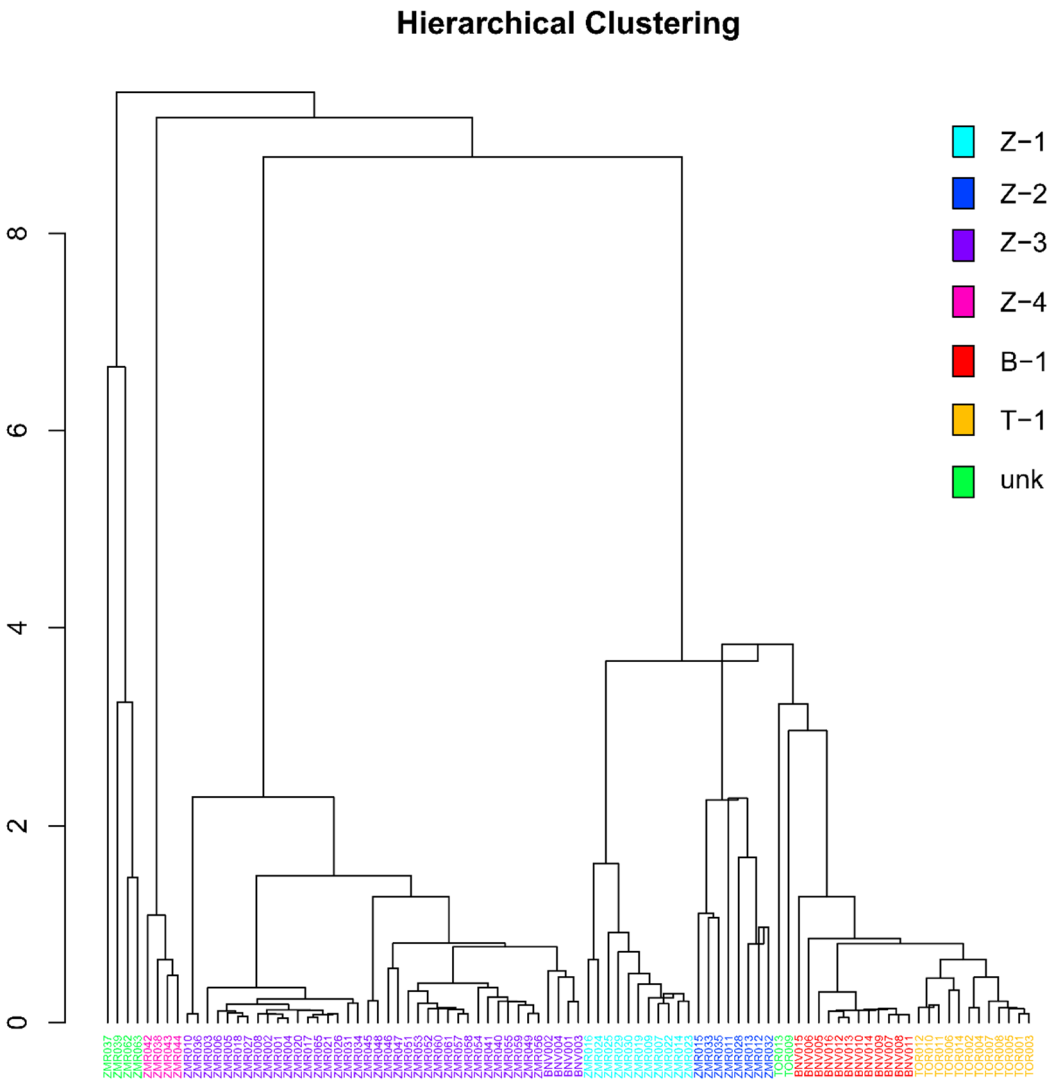

6.12. irudia. Euklidear distantzia karratua eta zentroidearen algoritmoa erabiliz lortutako Toroko hainbat lekutako, Zamorako eta Benaventeko 93 zeramiken dendrograma, hurrengo azpi-konposiziorako: neurtutako 42 konposatuak Co, Cu, Ni, P_2O_5, Pb, Sn, Ta, U eta Zn izan ezik, batezbesteko geometrikoaz zatituz. Z-1, Z-2 eta Z-3= Olivareseko ekoizpenen erreferentzia-taldeak; B-1= Benaventeko ekoizpenaren erreferentzia-taldea; T-1= Toroko ekoizpenaren erreferentzia-taldea; Z-4= Eskualdeko jatorriko PCRU-a

6.1.4. Erreferentzia-taldeen eta PCRU-en karakterizazioa

Erreferentzia-taldeak eta PCRU-ak identifikatu ondoren, fase mineralak eta ekoizpen-fabrikak identifikatu dira XRD analisien bidez. Fabrikak erre ziren Erreketa Tenperatura Baliokidea (EFT) ere Heimann (2010 eta bertako erreferentziak)-en behaketen arabera ebaluatu da. 1. kapituluan aipatu den bezala, fabrika bat pasta iristen den azken emaitza da, zeramika egiteko prozesu teknologikoa osatu ondoren (Buxeda i Garrigós eta Cau, 1995; Buxeda i Garrigós eta

Madrid i Fernández, 2017) eta konposizio mineralogikoaren eta pasten testuren arabera identifikatu daitezke.

Gainera, SEM-EDS eta Raman analisiak ere egin dira zeramika batzuetan, Z-1, Z-2, Z-3, T-1 eta B-1 erreferentzia-taldeak sakonago karakterizatzeko, beraien mikroegitura eta beiraduren konposizioa ikertuz.

Z-1 erreferentzia-taldea

Z-1, batez ere, beiradurarik gabeko 2 zeramikaz eta beiradura zeharrargidun 9 zeramikaz osatua dago. Denek pasta gorria dute, batek izan ezik (beltza du, kiskalita dagoelako) (6.3. taula). Platerak, eltzeak eta pitxerrak daude batik bat eta horietatik bost akastun piezak dira (beiradura gordina edota kiskalita dutenak). Kronologikoki, multzo honetako zeramikak XIX. mende amaiera eta XX. mende hasierakoak dira (ikus 6.2. taula). Zeramika hauek kaltzio eduki baxukoak dira, eta batezbesteko CaO kontzentrazioa % 1-ekoa da (masan) (ikus 6.3. taula). Gainera, Z-1 zeramiken SiO_2 eta Zr edukia gainerako Olivares (Z-2, Z-3) ekoizpenena baino altuagoa da.

6.3. taula. Erreferentzia-talde eta PCRU bakoitzaren konposizio kimikoa eta talde bakoitzari dagozkion zeramikak, hauen tipologia eta pasta-kolorearekin batera. Elementuen kontzentrazioak ng/g-tan adierazten dira, eta oxidoenak, berriz, masa %-tan

Laginak	Taldea	Tipologia	Pastaren kolorea	Al_2O_3	Ba	CaO	Ce	Co	Cr	Cs	Cu	Dy	Er	Eu	Fe_2O_3	Gd
ZMR007; ZMR009; ZMR014; ZMR016; ZMR019; ZMR022-ZMR025; ZMR029-ZMR030	Z-1	Beiraztatu gabea (2), beiradura zeharrargiduna (9)	Gorria (10), beltza (1)	13.1	297	0.989	75.0	29.8	63.4	9.50	-	4.85	2.73	1.17	4.31	5.56
ZMR011-ZMR013; ZMR015; ZMR028; ZMR032-ZMR033; ZMR035	Z-2	Mikatsua beiraztatu gabea (2), beiradura zeharrargidun zeramika mikatsua (6)	gorria (6), gorria eta grisa (1), beltza (1)	19.2	403	1.46	76.4	26.9	48.2	12.2	-	5.01	2.33	1.74	4.27	7.07
ZMR001-ZMR006; ZMR008; ZMR010; ZMR017-ZMR018; ZMR020-ZMR021; ZMR026-ZMR027; ZMR031; ZMR034; ZMR036; ZMR040-ZMR041; ZMR045-ZMR049; ZMR051-ZMR061; ZMR065; BNV001-BNV004;	Z-3	Beiraztatu gabea (10), eztainu-berunez beiraztatua (30)	beixa (6), beix/arrosa (28), gorriska eta grisa (2), gorriska (4)	12.3	404	12.7	67.3	21.1	50.3	5.37	48.2	4.53	2.49	1.24	4.13	5.55
ZMR038; ZMR042-ZMR044	Z-4	Mikatsua beiraztatu gabea (4)	beixa (1), grisa eta beixa (3)	24.7	305	3.55	47.7	15.9	21.8	30.7	6.09	5.68	3.07	0.940	2.48	5.68
BNV005-BNV016	B-1	Beiraztatu gabea (12)	gorria (11), gorriska (1)	23.7	660	1.83	86.4	29.0	123	8.25	24.3	5.62	2.91	1.93	8.35	7.41
TOR001-TOR008; TOR010-TOR012; TOR014	T-1	Beiraztatu gabea (6), beiradura zeharrargiduna (6)	gorria (12)	19.5	591	1.45	95.5	20.6	86.0	9.07	23.9	6.20	3.12	1.97	6.21	7.78

(jarraipena)

Laginak	Taldea	Tipologia	Pastaren kolorea	Hf	Ho	K_2O	La	Lu	MgO	MnO	Na_2O	Nb	Nd	Ni	P_2O_5	Pb	Pr	Rb	SiO_2	Sm
ZMR007; ZMR009; ZMR014; ZMR016; ZMR019; ZMR022-ZMR025; ZMR029-ZMR030	Z-1	Beiraztatu gabea (2), beiradura zeharrargiduna (9)	Gorria (10), beltza (1)	7.79	0.826	1.77	38.0	0.406	0.466	0.0241	0.763	16.7	35.3	-	-	595	8.50	98.8	77.3	6.79
ZMR011-ZMR013; ZMR015; ZMR028; ZMR032-ZMR033; ZMR035	Z-2	Mikatsua beiraztatu gabea (2), beiradura zeharrargidun zeramika mikatsua (6)	gorria (6), gorria eta grisa (1), beltza (1)	3.30	0.779	2.88	36.8	0.272	0.697	0.0222	0.851	12.6	44.8	-	-	1.00E+04	10.4	136	67.8	8.84
ZMR001-ZMR006; ZMR008; ZMR010; ZMR017-ZMR018; ZMR020-ZMR021; ZMR026-ZMR027; ZMR031; ZMR034; ZMR036; ZMR040-ZMR041; ZMR045-ZMR049; ZMR051-ZMR061; ZMR065; BNV001-BNV004;	Z-3	Beiraztatu gabea (10), eztainu-berunez beiraztatua (30)	beixa (6), beix/arrosa (28), gorriska eta grisa (2), gorriska (4)	5.15	0.766	3.19	33.3	0.337	2.16	0.0618	0.892	13.4	32.4	20.5	1.57	5.04E+03	8.04	117	58.6	6.19

Laginak	Taldea	Tipologia	Pastaren kolorea	Hf	Ho	K_2O	La	Lu	MgO	MnO	Na_2O	Nb	Nd	Ni	P_2O_5	Pb	Pr	Rb	SiO_2	Sm
ZMR038; ZMR042-ZMR044	Z-4	Mikatsua beiraztatu gabea (4)	beixa (1), grisa eta beixa (3)	4.86	0.932	3.48	22.7	0.375	0.895	0.0402	0.618	24.6	22.2	9.92	0.460	61.0	5.67	440	67.6	5.07
BNV005-BNV016	B-1	Beiraztatu gabea (12)	gorria (11), gorriska (1)	4.91	0.864	3.68	44.3	0.469	1.38	0.0437	0.614	20.4	41.1	36.4	0.101	60.7	10.3	173	65.8	7.61
TOR001-TOR008; TOR010-TOR012; TOR014	T-1	Beiraztatu gabea (6), beiradura zeharrargiduna (6)	gorria (12)	5.26	0.916	3.77	48.5	0.483	1.14	0.0348	0.481	18.3	45.5	33.4	0.125	1.10E+03	11.6	172	65.1	8.25

(jarraipena)

Laginak	Taldea	Tipologia	Pastaren kolorea	Sn	Sr	Ta	Tb	Th	TiO_2	Tm	U	V	Yb	Zn	Zr
ZMR007; ZMR009; ZMR014; ZMR016; ZMR019; ZMR022-ZMR025; ZMR029-ZMR030	Z-1	Beiraztatu gabea (2), beiradura zeharrargiduna (9)	Gorria (10), beltza (1)	8.35	85.3	1.90	0.862	14.5	0.926	0.417	3.34	59.7	2.78	-	367
ZMR011-ZMR013; ZMR015; ZMR028; ZMR032-ZMR033; ZMR035	Z-2	Mikatsua beiraztatu gabea (2), beiradura zeharrargidun zeramika mikatsua (6)	gorria (6), gorria eta grisa (1), beltza (1)	20.9	154	2.15	1.01	9.77	0.447	0.319	2.64	57.5	2.10	-	122
ZMR001-ZMR006; ZMR008; ZMR010; ZMR017-ZMR018; ZMR020-ZMR021; ZMR026-ZMR027; ZMR031; ZMR034; ZMR036; ZMR040-ZMR041; ZMR045-ZMR049; ZMR051-ZMR061; ZMR065; BNV001-BNV004;	Z-3	Beiraztatu gabea (10), eztainu-berunez beiraztatua (30)	beixa (6), beix/arrosa (28), gorriska eta grisa (2), gorriska (4)	40.0	260	1.32	0.601	12.5	0.591	0.391	3.1	58.9	2.49	48.8	251
ZMR038; ZMR042-ZMR044	Z-4	Mikatsua beiraztatu gabea (4)	beixa (1), grisa eta beixa (3)	33.8	107	7.72	0.446	8.41	0.284	0.503	-	24.2	2.96	62.9	211

Laginak	Taldea	Tipologia	Pastaren kolorea	Sn	Sr	Ta	Tb	Th	TiO_2	Tm	U	V	Yb	Zn	Zr
BNV005-BNV016	B-1	Beiraztatu gabea (12)	gorria (11), gorriska (1)	3.26	127	1.89	0.425	18.4	0.825	0.496	-	116	3.02	56.0	263
TOR001-TOR008; TOR010-TOR012; TOR014	T-1	Beiraztatu gabea (6), beiradura zeharrargiduna (6)	gorria (12)	4.30	182	1.88	0.428	18.0	0.719	0.522	-	93.0	3.21	52.5	280

XRD bidezko teknologiaren azterketa

Gainera, analisi mineralogikoen bidez, bost fabrika identifikatu dira erreferentziako talde honetan, F-I, F-II_a, F-II_b, F-III, F-IV eta F-V, hurrenez hurren (6.4. taula). Bost fabrikek hematita dute beren pastetan, pastaren kolore gorriarekin erlazionatzen den minerala, alegia (Heimann, 2010; Molera et al., 1998, 2015). Honez gain, F-I eta F-II-n illita dago (erreketa-tenperatura baxua adierazten duen fasea), eta F-I eta F-II-ko zeramikentzat 800 °C inguruko erreketa-tenperatura (EFT) adierazten du. Bestalde, F-II-an feldespato potasikoaren agerpenak tenperatura altuagoa (800-850 °C) iradoki dezake F-II-ko zeramikentzat. F-II_a eta F-II_b kaltzitaren agerpenagatik desberdintzen dira (F-II_b-k dauka). Kaltzita 650 °C-tik gora deskonposatzen denez, litekeena da kaltzita horrek lotura izatea birkarbonatazio-prozesuekin edota jalkitze-osteko denbora horretan gerta litezkeen bigarren mailako prezipitazio-prozesuekin (Buxeda eta Cau, 1995) (ikus 5. kapitulua, 5.4. atala). Honez gain, F-III zeramika batek bakarrik osatzen du (ZMR007), zeinak dagoeneko erakusten baitu illitaren deskonposizioa, feldespato potasikoaren eta hematitaren agerpenarekin batera. Beraz, fabrika honentzat 850-900 °C-ko EFT proposatzen da. Azkenik, F-IV-ak plagioklasaren kristalizazioa erakusten du erreketa-fase gisa, eta, gainera, F-IV-ak eta F-V-ak, mullita dute. Beraz, fase hauek 1.000 °C-tik gorako EFT bat iradoki dezakete; ziur aski, tenperatura baxuagoa izango da F-IV-rentzat (1000-1050 °C), eta tenperatura altuagoa F-V-rentzat (1050-1100 °C, gutxienez) (6.4. taula eta 6.13. irudia).

6.4. taula. Fabrika bakoitzari dagokion konposizio mineralogikoa eta Erreketa-Tenperatura Baliokidea (EFT), eta talde bakoitzari dagozkion zeramikak, hauen tipologia eta pasta-kolorea. Qz= kuartzoa; Kfs= feldespato potasikoa; Pl= plagioklasa; Cal= kaltzita; Ak-Gh= akermanita-gehlenita; Di= diopsidoa; Ilt= illita; Hem= hematita; Mul= mullita; Crs= kristobalita, laburdurak Whitney eta Evans (2010)-en arabera

Talde a	Tipologia	Pasta-kolore a	Laginak	Fab rika	Qz	Kfs	Pl	Cal	Ak-Gh	Di	Ilt	Hem	Mul	Crs	EFT (° C)
Z-1	beiraztatu gabea (1), beiradura zeharrargidu na (1)	gorria (2)	ZMR009; ZMR019	F-I	x						x	x			800
	beiradura zeharrargidu na (3)	gorria (3)	ZMR022-ZMR023; ZMR025	F-II_a	x	x					x	x			800-850
	beiradura zeharrargidu na (1)	gorria (1)	ZMR029	F-II_b	x	x		x			x	x			800-850
	beiraztatu gabea (1)	gorria (1)	ZMR007	F-III	x	x						x			850-900

	beiradura zeharrargidu na (1)	beltza (1)	ZMR030	F-IV	x	x	x					x	x		1000 - 1050
	beiradura zeharrargidu na (3)	gorria (3)	ZMR014; ZMR016; ZMR024	F-V	x	x						x	x		1050
Talde a	**Tipologia**	**Pasta-kolore a**	**Laginak**	**Fab rika**	**Qz**	**Kfs**	**Pl**	**Cal**	**Ak-Gh**	**Di**	**Ilt**	**Hem**	**Mul**	**Crs**	**EFT (° C)**
Z-2	mikatsua beiraztatu gabea (1), beiradura zeharrargidu n zeramika mikatsua (2)	gorria (3)	ZMR011-ZMR012; ZMR035	F-I_a	x	x					x	x			800-850
	mikatsua beiraztatu gabea (1)	gorria eta grisa (1)	ZMR013	F-I_b	x	x					x				800-850
	beiradura zeharrargidu n zeramika mikatsua (1)	gorria (1)	ZMR028	F-I_c	x	x		x			x	x			800-850
	beiradura zeharrargidu n zeramika mikatsua (1)	beltza (1)	ZMR033	F-II	x	x						x	x		1050
	beiradura zeharrargidu n zeramika mikatsua (1)	gorria (1)	ZMR015	F-III	x	x				x		x	x	x	1050 - 1100
	beiradura zeharrargidu n zeramika mikatsua (1)	gorria (1)	ZMR032	F-IV	x							x	x	x	1100
Talde a	**Tipologia**	**Pasta-kolore a**	**Laginak**	**Fab rika**	**Qz**	**Kfs**	**Pl**	**Cal**	**Ak-Gh**	**Di**	**Ilt**	**Hem**	**Mul**	**Crs**	**EFT (° C)**
Z-3	beiraztatu gabea (2), eztainu-berunez beiraztatua (2)	gorriska eta grisa (2), gorriska (2)	ZMR010; ZMR036; BNV001; BNV003	F-I	x	x	x	x			x				850
	beiraztatu gabea (3), eztainu-berunez beiraztatua (13)	beixa (2), beix/arrosa (12), gorriska (2)	ZMR001-ZMR006; ZMR008; ZMR020; ZMR027; ZMR045; ZMR048; ZMR051-ZMR052; ZMR058; ZMR061; ZMR065	F-II_a	x	x	x	x	x	x	x				850-900
	beiraztatu gabea (1)	beixa (1)	ZMR031	F-II_b	x	x	x		x	x	x				850-900
	beiraztatu gabea (2), eztainu-berunez	beix/arrosa (2), beixa (1)	ZMR017; ZMR021; ZMR034	F-III	x	x	x			x	x				900

	beiraztatua (1)														
	eztainu-berunez beiraztatua (6)	beix/arrosa (6)	ZMR040-ZMR041; ZMR049; ZMR054-ZMR056	F-IV_a	x	x		x	x	x					900-950
	eztainu-berunez beiraztatua (4)	beix/arrosa (3), beixa (1)	ZMR053; ZMR057; ZMR059-ZMR060	F-IV_b	x	x	x	x	x	x					900-950
	eztainu-berunez beiraztatua (4)	beix/arrosa (3), beixa (1)	ZMR046-ZMR047; BNV002; BNV004	F-V	x	x	x		x	x					950
	beiraztatu gabea (2)	beix/arrosa (2)	ZMR018; ZMR26	F-VI	x	x	x	x	x	x					950-1000
Taldea	**Tipologia**	**Pasta-kolorea**	**Laginak**	**Fabrika**	**Qz**	**Kfs**	**Pl**	**Cal**	**Ak-Gh**	**Di**	**Ilt**	**Hem**	**Mul**	**Crs**	**EFT (° C)**
Z-4	mikatsua beiraztatu gabea (4)	beixa (1), grisa eta beixa (3)	ZMR038; ZMR042-ZMR044	F-I	x	x	x	x			x				850-900
Taldea	**Tipologia**	**Pasta-kolorea**	**Laginak**	**Fabrika**	**Qz**	**Kfs**	**Pl**	**Cal**	**Ak-Gh**	**Di**	**Ilt**	**Hem**	**Mul**	**Crs**	**EFT (° C)**
B-1	beiraztatu gabea (5)	gorria (4), gorriska (1)	BNV006; BNV009; BNV012-BNV014	F-I	x	x		x			x	x			800-850
	beiraztatu gabea (3)	gorria (3)	BNV005; BNV010; BNV015	F-II	x	x						x			850-900
	beiraztatu gabea (4)	gorria (4)	BNV007-BNV008; BNV011; BNV016	F-III	x	x						x	x		1050
Taldea	**Tipologia**	**Pasta-kolorea**	**Laginak**	**Fabrika**	**Qz**	**Kfs**	**Pl**	**Cal**	**Ak-Gh**	**Di**	**Ilt**	**Hem**	**Mul**	**Crs**	**EFT (° C)**
T-1	beiraztatu gabea (5), beiradura zeharrargidu na (3)	gorria (8)	TOR002-TOR004; TOR005-TOR008; TOR012	F-I	x	x		x			x	x			800-850
	beiraztatu gabea (1), beiradura zeharrargidu na (3)	gorria (4)	TOR001; TOR010-TOR011; TOR014	F-II	x	x					x	x			850-900

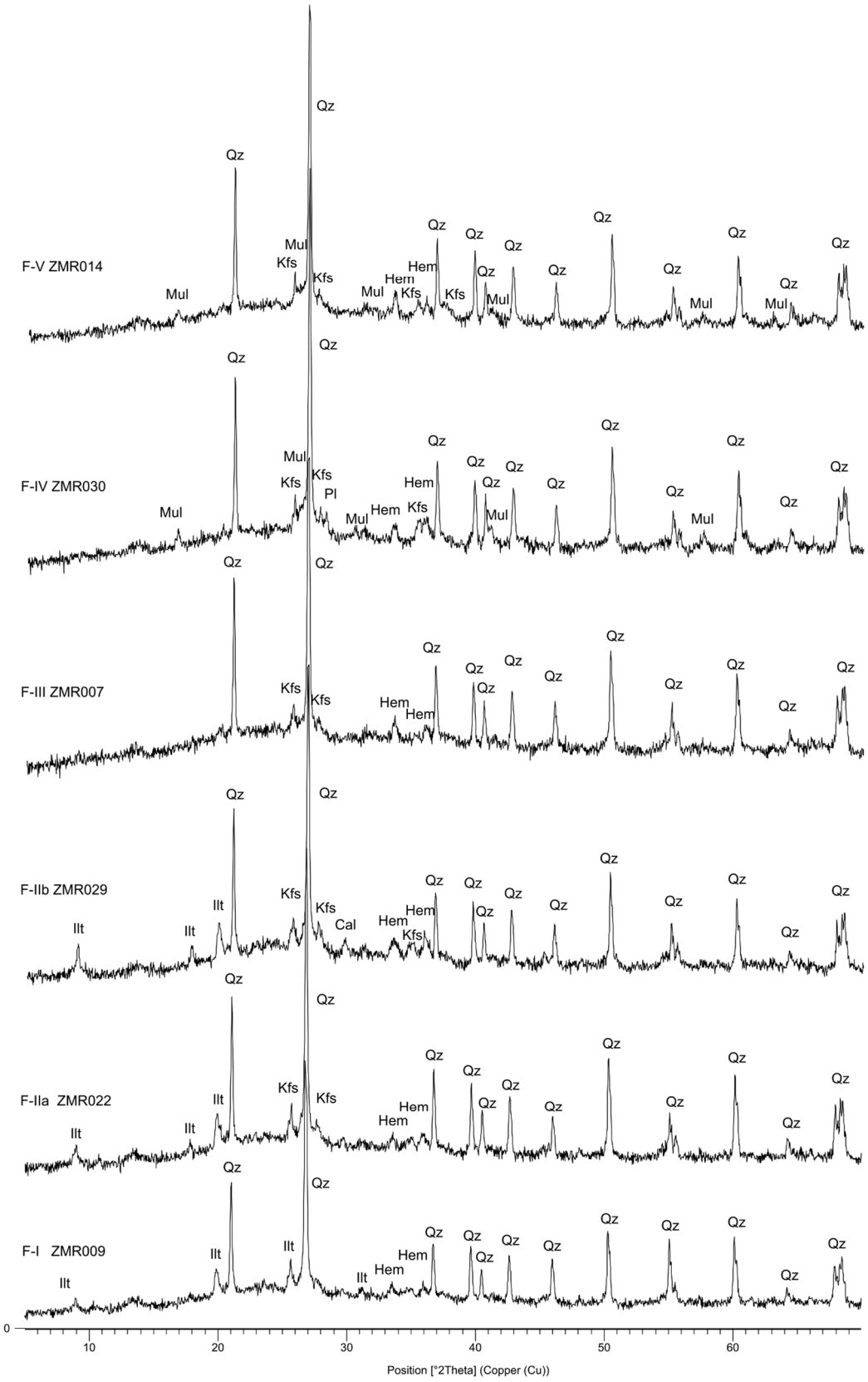

6.13. irudia. Z-1 erreferentzia-taldeko fabriken erreferentziazko difraktogramak. Qz = kuartzoa; Ilt = illita; Kfs = feldespato potasikoa; Pl = plagioklasa; Hem = hematita; Cal = kaltzita; = mullita, laburdurak Whitney eta Evans (2010)-en arabera

SEM-EDS bidezko azterketa

SEM-EDS analisietarako 3 zeramika hautatu ziren: ZMR009 beiraztatu gabea (F-I), ZMR025 (zeharrargia, F-II_a) eta ZMR014 (zeharrargia, F-V) (6.14. irudia). Lehenik eta behin, ZMR009-k bitrifikazio-maila baxuko pasta erakusten du, gainazal lauko eremu isolatuak agertzen direlako (Maniatis eta Tite, 1978). Bestalde, ZMR014 Z-1 taldeko tenperatura-tarte altuena duen fabrikari dagokio, eta etengabeko bitrifikazioa erakusten du. Gainera, ZMR025 eta ZMR014 laginek beiraduren mikroegiturak erakusten dituzte. Z-1-eko zeramikak Pb eta Si-ren nahasketa bat erabiliz beiraztatu ziren, ziurrenik fritaduraren teknika erabiliz, literaturaren arabera (Iñañez, 2007). Honez gain, beiradura zeharrargiari kolore marroia (ezti kolorea) Fe ioiek eta errekuntza-baldintza oxidatzaileek ematen diote. Hau eltzegileek nahita egiten zuten hautu teknologikoa zen (Molera et al., 2015).

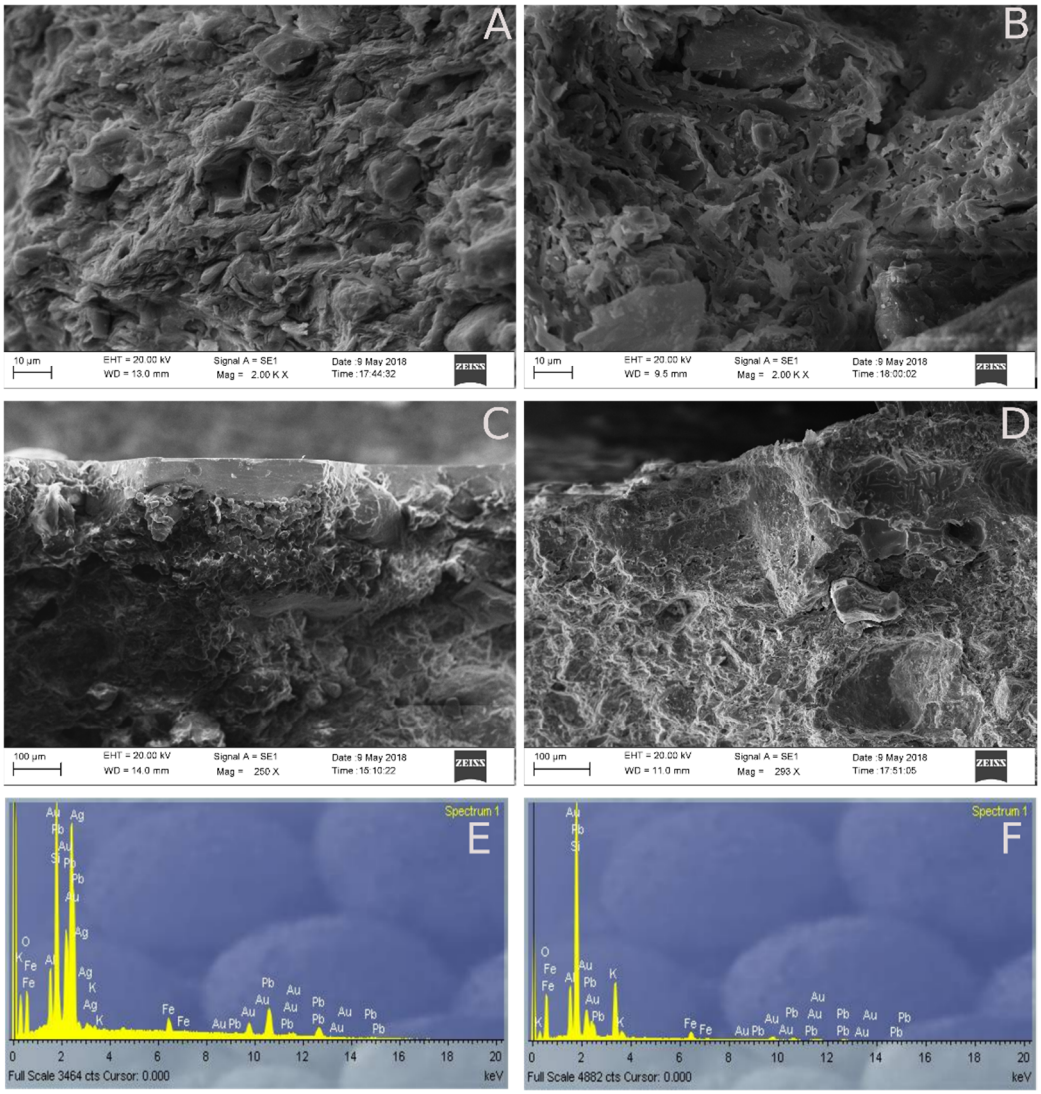

6.14. irudia. Z-1 taldeko zeramiken SEM-SED mikrofotografiak eta SEM-EDS mikroanalisiak: **(a)** ZMR009-ren pasta; **(b)** ZMR014-ren pasta; **(c)** ZMR025-en beiradura; **(d)** ZMR014-ren beiradura; **(e)** ZMR025 beiraduraren EDS espektroa; **(f)** ZMR014 beiraduraren EDS espektroa

Z-2 erreferentzia-taldea

Z-2 taldea 8 zeramika mikatsuz osatuta dago. Horietako 6-k beiradura zeharrargia dute (eta horietatik 4 akastun zeramikak dira). Kronologikoki, multzo honetako zeramikak XIX. mende amaiera eta XX mende hasierakoak dira (ikus. 6.2. taula). Zeramika mikatsu hauek aluminioan eduki altua dute eta kaltzioan eduki baxua, batezbeste % 19 Al_2O_3-n eta % 1 CaO-n (masan) (ikus. 6.3. taula). Begiz ikusten den itxura eta aluminio-eduki altua filosilikatoen (adibidez, mika) eduki altuari dagozkio, eta horrek talka termikoari aurre egiteko ezaugarri tekniko ezin hobeak ematen dizkie zeramika horiei. Lehengaiak hiriaren inguruan dauden kanbriar

garaiko kuartzitazko formakuntzetatik erauztea posible zen, hauek buztin illitikoz eta mikaz eratuta baitaude (Corrochano, 1980; Corrochano et al., 1976).

XRD bidezko teknologiaren azterketa

Lau fabrika desberdin identifikatu dira Z-2 taldean, F-I_a, F-I_b, F-I_c, F-II, F-III eta F-IV, hurrenez hurren. F-I-en hiru azpitaldetan desberdintasun txikiak daude, eta, orokorrean, F-I illitaren presentziak bereizten du, erreketa-tenperatura baxua izan zela iradokiz, segur aski 800-850 °C ingurukoa. Gainera, F-I_b-k ez bezala, F-I_a-k eta F-I_c-ek, biek hematita dute beren difraktogrametan, eta F-I_c-n ere kaltzita sekundarioa dago (6.4. taula). F-I_b-ko difraktogrametan hematita ez agertzeak ez du esan nahi hematita ez dagoenik. Gainera, F-I_b-n Fe_2O_3-ren kontzentrazioa % 4 ingurukoa da; beraz, hematita ager daiteke, baina ez ondo kristalizatuta, edo DRX-ak identifikatzen ez duen kontzentrazio baxu batean (burdin konposatuaren % 4 kontzentrazio hori ere burdin silikatoei edota mineralei dagokie). Hala ere, kontzentrazio txikia nahikoa da pastari kolore gorria emateko (Pollard et al., 2007). Bestalde, F-II-k mullita dauka, eta horrek 1050 °C inguruko EFT bat iradokitzen du. Honez gain, F-III-k diopsidoa, mullita eta kristobalita ditu. Azkena, kuartzoaren polimorfoa da, eta kuartzoan tenperatura altuetan gertatzen diren inbertsioen ondorioz agertzen da, eta 1050-1100 °C-ko EFT bat iradokitzen du. Azkenik, F-IV-ak, besteek ez bezala, ez du feldespato potasikorik. Gainera, tenperatura altuko faseak

ditu, hala nola kuartzoa, hematita, mullita eta kristobalita, eta 1100 °C inguruko EFT bat iradokitzen du (6.4. taula eta 6.15. irudia).

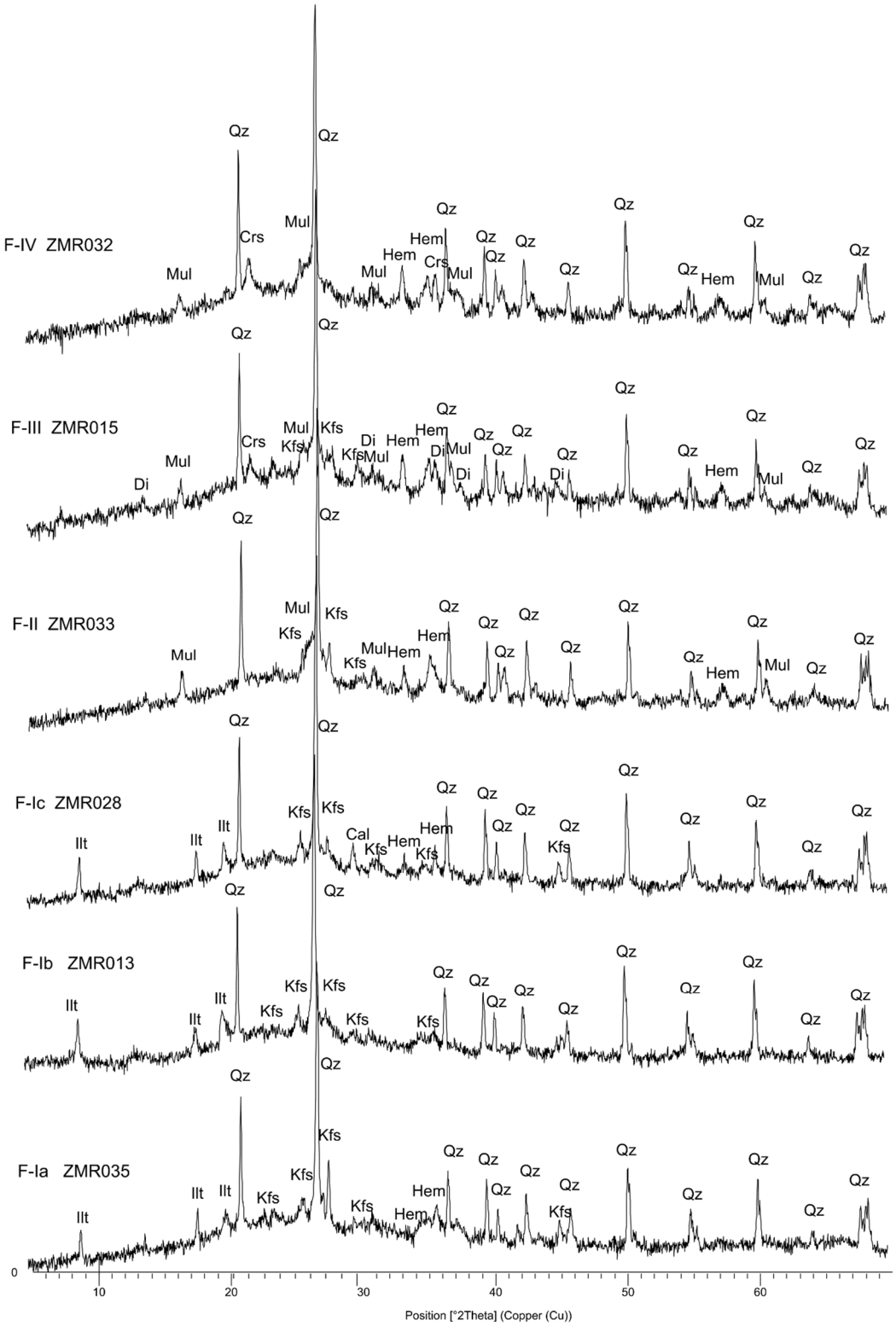

6.15. irudia. Z-2 erreferentzia-taldeko fabriken erreferentziazko difraktogramak. Qz = kuartzoa; Ilt = illita; Kfs = feldespato potasikoa; Hem = hematita; Cal = kaltzita; Mul = mullita; Di = diopsidoa; Crs = kristobalita, laburdurak Whitney eta Evans- (2010)-en arabera

SEM-EDS bidezko azterketa

Z-2-ko hiru zeramika aztertu dira SEM-EDS bidez. 6.16. irudian ZMR013-k (F-I_b) bitrifikazio maila baxua erakusten du eta ZMR015-ek, berriz, (F-III) etengabeko bitrifikazioa, erretze-tenperatura altu eta iraunkorrengatik. Gainera, ZMR015 eta ZMR033 zeramiken beiraduren EDS espektroak ere ikus daitezke 6.16 irudian. Hauetan ikus daiteke beiradura horiek (taldeko gainerako beiradurak bezala) beiradura zeharrargiak direla, kolore marroiekoak, Z-1 taldekoak bezalakoak.

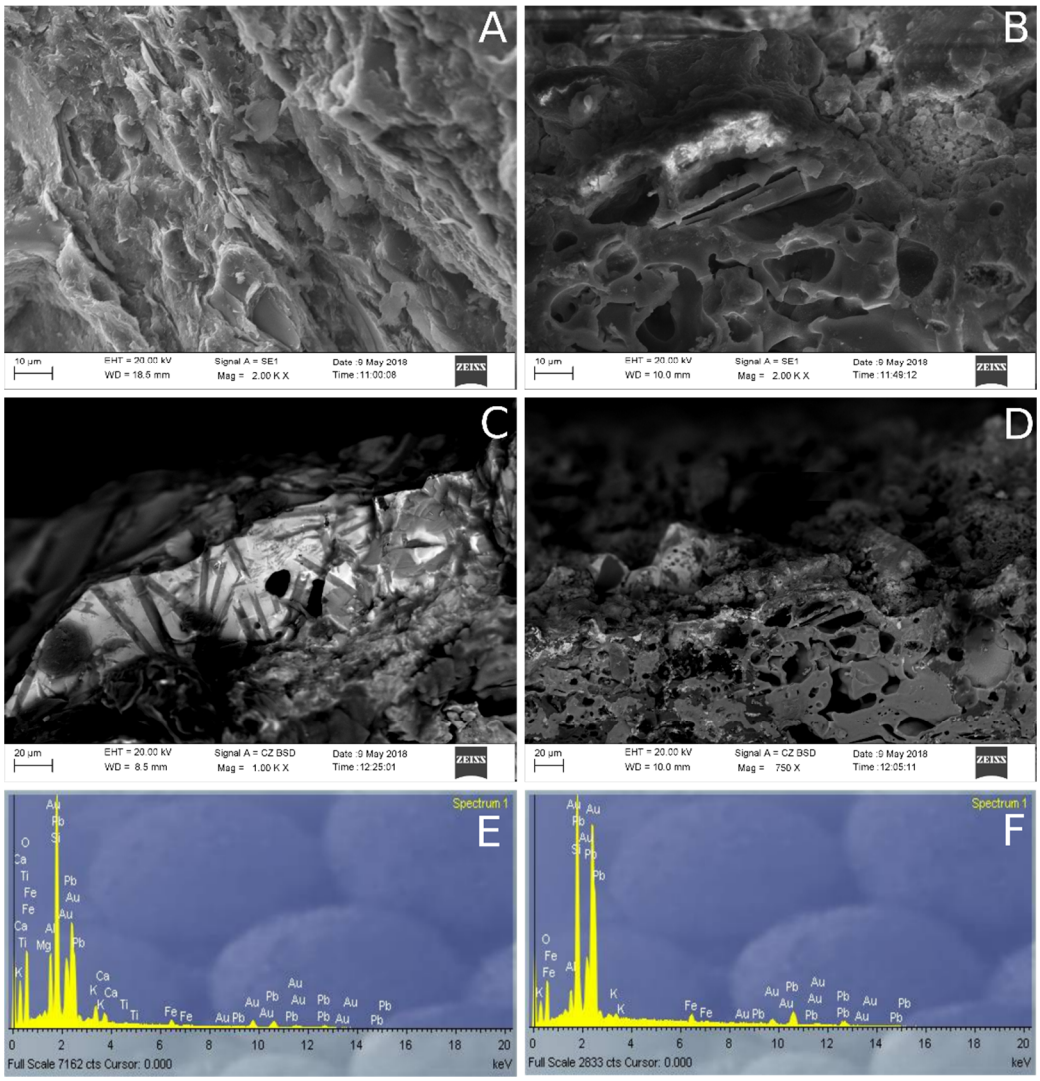

6.16 irudia. Z-2 taldeko SEM-SED (a,b) eta SEM-BSD (c,d) mikrofotografiak eta SEM-EDS mikroanalisiak: **(a)** ZMR013-ren pasta; **(b)** ZMR015-ren pasta; **(c)** ZMR033-ren beiradura; **(d)** ZMR015-ren beiradura; **(e)** ZMR033 beiraduraren EDS espektroa; **(f)** ZMR015 beiraduraren EDS espektroa

Z-3 reference group

Finally, Z-3 group is made out of 30 tin-lead glazed and 10 biscuit ceramics (from which 4 are kiln furniture, see Table 6.2.). Chronologically, the ceramics of this group correspond to the 15^{th}-20^{th} centuries. This group is high-calcareous, averaging to 13 wt % of CaO. Moreover, the set also contains higher concentrations of MgO than the rest groups, averaging to 2 wt % (see Table 6.3.). It is possible that potters from Olivares used raw materials from the Terciary marl and limolite crops nearby the city of Zamora, just at 3 km SW, for this Z-3 production (Corrochano, 1980; Corrochano et al., 1976).

Technological assessment by XRD

Additionally, six different fabrics were defined in Z-3, F-I, F-II_a, F-II_b, F-III, F-IV_a, F-IV_b, F-V and F-VI, respectively (Table 6.4. and Figure 6.17.). The EFT of F-I is suggested to be around 850 °C, due to the presence of illite. The curious detail of this fabric is that, although the ceramic pastes are reddish and greys and reddish, hematite has not been identified by XRD. However, as explained before, this fact does not necessarily mean that hematite is not present; indeed, this mineral might not has been good crystallised. In addition, the CaO amount is high, 7 wt % for ZMR010 and ZMR036, and around 14 wt % for BNV001 and BNV003 (all from F-I_b). In addition, F-II is also divided in two subgroups, due to the identification of calcite in F-II_a. F-II shows incipient diffraction peaks of akermanite-gehlenite solid solution and diopside, therefore, suggesting an EFT in the range of 850-900 °C, since illite has not been fully decomposed yet. In addition, 900 °C is the suggested EFT for F-III, since although illite peaks are identified, they show low intensity at 5 Å and 10 Å (basal reflections), which indicate that dehydroxilation of illite has been not fully completed. Besides, F-IV has no evidence of illite reflections, suggesting an EFT in the range of 900-950 °C (Table 6.4.). This fabric contains two subgroups, F-IV_a and F-IV_b, due to the presence of plagioclase in the latter. In addition, F-V is very similar to F-IV, but it does not contain calcite, thus suggesting an EFT of 950 °C. Finally, although F-VI contains the same phases of F-IV_b, the EFT of the former is of 950-1000 °C, and the reasons are the much more intense signals of plagioclase. In addition, the appearance of calcite in F-VI is probably related to a re-carbonation.

It is important to highlight that F-I fabric contains reddish and grey and reddish pastes, whereas the rest contain beige or buff-coloured and some reddish

pastes. This is a technological empirical choice performed by potters. The high amounts of CaO, along with relatively low Fe_2O_3 contents, provide buff-colour to the ceramic pastes in oxidizing conditions (Molera et al., 1998, 2015). Heimann (2010) explains that the colour change depends on the size of the calcite grain, because it controls the ratio of diopside to anorthite in the oxidizing fired product. Diopside can incorporate Fe^{3+} ions into its crystal structure, while anorthite is unable to incorporate large amounts of them. Therefore, a low diopside/anorthite ratio results in the formation of iron oxides phases, such as hematite, due to the free Fe^{3+}. Hematite (Fe_2O_3) is the responsible for the paste being red instead of buff. Therefore, ceramics from Z-3 group developed buff-coloured clay pastes, since the process of incorporation of iron oxides into calcium iron silicates has already occurred. This is usually a desirable condition for tin-lead glazed ceramics in order to avoid any strong coloured signal from the paste into the white opaque glaze, at the same time that it saves Sn raw material, an expensive commodity during post-Medieval period in the region (Molera et al., 1997, 1998). Contrarywise, ceramics from Z-1, Z-2, B-1 and T-1 groups show principally red pastes, mainly due to the presence of hematite (Fe_2O_3) and the low CaO content.

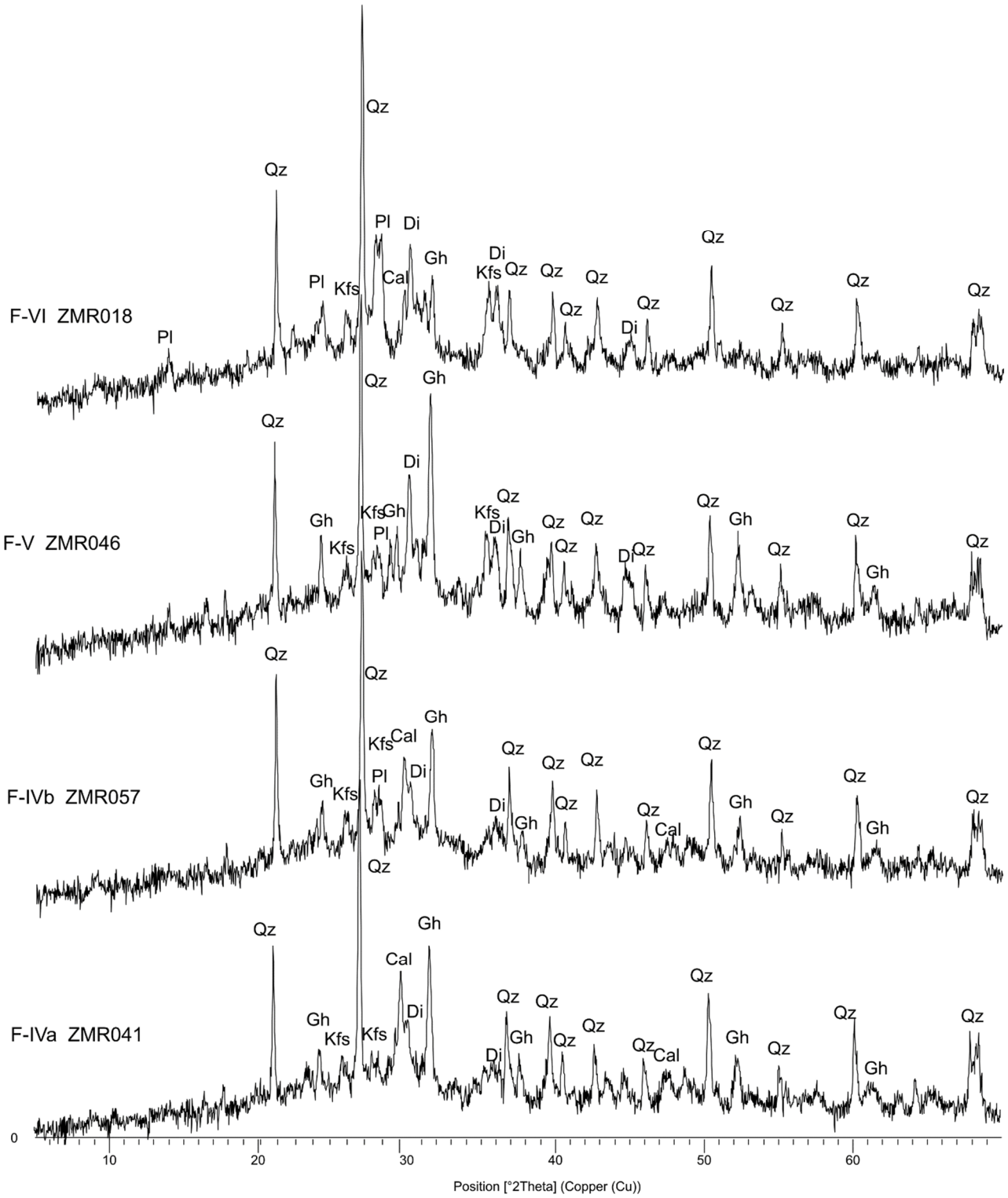
F-VI ZMR018
F-V ZMR046
F-IVb ZMR057
F-IVa ZMR041
Qz
Pl
Kfs
Cal
Gh
Di
0
10
20
30
40
50
60
Position [°2Theta] (Copper (Cu))

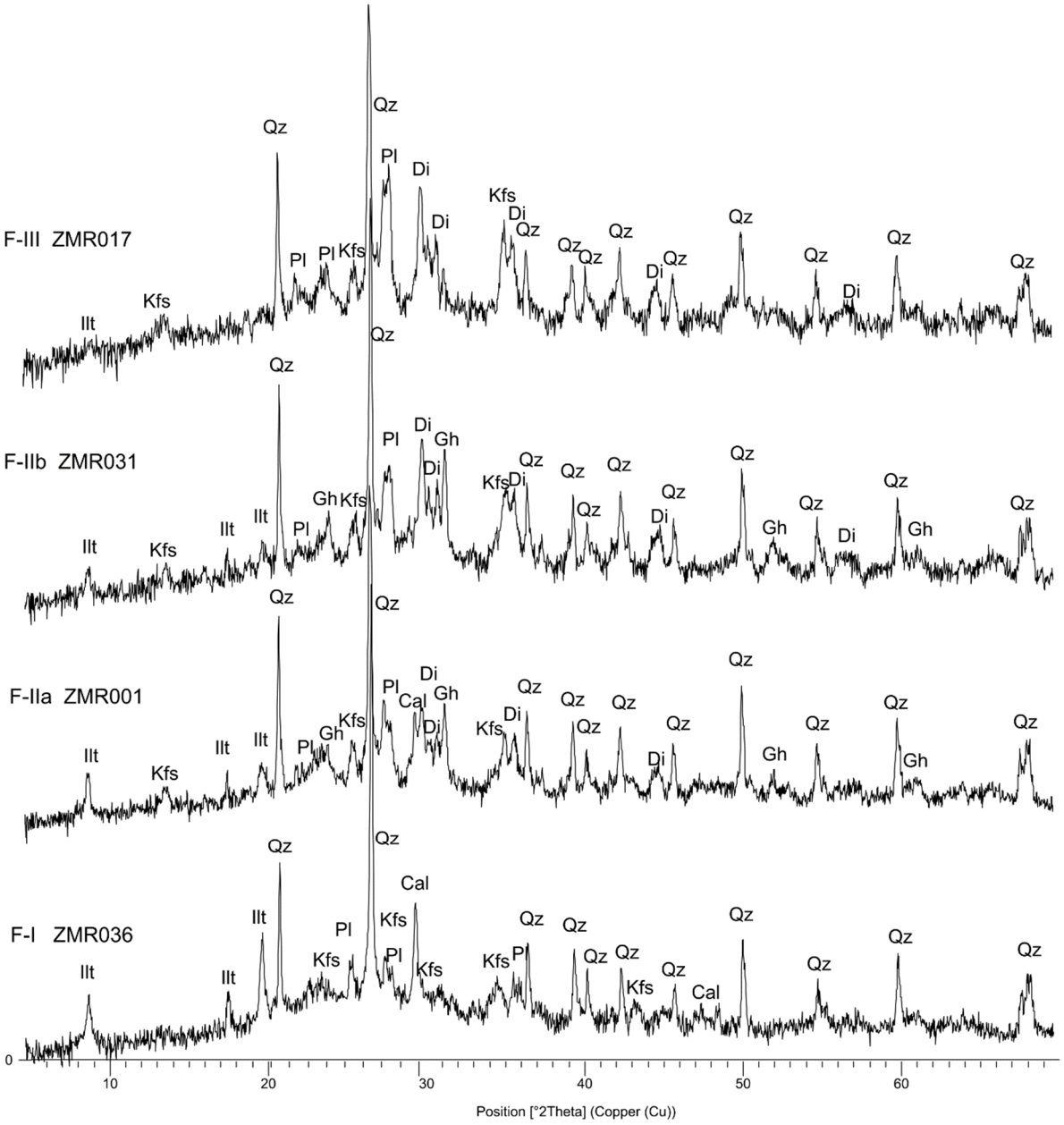

Figure 6.17. Reference diffractograms of the fabrics from Z-3 reference group. Qz = quartz; Ilt = illite; Kfs = potassium feldspar; Cal = calcite; Di = diopside; Pl = plagioclase; Ak-Gh = akermanite-gehlenite, abbreviations according to Whitney and Evans (2010)

SEM-EDS assessment

On the one hand, Figure 6.18. shows the early-initial vitrified clay structure of ZMR010 (F-I). This low vitrification state is in agreement with the temperature estimated by mineralogical analysis for F-I. On the opposite side, Figure 6.18. shows an important vitrified sinterization of ZMR026 (F-IV), fired at 950-1000 °C.

On the other hand, regarding the glaze composition of glazed ceramics from Z-3, all of them were glazed using a mixture of Pb and Si, probably using a frit before, as suggested by the literature (Iñañez, 2007) and as commented in the previous sections. In addition, SEM-EDS enables the identification of crystals including Sn particles distributed evenly within the glaze (Figure 6.18.c-f). These crystals are cassiterite (SnO_2) (this fact is confirmed by Raman, see the next section, "Raman results section"). Along with some relicts of quartz and sometimes feldspars, cassiterite helps achieving the opaque white colour diffracting and dispersing the incident light (Iñañez et al., 2013; Molera et al., 1999). According to SEM examinations, it can be confirmed that Zamoran potters used a two-firing technique for crafting their potteries. This fact is further supported by the existence of a very thin reaction area in the interface between glaze and clay body, which shows low crystallization in all the ceramics (Figure 6.18.c,e and Figure 6.19.a), as also evidenced by other authors (Molera et al., 1993, 2001). Furthermore, it is documented in historical written sources that majolica potters in Modern Era Spanish productions commonly employed a double firing technique: firstly, the modelled pot was fired, providing a fired pot known as biscuit; secondly, potters applied the glaze coating and decoration to the biscuit ceramic and fired it, usually at a lower temperature (Iñañez, 2007). Besides, biscuit and failure ceramic evidences have been unearthed at the Olivares workshops kiln dumps as well as in La Concepción, reinforcing the idea of a double firing process conducted in Zamora productions (Iñañez et al., 2018; Sanz et al., 2005). During the process of a second firing, the compounds from the glaze are still diffused into the ceramic body and vice versa. The Pb clearly diffuses into the clay body, while Sn does not, since particles are dispersed into the glaze and are not dissolved in it (Molera et al., 1999) (Figure 6.18.c-f). However, Sn compounds clearly influence the paste composition as explained in Chapter 4, section 4.4.2.

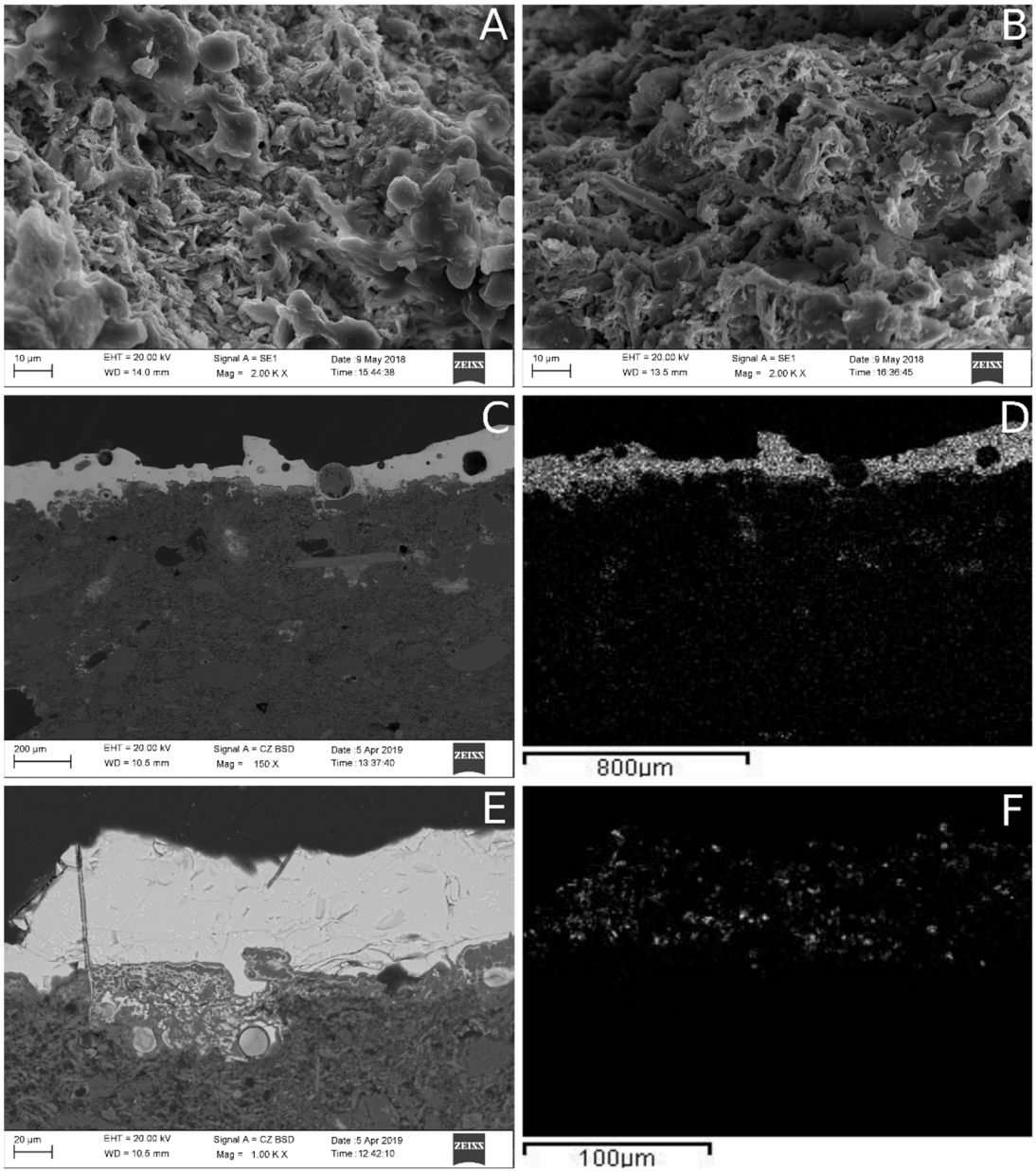

Figure 6.18. SEM-SED (a,b) and SEM-BSD (c,e) microphotographs and SEM-EDS microanalyses of Z-3 chemical group ceramics (from upper left to bottom right: **(a)** ZMR010 paste; **(b)** ZMR026 paste; **(c)** ZMR056 glaze; **(d)** elemental distribution of Pb in the region of (c) (ZMR056); **(e)** ZMR056 glaze; **(f)** elemental distribution of Sn in the region of E (ZMR056)

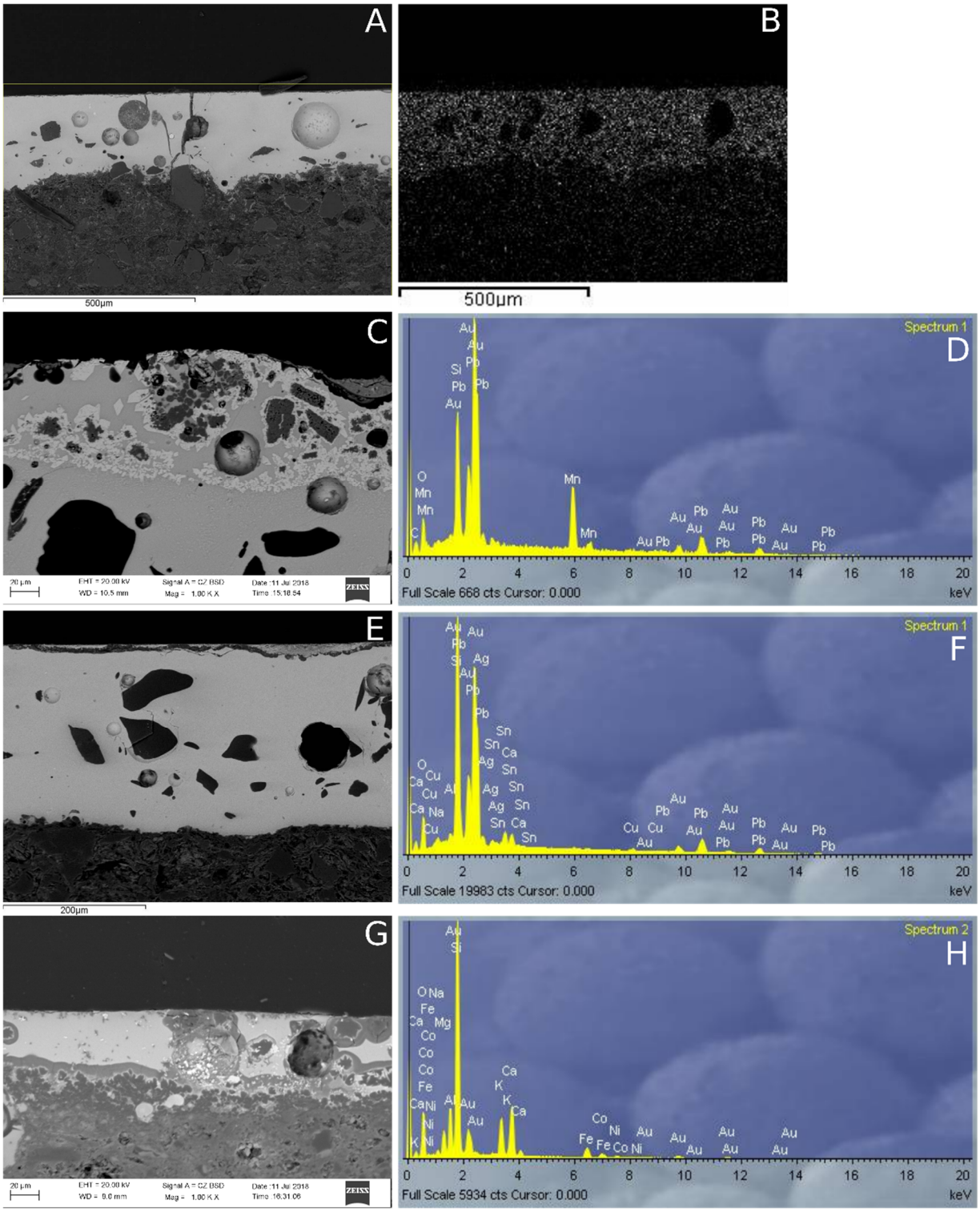

Figure 6.19. SEM-BSD microphotographs and SEM-EDS microanalyses of Z-3 chemical group ceramics (from upper left to bottom right: **(a)** ZMR052 glaze; **(b)** elemental distribution of Mn in the region of (a) (ZMR052) (black pigment); **(c)** ZMR045 glaze; **(d)** ZMR045 EDS spectrum, showing Mn for the brown colour; **(e)** ZMR045 glaze; **(f)** ZMR045 EDS spectrum, showing Cu for the green colour; **(g)** ZMR046 glaze; **(h)** ZMR046 EDS spectrum, showing Co and Fe for the blue colour

Moreover, regarding the black/brown colour decorations, remarkably, Mn compounds are unequivocally the responsible for obtaining these pigments. Moreover, this result is in accordance with other brown/black pigments in tin-lead glazes from the Iberian Peninsula dated back to the 11th century onwards (Coentro et al., 2012, 2018; Molera et al., 2013; Pradell et al., 2010). Besides, it can be seen that Mn particles are clearly evenly distributed within the black region of the glaze (black in Figure 6.19.a-d). It is supposed that for the rest of black/brown decorations from Z-3, Mn compounds were used too. However, the composition of these Mn-compounds remains unclear so far. According to Molera et al. (2013), the most common Mn-bearing crystals found at these kind of manufactures are hausmannite, braunite and kentrolite, as well as bustamite. Furthermore, Coentro et al. (2020) identified the inclusions observed by μ-Raman as braunite ($Mn^{2+}Mn_6^{3+}SiO_{12}$) in brown-coloured glazes.

Additionally, green pigments have been also identified by SEM-EDS. Green decorations follow traditional Hispano-Moresque recipes for green colour achievement, traditionally using Cu compounds. Accordingly, Cu content has been found dispersed in green areas by SEM-EDS (Figure 6.19.e,f). The fact that Sn also appears in the same region than green decoration leads us to think that Cu compound is applied over the white glaze in order to get green colour and not under the white coating. This is in agreement with previous studies for the main Post-Medieval production centres of Spain (Iñañez, 2007; Iñañez et al., 2013).

Besides, the blue decoration on Z-3 has been studied only in ceramics from La Concepción (Z-3). Interestingly, in the blue areas, Co-Fe-Ni particles are found under the glaze and directly in contact with the clay body, suggesting that the blue decoration was achieved at least by the use of Co, Ni and Fe (Figure 6.19.g,h). Coentro et al. (2020) identified Co, Fe and Ni inclusions corresponding to ferrite spinels (nickel ferrites, $NiFe_2O_4$ and cobalt ferrites, $CoFe_2O_4$) for blue pigments. Unexpectedly, this blue under coating decoration has been identified for the first time in the area of Zamora. However, this undercoating decoration technique has few parallels in other areas of the Iberian Peninsula, mainly in Valencia (Castro and Doménech, 1955; Roldán et al., 2006), in Teruel (Pérez-Arantegui et al., 2009b), in Seville (Pleguezuelo, 2011), in Catalonia (Pradell et al., 2010) and in Granada (García-Porras, 2012). Besides, interestingly, a K- and P-enriched layer related to these Co-Fe-Ni particulates has also been detected as an interphase between the paste and the glaze. Coentro et al. (2020) mention that potassium feldspars (mainly sanidine,

Molera et al. (1993)) may appear as an intermediate phase due to the reaction between lead-rich glazes and potassium-rich ceramic bodies at high temperatures. Phosphorous probably is related to post-depositional contaminations.

Raman assessment

On the one hand, the Raman study of the glaze ZMR054 allowed to identify the crystals containing Sn as cassiterite (SnO_2), giving the typical bands in Raman spectra, with the main maximum corresponding to 636 cm^{-1} (De Waal, 2009) (Figure 6.20.a).

Moreover, the study of ZMR056 ceramic by Raman microscopy enabled the identification of cerussite ($PbCO_3$), giving the typical bands in Raman spectra, with the main maximum corresponding to 1055 cm^{-1} (Wang et al., 2013) (Figure 6.20.b). Wolf et al. (2003) reported that, in the central Iranian mines, there was a tradition of mining cerussite rather than galena (PbS). Technically, such tradition might be explained due to the fact that cerussite has the advantage over galena of not requiring a previous roasting to make lead oxide for the production of a lead glaze. However, Molera et al. (2013) described that the lead glaze appears heavily altered due to the burial conditions, and cerussite, formed by carbonation of leached lead, is mainly present in the bubbles and cracks. Figure 6.20. shows an image of the glaze coat of ZMR056 taken by Raman spectrometry. In this figure, a bubble is evident, corresponding to cerussite after Raman identification. Given that cerussite has been found in a crack or bubble in the glaze, the most probable hypothesis is that the cerussite found in this glaze is not a primary compound, but the subproduct of the primary lead oxide after the alteration processes.

Finally, the ZMR058 glaze showed a yellowish tone on the white glaze, similar to a white cream colour. The study by Raman of this glaze enabled the identification of a lead-tin yellow type II ($PbSn_{1-x}Si_xO_3$) compound, giving the typical bands in Raman spectra, with the main maximum corresponding to the vibration of Pb-O at 138 cm^{-1} (Clark et al., 1995; Šefců et al., 2015) (Figure 6.20.c). The oldest references that mention the usage and preparation of lead-tin yellow pigments (lead-tin yellow type I and type II) in artworks can be found in medieval manuscripts, according to Šefců et al. (2015). Likewise, as Sandalinas et al. (2006), lead-tin oxides and lead-antimony oxides have been employed since antiquity as opacifiers and yellow colourings of glass, enamel and pottery production. For that, as mentioned in the

treatises wrote by the Persian potter Abu'l-Qasim Kashani in 1301 (Allan, 1973), one of the ancient production of the opaque glazes would have taken place in two stages (Matin et al., 2018): first, a mixture of lead and tin was calcined (oxidized) by heat to produce lead-tin yellow type I, also known as the "calx" powder, according to the next reaction (Šefců et al., 2015):

$$2Pb_3O_4 + 3SnO_2 \rightarrow 3Pb_2SnO_4 + O_2 \quad Eq.\ 6.1.$$

In the second stage, to produce the opaque yellow glaze, the "calx" powder was mixed with a source of silica (e.g., quartz) and heated. To produce the opaque white glaze, alkaline ashes were also added to the mixture of calx and silica and then again heated. The same technical strategy is reported by Piccolpasso in his treatise about Italian majolica pottery (Lightbown and Caiger-Smith, 1980). Nevertheless, the ceramic shard ZMR058 is not a yellow opaque glazed ware, but a white yellowish or white cream colored one. This is the reason why the hypothesis of the appearance of the lead-tin yellow type II compound could be due to a modification of the primary lead oxide compound of the glaze, in accordance with the next possible alteration way: when silica (SiO_2) is added to the lead-tin-oxide type I and the mixture is fused between 800 °C and 950 °C, the lead-tin yellow type I compound, with orthorhombic crystal structure, can be transformed into the lead-tin yellow type II compound, which has a cubic crystal structure (Šefců et al., 2015). During this process, Pb_2SnO_4 incorporates variable amounts of SiO_2, substituting the SnO_2 compounds, according to the next reaction (Matin et al., 2018; Šefců et al., 2015):

$$Pb_2SnO_4 + SiO_2 \rightarrow PbSn_{1-x}Si_xO_3 \quad Eq.\ 6.2.$$

Šefců et al. (2015) proved that it is possible to find the primary substances in the final mixture if the firing temperature is lower than necessary.

Considering this reaction and taking into account that ZMR058 glaze is not a yellow opaque glaze one, but a white yellowish or white cream coloured one, the following hypothesis is contemplated: the potters used the same technical strategy as mentioned in the treatises of Abu'l-Qasim Kashani and Piccolpasso (Allan, 1973; Lightbown and Caiger-Smith , 1980), that is, they first calcined a mixture of lead and tin to produce the lead-tin yellow type I compound, and, secondly, they mixed this matter with a source of silica (e.g. sand) and alkaline substances (e.g. plant ashes or some kind of salt). This latter is in agreement with the Hispano-Moresque technological tradition (Tite et al., 1998) and the recipes listed by Piccolpasso (Lightbown and Caiger-Smith, 1980). Then, the high firing temperatures enabled the

reaction mentioned, so that the lead-tin yellow type I was partly transformed into the lead-tin yellow type II, likely, not intentionally. Thus, the relicts of such crystallites seem to deliver a yellowish tone to the overall amorphous tin-lead glaze matrix. Oppositely, this compound has not been identified so far in other ceramics from the sample, thus showing a much whiter opaque glaze (see images in Figure 4.3. from Chapter 4).

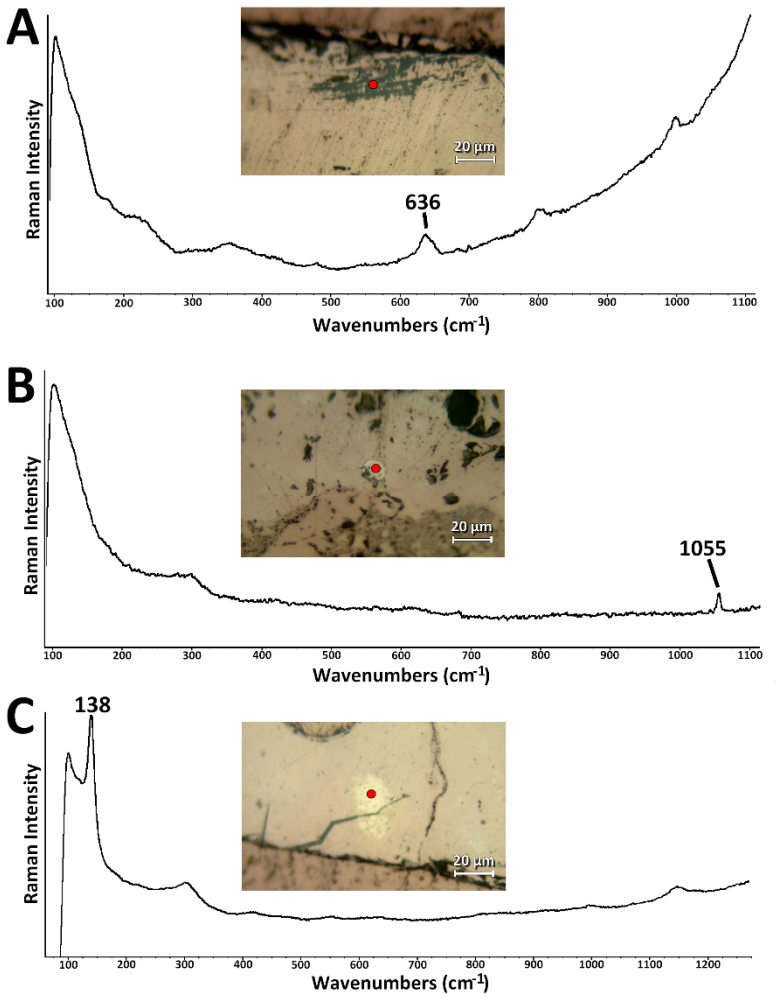

Figure 6.20. **(a)** Photomicrograph and Raman spectrum of cassiterite in the glaze ZMR054 by Raman microscopy; **(b)** Photomicrograph and Raman spectrum of cerussite in a bubble or crack of the ZMR056 glaze by Raman microscopy; **(c)** Photomicrograph and Raman spectrum of lead-tin yellow type II compound in ZMR058 glaze by Raman microscopy

Finally, the elemental characterization of Ethnographic Museum ceramics from Z-3 shows some differences with respect to the rest of ceramics in the case of P_2O_5: the concentration of this compound is higher in the Ethnographic Museum ceramics than in the rest (see Table 6.1.). The post-depositional context could be a reason for the higher presence of this compound. According to the elemental distribution observed in Figure 6.21.a-l, the presence of phosphorous is accompanied by calcium, both in the ceramic paste and in the glaze. One of the hypotheses is that this could occur due to the post-depositional contamination, subjected to the existence of phosphorous compounds in soil waters. These soil waters could penetrate into the ceramic glaze and clay in more than one way: (i) spreading through the glaze and forming Liesegang rings-like degradation and (ii) taking advantage of one crack to penetrate into the ceramic body (Calparsoro, 2019). The concentration of this element in the ceramic pastes might vary depending on the exact burial location of the ceramics (Freestone et al., 1985).

As is shown in Figure 6.21.a-c, there are some cases in which cracks appear in the glaze while they do not occur in other cases (Figure 6.21.d-i). In addition, there are some cases where phosphorus and calcium forming perfectly defined spheres could be seen (Figure 6.21.j-l). The reason for this phenomenon could be the strong correlation between P_2O_5 and CaO, according to Freestone et al. (1985). The trend of this correlation suggested the addition of a phase with a constant Ca/P ratio corresponding to $CaO{\cdot}P_2O_5$ towards the surfaces of the shard, forming apatite ($Ca_5(PO_4)_3(Cl,F,OH)$) or brushite ($Ca(HPO_4){\cdot}2H_2O$), but they can form also a compound such as monocalcium phosphate monohydrate (MCPM, $Ca(H_2PO_4)2{\cdot}H_2O$), as Jones and Smith (1962) proposed. Even if the initial mechanism of phosphate fixation could be absorption, reaction and compound formation take place later (Freestone et al., 1985). Therefore, calcium and phosphorus represent environmental contamination of the shard.

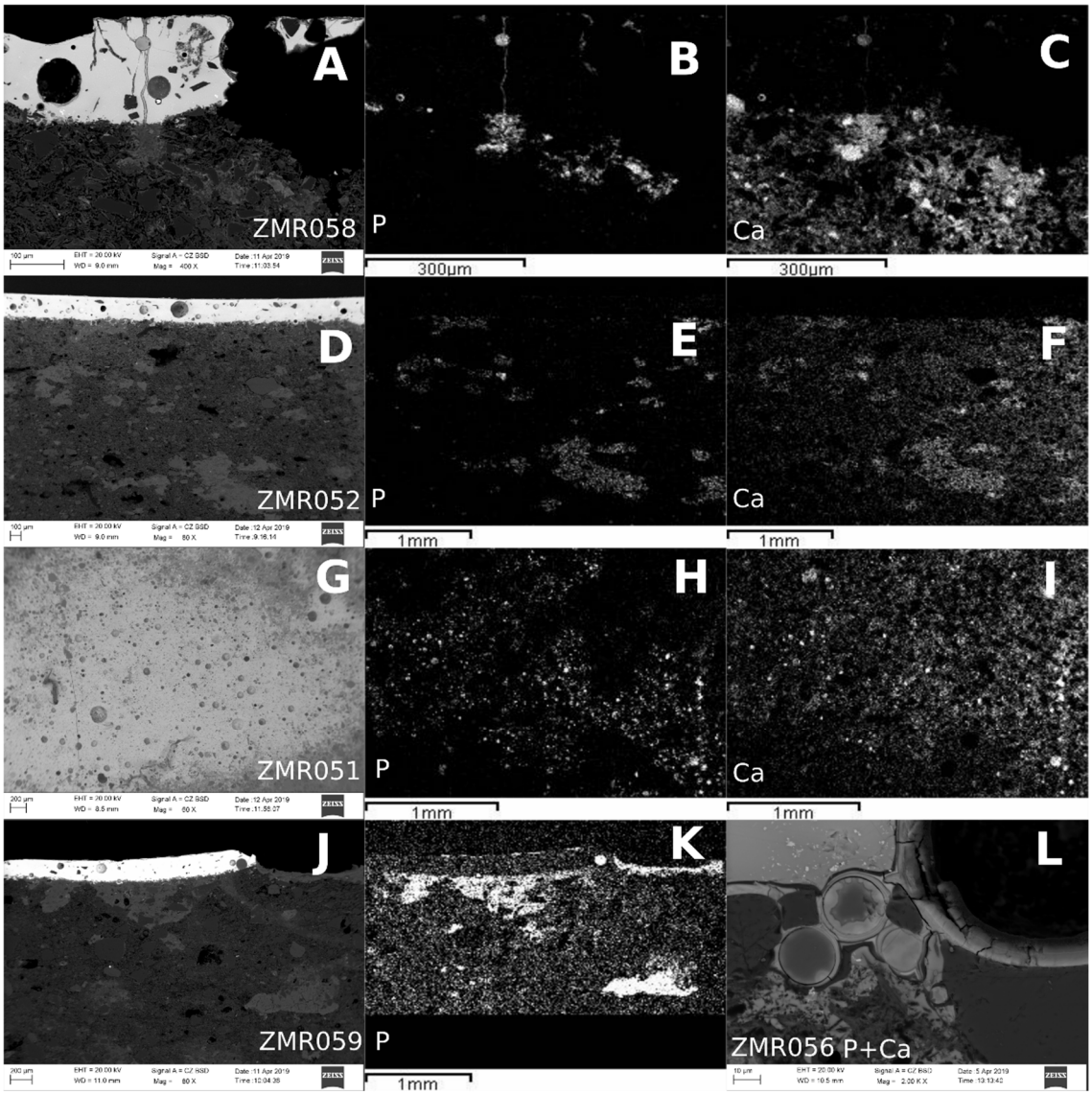

Figure 6.21. (a) SEM-BSD images of ZMR058; **(b-c)** elemental distribution of P and Ca in the region of (a) (ZMR058); **(d)** SEM-BSD image of ZMR052; **(e-f)** elemental distribution of P and Ca in the region of (d) (ZMR052); **(g)** SEM-BSD image of ZMR051 surface; **(h-i)** elemental distribution of P and Ca in the region of (g) (ZMR051); **(j)** SEM-BSD image of ZMR059; **(k)** elemental distribution of P in the region of (j) (ZMR059); **(l)** SEM-BSD image of ZMR056: phosphorus and calcium forming spheres in the interphase of the glaze

Z-4 PCRU

Z-4 is formed by 4 micaceous unglazed ceramics. Chronologically, the ceramics of this group correspond to the 15th-16th centuries (see Table 6.2.). This group shows a low-calcareous clay paste, with CaO concentration around 4 wt % (see Table 6.3.). In addition, Z-4 group shows high amounts of Al_2O_3 (25 wt %), clearly linked to the high quantity of phyllosilicates (e.g. mica) and due to its optimal technical properties for thermal shock resistance.

Technological assessment by XRD

In this group, one mineralogical fabric has been identified, F-I (Table 6.4. and Figure 6.22.) and the EFT for this is in the range of 850-900 °C.

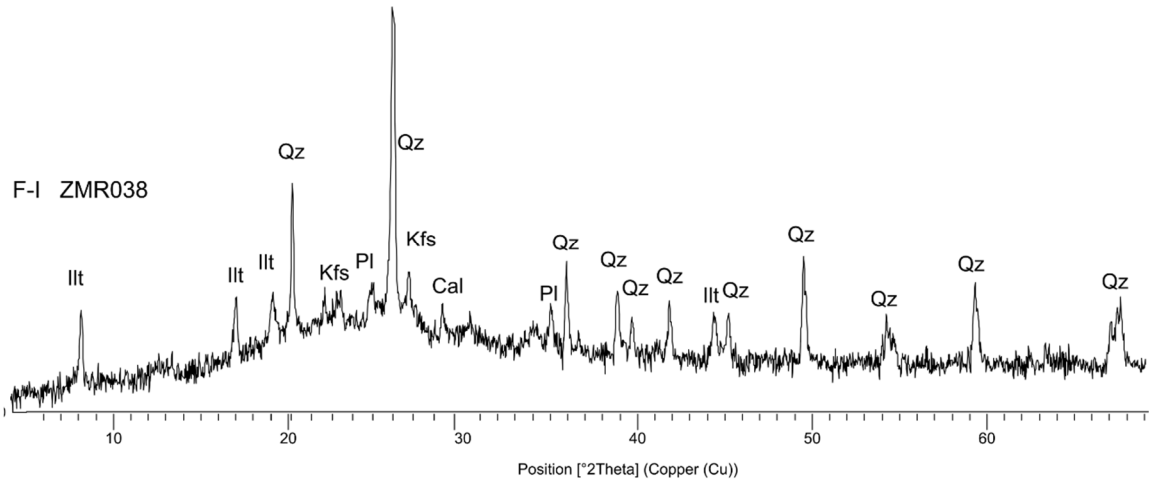

Figure 6.22. Reference diffractograms of the fabric from Z-4 reference group. Qz = quartz; Ilt = illite; Kfs = potassium feldspar; Cal = calcite; Pl = plagioclase, abbreviations according to Whitney and Evans (2010)

B-1 reference group

B-1 is formed by 12 unglazed redware. Chronologically, the ceramics of this group correspond to the 16th-18th centuries (see Table 6.2.). The group includes jugs, pitchers and small jars and the ceramics are low-calcareous, averaging to 2 wt % in CaO concentration. In addition, this group contains 8 wt % of Fe_2O_3, much more than Z-1, Z-2, Z-3 and Z-4, which probably is related to the red colour of the pastes.

Technological assessment by XRD

Besides, the group includes three fabrics, F-I, F-II and F-III, respectively (Table 6.4. and Figure 6.23.). Since F-I contains illite, the EFT is suggested to be 800-850 °C. Moreover, since illite has been decomposed in F-II, the EFT is suggested to be 850-900 °C, and around 1050 for F-III, due to the presence of mullite.

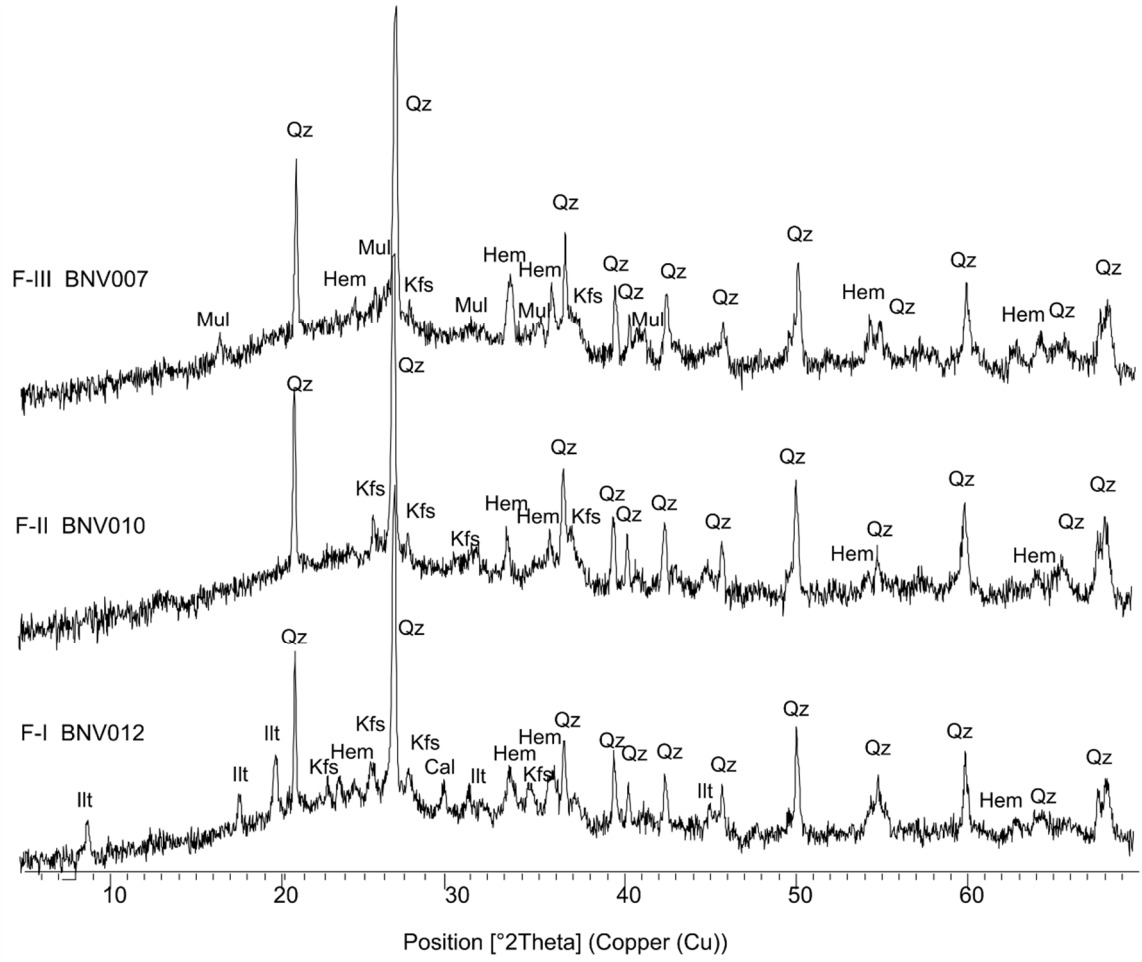

Figure 6.23. Reference diffractograms of the fabrics from B-1 reference group. Qz = quartz; Ilt = illite; Kfs = potassium feldspar; Cal = calcite; Mul = mullite; Hem = hematite, abbreviations according to Whitney and Evans (2010)

T-1 reference group

T-1 is formed by 6 unglazed and 6 translucent-glazed redware and the set includes several forms, such as mugs, small jars, chamber pots, pitchers, lids, cups and pipes. Chronologically, the ceramics of this group correspond to the 17th century (see Table 6.2.). The ceramics are low-calcareous, averaging to 1 wt % in CaO concentration. In addition, this group contains 6 wt % of Fe_2O_3, less than B-1 but

more than Z-1, Z-2, Z-3 and Z-4, which probably is also related to the red colour of the pastes.

Technological assessment by XRD

The group includes two fabrics, F-I and F-II, respectively (Figure 6.24.). Since illite is present in F-I, the EFT is suggested to be around 800-850 °C. Moreover, F-II contains very few amounts of illite, so its EFT is around 850-900 °C.

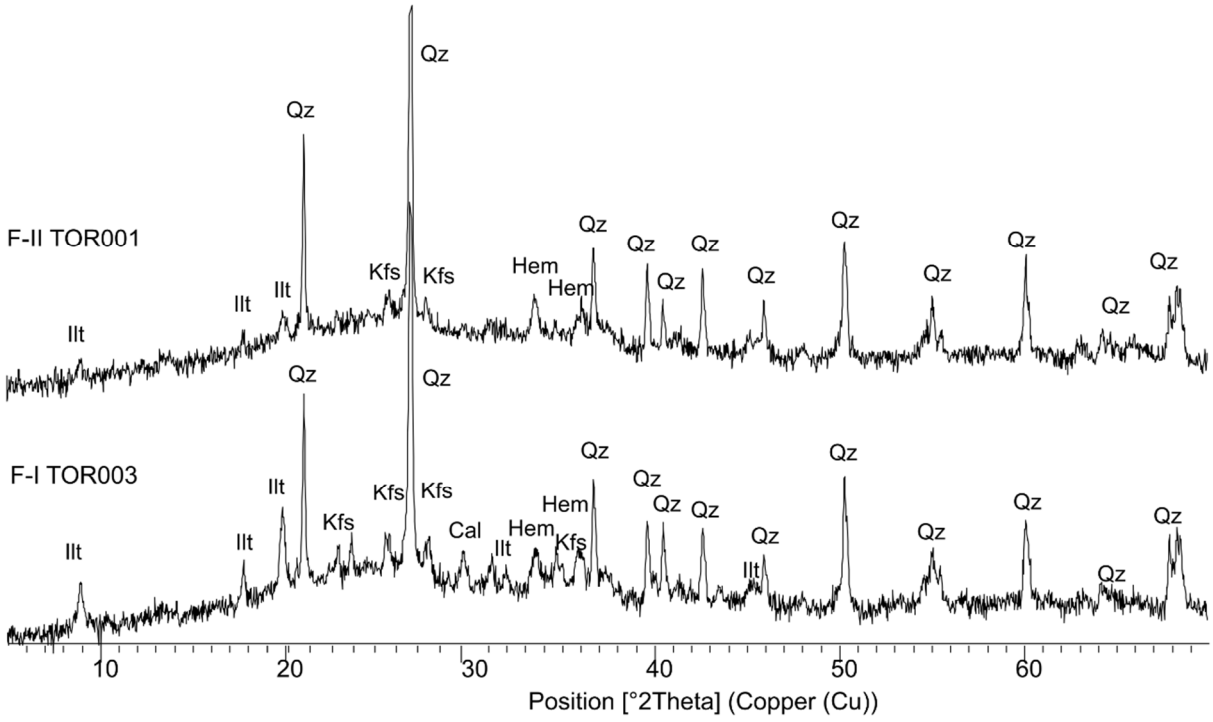

Figure 6.24. Reference diffractograms of the fabrics from T-1 reference group. Qz = quartz; Ilt = illite; Kfs = potassium feldspar; Cal = calcite; Hem = hematite, abbreviations according to Whitney and Evans (2010)

Furthermore, SEM-EDS analyses from Figure 6.25. show that these glazes (like the rest of the glazes of the group), were coated with a translucent honey-glaze, like their counterparts from Z-1 and Z-2 groups.

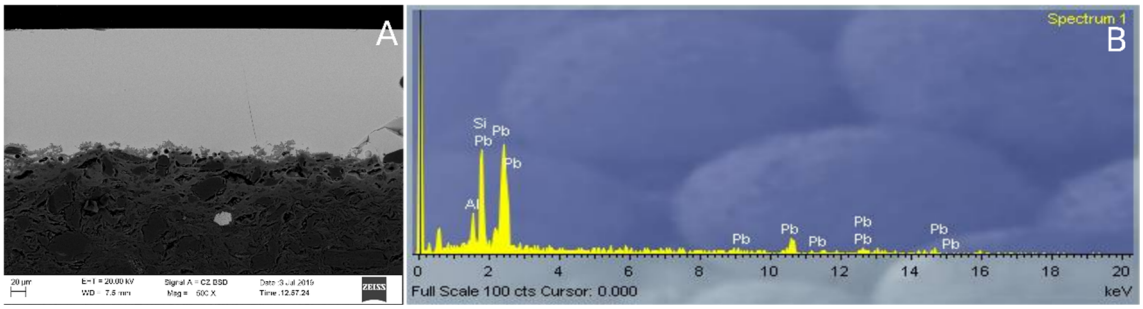

Figure 6.25. SEM-BSD microphotograph and SEM-EDS microanalysis of TOR001 ceramic from T-1 chemical group (from left to right: **(a)** TOR001 glaze; **(b)** TOR001 glaze EDS spectrum

Finally, Figure 6.26. and 6.27. show the general chemical tendency of each group. Thus, Figure 6.26. displays that Z-3 is richer in CaO, MgO, Sr and MnO than the rest of the groups, due to its high-calcareous beige and buff-coloured pastes. In addition, the micaceous Z-4 group is richer in components such as Cs and Rb than the rest. Besides, despite the fact that Z-1 is a group with translucent-glazed red ceramics and Z-2 is micaceous, they are more similar than Z-2 and Z-4 are. This is an interesting fact, because it might give clues about Olivares production: since Z-1 and Z-2 have similarities, they may be clays which were in the same geological region or even same outcrop. Thus, Z-2 production group migh have been taken place in Olivares workshops, and not in an exogenous workshop, as it was suggested earlier. Besides, Figure 6.27. depicts that although there are little similarities, B-1 and T-1 are different reference groups, T-1 being richer in Sn and Sr, and B-1 in MnO.

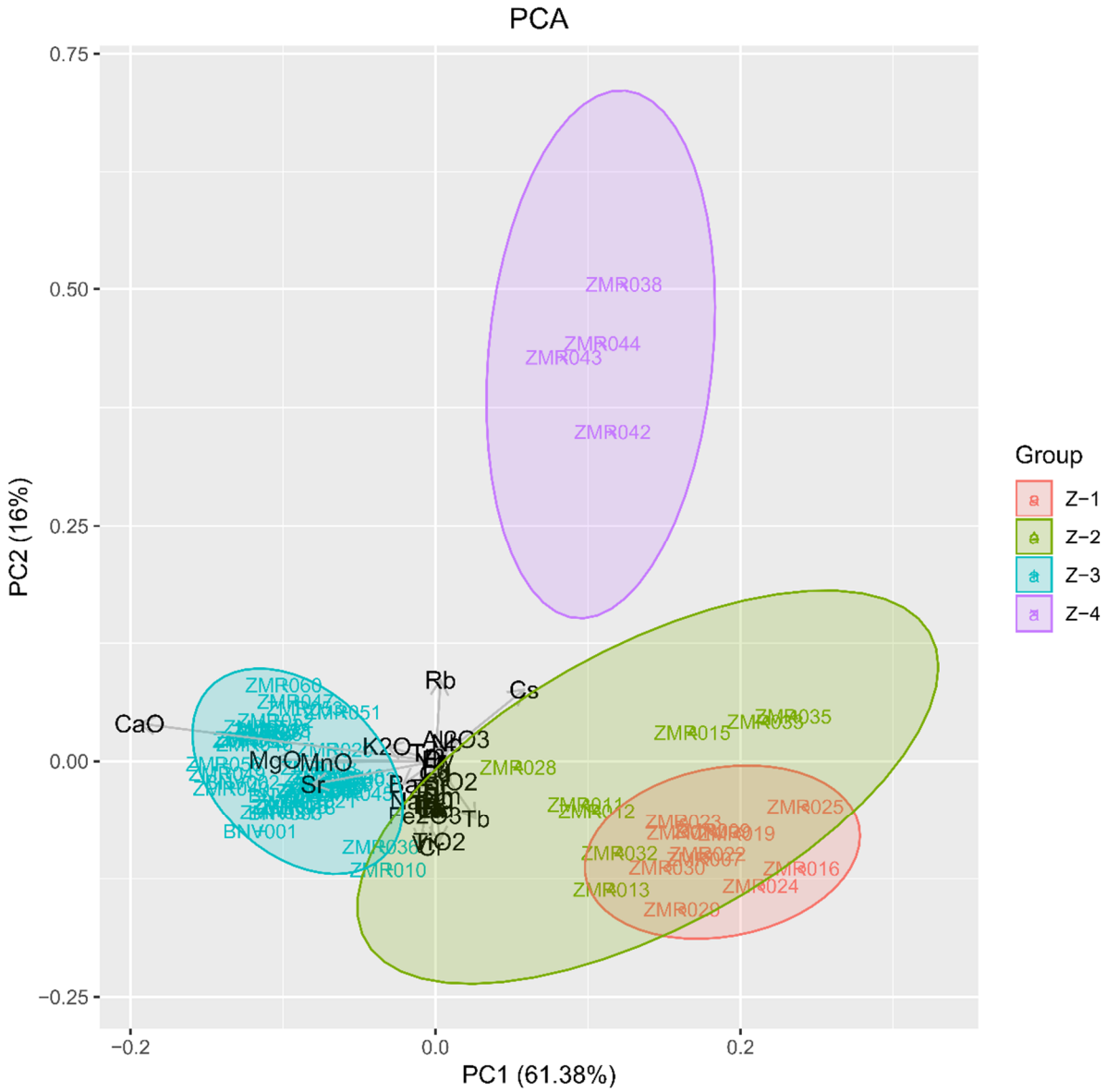

Figure 6.26. Principal Component Analysis of shards from different sites of Zamora, corresponding to Z-1, Z-2, Z-3 and Z-4 chemical groups, on the sub-composition of all the measured components (42) (with the exception of Co, Cu, Ni, P_2O_5, Pb, Sn, Ta, U and Zn). Ho has been used as divisor

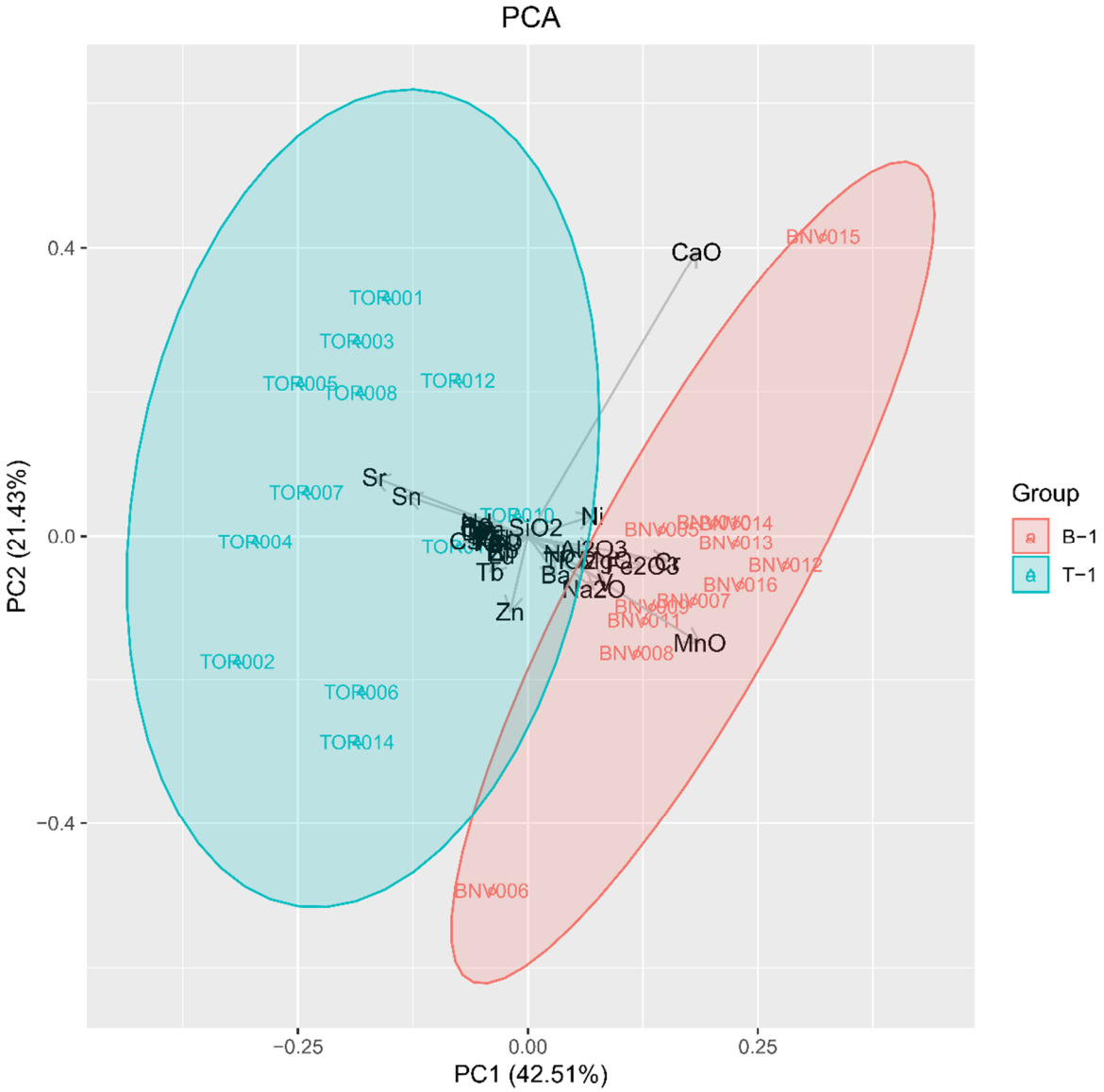

Figure 6.27. Principal Component Analysis of shards from Toro and Benavente, corresponding to T-1 and B-1 chemical reference groups, on the sub-composition of all the measured components (42) (with the exception of Co, Cu, P_2O_5, Pb, Ta and U). Th has been used as divisor

6.2. Aveiro

The concentrations of each component and their relative average expanded uncertainties (U %) for the 28 ceramics analysed by ICP-MS, are presented in Table 6.5. The expanded uncertainty of the results has been calculated in the same way as for the 11 ceramics of the Ethnographic Museum, following the Guide to the Expression of Uncertainty in Measurement (GUM) with k = 2, which is equivalent to a 95 % confidence level, considering the whole analytical procedure (see Chapter 4, section 4.4.3.). Since the type of calibration was the same for the whole set of Aveiro ceramics, an approximation has been made: the uncertainties calculated for 25 ceramics of Aveiro (U % for AVR021, AVR027 and AVR028 was not calculated) are extrapolated to the rest of ceramics (see Table 6.5.). It should be highlighted that the calculated U % values for the Ethnographic Museum ceramics are not useful for Aveiro ceramics, because the calibration curves of Aveiro ceramics were obtained using 12 concentration values and not using 4, as has been done for Zamoran ceramics.

Table 6.5. Elemental concentrations and their relative average expanded uncertainties (U %) for the 30 ceramics analysed by ICP-MS. Some values of P_2O_5 and Zn were omitted since they showed values below the quantification limit. The concentrations of the elements are expressed in ng/g and of the oxides in wt %. The calcareous or high-calcareous ceramics are marked in bold (those with CaO ≥ 6 %)

Samples	Al_2O_3	Ba	CaO	Ce	Co	Cr	Cs	Cu	Dy	Er	Eu	Fe_2O_3	Gd	Hf	Ho	K_2O	La	Lu	MgO	MnO	Na_2O
AVR001	17.9	371	3.08	96.3	38.7	39.1	26.9	4.80	5.19	2.66	1.16	4.54	6.41	6.41	0.743	4.08	48.3	0.418	1.59	0.0171	0.465
AVR002	15.2	385	4.61	73.9	35.6	30.0	23.3	5.60	4.33	2.22	1.09	3.68	5.02	5.05	0.641	4.60	36.7	0.351	1.35	0.0168	0.759
AVR003	17.3	408	4.23	108	36.8	39.8	26.7	12.5	5.62	2.91	1.40	5.10	7.32	6.67	0.786	4.40	54.8	0.442	1.70	0.0190	0.501
AVR004	16.4	434	4.91	88.8	32.2	22.9	26.4	12.8	4.08	2.24	1.17	4.51	5.55	5.29	0.596	5.72	44.2	0.314	1.59	0.0349	1.11
AVR005	18.4	380	4.17	104	42.7	46.7	28.7	3.00	5.44	2.86	1.17	4.94	6.68	6.89	0.749	4.47	52.3	0.447	1.72	0.0176	0.710
AVR006	15.4	370	4.50	71.5	23.5	30.1	23.9	11.8	3.84	2.06	1.00	3.74	4.90	5.18	0.577	4.37	37.1	0.312	1.61	0.0142	0.735
AVR007	18.0	365	4.75	104	28.1	44.4	28.5	4.62	5.31	2.85	1.18	5.13	6.53	6.81	0.743	4.62	51.8	0.420	1.88	0.0177	0.648
AVR008	17.7	419	4.93	104	19.5	45.4	27.6	3.48	5.07	2.62	1.23	4.67	6.57	5.86	0.722	5.04	50.2	0.440	2.09	0.0221	0.680
AVR009	17.7	383	3.70	96.0	16.5	40.1	25.4	9.63	4.87	2.68	1.15	4.87	6.02	6.68	0.690	4.45	48.2	0.403	1.67	0.0179	0.482
AVR010	15.0	372	3.62	76.1	30.2	25.8	23.9	8.62	4.47	2.32	1.12	4.36	5.15	5.84	0.655	4.72	36.4	0.353	1.56	0.0172	0.797
AVR011	16.1	403	5.66	84.8	88.6	33.6	25.5	10.5	4.64	2.34	1.04	4.37	5.69	5.52	0.683	4.73	42.4	0.379	1.69	0.0233	0.671
AVR012	16.6	475	4.66	96.5	27.1	38.1	24.7	11.7	5.12	2.45	1.33	4.66	6.30	5.70	0.700	4.37	46.0	0.397	1.74	0.0195	0.585
AVR013	16.9	389	3.92	104	17.5	34.3	26.1	9.23	4.86	2.34	1.23	4.24	6.17	5.37	0.668	4.44	46.7	0.405	1.74	0.0175	0.643
AVR014	16.4	406	3.67	93.4	19.6	45.9	25.3	5.63	4.63	2.22	1.15	4.03	5.49	5.61	0.668	4.50	42.4	0.405	1.64	0.0227	0.644
AVR015	18.0	395	3.82	96.7	31.5	47.0	26.8	20.7	5.40	2.65	1.14	4.97	6.07	6.55	0.750	4.48	49.9	0.463	1.71	0.0185	0.847
AVR016	17.7	409	3.64	110	27.9	44.1	26.7	3.44	5.91	2.85	1.41	5.22	7.21	6.59	0.829	4.47	54.9	0.489	1.80	0.0205	0.538
AVR017	21.2	451	5.06	117	18.1	62.6	27.5	32.5	6.70	3.10	1.83	4.59	8.06	5.93	0.946	4.36	54.8	0.503	2.22	0.0304	0.452
AVR018	17.9	419	4.28	110	26.5	54.4	23.0	10.8	6.31	3.02	1.56	5.32	7.33	6.36	0.886	3.99	51.0	0.506	1.89	0.0323	0.441
AVR019	19.0	430	3.58	84.5	19.5	68.8	20.7	30.0	5.47	2.76	1.23	7.26	5.77	6.86	0.805	4.14	43.5	0.498	1.84	0.0213	0.365
AVR020	19.1	427	3.52	85.0	19.0	74.8	21.1	6.55	5.42	2.82	1.31	7.62	5.99	6.82	0.849	4.40	43.5	0.528	1.94	0.0224	0.390
AVR021	22.6	459	4.64	287	11.9	24.6	69.0	15.9	18.3	7.20	4.15	4.54	23.5	10.9	2.22	4.77	124	1.20	1.32	0.0462	1.72
AVR022	18.3	364	3.96	90.5	16.0	45.0	27.1	12.2	5.10	2.64	1.08	4.74	5.64	6.31	0.746	4.39	47.0	0.436	1.72	0.0174	0.430
AVR023	21.5	450	3.41	121	24.5	47.8	32.5	14.7	6.21	2.95	1.68	5.02	7.79	6.43	0.867	5.10	60.3	0.495	2.02	0.0218	0.695
AVR024	18.1	413	3.28	99.2	21.0	42.5	26.8	9.14	5.08	2.61	1.30	4.97	6.31	6.72	0.770	4.82	50.3	0.457	1.65	0.0169	0.561
AVR025	20.6	447	3.49	107	45.7	51.5	31.2	12.8	5.62	2.77	1.45	6.08	7.05	6.17	0.795	4.62	54.5	0.481	1.92	0.0208	0.499
AVR026	20.5	412	5.21	121	27.7	57.5	30.5	37.1	6.50	3.18	1.49	6.66	7.80	8.18	0.914	4.64	59.5	0.585	1.83	0.0208	0.500
AVR027	29.4	366	3.57	125	20.7	75.0	29.4	41.2	6.74	3.07	2.13	3.28	8.62	5.63	0.943	1.89	59.1	0.524	0.87	0.00813	0.255

	Al_2O_3	Ba	CaO	Ce	Co	Cr	Cs	Cu	Dy	Er	Eu	Fe_2O_3	Gd	Hf	Ho	K_2O	La	Lu	MgO	MnO	Na_2O
AVR028	16.3	409	**22.6**	100	15.9	78.8	9.71	74.5	6.94	3.58	1.73	3.42	7.91	7.74	1.04	1.78	52.4	0.606	4.97	0.0579	0.366
ANG030	18.1	411	2.95	105	39.9	53.5	26.9	4.74	6.44	2.97	1.49	5.20	6.97	4.24	0.976	4.41	47.8	0.356	2.05	0.0256	0.499
ANG031	17.5	396	2.51	93.7	29.3	62.6	25.6	3.32	5.31	2.61	1.27	5.30	5.84	4.48	0.751	4.14	45.6	0.349	1.81	0.0229	0.496
U (%)	6	5	84	6	26	38	4	24	13	22	11	8	10	6	20	4	5	17	18	28	34

(continues)

Samples	Nb	Nd	Ni	P_2O_5	Pb	Pr	Rb	SiO_2	Sm	Sn	Sr	Ta	Tb	Th	TiO_2	Tm	U	V	Yb	Zn	Zr
AVR001	21.6	41.1	15.6	-	37.4	10.9	301	69.6	6.97	18.7	86.2	3.50	0.874	18.8	0.727	0.439	5.11	56.6	2.65	-	235
AVR002	16.2	31.4	14.3	-	52.2	8.52	291	75.0	5.74	13.2	86.4	2.64	0.682	14.5	0.636	0.351	3.58	44.0	2.19	-	192
AVR003	21.0	48.6	14.8	-	36.0	12.9	300	71.9	8.74	17.7	95.2	3.42	0.966	18.4	0.737	0.433	4.69	58.8	2.74	-	241
AVR004	15.8	35.9	11.4	-	74.2	9.72	319	74.9	5.93	12.3	125	2.38	0.711	15.5	0.614	0.329	4.38	40.1	2.10	-	192
AVR005	22.2	44.4	28.4	-	37.0	11.8	316	72.2	7.78	17.7	85.9	3.47	0.854	19.5	0.786	0.443	5.33	63.2	2.73	-	246
AVR006	16.8	30.8	12.2	-	37.6	8.32	292	70.2	5.40	12.8	86.7	2.45	0.614	13.8	0.598	0.322	3.52	42.7	2.04	-	180
AVR007	22.4	43.1	17.8	-	37.9	11.9	310	75.6	7.42	16.4	80.2	3.39	0.820	18.6	0.788	0.437	5.18	60.7	2.67	-	234
AVR008	19.1	43.4	12.9	-	49.0	11.7	311	75.0	7.59	15.2	95.8	2.81	0.828	17.4	0.698	0.412	4.54	51.3	2.52	-	203
AVR009	21.7	40.5	18.1	-	42.5	10.9	288	73.9	7.14	17.5	87.9	3.27	0.811	17.7	0.768	0.409	4.84	48.9	2.48	-	238
AVR010	15.4	33.0	9.78	-	54.1	8.59	294	73.9	5.90	12.2	81.9	2.33	0.695	13.3	0.593	0.340	3.47	42.2	2.29	-	214
AVR011	18.2	36.8	13.5	-	48.1	9.71	304	76.7	6.66	15.5	87.6	2.80	0.756	15.5	0.673	0.367	4.39	47.2	2.28	-	205
AVR012	18.8	43.0	19.1	-	39.5	10.7	287	71.3	7.60	16.6	85.3	2.88	0.825	15.4	0.671	0.386	3.98	51.0	2.39	-	201
AVR013	18.2	40.8	11.4	-	41.1	10.9	298	68.8	7.59	14.7	87.7	2.80	0.800	16.6	0.633	0.379	4.26	47.1	2.36	-	198
AVR014	18.8	36.2	17.4	-	40.9	9.50	302	74.5	6.69	15.5	86.1	2.98	0.760	15.7	0.658	0.356	4.58	49.6	2.32	-	208

	Nb	Nd	Ni	P_2O_5	Pb	Pr	Rb	SiO_2	Sm	Sn	Sr	Ta	Tb	Th	TiO_2	Tm	U	V	Yb	Zn	Zr
AVR015	22.1	40.9	12.3	-	36.4	10.9	302	75.6	7.44	17.5	89.1	3.46	0.883	18.8	0.771	0.433	5.23	62.5	2.69	-	247
AVR016	21.5	49.5	14.9	-	43.5	12.8	305	76.1	9.09	17.6	93.9	3.35	0.994	18.3	0.750	0.452	5.00	59.1	2.65	-	255
AVR017	20.1	52.7	17.6	-	60.2	13.5	288	70.1	10.1	17.0	88.8	2.91	1.12	17.9	0.741	0.493	6.26	88.7	3.10	-	213
AVR018	21.7	46.9	18.9	-	45.7	11.9	269	70.1	9.13	16.5	82.6	2.85	1.05	16.6	0.777	0.516	5.07	78.8	2.96	-	238
AVR019	22.6	36.4	20.7	-	33.9	9.45	254	66.8	6.87	13.0	74.6	2.72	0.855	16.2	0.898	0.491	6.20	94.0	3.05	-	264
AVR020	22.9	37.0	17.9	-	32.1	9.59	252	70.6	6.93	11.3	76.3	2.64	0.858	16.3	0.941	0.503	6.33	96.7	3.01	-	260
AVR021	30.3	148	5.29	-	54.9	35.8	434	65.4	30.1	30.2	120	5.26	3.25	46.6	0.795	1.22	22.8	50.0	6.60	-	426
AVR022	22.1	37.1	19.2	-	39.9	10.0	307	70.7	6.76	16.9	88.6	3.13	0.795	18.6	0.772	0.438	8.07	59.2	2.72	-	232
AVR023	23.0	51.3	16.8	-	49.1	13.4	362	82.1	9.90	19.1	106	3.38	1.03	20.3	0.765	0.479	8.96	66.1	2.82	-	240
AVR024	21.5	41.3	12.1	-	36.2	11.0	323	83.5	7.47	15.7	91.5	3.24	0.808	18.3	0.782	0.443	5.47	56.2	2.63	-	256
AVR025	22.7	46.3	32.3	-	38.4	11.9	347	77.2	8.18	18.0	96.7	3.25	0.890	18.9	0.776	0.431	5.41	64.7	2.61	-	232
AVR026	25.4	52.4	15.6	-	39.0	13.6	337	77.1	9.31	22.8	101	3.70	1.10	21.0	0.836	0.493	5.91	68.3	3.06	-	316
AVR027	26.2	55.9	13.0	-	88.9	14.4	177	78.2	10.7	13.9	80.1	3.05	1.15	15.2	0.926	0.496	7.84	75.3	3.01	-	198
AVR028	20.8	52.0	26.7	-	7.27E+03	13.0	79.3	69.4	9.75	27.6	372	2.70	1.16	14.6	0.996	0.578	6.07	86.5	3.44	-	284
ANG030	21.7	42.8	5.01	0.0651	33.2	10.9	291	72.9	7.79	17.8	81.9	3.63	1.03	16.6	0.663	0.390	3.68	56.7	2.88	46.2	154
ANG031	21.7	38.4	4.56	0.0767	15.8	9.69	274	74.2	6.64	23.5	85.1	3.63	0.885	16.7	0.662	0.400	4.39	60.2	2.57	33.4	168
U (%)	4	6	82	-	63	5	3	5	6	81	19	8	8	13	9	22	17	16	19	-	6

The interpretation of the chemical results obtained by ICP-MS with a view to identifying the compositional groups has followed the statistical procedure explained in Chapter 4, section 4.5., like in the case of Zamoran ceramics. As has been done for the latter ceramics, for Aveiro ceramics Co, Ta, Pb, Sn and Cu were omitted in the statistical procedure to minimize the analytical variance. In addition, P_2O_5 and Zn were omitted because they showed values below the quantification limit.

As described in Chapter 4, the 28 analysed ceramics correspond to production and consumption centres. In the next lines, the study of the 28 ceramics in order to define the reference groups will be done in two parts: first, 28 ceramics corresponding to Aveiro city, rescued in Santo António church, in wasters and in Ria de Aveiro A shipwreck will be studied (section 6.2.1.). Then, the study of two ceramics corresponding to Angra D shipwreck will be carried out (section 6.2.2.). Once the reference groups are defined, they will be described in section 6.2.3.

6.2.1. Ceramics recovered in Aveiro city

In this case, the homogeneous set (referring to the typology, because all are unglazed, excepting AVR027 and AVR028, which are glazed) of 28 ceramics recovered in Aveiro (AVR001-AVR016 from RAVA, AVR017-AVR026 from Santo António church and AVR027-AVR028 from wasters) (see Table 4.1. from Chapter 4) shows a relatively high vt (3.32). This vt reveals the high contribution of specially Pb, Cu and Co (Figure 6.28.a), and suggests that the dataset is polygenic, that is, the presence of several compositional groups is probable (Buxeda i Garrigós and Kilikoglou, 2003). The variability of Pb is probably linked to the lead glazes of AVR027 and AVR028 (the former is translucent-glazed and the latter tin-lead glazed). Cu and Co, on the contrary, are likely to be related to contaminations (Cu to post-depositional contaminations and Co to sample preparation alterations). Then, Pb, Sn, Co, Ta and Cu, in addition to Na_2O, are omitted. Na_2O is not considered because salt crystallization in porous materials (such as ceramics) is one of the primary causes of their deterioration, especially in marine environments (López-Arce et al., 2013). When those components are omitted from the statistical routine, the vt decreases to 1.44, still a high value, considering that they are only 28 ceramics and most of them have the same typology. Therefore, this supports the hypothesis of a polygenic set (Figure 6.28.b).

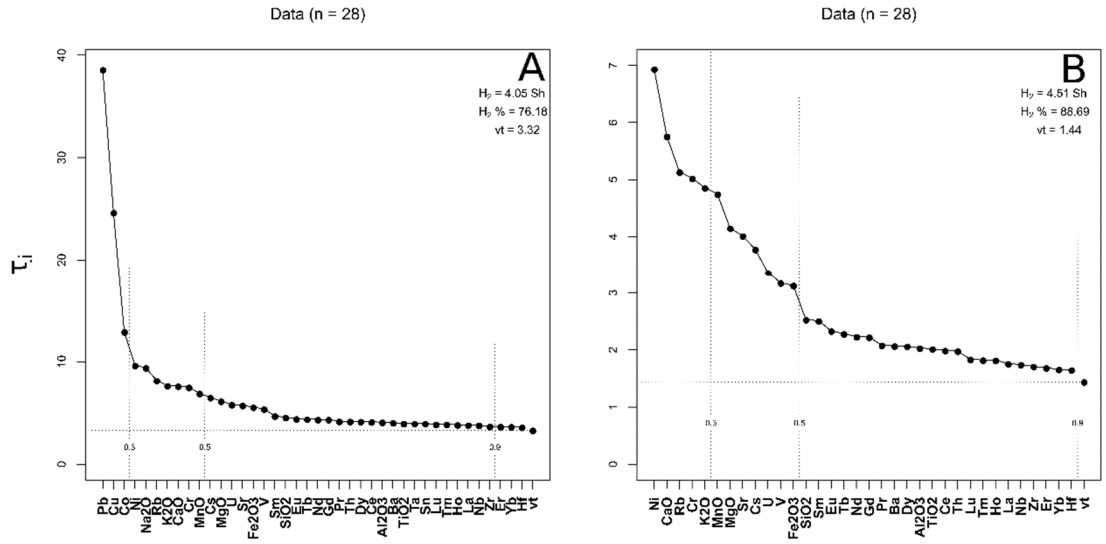

Figure 6.28. Graphical representations of the evenness of the compositional variability of 28 analysed ceramics, recovered in Aveiro, by ICP-MS: **(a)** P_2O_5 and Zn were omitted because their values are below the quantification limit; **(b)** Co, Cu, Na_2O, Pb, Sn, and Ta were omitted due to their potential effect for alterations, in addition to P_2O_5 and Zn. (y-axis (τ.i) = the individual contribution of the variability from each element to the whole dataset, from the highest to the lowest; vt = Total variability; H_2 = information entropy; H_2% = percentage of information entropy over the maximum possible; n = number of specimens)

Additionally, since Aveiro was a production centre (see Chapter 2, section 2.2.), first, the 12 ceramics recovered in Santo António church have been evaluated performing a Hierarchical Cluster Analysis (HCA), in order to identify the potential reference groups (RF) for this production centre (Figure 6.29.). The dendrogram of Figure 6.29. demonstrates that, excepting AVR021, the rest (n=11) correspond to the same PCRU. In the case of AVR021, this fact is evidenced by the lower content on some Rare Earth Elements such as Eu, Pr, Ce, Sm, Tb, Dy, Gd, and Nd (Table 6.5.). Since ceramics recovered in the upper choir of the church are considered made in Aveiro, this PCRU is defined as A-1 reference group of the production from Aveiro. AVR021 might be also another type of production from Aveiro, but as there are not more similar ceramics for comparison, it will be treated as an unkown ceramic.

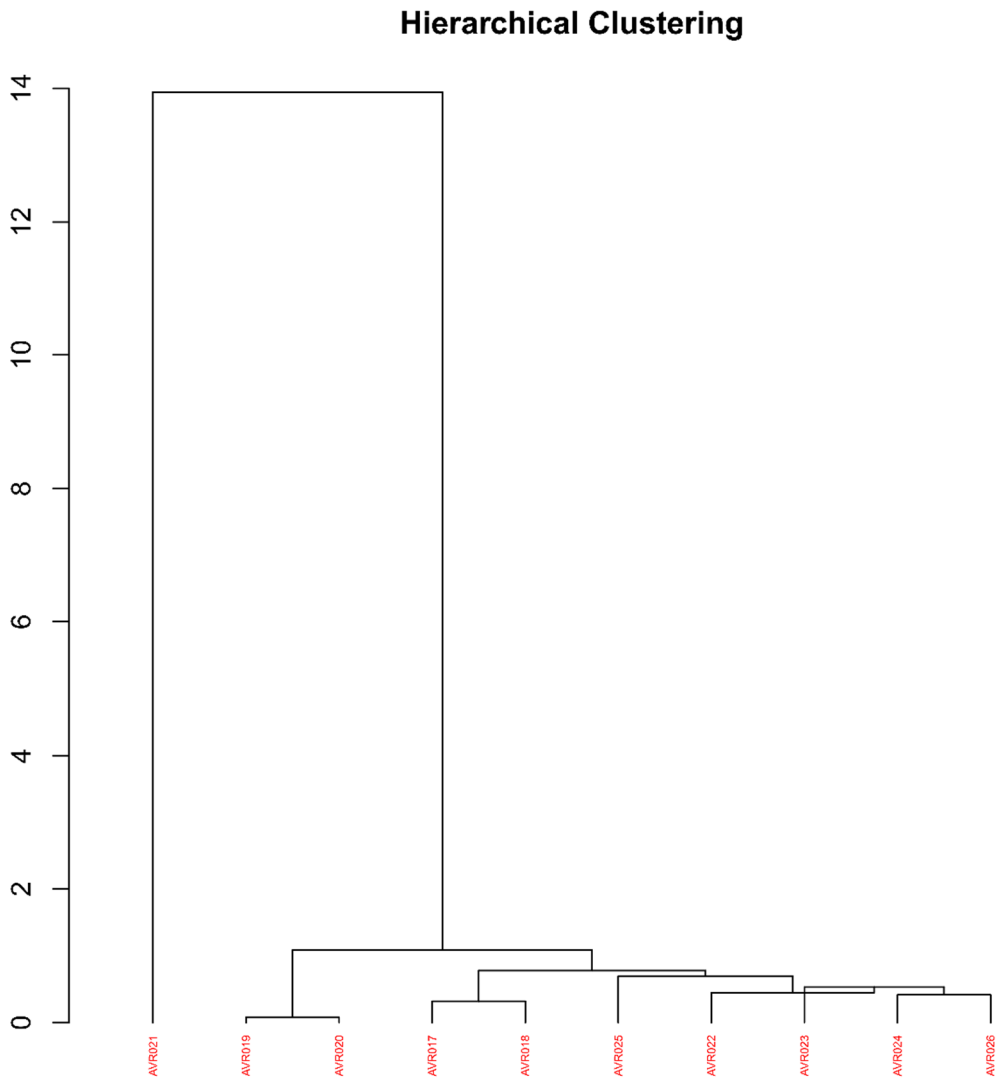

Figure 6.29. Dendrogram of Euclidean squared distances using centroid algorithm of 10 individuals from Santo António church (Aveiro) on the sub-composition of all the measured components (42) (with the exception of Co, Cu, Na_2O, P_2O_5, Ta and Zn) divided by the geometric mean

After that, a Hierarchical Cluster Analysis (HCA) was performed to evaluate the aggrupations of the rest 16 ceramics recovered in RAVA and wasters, having as a reference the A-1 reference group (Figure 6.30.). Examination of the resulting dendrogram shows a well-defined single-group structure that corresponds to the A-1 production identified in Aveiro (see Table 6.6.). This fact is in accordance with the article published by Alves et al. (1998). In that work, the authors catalogued ceramics from RAVA as local products after comparing them with the ceramics recovered in Bairro das Olarias (Aveiro) and Casa do Infante (Porto) by means of X-Ray Fluorescence (XRF). All ceramics from A-1 are unglazed black and red ceramics

and are, basically, cooking pots, ceramics for transport and serving vessels. Upon further examination, Figure 6.30. also reveals the existence of three ceramics (AVR021, AVR027 and AVR028) that do not match the A-1 reference group. In the case of AVR028, this fact is evidenced principally by the higher content on CaO, because it is the only calcareous ceramic of the set (Table 6.5.). Contrariwise, AVR027 highlights because of its lower content on MgO and MnO. It is not clear where AVR021 comes from, but one possibility is that it was produced in Vila Real district (Portugal), since its production was only black ceramic production (Fernandes and Castro, 2012). Besides, AVR027 translucent yellow glazed ceramic might have been produced in Coimbra (Portugal) (Silva, 2015), whereas AVR028 in Lisbon (Vieira et al., 2013) due to their similarity to the ceramics from these places.

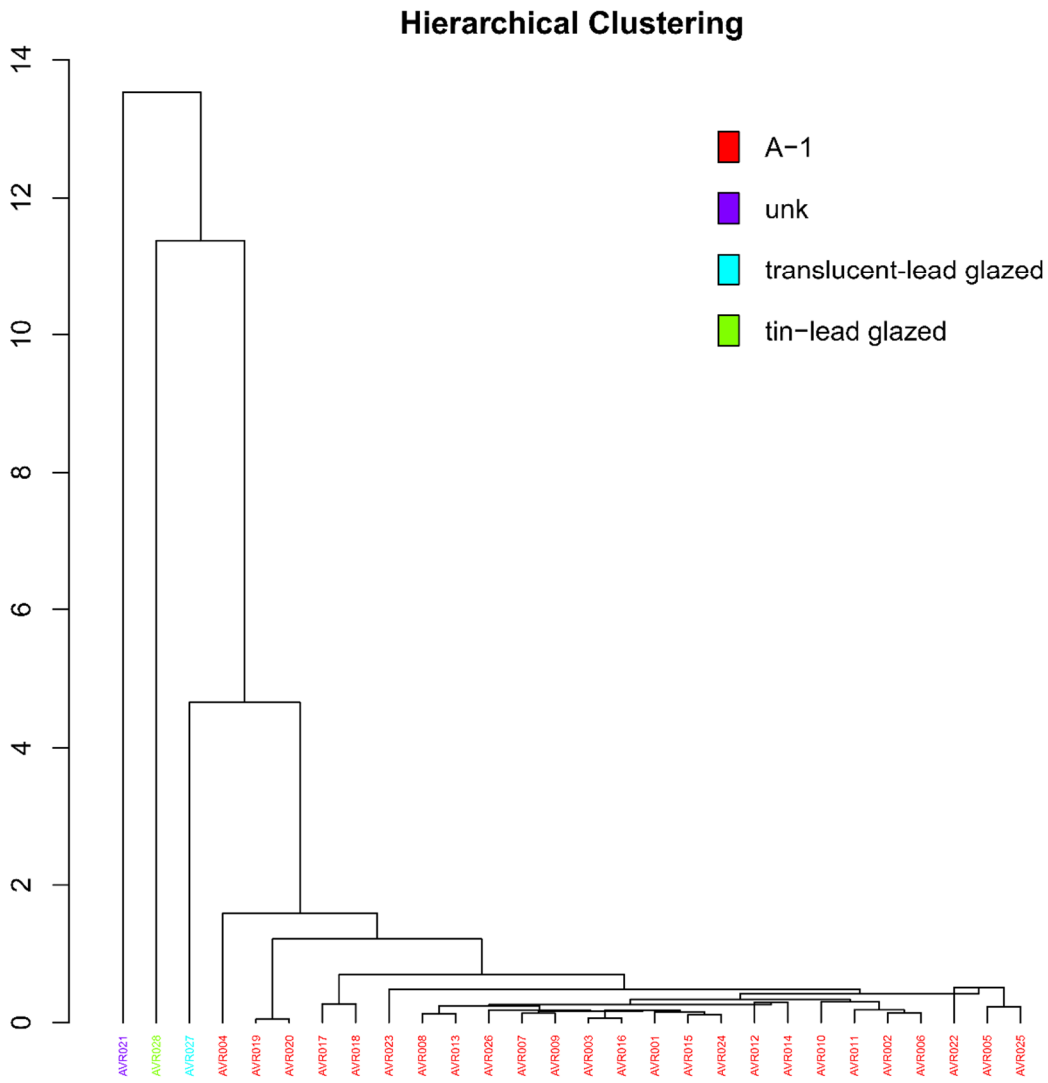

Figure 6.30. Dendrogram of Euclidean squared distances using centroid algorithm of 28 individuals from different sites of Aveiro (Santo António church, RAVA, and wasters) indicated by the reference groups they correspond to, on the sub-composition of all the measured components (42) (with the exception of Co, Cu, Na_2O, P_2O_5, Pb, Sn, Ta and Zn) divided by the geometric mean

Table 6.6. Samples, village, the archaeological site and the context where ceramics were rescued, in addition to their typology, colour decoration of the glazes, form, chronology, the reference group they belong to and their paste and surface colours. AVR = ceramics recovered in Aveiro city; ANG= ceramics recovered in Angra D; unk = ceramics with unkown reference group

Samples	Village	Archaeological site	Context	Typology	Colour decoration	Form	Chronology	Group	Paste colour	Surface colour
AVR001	Aveiro	Ria de Aveiro A	RAVA	unglazed	-	basin	16th-17th	A-1	Beige	Black matte
AVR002	Aveiro	Ria de Aveiro A	RAVA	unglazed	-	basin	16th-17th	A-1	Black	Black matte
AVR003	Aveiro	Ria de Aveiro A	RAVA	unglazed	-	plate	16th-17th	A-1	Black	Shiny black and beige
AVR004	Aveiro	Ria de Aveiro A	RAVA	unglazed	-	mug	16th-17th	A-1	Beige	Beige
AVR005	Aveiro	Ria de Aveiro A	RAVA	unglazed	-	storage jar	16th-17th	A-1	Black	Shiny black
AVR006	Aveiro	Ria de Aveiro A	RAVA	unglazed	-	bowl	16th-17th	A-1	Red	Red
AVR007	Aveiro	Ria de Aveiro A	RAVA	unglazed	-	bowl	16th-17th	A-1	Red	Red
AVR008	Aveiro	Ria de Aveiro A	RAVA	unglazed	-	basin	16th-17th	A-1	Beige	Beige
AVR009	Aveiro	Ria de Aveiro A	RAVA	unglazed	-	bowl	16th-17th	A-1	Beige	Beige
AVR010	Aveiro	Ria de Aveiro A	RAVA	unglazed	-	mug	16th-17th	A-1	Red	Red
AVR011	Aveiro	Ria de Aveiro A	RAVA	unglazed	-	mug	16th-17th	A-1	Red	Red
AVR012	Aveiro	Ria de Aveiro A	RAVA	unglazed	-	pitcher	16th-17th	A-1	Red	Black matte
AVR013	Aveiro	Ria de Aveiro A	RAVA	unglazed	-	basin	16th-17th	A-1	Red	Red and black matte
AVR014	Aveiro	Ria de Aveiro A	RAVA	unglazed	-	basin	16th-17th	A-1	Red	Red
AVR015	Aveiro	Ria de Aveiro A	RAVA	unglazed	-	plate	16th-17th	A-1	Black	Shiny black
AVR016	Aveiro	Ria de Aveiro A	RAVA	unglazed	-	plate	16th-17th	A-1	Dark red	Shiny black
AVR017	Aveiro	Santo António church	upper choire dome	unglazed	-	olive jar (*anforeta/botija*)	16th	A-1	Red	White

AVR018	Aveiro	Santo António church	upper choire dome	unglazed	-	sugar mould (*forma de açúcar*)	16th	A-1	Red	Black matte
AVR019	Aveiro	Santo António church	upper choire dome	unglazed	-	sugar mould (*forma de açúcar*)	16th	A-1	Red	Black matte
AVR020	Aveiro	Santo António church	upper choire dome	unglazed	-	sugar mould (*forma de açúcar*)	16th	A-1	Red	Black matte
AVR021	Aveiro	Santo António church	upper choire dome	unglazed	-	cooking pot	16th	unk	Black	Black matte
AVR022	Aveiro	Santo António church	upper choire dome	unglazed	-	cooking pot	16th	A-1	Red	Black matte
AVR023	Aveiro	Santo António church	upper choire dome	unglazed	-	bowl	16th	A-1	Red	Red
AVR024	Aveiro	Santo António church	upper choire dome	unglazed	-	pitcher	16th	A-1	Red	Red
AVR025	Aveiro	Santo António church	upper choire dome	unglazed	-	pitcher	16th	A-1	Red	Black matte
AVR026	Aveiro	Santo António church	upper choire dome	unglazed	-	mug	16th	A-1	Red	Red
AVR027	Aveiro	Wasters	dump	translucent-glazed	yellow	bowl	16th-17th	unk	Beige	Translucent-glazed (yellow)
AVR028	Aveiro	Wasters	dump	tin-lead glazed	white and blue	plate	16th-17th	unk	Beige	Tin-lead glazed (white and blue)
ANG030	Angra	Angra D	Angra D	unglazed	-	plate	17th	A-1	Red	Red
ANG031	Angra	Angra D	Angra D	unglazed	-	plate	17th	A-1	Red	Red

6.2.2. Ceramics recovered in Angra D

Terceira Island (Azores Archipelago, Portugal), precisely Angra, was the main Atlantic port of call through the whole sixteenth and part of the seventeenth century. It became a deep-sea harbour for Portuguese and Castilian ships returning to Europe (Meneses 2005, 2008) (Figure 6.31.).

Figure 6.31. Angra D geographical location

The first archaeological underwater studies with acceptable scientific standards were conducted between 1995-2001 and led to the survey of several wrecks (like Angra A and B) and the rescue excavation of two wrecks, Angra C and Angra D (Garcia and Monteiro 2001; Garcia et al. 1999).

Iñañez and collaborators (2020) characterized archaeometrically a set of 34 archaeological ceramics, from seventeenth century Angra D shipwreck, including olive jars, translucent green lead glazed, tin-lead glazed and unglazed ceramics. The main goal of this study was shedding light to the historical understanding of the Angra D shipwreck through its ceramic cargo. According to botanical and archaeological evidences, the ship was returning from the Americas. Moreover, it corresponds to a Spanish ship operating on the Atlantic. It would have commercial functions and, at some stage of its last journey, touched in Central or South America. Its last location should relate with a technical stopover in the Angra port (Iñañez et al., 2020). For that, chemical and mineralogical analyses of the ceramics were carried out by Inductively Coupled Plasma-Mass Spectrometry (ICP-MS) and X-Ray Diffraction (XRD), and microstructural analysis by Scanning Electron Microscopy-Energy Dispersive Spectrometry (SEM-EDS) analytical techniques. The authors suggested that the ceramic provenance is mainly from Seville origin (southern Spain) and, at a lesser extent, from the north of Portugal, piling up evidences to suggest a Spanish ship. Indeed, ANG030 and ANG031 unglazed red pots were classified as ceramics corresponding to A-1, that is, produced in Aveiro, something that is shown in Figure 6.32. Chemical results of ANG030 and ANG031 are shown in Table 6.5.

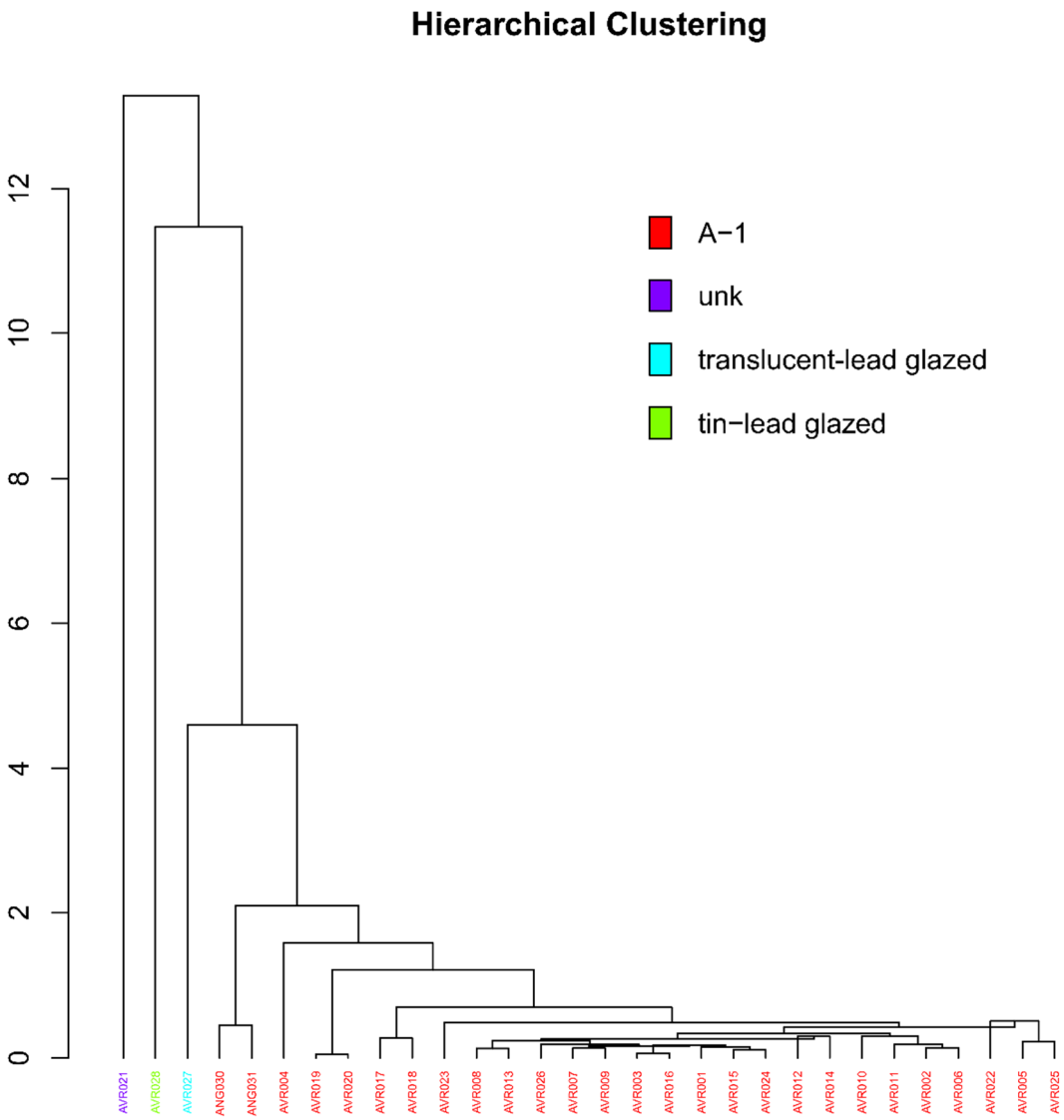

Figure 6.32. Dendrogram of Euclidean squared distances using centroid algorithm of 30 individuals recovered in Aveiro (Santo António church, RAVA and wasters) and in Angra D, on the sub-composition of all the measured components (42) (with the exception of Co, Cu, Na_2O, P_2O_5, Pb, Ta, Sn and Zn) divided by the geometric mean

6.2.3. Characterization of the reference groups

A-1 reference group

After identifying the A-1 reference group, the mineral phases and different production fabrics were identified, by means of XRD analyses. All the ceramics studied in the present Doctoral Thesis were analysed by XRD. Like for Zamora region ceramics, the Equivalent Firing Temperature (EFT) in which the fabrics were fired

was also evaluated according to Heimann (2010 and references therein) observations.

Besides, SEM-EDS analyses were carried out to make the microstructural characterization and examination of the extent of vitrification, alterations and contaminations of the ceramics.

Regarding the main chemical features of A-1 reference group, it can be said that it is a low-calcareous group, averaging around 4 wt % of CaO. The forms dominating in this group are all unglazed olive jars, pots, cups, sugar moulds, plates and bowls, developing reddish and, in some cases, black pastes to visual appearance. The difference between the three sample sets (RAVA, church and Angra D) are those which could be seen in a macroscale: while the ceramics retrieved in the church and Angra D have only red pastes and do not show shiny black surface and vitrified material, ceramics from RAVA show also black pastes and a shiny finish as well as some concretions or alterations in the paste (see Table 6.7.).

Table 6.7. The chemical composition of A-1 group, in addition to the ceramics belonging to each group, their typology and paste colour

Samples	Group	Typology	Paste colour	Al_2O_3	Ba	CaO	Ce	Co	Cr	Cs	Cu	Dy	Er	Eu	Fe2O3	Gd
AVR001-AVR020; AVR022-AVR028; ANG030-ANG031	A-1	unglazed (27)	Beige (4), black (4), red (19)	17.9	407	4.04	97.8	29.7	45.5	26.3	11.6	5.29	2.66	1.28	5.03	6.36

(continues)

Samples	Group	Typology	Paste colour	Hf	Ho	K_2O	La	Lu	MgO	MnO	Na_2O	Nb	Nd	Ni	Pb	Pr	Rb	SiO_2	Sm	Sn	Sr
AVR001-AVR020; AVR022-AVR028; ANG030-ANG031	A-1	unglazed (27)	Beige (4), black (4), red (19)	6.09	0.759	4.54	48.1	0.431	1.78	0.0211	0.598	20.6	41.6	15.7	41.9	10.9	301	73.7	7.51	16.4	89.4

(continues)

Samples	Group	Typology	Paste colour	Ta	Tb	Th	TiO_2	Tm	U	V	Yb	Zn
AVR001-AVR020; AVR022-AVR028; ANG030-ANG031	A-1	unglazed (27)	Beige (4), black (4), red (19)	3.07	0.863	17.2	0.730	0.421	5.10	59.8	2.61	224

Technological assessment by XRD

The ceramics from Aveiro form five different production fabrics (F-I_a, F-I_b, F-I_c, F-II_a, F-II_b, F-III_a, F-III_b, F-IV, F-V_a and F-V_b) (Table 6.8.). The main mineral phases of these five fabrics are quartz, potassium feldspar (principally microcline, sanidine and orthoclase) and plagioclase (principally albite and anorthite). The main differences between the fabrics are the existence or not of illite, hematites and hercynite, all depending on the firing temperatures and oxidizing/reducing conditions (Broekmans et al., 2008; Cianchetta et al., 2015; Nodari et al., 2004).

Table 6.8. The composition of each fabric and summary of the results obtained by XRD (the EFT, subgroups, ceramics and typology and composition of each fabric). Qz= quartz; Ilt= illite; Kfs= potassium feldspar; Pl= plagioclase; Hem= hematite; Hc= hercynite; Py= pyrite; Hl= potassium halite; Cal= calcite, abbreviations according to Whitney and Evans (2010)

Fabric	Ceramics	Paste	Qtz	Ilt	Kfs	Pl	Hem	Hc	Py	Hl	Cal	EFT (°C)
F-I_a	AVR001	beige (1)	X	X	X	X	X					800
F-I_b	AVR004	beige (1)	X	X	X	X	X		X			800
F-I_c	AVR008; AVR009	beige (2)	X	X	X	X	X					800
F-II_a	AVR013; AVR017; AVR025	red (3)	X	X	X	X	X				X (surface of AVR017)	800-850
F-II_b	AVR006	red (1)	X	X	X	X	X					800-850
F-III_a	ANG030-ANG031	red (2)	X		X		X					850-900
F-III_b	AVR007; AVR010-AVR012; AVR014; AVR018-AVR020; AVR022-AVR024; AVR026	red (12)	X		X	X	X					900
F-IV	AVR002	Black paste and black matte surface (1)	X	X	X	X		X				850-900
F-V_a	AVR016	Dark red paste and black shiny surface (1)	X		X	X	X	X				950

F-V_b	AVR003; AVR005; AVR015	Black paste and black shiny surface (3)	X		X	X		X		X (AVR003)		950

As regards the F-I group, it is completed with beige paste ceramics from RAVA and is divided in three subgroups: F-I_a, F-I_b and F-I_c (Table 6.8.). The common phases are quartz, illite, potassium feldspars, hematite and plagioclases. On the other hand, the differences between these three groups are the amount of potassium feldspars, plagioclases, hematite and the appearance of secondary phases (pyrite). It has to be highlighted that the ceramic that forms the F-I_a subgroup, is the only one that has a black matte surface in F-I. F-I_b seems to have more potassium feldspars and plagioclases than the rest, whereas the main difference between F-I_a, F-I_b and F-I_c is the amount of hematite: F-I_c has much more hematite than the others do. This fact could be related to the reduction of hematite in marine environments, suggesting that the iron of the hematite (Fe^{3+}) of F-I_a and F-I_b is lower because it was reduced to the iron of pyrite and/or jarosite (Fe^{2+}), whereas F-I_c did not suffer any or not many hematite reducing reactions (see the part called "Marine environments") (Secco et al., 2011). This fact could be proven by the appearance of pyrite in the F-I_b fabric. Therefore, in the fabric F-I, the high presence of illite and the appearance of potassium feldspar allow establishing an Equivalent Firing Temperature (EFT) of 800 °C (Figure 6.33.).

The fabric F-II is formed by red paste ceramics and divided in two subgroups: F-II_a and F-II_b, completed by ceramics from RAVA and the church. The common phases are quartz, illite, plagioclases, potassium feldspars and hematite and the differences between these two subgroups is that F-II_a contains much more illite than F-II_b. Moreover, inside the group of F-II_a, ceramics from the church (AVR017 and AVR025) show more hematite than ceramics from RAVA (AVR013). This could be in accordance with the fact that in marine environment hematite could be reduced (Secco et. al., 2011). As illite is present but is decreasing in the amount, the EFT of the fabric F-II is in the range of 800-850 °C (Figure 6.33.).

When it comes to the fabric F-III, F-III_a is formed by red ceramics from Angra D and F-III_b by red ceramics from RAVA and the church. The fabric presents quartz, potassium feldspars and hematite. In addition, F-III_b contains plagioclases. As the

no appearance of illite suggests its decomposition, the EFT is of 900 °C and a little bit lower, around 850-900 °C in the case of F-III_a ceramics (Figure 6.33.).

The F-IV fabric is formed by one black matte ceramic (surface and paste) from RAVA and it presents quartz, little illite, plagioclases, potassium feldspars and hercynite. There is no hematite, and this fact could suggest that the hematite could have been reduced to hercynite, in addition to the reductions that could happen in the marine environment (Broekmans et al., 2008; Cianchetta et al., 2015; Nodari et al., 2004). The total reduction of hematite could be explained by the black colour of AVR002 ceramic shard. In this fabric, the presence of a little amount of illite, potassium feldspar and hercynite permits establishing an EFT in the range of 850-900 °C (Figure 6.33.).

Finally, F-V fabric, divided in two subgroups, is formed by four metallic shiny black surface ceramics from RAVA, showing quartz, potassium feldspars, plagioclases and hercynite. F-V_a is formed by a ceramic which shows a dark red paste, whereas F-V_b is formed by ceramics with black paste. The main difference between these two subfabrics is the appearance of hematite in F-V_a, suggesting that the reduction conditions were not fully achieved in AVR016 ceramic (see "The glassy-layer" part in the next section). Additionally, some secondary phases in some shards, as well, were identified, like potassium halite (AVR003). According to literature, sodium-potassium chloride (potassium halite) was also detected in an Italic amphora recovered in an underwater marine environment (López-Arce et al., 2013). Given these conditions, the EFT of this fabric is of 950 °C. The amount of hercynite particularly draws the attention in F-V_b, because it is the highest peak in comparison with the rest of the fabrics (Figure 6.33.).

Additionally, the white slip of AVR017 ceramic (olive jar) has been analysed. The phases that are clearly differentiated are quartz, calcite and clay minerals (Figure 6.33.). Thus, this slip was made mainly by a calcareous substrate likely mixed with clay to facilitate bonding to the ceramic surface while providing a white surface that covered the whole piece. However, the reason for applying such slip, beyond aesthetic features or for marking specific product containing the olive jar, remains unknown.

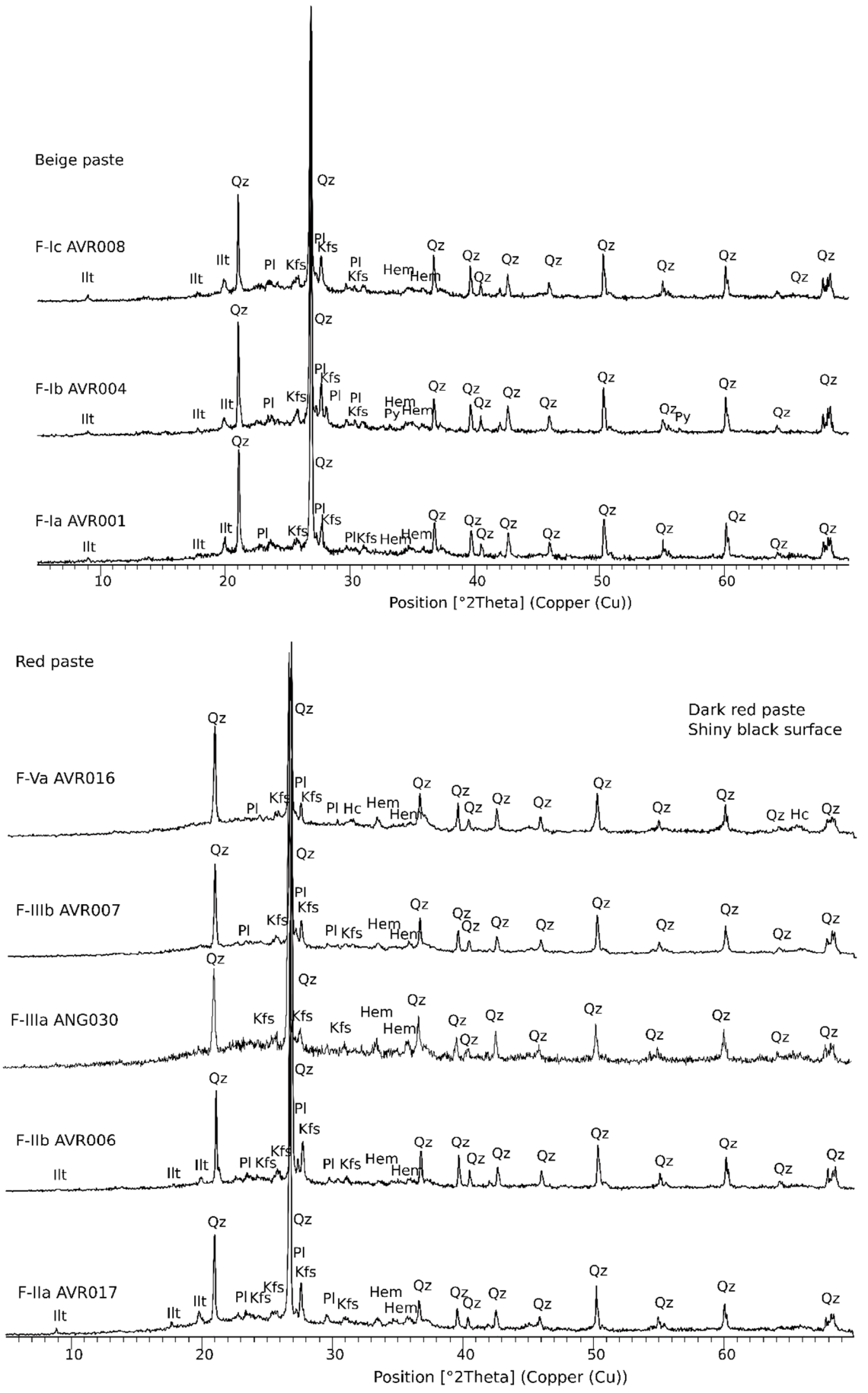
Beige paste
F-Ic AVR008
F-Ib AVR004
F-Ia AVR001
Red paste
Dark red paste
Shiny black surface
F-Va AVR016
F-IIIb AVR007
F-IIIa ANG030
F-IIb AVR006
F-IIa AVR017
Qz
Pl
Kfs
Ilt
Hem
Hc
Py
10
20
30
40
50
60
Position [°2Theta] (Copper (Cu))

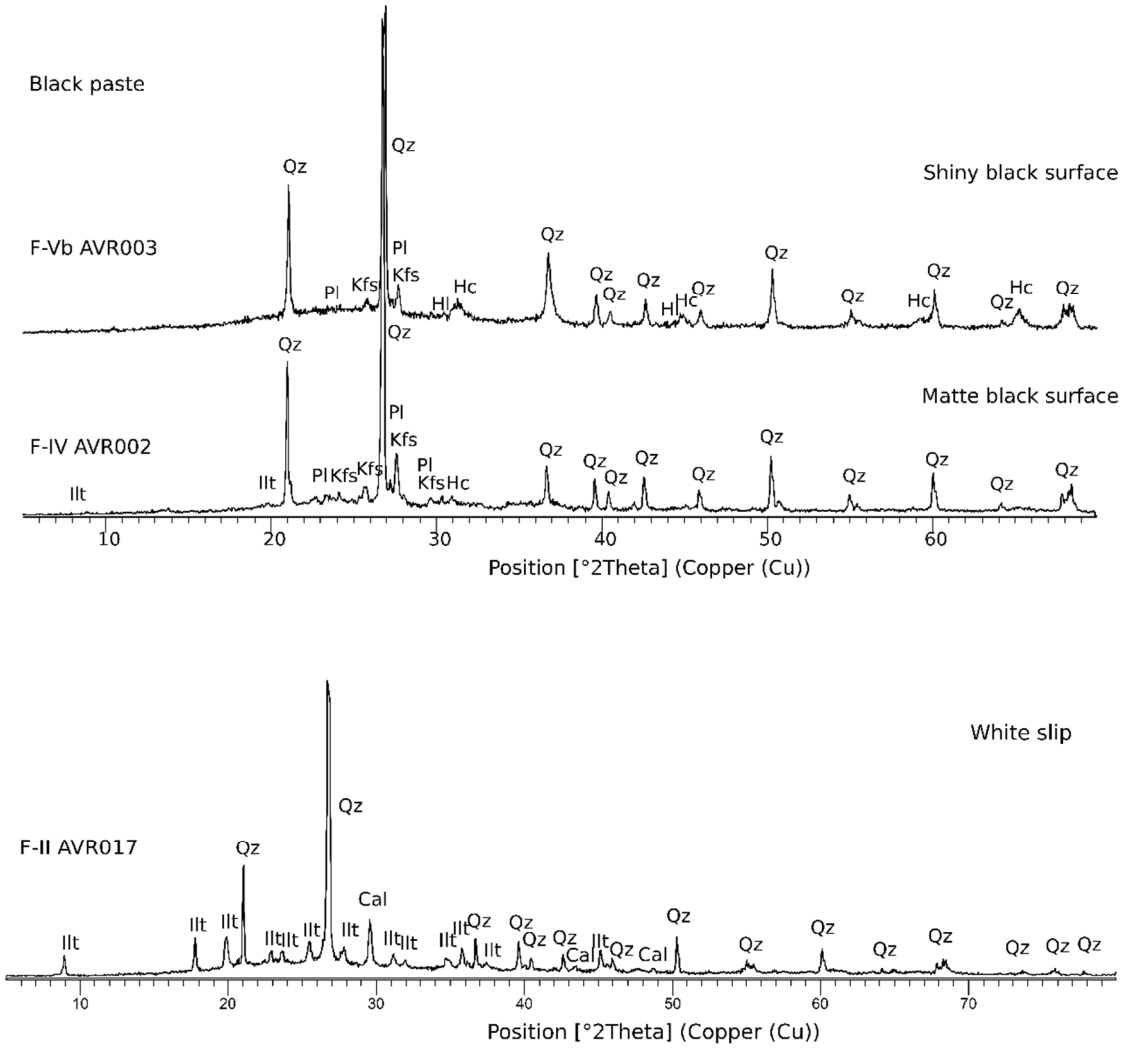

Figure 6.33. Reference diffractograms of the fabrics divided by the colour of the pastes (beige paste, red paste and black paste) and the diffractogram of the white slip of AVR017. Qz= quartz; Ilt= illite; Kfs= potassium feldspar; Pl= plagioclase; Hem= hematite; Hc= hercynite; Py= pyrite; Hl= potassium halite; Cal= calcite, abbreviations according to Whitney and Evans (2010)

Black ceramic production

The ICP-MS analyses allowed to know that the source of clay used for the manufacture of these 27 ceramics was the same. Additionally, as it could be noticed by XRD analyses, the pastes are not the same, so the only reason for this fact that one can think about, is the different technology (e.g. different atmosphere conditions during firing, different finishing) applied with a view to obtaining red and black pastes. According to the literature, the black coloration of ancient ceramics was obtained mainly in three ways: using carbon, adding manganese oxides to the clays and reducing iron oxides in a reducing atmosphere during firing (Edwards and Chalmers, 2005; Gillies and Urch, 1983). The first case (the use of carbon) is based on

using clays naturally rich in organic material or to which carbonaceous material has been added. Then, they are fired in reducing conditions and carbon is formed. This gives the black colour to the ceramic (Gillies and Urch, 1983). The third case (firing in reducing conditions) is probably the oldest of all ceramic-decoration processes (Noll et al., 1975). When iron oxides are fired, their colour is affected by temperature, duration of heating and atmosphere (Shepard, 1956). In an oxidizing atmosphere, iron oxides are mainly in the form of hematite. However, in a reducing atmosphere, iron oxides form spinel phases, like hercynite ($FeO{\cdot}Al_2O_3$) and magnetite (Fe_3O_4), which are predominantly black (Longworth and Tite, 1979; Maggetti et al., 1981; Noll et al., 1975). One of the hypotheses of the black ceramics that form F-IV and F-V, is that they were fired in reducing conditions in order to get the black colour. This black colour could have been obtained due to the reduction of hematite (Fe_2O_3) to hercynite, indicating strong reducing firing conditions (Ibarra, 2006; Nodari et al., 2004).

According to archaeological evidence, it was common in Aveiro to produce these black ceramics for the forms related to kitchen wares, like cooking pots (Carvalho and Bettencourt, 2012; Fernandes and Castro, 2012; Ibarra, 2006). The reason for doing this could have been the good qualities that the ceramics obtain in these reducing firing conditions: the carbon element that is caught in the ceramic paste during the process decreases the permeability of the paste, so that these shards are suitable for retaining liquids. The same circumstances provide also better and more hygienic food preservation because the dirt and bacteria are not able to pierce in the pores, preventing the ceramic pastes, in this way, from the reproduction of these microorganisms (Sempere, 1982). On the other hand, the reduced wares are harder than the common wares, so that they are more resistant in the use (Sempere, 1982).

SEM-EDS assessment

Extent of vitrification

Five freshly fractured surface ceramics were selected for SEM analysis, because their SEM examination provides information about the internal morphology developed during the original firing, the extent of vitrification and pore structure (Maniatis and Tite, 1978). Among the selected ceramics, two are from F-I

(AVR008, AVR009), one from F-II (AVR017), one from F-IV (AVR002), and one from F-V (AVR003) (Table 6.8.). In this way, the results of SEM demonstrate that the F-I and F-II fabrics show an early initial vitrification due to the appearance of isolated smooth-surfaced areas, whereas the F-IV shows a medium vitrification (Maniatis and Tite, 1978). Finally, the F-V shows a continuous vitrification, because a continuous smooth vitrified layer is formed over the whole fracture surface (Figure 6.34.) (Maniatis and Tite, 1978). All these results are in accordance with their EFTs.

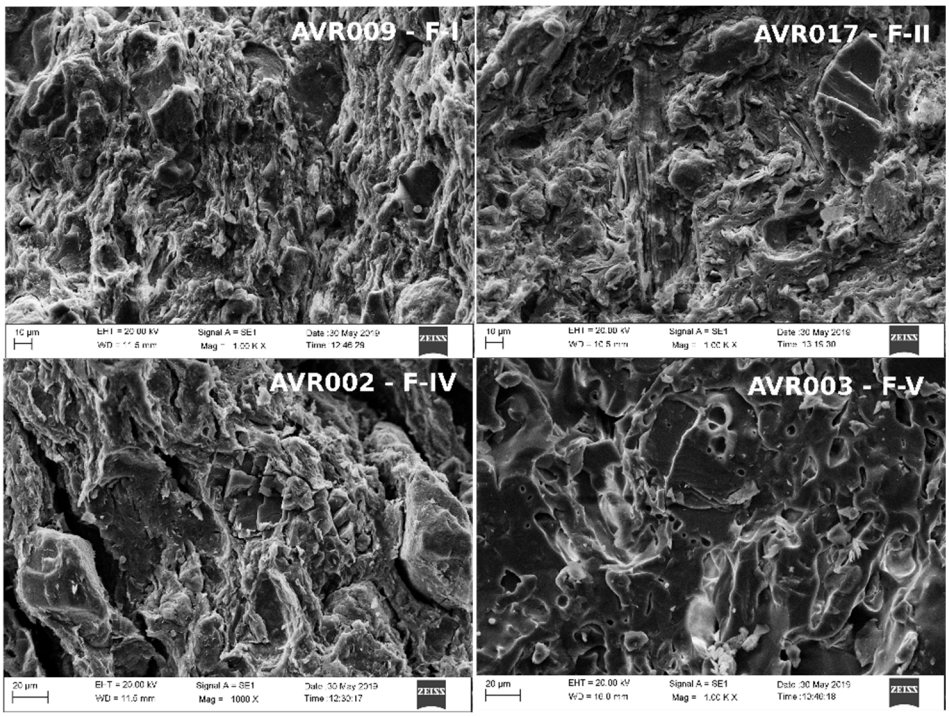

Figure 6.34. SEM-SED images showing the grade of vitrification of: **(a)** F-I (ceramic AVR009); **(b)** F-II (ceramic AVR017); **(c)** F-IV (ceramic AVR002) and **(d)** F-V (AVR003)

Additionally, 11 transversally cut and polished pieces were selected for SEM-EDS analyses: 2 from F-I (AVR004, AVR008), 1 from F-II (AVR017), 4 from F-III (AVR007, AVR014, AVR016, AVR018) and 4 from F-V (AVR003, AVR005, AVR015, AVR016).

The glassy-layer

According to SEM-EDS results, none of the ceramics has any alkaline or tin-lead glaze, although a glassy-layer is observed in the shiny black ceramics from F-V (Figure 6.35.). For the ceramics of F-V_b a glassy-layer that contains vacuoles could be observed, whereas for F-V_a (AVR016), the vacuoles are less abundant. The reason for the appearance of the glassy-layer could be that, at high temperatures, iron compounds may act as a flux when they are exposed to a reducing atmosphere, resulting in the change of the colour of the shard (from red to black) and also in the formation of a glassy-layer in the surface (Rice, 2015). Additionally, Noll et al. (1975) explain that, for example, Cretan wares black painting was obtained reducing (by the iron reduction technique) iron-rich clays, which were added as a slip. The authors explain that in Cretan wares a high content of vacuoles were formed in the black paint layer. These vacuoles could have been formed due to the fact that during firing, some gases were formed in the form of bubbles (e.g. carbon dioxide) that attempt to escape through the layer. At higher temperatures, more of this glassy-layer is formed and the large number of bubbles/vacuoles could indicate a relatively high firing temperature (Noll et al., 1975). Thus, the existence of the vacuoles in the ceramics from Aveiro could be explained by the fact that Noll and collaborators report in their study. In these lines, a hypothesis is thought for AVR016 ceramic; it is from F-V_a subgroup, which shows a dark red paste and fewer vacuoles in the glassy-layer. Thus, this ceramic probably was red in origin but it was refired during the firing produced in the ship. As the firing environment around the ceramic cargo was probably a reducing environment (because they were covered), the hematite of the paste was reduced partially to hercynite, as it has been reported in Chapter 6, section 6.2.3., "Technological assessment by XRD". Thus, the fewer vacuoles of the glassy-layer and the partial reduction of hematite to hercynite could suggest that the interaction between the ceramic and the fire was not very strong when time exposed and temperature reached are considered. On the contrary, a strong interaction case could be that of AVR005; this ceramic was probably red in origin as well, but the reduction of hematite in this case was a total reduction. Moreover, the reason for thinking that AVR005 was red in origin, is that there is no archaeological evidence for black storage jars in Aveiro A excavation context. All storage jars recovered are red.

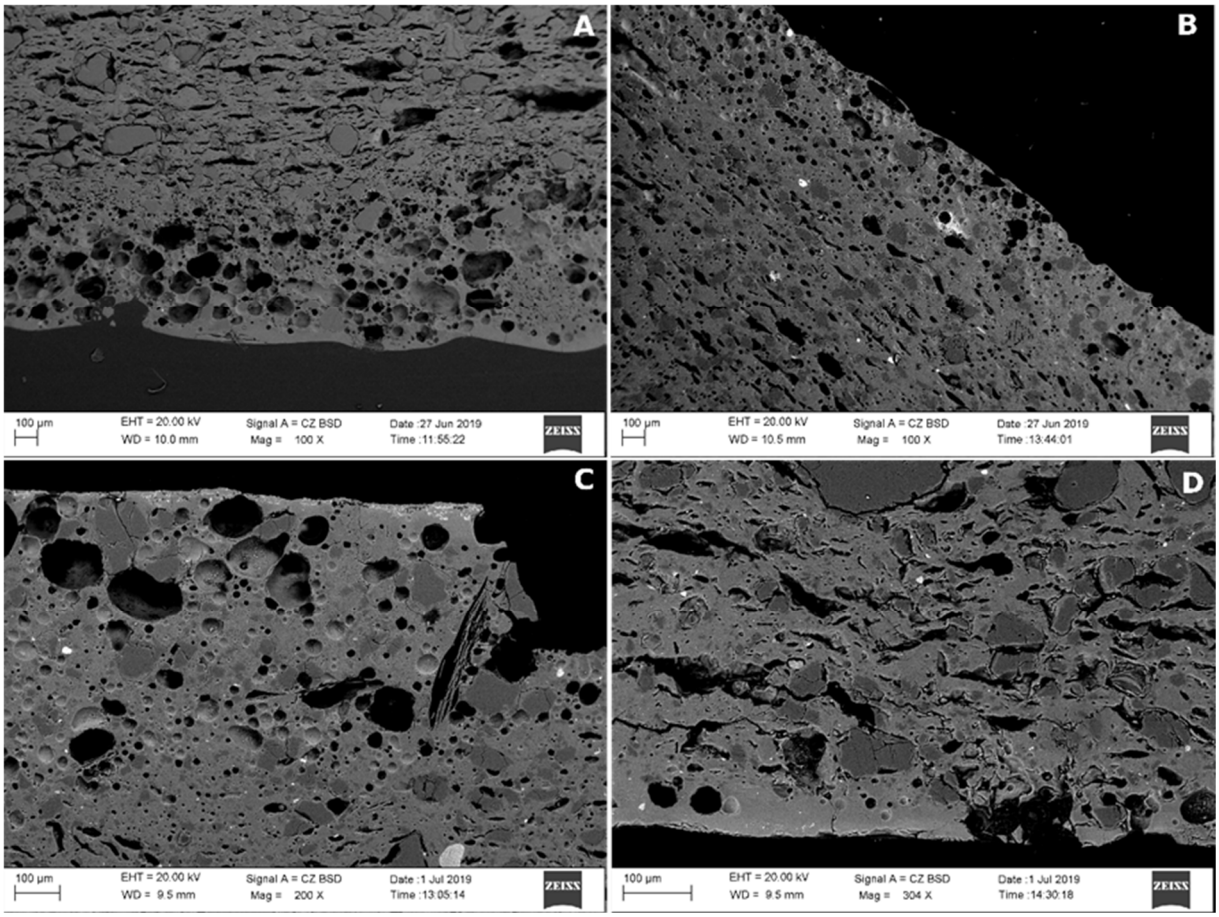

Figure 6.35. SEM-BSD images of four ceramic pieces from F-V showing a glassy-layer: **(a)** AVR003; **(b)** AVR005; **(c)** AVR015 and **(d)** AVR016

The shiny black surface

The shiny black surface finishes found on ceramics studies here, have been applied in pottery from their earliest production. The reasons for applying them were both practical -because they provide more impermeable surface layer- and decorative (Tite et al., 1982). In some cases, the fine particle fraction of the body clay has been used to produce the black coating (in the case of Greek Attic black ceramics, for example) (Gillies and Urch, 1983). This is not the case of our ceramics, as no clay slip has been identified by SEM-EDS. In other cases, the metallic shiny black surface has been achieved by applying a burnished finishing in addition to the firing in high temperatures and reducing atmosphere. In this way, the shiny black surface is produced due to the alignment of the clay particles in the surface region on account of reducing firing conditions and burnishing (Gillies and Urch, 1983). According to Berg (2008), burnishing consists of the use of a hard, smooth object like wood, stone or bone, to rub the ceramic surface, often resulting in narrow parallel

facets. By compressing the clay, burnishing creates a characteristic luminous shine (Berg, 2008). Burnishing produces a uniform and compact surface, and it causes specular reflection, giving to the ceramics a "lustrous", "shiny" or "glossy" surface like that obtained by different coatings (e.g. paints, slips, glazes). Contrariwise, smoothing makes ceramics appear "matte" or "dull" and this difference is because of different light reflections; the uniform surface allows for a large amount of light to be reflected directly back to the observer and thus the surface appears "lustrous" or "shiny" (Ionescu et al., 2014). This is the case for some black ceramics from Marginea (Romania) (Ionescu et al., 2014), Orsett (Essex, England) (Gillies and Urch, 1983), Indian "Northern Black Polished Ware" (Gillies and Urch, 1983) and Attic ceramics (Maniatis et al., 1993). Regarding the present case, burnished ceramics are well documented in Aveiro red and black ceramics, sometimes in vertical and crossed lines, creating geometric motifs in some of the closed forms (mugs, jugs/water jugs and storage jars) (Bettencourt and Carvalho, 2007-2008; Carvalho and Bettencourt, 2012). Additionally, Fernandes (2012) studies the black ceramic production from Portugal in her doctoral thesis and mentions that burnishing the surface of the pieces was, and still is, a technique widely used to decorate the surfaces of black or red pottery, leaving the surface shiny (Fernandes, 2012). Therefore, according to the literature presented, ceramics from F-V have been probably burnished because of the appearance of their shiny black surface.

Salt-glaze hypothesis

Additionally, the elements Na and Cl have been identified in an aggregate of AVR009, in the surfaces of AVR004 and AVR005 and in the ceramic body of AVR015 (Figure 6.36.). Moreover, Na has been identified in the surface and body of some ceramics (AVR003, AVR004, AVR005, AVR006, AVR007, AVR008, AVR014, AVR015, AVR016) (Figure 6.36.). Potassium halite has been identified as described in Chapter 6, section 6.2.3., "Technological assessment by XRD", as well. Although the sodium could be related to the sodium feldspars, especially in the ceramics that do not have a glassy-layer, the NaCl or Na could be related to the salt of the water environment from RAVA. But it could also be related to the salt production and trade of Aveiro because fragments of a wood piece belonging to the shipwreck were discovered in the archaeological site of Ria de Aveiro A. By comparison with materials from other underwater contexts, it was recognized as a part of a shovel made of a single piece of log. It seems that the shovels were destined to load, unload and move the salt,

although another function on board is not excluded. A similar shovel was also recovered in Newfoundland, associated with the conservation treatment of fish caught by European fishers who move there annually (Bettencourt and Carvalho, 2007-2008). Therefore, it could be thought that the ship was carrying salt in a location next to the ceramics or above them.

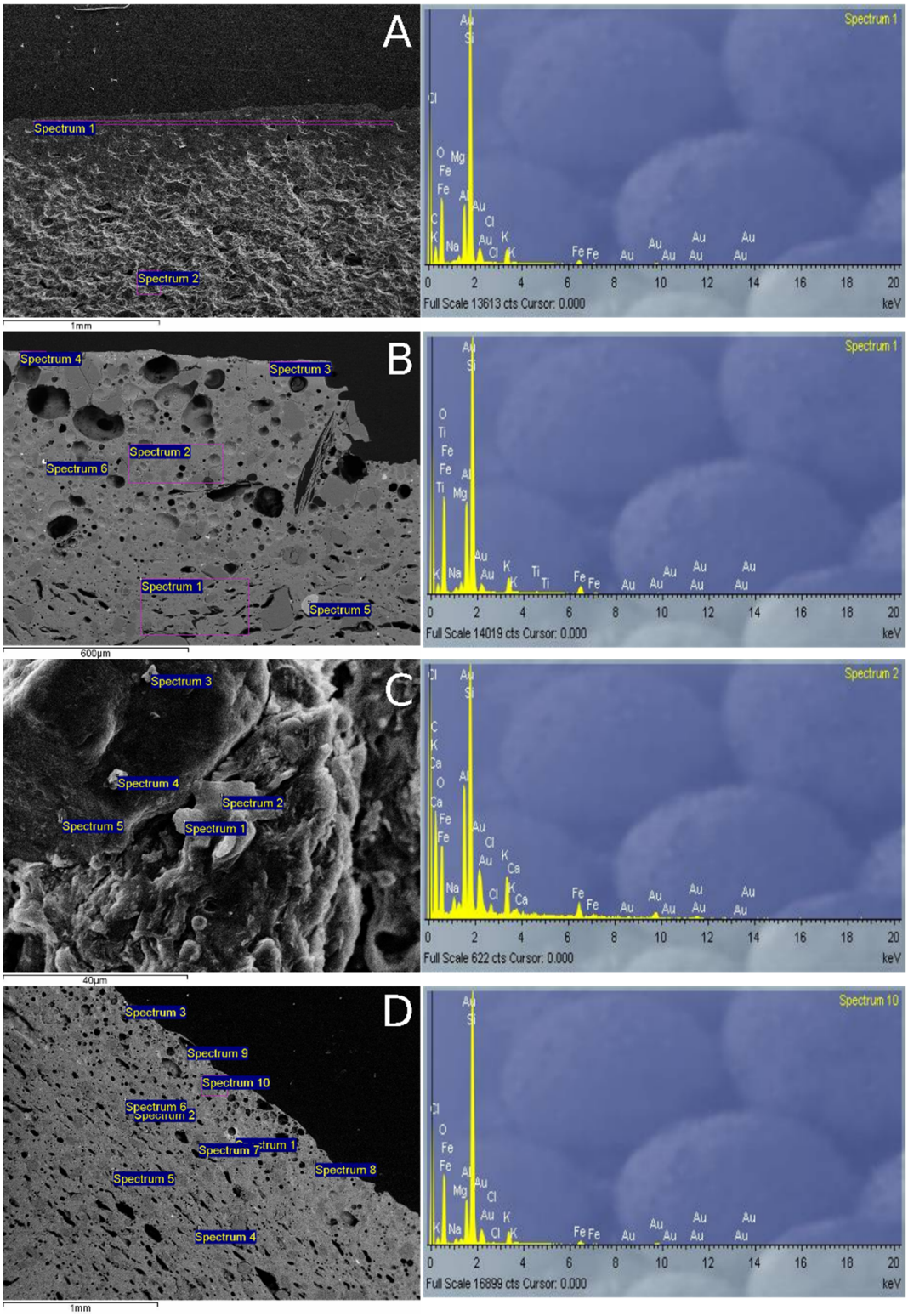

Figure 6.36. SEM-BSD (a,b,d), SEM-SED (c) images and their SEM-EDS analyses: **(a)** Na and Cl in the Surface of AVR004; **(b)** Na in the body of AVR015; **(c)** Na and Cl in an aggregate of AVR009; **(d)** Na and Cl in the surface of AVR005

Besides, as has been reported in Chapter 2, several indications of a fire on board have been documented. In this context, it is possible to hypothesize about the presence of the salt and the fire on board affecting the ceramics. As the fire started in the ship, the salt could have reacted with the water in high temperatures (the temperatures of the fire), giving hydrogen chloride and sodium oxide (alkaline flux) as a product, according to the following reaction (Rice, 1987):

$$2NaCl + H_2O \rightarrow 2HCl\uparrow + Na_2O \quad Eq.\,6.3.$$

The important role of the alkaline fluxes is to lower the very high melting point of silica, which is normally 1710 °C (Rice, 1987). Hence, this alkaline flux could have reacted with the silica of the pot surface ($Al_2O_3{\cdot}4SiO_2$), giving a glassy-layer as a product ($Na_2O{\cdot}Al_2O_3{\cdot}4SiO_2$):

$$Na_2O + Al_2O_3 \cdot 4SiO_2 = Na_2O \cdot Al_2O_3 \cdot 4SiO_2 \quad Eq.\,6.4.$$

The adiabatic flame temperature is the highest temperature achieved without any heat loss or any other external factor affecting the combustion process and, in the case of wood, the calculated adiabatic value is 1980°C (Annamalai and Puri, 2006; Nolan, 2000). However, in a real fire event, like the underwent by the RAVA shipwreck, many factors play a role when determining the temperature (e.g. timber thickness and density, amount of available combustible material, humidity, atmospheric pressure, oxygen supply, among others). In any case, flame temperature can be around 1000°C (Elvira Martin, 1984; Stroup et al., 2013), or even higher if it is an enclosed fire, in which flame temperature easily reaches 900C° but showing peak temperatures up to 1200°C depending on the size of the fire (Babrauskas and Williamson, 1979). However, when considering pottery firing, flame temperature is not the only factor to consider; surrounding gas temperature should be also of importance regarding the effect of firing. In this regard, and according to software simulations, the expected gas temperature in the near field of a wood fire will vary between 600 – 1100 °C (Degler and Eliasson, 2015; Kawagoe and Sekine, 1963). Moreover, in enclosure fires, gas temperature may easily exceed a temperature above 1000°C (Elvira Martin, 1984), sustaining the gas temperature for over 50 min under optimal conditions of amount of combustible, humidity and oxygen (Karlsson and Quintiere, 2000). Therefore, temperature achieved during a fire like the one in the RAVA shipwreck might be high enough and sustained long enough as to produce vitrification and glassy-layers on the vessel surfaces, probably with a rapid temperature increase when the vegetable cover that wrapped the cargo ignited.

Those reactions can explain the presence of Na and not Cl in some ceramics and some concretions of some ceramics as well as the vacuolar aspect of the glassy-layers: the Cl was evaporated in the form of hydrogen chloride, leaving holes where before were bubbles. This reaction and the formation of a glassy-layer also can be explained by the compositional difference of Na between the surface and the body of the ceramics that have the glassy-layer (Figure 6.37. and Table 6.9.). The values of Table 6.9. demonstrate that the concentration of Na is higher in the surface than in the body, due to probably the formation of Na_2O in the surface. The difference in the concentration of Na also occurs in a lesser degree, that is, not with big differences, in other ceramics that do not have a glassy-layer (e.g. AVR014), but not in all of them (e.g. AVR004). Moreover, this hypothesis can also explain the case of AVR005: the two ceramics that were next to each other in the ship could have reacted with the salt following the reaction explained, so that finally they got stuck.

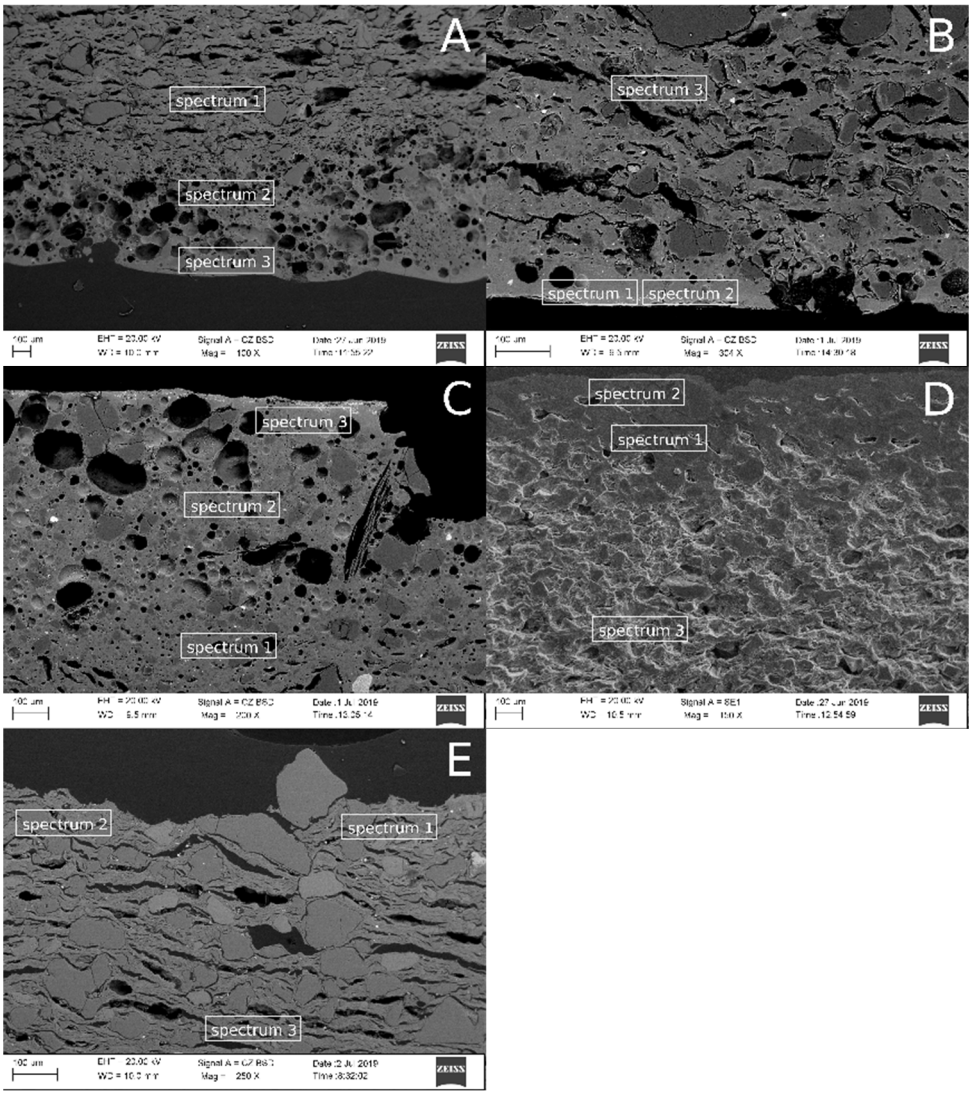

Figure 6.37. SEM-BSD (a,b,c,e) and SEM-SED (d) images showing the elemental analyses carried out in different regions (surface, lower than the surface and body) of: **(a)** AVR003; **(b)** AVR016; **(c)** AVR015; **(d)** AVR004; **(e)** AVR014, marked by the name of the spectrum

Table 6.9. Elemental concentrations of Na (in wt %) in different regions obtained by SEM-EDS of the ceramics shown in Figure 6.37.

Samples	Glassy-layer	Spectrum	Position	Na
A. AVR003	Yes	Spectrum 3	Surface	9.99
		Spectrum 2	Lower than the surface	1.97
		Spectrum 1	Body	0.29
B. AVR016	Yes	Spectrum 1	Surface	5.37
		Spectrum 2	Surface	6.03
		Spectrum 3	Body	0.64
C. AVR015	Yes	Spectrum 3	Surface	5.87
		Spectrum 2	Lower than the surface	2.79

		Spectrum 1	Body	0.77
D. AVR004	No	Spectrum 4	Surface	0.41
		Spectrum 3	Body	0.43
E. AVR014	No	Spectrum 1	Surface	0.39
		Spectrum 2	Surface	0.26
		Spectrum 3	Body	0.17

Marine environments

Some aggregates composed by Fe, S, and in some cases, K have also been identified in the cavities and cracks of the ceramics (Figure 6.38.).

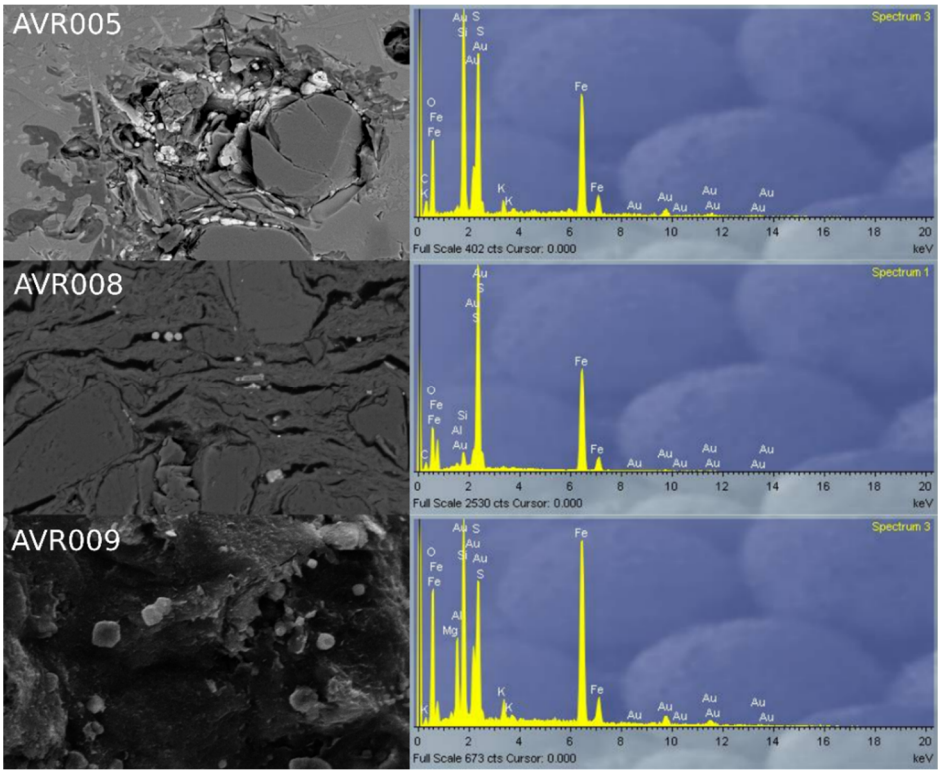

Figure 6.38. SEM-BSD and SEM-EDS images of the aggregates in the cracks and cavities of AVR005, AVR008 and AVR009 composed mainly by Fe and S, and, sometimes, K

According to the literature, these aggregates could be pyrite (FeS_2) and/or jarosite [(K, Na)$Fe_3(SO_4)_2(OH)_6$] (Secco et al., 2011). The presence of these two aggregates is a common alteration in marine environment ceramics, produced due to the decomposition of hematite (Fe_2O_3), from ferric ion (Fe^{3+}) to ferrous ion (Fe^{2+}), by the reduction and solubilisation with hydrogen sulphide (H_2S) in water solution (Secco et al., 2011). In saline water environments, the microorganisms can reduce sulphate ions (SO_4^{2-}) to sulphur (S) or hydrogen sulphide, in the presence of

sulphate-reducing bacteria (*Desulfovibrio desulfuricans*) (Neal et al., 2001; Secco et al., 2011). Then, this H_2S is the responsible for hematite being reduced. Two main mechanisms could happen for this reduction, giving as a product framboidal aggregates or euhedral crystals of pyrite (Secco et al., 2011). On the one hand, hematite could hydroxilate to goethite (FeOOH), and subsequently, goethite could be reduced by H_2S to Fe^{2+}. On the other hand, hematite could be reduced directly to Fe^{2+} in the presence of H_2S. After these two reduction mechanisms, the ferrous ion reacts with additional hydrogen sulphide and forms pyrite as euhedral crystals or framboidal aggregates depending on the different sequences of reactions and the amount of organic matter and hydrogen sulphide (Neal et al., 2001; Schoonen, 2004; Secco et al., 2011). Then, jarosite could be formed due to the oxidation of pyrite and reaction with dissolved alkali (Secco et al., 2011). A good example of this phenomenon is showed in the study carried out by Iñañez et al. (2020). The authors identified framboidal aggregates of Fe and S by SEM-EDS in some of the translucent green lead glazed and tin-lead glazed ceramics recovered in Angra D shipwreck (Figure 6.39.), suggested to be pyrite neoformed crystallite.

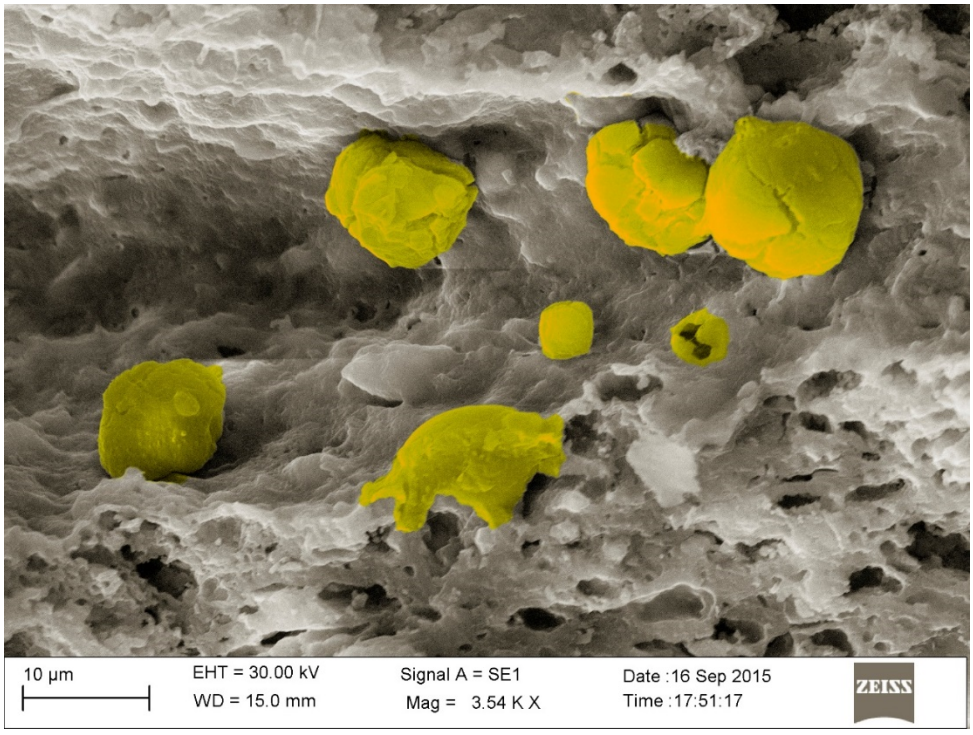

Figure 6.39. False coloured SEM-SED microphotograph at 3500× magnification of ANG014 ceramic recovered in Angra D shipwreck (Iñañez et al., 2020) showing framboidal aggregates (in yellow). Fe and S are major components according to point EDS microanalysis (see Iñañez et al., 2020 for a thorough discussion)

6.3. Lead isotopic study of ceramics recovered in Zamora city

In the present work, the glazes of 24 ceramics from Zamora region have been studied by lead isotope analyses to assess the supply of metals (lead and, after indirect evidences, tin) for ceramic glazing in the Zamora region, enhancing the knowledge of ancient mining and trade routes. Moreover, elemental data were gathered for 7 artefacts. Additionally, Zamoran and surrounding 15 lead ores have also been analysed in order to extend the currently available lead isotope database and use this as a tool for lead provenancing. It should be noted that I am aware of the fact that the data obtained from the galena deposits is scarce. That is, only one sample from each mine has been measured and, consequently, the natural variability on the isotopic ratio in each deposit is unknown. However, since there is no known lead isotope analysis conducted on Zamora and surrounding regions lead mines, and the hypothesis of a domestic origin of the lead used for manufacturing the studied glazes must be tested, I decided to carry out a first preliminary approach on historical mines for comparison purposes.

Lead isotope compositions and elemental data of the glazes were determined by Laser Ablation-Multi Collector-Inductively Coupled Plasma-Mass Spectrometry and Laser Ablation- Single-Collector High-Resolution ICP-MS (LA-MC-ICP-MS and LA-HR-ICP-MS) and lead isotope compositions of lead ore samples and some glazes were also determined by solution MC-ICP-MS (see Chapter 4, section 4.3.). The studied ceramics are summarized in Table 6.10.

Table 6.10. Ceramics studied in the present work, with the information about the village and the archaeological site where they were recovered, in addition to their typology, colour decoration of the glaze, form, chronology (centuries) and the reference group they belong to

Samples	Village	Archaeological site	Typology	Colour decoration	Form	Chronology	Group
ZMR024	Zamora	Olivares	translucent-glazed	green	cooking pot	late 19th-early 20th	Z-1
ZMR025	Zamora	Olivares	translucent-glazed	brown	cooking pot	late 19th-early 20th	Z-1
ZMR029	Zamora	Olivares	translucent-glazed	beige (raw glaze)	small jar	late 19th-early 20th	Z-1
ZMR012	Zamora	Olivares	micaceous translucent-glazed	beige (raw glaze)	large jar	late 19th-early 20th	Z-2
ZMR032	Zamora	Olivares	micaceous translucent-glazed	brown	large jar	late 19th-early 20th	Z-2
ZMR035	Zamora	Olivares	micaceous translucent-glazed	blackish (burnt)	handle	late 19th-early 20th	Z-2
BNV001	Benavente	Casa del Tinte	tin-lead glazed	white and blue	bowl	17th-18th	Z-3
BNV002	Benavente	Casa del Tinte	tin-lead glazed	white	plate	17th-18th	Z-3
BNV003	Benavente	Casa del Tinte	tin-lead glazed	white	bowl	17th-18th	Z-3
BNV004	Benavente	Casa del Tinte	tin-lead glazed	white and green	chamber pot	17th-18th	Z-3
ZMR002	Zamora	Olivares	tin-lead glazed	white and blue	plate	late 19th-early 20th	Z-3
ZMR005	Zamora	Olivares	tin-lead glazed	white and blue	plate	late 19th-early 20th	Z-3
ZMR008	Zamora	Olivares	tin-lead glazed	white	porringer	late 19th-early 20th	Z-3
ZMR045	Zamora	La Concepción	tin-lead glazed	green and black on white	bowl	15th-16th	Z-3
ZMR046	Zamora	La Concepción	tin-lead glazed	white and blue	bowl	15th-16th	Z-3
ZMR047	Zamora	La Concepción	tin-lead glazed	white and blue	bowl	15th-16th	Z-3
ZMR048	Zamora	La Concepción	tin-lead glazed	green and brown on white	plate	15th-16th	Z-3
ZMR052	Zamora	Ethnographic Museum	tin-lead glazed	white, green and black	bowl	16th	Z-3
ZMR053	Zamora	Ethnographic Museum	tin-lead glazed	white and green	bowl	17th-18th	Z-3
ZMR055	Zamora	Ethnographic Museum	tin-lead glazed	white and blue	plate	17th-18th	Z-3
TOR002	Toro	Cuesta del Negrillo No.11	translucent-glazed	brown	small jar	17th	T-1
TOR010	Toro	Cuesta del Matadero	translucent-glazed	brown	pitcher	17th	T-1
TOR011	Toro	Cuesta del Matadero	translucent-glazed	brown	lid	17th	T-1
TOR012	Toro	Cuesta del Matadero	translucent-glazed	brown	cup	17th	T-1

As explained in Chapter 1, these objectives are possible because the lead isotope ratios of minerals such as galena (PbS), cerussite ($PbCO_3$) or anglesite ($PbSO_4$) (minerals from which lead was extracted), which are denominated as "common lead minerals", remain constant over time (Hunt, 2003), giving the opportunity to constrain the origin and age of their source (Dickin, 2018). When the isotope field in Pb/Pb space of particular mineral deposits or zones overlaps with the lead isotope ratios of the objects in the graphs ($^{207}Pb/^{204}Pb$ vs $^{206}Pb/^{204}Pb$ and $^{208}Pb/^{204}Pb$ vs $^{206}Pb/^{204}Pb$ in the present work), the lead of the object is "consistent" with, or "matches", the composition of the deposit/zone (Hunt, 2003). If there is no overlap or there is an overlap only in one graph, it is stated that the object could not have been made with lead from this particular deposit/zone. However, different metal ores or geologic areas may show similar lead isotope compositions; in consequence, an isotopic match between the archaeological materials and the geologic areas or metal ores might not be conclusive (García de Madinabeitia and Gil Ibarguchi, 2019; Hunt, 2003; Santos Zalduegui et al., 2004). Furthermore, it is possible that the analysed lead represents a mixture of source materials. In this case, the isotope composition of the archaeologic material would be a mixture between the isotope compositions of the source materials. To manage these problems, it is necessary to have extensive information about the isotopic features of different metal ores or geological zones coupled with the knowledge about the historical period in which the metal ores have been exploited (Santos Zalduegui et al., 2004; Stos-Gale et al., 1995). Moreover, the possible import-export commercial routes into the Iberian Peninsula or other continents are also of great importance for the interpretation of isotopic and other results. Several authors have collected lead isotope compositions of ores from the Iberian Peninsula. Santos Zalduegui et al. (2004) analysed galena samples from the Alcudia Valley, Linares-La Carolina and Los Pedroches batholith areas. Additionally, Velasco et al. (1996) presented lead isotope data of galena samples from the Pyrenees, Basque-Cantabrian basin and Demanda ranges. Marcoux (1997) analysed samples from Spanish and Portuguese volcanogenic massive sulphide deposits and Tornos and Chiaradia (2004) published data from the Ossa-Morena zone. Montero-Ruiz (2018) published a comprehensive review about these works and Stos-Gale and Gale (2009) assembled the Oxford lead isotope database (named as "OXALID") of the European ore deposits, metals and artefacts at the Isotrace Laboratory at the Research Laboratory for Archaeology and the History of Art in Oxford. Recently, García de Madinabeitia et al. (2021) have also published a compilation of Pb isotope data called "IBERLID". This publication

includes compiled analytical data for nearly 3000 samples from the Iberian Peninsula and Balearic Islands with references given to about 140 articles, monographs, etc. In the present study, the studied artefact results have been compared with information from available databases comprising reference data not only from mineralizations across the Iberian Peninsula, but also from other European countries.

Besides, tin is a pivotal component in opaque white glazes. Therefore, the question where the tin comes from is an important issue to consider regarding the study of ancient trade routes. Tin is almost always mined from cassiterite (SnO_2), often occurring at elevated concentrations in large granite massifs (granite batholiths), and related pegmatites. The Iberian Peninsula is rich in tin mineralizations, and it has been suggested that early tinworks exploited mainly alluvial deposits (Comendador-Rey et al., 2017). This was a system of mining that has left very few, if any, remains. In addition, more recent mining works (e.g., for tungsten and tin in the 20th century) may have destroyed evidence of earlier mining, which makes it difficult to determine if tin mining occurred earlier than what is known from historical records. It is also important to note that tin mining during Medieval times is known from other countries in Europe, such as Germany (Erzgebirge in Saxony) and England (Devon and Cornwall) (Taylor, 1983; Gerrard, 2000). Most tin deposits are found in the north-western part of the peninsula, and among the more well-known examples are the Panasqueira (Kelly and Rye, 1979) deposits in the Central Iberian zone. It is noteworthy that lead is rarely an associated metal with Sn deposits (i.e. the lead concentration in a tin ore concentrate is typically very low). This implies that the addition of tin to the glaze is not likely to have contributed to the lead budget. Hence, as a first order assumption, the obtained lead isotope compositions of glazes are assumed to solely reflect the lead ore used for manufacturing the objects. Yet, the establishment of the origin of the tin component is another piece of information that helps understand the trading routes at the time of the pottery production.

In this study, the lead isotope compositions of the glazes were determined by LA-MC-ICP-MS. The main benefits of this technique, compared to solution multi-collector (MC)-ICP-MS, are the minimal destruction of the sample, the lack of sample preparation requirement and the rapidity and precision of the analyses (Iñañez et al., 2016). A disadvantage is that LA-MC-ICP-MS generally requires a suitable reference material with similar matrix to the samples for calibration. Such

material is not available for glazes. Instead, glass materials are commonly used for such analyses (Resano et al., 2005) and, therefore, CRM NIST 610 and 612 glass wafers were chosen in this study. In addition, glazes may show a certain degree of heterogeneity, so the elemental result emanating from the ablated part may not be representative of the whole glaze composition. However, since lead has passed through a liquid phase during the glaze preparation, the lead isotope composition is assumed to be homogeneous within the glaze. Lead is, along with silica, the main component of these glaze matrices, and plays the role of a flux, that is decreasing the silica fusion temperature enabling the transformation into a glassy network. Tin is the principal responsible component for achieving the opaque white coating, given that tiny tin oxide recrystallizations within the glaze during firing scatter and diffract the incident light (Molera et al., 1999; Tite et al., 1998). Accordingly, SEM-BSD examinations (Figure 6.40.) reveal the common presence of nano- and micrometric crystals of cassiterite (SnO_2) forming small clusters, in addition to quartz, feldspar and sometimes lead inclusions. Such inclusions are usually well-distributed within the glaze due to the technological resource of using a fritting method (see Chapter 1, section 1.1.).

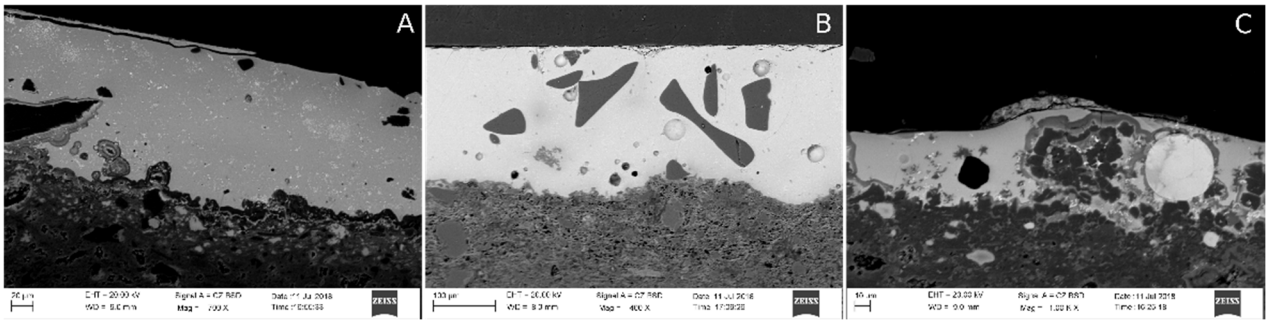

Figure 6.40. SEM-BSD images of: **(a)** ZMR046, where cassiterite clusters are visible (white spots); **(b)** ZMR048 glaze, where quartz and feldspar inclusions are visible; **(c)** ZMR046, where a big lead inclusion (white circle) is visible

6.3.1. Ores and mining history of the Iberian Peninsula

The Iberian Peninsula is divided in different geological zones, which are shown in Figure 6.41. One such zone is the Iberian Pyrite Belt, which hosts a large number of metal deposits and has been an important producer of especially copper for several millenniums. Its ore deposits are rich in base metals (Zn-Cu-Pb), with significant amounts of silver and gold, and occur as massive ore lenses in volcanic rocks of Devonian age (Tornos, 2003, Tornos et al., 1999). Besides, the Ossa-Morena Zone is an area in the south-west with a complex geology, which hosts a variety of ore types of different ages (Tornos et al., 2004). In addition to iron, and Cu-Ni-rich occurrences, there are lead-bearing base metal deposits hosted by rocks having different ages (from Cadomian to Carboniferous). This age range, spanning roughly a period between ca 700 and 300 million years, has led to pronounced lead isotope distinctions between different ore deposits found within this district, such as Nava-Paredón. In addition, the South Portuguese Zone also carries volcanic-hosted deposits in basins equivalent to those found at the Ossa-Morena Zone (Onézime et al., 2003). Besides, the existing Pb-Zn mesothermal veins in the Central Iberian Zone are mostly small but widely extended. Ores in that area are often of a vein-type that formed as a result of processes during the Alpine orogeny that started about 65 million years ago (Lillo, 1992). Besides, the Betic Ranges were also developed due to Alpine processes, and their eastern section is among the most intensely mineralized regions of Europe (Arribas and Tosdal, 1994). Additionally, ores in the Cartagena Ranges district are typically hosted by limestones (Sabaté et al., 2015). Moreover, the Iberian Ranges are mainly formed by predominantly calcareous Mesozoic and Tertiary age rocks. They contain abundant Pb-Zn-(Ag)- and Ba-dominated low temperature veins formed during the Mesozoic (Subías et al., 2010). Besides, most of the several ancient mining areas of the Catalonian Coastal Ranges consist of Pb-Zn vein deposits hosted by Paleozoic rocks (Alfonso et al., 2012). Moreover, in the West Asturian Leonese zone, strata bound deposits of Zn-Pb-(Ag) in the Cambrian limestones are very frequent (Perez Estaun et al., 1990a). In addition, in the Cantabrian zone, there are little occurrences of Permian epithermal Pb-Zn deposits related to late Variscan fractures (Perez Estaun et al., 1990b). Finally, regarding the Basque-Cantabrian Basin (BCB), there are two types of deposits with Pb-Zn: epithermal veins related with faults and strata bound deposits related with Mesozoic limestones (which are the most important) (Ábalos, 2016; Cámara 1997; García-Mondéjar et al. 1996; Gómez et al. 2002; Mangin and Rat 1962; Rat 1988). For

more details of the Iberian geology, the reader is referred to works of e.g. Julivert et al. (1992) and Tornos (2003). Besides, as several of the geological zones carry great mineralizations, further information about important mineral deposits is found in works by e.g. Arribas and Tosdal (1994), Klein et al. (2009), Marcoux (1997), Santos Zalduegui et al. (2004), Subías et al. (2010), Tornos (2003), Tornos and Chiaradia (2004) and Velasco et al. (1996).

In addition, tin deposits, with respect to the Iberian Peninsula, are commonly of the "greisen-type" which refers to a coarse-grained quartz-muscovite rock without feldspar, which is typically associated with tin ± tungsten mineralization. On the other hand, regarding the geology of Zamora province, two large geological regions or groups of different rocks can be found: the basement that constitutes the Iberian Massif, which occupies the entire western edge, and the sedimentary materials of the Duero Basin that emerge in the eastern half. Each one represents a stage in the long geological history of the Peninsula, in total some 600 million years of stratigraphic record, in which two important orogenic periods, the Hercynian and the Alpine, followed one another (Fadón, 2011).

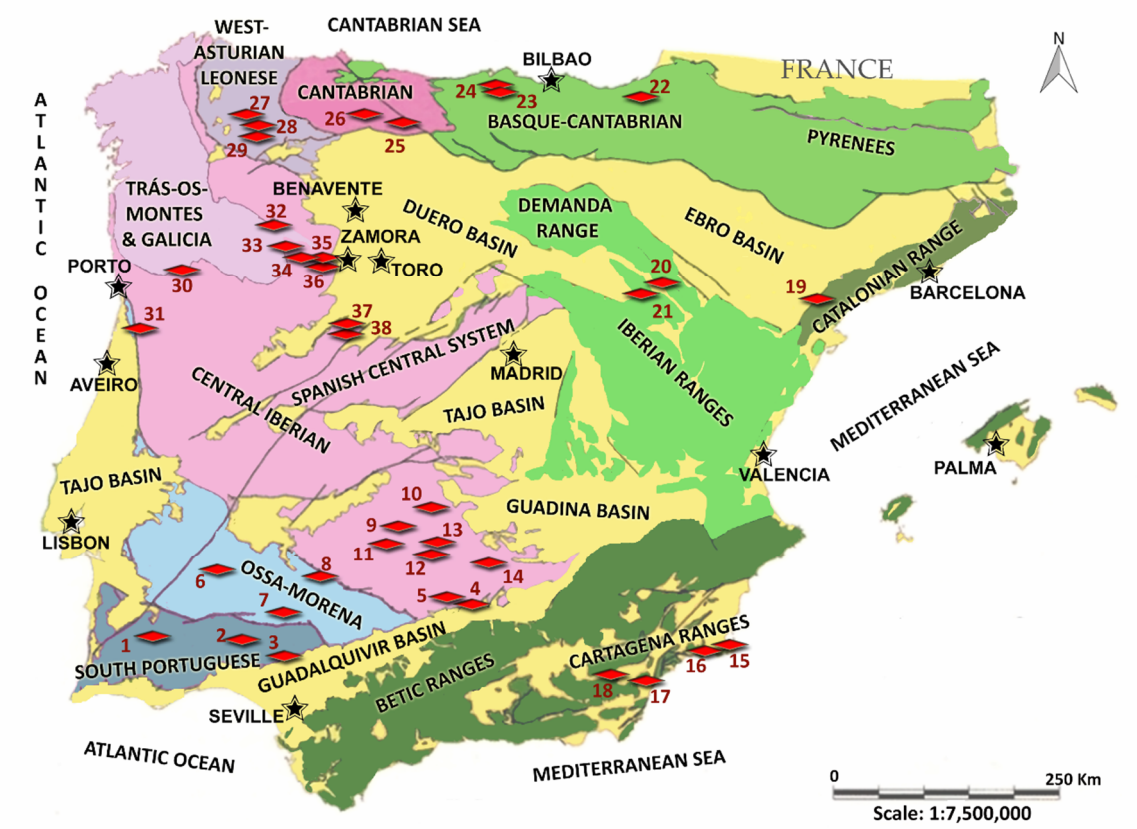

Figure 6.41. An overview of the geological zones and the location of some relevant mines: 1. Neves Corvo (Beja, Pt). 2. Rio Tinto (Huelva, Es). 3. Aznalcollar (Sevilla, Es). 4. Linares (Jaén, Es). 5. La Carolina (Jaén, Es). 6. La Infanta (Huelva, Es). 7. Nava-Paredón (Córdoba, Es). 8. Azuaga (Badajoz, Es). 9. Pedroches (Córdoba, Es). 10. Alcudia (Ciudad Real, Es). 11. Los Eneros (Córdoba, Es). 12. Navalmedio (Ciudad Real, Es). 13. Mina Vieja (Córdoba, Es). 14. El Hoyo (Ciudad Real, Es). 15. La Unión (Murcia, Es). 16. Mazarrón (Murcia, Es). 17. Almagrera (Almería, Es). 18. Gador (Almería, Es). 19. Priorat ((Molar Bellmunt Falset, MBF), Tarragona, Es). 20. La Pedraza (Zaragoza, Es). 21. Juan de Austria (Soria, Es). 22. Troya (Gipuzkoa, Es). 23. Reocín (Cantabria, Es). 24. San José (Cantabria, Es). 25. Valdetriollo (Palencia, Es). 26. Velilla (León, Es). 27. Rubiales (Lugo, Es). 28. Antonina-Santa Bárbara (León, Es). 29. Valentín (León, Es). 30. Vila Pouça (Vila Real, Pt). 31. Braçal (Aveiro, Pt). 32. Nuez (where Mina San Blás is located) (Zamora, Es). 33. Latedo-Manzanas (where Mina Tertiñan is located) (Zamora, Es). 34. San Martín del Pedroso (Bragança, Pt/Zamora, Es). 35. Losacio-Marquiz (where Mina Clara is located) (Zamora, Es). 36. Carbajales (Zamora, Es). 37. Goviendes-La Tala (Salamanca, Es). 38. Los Santos (Salamanca, Es). (Pt=Portugal; Es=Spain; Black stars= main cities and villages; red spots=areas with lead mines or specific galena ores)

In addition to hosting a large number of metalliferous deposits across the country, the Iberian Peninsula has a long mining history. Ancient mining may have started already around 4000 BC (Montero-Ruiz et al., 2021) in the Iberian Pyrite Belt, whereas ores in the Linares-La Carolina (within the Central Iberian Zone) and the Cartagena ranges (within the Betic ranges) were mined already during the Roman

Empire and earlier (Santos Zalduegui et al., 2004). Sánchez (1989) gave an overview of all mineral deposits that existed in the Castille and Navarre Kingdoms from 1450-1610. Tornos (2003) described that Spain became the world's leading producer of copper, pyrite (an iron sulphide) and lead more recently, in the 18th-19th centuries and the most important exploited ores were those of Gádor ranges (1800-1870), Almagrera ranges (middle 19th century), Linares-La Carolina (1880-1970), Alcudia (1840-1935) and Azuaga (late 19th century-early 20th century).

Of particular interest are a number of historical minor deposits (see Figure 6.41.), known to carry lead, which occurs relatively close to or within the Zamora region. This spatial relationship between the production centres and mines merits a brief summary of their ore characteristics. The lead mineralizations at the Zamora province, some of which have been sampled for this study, were formed during late-Hercynian hydrothermal events. They comprise a set of small mines, mainly quartz vein-type deposits and a scarce portion of sedimentary-exhalative deposits, which are hosted by the Variscan Massif at the border of Galicia/Tras-os-Montes and Central Iberian Zone. A few major deposits are also known, such as Mina Clara (located in the village of Losacio), which became the second national producer of lead in the middle of the 19th century, only surpassed by the District of Linares-La Carolina (Fadón, 2011). Additionally, there is historical documentation about lead mining activity in the 17th century in some other mines in the Zamora province, such as those located in Alcañices, Carbajales and Nuez (De la Escosura, 1846; Martín, 2018; SIEMCALSA, 2007). González (1832) documents that lead was exploited in the mine of Nuez as early as 1575 and that new deposits of *alcohol* were discovered and exploited in that area. *Alcohol* is the ancient name given to galena used for manufacturing the glazes of the ceramics (Sánchez, 1989). Martín (2018) explains that the activity in these mines was directed to the needs of the surrounding commercial activity.

Analysed ore galena samples

To increase the knowledge of lead isotope fingerprints of the possible mineral supply to Zamoran potters, a set of 15 new ore galena samples from the following known historic mines and mine districts has been analysed (see Figure 6.41.): in the province of Zamora, Latedo (Mina Tertiñan, Figure 6.41., 33), Losacio (Mina Clara, Figure 6.41., 35), Nuez (Mina San Blás, Figure 6.41., 32) and San Martín del

Pedroso (Mina Manzanas, Figure 6.41., 34). In addition, there are deposits in the provinces of León and Lugo. One example of these deposits is the Valentín mine (province of León, Figure 6.41., 29). Continuing with the more northern deposits, there are deposits such as Valdetriollo (province of Palencia, Figure 6.41., 25) and Velilla (province of León, Figure 6.41., 29). Most of the mines from the Zamora and Salamanca areas are small, but there are some very important mineralizations. In those mines, zinc dominates over lead like in the San José mine (province of Cantabria, Figure 6.41., 24). In addition, the Central Iberian Zone hosts mineralizations in Salamanca, Ciudad Real (Alcudia Valley) and Córdoba (Sinclinal de Guadalmez). Samples from Goviendes (Figure 6.41., 37) and Los Santos (Figure 6.41., 38) mines were taken from the mines of the province of Salamanca. Los Santos is best known for its tungsten mineralizations, but lead seams are also present. From the Alcudia Valley mineralizations, in the province of Ciudad Real, a sample from El Hoyo mine (Figure 6.41., 14),and other samples from the mineralizations of the Sinclinal de Guadalmez (province of Córdoba), the Vieja mine in Santa Eufemia (Figure 6.41., 13) have been analysed. In the Ossa-Morena Zone, one of the most significant is Los Eneros mine (province of Córdoba, Figure 6.41., 11). The mineralizations on the edges of the Iberian System, such as the La Pedraza (province of Zaragoza, Figure 6.41., 20) and Juan de Austria mines (province of Soria, Figure 6.41., 21) are associated with quartz veins.

6.3.2. Analytical Methodology

As commented, lead isotope compositions of the glazes were determined by means of LA-MC-ICP-MS and solution MC-ICP-MS. This last was also used for analysing lead isotope compositions of lead ore samples. Moreover, chemical analyses of the glazes were carried out by LA-HR-ICP-MS (see Chapter 4, sections 4.3.5. and 4.3.6., for sample preparation and measurement details). In the case of LA-MC-ICP-MS analyses, internal precision (the precision of each measurement, repeatability) and external precision (the precision between each measurement, reproducibility or RSD %) for replicate analyses of NIST 610 (n=79) are for $^{20x}Pb/^{204}Pb$ (with x being 6, 7 or 8) 0.003-0.02 and 0.03-0.04 %, respectively. In Addition, for $^{207}Pb/^{206}Pb$ and $^{208}Pb/^{206}Pb$ the internal precision is $5{\cdot}10^{-5}$ – $9{\cdot}10^{-4}$ and the external precision is 0.01-0.02 %. In addition, in the case of solution MC-ICP-MS, the external precision (reproducibility) of the standard solutions was better than 0.08 % (2 σ, n=16), 0.18 % (2 σ, n=4) and 0.13 % (2 σ, n=2), respectively, and accurate within 0.04 %,

0.15 % and 0.10 % of their respective literature values (Todt et al., 1996; Woodhead and Hergt, 2000). This approach allowed the assessment of the LA-MC-ICP-MS results obtained on potentially heterogeneous glaze materials. Given the absence of matrix-matched reference materials for ceramic glazes, the solution data were also used to verify the accuracy of the laser ablation results. Nine glaze samples were dissolved; two of them were taken from the inner and outer glazed surfaces of the ZMR047 ceramic piece and other two from two different places of the same surface of BNV003. The unknowns were run as duplicates to ensure the significance of the results. Moreover, the solution isotope data was compared with laser ablation isotope data corrected in two different ways; either the latter results were corrected only for mass bias (Tl correction) or corrected both for mass bias and to compensate for the deviation between Tl-corrected NIST 610 data and corresponding published data. There was a systematic offset (of about 0.04 units for e.g. $^{206}Pb/^{204}Pb$) between solution data and Tl+NIST corrected laser data, whereas the former yielded, within error, identical values to the Tl-only corrected set of laser data (Table 6.11. and Figure 6.40.a,b). The reason for this discrepancy is unknown, but it may be due to a matrix mis-match given the large contrast between lead concentration in NIST 610 (around 430 μg/g) and glazes (from ca 20 to above 90 %; Table 6.14., later). For consistency and taking the noted data discrepancies into account, the complete set of glaze results given in Table 6.12. are corrected for mass bias only (Tl correction) and shown as averages of laser ablation data obtained from nearby rastered lines. These tabulated results are also plotted in associated diagrams.

Table 6.11. Tl correction and Tl+NIST correction (marked with *) LA-MC-ICP-MS data

Samples	$^{206}Pb/^{204}Pb$	$^{207}Pb/^{204}Pb$	$^{208}Pb/^{204}Pb$	$^{207}Pb/^{206}Pb$	$^{208}Pb/^{206}Pb$
ZMR002	18.245	15.622	38.374	0.856270	2.10318
ZMR002*	18.205	15.595	38.320	0.856660	2.10502
ZMR005	18.240	15.629	38.390	0.856898	2.10475
ZMR005*	18.194	15.595	38.313	0.857159	2.10596
ZMR008	18.292	15.633	38.430	0.854568	2.10075
ZMR008*	18.246	15.597	38.347	0.854781	2.10172
ZMR012	18.218	15.622	38.369	0.857525	2.10609
ZMR012*	18.162	15.577	38.264	0.857678	2.10685
ZMR024	18.243	15.621	38.367	0.856250	2.10313
ZMR024*	18.183	15.574	38.259	0.856536	2.10419
ZMR025	18.215	15.617	38.348	0.857383	2.10532
ZMR025*	18.156	15.572	38.246	0.857704	2.10656
ZMR029	18.237	15.620	38.368	0.856546	2.10361
ZMR029*	18.188	15.585	38.294	0.856870	2.10521
ZMR032	18.229	15.628	38.387	0.857284	2.10573
ZMR032*	18.172	15.581	38.275	0.857392	2.10625
ZMR035	18.239	15.634	38.414	0.857010	2.10519
ZMR035*	18.182	15.588	38.303	0.857124	2.10575
ZMR045	18.716	15.667	38.850	0.837120	2.07589
ZMR045*	18.668	15.630	38.763	0.837293	2.07669
ZMR046	18.568	15.666	38.739	0.843690	2.08624
ZMR046*	18.521	15.631	38.658	0.843885	2.08723
ZMR047	18.645	15.665	38.789	0.840172	2.08038
ZMR047*	18.601	15.632	38.717	0.840420	2.08162
ZMR048	18.373	15.662	38.486	0.852482	2.09479
ZMR048*	18.327	15.627	38.404	0.852682	2.09572
ZMR052	18.427	15.637	38.435	0.848563	2.08573
ZMR052*	18.377	15.597	38.341	0.848715	2.08643

Samples	$^{206}Pb/^{204}Pb$	$^{207}Pb/^{204}Pb$	$^{208}Pb/^{204}Pb$	$^{207}Pb/^{206}Pb$	$^{208}Pb/^{206}Pb$
ZMR053	18.276	15.640	38.395	0.855815	2.10085
ZMR053*	18.233	15.608	38.321	0.856026	2.10191
ZMR055	18.405	15.636	38.402	0.849541	2.08645
ZMR055*	18.364	15.605	38.334	0.849785	2.08767
TOR002	18.241	15.625	38.382	0.856551	2.10415
TOR002*	18.180	15.590	38.284	0.857476	2.10601
TOR010	18.205	15.617	38.367	0.857881	2.10763
TOR010*	18.159	15.581	38.282	0.858024	2.10822
TOR011	18.204	15.620	38.377	0.858010	2.10811
TOR011*	18.157	15.582	38.286	0.858108	2.10856
TOR012	18.246	15.630	38.405	0.856585	2.10482
TOR012*	18.199	15.592	38.317	0.856722	2.10547
BNV001	18.462	15.640	38.446	0.847155	2.08245
BNV001*	18.406	15.595	38.333	0.847202	2.08269
BNV002	18.469	15.647	38.470	0.847217	2.08290
BNV002*	18.413	15.602	38.357	0.847262	2.08313
BNV003	18.313	15.636	38.357	0.853799	2.09453
BNV003*	18.261	15.592	38.249	0.853877	2.09480
BNV004	18.450	15.636	38.476	0.847522	2.08542
BNV004*	18.398	15.593	38.372	0.847618	2.08578

6.3.3. Results

Distribution of lead isotope ratios of studied glazes

The Pb isotope compositions of analysed glazes of Zamora region ceramics are illustrated in Figure 6.42. and reported in Table 6.12. Although individual results from nearby rastered areas are not given in Table 6.12., it is clear that on the scale of a specific glazed area, there are no significant isotope differences. It is also evident when comparing laser and solution results, emanating from different parts of a glaze of a certain colour, that glazes are isotopically homogeneous (Figure 6.42.a,b). The glaze results of the ZMR047 (Z-3 La Concepción group) are complex (Figure 6.42.a,b). Two solution-mode analyses were carried out on tin-glazed material from different parts of this sample, which corresponds to a bowl that has an inner blue- and an outer white-coloured surface. Results from the white part are identical with the laser ablation results, which also relate to a white surface. However, the other solution-mode analysis, involving the bluish part, yielded much more radiogenic compositions. Since the former was sampled from the white glazed area and the latter from a bluish area, this deviation is likely affected by blue pigment interference. Contribution of such pigment to the isotope composition cannot really be constrained. In addition, this significant difference between both analyses does not have a clear archaeological explanation. Taking these facts into account, and because only white and translucent glazed areas of the glazes are considered in this work, it has been decided to omit this radiogenic result from the discussion. Additionally, as indicated in Figure 6.42.c,d, three main populations can be defined and they are illustrated by fields in different colours. A conspicuous feature is the tendency for the development of a linear data array formed by data from the tin-lead glazed Z-3 La Concepción samples (blue field). These data are characterized by a wide range in $^{206}Pb/^{204}Pb$ coupled with relatively elevated $^{207}Pb/^{204}Pb$ and $^{208}Pb/^{204}Pb$ values. A second, major population plotting in a comparatively low-radiogenic part of the diagrams (green field) is defined by all translucent-glazed ceramics (Z-1, Z-2 and Toro) along with tin-lead glazed Z-3 Olivares samples. Finally, tin-lead glazed Z-3 Benavente and Z-3 Ethnographic Museum samples form a third population (violet field). However, there are two samples (BNV003 and ZMR053) that differ from the other ceramics of this sample group and plot closer to translucent-glazed and Z-3 Olivares ceramics. The red encircled field covers the complete data field defined by results from Benavente and the Museum group of Z-3 samples.

Table 6.12. Averages of laser ablation data, with its precision (2σ), obtained from nearby rastered lines (in the white coloured parts of tin-lead glazed and translucent-glazes ceramics) and solution-mode MC-ICP-MS data (marked with a *); the exception is the ZMR047(b)* sample, for which the blue colour was rastered

Samples	Site	$^{206}Pb/^{204}Pb$	2σ (mean)	$^{207}Pb/^{204}Pb$	2σ (mean)	$^{208}Pb/^{204}Pb$	2σ (mean)	$^{207}Pb/^{206}Pb$	2σ (mean)	$^{208}Pb/^{206}Pb$	2σ (mean)
ZMR002	Olivares	18.245	6.07E-03	15.622	6.13E-03	38.374	2.48E-02	0.856270	3.617E-04	2.10318	1.475E-03
ZMR005	Olivares	18.240	4.19E-03	15.629	4.81E-03	38.390	1.72E-02	0.856898	1.866E-04	2.10475	7.835E-04
ZMR008	Olivares	18.292	3.82E-03	15.633	4.60E-03	38.430	1.55E-02	0.854568	1.311E-04	2.10075	5.668E-04
ZMR012	Olivares	18.218	7.20E-03	15.622	7.27E-03	38.369	3.28E-02	0.857525	5.053E-04	2.10609	2.101E-03
ZMR024	Olivares	18.243	5.66E-03	15.621	6.76E-03	38.367	2.27E-02	0.856250	1.778E-04	2.10313	8.134E-04
ZMR025	Olivares	18.215	6.48E-03	15.617	8.11E-03	38.348	2.66E-02	0.857383	1.768E-04	2.10532	8.257E-04
ZMR029	Olivares	18.237	1.06E-02	15.620	1.29E-02	38.368	4.34E-02	0.856546	3.475E-04	2.10361	1.507E-03
ZMR032	Olivares	18.229	4.95E-03	15.628	6.10E-03	38.387	2.02E-02	0.857284	1.494E-04	2.10573	6.787E-04
ZMR035	Olivares	18.239	1.16E-02	15.634	9.17E-03	38.414	3.53E-02	0.857010	5.239E-04	2.10519	2.148E-03
ZMR045	La Concepción	18.716	3.82E-03	15.667	3.95E-03	38.850	1.46E-02	0.837120	1.716E-04	2.07589	7.345E-04
ZMR045*	La Concepción	18.709	1.86E-04	15.660	2.19E-04	38.833	6.55E-04	0.837003	5.920E-06	2.07563	2.345E-05
ZMR046	La Concepción	18.568	3.51E-03	15.666	3.99E-03	38.739	1.48E-02	0.843690	1.801E-04	2.08624	7.477E-04
ZMR046*	La Concepción	18.577	1.59E-04	15.663	1.77E-04	38.740	6.10E-04	0.843128	4.990E-06	2.08536	2.185E-05
ZMR047	La Concepción	18.645	5.60E-03	15.665	6.27E-03	38.789	2.30E-02	0.840172	2.809E-04	2.08038	1.182E-03
ZMR047*	La Concepción	18.643	1.89E-04	15.663	2.04E-04	38.786	6.44E-04	0.840153	5.295E-06	2.08043	2.255E-05
ZMR047(b)*	La Concepción	19.766	1.54E-04	15.771	1.59E-04	38.880	5.19E-04	0.797894	3.550E-06	1.96703	1.740E-05

Samples	Site	$^{206}Pb/^{204}Pb$	2σ (mean)	$^{207}Pb/^{204}Pb$	2σ (mean)	$^{208}Pb/^{204}Pb$	2σ (mean)	$^{207}Pb/^{206}Pb$	2σ (mean)	$^{208}Pb/^{206}Pb$	2σ (mean)
ZMR048	La Concepción	18.373	5.01E-03	15.662	5.97E-03	38.486	2.04E-02	0.852482	1.684E-04	2.09479	7.568E-04
ZMR052	Ethnographic Museum	18.427	3.73E-03	15.637	4.07E-03	38.435	1.50E-02	0.848563	1.820E-04	2.08573	7.604E-04
ZMR053	Ethnographic Museum	18.276	3.70E-03	15.640	4.33E-03	38.395	1.47E-02	0.855815	1.360E-04	2.10085	5.754E-04
ZMR053*	Ethnographic Museum	18.271	1.98E-04	15.637	2.22E-04	38.390	7.32E-04	0.855829	5.075E-06	2.10118	2.295E-05
ZMR055	Ethnographic Museum	18.405	3.46E-03	15.636	4.19E-03	38.402	1.48E-02	0.849541	1.478E-04	2.08645	6.479E-04
TOR002	Cuesta del Negrillo No. 11	18.241	3.13E-03	15.625	3.72E-03	38.382	1.27E-02	0.856551	1.233E-04	2.10415	5.318E-04
TOR010	Cuesta del Matadero	18.205	3.44E-03	15.617	4.30E-03	38.367	1.45E-02	0.857881	1.134E-04	2.10763	5.014E-04
TOR010*	Cuesta del Matadero	18.194	1.61E-04	15.606	2.04E-04	38.335	6.28E-04	0.857769	5.370E-06	2.10708	2.175E-05
TOR011	Cuesta del Matadero	18.204	3.59E-03	15.620	4.49E-03	38.377	1.61E-02	0.858010	1.509E-04	2.10811	6.608E-04
TOR011*	Cuesta del Matadero	18.194	1.60E-04	15.607	1.83E-04	38.341	6.45E-04	0.857799	4.505E-06	2.10730	2.105E-05
TOR012	Cuesta del Matadero	18.246	2.71E-03	15.630	3.36E-03	38.405	1.19E-02	0.856585	1.222E-04	2.10482	5.163E-04
BNV001	Casa del Tinte	18.462	3.44E-03	15.640	3.58E-03	38.446	1.54E-02	0.847155	2.407E-04	2.08245	9.867E-04
BNV002	Casa del Tinte	18.469	2.64E-03	15.647	2.99E-03	38.470	1.05E-02	0.847217	1.198E-04	2.08290	4.926E-04
BNV003	Casa del Tinte	18.313	6.38E-03	15.636	4.58E-03	38.357	2.29E-02	0.853799	4.163E-04	2.09453	1.724E-03
BNV003_1*	Casa del Tinte	18.315	1.41E-04	15.631	1.54E-04	38.319	4.96E-04	0.853452	3.935E-06	2.09225	1.690E-05
BNV003_2*	Casa del Tinte	18.312	1.22E-04	15.630	1.38E-04	38.316	4.18E-04	0.853525	3.930E-06	2.09235	1.620E-05
BNV004	Casa del Tinte	18.450	2.97E-03	15.636	2.90E-03	38.476	1.18E-02	0.847522	1.714E-04	2.08542	7.213E-04

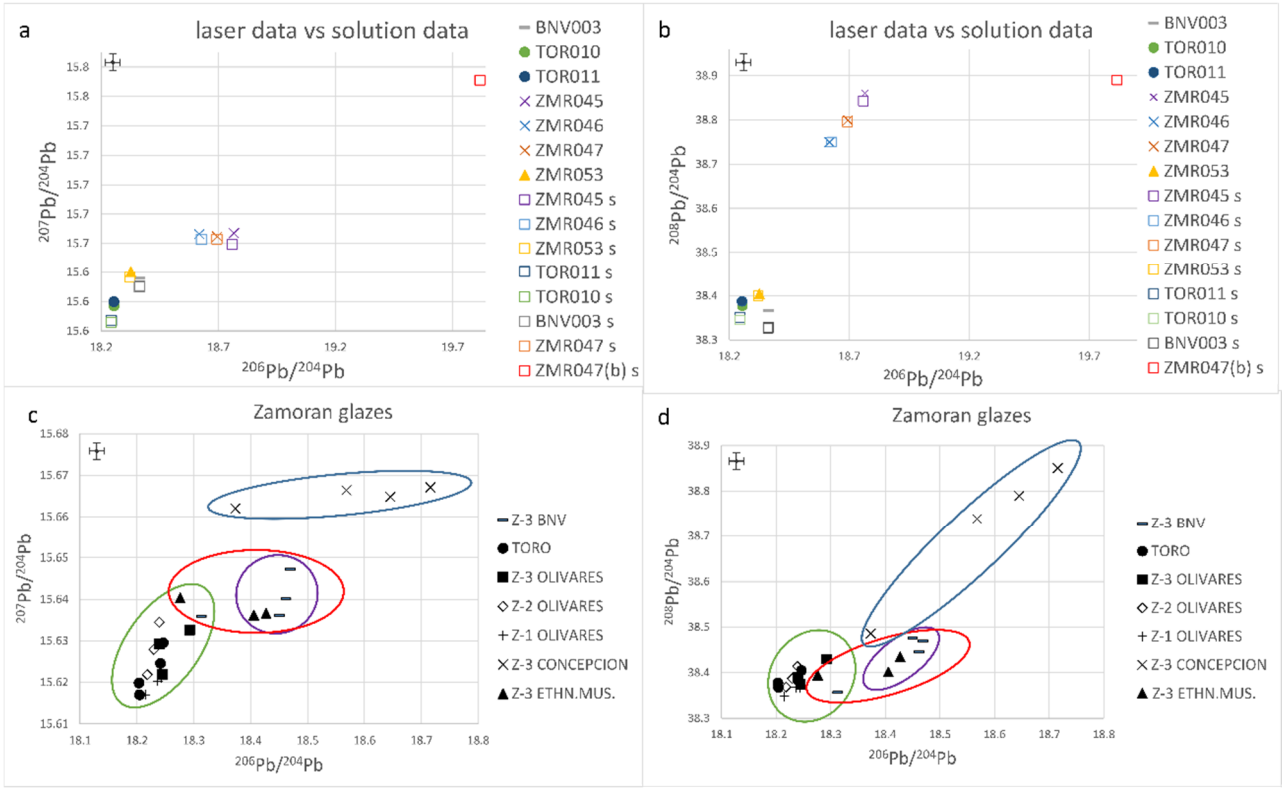

Figure 6.42. Averages of Pb isotope ratios of Zamoran glazes: **(a,b)** solution and laser ablation mode analyses. The sample names containing an "s" are those analyzed in solution mode. ZMR047(b) is the sample for which the blue colour was rastered; **(c,d)** data obtained by LA-MC-ICP-MS. Blue field: tin-lead glazed Z-3 La Concepción samples; green field: all translucent-glazed ceramics (Z-1, Z-2 and Toro) along with tin-lead glazed Z-3 Olivares samples; violet field: tin-lead glazed Z-3 Benavente and Z-3 Ethnographic Museum samples; red field: it covers the complete data field defined by results from Benavente and the Museum group of Z-3 samples. Measurement precision (2σ) is smaller than displayed symbols and represented by the average precision bars shown in the upper left corner of the diagram

Pb ore data of galenas from the Zamoran and surrounding areas

The obtained (solution mode) data for the galenas of more local and regional relevance are shown in Table 6.13. and Figure 6.43. Taken all local and regional data into account, data shows a very large spread with e.g. $^{206}Pb/^{204}Pb$ between 17.26 and 20.39; that is, a range that covers the glaze data. Yet, data are scarce and it is impossible to add contours for data fields that are believed to be significant for a local area.

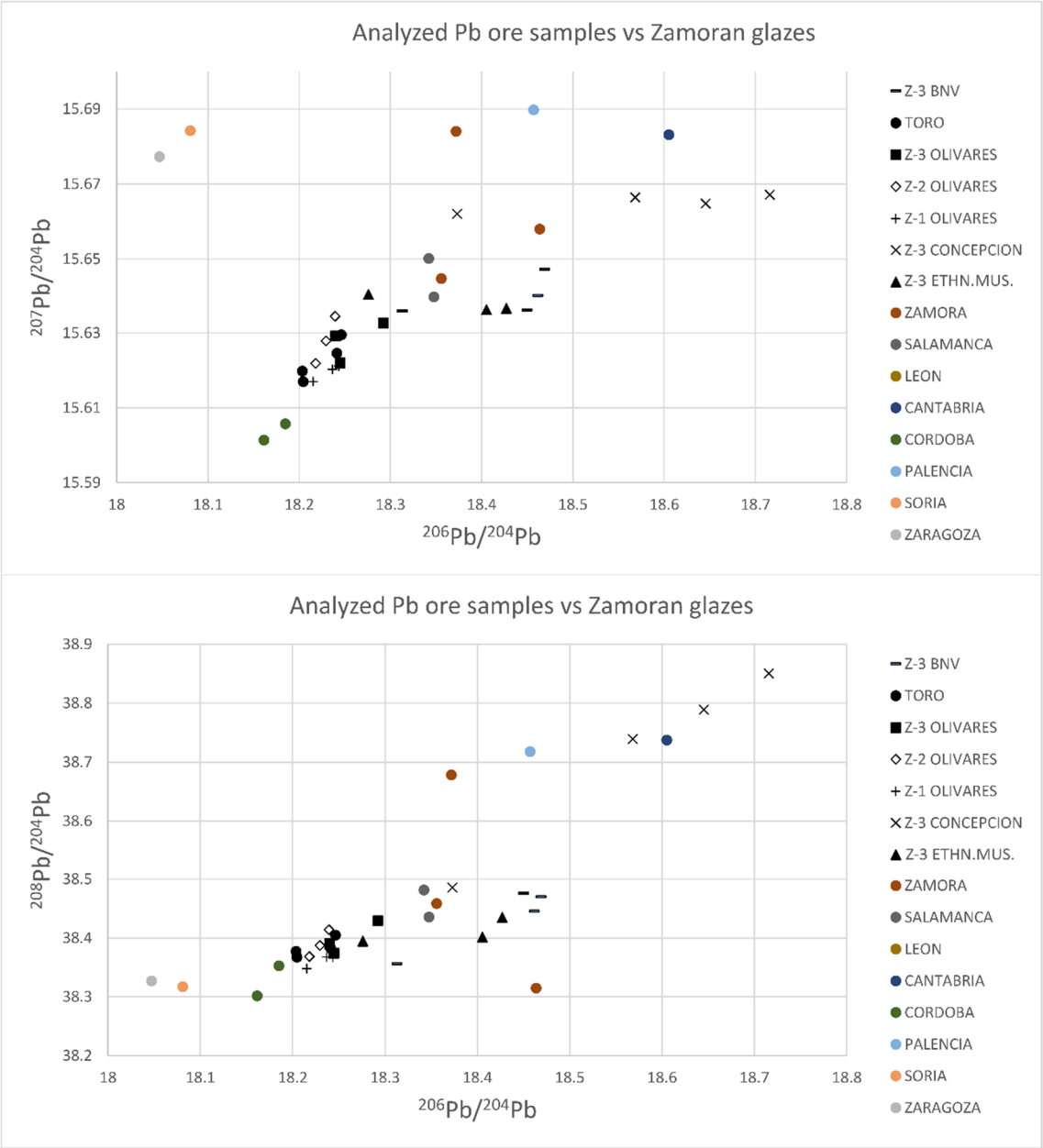

Figure 6.43. Isotope data of galenas of more local and regional relevance, obtained by solution MC-ICP-MS. For clarity, the extreme data points are not shown in this diagram. The reader is referred to Table 6.13. for this data

Table 6.13. Solution data for the galenas, with its precision (2σ), of more local/regional relevance

Samples	Mine	Village	Province	$^{206}Pb/^{204}Pb$	2σ (mean)	$^{207}Pb/^{204}Pb$	2σ (mean)	$^{208}Pb/^{204}Pb$	2σ (mean)	$^{207}Pb/^{206}Pb$	2σ (mean)	$^{208}Pb/^{206}Pb$	2σ (mean)
PbS001	Mina Manzanas	San Martín del Pedroso	Zamora	18.356	4.02E-03	15.645	4.64E-03	38.459	1.18E-02	0.852305	2.092E-04	2.09508	5.455E-04
PbS002	Mina de Velilla	Fontún de la Tercia	León	20.391	8.70E-03	15.784	5.80E-03	38.742	2.00E-02	0.774047	2.092E-04	1.89988	5.455E-04
PbS003	Mina San José	Novales	Cantabria	18.605	4.02E-03	15.683	4.64E-03	38.738	1.18E-02	0.842955	2.092E-04	2.08202	5.455E-04
PbS004	Mina Vieja	Santa Eufemia	Córdoba	18.161	4.02E-03	15.601	4.64E-03	38.302	1.18E-02	0.859045	2.092E-04	2.10887	5.455E-04
PbS005	Mina Valdetriollo	Triollo	Palencia	18.457	4.02E-03	15.690	4.64E-03	38.718	1.18E-02	0.850074	2.092E-04	2.09763	5.455E-04
PbS006	Mina Juan de Austria	Peñalcazar	Soria	18.081	4.40E-03	15.684	1.00E-02	38.317	3.10E-02	0.867453	3.700E-04	2.11915	1.200E-03
PbS007	Mina Valentín	San Tirso de Cabarcos	León	17.794	7.60E-03	15.596	1.10E-02	37.939	3.70E-02	0.876464	2.500E-04	2.13199	1.170E-03
PbS008	Mina La Pedraza	Bubierca	Zaragoza	18.047	4.02E-03	15.677	4.64E-03	38.327	1.18E-02	0.868686	2.092E-04	2.12363	5.455E-04
PbS011	Mina Los Santos	Los Santos	Salamanca	18.342	4.02E-03	15.650	4.64E-03	38.482	1.40E-02	0.853242	2.092E-04	2.09791	5.455E-04
PbS012	Mina Goviendes	La Tala	Salamanca	18.348	1.00E-02	15.640	1.78E-02	38.435	5.60E-02	0.852414	5.100E-04	2.09477	1.900E-03

Samples	Mine	Village	Province	$^{206}Pb/^{204}Pb$	2σ (mean)	$^{207}Pb/^{204}Pb$	2σ (mean)	$^{208}Pb/^{204}Pb$	2σ (mean)	$^{207}Pb/^{206}Pb$	2σ (mean)	$^{208}Pb/^{206}Pb$	2σ (mean)
PbS013	Mina Tertiñan	Latedo	Zamora	18.372	4.02E-03	15.684	4.64E-03	38.678	1.18E-02	0.853701	2.092E-04	2.10520	5.455E-04
PbS014	Mina San Blas	Nuez	Zamora	17.265	4.02E-03	15.535	4.64E-03	37.082	1.18E-02	0.899846	2.092E-04	2.14776	5.455E-04
PbS015	Mina Clara	Losacio	Zamora	18.464	4.02E-03	15.658	4.64E-03	38.315	1.18E-02	0.848048	2.092E-04	2.07508	5.455E-04
PbS018	Mina Los Eneros	Fuenteovejuna	Córdoba	18.185	4.02E-03	15.606	4.64E-03	38.353	1.18E-02	0.858173	2.092E-04	2.10898	5.455E-04
PbS022	Mina El Hoyo	Mestanza	Ciudad Real	20.388	9.10E-03	15.781	1.20E-02	38.736	3.90E-02	0.774010	2.092E-04	1.89985	1.000E-03

Elemental data of glazes

Table 6.14. lists concentration data for the analysed major elements in translucent-glazed parts and white coloured parts of tin-lead glazed ceramics. Reproducibility is usually in the range of ± 10 % and the absolute numbers must be considered with some caution, as the data is semi-quantitative. There are some unlikely values (exceeding 1.000.000 μg/g) obtained for the lead concentration, which may be caused by the extreme Pb concentrations in the glazes compared to the NIST glasses. Interestingly, concentrations of elements, including lead, may occasionally differ substantially between nearby spots representing a common colour. Thus, partial compositional heterogeneities are evident from these analyses. As seen in Figure 6.40., several inclusions (e.g. quartz and feldspars) can easily be identified within the glaze. In addition, as explained above, tin is connected to small cassiterite clusters and, therefore, the obtained tin concentrations may show a high spread even within the same sample depending on whether or not the analysed spot area overlaps with such clusters. Moreover, lead is one of the main components of the glaze and, therefore, shows high contents in all analysed ceramics, occasionally reaching above 90 % (Table 6.14.). The reason for this could be that a lead inclusion has been ablated (see Figure 6.40.).

Table 6.14. Elemental data (in μg/g) with its precision (2σ), for analysed glazes. Three analyses have been made in adjoining spots in translucent-glazed parts and white parts of tin-lead glazed ceramics. (<DL refers to values below the quantification limit)

Samples	Na	2 σ	Mg	2 σ	Al	2 σ	Si	2 σ	P	2 σ	K	2 σ	Ca	2 σ
ZMR002_1	2.06E+04	2.3E+03	3.39E+03	3.3E+02	1.47E+04	1.5E+03	2.99E+05	2.7E+04	2.12E+02	2.4E+01	2.19E+04	1.8E+03	1.00E+04	8.8E+02
ZMR002_2	1.16E+04	2.0E+03	2.79E+03	4.9E+02	9.70E+03	2.0E+03	1.83E+05	3.3E+04	4.60E+02	1.9E+02	1.36E+04	2.2E+03	8.20E+03	1.4E+03
ZMR002_3	1.46E+04	3.6E+03	1.96E+03	5.3E+02	8.80E+03	2.0E+03	1.87E+05	4.6E+04	2.20E+02	1.3E+02	1.49E+04	3.6E+03	6.40E+03	1.6E+03
ZMR012_1	2.06E+03	3.1E+02	4.70E+03	1.1E+03	2.58E+04	3.7E+03	1.94E+05	2.4E+04	3.22E+03	4.6E+02	4.95E+04	7.6E+03	2.30E+04	4.8E+03
ZMR012_2	2.12E+03	6.4E+02	3.47E+03	5.5E+02	2.82E+04	3.2E+03	2.07E+05	2.7E+04	3.12E+03	5.0E+02	5.36E+04	5.1E+03	2.11E+04	4.0E+03
ZMR012_3	3.07E+03	7.3E+02	6.70E+03	1.6E+03	4.82E+04	7.0E+03	2.50E+05	2.6E+04	4.40E+03	1.6E+03	6.69E+04	7.0E+03	3.30E+04	1.1E+04
ZMR046_1	9.20E+03	1.1E+03	1.94E+03	1.6E+02	1.29E+04	1.0E+03	3.63E+05	3.1E+04	1.37E+02	3.3E+01	9.90E+04	1.1E+04	1.27E+04	1.0E+03
ZMR046_2	9.20E+03	1.5E+03	2.67E+03	2.8E+02	1.41E+04	1.1E+03	3.65E+05	3.4E+04	9.80E+01	1.6E+01	1.08E+05	1.3E+04	1.74E+04	1.6E+03
ZMR046_3	8.75E+03	7.6E+02	3.06E+03	2.7E+02	1.38E+04	1.6E+03	3.50E+05	3.1E+04	1.76E+02	6.4E+01	9.38E+04	8.5E+03	1.84E+04	1.5E+03
ZMR048_1	9.80E+03	1.3E+03	2.05E+03	1.6E+02	3.34E+03	4.6E+02	1.98E+05	2.3E+04	1.28E+04	5.5E+03	1.67E+04	1.6E+03	3.30E+04	1.1E+04
ZMR048_2	9.97E+03	9.7E+02	1.98E+03	2.3E+02	3.99E+03	3.9E+02	1.96E+05	1.6E+04	8.40E+02	2.8E+02	1.74E+04	1.6E+03	1.29E+04	1.2E+03
ZMR048_3	1.20E+04	1.2E+03	1.65E+03	2.0E+02	3.77E+03	3.7E+02	2.40E+05	1.9E+04	4.90E+03	3.5E+03	2.24E+04	1.6E+03	1.49E+04	3.3E+03
ZMR052_1	5.62E+03	7.6E+02	4.23E+02	5.9E+01	8.56E+03	1.3E+03	1.15E+05	1.7E+04	<DL		6.44E+03	8.3E+02	2.74E+03	3.3E+02
ZMR052_2	3.92E+03	5.5E+02	4.92E+02	7.6E+01	4.35E+03	5.2E+02	8.06E+04	1.2E+04	1.32E+02	5.9E+01	4.00E+03	7.1E+02	1.94E+03	2.3E+02
ZMR052_3	8.58E+03	1.1E+03	5.58E+02	9.8E+01	9.36E+03	1.3E+03	1.62E+05	1.8E+04	2.39E+02	6.4E+01	1.03E+04	1.3E+03	3.73E+03	5.6E+02
TOR010 _1	1.06E+03	1.1E+02	2.12E+03	1.4E+02	6.27E+04	2.4E+03	3.11E+05	1.8E+04	2.62E+02	1.7E+01	6.30E+03	3.8E+02	3.14E+03	2.6E+02

Samples	Na	2 σ	Mg	2 σ	Al	2 σ	Si	2 σ	P	2 σ	K	2 σ	Ca	2 σ
TOR010 _2	1.22E+03	1.1E+02	2.35E+03	2.0E+02	6.85E+04	4.1E+03	3.26E+05	1.8E+04	2.76E+02	1.7E+01	6.33E+03	3.9E+02	3.86E+03	3.6E+02
TOR010 _3	1.23E+03	1.3E+02	2.17E+03	1.0E+02	6.56E+04	2.9E+03	3.60E+05	1.4E+04	3.12E+02	2.3E+01	6.27E+03	2.6E+02	3.77E+03	3.3E+02
BNV001_1	1.68E+04	1.4E+03	4.98E+02	4.2E+01	1.54E+04	1.3E+03	2.64E+05	1.7E+04	2.73E+03	1.7E+03	2.14E+04	1.5E+03	7.12E+03	2.1E+03
BNV001_2	1.24E+04	1.7E+03	1.11E+03	1.3E+02	1.61E+04	1.5E+03	2.83E+05	2.1E+04	1.20E+04	6.7E+03	1.89E+04	2.1E+03	2.03E+04	8.6E+03
BNV001_3	1.48E+04	2.0E+03	6.85E+02	9.1E+01	1.50E+04	1.2E+03	2.85E+05	2.1E+04	6.21E+03	2.6E+03	2.33E+04	1.4E+03	1.14E+04	2.7E+03
BNV002_1	9.85E+03	2.7E+03	1.24E+03	3.6E+02	1.23E+04	2.3E+03	3.21E+05	5.9E+04	1.17E+03	5.2E+02	3.18E+04	8.5E+03	1.56E+04	3.9E+03
BNV002_2	1.58E+04	2.0E+03	1.80E+03	1.8E+02	1.39E+04	5.0E+02	3.94E+05	2.7E+04	4.73E+02	1.2E+02	5.24E+04	7.4E+03	2.20E+04	2.4E+03
BNV002_3	1.42E+04	1.2E+03	1.33E+03	7.6E+01	1.36E+04	7.9E+02	3.62E+05	2.4E+04	1.62E+02	8.2E+01	4.65E+04	4.5E+03	1.77E+04	1.1E+03

(continues)

Samples	Mn	2 σ	Fe	2 σ	Co	2 σ	Ni	2 σ	Cu	2 σ	As	2 σ	Sn	2 σ	Pb	2 σ
ZMR002_1	4.91E+02	3.5E+01	4.61E+03	3.6E+02	1.07E+01	1.3E+00	2.78E+01	4.1E+00	1.80E+03	2.8E+02	3.65E+02	2.8E+01	8.37E+04	7.1E+03	6.98E+05	3.6E+04
ZMR002_2	3.54E+02	6.2E+01	2.55E+03	5.1E+02	6.40E+00	1.4E+00	1.63E+01	3.0E+00	9.40E+02	1.7E+02	1.61E+02	2.5E+01	6.91E+04	7.7E+03	4.11E+05	6.1E+04
ZMR002_3	4.50E+02	1.1E+02	2.51E+03	6.6E+02	5.90E+00	2.3E+00	1.61E+01	4.7E+00	8.10E+02	2.5E+02	2.02E+02	5.1E+01	6.60E+04	1.8E+04	4.10E+05	9.4E+04
ZMR012_1	3.55E+02	5.3E+01	1.34E+04	2.0E+03	6.00E+00	8.7E-01	2.34E+01	5.1E+00	2.23E+03	3.6E+02	5.70E+01	8.3E+00	1.72E+02	2.2E+01	3.94E+05	4.4E+04
ZMR012_2	4.70E+02	1.0E+02	2.03E+04	2.3E+03	6.10E+00	1.2E+00	1.68E+01	3.3E+00	1.08E+03	2.2E+02	5.71E+01	7.2E+00	1.87E+02	2.4E+01	4.09E+05	5.6E+04

Samples	**Mn**	**2 σ**	**Fe**	**2 σ**	**Co**	**2 σ**	**Ni**	**2 σ**	**Cu**	**2 σ**	**As**	**2 σ**	**Sn**	**2 σ**	**Pb**	**2 σ**
ZMR012_3	5.00E+02	1.0E+02	2.15E+04	1.8E+03	8.10E+00	1.6E+00	2.45E+01	7.1E+00	2.59E+03	4.1E+02	6.09E+01	6.7E+00	2.11E+02	2.5E+01	5.26E+05	4.2E+04
ZMR046_1	6.11E+01	6.5E+00	1.20E+03	3.8E+02	3.98E+01	6.5E+00	2.71E+01	6.1E+00	1.41E+03	2.4E+02	2.86E+01	5.4E+00	3.39E+04	4.2E+03	4.98E+05	4.4E+04
ZMR046_2	9.15E+01	9.8E+00	2.01E+03	3.5E+02	2.65E+01	3.6E+00	2.82E+01	4.9E+00	1.66E+03	2.3E+02	2.61E+01	2.5E+00	2.54E+04	3.3E+03	4.90E+05	3.5E+04
ZMR046_3	9.20E+01	1.1E+01	2.35E+03	4.1E+02	3.29E+01	5.7E+00	2.79E+01	3.5E+00	1.40E+03	2.0E+02	4.81E+01	4.2E+00	3.28E+04	4.9E+03	5.11E+05	4.4E+04
ZMR048_1	2.50E+02	2.8E+01	3.23E+03	6.5E+02	5.08E+00	5.3E-01	2.66E+01	3.6E+00	2.73E+03	3.0E+02	3.40E+01	1.3E+01	1.25E+05	3.9E+04	6.81E+05	4.2E+04
ZMR048_2	2.08E+03	3.1E+02	2.68E+03	4.0E+02	7.50E+00	1.0E+00	3.05E+01	4.2E+00	3.17E+03	3.0E+02	7.29E+00	8.8E-01	9.40E+04	2.8E+04	5.38E+05	3.3E+04
ZMR048_3	3.80E+03	5.1E+02	3.02E+03	7.3E+02	8.40E+00	1.8E+00	2.50E+01	4.4E+00	3.79E+03	5.4E+02	1.17E+01	3.9E+00	7.50E+04	2.1E+04	6.85E+05	4.7E+04
ZMR052_1	2.41E+01	2.6E+00	9.05E+02	9.8E+01	2.48E+00	3.5E-01	<DL		4.79E+02	7.9E+01	5.50E+01	1.1E+01	4.24E+04	5.3E+03	2.17E+05	2.1E+04
ZMR052_2	1.85E+01	2.6E+00	6.74E+02	1.2E+02	1.76E+00	3.6E-01	<DL		2.27E+02	3.3E+01	2.76E+01	5.6E+00	3.00E+04	4.4E+03	1.80E+05	2.6E+04
ZMR052_3	3.14E+01	4.8E+00	1.29E+03	2.1E+02	2.89E+00	6.1E-01	<DL		4.74E+02	8.0E+01	4.26E+01	7.9E+00	5.12E+04	7.0E+03	3.44E+05	3.9E+04
TOR010_1	1.38E+02	8.2E+00	2.33E+04	1.2E+03	7.11E+00	4.4E-01	<DL		1.47E+02	7.7E+00	4.24E+01	2.3E+00	1.07E+01	7.6E-01	7.97E+05	4.1E+04
TOR010_2	1.42E+02	1.1E+01	2.53E+04	2.1E+03	7.30E+00	5.5E-01	<DL		1.51E+02	1.1E+01	4.17E+01	2.9E+00	1.22E+01	1.0E+00	8.11E+05	5.6E+04

Samples	Mn	2 σ	Fe	2 σ	Co	2 σ	Ni	2 σ	Cu	2 σ	As	2 σ	Sn	2 σ	Pb	2 σ
TOR010_3	1.45E+02	9.4E+00	2.62E+04	2.1E+03	7.79E+00	5.9E-01	<DL		1.78E+02	1.0E+01	4.98E+01	1.8E+00	1.08E+01	1.1E+00	9.61E+05	5.6E+04
BNV001_1	2.97E+01	2.3E+00	1.71E+03	1.8E+02	3.09E+01	3.0E+00	4.48E+01	3.3E+00	1.21E+03	5.3E+01	1.22E+03	1.2E+02	8.64E+04	1.3E+04	7.29E+05	3.9E+04
BNV001_2	2.55E+01	5.6E+00	3.42E+03	5.2E+02	1.18E+01	2.4E+00	2.83E+01	4.8E+00	8.24E+02	1.0E+02	1.18E+03	3.9E+02	7.94E+04	1.2E+04	5.83E+05	4.7E+04
BNV001_3	3.14E+01	3.5E+00	1.76E+03	1.7E+02	1.88E+01	2.3E+00	3.00E+01	3.3E+00	9.68E+02	8.6E+01	1.18E+03	1.7E+02	8.56E+04	8.2E+03	6.48E+05	5.6E+04
BNV002_1	1.32E+02	2.7E+01	3.09E+03	7.1E+02	4.11E+00	8.8E-01	<DL		3.76E+02	1.3E+02	1.05E+01	1.8E+00	4.42E+04	1.3E+04	3.11E+05	7.9E+04
BNV002_2	1.80E+02	1.8E+01	5.15E+03	5.5E+02	6.29E+00	7.1E-01	3.41E+01	5.5E+00	7.14E+02	8.6E+01	1.23E+01	1.5E+00	8.94E+04	2.4E+04	5.17E+05	5.2E+04
BNV002_3	1.56E+02	1.1E+01	4.44E+03	2.6E+02	4.33E+00	3.3E-01	<DL		5.92E+02	4.8E+01	1.55E+01	1.2E+00	4.64E+04	1.1E+04	4.80E+05	3.8E+04

6.3.4. Discussion

The Pb isotope results for glazes of ceramics from the Zamora region show a significant compositional range, and three main data populations can be distinguished (Figure 6.42.). In the following sections, glaze data is aimed to match with reference data from ore districts known to have provided lead and other base metals. For isotopic provenance assignment, all available literature relevant to the different lead isotope fields have been used in the statistical study (see section 6.3.), although only the matching groups are depicted in the example diagrams. It is likely that the spread in data, with e.g. $^{206}Pb/^{204}Pb$ values between ca. 18.21 and 18.72, requires a supply of metals from several ore districts. Another important factor to consider concerns possible changes in trading routes over time.

Pb isotope matching: glazes vs galenas from sites across the Iberian Peninsula

A first isotopic comparison will focus on ore deposits from the Iberian Peninsula bearing in mind the important, ancient base metal mining activity in this large area. Figure 6.44. presents Pb isotope compositions of selected Iberian ore regions having isotope ratios that overlap with data of Zamoran glazes. The figure does not include galena data obtained in the present study involving mineralizations located at local or semi-regional sites in relation to the city of Zamora, because no good isotopic matches exist. However, only few data are available (Table 6.13.) so it is premature to reject the possibility that local ores were used by the artisans producing the ceramics. The lead isotope results of the glazes can be divided into three data populations.

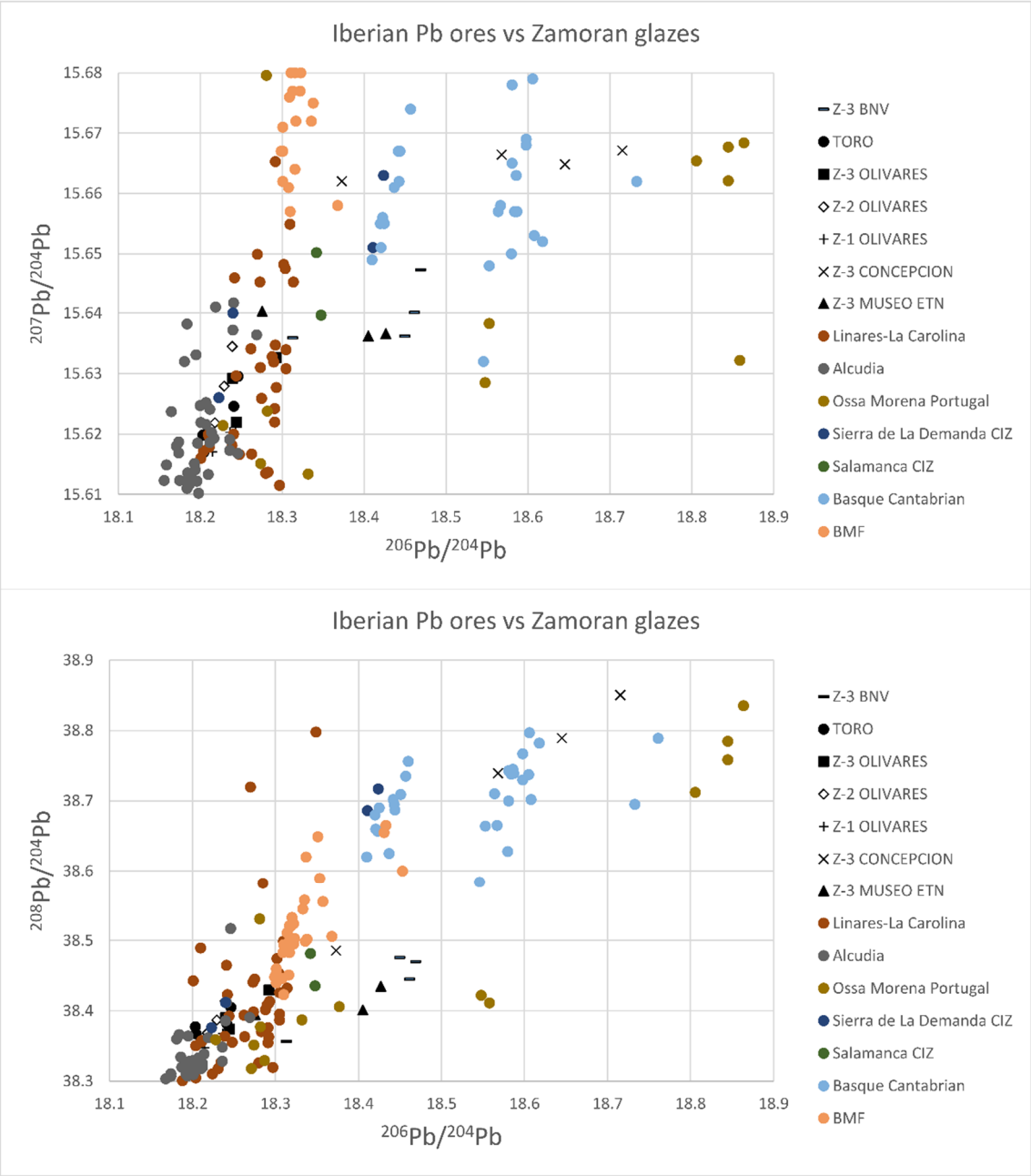

Figure 6.44. Pb isotope compositions of selected Iberian ore regions having isotope ratios that overlap with data of Zamoran glazes

Population 1: La Concepción (tin-lead glazes; 15th-16th centuries)

Data from La Concepción form a distinct pattern (Figure 6.42.; blue Z-3 population) characterized by a large compositional range with considerably higher $^{207}Pb/^{204}Pb$ and $^{208}Pb/^{204}Pb$ than other glazes. The linearity of this population is striking and is seen in both types of lead isotope diagrams. This linear trend can be explained in two ways; either there exists one or several ore districts that are

characterized by heterogeneous lead isotope compositions that encompass the range of glaze data, or the data range represents a mixture, involving different proportions of two end-member components. In the used diagram types, such mixing would lead to an alignment of data along a straight line; that is, a mixing line that connects the extreme ends of the data range. Regardless of the preferred explanation, any potential lead supplier(s) must be characterized by isotope data that match the blue-coloured linear population in Figure 6.42. The Basque-Cantabrian ore zone is of particular interest (Figure 6.44.), because galena data from this zone straddles the obtained glaze data. Regarding a mixing hypothesis involving two end-members, the elevated $^{208}Pb/^{204}Pb$ and $^{207}Pb/^{204}Pb$ values for the glazes suggest that Ossa-Morena could constitute a high-end (radiogenic) component, whereas the lower end (less radiogenic) component could be sought either in the Molar-Bellmunt-Falset area (MBF, in Tarragona, Catalonia) or in the region of Linares-La Carolina.

Population 2: a dominant group of less radiogenic tin-lead and translucent-glazes (17th-20th centuries)

A large population of less radiogenic data (green field in Figure 6.42.) comprises all translucent-glazed ceramics (Z-1, Z-2 and Toro) along with tin-lead glazed Z-3 Olivares samples. With respect to the data population involving artefacts from Benavente and the Ethnographic Museum, these data appear to define two fields; the majority of samples form a separate data field (population 3) and their significance is discussed separately. Two other samples from Benavente and the Ethnographic Museum (BNV003 and ZMR053) overlap with the main population 2. The reason for this differentiation cannot be linked to typological or chronological features, and perhaps the recognition of dual populations is due to a manufacturing process involving isotopically different raw materials.

The relatively narrow range of lead isotope compositions of the large data population, constrained by $^{206}Pb/^{204}Pb$ of less than 18.4, is consistent with all samples being prepared with lead from the same geological zone. Probable source candidate(s), showing a good overlap with population 2, are deposits at Linares-La Carolina and Alcudia. In addition, some of the deposits from Ossa-Morena (Portugal zone), Central Iberian Zone (Salamanca) and Sierra de La Demanda show data ranges in the same isotopic region. However, there are relatively few ore reference

data from the latter zones that match with this glaze data population. Keeping in mind that Alcudia was the major producer of *alcohol* in the Castilian Kingdom already in the 15th-16th centuries and that such production also took place at Linares-La Carolina, one or both of these geological zones may have delivered lead corresponding to population 2.

Population 3: tin-lead glazes from Benavente and the Ethnographic Museum (16th-18th centuries)

The dominant Z-3 data population from Benavente and the Ethnographic Museum with $^{206}Pb/^{204}Pb$ values in the range 18.4-18.5 (violet field in Figure 6.42.) does not match with any existing Spanish or Portuguese galena ore data. Additional data from the Iberian Peninsula may provide an isotopic overlap, but given that many of the most distinguished historical ore districts are covered by numerous lead isotope investigations, this option seems less feasible. Of considerable interest is that historical documentation refers to the possibility that lead and other metals occasionally were imported. Although the Castilian Kingdom was able to supply itself with lead for long periods of time, the downward trend in the total production of lead during the 16th century, in addition to the increase in military demand, made it necessary to rely on imports from northern Europe, specifically during the period 1566-1577 (Sánchez, 1989).

One of the most probable origins that can be thought of is England, because there is a good isotopic overlap between population 3 results and published data from e.g. Derbyshire and Cornwall (Figure 6.45.). Another circumstance in favour of a British origin for lead used for part of the ceramics found in Benavente and the Ethnographic Museum is that the population 3 data are similar to the lead isotopic compositions obtained from some Portuguese glazes from Coimbra and Lisbon (Iñañez, pers. comm. 2021). The documentation of the latter will be published elsewhere, but it is important to recall that there is a great historical documentation about the trade between Portugal and England (see for example Childs, 1992 and references therein). Hence, a logical suggestion is that the lead used for both population 3 ceramics (this study) and some specific ones in Portugal have a common origin and were derived from Britain (see for example Sebastian, 2010 pp.339).

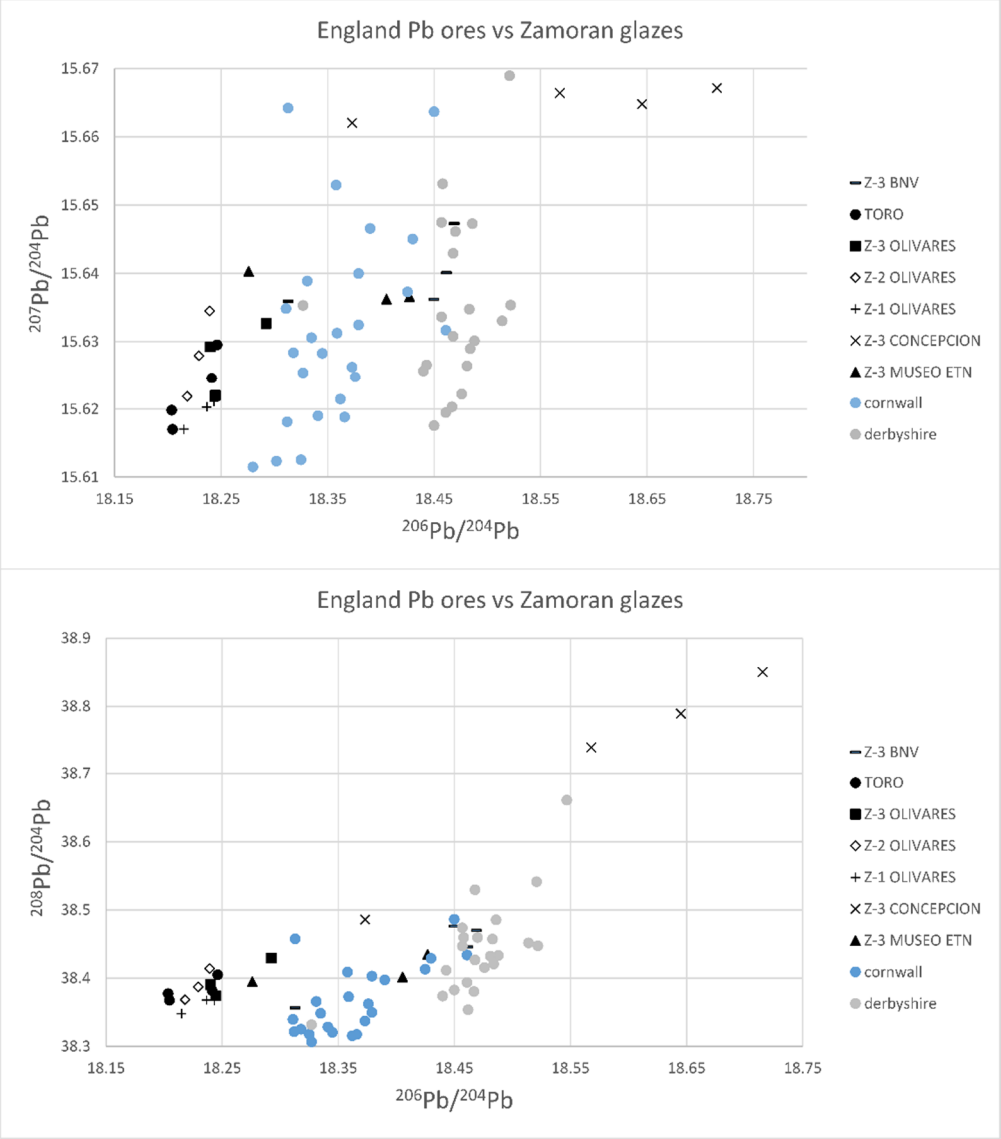

Figure 6.45. Cornwall and Derbyshire lead data matching the studied samples

Elemental data and tin issue

A number of 9 LA-ICP-MS elemental analyses have been carried out on translucent-glazed parts of ceramics and in white-coloured parts of tin-lead glazed ceramics (Table 6.14.). The concentration of lead shows large differences, both among samples from the same workshop and occasionally also among different parts of the same object (Pb from 1.8E+05 to 9.61E+05 μg/g). To some extent, this variation may be due to the nature of different mineral inclusions (e.g quartz and feldspars) that may have been hit by the laser beam. The observed variability in the

lead contents could be a result of a less effective mixing of the glaze ingredients, or it could be due to the effect of mixing raw material of different origin and metal grade. The latter explanation would imply that certain data patterns derived from lead isotope analyses are due to the effect of mixing isotopically contrasting raw materials.

As mentioned above, the distinction between tin-lead and translucent-glazes is clear based on the tin content. For the translucent-glazes, tin is almost inexistent (1.01E+02 μg/g), while white opaque glazes show an important amount of tin (6.44E+04 μg/g). As tin is necessary component in opaque white glazes, the question of where the tin component derived from is also important to consider and may help to further understanding of existing trading routes at the time. Given the extant historical knowledge regarding tin trade in Medieval and Post-Medieval periods in Europe, it is relevant noticing the existence of two important mining districts that supplied tin during this period: Erzgebirge (Germany) and Devon and Cornwall (England) (Gerrard, 2000; Taylor, 1983). Notably, performing an indirect approach, if Cornwall is a possible source of lead in some samples from Benavente and the Ethnographic Museum (population 3), it is reasonable to suggest that the tin component in these glazes originated from the same area. Moreover, Piccolpasso mentions on his treatise on pottery that Flanders tin was recommended for opacifying lead glazes, but it is important to note that the source of this tin was south-west England (Lhôte, 2007; McSweeney, 2011; Métreau et al., 2021).

Insights into trading routes transporting metals to northern Spain (Zamora region)

The chronology of the studied ceramics spans from the 15th to the early 20th centuries, and this long time interval implies that metals may have been transported along different routes. At present, there is no clear isotope evidence to suggest that lead from local ores played a significant role in the production of the studied ceramics; at least such deposits do not seem to have been the sole source of lead. However, the available data collected from local ores are still few (less than fifteen analyses dispersed among a number of mineralizations; Table 6.13.). As such, it is possible that several workshops relied on metal supply from local ores, however, further investigations are required before conclusions can be drawn.

The earliest documented ceramics are those found in La Concepción, which date back to the 15th-16th centuries. The Pb isotope data showed a unique pattern (blue field in Figure 6.42.) and one interpretation of the data range is that it represents a metal origin in the Basque-Cantabrian region. Little is known about the old mining in the Basque-Cantabrian region, although the large Reocín mine, located near Santander, was an important lead producer with mining documented in the late 19th century. However, Velasco et al., (2003) stated that other deposits in the region such as Udías, Novales, La Florida, Mercadal, Comillas, and Punta Calderón may have been mined much earlier. In addition, there is historical documentation about the trade between Zamora and Basque Country already from the 14th century. Several authors explain that micaceous ceramics from villages from Zamora were sent to the Basque workshops in order to be tin-lead glazed. The workshops from Zegama and Segura are one example, and so are the workshops from Elosu, Durango and Ametzaga (Ibabe, 1995a; Solaun, 2005; Villanueva, 2011). However, this type of trade also existed on a local scale inside Zamora; micaceous ceramics from Muelas del Pan were transported to the nearby Olivares workshops to become glazed (Moratinos and Villanueva, 2006; Villanueva, 2011).

The alternative explanation for La Concepción data is mixing, and the radiogenic end-member may correspond to ores in the Ossa Morena (Portugal), whereas the less radiogenic end-member could be sought either among the Molar-Bellmunt-Falset mines (Catalonia) or in the La Carolina-Linares (Andalucía) district. Although Pb-Ag veins were exploited already in Roman times, and some minor workings of Pb and Cu veins existed during the 16th century, little evidence for pre-18th century mining is known from the Ossa Morena Zone (Tornos et al., 2004). On the other hand, it is well known that mining was active in the famous and historic La Carolina-Linares district in Medieval times. Similarly, historical evidence supports that the Molar-Bellmunt-Falset area (e.g. Bellmunt de Ciurana near Tarragona; Catalonia) was active at approximately the same time period (ca. 15th century) (Abella i Creus et al., 2001). The latter had an abundant production and served, along with other production centres such as Jabalcol in Granada, not only to supply national consumption, but also to export excess product to North Africa (Vallvé, 1996). These authors also documented that galena was extracted in another mine near Tarragona (Bellmunt del Priorat) already in the middle of the 15th century (see Figure 6.41.). Nevertheless, a mixing scenario is considered less feasible for the

La Concepción data trend as it implies that artisans used a mix of raw material that was delivered more or less simultaneously from deposits being located at a considerable distance from each other. Thus, an explanation where the studied glazes contain a dominant lead type from the Basque-Cantabrian area is advocated.

Chronologically, the next group of shards is characterized by tin-lead glazes from the 16th-18th centuries (violet field, Figure 6.42.). Presently, no lead isotope match exists for this group, but an English origin is plausible. A shortage of lead and other metals existed at different times in Spain and Portugal, forcing an import of metals, not only during the 1566-1577 period (Sánchez, 1989). Another reason for more acute needs of lead was for making war ammunition, and e.g. Abella i Creus et al. (2001) described that the Bellmunt mines (west of Tarragona) were exploited intensively in 1838, during the first Carlist War (a civil war over the succession to the Spanish Throne, 1833-1840), sending the lead metal to the ammunition factories of Tarragona. Another argument for an English origin for lead used for part of the ceramics found in Benavente and the Ethnographic Museum is that the population 3 data are similar to the lead isotope compositions obtained from some Portuguese glazes from Coimbra and Lisbon (Iñañez, 2021, pers. comm.). As commented, there is extensive historical documentation about the trade between Portugal and England. As such, it is probable that the lead used for both population 3 ceramics and some specific ones in Portugal have a common origin; being mined in England and transported first to ports in Portugal (Lisbon and Aveiro; see for example Sebastian, 2010 pp.339) and traded into Zamora from Portugal. Alternatively, another possibility is that lead was exploited in Portuguese lead mines near Aveiro (NNW of Coimbra), in areas such as Vila Pouça de Aguiar and Braçal (indicated on Figure 6.41.; Martins, 2010; Wahl, 1998). Moreover, if an English origin is preferred, it is important to point out that the span of data from e.g. Cornwall (Figure 6.45.) actually overlaps with the total population of Benavente + Ethnographic Museum samples (red field, Figure 6.42.), implying that all these samples may contain lead originating from England.

The main group of samples (population 2) spans a period from approximately the 17th to the 20th centuries (green field, Figure 6.42.). There is a good isotopic overlap between population 2 samples and data from Linares-La Carolina and Alcudia supporting a lead supply from these areas. Moreover, the historical documentation reinforces that Linares-La Carolina and Alcudia zones featured

more or less continuous mining from Antiquity to the end of the 20th century (García and Martínez, 1992; Pérez and Carriazo 2010; Sánchez, 1989; Santos Zalduegui et al., 2004 and references therein) and were the most probable lead suppliers to workshops in, and nearby, Zamora. In addition, De La Mata (1989) suggested that for glazing the ceramics manufactured in Benavente, the potters used imported lead from Linares-La Carolina district in the 18-19th centuries, but he did not elaborate further. Sánchez (1989) stated that lead extraction was active, at least from the 12th century, in Linares and in Alcudia. Considering the significant production of *alcohol* in both regions and that *alcohol* was the term for galena used for the ceramics glazing (Sánchez, 1989), the potential importance of these regions as suppliers of lead to Zamora glazes becomes evident.

CHAPTER 7: CONCLUSIONS

The results obtained in the present Doctoral Thesis can be divided into two fields. On the one hand, there are results that carried an important progress on the methodology and the elucidation of current archaeometrical challenges, such as the post-depositional alteration processes in buried ceramics. These results derive from the archaeometrical approach carried out in manufactured ceramics buried in water environments at the laboratory, addressed in Chapter 5. Moreover, the optimization of calibration curves for the chemical analyses by ICP-MS and the thorough explanation about the importance of the estimation of the uncertainty of the results and, thus, of presenting these chemical results with their uncertainty (see both issues in Chapter 4, sections 4.4.1 and 4.4.3.) make a relevant contribution for obtaining accurate results. This contribution is not limited exclusively to the field of archaeometric analyses in ceramics. In fact, these considerations can be extended to other types of analyses involving compositional data. Moreover, this work has also been effective for confirming the usefulness of LA-MC-ICP-MS for lead provenancing of glazes. On the other hand, the results obtained from the study of pottery production centres of Zamora, Toro, Benavente and Aveiro entailed an important contribution to the archaeometric and archaeological knowledge about the ceramic productions of Zamora and Aveiro regions in Medieval and Post-Medieval periods, as is addressed in Chapter 6. Besides, lead isotope analyses in Zamoran glazes added deeper knowledge about lead mining and trade in Zamora region and surroundings.

Regarding the results that carried an important progress on the elucidation of current archaeometrical challenges, the aging experiment carried out in the laboratory has demonstrated that the modelling of experimental approaches can be very useful for the research of post-depositional alterations in ceramics. This fact was proven as well in previous experiences on this topic, mentioned in Chapter 1, section 1.3.2. The present experiment builds on previous research as cited in the literature and, with respect to the proposed objectives and the laboratory approach, it is the first experiment carried out in tap water and simulated seawater to model, simultaneously, alterations in archaeological calcareous, low-calcareous and micaceous ceramics. Additionally, it is important to emphasize that the aging study not only explains post-depositional alteration ways, but also it refers to several studies to explain firing alteration ways occurred in these samples. Regarding the specific results, on the one hand, it was observed that, in several and different types

of samples, the same type of aggregate was identified with different crystallization grades. In some cases, samples immersed for less time showed more aggregates, or better crystalized aggregates, than samples immersed for a longer time. This fact demonstrates that the crystallization grade, in many cases, is not related to the immersion period. Moreover, a great amount of NaCl aggregates was identified in PT (high-calcareous) samples and AP (micaceous) fired at 1100 °C and submerged in the marine environment, in comparison with ceramics fired at lower temperatures. However, this fact was expected to occur the other way round (that is, in samples fired at lower temperatures), since ceramics fired at lower temperatures are more porous. Besides, it was demonstrated that the same type of aggregates such as halite, calcium sulphate and the sponge-like aggregates containing mainly Ca and F, can be present in very different pastes. On the other hand, the presence of more NaCl cubes in the samples immersed in the marine environment was also expected; however, although they were identified, other aggregates, such as those containing mainly Ca and F, were found in higher amounts. Paying attention to the NaCl issue, interestingly, it seems that NaCl did not penetrate as much as expected, precipitating mainly on the surface. This fact is in accordance with Maritan (2020), who documented that the presence of halite has rarely been reported in similar works (Béarat et al. 1989; Montana et al. 2014b; Schwedt et al. 2006). In addition, concentrating on the occurrence of aggregates composed mainly of Ca and F, it is something that should be taken into account in the desalination protocols of the ceramics. According to the literature, desalinization protocols for ceramics routinely include the immersion of these artefacts in big pools with tap water for certain periods of time and/or after checking that the salinity of the water decays to tap water values (Zornoza-Indart, 2012). However, the tap water available in the majority of countries contains fluorine for public health reasons. Along these lines, fluorine can penetrate into the ceramic clayous structure and can replace OH^- groups, forming HF. Then, this compound can react with calcite, forming fluorite (CaF_2) and affecting the original elemental composition of the ceramics. This effect might be traceable with the presence of sponge-like structures formed by Ca and F, suggested to be cuspidine [$Ca_4Si_2O_7(F,OH)_2$] or normandite [$NaCa(Mn,Fe)(Ti,Nb,Zr)(Si_2O_7)OF$], due to the presence of Mn in the aggregate. Furthermore, it should be emphasized that, the proper identification of aggregates by SEM–EDS in ceramics depends on several factors. One of these factors is how the artefact has been cut (e.g., parallel or transversal to the wheel-thrown marks of the

ceramic pot) in addition to which part of the artefact is being analysed (e.g., handle, rim, bottom) and the direction or plane that the artefact is being observed by the microscope. Moreover, it is important to know which part of the artefact is being looked at (the inner or outer side), because secondary aggregates would not be evenly and homogeneously distributed. Finally, it is shown in this work that the repeatability was low for some elements of this experiment (e.g. Ni and Cu). This suggests that, although there is a certain degree of probability of identifying the same type of alterations in real case studies with very similar conditions to the experiment, these reaction paths are difficult to reproduce, even in controlled conditions. Therefore, it is important to highlight that many other factors may play a role when affecting real archaeological ceramics given their post-depositional context (e.g. water temperature, salinity, open sea or closed harbour with high organic matter amounts), ceramic nature (e.g., calcareous, low-calcareous or micaceous) and time of deposition. Hence this work serves as a valuable contribution towards the identification of post-depositional alterations in archaeological ceramics that have undergone a considerable amount of time in a seawater and tap water environment, piling up data on the extant literature. In addition, it provides curatorial and conservation stakeholders and researchers with an interesting piece of information regarding the effects on archaeological ceramics after using tap water with a certain amount of fluorine for desalinization purposes.

Moreover, within the progress made on methodology, first, the calibration curves have been optimized for the chemical analyses by ICP-MS. At first, calibration curves with 4 calibration solutions were used. Then, after several observations of the calibrations and the sample concentration, the optimization consisted on the change of using 12 different calibration solutions instead of 4. Therefore, external calibrations with wider concentration ranges were obtained, improving the curves. Secondly, it has been concluded that the estimation of the uncertainty is a must when comparing data in the same laboratory as well as between different laboratories, as every measurement is subject to some uncertainty. In this way, the results will be comparable to other results from the literature, since it sets the limits for considering a result as accurate (Nelms, 2005). Furthermore, once the sources of the uncertainty are evaluated and the uncertainty calculated, the pie chart shown in Figure 4.13. (chapter 4), could be useful for improving the analytical procedure after identifying the major contributors. It

demonstrates that the major contributors to the uncertainty are the uncertainty of the calibration and the uncertainty of the first reference concentration, suggesting that, in my particular case, the major source of uncertainty is in the calibration curves. The nearer the concentrations of the samples are to the centroid of the calibration curve, the lower should be the calibration uncertainty. This fact reinforces the initiative of optimizing the calibration curves in the present work. In fact, the uncertainty improves in most of the components (with the exception of CaO, Pb and Ni, in which it gets worse) when calibrations are made with 12 calibration solutions (see Table 6.1. and Table 6.5., chapter 6, the cases of Zamora and Aveiro, respectively). However, the calculation of the standard uncertainty of each input (the values shown in Table 4.11., chapter 4) can be an arduous work, which requires knowing the proper values and equations for its calculation. Despite this laborious calculation process, once the sources of the uncertainty are evaluated and the uncertainty properly calculated, the evaluation of the contribution of each input to the combined variance becomes pivotal for improving the analytical procedure, therefore, the effort is worth it. Finally, Pb isotope analyses were conducted on the lead-bearing glazes by LA-MC-ICP-MS complemented by solution MC-ICP-MS analyses of some selected samples to verify the laser ablation results. This showed that laser ablation raw data, corrected for mass bias only (Tl normalisation) was identical to the solution results, demonstrating that the LA-MC-ICP-MS approach on potentially non-homogeneous glaze materials gives reliable results (see Table 6.11 and Figure 6.42.).

When it comes to the general results obtained from the study of pottery production centres of Zamora region, these have been obtained by a systematic archaeometric characterization, carried out for the first time in Medieval and Post-Medieval ceramics in these regions. Regarding Zamoran ceramics, in conclusion, the results have permitted establishing 5 reference compositional groups (Z-1, Z-2, Z-3, B-1 and T-1) and one PCRU (Z-4).

Z-1 is a low-calcareous (CaO around 1 wt %) red production from the late 19th-early 20th centuries, with biscuit and translucent-glazed ceramics and firing temperatures ranging from 800 °C to 1050 °C. These ceramics were glazed using a mixture of Pb and Si, probably using a frit before, and the honey colour of the translucent-glaze coating was provided by the presence of Fe ions in the glaze mixture and oxidizing firing conditions. In addition, Z-2 is a micaceous low-

calcareous (CaO around 1 wt %) reddish production from the late 19th-early 20th centuries, with non-glazed and translucent-glazed ceramics and firing temperatures ranging from 800 °C to 1100 °C. The SEM-EDS results of Z-2 show that the glazes were glazed with a translucent honey-glaze, like their counterparts from Z-1 group. Z-3, on the contrary, is a high-calcareous (CaO around 13 wt %) production from the 15th-early 20th centuries, with biscuit and tin-lead glazed ceramics, with reddish, buff-coloured and beige pastes and firing temperatures ranging from 850 °C to 1000 °C. All of the Z-3 ceramics were glazed using the two-firing technique and using a mixture of Pb and Si (fritting them), and adding cassiterite (SnO_2) for obtaining opaque glazes. Additionally, although most of the pigments were applied over the glaze, blue pigments (ferrite spinels, such as nickel ferrites and cobalt ferrites) were applied under the glaze, at least in La Concepción ceramics. On the contrary, the brown and black pigments were probably obtained with Mn compounds, such as braunite, and green pigments with components containing Cu. Moreover, Z-4 is a micaceous low-calcareous (CaO around 4 wt %) grey and beige production from the 15th-16th centuries, with non-glazed ceramics and firing temperatures ranging from 850 °C to 900 °C. Then, B-1 is a low-calcareous (CaO around 2 wt %) production from the 16th-18th centuries, with non-glazed ceramics, red pastes and firing temperatures ranging from 800 °C to 1050 °C. Finally, T-1 is a low-calcareous red production from the 17th century, with unglazed and translucent-glazed ceramics and firing temperatures ranging from 800 °C to 900 °C. The SEM-EDS results of T-1 show that the ceramics were glazed with a translucent honey-glaze, like ceramics from Z-1 and Z-2 groups.

Among the 5 groups, Z-1, Z-3, T-1 and B-1 are from local origin. The local origin of the production of micaceous ceramics from Z-2 was not clear but the study of the chemical composition enables suggesting that ceramics from Z-1 and Z-2 (reddish low-calcareous and micaceous pastes, respectively) may have clays that share a similar geological origin, because they have more in common than Z-2 and Z-4, both micaceous (Figure 6.26.). This fact can lead to think that ceramics from Z-2 are also a production from Olivares and not from an exogenous workshop such as Pereruela or Muelas del Pan. Besides, Z-4 is ascribed to an exogenous origin, probably from Muelas del Pan, Moveros or Pereruela. Finally, the provenance of 7 ceramics (ZMR037, ZMR039, ZMR050, ZMR062, ZMR063, TOR009 and TOR013) remains undetermined.

Therefore, the present work demonstrates that the workshops remains of Olivares represent the only archaeological well-known evidence of pottery production in the city of Zamora, showing a chronology of activity from the late 15th century to the 1940s, thus, shedding light on the continuation of the pottery tradition since Medieval Era until Modern Era, in accordance with the suggestion of Martín et al. (1997). The authors suggested a continuity of the ceramic manufacturing over a long period in the workshops of Olivares, approximately between the late 15th and the first half of the 20th centuries. Eventually, as ocurred for many other traditional activities, the end of the pottery making activity in the city is in direct relationship with the industrialization blossom, beginning in the last decades of the 19th century, which propitiated the depopulation from the rural areas of Zamora region towards the more industrialized capitals of northern and central Spain. In addition, the clays exploited during the last decades of activity by the potters from Olivares might be the same or, at least, of a very similar geological origin than the ones employed in precedent centuries. This fact suggests a continuation of the exploitation of the clays located nearby the riverbank in the Olivares quarter. When it comes to the ceramics unearthed at La Concepción (15th-16th centuries), the consumption of pottery by the people who inhabited and worked in the goldsmithing workshop during the 15th and early 16th centuries show mainly a local pattern. In this way, the use of local Zamoran ceramics (tin-lead glazed produced in Olivares, from Z-3), as well as micaceous ceramics from regional contexts (corresponding to Z-4), is predominant in this site. However, two micaceous ceramics (ZMR037 and ZMR039) and one ceramic archaeologically described as *Duque de la Victoria* type (ZMR050, ascribed probably to Valladolid), unearthed at La Concepción, demonstrate that in the 15th-16th centuries Zamora city kept a regional trade with Valladolid and villages producing micaceous ceramics in Zamora region. Regarding the ceramics unearthed at the Ethnographic Museum (16th-18th centuries), it is important to remember that these ceramics correspond to the period that the Royal Prison was active (1583-18th century). During the Modern Era, in the Royal Prisons of the Kingdom of Castile, the families of the prisoners were the ones in charge of supplying their needs, so the belongings of the prisoners depended on how wealthy their families were (De Las Heras, 1991). So, based on the fact that the ceramics from this site belong stratigraphically to the Royal Prison period, it is apparent that the Royal Prison of Zamora had a high diversity among prisoners or between the prison garrison and the inmates, in terms of their economic and social status. Thus, some

prisoners were much wealthier than others, and the decorated tin-lead glazed pottery analysed in this study may had belonged to some of the most accommodated inmates. In addition, ceramics from Toro (17th century) demonstrated that Toro had a local production for the local consumption, but the village also consumed ceramics from exogenous provenance, as it is suggested by the two unggrouped ceramics unearthed at Toro (TOR009 and TOR013). Besides, regarding ceramics unearthed at Benavente (16th-18th centuries), they demonstrate that Benavente also had its own low-calcareous reddish production but it also carried tin-lead glazed tableware produced in Olivares. Along these lines, in light of the archaeometric results, most of the ceramics produced in Olivares, translucent-glazed and tin-lead glazed ones, were consumed in the city and in a regional scale (like in Benavente). Besides, local production from Zamora region, including productions from Benavente and Toro, clearly predominates in such cities' consumption pattern.

Regarding the work about lead isotope analyses conducted in Zamoran glazes, the studied ceramics can be grouped both with respect to the character of the clay paste used and their chronology (spanning between late 15th-early 20th centuries). The studied glazes carry isotopically different types of lead, forming three main data populations. Although it is difficult to draw definite conclusions regarding the sources of lead, at least three lead districts have played a role in Zamoran glazed ceramic productions. Most evidences suggest that the oldest tin-lead glazed ceramics (recovered at La Concepción, 15th-16th centuries) contain lead from Basque-Cantabrian ores that are geographically located relatively close to Zamora. Yet, a mixed origin involving lead from Ossa Morena (Portugal) and Molar-Bellmunt-Falset area (Catalonia) or the Linares-La Carolina district (Andalucía) cannot be excluded. Considering a later stage of Zamoran ceramic production (tin-lead glazed ceramics from Benavente and those recovered at the Ethnographic Museum, 16th-18th centuries), the lead component was probably intermittently supplied from England (e.g. Derbyshire and Cornwall), during a period characterized by a shortage of lead in Spain and Portugal. At times, lead was needed for making war ammunition and it is possible that metal was re-used by melting of lead pipes and household objects, among other lead items (Sánchez, 1989). Finally, tin-lead glazes and translucent-glazes from the 17th-early 20th centuries (from Toro, Olivares, one from Benavente and one recovered at the Ethnographic Museum), were

probably made with lead from the Linares-La Carolina and Alcudia areas. These areas have a long tradition of continuous lead mining since Antiquity, and are known for their large production of *alcohol*, that is, the ancient name given to galena used for manufacturing the glazes. In addition, tin deposits are numerous in Spain and Portugal, but only meagre evidence exists to support early mining. Considering that the lead metal is believed to have been imported from Cornwall during certain periods, it is plausible there was an associated import of tin from this area.

Therefore, the lead isotope evidence suggests that trading routes have changed over time. Considering the known chronology of the studied ceramics, it seems that domestic resources of lead were used whenever available, whereas during periods of shortage the Castilian Kingdom relied on import from northern Europe. Along these lines, a relationship between Zamora and Aveiro can be drawn in terms of lead supply. Therefore, evidences of English lead found in Zamoran glazes suggest a trading route between near Portugal markets and Zamora, likely through the important trade-port of Aveiro. There are also indications that the oldest set of ceramics (15th-16th centuries) contains lead from nearby regional ores (Basque Country-Cantabria) and that long-distance transport ways from the southern and south-eastern parts of Spain became more important later on (Linares-La Carolina, and Alcudia).

When it comes to the general results obtained from the study of pottery production centres of Aveiro region, this study provides a deeper understanding of pottery production and trade in Aveiro during the Post-Medieval period after the archaeometric characterization performed on 30 ceramics (unglazed red and black low-calcareous, translucent yellow-glazed and tin lead-glazed) unearthed at the RAVA and Angra D shipwrecks, the Santo António church and wasters. Thus, chemical analyses allowed stablishing the provenance of 27 unglazed ceramics as belonging to A-1 local reference group, which is related to the local pottery production of Aveiro during the 16th to the beginning of the 17th centuries. These results are in accordance with the study carried out by Alves et al. (1998). However, three ceramics probably are of exogenous provenance: the black ware could be from a different production type of Aveiro, or it might have been produced in the Vila Real district of Portugal; the translucent-yellow-glazed ceramic probably was produced in Coimbra and the tin-lead glazed ceramic probably in Lisbon. These

facts can suggest that these type of ceramics were transported to Aveiro in order to be sold there to local people or foreigners (because Aveiro was an important port due to the salt commerce).

As far as the manufacture technology is concerned, two main paste colours are distinguished among the ceramics from A-1 reference group: low-calcareous red and black, fired at temperatures ranging from 800 °C to 950 °C. Considering that all ceramics are formed with the same clays, the difference in the colour suggests that there is no specialization of raw materials procurement concerning the paste. Instead, in the first place, potters played with the temperature and the atmosphere of the kiln to obtain the colour of the paste they desired and, in the second place, they played with the different finishing of the ceramics. Thus, probably, they applied reducing conditions and high firing temperatures (850-950 °C) for AVR002, AVR003 and AVR015 ceramics and this fact would be explained by the appearance of hercynite -after the reduction of hematite- in all of these ceramics. Echallier (1984) states that black pastes should therefore not be considered a priori as an indubitable index of technological poverty, but, on the contrary, as a conscious mastery of a simple and effective technique. However, two ceramics, which form the F-V fabric (AVR005 and AVR016), present a different case study; probably, they were red ceramics in origin, however, the reducing firing conditions of the fire of the ship turned their surfaces to black. On the other hand, with respect to the shiny finishing of the ceramics, the potters probably burnished the shiny black shards of F-V fabric (AVR003, AVR005, AVR015 and AVR016), evidencing the burnishing technique in ceramics with red and black pastes (Fernandes, 2012). However, AVR002 from F-IV draws the attention because of its black matte surface. In order to obtain the metallic black finishing the potters used the technique of burnishing, as it produces an even and compact surface, which causes specular reflection and gives to the ceramics a shiny surface (Ionescu et al., 2014). Therefore, the reasons for this difference could be that, maybe they did not give this finishing to AVR002 or that, AVR002 could have been smoothed instead of burnished because, according to the literature, smoothing makes ceramics appear matte.

Besides, SEM-EDS analyses have also facilitated the identification of the nature of a glassy-layer mainly of vacuolar aspect. One of the reasons for the formation of that layer is that iron compounds may act as a flux when they are exposed to a reducing atmosphere at high temperatures (Rice, 2015). In this case, the

vacuoles could have been formed because of the gases (such as the carbon dioxide) formed during the original firing of high temperature or due to the fire produced in the ship. Therefore, the thickness of the glassy-layer would depend on the contact between the fire and the shards. On the other hand, the glassy-layer could have also been produced because of the reaction between the salt (NaCl) and the water. If the salt (that was transported in the ship) reacted with seawater (thanks to the high temperature of the fire), HCl and sodium oxide would be formed according to the reaction of Rice (1987). Then, sodium oxide could have reacted with the silica of the ceramics, lowering its melting point, and giving as a product a glassy-layer. The vacuoles could be the product of the evaporation of HCl. Therefore, in this case, the thickness of the glassy-layer would depend on the amount of salt that reacted with the ceramics. The clear example would be the AVR005 ceramic, which has two ceramics stuck together: they were fused and melted together during the process. Furthermore, it is probable that the layers of the rest of the ceramics from F-V were also formed due to this reaction, as the higher concentration of Na in the surface of F-V ceramics suggested, probably due to the formation of Na_2O in the surface.

Moreover, the fire produced in the ship possibly did not act with the same intensity on all the shards, so some black spots may have appeared because the fire impacted directly on them (like in the case of AVR001, AVR012 or AVR013). Maybe, as with AVR005 and AVR016 happened, AVR002 was also burnt by the fire developed in the ship. Additionally, the beige surface of AVR003 could have been reoxidized during this process (Gillies and Urch, 1983).

Finally, the present work reinforces the idea that local production from Aveiro, included in A-1 compositional group, clearly predominates in the city production pattern and was also a valuable object in the Atlantic trade. The fact that the ceramics from RAVA show a chemical fingerprint compatible with ceramics from the church, reinforces the conclusion of the study carried out by Carvalho and Bettencourt (2012); that ceramics from RAVA were from a latter period than it was thought, despite the ship being dated to the mid-15th century (Alves et al., 2001). Besides, two ceramics produced in Aveiro were found in Angra D, the ship that was returning from the Americas. Probably, these ceramics were used daily on board. The presence of everyday use Aveiro ceramics is also documented elsewhere, like in the Caribbean, as demonstrated by the study of the Tortugas shipwreck ceramic assemblage and other colonial sites (Deagan, 1987; Stemm et al., 2013), in the United

Kingdom (Casimiro, 2014; Gutiérrez, 2007), África (Casimiro, 2018, 2020), Brazil (Orser, 2002), Madeira (Sousa, 2006) or even in Newfoundland (Newstead, 2008).

Moreover -and linking the aging laboratory experiment with the Aveiro and Zamora case studies-, the results of the laboratory experiment in addition to the experiments cited in Chapter 1, section 1.3.2, have been relevant and very useful for the proper identification of the chemical variability and secondary phases present in the case studies. For instance, in ceramics recovered in RAVA, the presence of some secondary phases, such as pyrite or jarosite and evidences of potassium halite, have been identified, all related to alterations and contaminations of the ceramics in the post-depositional scenery (López-Arce et al., 2013; Secco et al., 2011). Furthermore, the elemental characterization of Ethnographic Museum ceramics from Z-3 shows high concentrations in P_2O_5, accompanied by calcium, both in the ceramic paste and in the glaze. One of the hypotheses is that this could occur due to the post-depositional contamination, subjected to the existence of phosphorous compounds in soil waters. These soil waters could penetrate into the ceramic glaze and clay in more than one way: (i) spreading through the glaze and forming Liesegang rings-like degradation and (ii) taking advantage of one crack to penetrate into the ceramic body (Calparsoro, 2019). The concentration of this element in the ceramic pastes might vary depending on the exact burial location of the ceramics (Freestone et al., 1985). Besides, in La Concepción glazes, a K- and P-enriched layer related to the Co-Fe-Ni particulates of the blue pigment has been also detected as an interphase, between the paste and the glaze, probably, related to the reaction between lead-rich glazes and potassium-rich ceramic bodies at high temperatures (for the case of potassium) and some post-depositional contaminations (for the case of phosphorous). Finally, cerussite ($PbCO_3$) and a lead-tin yellow type II ($PbSn_{1-x}Si_xO_3$) have been identified in two different glazes (one compound in one glaze and the other compound in the other glaze) from the Ethnographic Museum ceramics. These compounds, probably, have been a subproduct of the primary lead oxide after the alteration processes.

Finally, as attributed to Isaac Newton when he said that he was standing on the shoulder of giants, this Doctoral Thesis has been possible thanks to all the advances made by many other researchers working on all the issues related to Archaeometry. In this regards, I have provided a deeper insight in some different aspects of the field, as developed above. Therefore, this work is a valid contribution

to the interdisciplinary methodology in Archaeology as well as to the knowledge about the human cultural history. Besides, it represents a further example of the value of Archaeometry to address both simple and complex archaeological questions.

Bibliografia / Bibliography

Ábalos, B., 2016. Geologic map of the Basque-Cantabrian Basin and a new tectonic interpretation of the Basque Arc. Int J Earth Sci (Geol Rundsch). 105, 2327–2354. https://doi.org/10.1007/s00531-016-1291-6

Abella i Creus, J., Curto, C., Fabre, J., 2001. Bellmunt del Priorato. Un yacimiento histórico en Cataluña. Bocamina. 7, 28-63.

Abubakar, M., Muthuraja, A., Rajak, D.K., Ahmad, N., Pruncu, C.I., Lamberti, L., Kumar, A., 2020. Influence of Firing Temperature on the Physical, Thermal and Microstructural Properties of Kankara Kaolin Clay: A Preliminary Investigation. Materials. 13, 1872, doi:10.3390/ma13081872.

Aitchison, J., 1982. The statistical analysis of compositional data. J. R. Stat. Soc. Ser. B Methodol. 44, 2, 139-177.

Aitchison, J., 2008. The single principle of compositional data analysis, continuing fallacies, confusions and misunderstandings and some suggested remedies, in: CoDaWork, Girona. pp. 1-28.

Albarède, F., Desaulty, A. M., Blichert-Toft, J., 2012. A geological perspective on the use of Pb isotopes in archaeometry. Archaeometry. 54, 853–67.

Alfonso, P., Canet, C., Melgarejo, J.C., Mata-Perelló, J.M., Fallick, A.E., 2012. Stable isotope geochemistry of the Ulldemolins Pb-Zn-Cu deposit (SW Catalonian Coastal Ranges, Spain). Geologica Acta, Vol.10, Nº2, June 2012, 145-157. DOI: 10.1344/105.000001707

Allan, J.W., 1973. Abu'l-Qasim's treatise on ceramics. Journal of Persian Studies. 11, 111-120. DOI: 10.2307/4300488

Aloupi-Siotis, E., 2020. Ceramic technology. How to characterise black Fe-based glass-ceramic coatings. Archaeol Anthropol Sci. https://doi.org/10.1007/s12520-020-01134-x

Alves, F., Castro, F., Labrincha, J., 1998. Physical and chemical characterisation of archaeological ceramics found in a mid-15th century shipwreck in Ria de Aveiro, in Conference on Materials in Oceanic Environment (Euromat'98), Lisbon. 2, 223-232

Alves, F., Rodrigues, P., Aleluia, M., Rodrigo, R., Garcia, C., Rieth, E., Riccardi, E., 2001. Ria de aveiro A: A shipwreck from Portugal dating to the mid15th century; a preliminary report. The International Journal of Nautical Archaeology. 30, 1, 12-36. doi: 10.1111/j.1095-9270.2001.tb01353.x.

Amadori, M.L., Fabbri, B., Gualtieri, S., 1998. Alteration forms in majolica tiles from the church of Plattelletti in Fano (Central Italy), in: Metodi Chimici, Fisici e Biologici per la Salvaguardia dei Beni Culturali; Publisher: Abaco Edizioni. Rome, Italy.

Amorim, I., 2011. Sea Salt and Land Salt. The language of salt and technology transfer (Portugal since the Second Half of the 18th century), in: Marius Alexianu, Oliver Weller and Roxana-Gabriela Curcâ (Eds.), Archaeology and Anthropology of Salt: A Diachronic Approach. Proceedings of the International Colloquium, Cuza University. BAR S2198, 187-192.

Amorim, I., 2019. O comércio do sal de Aveiro na configuração de relações transfronteiriças do noroeste peninsular Ibérico (1692-1714), in: Manuel-Reyes García Hurtado (Eds.) Soltando amarras. La costa noratlántica ibérica en la Edad Moderna. A Coruña, Universidade da Coruña, 73- 101.

Amosova, A.A., Panteeva, S.V., Chubarov, V.M., Finkelshtein, A.L., 2016. Determination of major elements by wavelength-dispersive X-ray fluorescence spectrometry and trace elements by inductively coupled plasma mass spectrometry in igneous rocks from the same fused sample (110 mg). Spectrochimica Acta Part B, 122, 2016, 62–68. doi: 10.1016/j.sab.2016.06.001.

Annamalai, K., Puri, I., 2006. Combustion Science and Engineering. CRC Press, Boca Raton.

Antunes, C., 2008a. The commercial relationship between Amsterdam and the Portuguese Salt-Exporting Ports: Aveiro and Setúbal, 1580-1715, in: A articulação do sal português aos circuitos mundiais: antigos e novos consumos. Porto: Instituto de História Moderna - Universidade do Porto, 161-181.

Antunes, C., 2008b. The Commercial Relationship between Amsterdam and the Portuguese Salt-Exporting Ports: Aveiro and Setubal, 1580-1715. Journal of Early Modern History. 12, 25-53. 10.1163/138537808X297144.

Aras, A., 2004. The change of phase composition in kaolinite- and illite-rich clay-based ceramic bodies. Appl. Clay Sci. 24, 257–269, doi:10.1016/j.clay.2003.08.012.

Arcifa, L., Bagnera, A., 2018. Palermo in the Ninth and Early Tenth Century: Ceramics as Archaeological Markers of Cultural Dynamics, in: Anderson, G.D., Fenwick, C., Rosser-Owen, M. (Eds), The Aghlabids and their Neighbors: Art and Material Culture

in Ninth-Century North Africa. Series: Handbook of Oriental Studies. Section 1 The Near and Middle East. Vol. 122, p. 382–404.

Arnau, B.E., 1997. Noticia de la actuación arqueológica en el solar de la que fue "Casa del Tinte" de Benavente. Brigecio, estudios de Benavente y sus tierras. Centro de estudios benaventanos "Ledo del pozo". 7, 91-106.

Arribas, A.J., Tosdal, R.M., 1994. Isotopic Composition of Pb in Ore Deposits of the Betic Cordillera, Spain: Origin and Relationship to Other European Deposits. Economic Geology. 89, 1074-1093.

Artoli, G.,Canovaro, C., Nimis, P., Angelini, I., 2020. LIA of prehistoric metals in the central mediterranean area: a review. Archaeometry. 62, Suppl.1, 53-85. DOI: 10.1111/arcm.12542.

Astarloa, E., Aranburu, I., Arrate, B., Laskibar, N., Baztarrika, P., Gomez, B. Zeramika Hiztegia. Eusko Jarurlaritzaren Argitalpen Zerbitzu Nagusia, Vitoria-Gasteiz, 2016. ISBN 978-84-457-3400-1.

Babrauskas, V., and Williamson R.B., 1978. Post-Flashover Compartment Fires. Fire and Materials. 2, 39–53.

Barbosa, T., Casimiro, T.M., Manaia, R., 2009. A late medieval household pottery group from Aveiro, Portugal. Medieval Ceramics, 30, 119-136.

Béarat, H., Dufournier, D., Nguyen, Y., Raveau, B., 1989. Influence de NaCl sur la couleur et la composition chimique de pâtes céramiques calcaires au cours de leurs caisson. Revue d'Archéométrie. 13, 43–53.

Béarat, H., Dufournier, D., Nouet, Y., 1992. Alterations of ceramics due to contact with seawater. Archaeologia Polona. 30, 151-162.

Beauvoit, E., Ben Amara, A., Tessier-Doyen, N., Frugier, C., Lemasson, Q., Moignard, B., Pacheco, C., Pichon, L., Chapoulie, R., Gratuze, B., 2021. Chemical and Mechanical Characterisation of White Earthenware Glazes from the Johnston-Vieillard Manufactory (France, 19th Century). Archaeometry. 63: 941– 959. https://doi.org/10.1111/arcm.12656.

Bell, S., 2001. The Beginner's Guide to Uncertainty of Measurement. Good Practice Guide Nº 11 (Issue 2). National Physical Laboratory (NPL)

Belfiore, C.M., La Russa, M.F., Randazzo, L., Montana, G., Pezzino, A., Ruffolo, S.A., Aloise, P., 2014. Laboratory tests ad-dressed to realize customized restoration procedures of underwater archaeological ceramic finds. Appl Phys A. 114, 741-752. DOI: 10.1007/s00339-013-7878-x.

Ben Amara, A., Schvoerer, M., Daoulatli, A., Rammah, M., 2011. "Jaune de Raqqada" et autres couleurs de céramiques glaçurées aghlabides de Tunisie (IXe-Xe siècles). Revue d'Archéometrie. 25, 179–186.

Berducou, M. C.,1990. La céramique archéologique, in: Berdocou, M. C. (coord.) La conservation en archéologie, pp. 78-119. Ed. Masson, París.

Berg, I., 2008. Looking through pots: recent advances in ceramics X-radiography. Journal of Archaeological Science. 35, 5, 1177–88.

Bettencourt, J., 2009. Arqueologia marítima da Ria de Aveiro: uma revisão dos dados disponíveis, in: Octávio Lixa Filgueiras. Arquitecto de Culturas Marítimas. Lisboa, Âncora Editora, 137-160.

Bettencourt, J. and Carvalho, P., 2007-2008. A carga do navio Ria de Aveiro A (Ílhavo, Portugal): uma aproximaçao preliminar ao seu significado histórico-cultural. Cuadernos de estudios borjanos, 50-51, 257-287.

Blanco-Zubiaguirre, L., Ribechini, E., Degano, I., La Nasa, J., Carrero, J.A., Iñañez, J., Olivares, M., Castro, K., 2018. GC–MS and HPLC-ESI-QToF characterization of organic lipid residues from ceramic vessels used by Basque whalers from 16th to 17th centuries. Microchemical Journal. 137, 190-203. DOI: 10.1016/j.microc.2017.10.017.

Blanco-Zubiaguirre, L., Olivares, M., Castro, K., Carrero, J.A., García-Benito, C., García-Serrano, J.A., Pérez-Pérez, J., Pérez-Arantegui, J., 2019. Wine markers in archeological potteries: detection by GC-MS at ultratrace levels. Anal Bioanal Chem. 411, 6711–6722. DOI: 10.1007/s00216-019-02044-1

Blet-Lemarquand, M., Gratuze, B., 1997. Archaeological Ceramic Glazes Characterization by Laser Ablation - Inductively Coupled Plasma - Mass Spectrometry (LA-ICP-MS). Key Engineering Materials - KEY ENG MAT. 132-136. 1466-1469.

Blomster, J.P., Neff, H., Glascock, M.D., 2005. Olmec pottery production and export in ancient Mexico determined through elemental analysis. Science, 307, 1068-1072. DOI:10.1126/science.1107599

Boulanger, M. T., Fehrenbach, S. S., Glascock, M. D., 2013. Experimental evaluation of sample-extraction methods and the potential for contamination in ceramic specimens. Archaeometry. 55, 5, 880–892, 2013. ISSN 0003813X. DOI: 10.1111/j.1475-4754.2012.00706.x.

Brill, R.H., Wampler, J.M. 1967. Isotope studies of ancient lead. Am J Archaeol. 71, 63–77

Brill, R.H., Barnes, I.L., Tong, S.S.C., Joel, E.C., Murtagh, M.J., 1987. Laboratory studies of some European artifacts excavated on San Salvador Island, in: Gerace, D.T. (ed) First San Salvador conference: Columbus and his world. CCFL Field Station, Fort Lauderdale, pp 247–292

Broekmans, T., Adriaens, A., Pantos, E., 2008. Insights into the production technology of north-mesopotamian bronze age pottery. Appl Phys A. 90, 1, 35-42. doi: 10.1007/s00339-007-4227-y.

Bulska E., Wagner, B., 2016. Quantitative aspects of inductively coupled plasma mass spectrometry. Philosophical Transactions Royal Society A, 374: 20150369. doi: 10.1098/rsta.2015.0369.

Buxeda i Garrigós, J., 1994. La caracterització arqueomètrica de la ceràmica de Terra Sigillata Hispanica Avançada de la ciutat romana de Clunia i la seva contrastació amb la Terra Sigillata Hispanica d'un centre productor contemporani, el taller d'Abella. Universitat de Barcelona.

Buxeda i Garrigós, J., 1999. Alteration and contamination of archaeological ceramics: The perturbation problem. Journal of Archaeological Science. 26, 3, 295-313. DOI: 10.1006/jasc.1998.0390

Buxeda i Garrigós, J., 2008. Revisiting the compositional data. Some fundamental questions and new prospects in Archaeometry and Archaeology. Proceedings of CODAWORK08. The 3rd Compositional Data Analysis Workshop May 2730 University of Girona Girona Spain, pages 1–18.

Buxeda i Garrigós, J., Cau Ontiveros, M. A., 1994. Identificación y significado de la calcita secundaria en cerámicas arqueo-lógicas. Complutum. 5, 293.

Buxeda i Garrigós, J., Cau, M.A., 1995. Identificación y significado de la calcita secundaria en cerámicas arqueológicas. Complutum. 6, 293-309.

Buxeda i Garrigós, J., Kilikoglou, V., 2003. Total variation as a measure of variability in chemical data sets, in: van Zelst, L. (Ed.), Patterns and Process. A Festchrift in Honor to Dr. Edward Sayre. Smithsonian Center for Materials Research and Education, Suitland, Maryland, pp. 185-198.

Buxeda i Garrigós, J., Madrid i Fernández, M., 2017. Designing Rigorous Research: Integrating Science and Archaeology, in: The Oxford Handbook of Archaeological Ceramics, chapter Part II. R, pages 19–47. Oxford University Press, Oxford, oxford han edition

Buxeda i Garrigós, J., Cau, M., Gurt, J. M., Tuset, F., 1995. Análisis tradicional y análisis arqueométrico en el estudio de las cerámicas comunes de época romana. Monografies Empuritanes, 8, 39–60.

Buxeda i Garrigós, J., Kilikoglou, V., Day, P. M., 2001. Chemical and mineralogical alteration of ceramics from a Late Bronze Age kiln at Kommos, Crete: The effect on the formation of a reference group. Archaeometry. 43, 3, 349-371. DOI: 10.1111/1475-4754.00021

Buxeda i Garrigós, J., Mommsen, H., Tsolakidou, A., 2002a. Alterations of Na, K and Rb concentrations in mycenaean pottery and a proposed explanation using X-ray diffraction. Archaeometry. 44, 2, 187-198. DOI: 10.1111/1475-4754.t01-1-00052.

Buxeda i Garrigós, J., Cau Ontiveros, M. A., Madrid i Fernández, M., Toniolo, A., 2002b. Roman Amphorae from the Iulia Felix Shipwreck: Alteration and Provenance, in: Hars and Burke (Ed.), Proceedings of the 33rd International Symposium on Archaeometry. Amsterdam.

Buxeda i Garrigós, J., Cau, M.A., Kilikoglou, V., 2003. Chemical variability in clays and pottery from a traditional cooking pot production village: testing assumptions in Pereruela. Archaeometry. 45, 1-17. https://doi.org/10.1111/1475-4754.00093.

Buxeda i Garrigós, J., Madrid i Fernández, M., Iñañez, J. G., Vila Socias, L., 2010. Mayor Conocimiento, Mejores Interpretaciones: La Arqueometría Cerámica. CVDAS Revista de arqueología e historia

Buxeda i Garrigós, J., Madrid i Fernández, M., Iñañez, J.G., Fernández de Marcos, C., 2015. Archaeometry of the technological change in societies in contact. First examples for modern ceramics from the Crowns of Castile and Aragon.

GlobalPottery 1. Historical Archaeology and Archaeometry for Societies in Contact, BAR International Series 2761, Archaeopress, 3-25.

Calparsoro, E., 2019. Transdisciplinar methodologies on Medieval and Post-Medieval pottery analysis: an archaeometric approach to Basque and Riojan Productions. Doctoral Thesis. University of the Basque Country (UPV/EHU), Vitoria-Gasteiz, Spain

Calparsoro, E., GitHub Website, 2021. URL https://github.com/esteful/arch_flow

Calparsoro, E., Sanchez-Garmendia, U., 2021. Ikerketa berregingarria analisi arkeometrikoan, kode irekia eta R. IV. Ikergazte. Nazioarteko ikerketa euskaraz. Kongresuko artikulu bilduma. Giza Zientziak eta Artea. UEU arg. https://dx.doi.org/10.26876/ikergazte.iv.01.16

Calparsoro, E., Maguregui, M., Morillas, H., Arana, G., Iñañez, J.G., 2019a. Non-destructive screening methodology based on ED-XRF for the classification of medieval and post-medieval archaeological ceramics. Ceramics International, 45, 10672-10683. doi: 10.1016/j.ceramint.2019.02.138.

Calparsoro, E., Sanchez-Garmendia, U., Arana, G., Maguregui, M., Iñañez, J.G., 2019b. An archaeometric approach to the majolica pottery from alcazar of Nájera archaeological site. Herit. Sci. 7, 33. https://doi.org/10.1186/s40494-019-0275-9.

Calparsoro, E., Arana, G., Iñañez, J.G., 2019c. Pottery from Orduña Village in the 17th–19th centuries: An archaeometrical approach. Journal of Archaeological Science Reports, 23, 304-323. doi: 10.1016/j.jasrep.2018.10.019.

Calparsoro, E., Iñañez, J.G., Arana, G., Glascock, M.D., 2021. Pottery making tradition in Logroño: an archaeometric approach to the Late Medieval workshops. Archaeol Anthropol Sci. 13, 85. https://doi.org/10.1007/s12520-021-01311-6

Cámara, P., 1997. The Basque-Cantabrian basin's Mesozoic tectono-sedimentary evolution. Mémoires de la Société géologique de France, 171:187-191

Carvalho, P. and Bettencourt, J., 2012. De Aveiro para as margens do Atlântico: a carga donavio Ria de Aveiro A e a circulação de cêramica na Época Moderna, In: Velhos e Novos Mundos. Estudos de Arqueologia Moderna Old and New Worlds. Studies on Early Modern Archaeology, Volume 2. Lisbon, 733-746

Carvalho, P., Bettencourt, J., Coelho, I., 2014. The maritime cultural landscape of the ria de aveiro lagoon (portugal) in the early modern period, in: Proceedings of the 5th International Congress on Underwater Archaeology, Cartagena. 368-378.

Casimiro, T.M., 2014. Portuguese Redwares and Coarse Wares in Historical Archaeology, in: Smith C. (eds), Encyclopedia of Global Archaeology. Springer, New York, NY. https://doi.org/10.1007/978-1-4419-0465-2_2306

Casimiro, T.M., 2018. Material Culture from the Al Hallaniyah Island Early 16th Century Portuguese Indiaman Wrecksite. International Journal of Nautical Archaeology. 47, 1, 182-202. DOI: 10.1111/1095-9270.12291

Casimiro, T.M., 2020. Globalization, trade, and material culture: Portugal's role in the making of a multicultural Europe (1415–1806). Post-Medieval Archaeology. 54, 1, 1-17. DOI: 10.1080/00794236.2020.1750239

Castro, E.A., Doménech, M.T.C., 1995. Aproximación al examen científico de la cerámica medieval de manises. Caracterización mineralógica mediante microscopía electrónica y difracción de rayos X, in: Spanish Medieval Ceramis in Spain and the British Isles, BAR International Series, Archaeopress, Oxford.

Castro, K., Pérez-Alonso, M., Rodríguez-Laso, M.D., Fernández, L.A., Madariaga, J.M., 2005. On-line FT-Raman and dispersive Raman spectra database of artists' materials (e-VISART database). Anal Bioanal Chem. 382, 248–258. DOI: 10.1007/s00216-005-3072-0

Cau Ontiveros, M.A., Day, P.M., Montana G., 2002. Secondary calcite in archaeological ceramics: evaluation of alteration and contamination processes by thin section study, in: Kilikoglou, Hein, Maniatis (Ed.), Modern Trends in Scientifis Studies on Ancient Ceramics. Oxford.

Centeno, S., Williams, V., Little, N., Speakman, R.J., 2012. Characterization of surface decorations in Prehispanic archaeological ceramics by Raman spectroscopy, FTIR, XRD and XRF. Vibrational Spectroscopy. 58, 119–124. 10.1016/j.vibspec.2011.11.004.

Cerdà, J.A., 2021. Els Escudellers i la producció de Pisa a Barcelona (segles XV-XIX). Doctoral Thesis. Universitat Autònoma de Barcelona.

Chan Kim, J., Chang, Y., 2021. Evidence of human movements and exchange seen from curated obsidian artifacts on the Korean Peninsula. Journal of Archaeological

Science: Reports. 39,103184, ISSN 2352-409X, https://doi.org/10.1016/j.jasrep.2021.103184.

Chiarantini, L., Gallo, F., Rimondi, V., Benvenuti, M., Costagliola, P., Dini, A., 2014. Early Renaissance production recipes for Naples Yellow pigment: A mineralogical and lead isotope study of Italian Majolica from Montelupo (Florence). Archaeometry. 57, 5, 879–896. ISSN 14754754. DOI: 10.1111/arcm.12146.

Childs, R.W., 1992. Anglo-Portuguese trade in the fifteenth century. Transactions of the Royal Historical Society. 2, 195-219.

Cianchetta, I., Trentelman, K., Maish, J., Saunders, D., Foran, B., Walton, M., Sciau, Ph., Wang, T., Pouyet, E., Cotte, M., Meirer, F., Liu, Y., Pianetta, P., Mehta, A., 2015. Evidence for an unorthodox firing sequence employed by the berlin painter: Deciphering ancient ceramic firing conditions through high-resolution material characterization and replication. Journal of Analytical Atomic Spectrometry. 30, 3, 666-676. DOI: 10.1039/c4ja00376d.

Clark, J.H.R., Cridland, L., Kariuki, B.M., Harris, K.D.M., Withnall, R., 1995. Synthesis, Structural Characterisation and Raman Spectroscopy of the Inorganic Pigments Lead Tin Yellow Types I and II and Lead Antimonate Yellow: Their Identification on Medieval Paintings and Manuscripts. J. Chem. Soc. Dalton Trans. 16, 2577-2582. https://doi.org/10.1039/DT9950002577.

Coentro, S., Lima, A.M., Silva, A.S., Pais, A.N., Mimoso, J.M., Muralha, V.S.F., 2012. Pigments and pigment mixtures in Portuguese 17th century Azulejos. J. Eur. Ceram. Soc. 32, 1, 37–48.

Coentro, S., Relvas, C., Ferreira, T., Mirão, J., Trindade, R.A.A., Pleguezuelo, A., da Silva, R.C., Muralha, V.S.F., 2018. Mineralogical characterization of hispano-moresque glazes: a μ-Raman and scanning electron microscopy with X-ray energy dispersive spectrometry (SEM-EDS) study. Microsc. Microanal. 24, 3, 300–309.

Coll Conesa, J., 2009. Cobalt blue in medieval ceramic production in the Valencian workshops. Manises, Paterna and Valencia, Spain. Medieval Ceram. 31, 11–24.

Colomban, P., 2003. Polymerization degree and Raman identification of ancient glasses used for jewelry, ceramic enamels and mosaics. Journal of Non-Crystalline Solids. 323, 1-3, 180–187. ISSN 00223093.

Colomban, P., 2008. On-site Raman identification and dating of ancient glasses: A review of procedures and tools. ISSN 12962074.

Colomban, P., Treppoz, F., 2001. Identification and differentiation of ancient and modern European porcelains by Raman macro- and micro-spectroscopy. Journal of Raman Spectroscopy. 32, 2, 93–102. ISSN 03770486. doi: 10.1002/jrs.678.

Colomban, P., Milande, V., Lucas, H., 2004. On-site Raman analysis of Medici porcelain. Journal of Raman Spectroscopy. 35, 1, 68–72. ISSN 03770486. doi: 10.1002/jrs.1085.

Colomban, P., Ngo, A., Edwards, H.G.M., Prinsloo, L.C., Esterhuizen, L.V., 2021. Raman identification of the different glazing technologies of Blue-and-White Ming porcelains. Ceramics International. ISSN 0272-8842. https://doi.org/10.1016/j.ceramint.2021.09.246.

Colombini, M.P., Giachi, G., Modugno, F., Ribechini, E., 2005. Characterisation of organic residues in pottery vessels of the Roman age from Antinoe (Egypt). Microchemical Journal. 79, 1-2, 83-90

Comendador-Rey, B., Meunier, E., Figueiredo, E., Lackinger, A., Fonte, J., Fernández, C., Lima, A., Mirao, J., Silva, R.J.C., 2017. North-West Iberia tin mining from Bronze Age to modern times: an overview. Conference: The Tinworking Landscape of Dartmoor in a European Context - Prehistory to 20th Century. Volume: Phil Newman (Editor).

Corrochano, C., 1980. Memoria de la Hoja nº 397 (Zamora). Mapa Geológico de España E. 1:50.000. Segunda Serie (MAGNA), Primera edición. IGME, Madrid.

Corrochano, A., León Gómez, C., Quinquer Agut, R., 1976. Mapa geológico de la Hoja nº 397 (Zamora). Mapa Geológico de España E. 1:50.000. Segunda Serie (MAGNA), Primera edición. IGME, Madrid.

Cremaschi, M., 2000. Manuale di Geoarcheologia. Laterza, Bari

De Benedetto, G., Catalano, F., Sabbatini, L., Zambonin, P.G., 1998. Analytical characterisation of pigments on pre-Roman pottery by means of spectroscopic techniques Part I: white coloured shards. Fresenius J Anal Chem. 362, 170–175. https://doi.org/10.1007/s002160051052

De Bonis, A., Cultrone, G., Grifa, C., Langella, A., Morra, V., 2014. Clays from the Bay of Naples (Italy): New insight on ancient and traditional ceramics. J. Eur. Ceram. Soc. 34, 3229–3244, doi:10.1016/j.jeurceramsoc.2014.04.014.

De la Escosura, L., 1846. Descripción de las minas de la provincia de Zamora. Madrid.

De la Fuente, G.A., 2008. Post-Depositional Chemical Alterations in Archaeological Ceramics: a critical review and implications for their conservation. Boletín del Laboratorio de Petrología y Conservación Cerámica. 1, 2, 21-37.

De La Mata, J.C., 1989. La Alfarería popular de Benavente. Brigecio, estudios de Benavente y sus tierras. Centro de estudios benaventanos "Ledo del pozo". 1, 229-238.

De Laeter, J.R., Bohlke, J.K., Bievre, P.D., Hidaka, H., Peiser, H.S., Rosman, K.J.R., Taylor, P.D.P., 2003. Atomic weights of the elements: review 2000. Pure and Applied Chemistry. 75, 6, 683-800.

De Las Heras, J.L., 1991. La justicia penal de los Austrias en la corona de Castilla, first ed. Salamanca, Spain.

De Lapérouse, J.F., 2020. Ceramic musealisation: how ceramics are conserved and the implications for research. Archaeol Anthropol Sci. https://doi.org/10.1007/s12520-020-01139-6

De Stefano, C., Foti, C., Sammartano, S., Gianguzza, A., Rigano, C., 1994. Equilibrium Studies in Natural Fluids. Use of Synthetic Seawaters and Other Media as Background Salts. Ann. Chim. 84, 159–175.

De Waal, D., 2009. Micro-Raman and portable Raman spectroscopic investigation of blue pigments in selected Delft plates (17–20th Century). Journal of Raman Spectroscopy. 40, 2162-2170. DOI 10.1002/jrs.2389.

Deagan, K., 1987. Artifacts of the Spanish colonies of Florida and the Caribbean, 1500-1800. Volume I: ceramics, glassware and beads. Washington (DC): Smithsonian Institution Press.

Degler, J., Eliasson, A., 2015. A Priori Modeling of the Tisova Fire Test in FDS. Fire Protection Engineer Bachelor's Thesis, Luleå University of Technology.

Dickin, A.P., 2018. Radiogenic Isotope Geology, Cambridge University Press. DOI: https://doi.org/10.1017/9781316163009.

Downs, R.T., Hall-Wallace, M., 2002. 18th General Meeting of the International Mineralogical Association. Programme with Abstracts, Edinburgh, Scotland, p. 128.

Dunstan, L.P., Gramlich, J.W., Barnes, I.L., 1980. Absolute Isotopic Abundance and the Atomic Weight of a Reference Sample of Thallium. Journal of Research of the National Bureau of Standards. 85, 1, 1-10.

Dussubieux, L., 2020. Inductively Coupled Plasma-Mass Spectrometry (ICP-MS): Applications in Archaeology, in: Smith, C. (eds) Encyclopedia of Global Archaeology. Springer, Cham. https://doi.org/10.1007/978-3-030-30018-0_338

Dussubieux, L., Golitko, M., Gratuze, B., 2016. Recent Advances in Laser Ablation ICP-MS for Archaeology. Springer, Berlin

Echallier, J.C., 1984. Éléments de technologie céramique et d'analyse des terres cuites archéologiques. Documents d'Archéologie Méridionale, Serie Méthodes et Techniques, 3.

Edwards, H. G. M., Chalmers, J. M., 2005. Raman spectroscopy in archaeology and art history. Cambridge, UK: Royal Society of Chemistry.

Edwards, H.G.M., Vandenabeele, P., 2016. Raman spectroscopy in art and archaeology. Phil. Trans. R. Soc. A.3742016005220160052 http://doi.org/10.1098/rsta.2016.0052

Eggins, S.M., Woodhead, J.D., Kinsley, L.P.J., Mortimer, G.E., Sylvester, P., McCulloch, M.T., Hergt, J.M., Handler, M.R., 1997. A simple method for the precise determination of 40 trace elements in geological samples by ICPMS using enriched isotope internal standardization. Chemical Geology, 134, 311-326.

El Ouahabi, M., Daoudi, L., Hatert, F., Fagel, N., 2015. Modified Mineral Phases During Clay Ceramic Firing. Clays Clay Miner. 63, 404–413, doi:10.1346/ccmn.2015.0630506.

Ellison, S.L.R., Williams, A., 2012. Quantifying Uncertainty in Analytical Measurement. EURACHEM/CITAC Guide CG-4, QUAM:2012.P1. EURACHEM, Third edition, URL http://www. eurachem.org.

Elvira Martín, L. M., 1984. Informes de la Construcción. 35, 358, 63-72.

Eramo, G., 2020. Ceramic technology. How to recognize clay processing. Archaeol Anthropol Sci. https://doi.org/10. 1007/s12520-020-01132-z

Escribano, S., 2014. Genealogía del registro cerámico alavés de época preindustrial (siglos XIV al XVII), tesis doctoral, Universidad del País Vasco (UPV/EHU), Vitoria-Gasteiz.

Evershed, R.P., 2008. Organic residue analysis in archaeology: the archaeological biomarker revolution. Archaeometry. 50, 6, 895-924. DOI: https://doi.org/10.1111/j.1475-4754.2008.00446.x

Fabbri, B., Gualtieri, S., Shoval, S., 2014. The presence of calcite in archeological ceramics. J. Eur. Ceram. Soc. 34, 1899–1911, doi:10.1016/j.jeurceramsoc.2014.01.007.

Fadón, O., 2011. Geología de Zamora.

Fantuzzi, L., 2010. La alteración posdeposicional del material cerámico. Agentes, procesos y consecuencias para su preser-vación e interpretación arqueológica. Comechingonia Virtual. 4, 1 27-59.

Faure, G., Mensing, T.M., 2004. Isotopes: Principles and Applications, 3rd Edition. John Wiley & Sons, Inc. 897 pp.

Fernandes, I. M., 2012. A loiça preta em Portugal: Estudo histórico, modos de fazer e de usar, in: Universidade do Minho.

Fernandes, I. M. and Castro, F., 2012. As produções de louça preta em Trás-os-Montes: caracterização etnográfica e química; seu interesse para o estudo das cerâmicas arqueológicas, In: Velhos e Novos Mundos. Estudos de Arqueologia Moderna Old and New Worlds. Studies on Early Modern Archaeology, Volume 2. Lisbon, 975-982.

Fernández, A., Moreda, J., Martín, M.A., 1991. Excavaciones arqueológicas en el casco urbano de Valladolid. Casa de Galdo. Codex aquilarensis: Cuadernos de investigación del Monasterio de Santa María la Real. ISSN 0214-896X, 4, 29-62.

Fernández de Marcos, C., 2018. Sevilla i l'expansió atlàntica en els s. XVI i XVII. Un estudi arqueomètric i arqueològic del principal centre productor ceràmic d'Europa. PhD thesis, Universitat de Barcelona.

Ferrer, P., 2014. Una contribución a la investigación de la espectroscopia Raman en el análisis de pigmentos: resultados teóricos y experimentales. Tesi doctoral, UPC, Departament de Teoria del Senyal i Comunicacions

Forster, N., Grave, P., Vickery, N., Kealhofer, L., 2011. Non-destructive analysis using PXRF: methodology and application to archaeological ceramics. X-Ray Spectrometry. 40, 5, 389–398. ISSN 00498246. doi: 10.1002/xrs.1360. URL http://doi.wiley.com/10.1002/xrs.1360.

Frackiewicz, K., Kiegiel, K., Herdzik-Koniecko, I., Chajduk, E., Zakrzewska-Trznadel, G., Wokowicz, S., Chwastowska, J., Bartosiewicz, I., 2012. Extraction of uranium from low-grade Polish ores: dictyonemic shales and sandstones. Nukleonika, 58, 4, 451-459.

Franklin, U.M., Vitali, V., 1985. The environmental stability of ancient ceramics. Archaeometry. 27, 1, 3-15.

Freestone, I. C., 2001. Post-depositional changes in archaeological ceramics and glasses, in: Brothwell and Pollard (Ed.), Handbook of Archaeological Sciences. Wiley & Sons, LTD.

Freestone, I. C., Meeks, N. D., and Middleton, A. P., 1985. Retention of phosphate in buried ceramics: an electron microbeam approach. Archaeometry. 27, 2, 161-177. DOI: 10.1111/j.1475-4754.1985.tb00359.x.

Freeth, S.J. A Chemical Study of Some Bronze Age Pottery Sherds. Archaeometry 1967, 10, 104–119, doi:10.1111/j.1475-4754.1967.tb00621.x.

Fuentes de Guerra, R., 1964. Toponimia cerámica española, in: Boletín de la Sociedad Española de Cerámica y Vidrio, 3, 6, 611-613. ISSN 0366-3175

Galli, A., Sibilia, E., Martini, M., 2020. Ceramic chronology by luminescence dating. How and when it is possible to date ceramic artefacts. Archaeol Anthropol Sci. https://doi.org/10.1007/s12520-020-01140-z

Garcia, C., Monteiro, P., 2001. The excavation and dismantling of Angra D, a probable Iberian seagoing ship, Angra bay, Terceira Island, Azores, Portugal. Preliminary assessment. Proceedings, Int. Symp. Archaeol. Mediev.Mod. Ships Iberian-Atlantic Tradit. hull Remain. manuscripts, Ethnogr. sources a Comp. approach 431–447

Garcia, C., Monteiro, P., Phaneuf, E., 1999. Os destroços dos navios Angra C e D descobertos durante a intervenção arqueológica subaquática realizada no quadro do projecto de construção de uma marina na baía de Angra do Heroísmo (Terceira, Açores). Rev Port Arqueol 2: 211–232

García, J., Martínez, J., 1992. Recursos minerales de España. CSIC, Madrid.

García de Madinabeitia, S., Gil Ibarguchi, J.I., 2019. Geoquímica isotópica en arqueología: los isótopos de Pb en los estudios de procedencia de muestras arqueológicas. XII Congresso Ibérico de Geoquímica.

García de Madinabeitia, S., Sánchez-Lorda, M.E., G. Ibarguchi, J.I., 2008. Simultaneous determination of major to ultratrace elements in geological samples by fusion-dissolution and inductively coupled plasma mass spectrometry techniques. Anal. Chim. Acta, 625, 2, 117-130. doi: 10.1016/j.aca.2008.07.024.

García de Madinabeitia, S., Sánchez-Lorda, M.E., G. Ibarguchi, J.I., Badillo, J.M., 2017. Elemental and PB Isotopic analysis of archaeological metals by laser ablation-Q/MC-ICP-MSMethods restrictions and application example, in: Montero-Ruiz. I., Perea, A., Instituto de História (eds), Archaeometallurgy in Europe IV. ISBN 9788400102876, pp. 7-18

García de Madinabeitia, S., Gil Ibarguchi, J.I., Santos Zalduegui, J.F., 2021. IBERLID: A lead isotope database and tool for metal provenance and ore deposits research. Ore Geology Reviews. 137. DOI: 10.1016/j.oregeorev.2021.104279.

García-Castrillo, G., Lanuza, P., López, G., 2003. El entorno marino de los restos arqueológicos, In Monte Buciero 9, La conservación del material subacuático; Publisher: Excmo. Ayuntamiento de Santoña. Santoña, Spain. pp. 95–109.

García-Heras, M., Blackman, M. J., Fernández-Ruiz, R., Bishop, R. L., 2001. Assessing Ceramic Compositional Data: A Comparison of Total Reflection X-ray Fluorescence and Instrumental Neutron Activation Analysis On Late Iron Age Spanish Celtiberian Ceramics. Archaeometry. 43, 3, 325–347. doi: 10.1111/1475-4754.00020.

García-Mondéjar, J., Agirrezabala, L.M., Aranburu, A., Fernández-Mendiola, P.A., Gómez-Pérez, I., López-Horgue, M. Rosales, I., 1996. Aptian-Albian tectonic pattern of the Basque-Cantabrian Basin (Northern Spain). Geol. J. 31, 13-45. https://doi.org/10.1002/(SICI)1099-1034(199603)31:1<13::AID-GJ689>3.0.CO;2-Y

García-Oses, I., 2018. Les relacions urbanes i interurbanes dels ceramistes de barcelona. La confraria de sant hipòlit, 1531-1813. PhD thesis, Universitat de Barcelona.

García-Porras, A., 2012. El azul en la producción cerámica bajomedieval de las áreas islámica y cristiana de la Península Ibérica, IX Congreso Internacional de Cerámica Medieval en el Mediterráneo, Florencia, 2012.

García-Ten, J., Monfort, E., Gomez, P., Gomar, S., 2006. Influence of calcite content on fluorine compound emissions during ce-ramic tile firing. J. Ceram. Process. Res. 7, 75–82.

Gerrard, S., 2000. The Early British Tin Industry. The History Press LTD

Gillies, K. J. S., Urch, D.S., 1983. Spectroscopic studies of iron and carbon in black surfaced wares. Archaeometry. 25, 1, 29-44. doi: 10.1111/j.1475-4754.1983.tb00659.x.

Gilstrap, W.D., Meanwell, J.L., Paris, E.H., López Bravo, R., Day, P.M., 2021. Post-Depositional Alteration of Calcium Carbonate Phases in Archaeological Ceramics: Depletion and Redistribution Effects. Minerals. 11, 749. https://doi.org/10.3390/min11070749

Giussani, B., Monticelli, D., Rampazzi, L., 2009. Role of laser ablation-inductively coupled plasma-mass spectrometry in cultural heritage research: A review. Analytica Chimica Acta, 635, 1, 6–21. ISSN 00032670. doi: 10.1016/j.aca.2008.12.040.

Glascock, M. D., 1992. Characterization of Archaeological Ceramics at MURR by Neutron Activation Analysis and Multivariate Statistics. In Chemical Characterization of Ceramic Pastes in Archaeology, number August. Prehistory Press, 1992. ISBN 1055-2316.

Glascock, M.D., 2002. Geochemical Evidence for Long-Distance Exchange. Greenwood Publishing Group, USA

Glascock, M.D., 2014. Neutron Activation Analysis (NAA): Applications in Archaeology. In C. Smith (Ed.), Encyclopedia of Global Archaeology. Springer, New York, NY. doi: 10.1007/978-1-4419-0465-2_337

Glascock, M.D., 2016. Compositional Analysis in Archaeology, in: Oxford Handbooks, pages 1–25. Oxford Handbooks Online, Oxford. doi: 10.1093/oxfordhb/9780199935413.013.8Abstract.

Gliozzo, E., 2020a. Ceramics investigation, Research questions and sampling criteria. Archaeol Anthropol Sci. DOI: https://doi.org/10.1007/s12520-020-01128-9

Gliozzo, E., 2020b. Ceramic technology. How to reconstruct the firing process. Archaeol Anthropol Sci. https://doi.org/10.1007/s12520-020-01133-y

Goldstein, J.I., Newbury, D.E., Echlin, P., Joy, D.C., Lyman, C.E., Lifshin, E., Sawyer, L., Michael, J.R., 2003. Scanning Electron Microscopy and X-Ray Microanalysis. 3rd edition. Springer

Golitko, M., Dussubieux, L., 2016. Inductively Coupled Plasma-Mass Spectrometry (ICP-MS) and Laser Ablation Inductively Coupled Plasma-Mass Spectrometry (LA-

ICP-MS), in: Hunt, A. (Ed.), The Oxford Handbook of Archaeological Ceramic Analysis, Oxford University Press. 10.1093/oxfordhb/9780199681532.013.23

Golitko, M., McGrath, A., Kreiter, A., Lightcap, I.V., Duffy, P.R., Parditka, G.M., Giblin, J.I., 2021. Down to the Crust: Chemical and Mineralogical Analysis of Ceramic Surface Encrustations on Bronze Age Ceramics from Békés 103, Eastern Hungary. Minerals. 11, 436. https://doi.org/10.3390/min11040436

Gómez, M., Vergés, J., Riaza, C., 2002. Inversion tectonics of the northern margin of the Basque Cantabrian Basin. Bulletin de la Société Géologique de France. 173, 5, 449–459. doi: https://doi.org/10.2113/173.5.449

González, T., 1832. Registro y relación general de minas de la corona de Castilla. Madrid.

González-Menéndez, L., Gallastegui, G., Cuesta, A., Heredia, N., Rubio-Ordóñez, A., 2013, Petrogenesis of Early Paleozoic basalts and gabbros in the western Cuyania terrane: Constraints on the tectonic setting of the southwestern Gondwanamargin (Sierra del Tigre, Andean Argentine Precordillera). Gondwana Research, 24, 359–376. doi: 10.1016/j.gr.2012.09.011

González-Ruibal, A., Ayán Vila, X., 2018. Arqueología. Una introducción al estudio de la materialidad del pasado. Alianza Editorial, Madrid. ISBN 9788491812357

Grassi, F., Quirós, J. A., 2018. Arqueometría de los materiales cerámicos de época medieval en España (Documentos de Arqueología Medieval 12). ISBN 9788490829073.

Gualtieri, S., 2020. Ceramic raw materials. How to establish the technological suitability of a raw material. Archaeol Anthropol Sci. https://doi.org/10.1007/s12520-020-01135-w

Guevara Muñoz, M.E., 2001. Conservación preventiva de objetos cerámicos en excavaciones arqueológicas, in: Schneider Glantz, R. (comp.) Conservación in situ de materiales arqueológicos. Un manual. pp. 89-100. INAH, México.

Guimerà, J., Álvaro, M., 1990. Structure et évolution de la compression alpine dans la Chaîne Ibérique et la Chaîne côtière catalane (Espagne). Bulletin de la Société Géologique de France. 8, VI (2), pp. 339-340

Gutiérrez, A., 2007. Portuguese coarsewares in early modern England: reflections on an exceptional pottery assemblage from Southampton. Post Medieval Archaeology. 41, 64-79.

Habicht-Mauche, J.A., Glenn, S.T., Milford, H., Flegal, A.R., 2000. Isotopic tracing of prehistoric Rio Grande glaze-paint production and trade. J Archaeol Sci. 27, 709–713

Habicht-Mauche, J.A., Glenn, S.T., Schmidt, M.P., Franks, R., Milford, H., Flegal, A.R., 2002. Stable lead isotope analysis of Rio Grande glaze paints and ores using ICP-MS: a comparison of acid dissolution and laser ablation techniques. J Archaeol Sci. 29, 1043–1053

Hall, E.T., 1960. X-ray fluorescent analysis applied to archaeology. Archaeometry. 3, 29-37.

Harris, E.C., 1979. Principles of Archaeological Stratigraphy. Academic Press, New York

Heimann, R. B., 1989. Assesing the Technology of Ancient Pottery: The Use of Ceramic Phase Diagrams. Archaeomaterials. 3, 123–148.

Heimann, R.B., 2010. Classic and Advanced Ceramics: From Fundamentals to Applications, first ed. Görlitz, Germany. DOI: 10.1002/9783527630172

Heimann, R. B., Maggetti, M., 1981. Experiments on simulated burial of calcareous terra sigillata (mineralogical change). Preliminary results. British Museum Occasional Paper. 19, 163-177.

Heimann, R.B., Kreher, U., Spazier, I., Wetzel, G., 2002. Mineralogical And Chemical Investigations Of Bloomery Slags From Prehistoric (8th Century Bc To 4th Century Ad) Iron Production Sites In Upper And Lower Lusatia, Germany. Archaeometry. 43, 227 - 252. 10.1111/1475-4754.00016

Hein, A., Kilikoglou, V., 2017. Compositional variability of archaeological ceramics in the eastern Mediterranean and implications for the design of provenance studies. Journal of Archaeological Science: Reports. ISSN 2352409X. DOI: 10.1016/j.jasrep.2017.03.020.

Hein, A., Kilikoglou, V., 2020. Ceramic raw materials. How to recognize them and locate the supply basins Chemistry. Archaeol Anthropol Sci. https://doi.org/10.1007/s12520-020-01129-8

Hein, A., Tsolakidou, A., Iliopoulos, I., Mommsen, H., Buxeda i Garrigós, J., Montana, G., Kilikoglou, V., 2002. Standardisation of elemental analytical techniques applied to provenance studies of archaeological ceramics –an inter laboratory calibration study. The Analyst. 127, 542-553. DOI: 10.1039/b109603f.

Henderson, J., Ma, H., Cui, J., Ma, R., Xiao, H., 2020. Isotopic investigations of Chinese ceramics. Archaeol Anthropol Sci. https://doi.org/10.1007/s12520-020-01138-7

Herrero, B.F., 2016. De cárcel a museo: la cárcel real de Zamora. Revista de Estudios Penitenciarios. 259, 257-342.

Hill, S.J., 2007. Inductively Coupled Plasma Spectrometry and its Applications. Blackwell Publishing Ltd, oxford

Holliday, V.T., 1992. Soil formation, time, and archaeology, in: Holliday, V.T. (ed) Soils in Archaeology: landscape evolution and human occupation, pp. 101–117. Smithsonian Institution Press, Washington.

Hunt, M., 2003. Prehistoric Mining and Metallurgy in South West Iberian Peninsula. BAR International Series 1188, Oxford.

Hunt, M., 2016. The Oxford handbook of archaeological ceramic analysis. 2016. ISBN 9780199681532.

Hunt, M., Speakman, R.J., 2015. Portable XRF analysis of archaeological sediments and ceramics. Journal of Archaeological Science, 53, 626-638.

Ibabe, E., 1995a. Ceramica popular vasca. Fundación BBK. ISBN 84-89476-09-8.

Ibarra, J.L., 2006. Productos de alfarería negra posmedieval recuperados en contextos arqueológicos de Vizcaya. Kobie (Serie Antropología Cultural). 12, 299-337.

Igea, J., Pérez-Arantegui, J., Lapuente, P., Saiz, M.E., Burillo, F., 2013. Producciones de cerámica Celtibérica procedentes del sistema Ibérico Central (España): Caracterización química y petrográfica. Boletín de la Sociedad Española de Cerámica y Vidrio, 52, 1, 1-14. doi: 10.3989/cyv.12013

Iñañez, J. G., 2007. Caracterització Arqueomètrica De La Ceràmica Vidriada Decorada De La Baixa Edat Mitjana Al Renaixement Als Centres Productors De La Península Ibèrica. PhD thesis, Universitat de Barcelona.

Iñañez, J.G., 2021. Personal communication

Iñañez, J.G., Speakman, R.J., Buxeda i Garrigós, J., Glascock, M.D., 2008. Chemical characterization of majolica from 14th-18th century production centers on the Iberian Peninsula: a preliminary neutron activation study. Journal of Archaeological Science, 35, 425-440

Iñañez, J.G., Speakman, R.J., Buxeda i Garrigós, J., Glascock, M.D., 2009. Chemical characterization of tin-lead glazed pottery from the Iberian Peninsula and the Canary Islands: Initial steps toward a better understanding of Spanish Colonial pottery in the Americas. Archaeometry. 51, 4, 546–567. ISSN 0003813X. doi: 10.1111/j.1475-4754.2008.00431.x.

Iñañez J.G., Bellucci, J.J., Rodríguez-Alegría, E., Ash, R., McDonough, W.F., Speakman, R.J., 2010. Romita pottery revisited: a reassessment of the provenance of ceramics from Colonial Mexico by LA-MC-ICP-MS. J. Archaeol. Sci. 37, 2698–2704.

Iñañez, J.G., Madrid-Fernández, M., Molera, J., Speakman, R.J., Pradell, T., 2013. Potters and pigments: Preliminary technological assessment of pigment recipes of American majolica by synchrotron radiation micro-X-ray diffraction (Sr-μXRD). Journal of Archaeological Science. 40, 2, 1408–1415. ISSN 03054403

Iñañez J.G., Bellucci, J.J., Martín, J.G., Ash, R., McDonough, W.F., Speakman, R.J., 2016. Pb Isotopic Composition of Panamanian Colonial Majolica by LA-ICP-MS, in: Recent Advances in Laser Ablation ICP-MS for Archaeology, Dussubieux, L., Golitko, M., Gratuze, B., (Eds.), Chicago.

Iñañez, J.G., Sanchez-Garmendia, U., Calparsoro, E., Arana, G., 2018. Zamora and the pottery from Olivares workshops: long-tradition pottery manufacturing in the heart of Spain. 42nd International Symposium on Archaeometry ISA 2018, 166. Ruvalcaba, José Luís, Mexico.

Iñañez, J. G., Bettencourt, J., Pinto, I., Teixeira, A., Arana, G., Castro, K., Sanchez-Garmendia, U., 2020. Hit and sunk: provenance and alterations of ceramics from 17th century Angra D shipwreck. Archaeological and Anthropological Sciences. (In Press). doi: 10.1007/s12520-020-01109-y.

Iñañez, J., Bento Torres, J., Teixeira, A., Sanchez-Garmendia, U., Calparsoro, E., Arana, G., 2021. The supply of ceramics to Portuguese North African strongholds in the 15th and 16th centuries: New archaeometric data from Ksar Seghir and Ceuta. Journal of Archaeological Sciences: Reports. 37. https://doi.org/10.1016/j.jasrep.2021.102908

Ionescu, C., Hoeck, V., 2020. Ceramic technology, How to investigate surface finishing. Archaeol Anthropol Sci. https://doi.org/10.1007/s12520-020-01144-9

Ionescu, C., Hoeck, V., Crandell, O. N., Šarić K., 2014. Burnishing versus smoothing in ceramic surface finishing: A SEM study. Archaeometry. 57, 1, 18-26. doi: 10.1111/arcm.12089

Joel, E.C., Olin, J.S., Blackman, M.J., Barnes, I.L., 1988. Lead isotope studies of Spanish, Spanish-Colonial and Mexican Majolica, in: Farquhar RM, Hancock RGV, Pavlish LA (eds) Archaeometry 88, Proceedings of the 26th international archaeometry symposium. University of Toronto, Toronto, pp 188–195

Jones, D.W., Smith, J.A., 1962. Hydrogen bonding in calcium orthophosphates. Nature. 195, 1090-1091.

Julivert, M., Fontboté, J.M., Ribeiro, A. y Nabais-Conde, L.E., 1972. Mapa Tectónico de la Península Ibérica y Baleares 1:1.000.000. IGME.

Kawagoe, K., Sekine, T., 1963. Estimation of Fire Temperature-Time Curve in Rooms. 23p, BRI Research Paper, Building Research Institute, Japan.

Karlsson B., Quintiere, G. J., 2000. Enclosure Fire Dynamics, CRC Press.

Kelloway, S.J., VanValkenburgh, P., Astuhuamán, C., Gonzáles, A., Bedoya, D., 2019. International Pots of Mystery: Using PXRF spectroscopy to identify the provenance of botijas from 16th Century sites on Peru's north coast. Journal of Archaeological Sciences: Reports, 27. doi: 10.1016/j.jasrep.2019.101974

Kelly, W.C., Rye, R.O., 1979. Geologic, fluid inclusion, and stable isotope studies of the tin-tungsten deposits of Panasqueira, Portugal. ECON. GEOL. 74, 1721-1822.

Klein, S., Domergue, C., Lahaye, Y., Brey, G.P., von Kaenel, H.M., 2009. The lead and copper isotopic composition of copper ores from the Sierra Morena (Spain). Journal of Iberian Geology. 35, 1, 59-68.

Knappett, C., 2013. Network analysis in Archaeology: new approaches to regional interaction. Oxford University Press, Oxford, 350 pp

Larrén Izquierdo, H., 1991. Hallazgos cerámicos en la ciudad de Toro. Anuario del Instituto de Estudios Zamoranos Florián de Ocampo. 8, 75-113.

Larrén Izquierdo, H., 1992. Hallazgos cerámicos en la ciudad de Toro (II): el conjunto del “Patio del Siete”. Anuario del Instituto de Estudios Zamoranos Florián de Ocampo. 9, 163-174.

Larrén Izquierdo, H., 1997-1998. Zamora. Numantia. 8, 371-392.

Lemoine, C., Picon, M., 1982. La fixation du phosphore par les céramiques lors de leur enfouissement et ses incidences analytiques. Rev. d’Archéom. 6, 101-112.

Lemoine, C., Meille, E., Poupet, P., Barandon, J.N., Borderie, B., 1981. Etude de quelques alterations de composition chimique des ceramiques en milieu marin et terrestre. Revue d’Archeometrie. 3, 349-60.

Lhôte, J.M., 2007. Les trois livres de l’art du potier, Traduction de: “Li tre libri dell’arte del Vasaio”, Fac-similé du manuscrit de Cipriano Piccolpasso Casteldurante, 1557. Ed. de la Revue de la céramique et du verre, Vendin-le-Vieil.

Lightbown, R., Caiger-Smith, A., 1980. The three books of the potter’s art: a facsimile of the manuscript in the Victoria and Albert Museum, 2 vol., Scolar Press, London.

Lillo, J., 1992. Vein-type base metal ores in Linares-La Carolina (Spain): ore-lead isotopic constraints. European J. of Mineralogy 4, 337-343.

Liritzis, I., Zacharias, N., 2011. Portable XRF of archaeological artefacts: current research, protocols and limitations, in: M.S. Shackley (ed.) Archaeological obsidian studies: method and theory: 109-42. New York: Plenum Press.

Liritzis, I., Xanthopoulou, V., Palamara, E., Papageorgiou, I., Iliopoulos, I., Zacharias, N., Vafiadou, A., Germanos Karydas, A., 2020. Characterization and provenance of ceramic artifacts and local clays from Late Mycenaean Kastrouli (Greece) by means of p-XRF screening and statistical analysis. Journal of Cultural Heritage, 46, 61-81. DOI: 10.1016/j.culher.2020.06.004

Longworth, G., Tite, M. S., 1979. Mössbauer studies on the nature of the red or black glazes on Greek and Indian painted ware. Le Journal de Physique Colloques. 40, C2, C2-461. doi: 10.1051/jphyscol:19792160.

López-Arce, P., Zornoza-Indart, A., Gomez-Villalba, L., Pérez-Monserrat, E. M., Álvarez de Buergo, M., Vivar, G., Fort, R., 2013. Archaeological ceramic amphorae from underwater marine environments: Influence of firing temperature on salt crystallization decay. Journal of the European Ceramic Society. 33, 10, 2031-2042. http://dx.doi.org/10.1016/j.jeurceramsoc.2013.03.009.

Lucarini, G., Barca, D., Manzo, A., 2020. The provenance of obsidian artefacts from the Middle Kingdom harbour of Mersa/Wadi Gawasis, Egypt, and its implications for Red Sea trade routes in the 2nd millennium BC. Quaternary International. 555, Pages 85-95. ISSN 1040-6182, https://doi.org/10.1016/j.quaint.2020.03.015.

Lydzba-Kopczynska, B., Madariaga, J.M., 2016. Applications of Raman spectroscopy in art and archaeology. J. Raman Spectrosc. 47, 1404– 1407. doi: 10.1002/jrs.5067.

Madrid i Fernández, M., 2006. Estudi arqueològic i caracterització arqueomètrica de la "terra sigillata" de la ciutat de Baetulo (Badalona), Tesis Doctoral de la Universidad de Barcelona, Barcelona https://www.tesisenred.net/handle/10803/2591#page=1.

Madrid i Fernández, M., Buxeda i Garrigós, J., 2007. Qualitat i consum ceràmic de la sigillata augustal, Noves vies d'estudi i interpretació a partir de l'arqueometria. Empúries. 55, 53–66.

Madrid i Fernández, M., Buxeda i Garrigós, J., 2014. Hispanic terra sigillata Productions Documented on the Catalan Coast: Some Unexpected Results and New Issues, in: Martinón-Torres, M. (ed), Craft and Science: International Perspectives on Archaeological Ceramics. UCL Qatar Series in Archaeology and Cultural Heritage, 1 (Doha: Bloomsbury Qatar Foundation), 101–108.

Madrid i Fernández, M., Sinner, A.G., 2019. Analysing technical choices: improving the archaeological classification of Late Republican Black Gloss pottery in north-eastern Hispania consumption centres. Archaeol Anthropol Sci. 11, 3155–3186. https://doi.org/10.1007/s12520-018-0748-x

Madrid i Fernández, M., Sinner, A.G., 2021. La vajilla de barniz negro en Empúries y la Layetania: Origen y técnica de producción a partir de su caracterización arqueométrica. Archivo español de arqueología, ISSN 0066-6742, 94.

Madrid i Fernández, M., Comas i Solà, M., Padrós i Martí, P., 2005. Étude archéologique et analise archéométrique de la céramique sigillée sud-gauloise documentée a la ville romaine de Baetulo (Badalone, Barcelone), in: Nieto, X. Roca, M., Vernhet, A., Sciau, P. (eds), La difusió de la terra sigillata sudgàl·lica al nord d'Hispania (Barcelona: Monografies del Museu d'Arqueologia de Catalunya), 179–197.

Magaña, H.O., Grimaldi, D.M., Meurs, V.M., 2001. La conservación de los materiales arqueológicos durante los procesos de registro, excavación y extracción, in:

Schneider Glantz, R. (comp.) Conservación in situ de materiales arqueológicos. Un manual, pp. 9-18. INAH, México.

Maggetti, M., 1981. Composition of Roman pottery from Lousonna (Switzerland). In Scientific studies in ancient ceramics. British Museum Research Laboratory, London.

Maggetti, M., 1982. Phase Analysis and Its Significance for Technology and Origin, in: Olin, J. S. and Franklin, A. D. (eds), Archaeological Ceramics (Washington D.C.: Smithsonian Institution Press), 121–133.

Maggetti, M., Galetti, G., Schwander, H., Picon, M., Wessicken, R., 1981. Campanian pottery; the nature of the black coating. Archaeometry. 23, 2, 199-207. doi: 10.1111/j.1475-4754.1981.tb00306.x.

Maguregui, M., Prieto-Taboada, N., Trebolazabala, J., Goienaga, N., Arrieta, N., Aramendia, J., Gomez-Nubla, L., Sarmiento, A., Olivares, M., Carrero, J.A., Martinez-Arkarazo, I., Castro, K., Arana, G., Olazabal, M.A., Fernandez, L.A., Madariaga, J.M., 2010. CHEMCH 1st International Congress Chemistry for Cultural Heritage, Ravenna.

Maguregui, M., Morillas, H., Marcaida, I., García-Florentino, C., Ortiz de Errazti, I., Aransay, C., Madariaga, J.M., 2018. A non-invasive in situ methodology to characterise the lacquers and metals from the Edo period Japanese armour. Microchemical Journal. 137, 160-167. ISSN 0026-265X, https://doi.org/10.1016/j.microc.2017.10.009.

Mangin, Ph., Rat, P., 1962. L' evolution post-hercynienne entre Asturies et Aragon (Espagne). Mem. Soc. France (Livre a la memoíre du Prof P. Fallot) t. 1, pp. 333-349

Maniatis, Y., Tite, M.S., 1978. Ceramic technology in the Aegean world during the Bronze Age. Thera Aegean World. 1, 483–492.

Maniatis, Y., Tite, M. S., 1981. Technological examination of Neolithic-Bronze Age pottery from central and southeast Europe and from the Near East. Journal of Archaeological Science. 8, 1, 59–76. ISSN 10959238. DOI: 10.1016/0305-4403(81)90012-1.

Maniatis, Y., Aloupi, E., Stalios, A.D., 1993. New evidence for the nature of the attic black gloss. Archaeometry. 35, 1, 23-34. DOI: 10.1111/j.1475-4754.1993.tb01021.x

Marcaida, I., Maguregui, M., Morillas, H., Veneranda, M., Prieto-Taboada, N., Fdez-Ortiz de Vallejuelo, S., Madariaga, J.M., 2018. Raman microscopy as a tool to discriminate mineral phases of volcanic origin and contaminations on red and yellow ochre raw pigments from Pompeii. J Raman Spectrosc. 50, 143– 149. https://doi.org/10.1002/jrs.5414

Marcoux, E., 1997. Lead isotope systematics of the giant massive sulphide deposits in the Iberian Pyrite Belt. Mineralium Deposita. 33, 45-58.

Maritan L., 2020. Ceramic abandonment. How to recognise postdepositional transformations. Archaeol Anthropol Sci. 12, 199. DOI: 10.1007/s12520-020-01141-y.

Maritan, L., Mazzoli, C., 2004. Phosphates in archaeological finds: implications for environmental conditions of burial. Archaeometry. 46, 673–683.

Martín, J.I., 2018. Minería en Zamora. Una aproximación al siglo XVI y primer tercio del XVII. Brigecio, estudios de Benavente y sus tierras. Centro de estudios benaventanos "Ledo del pozo". 28, 61-89.

Martín, M. A., Marcos, G. J., Sanz, F. J., Misiego, J.C., Villanueva, L. A., Sandoval, A. M., García, P.F., 1997. La excavación arqueológica en el solar del museo Etnográfico de Zamora: la transformación urbana de este espacio desde la Edad Moderna. Numantia, 8, 245-270.

Martín, M.A., Villanueva, L.A., Sanz F.J., Marcos, G.J., Misiego, J.C., García, M.I., del Caño García, L.A., 2002. Trabajos arqueológicos en el solar del antiguo Convento de La Concepción, en Zamora, in: Anuario 2002 del Instituto de Estudios Zamoranos “Florián de Ocampo”. Zamora, 19, pp. 115-139.

Martín, M.A., Sanz, F.J., Misiego, J.C., Marcos, G.J., Villanueva, L.A., Fernández, E., García, M.I., García, P.F., 2003. Las excavaciones arqueológicas en la Iglesia y el Convento de La Concepción, in: 389 años del Convento de La Concepción. Junta de Castilla y León, Consejería de Educación y Cultura, Zamora.

Martín-Fernández, J. A., Buxeda i Garrigós, J., Pawlowsky-Glahn, V., 2015. Logratio Analysis in Archeometry: Principles and Methods. In Mathematics and Archaeology, volume Science Pu, pages 178–189. Science Publishers, Boca Raton., bogdanovic edition.

Martins, C., 2010. The Mining Complex of Braçal and Malhada, Portugal: Lead Mining in Roman Times and Linking Historical Social Trends – Amphitheatre Games. European Journal of Archaeology. 13, 2, 195-216. doi:10.1177/1461957109359975

Marzo, P., Laborda, F., Pérez-Arantegui, J., 2007. A Simple Method for the Determination of Lead Isotope Ratios in Ancient Glazed Ceramics Using Inductively Coupled Plasma - Quadrupole Mass Spectrometry. Atomic Spectroscopy. 28, 6.

Mas, J.L., Villa, M., Hurtado, S., García-Tenorio, R., 2012. Determination of trace element concentrations and stable lead, uranium and thorium isotope ratios by quadrupole-ICP-MS in NORM and NORM-polluted sample leachates. Journal of Hazardous Materials, 205-206, 198-207. doi: https://doi.org/10.1016/j.jhazmat.2011.12.058

Mason, R.B., Farquhar, R.M., Smith, P.E., 1992. Lead-isotope analysis of Islamic glazes: an exploratory study. Muqarnas. 9, 67–71

Matin, M., Tite, M., Watson, O., 2018. On the origins of tin-opacified ceramic glazes: New evidence from early Islamic Egypt, the Levant, Mesopotamia, Iran, and Central Asia. Journal of Archaeological Science. 97, 42-66. https://doi.org/10.1016/j.jas.2018.06.011.

McSweeney, A., 2011. The tin trade and medieval ceramics: tracing the sources of tin and its influence on Mediterranean ceramics production. Al-Masaq 23, 155–169.

Medeghini, L., Fayek, M., Mignardi, S., Coletti, F., Contino, A., De Vito, C., 2020. A provenance study of Roman lead-glazed ceramics using lead isotopes and secondary ion mass spectrometry (SIMS). Microchemical Journal. 154

Meneses, A., 2005. A economia e as finanças. In: Matos A (ed) Colonização Atlântica. Nova História Da Expansão Portuguesa. Editorial Estampa, Lisboa, pp 331–445

Meneses, A., 2008. Novas escalas ocasionais e relacionamentos exteriores, in: Leite, J., Matos, A., Meneses, A. (Eds.), História Dos Açores. Dos Descobrimentos Ao Século XX. Instituto Açoriano de Cultura, Angra do Heroísmo, pp. 297–324

Métreau, L., Cattin, F., Maria Villa, I., André, P., Chateau-Smith, C., 2021. Lead provenance for medieval decorated tile glazes from Brittany and Anjou (13th-14th c.). Journal of Archaeological Science: Reports. 38 https://doi.org/10.1016/j.jasrep.2021.103037

Millhauser, J. K., Rodríguez-Alegría, E., and Glascock, M. D., 2011. Testing the accuracy of portable X-ray fluorescence to study Aztec and Colonial obsidian supply at Xaltocan, Mexico. Journal of Archaeological Science. 38, 11, 3141–3152. ISSN 03054403. DOI: 10.1016/j.jas.2011.07.018. URL http://dx.doi.org/10.1016/j.jas.2011.07.018.

Mise, M., Quinn, P.S., Glascock, M.D., 2021. Lost at sea: Identifying the post-depositional alteration of amphorae in ancient shipwrecks. Journal of Archaeological Science. 134. https://doi.org/10.1016/j.jas.2021.105463.

Misiego, J.C., Villanueva, L.A., Marcos, G.J., Martín, M.A., Sandoval, A.M., García, P.F., Sanz, F.J., 1997-1998. La excavación arqueológica en el solar del museo Etnográfico de Zamora la transformación urbana de este espacio desde la Edad Moderna. Numantia: Arqueología en Castilla y León. pp. 245-270.

Molera, J., 1997. Evolució mineralògica i interacció de lespastes càlciques amb els vidrats de plom: implicacionsarqueomètriques. Tècniques de fabricació de la ceràmica islàmica i mudèjar, Col·lecció de Tesis Doctorals Microfitxades [3134], Universitat de Barcelona, Barcelona

Molera, J., Pradell, T, Martínez Manent, S., Vendrell-Saz, M., 1993 The growth of sanidine crystals in the lead of glazes of Hispano-Moresque pottery. Applied Clay Science. 7, 483-491.

Molera, J., Vendrell-Saz, M., García-Vallés, M., and Pradell, T., 1997. Technology and colour development of Hispano-Moresque lead-glazed pottery. Archaeometry. 39, 1, 23–39. ISSN 0003813X

Molera, J., Pradell, T., Vendrell-Saz, M., 1998. The colours of Ca-rich ceramic pastes: origin and characterization. Applied Clay Science. 13, 3, 187-202. https://doi.org/10.1016/S0169-1317(98)00024-6.

Molera, J., Pradell, T., Salvado, N., Vendrell-Saz, M., 1999. Evidence of tin oxide recrystallization in opacified lead glazes. Journal of the American Ceramic Society. 82, 10, 2871–2875. ISSN 00027820. doi: 10.1111/j.1151-2916.1999.tb02170.x.

Molera, J., Pradell, T., Salvado, N., 2001. Interactions between clay bodies and lead glazes. Journal of the American Ceramic Society. 84, 5, 1120–1128. ISSN0002-7820. DOI: 10.1111/j.1151-2916.2001.tb00799.x

Molera, J., Coll, J., Labrador, A., Pradell, T., 2013. Manganese brown decorations in 10th to 18th century Spanish tin glazed ceramics. Applied Clay Science. 82, 86-90. 86-90. 10.1016/j.clay.2013.05.018.

Molera, J., Iñañez, J., Molina, G., Burch, J., Alberch, X., Glascock, M. D., Pradell, T., 2015. Lustre and glazed ceramic collection from Mas Llorens, Salt 16-17th centuries (Girona). Provenance and technology. Periodico di Mineralogia. 84, 1. DOI 10.2451/2015PM0004.

Molina, G., 2014. Colour and technology in historic decorated glazes and glasses. Tesi doctoral, UPC, Departament de Física i Enginyeria Nuclear

Montana, G., 2020. Ceramic raw materials. How to recognize them and locate the supply basins. Mineralogy, petrography. Archaeol Anthropol Sci. https://doi.org/10.1007/ s12520-020-01130-1

Montana, G., Randazzo, L., Belfiore, C.M., La Russa, M.F., Ruffolo, S.A., De Francesco, A.M., Pezzino, A., Punturo, R., Di Stefano, V., 2014a. An original experimental approach to study the alteration and/or contamination of archaeological ceramics originated by seawater burial. Periodico di Mineralogia. 83, 1, 89-120. DOI: 10.2451/2014PM0006.

Montana, G., Randazzo, L., Castiglia, A., La Russa, M.F., La Rocca, R., Bellomo, S., 2014b. Different methods for soluble salt removal tested on late-Roman cooking ware from a submarine excavation at the island of Pantelleria (Sicily, Italy). J Cult Herit. 15, 403–413

Montero-Ruiz, I., 2018. La procedencia del metal: consolidación de los estudios con isótopos de plomo en la Península Ibérica. Revista d'Arqueologia de Ponent. 28, 313-330. DOI: 10.21001/rap.2018.28.17

Montero-Ruiz, I., Murillo-Barroso, M., Ruiz-Taboada, A., 2021. The Beginning of the Production and Use of Metal in Iberia: from Independent Invention to Technological Innovation. Eurasia Antiqua. 23

Moratinos, M., Villanueva, O., 2006. La alfarería en la Tierra de Zamora en época moderna. Instituto de Estudios Zamoranos "Florián de Ocampo", Diputación de Zamora, Zamora.

Morgado, P., Silva, R. C., Filipe, S., 2012. A cerâmica do açúcar de Aveiro: recentes achados na área do antigo bairro das olarias, in: Teixeira, A., Bettencourt, J. (Eds.), Velhos e novos mundos: estudos de arqueologia moderna. Lisboa, 2, 771–782.

Murillo-Barroso, M., Montero-Ruiz, I., Nieto, J.M., Camalich, M.M.D., Martín S.D., Martinón-Torres, M., 2019. Trace elements and lead isotopic composition of copper deposits from the eastern part of the Internal Zone of the Betic Cordillera (SE Iberia): application to provenance of archaeological materials. Journal of Iberian Geology, 45, 585-608.

Museo de Zamora, 2018. Bajo el suelo de Zamora, Ciudad, Arqueología, Museo. Exhibition Catalogue. Museo de Zamora (July-October 2018), Junta de Castilla y Leon, Zamora.

Museo Etnográfico, (01/11/2021). Museo Etnográfico de Castilla y León. https://museo-etnografico.com

Neal, A., Techkarnjanruk, S., Dohnalkova, A., McCready, D., Peyton, B., Geesey, G., 2001. Iron sulfides and sulfur species produced at hematite surfaces in the presence of sulfate-reducing bacteria. Geochimica et Cosmochimica Acta. 65, 223-235. DOI: 10.1016/S0016-7037(00)00537-8.

Neff, H., 2000. Neutron activation analysis for provenance determination in archaeology, in: John, W. (ed), Modern Analytical Methods in Art and Archaeology. Wiley, New York.

Neff, H., 2003. Analysis of Mesoamerican Plumbate Pottery Surfaces by Laser Ablation-Inductively Coupled Plasma-Mass Spectrometry (LA-ICP-MS). Journal of Archaeological Science. 30, 1, 21–35. ISSN 03054403. doi: 10.1006/jasc.2001.0801.

Neff, H., 2012. Laser Ablation ICP-MS in Archaeology, In: Handbook of Mass Spectrometry. John Wiley & Sons., New York.

Nelms, S.M., 2005. Inductively Coupled Plasma Mass Spectrometry Handbook. Blackwell Publishing Ltd. doi: 10.1002/9781444305463.

Neustupný, E., 1971. Whiter Archaeology?. Antiquity. 45, 177, 34–39. DOI: https://doi.org/10.1017/S0003598X00069027

Neustupný, E., 1993. Archaeological Method. Cambridge University Press

Newstead, S., 2008. Merida no more: Portuguese redware in Newfoundland. Unpublished Master's dissertation, Memorial University, Newfoundland.

Newstead, S., 2014. Cod, Salt and Wine: Tracing Portuguese Pottery in the English North Atlantic World. North Atlantic Archaeology. 3, 75-92.

Nodari, L., Maritan, L., Mazzoli, C., Russo, U., 2004. Sandwich structures in the etruscan-padan type pottery. Applied Clay Science. 27, 1, 119-128. http://dx.doi.org/10.1016/j.clay.2004.03.003.

Nodari, L., Marcuz, E., Maritan, L., Mazzoli, C., Russo, U., 2007. Hematite nucleation and growth in the firing of carbonate-rich clay for pottery production. J. Eur. Ceram. Soc. 27, 4665–4673, doi:10.1016/j.jeurceramsoc.2007.03.031.

Nolan, D.P., 2000. Encyclopedia of Fire Protection. Delmar Publishers, Albany, New York.

Noll, W., Holm, R., Born, L., 1975. Painting of ancient ceramics. Angewandte Chemie International Edition in English. 14, 9, 602-613. doi: 10.1002/anie.197506021

Nordenskiöld, G., 1893. The Cliff Dwellers of the Mesa Verde, Southwestern Colorado (Stockholm: P. A Norstedt and Söner)

Oakley, V., Jain, K., 2002. Essentials in the care and conservation of historical ceramic objects. 117 pp. Archetype Publications, Londres.

Onézime, J., Charvet, J., Faure, M., Bourdier, J.L., Chauvet, A., 2003. A new geodynamic interpretation for the South Portuguese Zone (SW Iberia) and the Iberian Pyrite Belt genesis. Tectonics 22, 1-17.

Orser, C. E., J.R., 2002. Portuguese colonialism, in: C.E. Orser, Jr. (ed.), Encyclopedia of historical archaeology: 490-494. London and New York: Routledge

Paterakis, A.B., 1987. The deterioration of ceramics by soluble salts and methods for monitoring their removal, in: Black, J. (ed.) Recent Advances in the Conservation and Analysis of Artifacts, pp. 67-72. Institute of Archaeology, University of London.

Paton, C., Hellstrom, J., Paul, B., Woodhead, J., Hergt, J., 2011. Iolite: Freeware for the visualisation and processing of mass spectrometric data. Journal of Analytical Atomic Spectrometry. 26, 2508-2518. DOI: 10.1039/C1JA10172B.

Papageorgiou, I., 2020. Ceramic investigation. How to perform statistical analyses. Archaeol Anthropol Sci. https://doi.org/10.1007/s12520-020-01142-x

Paynter, S., 2001. The development of vitreous materials in the ancient Near East and Egypt, PhD thesis, RLAHA, Oxford University

Pearson, K., 1987. Mathematical Contributions to the Theory of Evolution. - On a Form of Spurious Correlation Which May Arise When Indices Are Used in the Measurement of Organs. Proceedings of the Royal Society of London, 60:489–498. ISSN0370-1662. doi: 10.1098/rspl.1896.0076.

Pecci A., 2014. Organic Residue Analysis in Archaeology. In: Smith C. (eds) Encyclopedia of Global Archaeology. Springer, New York, NY. https://doi.org/10.1007/978-1-4419-0465-2_334

Peix Visiedo, J., Madrid i Fernández, M., Buxeda i Garrigós, J., 2021. The case of black and green tin glazed pottery from Barcelona between 13th and 14th century: Analysing its production and its decorations. Journal of Archaeological Science: Reports. 38. https://doi.org/10.1016/j.jasrep.2021.103100

Pérez, E. 1895 Guía de viajero en Zamora. Zamora

Pérez, J.A., Carriazo, J.L., 2010. Estudios de minería medieval en Andalucía. Universidad de Huelva.

Pérez-Arantegui, J., 2018. Métodos analíticos para el estudio de materiales de patrimonio histórico y artístico. In: Arqueometría de los materiales cerámicos de época medieval en España, 39–45. Universidad del País Vasco/Euskal Herriko Unibertsitatea.

Pérez-Arantegui, J., Resano, M., García-Ruiz, E., Vanhaecke, F., Roldán, C., Ferrero, J., Coll, J., 2008. Characterization of cobalt pigments found in traditional Valencian ceramics by means of laser ablation-inductively coupled plasma mass spectrometry and portable X-ray fluorescence spectrometry. Talanta. 74, 5, 1271–1280. ISSN 00399140. doi: 10.1016/j.talanta.2007.08.044.

Pérez-Arantegui, J., Montull, B., Resano, M., Ortega, J.M., 2009b. Materials and technological evolution of ancient cobalt-blue-decorated ceramics: Pigments and work patterns in tin-glazed objects from Aragon (Spain) from the 15th to the 18th century AD. J. Eur. Ceram. Soc. 29, 12, 2499–2509.

Perez Estaun, A., Bastida, F., Martinez Catalan, J.R., Gutierrez Marco, J.C., Marcos, A., Pulgar, J.A., 1990a., in: Dallmeyer, R. D., Martinez Garcia, E., (eds.), Pre-Mesozoic Geology of Iberia. pp. 92-102

Perez Estaun, Bastida, F., Rodriguez Fernandez, L. R., Heredia, N., 1990b., in: Dallmeyer, R. D., Martinez Garcia, E., (eds.), Pre-Mesozoic Geology of Iberia. pp. 55-71

Pernicka, 2011. Provenance determination of archaeological metal objects. Memorie del Museo Civico di Storia Naturale di Verona, 2.serie, Sezione Scienze dell'Uomo 11, 27-37

Picon, M., 1976. Remarques préliminaires sur deux types d'altération de la composition chimique des céramiques au cours du temps. Figlina. 1, 159-166.

Pingitore, N.E. Jr, Leach, J.D., Villalobos, J., Peterson, J.A., Hill, D.J., 1997. Provenance determination from ICP-MS elemental and isotopic compositions of El Paso area ceramics, in: Vandiver, P.B., Druzik, J.R., Merkel, J.F., Stewart, J. (eds) Material issue in art and archaeology V. MaterialsResearch Society, Pittsburgh, PA, pp 59–70

Pinto-Monte, M., 2021. Repensar la ceràmica valenciana d'època medieval i moderna des de l'arqueologia i l'arqueometria. Sistematització tipològica, producció i difusió, in: Tesis Doctorals en Xarxa, Barcelona.

Pinto-Monte, M., Madrid i Fernández, M., Buxeda i Garrigós, J., Coll, J., 2021. The medieval and post-medieval ceramics from Manises (Valencia). A reassessment from the new excavations at Barri d'Obradors. Journal of Archaeological Science: Reports. 39, 103135, ISSN 2352-409X, https://doi.org/10.1016/j.jasrep.2021.103135

Piñel, C., 1993. Cerámica producida en el Alfar de Olivares. Edad Moderna. Iglesia de Santo Tomé, in: Civitas. MC Aniversario de la Ciudad de Zamora, Catálogo de la exposición, Zamora, pp. 212-213.

Pleguezuelo, A., 2011. Lozas y azulejos de Triana – Coleccion Carranza. Ayto, Sevilla.

Pollard, M., Batt, C., Stern, B., Young, S.M.M., 2007. Analytical Chemistry in Archaeology. Cambridge University Press, Cambridge.

Ponting, M., Evans, J.A., Pashley, V., 2003. Fingerpriting of Roman mints using Laser-Ablation MC-ICP-MS Lead isotope analysis. Archaeometry. 45, 591–597

Pradell, T., Molera, J., 2020. Ceramic technology. How to characterize ceramic glazes. Archaeol Anthropol Sci. https://doi.org/10.1007/s12520-020-01136-9

Pradell, T., Vendrell-Saz, M., Krumbein, W.E., Picon, M., 1996. Altérations de céramiques en milieu marin: les amphores de l'épave romaine de la Madrague de Giens (Var). Revue d'achéométrie. 20, 47–56.

Pradell, T., Molera, J., Salvadó, N., Labrador, A., 2010. Synchrotron radiation micro-XRD in the study of glaze technology. Appl. Phys. A 99, 407–417.

Prieto-Taboada, N., Gómez-Laserna, O., Martínez-Arkarazo, I., Olazabal, M.Á., Madariaga, J.M., 2014. Raman Spectra of the Different Phases in the $CaSO_4$-H_2O System. Anal. Chem. 86, 10131–10137, doi:10.1021/ac501932f.

Pollard, A. M., Heron, C., 1996. Archaeological chemistry. Cambridge: The Royal Society of Chemistry

Possolo, A., 2015. Simple Guide for Evaluating and Expressing the Uncertainty of NIST Measurement Results. National Institute of Standards and Technology, 1297:1–20. ISSN 17426596. doi: 10.6028/NIST.TN.1900.

Possolo, A., 2016. Introducing a Simple Guide for the evaluating and expression of the uncertainty of NIST measurement results. Metrologia, 53, 17-24. doi:10.1088/0026-1394/53/1/S17.

Puig Barrachina, C., 2016. Les produccions ceràmiques del País Basc durant l'època baixmedieval i moderna. Una aproximació arqueomètrica, in: Tesis Doctorals en Xarxa, Barcelona.

Ramos, H. 1980 Cerámica popular de Zamora desaparecida. Valladolid

Rat, P., 1988. The Basque-Cantabrian Basin between the Iberian and European Plates. Some facts but still many problems. Rev. Soc. Geol. España, 1, 3-4.

Redondo, V., 2019. Personal communication.

Remesal, J.R, Revilla V.C., Martín-Arroyo Sánchez, D.J., Martín i Oliveras, A. (eds.)., 2019. Paisajes productivos y redes comerciales en el Imperio Romano / Productive landscapes and trade networks in the Roman Empire. Col·lecció Instrumenta ; 65. Edicions de la Universitat de Barcelona

Renfrew, C., Bahn, P., 1993. Arqueología: Teorías, métodos y práctica. Akal

Renson, V., Glascock, M.D., 2021. Lead Isotopes to Identify Underwater Ceramic Contamination: The Example of the Kyrenia Shipwreck (Cyprus). Minerals. 11, 625. https://doi.org/10.3390/min11060625

Resano, M., Perez-Arantegui, J., Garcia-Ruiz, E., and Vanhaecke, F., 2005. Laser ablation inductively coupled plasma mass spectrometry for the fast and direct

characterization of antique glazed ceramics. Journal of Analytical Atomic Spectrometry, 20(6):508–514.

Resano, M., Marzo, P., Perez-Arantegui, J., Aramendia, M., Cloquet, C., Vanhaecke, F., 2008. Laser ablation inductively coupled plasma-dynamic reaction cellmass spectrometry for the determination of lead isotope ratios in ancient glazed ceramics for discriminating purposes. J Anal Atom Spectrom. 23, 1182–1191

Reslewic, S., Burton, J.H., 2002. Measuring lead isotope ratios in Majolica from New Spain using a nondestructive technique, in: Jakes KA (ed) Archaeological chemistry: materials, methods, and meaning. American Chemical Society, Washington, DC, pp 36–47

Rice, P., 1987. Pottery Analysis: a Sourcebook. University of Chicago Press, Chicago

Rice, P., 2015. Pottery analysis: a sourcebook. University of Chicago Press, Chicago.

Richards, T.W., 1895. The composition of Athenian Pottery. American Chemical Journal. 17, 152-154.

Roca, E., 1994. Geodynamic evolution of the Catalan-Balearic Basin and neighbouring areas from Mesozoic to Recent (La evolucion geodinamica de la Cuenca Catalano-Balear y areas adyacentes desde el Mesozoico hasta la actualidad). Acta Geologica Hispanica. 29, 3– 25.

Roffet-Salque, M., Dunne, J., Altoft, D.T., Casanova, E., Cramp, L.J.E., Smyth, J., Whelton, H.L., Evershed, R.P., 2017. From the inside out: Upscaling organic residue analyses of archaeological ceramics. Journal of Archaeological Science: Reports. 16, 627-640. DOI: https://doi.org/10.1016/j.jasrep.2016.04.005

Roldán, C., Coll, J., Ferrero, J., 2006. EDXRF analysis of blue pigments used in Valencian ceramics from the 14th century to modern times. J. Cult. Heritage. 7, 134–138.

Roux, V., 2019. Introduction to Ceramic Technology. In Ceramics and Society, pages 1–14. Springer, Berlin.

Sabaté, A. A., Melgarejo, J.C., Tauler, E., Torró, L., Manteca, J.I., Arnold, M., 2015. Ore Deposits in La Unión-Portmán District: Mineralogical and Geochemical Characterization. 13th SGA Biennial Meeting 2015, Nancy, France, volume 1, 355-358.

Sabbatini, L., Tarantino, M., Zambonin, P., De Benedetto, G.E., 2000. Analytical characterization of paintings on pre-Roman pottery by means of spectroscopic techniques. Part II: Red, brown and black colored shards. Fresenius J Anal Chem. 366, 116–124. https://doi.org/10.1007/s002160050021

Salinas, E., Pradell, T., 2018. Primeros resultados del proyecto «La introducción del vidriado en al-Andalus: olas tecnológicas e influencias orientales», a partir de análisis arqueométricos, in: Arqueometría de los Materiales Cerámicos en España, pages 241–252. Servicio Editorial de la Universidad del País Vasco, 2018. ISBN 978-84-9082-907-3

Sánchez, J., 1989. De Minería, metalúrgica y comercio de metales. La minería no férrica en el Reino de Castilla 1450-1610. Ediciones Universidad de Salamanca, Salamanca.

Sánchez-Cortegana, J.M., 1994. El oficio de ollero en Sevilla en el siglo XVI. Sevilla: Diputación Provincial de Sevilla.

Sanchez-Garmendia, U., Calparsoro, E., Arana, G., Iñañez, J.G., 2018. Beneath sacred land: glazed pottery from the old church of La Concepción in Zamora, in: GlazeArt2018 Lisbon, Lisbon, pp. 361-379.

Sanchez-Garmendia, U., Calparsoro, E., Morillas, H., Arana, G., Iñañez, J.G., 2020a. Pottery from the Ethnographic Museum archaeological site of Zamora: an archaeometric approach. Journal of Archaeological Science Reports. 33. DOI: https://doi.org/10.1016/j.jasrep.2020.102514

Sanchez-Garmendia, U., Carvalho, P., Bettencourt, J., Silva, R.C., Arana, G., Iñañez, J.G., 2020b. Submerged and reused: an archaeometric approach to the Early Modern ceramics from Aveiro (Portugal). Journal of Archaeological Sciencie Reports, 34. doi: 10.1016/j.jasrep.2020.102648.

Sanchez-Garmendia, U., Iñañez, J.G., Arana, G., 2021a. Alterations and Contaminations in Ceramics Deposited in Underwater Environments: An Experimental Approach. Minerals. 11, 766. https://doi.org/10.3390/min11070766

Sanchez-Garmendia, U., Billström, K., Kielman, M., Bellucci, J., Kooijman, E., Arana G., Iñañez, J.G., 2021b. Zamorako zeramiken beiratua egiteko zeramikariek erabilitako galenaren jatorrizko meatzearen identifikazioa, berun isotopoen analisiaren bidez. IV. Ikergazte. Nazioarteko ikerketa euskaraz. Kongresuko artikulu

bilduma. Zientziak eta Natura Zientzia. UEU arg. https://dx.doi.org/10.26876/ikergazte.iv.05.05

Sandalinas, C., Ruiz-Moreno, S., López-Gil, A., Miralles, J., 2006. Experimental confirmation by Raman spectroscopy of a Pb-Sn-Sb triple oxide yellow pigment in sixteenth-century Italian pottery. Journal Raman Spectroscopy. 37, 1146–53. https://doi.org/10.1002/jrs.1580.

Santarelli, B., Goff, S., Killick, D., Schleher, K., Gonzales, D., 2019. Lead isotope ratios of Pueblo I lead-glazed ceramics and galena from Colorado and Pueblo II galena from Chaco Canyon, New Mexico. Journal of Archaeological Science: Reports. 23, 634–645. https://doi.org/10.1016/j.jasrep.2018.11.027

Santos Zalduegui, J.F., García de Madinabeitia, S., Gil Ibarguchi, J.I., 2004. A lead isotope database: the Los Pedroches – Alcudia area (Spain); implications for archaeometallurgical connections across southwestern and southeastern Iberia. Archaeometry. 46, 4, 625-634.

Sanz, F.J., Misiego, J.C., Marcos, G.J., Martín, M.A., Fernández, E., García, M.I., 2005. La actividad artesanal en el barrio de Olivares de Zamora. Los Hallazgos en el solar de la Plaza de San Claudio, 6 c/v a la Calle Mediodía, 2. Anuario 2005 del Instituto de Estudios Zamoranos "Florián de Ocampo", 22, pp. 229-240.

Sayre, E. V., Dodson, R. W., & Thompson, D. B., 1957. Neutron Activation Study of Mediterranean Potsherds. American Journal of Archaeology. 61, 1, 35–41. https://doi.org/10.2307/501078

Sayre, E.V., Harbottle, G., Bieber, A.M., Brooks, D., 1976. Application of Multivariative Techniques to Analytical Data on Aegean Ceramics. Archaeometry. 18, 1, 59–74. ISSN 0003-813X. doi: 10.1111/j.1475-4754.1976.tb00145.x.

Schiffer, M.B., 2011. Studying Technological Change: A Behavioral Approach. University of Utah Press, Salt Lake City

Schiffer, M.B., Skibo, J., 1989. A Provisional Theory of Ceramic Abrasion. American Anthropologist (New Series). 91, 1, 101-115.

Schoonen, M. A. A., 2004. Mechanisms of sedimentary pyrite formation. Geological Society of America. 379, 117-134. DOI: 10.1130/0-8137-2379-5.117

Schurr, M.R., Donohue, P.H., Simonetti, A., Dawson, E.L., 2018. Multi-element and lead isotope characterization of early nineteenth century pottery sherds from

Native American and Euro-American sites. Journal of Archaeological Science: Reports. 20, 390-399. https://doi.org/10.1016/j.jasrep.2018.05.014.

Schwedt, A., Mommsen, H., Zacharias, N., 2004. Post-depositional elemental alterations in pottery: neutron activation analyses of surface and core samples. Archaeometry. 46, 1, 85–101.

Schwedt, A., Mommsen, H., Zacharias, N., Buxeda i Garrigós, J., 2006. Analcime crystallization and compositional profiles - comparing approaches to detect post-depositional alterations in archaeological pottery. Archaeometry. 48, 2, 237–251.

Sciau, P., Sanchez, C., Gliozzo, E., 2020. Ceramic technology, How to characterise terra sigillata ware. Archaeol Anthropol Sci . https://doi.org/10.1007/s12520-020-01137-8

Sebastian, L., 2010. A produção oleira de faiança em Portugal (séculos XVI-XVIII). Dissertação de Doutoramento em História com especialidade de Arqueologia. Facultade de Ciências Sociais e Humanas, Universidade Nova de Lisboa.

Secco, M., Maritan, L., Mazzoli, C., Lampronti, G.I., Zorzi, F., Nodari, L., Russo, U., Mattioli, S.P., 2011. Alteration processes of pottery in lagoon-like environments. Archaeometry. 53, 809–829.

Šefců, R., Chlumská, S., Hostasová, A., 2015. An investigation of the lead tin yellows type I and II and their use in Bohemian panel paintings from the Gothic period. Heritage Science. 3, 16, 1-15. https://doi.org/10.1186/s40494-015-0045-2.

Sempere, E., 1982. Rutas a los alfares. Barcelona: Selbstverl.

Shepard, A.O., 1956. Ceramics for the Archaeologist. Number 609. Carnegie Institution of Washington Washington

Shortland, A.J., 2006. Application of lead isotope analysis to a wide range of late Bronze Age Egyptian materials. Archaeometry. 48, 657–669

SIEMCALSA, 2007. La Minería en Castilla y León. Junta de Castilla y León. Consejería de Economía y Empleo. ISBN: 978-84-9718-445-8.

Silva R.C., 2015. Late 16th century glazed ceramics from Coimbra (Portugal). Trabalho apresentado em XIth Congress on Medieval and Modern Period Mediterranean Ceramics of AIECM3.

Silva, R. C., 2018. Um carrego de abóbada na igreja quinhentista de Santo António (Aveiro, Portugal). Revista portuguesa de arqueologia. 21, 1, 181-195.

Skibo, J.M., 1992. Pottery Function. A use-alteration perspective. Plenum Press, New York.

Skibo, J.M., 2013. Understanding Pottery Function. Springer, New York

Skibo, J.M., Schiffer, M.B., 1987. The effects of water on processes of ceramic abrasion. Journal of Archaeological Science. 14, 83-96.

Skibo, J.M., Schiffer, M.B., 2008. People and things: A behavioral approach to material culture. Springer, New York

Solaun, J.L., 2005. Erdi Aroko zeramika Euskal Herrian (VIII.-XIII. Mendeak): ekoizpenaren sistematizazioa, bilakaera eta banaketa. Eusko Jaurlaritzaren argitalpen zerbitzu nagusia. ISBN 844572410X.

Sousa, E., 2006. A Cerâmica do Açúcar das cidades de Machico e do Funchal. Dados Históricos e Arqueológicos para a Investigação da Tecnologia e Produção do Açúcar em Portugal, in: E. Sousa (ed.), A Cerâmica do Açúcar em Portugal na Época Moderna: 10-31. Lisboa/Machico: Centro de Estudos de Arqueologia Moderna e Contemporânea.

Sousa, E., Silva, J., Gomes, C., 2005. Chemical and physical characterization of fragments from ceramic jars called “formas de açúcar” exhumed in the town of Machico, Madeira Island, in: Proceedings of the 7th European Meeting on Ancient Ceramics (EMAC’03).

Speakman, R.J., Glascock, M.D., 2007. Acknowledging Fifty Years of Neutron Activation Analysis in Archaeology. Archaeometry, 49, 2, 179–183.

Speakman, R.J., Neff, H., Glascock, M.D., Higgins, B.J., 2002. Characterization of archaeological materials by laser ablation-inductively coupled plasma-mass spectrometry, in: Jakes, K.A. (Ed), Archaeological Chemistry, Materials, methods and meaning. American chemical society, Washington

Speakman, R.J., Little, N.C., Creel, D., Miller, M.R., Iñañez, J.G., 2011. Sourcing ceramics with portable XRF spectrometers? A comparison with INAA using Mimbres pottery from the American Southwest. Journal of Archaeological Science, 38, 12, 3483-3496. doi: https://doi.org/10.1016/j.jas.2011.08.011

Stemm, G., Gerth, E., Flow, J., Guerra-Librero, C.E., Kingsley, S., 2013. The Deep-Sea Tortugas shipwreck, Florida: a Spanish-operated Navio of the 1622 Tierra Firme

Fleet. Part 2, the artifacts, odyssey marine exploration papers 27. Odyssey Marine Exploration

Stoner, W.D., Shaulis, B.J., 2021. Chemical Mapping to Evaluate Post-Depositional Diagenesis among the Earliest Ceramics in the Teotihuacan Valley, Mexico. Minerals. 11, 384. https://doi.org/10.3390/min11040384

Storey, J.M.V., Symonds, R.P., Hart, F.A. and Walsh, J.N., 1988. The chemical investigation of 'Colchester' Samian by means of inductively coupled plasma emission spectrometry. Journal of Roman Pottery Studies, 2, 33-43.

Stos-Gale, Z., Gale, H., 2009. Metal provenancing using isotopes and the Oxford archaeological lead isotope database (OXALID). J Archaeol Anthropol Sci. 1, 195–213

Stos-Gale, Z., Gale, N.H., Houghton, J., Speakman, R., 1995. Lead isotope data from the Isotrace Laboratory, Oxford: ARCHAEOMETRY data base 1, ores from the Western Mediterranean. Archaeometry. 37, 2, 407-415.

Stos-Gale, Z., Maliotis, G., Gale, N.H., Annetts, N., 1997. Lead isotope characteristics of the Cyprus copper ore deposits applied to provenance studies of copper oxhide ingots. Archaeometry. 39, 83–123

Stroup, D., Taylor, G., Hausman, G., Salley, M. H., 2013. Fire Dynamics Tools (FDTs) Quantitative Fire Hazard Analysis Methods for the U.S. Nuclear Regulatory Commission Fire Protection Inspection Program (NUREG-1805, Supplement 1, Volumes 1 & 2).

Subías, I., Fanlo, I., Mateo, E., Billström, K., Recio, C., 2010. Isotopic studies of Pb–Zn–(Ag) and barite Alpine vein deposits in the Iberian Range (NE Spain). Chemie der Erde. 70, 149-158.

Suda, Y., Adachi, T., Shimada, K., Osanai, Y., 2021. Archaeological significance and chemical characterization of the obsidian source in Kirigamine, central Japan: Methodology for provenance analysis of obsidian artefacts using XRF and LA–ICP–MS. Journal of Archaeological Science. 129, 105377, ISSN 0305-4403, https://doi.org/10.1016/j.jas.2021.105377.

Taylor, J.W., 1983. Erzgebirge tin: A closer look. Oxford Journal of Archaeology. 2, 295–298

Thér, R., 2020. Ceramic technology. How to reconstruct and describe pottery-forming practices. Archaeol Anthropol Sci. https://doi.org/10.1007/s12520-020-01131-0

Thibodeau, A.M., Killick, D.J., Ruiz, J., Chesley, J.T., Deagan, K., Cruxent, J.M., Lyman, W., 2007. The strange case of the earliest silver extraction by European colonists in the New World. Proc Natl Acad Sci USA. 104, 3663–3666

Thomas, J., Glass, D.H., White, A.W., Trandel, M.R., 1977. Fluoride content of clay minerals and argillaceous earth materials. Clays Clay Miner. 25, 278-284.

Tite M.S., 1995. Firing temperature determination–how and why?, in: Lindhal, A., Stilborg, O. (Eds.), The aim of laboratory analyses of ceramics in Archaeology. 37-42. Lund, Sweden, in honour of Birgitta Huthén, Stockholm: Kungl. Vitterhets historie och antikvitets akademien.

Tite, M. S., Freestone, I., Meeks, N., Bimson, M., 1982. The use of scanning electron microscopy in the technological examination of ancient ceramics. Smithsonian Institution Press, Washington D. C.

Tite, M.S., Freestone, I., Mason, R., Molera, J., Vendrell-Saz, M., Wood, N., 1998. Lead glazes in antiquity - Methods of production and reasons for use. Archaeometry, 1998. ISSN 0003813X. DOI: 10.1111/j.1475-4754.1998.tb00836.x

Todt, W., Cliff, R.A., Hanser, A., Hofmann, A.W., 1996. Evaluation of a 202Pb–205Pb double spike for high precision lead isotope analysis. In: A. Basu,S. Hart (Eds.), Earth Processes: Reading the Isotopic Code (1996), pp.429-437. American Geophysical Union Geophysical Monograph, 95

Tornos, F., 2003. Base metal deposits in Spain: mineralization in a diversity of environments. Irish Association for Economic Geology.

Tornos, F., Chiaradia, M., 2004. Plumbotectonic Evolution of the Ossa-Morena Zone, Iberian Peninsula: Tracing the Influence of Mantle-Crust Interaction in Ore-Forming Processes. Economic Geology. 99, 965-985.

Tornos, F.; Locutura, J., Martins, L., 1999. The Iberian Pyrite Belt Field trip guide. Joint SGA IAGOD International Meeting.

Tornos, F., Inverno, C.M.C., Oliveira, V., Gasquet, C., 2004. The metallogenic evolution of the Ossa-Morena Zone. Journal of Iberian Geology. 30, 143-181.

Trigger, B.G., 1988. Archaeology's relations with the physical and biological sciences: a historical review, in: R.M. Farquhar, R.G.V. Hancock & L.A. Pavlish (ed.) Proceedings of the 26th International Archaeometry Symposium: 1–9. Toronto: University of Toronto.

Tschegg, C., 2009. Post-depositional surface whitening of ceramic artifacts: Alteration mechanisms and consequences. Journal of Archaeological Science. 36, 10, 2155-2161. DOI: 10.1016/j.jas.2009.05.030

Tubb, A., Parker, A.J., Nickless, G., 1980. The analysis of Tomano-British pottery by Atomic Absorption Spectrophotometry. Archaeometry, 22, 2, 153-171.

Turina, A., 1994. Cerámica medieval y moderna de Zamora, first ed. Instituto De Estudios Zamoranos Florián De Ocampo, Zamora.

Vallvé, J., 1996. La minería en al-Andalus, in: Actas de las I Jornadas sobre Minería y Tecnología en le Edad Media Peninsular p. 56-64.

Velasco, F., Pesquera, A., Herrero, J.M., 1996. Lead isotope study of Zn-Pb ore deposits associated with the Basque-Cantabrian basin and Paleozoic basement, Northern Spain. Mineral Deposita. 31, 84-92.

Velasco, F., Herrero, J.M., Yusta, I., 2003. Geology and Geochemistry of the Reocín Zinc-Lead Deposit, Basque-Cantabrian Basin, Northern Spain. Economic Geology. 98, pp. 1371-1396.

Vendrell-Saz, M., Molera, J., Tite, M. S., 2000. Optical Properties of Tin-Opacified Glazes. Archaeometry. 42, 2, 325–340. ISSN 1475-4754. doi: 10.1111/j.1475-4754.2000.tb00885.x.

Vieira, L. F., Ferreira, I., Ferraria, A. M., Casimiro, T. M., Colomban P., 2013. Portuguese tin-glazed earthenware from the 16th century: A spectroscopic characterization of pigments, glazes and pastes. Applied Surface Science. 285, 144-152. doi: 10.1016/j.apsusc.2013.08.016.

Villanueva, L.A., Martín, M.A., Marcos, G.J., Sanz, F.J., Misiego, J.C., Fernández, E., 2000. Un taller de orfebrería de Época Bajomedieval y Moderna, bajo los restos de la Iglesia y Convento de Nuestra Señora de La Concepción, de Zamora, in: Anuario 2000 del Instituto de Estudios Zamoranos "Florián de Ocampo". Zamora, 17, pp. 79-112.

Villanueva, O., 2011. La Ollería y alcallería en la cuenca del Duero a lo largo de la Edad Media y Moderna, Manual de Cerámica Medieval y Moderna. Museo Arqueológico Regional, Madrid.

Wahl, J., 1998. Aspectos tecnológicos da indústria mineira e metalúrgica romana de Três Minas e Campo de Jales (Concelho de Vila Pouca de Aguiar), in: J.M. Brandão (coor.). Actas do Seminário Arqueologia e Museologia Mineiras. Lisboa, 57-68

Wang, L., Putnis, V.C., Ruiz-Agudo, E., King, E.H., Putnis, A., 2013. Coupled Dissolution and Precipitation at the Cerussite-Phosphate Solution Interface: Implications for Immobilization of Lead in Soils. Environ. Sci. Technol. 47, 23, 13502-13510. https://doi.org/10.1021/es4041946.

Wang, Y., Wei, G., Li, Q., Zheng, X., Wang, D., 2021a. Provenance of Zhou Dynasty bronze vessels unearthed from Zongyang County, Anhui Province, China: determined by lead isotopes and trace elements. Herit Sci 9, 97. https://doi.org/10.1186/s40494-021-00566-5

Wang, M., Wang, T., Wang, F., Hole, C., Cao, J., Zhu, J., Zhang, P., Shi, P., Sciau, P., 2021b. Raman study of rusty oil spotted glaze produced in Linfen kilns (Shanxi province, AD 1115–1368). J Raman Spectrosc. 1. https://doi.org/10.1002/jrs.6229

Weigand, P.C., Harbottle, G., Sayre, E.V., 1977. Turquoise sources and source analysis: Mesoamerica and the southwestern USA | University College London. Exchange Systems in Prehistory, pages 15–34. DOI: 10.1016/B978-0-12-227650-7.50008-0.

Whitney D.L., Evans B.W., 2010. Abbreviations for names of rock-forming minerals. Am Miner. 95, 1, 185–7.

Wolf, S., Stos, S., Mason, R., Tite, M.S., 2003. Lead isotope analyses of Islamic pottery glazes from Fustat, Egypt. Archaeometry. 45, 3, 405–420. https://doi.org/10.1111/1475-4754.00118.

Woodhead, J.D., Hergt, J. M., 2000. Pb-isotope analyses of USGS reference materials. Geostandards Newsletter, 24, 33–38

Yener, K.A., Sayre, E.V., Joel, E.C., Özbal, H., Barnes, I.L., Brill, R.H., 1991. Stable lead isotope studies of central Taurus ore sources and related artifacts from eastern Mediterranean Chalcolithic and Bronze Age sites. J Archaeol Sci. 18, 541–577

Young, S.M.M., Budd, P., Haggerty, R., Pollard, A.M., 1997. Inductively coupled plasma-mass spectrometry for the analysis of ancient metals. Archaeometry. 39, 379-392. https://doi.org/10.1111/j.1475-4754.1997.tb00814.x

Zornoza-Indart, A., 2012. Técnicas de Desalación, in: La Conservación de los Geomateriales Utilizados en el Patrimonio. Programa Geo-materiales: Madrid, Spain. pp. 143–154.

Eranskinak / Appendices

CHAPTER 1: INTRODUCTION

1.1. What are the ceramics?

Ceramics are among the most abundant materials found in the excavations across both geography and time thanks to their durable nature and because they were one of the main tools used by humanity since the Neolithic (Gliozzo, 2020a). The term "ceramic" comes from the *keramos* Greek word, translated as "burned stuff" or "earthenware". It describes a fired product rather than a clay raw material (Rice, 1987).

The ceramic body (called also as "ceramic paste") is composed by plastic and non-plastic (tempers) components and it is the result of the manipulation of the clay. The plastic components are phyllosilicates present in the raw materials (mainly clays like kaolinite, illite, montmorillonite, etc., and mica, among others), while the temper phases can be natural rocks and/or mineral fragments (e.g. feldspars, quartz, sand, crushed rock, etc.) as well as those from biological origin (e.g. plant fibres, shells, dung) or artificial inorganic materials (e.g. broken ceramics called also as "grog" or "chamotte", ashes, etc.) (Shepard, 1956). Tempers are materials added to the clay or clay-mixtures to neutralize excessive shrinkage during firing, in this way, preventing the cracking of the ceramic pieces (Astarloa et al., 2016). The mixture of plastic and non-plastic components provides specific properties to the ceramics, such as texture, colour, colloidal state, plasticity and particle size (Rice, 1987).

Although Medieval and Post-Medieval ceramics are grouped into a number of categories based on their composition, firing and surface treatments (e.g. terracottas, earthenwares, stonewares and porcelains), they are divided into two general groups: simple and complex (Figure 1.1.) (Buxeda i Garrigós and Madrid i Fernández, 2017). On the one hand, simple ceramics do not show any coating and are formed only by the materials of the body. In addition, they might be decorated with simple decorative forming techniques (such as polishing or incising). On the other hand, complex ceramics include decorations (pigments), glazes or slips, which are made of exogenous materials. A slip is a fluid suspension of clay in water, which is applied before firing to form a thin coating. Slips may also be called "engobes", but this term tends to be used primarily with reference to high-fired ceramics. Contrariwise, a glaze is a particular kind of glass, a non-crystalline substance cooled rapidly from a melt and fused with the surface of a vessel. Glazes are applied for the same reasons as slips, that is, to add colour or texture as well as to reduce permeability. Nevertheless, they are very different from slips because they are compositionally complex, high fired and they make the surface completely impermeable (Rice, 1987). The technology of glazing ceramics was introduced by the Islamic world into the Iberian Peninsula (Salinas and Pradell, 2018; Tite et al., 1998). Glazes may be opaque or translucent, shiny or matte, coloured or non-coloured, thick or thin, and occasionally they may develop a crystalline structure. Moreover, glazes were applied in several ways: 1) before the first firing of the artefact (using the called one firing method); 2) on the pre-fired ceramic body also known as "biscuit" (using the called two-firing method, called also as "biscuit firing"); or 3) in a third firing, which was used for luster pottery or *copperta* majolica technique, among others. Factors such as the thermal stability of the compounds used to cover the ceramic body, their shrinkage and expansion-coefficient will determine the adherence of the glaze with the clay body (Molera et al., 1997). The primary constituent used in ancient glazes was silica (silicon dioxide, SiO_2, commonly found in nature as quartz), and a component acting as a flux was added to lower the melting point of silica. These components were, for example, ashes (forming an ash glaze, or transparent alkali glaze, in which potassium and sodium were principal fluxing agents) or a lead (II) oxide (PbO). The lead was widely used in glazes because it has a similar coefficient of expansion to the clays present in the ceramic body. Contrariwise, when these coefficients are not similar, the glazes can peel off or crackle (Tite et al., 1998). Furthermore, metals such

as Cu (from copper metal debris or minerals like malachite and azurite), Co (from minerals like cobaltite, skutterudite and erythrite) and Mn (from minerals like braunite and hausmannite, among others), to obtain green, blues and brown/blacks, respectively, were sometimes added also as pigments. These pigments were applied following an over-glaze or under-glaze strategy, which was applying the coloured motifs on the biscuit ceramic and later covered by a glaze (*underglaze* technique) or applying first the glaze coating and the decoration on top of it (*overglaze*) (Molera et al., 1997; Rice, 1987). The underglaze technique in transparent glazes has been documented in Islamic ceramics from the 9th century (Coentro et al., 2020), for example in Raqqada (Ben Amara et al., 2011) and Palermo (Arcifa and Bagnera, 2018). Then, this technique started to develop in the 14th century in tin-lead glazed ceramics. According to the archaeological evidences, in white opaque glazes from Valencia, potters applied the blue pigments in the biscuit ceramic and then they fired the object for the first time (Coentro et al., 2020). Then, they applied the frit and fired the piece for the second time (Coll Conesa, 2009). This technology has been documented for example in ceramics from the 14th century from Granada (García-Porras, 2012).

Figure 1.1. Simple and complex ceramics unearthed at the region of Zamora, from left to right: biscuit beige ceramic (simple), biscuit red ceramic (simple), translucent-glazed (complex), white opaque glazed (complex) and decorated opaque glazed (complex). Scale bar: 8 cm

In traditional pottery, lead glazes have been extensively used since the 10th-11th centuries until the present (Molera et al., 2001; Rice, 1987; Tite et al., 1998). Since Medieval times, the translucent lead glazes (see Figure 1.1.) were produced in two ways: as a raw suspension and as a frit. The former consisted on making a powder mixture of lead compounds (could be lead (II) oxide (PbO), red lead (Pb_3O_4), white lead ($2PbCO_3{\cdot}Pb(OH)_2$) or galena (PbS)) and silica as a suspension in water. The lead oxides were obtained by melting metallic lead in a furnace or a domestic hearth and skimming off the oxide layer. Although it was possible to use galena directly, it was also common to first roast galena to form the oxide (Tite et al., 1998). However, this method produces a scum on the glaze during firing, and thus, the glaze appears powdery with patches of glaze mixed with regions showing undissolved glaze components (Paynter, 2001). The latter method, however, was consisted, in order to obtain a good homogeneous glaze, on first, melting together lead compound and silica, that is known as *fritting*, giving a *frit* as a product. This frit was then ground to a powder before being used to prepare the water suspension (Tite et al., 1998). Finally, the water suspension obtained from the two production ways was then applied over a dry unfired or biscuit ceramic body (normally red) and was melted at temperatures between 700 °C and 1000°C, depending on the composition. In the present work, when the term “translucent glaze” is used, it actually refers to “translucent lead glaze”.

Another kind of ceramic, known typically as “tin-lead glazed ceramic”, “majolica” or “faience” (see Figure 1.1.), which shows a white opaque glaze, had a more complicated production sequence. The names of majolica and faience purportedly have their origin in the trade networks of different regions. Mallorca is an island from which tin-glazed wares were shipped to Italy, so Italians named the pottery after the island, *maiolica* (in Italian); Faenza is a city in Italy from which Italian tin-glazed wares were exported to France, so the

French called the pottery *faïence* (in French) (Rice, 1987). The production sequence involved the preparation of a suspension containing, apart from a lead compound and silica, cassiterite (a tin dioxide, SnO_2, for obtaining the white opaque glaze) and an alkali. This mixture was also prepared previously as a frit and it was then powdered before being used to produce the water suspension, like in the procedure for translucent lead glazes (Tite et al., 1998). This suspension was generally applied to a biscuit ceramic (a ceramic that has been pre-fired) because it does not suffer expansion or contraction as a result of wetting and subsequent drying, and then, the ceramic was fired. Furthermore, a decorative layer including pigments was sometimes applied (as under-glazed decoration or over-glazed decoration).

1.1.1. The study of ceramics, what for?

Archaeology is the study of human societies through their material remains (González-Ruibal and Ayán Vila, 2018) and in the present work, the materials that are studied are ceramics. One of the reasons is that they are the most widespread materials in terms of chronological range and geographical distribution; moreover, they present optimal preservation conditions in the archaeological record (Fantuzzi, 2010).

Furthermore, ceramics present an inherent duality: the cultural and natural dimensions (Neustupný, 1971, 1993). The main motivation behind the examination of ceramics roots on their cultural dimension, in which the ceramics act as technological, socio-economical as well as socio-cultural and chronological indicators (Buxeda i Garrigós and Madrid i Fernández, 2017; Buxeda i Garrigós et al., 2010; Schiffer, 2011; Skibo, 2013; Skibo and Schiffer, 2008). For example, as regards the socio-economical aspect, the study of ceramics can provide the identification of daily-use objects (likely of moderate cost) and the precious items (from wealthy families). In this way, the researchers would be able to shed light on aspects such as the cultural characteristics and dietary habits of a specific population (Colombini et al., 2005; Evershed, 2008; Pecci, 2014; Roffet-Salque et al., 2017). Moreover, identifying the geographical localization of the ceramic workshops, it may also be possible to reconstruct commercial trading networks (e.g. determining issues such as short-range vs. long-range exchange, local consumption or export, etc.) and the type of route (terrestrial, riverine/ lacustrine or marine) used for the transportation of goods (Blomster et al., 2005; Glascock, 2002; Knappett, 2013; Remesal et al., 2019).

When it comes to the chronological aspect of ceramics, these materials can act as chronological indicators for the periodization of the stratigraphic sequence in the archaeological excavation. In this way, the most recent ceramic object found in a layer provides the term *post quem* for dating the layer (Harris, 1979; Renfrew and Bahn, 1993).

Finally, regarding the technological aspect, the study of the ceramic production provides to keep knowledge on the manufacturing technique used by the potters, which is determined by the technical skills, the traditions and the cultural frame of the society they lived in. For example, experimentation with new types of firing-structures (e.g. bonfire, single chamber kiln, double chamber kiln, etc.) was accompanied by developments in form and decoration, such as the application of functional coatings. In this regard, the transformation of raw materials on artefacts undergone in ceramics implies seeking certain physical properties, which will provide the final object the desired properties (malleability and fusibility) and the formal design in order to ensure that the final product can perform the wanted function (Buxeda i Garrigós and Madrid i Fernández, 2017; Gliozzo, 2020a; Heimann, 1989; Maggetti, 1982; Roux, 2019; Schiffer, 2011).

Some of the relevant questions that arise before starting to study ceramics, or while studying them, are the next ones: which kind of raw materials were used? Were different types of raw materials used depending on the use of the ceramic (e.g. tableware, transport, etc.)? How were the raw materials prepared? Was temper added? Why? What type of atmosphere (oxidizing or reducing) was obtained during firing? Which were the firing temperatures for the ceramics? Were the atmospheres obtained and temperatures reached intentional? Were the surfaces coated, decorated or glazed? How? Why? Which raw materials were used for the surface finish? Where they available onsite or imported? Is there a correlation between shape, composition and function? Was the ceramic destined for local use or to be exported, or both? Was a ceramic type used by poor or wealthy population or by both? Which is the provenance of that ceramics? Was there any pottery distribution? Any commercial trade? Which? Which dietary habits or other daily practices can be deduced from the ceramic evidence? As it can be noted, all these questions are resumed in technological, socio-economical, socio-cultural, provenance and chronological aspects of ceramics.

1.2. The principals of the archaeometric study

Archaeometry consists on the application of analytical techniques taken from experimental sciences, which allow analysing the cultural dimension of the artefact, through its natural dimension. Archaeometry answers archaeological questions, taking into account all the archaeological knowledge about the subject that is being studied.

Traditionally in Archaeology, the study of archaeological ceramics has consisted on classifications based on their morphological properties, paste colour and decorative characteristics. Admitting that this knowledge is of great value for the knowledge of a ceramic production, it is insufficient in some cases, especially when it comes to small fragments, often without decoration or clear typology, as well as unknown materials or those of uncertain origin. Along these lines, the questions about the provenance, technological, socio-economical as well as socio-cultural, and chronological aspects of ceramics require to be answered by means of the natural aspect they bear (using an archaeometric model) since they are material objects (Buxeda i Garrigós et al., 1995). Some relevant published articles about this model are those of Boulanger et al. (2013), Buxeda i Garrigós (1999) and Buxeda i Garrigós and Madrid i Fernández (2017). In the following lines, the principals of the archaeometric approach used in this Doctoral Thesis are explained. The followed approach is divided mainly in two complementary parts: the provenance and the study of the technology. Through them, socio-economical, socio-cultural and chronological aspects are also studied. It must be highlighted that the analysis of the ceramics can have a much broader perspective. In the present work other type of ceramic materials have been excluded from the present study, such as those related to construction (e.g. tiles) or the organic matter present in the residues of the ceramics, that can provide very valuable information regarding past human behaviour (e.g. Blanco-Zubiaguirre et al., 2018, 2019; Pecci, 2014).

The archaeometric model followed in this work is based on the one posed by Buxeda i Garrigós and Madrid i Fernández (2017), which is based on the *chaîne opératoire* of ceramics (Roux, 2019). The chain goes from of the as-received ceramic (its recovery in the archaeological site) to the area where the ceramist extracted the raw materials, which most probably was the same of the workshop (or nearby). Besides, it is important to note that in

Archaeology, ceramics are often referred to as calcareous or low-calcareous. In this work, the division of calcareous ($CaO \geq 6$ %) and low-calcareous ($CaO < 6$ %) has been made.

1.2.1. Provenance study

First, it should be clarified that the provenance of a ceramic is not necessarily the place where the artefact was rescued. The provenance is the place where the ceramics had been produced, since it is assumed that the place of origin of the clay was generally the same as that of production. That assumption is usually true during ancient times, given the costs that transport would entail, or even the impossibility of trading large amounts of raw materials, so the accessibility to raw materials imposed the location for the producing activity in most of the cases (Buxeda i Garrigós, 2010). Although when speaking about provenance I mainly refer to provenance studies of ceramic pastes, provenance studies can also carry out on ceramic lead-based glazes. Thus, hereafter all the allusions will be made to provenancing the ceramic pastes, unless the contrary is stated.

The first step for the identification of the provenance of archaeological ceramics of Medieval and Post-Medieval Eras, is to classify them into meaningful ceramic groups. Groups are defined through the material nature of the ceramics, analysing the chemical composition of ceramic pastes or making petrographic analyses (Buxeda i Garrigós and Madrid i Fernández, 2017) (Figure 1.2.). The determination of the origin of any material by means of chemical analysis is based on the *Provenience Postulate*, which assumes that the chemical differences within a single source of material are less than the chemical differences among different sources (Weigand et al., 1977). Thus, ceramics that were produced or transformed in a specific workshop and with a specific recipe will likely present a different chemical composition from those produced somewhere else, due to different raw materials and/or manufacturing methods used (Hein and Kilikoglou, 2017). The meaningful ceramic groups must be considered as the smallest unit of a chemically based classification, that is, the Paste Compositional Reference Unit (PCRU) (Buxeda i Garrigós and Madrid i Fernández, 2017). Additionally, although other relational and accidental properties, such as decorative motifs or potters' stamps are not used for defining the ceramic groups, they may play an important role in the background knowledge and evaluation of the archaeometric data (Buxeda i Garrigós and Madrid i Fernández, 2017). Then, the PCRUs are compared, using existing databases, with Reference Groups (RG). These are chemically established groups of pottery of known or assumed provenance and are representative of pottery ware types of a certain production area or workshops (Hein et al., 2002). If there is chemical similarity between a PCRU and a RG, they are considered part of the same reference group. On the contrary, if a PCRU is not similar to any of the known RGs, the PCRU cannot be ascribed either to a local origin or to an exogenous provenance, and it will be undetermined until a similarity is found with a new RG. Besides, it must be taken into account that the same workshop can present more than one reference group since it is possible that the ceramist had prepared pastes with different clays to manufacture various types of ceramics, for instance, one clay for tableware and another for cooking ware. For example, this is the case of the ceramics of the 13^{th}-15^{th} century from Logroño (La Rioja), which show different chemical reference groups diachronically within the same production centre (Calparsoro, et al., 2021). Additionally, it is possible that different workshops located at the same area used the same raw materials and prepared pastes in a similar way. In these cases, the ceramics produced in these multiple workshops will present similar chemical compositions and, therefore, it will be difficult or impossible to identify different RGs for each one of the workshops. This area is known as an area of incertitude or non-resolution space (Buxeda i

Garrigós and Madrid i Fernández, 2017), that is, the area in which it is not possible to distinguish analytically between the raw materials used by the various workshops, due to the fact that they present common characteristics, since they are in the same geological zone.

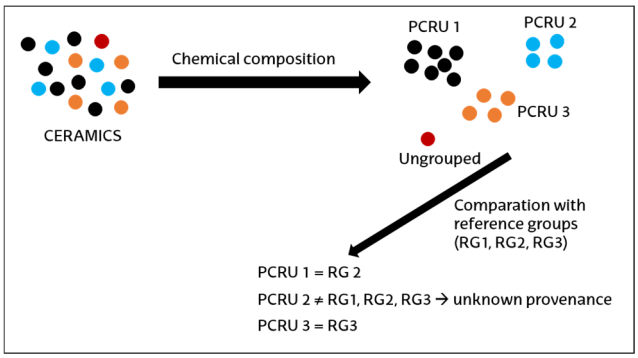

Figure 1.2. Graphical explanation of the provenance assessment

But, how are defined the reference compositional groups? This is possible because in the archaeological site, where an ancient pottery production centre (known also as workshop) was located, craft tools are usually rescued. The most direct evidences that can be preserved throughout time are evidences of ceramic kilns, permanent structures where ceramics were fired. Furthermore, more production tools such as trivets of kiln-tubes to separate the piece in the kiln (which started only being used after the introduction glazing technology, and were usually manufactured with the same clays of that used for the ceramics destined to consumption), pottery wheels and grinding wheels to grind frits can be found (Figure 1.3.). Moreover, fired or unfired ceramic pastes, misfired ceramics, ceramic wasters (full of ceramics that would be discarded, which depict a direct evidence of pottery production) as well as used raw materials, to name but a few, can also be found (Calparsoro, 2019). Thanks to this conjuncture, pottery production centres can be located geographically, or at least, the location can be suggested. What is more, carrying out the chemical analysis of trivets and misfired ceramics or ceramics that were in dumps, it is possible to characterize a given production centre (Buxeda i Garrigós and Madrid i Fernández, 2017). Since many factors such as refining of the raw materials, mixing, or tempering, complicate the direct comparison between the composition of the raw material and that of pottery, pottery is preferred over clay for the provenance study (Hein et al., 2002), a fact that has been demonstrated in the ethnoarchaeometric study carried out by Buxeda et al. (2003): the authors characterized chemically ceramics made by four ceramists, in addition to raw materials, and the results showed that the fired ceramics were clearly distinguished from raw materials. However, attention should be paid to the act of analysing waste materials (such as over-fired ceramics or kiln wasters). Since they were considered defective, they are very useful for provenance study, but it could be more difficult to understand the intended or desired performance characteristics of the vessel. Therefore, for this latter aspect, it is more convenient to study pottery from consumption centres (residence, towns, storage facilities, etc.) after their provenance assignment, rather than waste materials (Buxeda i Garrigós and Madrid i Fernández, 2017). Studying ceramics from consumption centres gives the opportunity to track technical/technological change of ceramics and to address intended performance characteristics as well as the interaction of vessels with things and people in the behavioural chain of use. Besides, the workshops can be diverse, including one

or several kilns (this is the case of the workshops of Olivares, Zamora, Sanz et al., 2005) and/or can be organized in guilds depending on the corresponding period (Solaun, 2005). The framework of this Doctoral Thesis covers traditional Medieval and Post-Medieval (late 15th-early 20th centuries) pottery activity from Zamora and Aveiro regions. Thus, hereafter all the allusions strictly apply to the mentioned period, unless it is not contrarily stated.

Figure 1.3. Two trivets (kiln furniture) unearthed at Olivares workshops in Zamora city. Scale bar: 8 cm

Regarding the provenance studies of lead-based glazes, this is possible because the lead isotope ratios of a mineral such as galena (PbS), cerussite ($PbCO_3$) or anglesite ($PbSO_4$), which are denominated as "common lead minerals", remain constant over time (Hunt, 2003). Lead has one non-radiogenic isotope (^{204}Pb) and three radiogenic isotopes (^{206}Pb, ^{207}Pb and ^{208}Pb), which are the final decay products of uranium and thorium. ^{206}Pb decays from ^{238}U, ^{207}Pb from ^{235}U and ^{208}Pb from ^{232}Th. Common lead minerals have a very low, or insignificant, U/Pb ratio and that is why their Pb isotopic composition change little, or not at all, with time, giving the opportunity to constrain the origin and age of their source (Dickin, 2018). Therefore, the isotope ratio of e.g. lead used for manufacturing the glazes, would be the same as its source (Figure 1.4.). Hence, it is possible to use databases containing lead isotope data of galena from various ore mining districts and compare these numbers with corresponding data obtained from the glazes. Ideally, such a comparison allows an identification of the geological source of the mineral, and in the best case, the exact mine from where the lead was extracted.

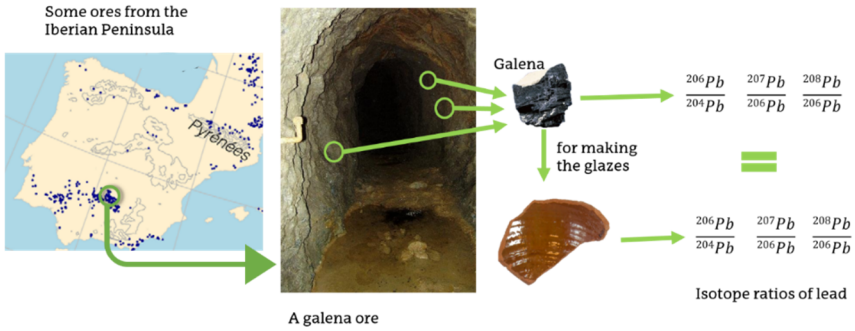

Figure 1.4. Graphical explanation of the principles of lead isotopic analyses

Traditionally Pb, U and Th isotope analyses have been used mainly in the field of Geochronology and Earth and Planetary Sciences to study the age of the formation of rocks and the age of the Earth and meteorites, among others (Albarède et al., 2012, Faure, 2004). Apart from investigations focused on geological issues, lead isotope analyses have been widely used in archaeometallurgy (summarized in: Artoli et al., 2020; García de Madinabeitia and Gil Ibarguchi, 2019; Montero-Ruiz, 2018) in order to trace the geological origin of raw materials and to study the metal flow in prehistoric or in more recent times (see the works from e.g. Ponting et al., 2003; Shortland 2006; Stos-Gale and Gale, 2009; Stos-Gale et al., 1997; Thibodeau et al., 2007; Yener et al., 1991). On the contrary, the study of lead glazes with the objective to shed more light on the possible provenance of the lead, to later propose possible commercial routes, is being carried out in the last years. Among the first works of this nature are those published by Brill et al. (Brill and Wampler 1967; Brill et al., 1987) and Joel et al. (1988), the latter focusing on the Pb isotopic fingerprinting of Spanish majolica pottery in the Americas. Since these initial publications, several more projects on Pb isotope provenance of glazed ceramics have been conducted. For example, the analyses of Islamic glazes by Mason et al. (1992) and Islamic and Hispano-Moresque ceramics by Resano et al. (2008), ceramics from the El Paso area by Pingitore et al. (1997), Rio Grande glazed ceramics by Habicht-Mauche et al. (2000, 2002) and majolica from eighteenth century New Spain prisons by Reslewic and Burton (2002), these latter ones in the southern USA region. Additionally, the works published by Wolf et al. (2003) and Marzo et al. (2007) are important. In the former study, Pb isotope compositions were obtained from 48 Islamic lead-glazed pottery from Fustat (Egypt), concluding that the lead used in glaze production by the Islamic potters at Fustat was obtained from distant ore sources. In the latter work, 12 lead-glazed ceramics from 11^{th}-16^{th} centuries from Aragon (Spain) were analysed. This work proves that relevant data can be derived from Inductively Coupled Plasma –Mass Spectrometry (ICP-MS) related to lead isotope ratios in vitreous materials. Furthermore, Iñañez et al. (2010) reported the lead isotope composition of Romita pottery glazes, in addition to majolica and non-tin-lead glazed ceramics from Spanish and Mexican production centres, comparing them with those of different lead ores from Central and South America and Europe. These data demonstrates that the production of Romita ceramics was conducted by Purépecha artisans, who successfully combined different ceramic traditions, in an effort to reproduce similar vessels than those of European origin, such as Spanish majolica in this case. Besides, Iñañez et al. (2016) also established the origin of the lead used in the manufacturing of Panamanian majolica. The results demonstrate that early majolica pottery production during the 16^{th}-17^{th} centuries used Pb obtained from the Andes. However, the Pb used in later majolica production in Panama is of Spanish origin. Continuing with the more recent works about lead isotope analyses, the work of Schurr et al. (2018) is one example. The authors carried out a lead isotope characterization of Native American and Euro-American pottery from the 19^{th} century, concluding that the lead was carried from England. In addition, Santarelli et al. (2019) studied lead isotopes of American Southwest glazes from ca. 750-850 CE and they concluded that the lead utilized by the potters was from the Galena District, in the Lake City (Utah) and Uncompahgre calderas, in the western San Juan Mountains of Colorado. Moreover, Medeghini et al. (2020) studied the lead isotopes of Roman lead-glazes for their provenancing, concluding that the lead was carried from British Isles and, finally, Métreau et al. (2021) studied Medieval decorated tile glazes from Brittany and Anjou for their provenancing, concluding that the lead was carried from Derbyshire (British Isles).

Besides, regarding the pottery provenancing, there are non-material sources (e.g. toponymy) as well for identifying pottery production centres. Note how in many villages, in Spain and Portugal, there are still streets called *Ollerías* (potter's workshops), depicting their

potters past (e.g. *Barrio das Olarias*, in Aveiro, Portugal). Furthermore, as another example, in Zamora there is a town called Alfaraz de Sayago, which refers to the red clays of the area (Fuentes Guerra, 1964). Moreover, written documentation including ethnographic works is a very good research point to start from. For instance, ethnographers such as Enrike Ibabe and Emili Sempere provided a general panorama about traditional pottery production in the Basque Country (Ibabe, 1995a) and Spain and Portugal (Sempere, 1982). On the one hand, Ibabe compiles the towns from the seven provinces of the Basque Country, in which a pottery activity was carried out. Moreover, the author gives details about the workshops and the artisans, including their names and details about their lives. In addition, the authors describes the type of clays that they used, the technology they used (e.g. how the wheels and the kilns were, how they fired the ceramics, etc.), how they applied the glaze, where they sold the pottery, and also shows a large collection of ceramics produced in each town. On the other hand, Sempere shows the reality of the 280 pottery centres that remained scattered throughout Spain and Portugal in 1982. In addition, the author makes evident both their similarities and the most pronounced differences between each of them with respect to material, technique and ovens.

1.2.2. The study of technology

The study of the technology is carried out once the compositional groups have been identified and it is done by means of mineralogical and microstructural analyses. Through the technological investigation of ceramics, it is possible to reconstruct the entire production cycle, from the manipulation of the raw materials to the finishing of the object. The technological aspect englobes each part that the complex ceramics exhibit, such as glazes, inclusions, porosity, and pigments. In addition, the study of the tools and infrastructures associated with production can be investigated too (Buxeda i Garrigós and Madrid i Fernández, 2017).

Already in 1301, the Persian potter Abu'l-Qasim Kashani wrote a treatise on the manufacture of ceramics (Allan, 1973). Additionally, in 1556, a treatise about the art of potters' craftwork, including the raw materials and manufacturing processes, was published by Cipriano Piccolpasso in his treatise about Italian majolica pottery (Lightbown and Caiger-Smith, 1980). The treatise is called *Le Tre Libri dell'Arte del Vasaio* (The Three Books of the Potter's Art). This compendium is regarded as the first written documentation of majolica pottery. In addition, recent findings of *Codice Calabranci* at Montelupo might be the earliest (written probably between 1456 and 1526) written manual of gathering the medieval pottery tradition in the western world (Chiarantini et al., 2014). In addition, there are also more recent and important documents, such as those of the potter's guilds ordinances, about the production technology in different cities (e.g. from Barcelona (García-Oses, 2018) and Sevilla (Fernández de Marcos, 2018)).

The paste is the result of the manipulation of the clay. These manipulations englobe actions such as the addition of tempers to the clay, the mixture of a clay with other clays or making combinations of these actions. These actions are carried out, as explained, in order to obtain a desired plasticity, shrinkage characteristics and resistance to thermal stress (Rice, 1987). Then, the paste will be converted into different fabrics due to the modelling, firing conditions, etc. In these lines, a fabric is the final result that reaches the paste, after completing the technological process of the fabrication of the ceramics (Buxeda i Garrigós and Cau, 1995; Buxeda i Garrigós and Madrid i Fernández, 2017), which can be observed by the array of mineralogical composition and paste textures. That is, the conversion step from

the paste to fabric involves changes in the chemistry (Hein and Kilikoglou, 2017), mineralogy (Maggetti, 1981) and micro-structure (Maniatis and Tite, 1981).

Therefore, studying the technology with which a ceramic was produced, it is possible to deep into the socio-economic factors of a certain population, since production cycles have been modified from time to time and adapted to fulfil the many social, technical and economic requirements of ancient (and modern) societies. In these lines, higher complexity in ceramics manufacture might imply higher social complexity in addition to the development of technology (Buxeda i Garrigós and Madrid i Fernández, 2017). Besides, the identification of the temper, for example, is considered important in archaeometric studies, due to the materials added might be distinctive of particular culture and periods. Thus, they might be useful in dating sites and tracing trade relationships (Rice, 1987).

1.2.3. State-of-the-art on ceramics Archaeometry

The interest on the topic of the archaeological analysis of ceramics has been growing during the last years with unprecedented number of publications and creation of specialized journals, such as *Archaeometry*, *Journal of Archaeological Science*, *Journal of Archaeological Science: Reports* and *Heritage Science*, among others (Figure 1.5.).

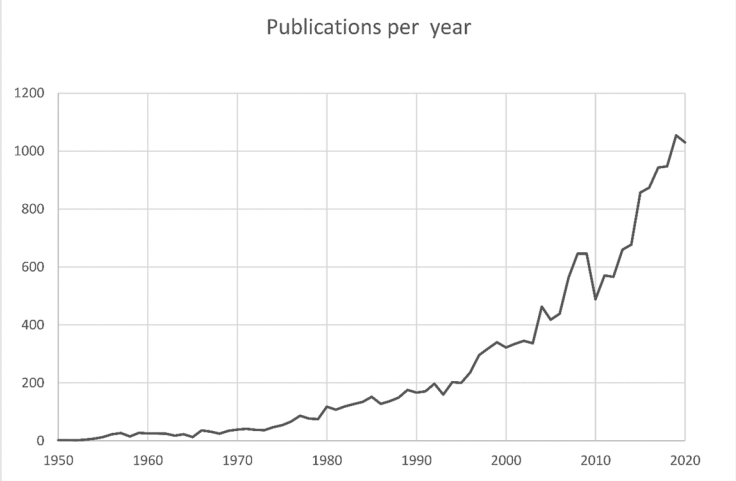

Figure 1.5. A chart showing results from the Web of Science database (consulted on the 17/11/2021), when "topic: archaeometr*", "AND topic: ceramic" and "OR topic: pottery" are entered, all together. The y-axis indicates the number of publications found when those terms are used, and the x-axis indicates the years of these publications (from 1950 to 2020)

In regards to describing the development of Archaeometry, three phases are established in the development of archaeometallurgy that can also be applied to Archaeometry of pottery (Pernicka, 2011): *the formative phase*, *the developing phase* and *the expansion phase*. With regard to the formative phase (18th century-1930), the first steps in the development of Archaeometry can be traced back to the 18th century, although it was not until the early 19th century that the first systematic studies were carried out. Thus, in 1752 the Comte de Caylus carried out a work that was, probably, the first "archeometric" application in order to identify what the black varnishes of Attic ceramics and the red varnishes of Roman terra sigillata were composed of (Maniatis et al., 1993). Then, M. Faraday

(1791-1867) identified the use of lead in the glazes of Roman pottery (Trigger, 1988). Additionally, the provenance of ceramics was also studied by petrography and chemical analysis. By petrography, Nordenskiöld (1893) published a collection of ceramics collected in Mesa Verde, Colorado, by means of the study of the thin-sections of ceramics. By chemical analysis, Richards (1895), investigated Athenian ceramics from the Boston Museum of Fine Arts. On the other hand, in the developing phase (1930-1970), the use of X-Ray Fluorescence (XRF) (e.g. Hall, 1960) and Neutron Activation Analysis (NAA) was increased (e.g. Sayre et al., 1957). In addition, a key work in the archaeometrical literature, was written by Shepard in 1956. This is called *Ceramics for the Archaeologist* and states the principals and research strategies of pottery analysis. Finally, the expansion phase (1970-present), is the phase in which the increase in instrumental measurement techniques, like those based on the application of Optical Emission Spectrometry (OES), ICP-MS, etc. takes place (Pernicka 2011; Pollard and Heron 1996; Pollard et al., 2007) and more works are published. In this phase Rice (1987, revised in 2015) wrote a book called *Pottery Analysis: a source-book*, which provides a complete reference guide covering more profoundly the properties of clays, production technologies and analysis of pottery. Moreover, a new phase, *non-destructive analyses phase* (2000-present), should be added, in which the development of non-destructive methods and techniques for the study of archaeological materials is being addressed (e.g. Calparsoro et al., 2019a; Liritzis and Zacharias, 2011; Neff, 2000, 2003, 2012).

Besides, the publications about ceramics including archaeometric approaches experimented a significant increase in the 1990s. This is demonstrated by the large volume of scientific works, including abundant theses. Focusing more on the Basque Country and Catalonia, on the one hand, examples of the studies and Doctoral Theses in archaeometric approaches on ceramic pastes, are those of the following lines. The reference Doctoral Thesis of Buxeda i Garrigós on Terra Sigilata of Clunia (Buxeda i Garrigós, 1994) and other works of the same author and colleagues (Buxeda i Garrigós, 2008; Buxeda i Garrigós and Kilikoglou, 2003; Buxeda i Garrigós and Madrid i Fernández, 2017; Buxeda i Garrigós et al., 1995, 2003, 2015) are some examples. In those latter works, topics such as compositional data and its variability, the archaeometric method, traditional and archaeometric analyses on Roman Age ceramics and ceramics from Seville and Barcelona and chemical variability in pottery from Pereruela are studied. In addition, the Doctoral Thesis of Calparsoro (2019) about the archaeometrical characterization of Basque and Riojan ceramic productions is relevant, along with the works of the same author and colleagues (Calparsoro et al., 2019b,c, 2021) in which Post-Medieval pottery from Orduña (Basque Country), Logroño and Nájera (La Rioja) are archaeometrically studied. Besides, the Doctoral Thesis of Iñañez (2007), in which the archaeometric characterisation of the Low Middle Ages ceramics of the Iberian Peninsula is carried out, and the studies of Iñañez and colleagues (Iñañez et al., 2008, 2009, 2018, 2020, 2021) are of special importance. In those latter works, Medieval and Post-Medieval pottery from the Iberian Peninsula, the Canary Islands, Ceuta, Morocco, Zamora and Angra D shipwreck are archaeometrically studied. Moreover, Madrid i Fernández also has relevant contributions: two about the archaeometric characterisation of Roman Late Republican Black Gloss pottery (Madrid i Fernández and Sinner, 2019, 2021) and other about the archaeometric characterization of terra sigillata productions commercialised during Augustan period (Madrid i Fernández and Buxeda i Garrigós, 2007). In addition, Hispanic terra sigillata dated back to the 1st century AD also was studied (Madrid i Fernández and Buxeda i Garrigós, 2014), as well as Southern Gaul sigillata ceramics documented in Baetulo (Badalona) Roman village (Madrid i Fernández et al., 2014). Moreover, before publishing the mentioned works, the author published a Doctoral Thesis about the archaeometric characterization of terra sigillata from Baetulo (Madrid i Fernández, 2006). In addition,

Doctoral Theses recently published by Puig Barrachina (2016), about Basque ceramics, Fernández de Marcos (2018) about Sevillan ceramics and Pinto-Monte (2021) about Valencian ceramics can be added to the list. On the other hand, an example of studies on ceramic pastes, glazes and the interaction between pastes and glazes is the Doctoral Thesis of Molera (1997). In addition, the works of that author and collaborators (Molera et al., 1997, 1998, 1999, 2001) should be mentioned, in which the technology and colour development of Hispano-Moresque lead-glazed pottery, the colours of Ca-rich ceramic pastes, the evidence of tin oxide recrystallization in opacified lead glazes and the interactions between clay bodies and lead glazes are studied. The Doctoral Theses of Molina and Ferrer should also be mentioned, the former about the color and technology of ancient glazes and glasses (Molina, 2014) and the latter about the yellow pigments of ceramics (Ferrer, 2014). In addition, Peix Visiedo et al. (2021), Salinas and Pradell (2018), Tite et al. (1998) and Vendrell-Saz et al. (2000) carried out studies on green and black tin-lead glazed pottery from Barcelona (13^{th}-14^{th} centuries), about the introduction of the glaze in Al-Andalus, about methods of productions and reasons for using lead glazes in antiquity and about the optical properties of tin-lead glazes, respectively. In these lines, some works about the study of pigments are those of Iñañez et al. (2013) and Pérez-Arantegui et al. (2008). In addition, there are also works about the provenancing of the lead from the glazes (Iñañez et al., 2010, 2016). Besides, there is a review of the archaeometric analysis on Medieval pottery published by Grassi and Quirós (2018).

Moreover, among the recently published reviews, the Topical Collection called *Ceramics: Research questions and answers*, aimed at guiding researchers in the study of archaeological ceramics from excavation to study and preservation in museum collections, has been published. Thus, research questions and sampling criteria are treated in Gliozzo (2020a). Then, some works deal with the investigation of raw materials: their chemical investigations are covered by Hein and Kilikoglou (2020) and mineralogical-petrographic investigation by Montana (2020).Moreover, Gualtieri (2020) writes about their technological character and suitability. Besides, Eramo (2020) published a work about the processing of clays, and in these lines, Thér (2020) treated the issue of the modelling of clays. Moreover, ceramic transformation issues, such as ceramic firing and the identification of post-depositional transformations have been handled by Gliozzo (2020b) and Maritan (2020), respectively. Moreover, the restoration and musealization of ceramics has been handled by de Lapérouse (2020). On the other hand, issues about the surface and coatings have been also published. In these lines, Ionescu and Hoeck (2020) wrote about surface finishing, whereas the investigation of different coatings such as black glass-ceramic, terra sigillata and glazes where treated by Aloupi-Siotis (2020); Pradell and Molera (2020) and Sciau et al. (2020), respectively. Additionally, the isotopic study of particular types of products such as Chinese high-fired ceramics were treated by Henderson et al. (2020) and the dating of ceramics by Galli et al. (2020). Finally, the Topical Collection concludes with a tutorial on statistical data processing (Papageorgiou, 2020).

Besides, it should be noted that more specific status of different issues are included in several parts of the present manuscript (e.g. the state-of-the-art of lead-based glazes in Chapter 1, section 1.2.1)

1.3. Current challenges in archaeometric research

The most important current challenges of archaeometric research are the development of non-destructive methodologies and the identification of the post-depositional alterations and contaminations.

1.3.1. Development of non-destructive methodologies

It should be noted that destructive analytical techniques such as Atomic Absorption Spectrometry (AAS) (e.g. Tubb et al., 1980), Inductively Coupled Plasma-Atomic Emission Spectrometry (ICP-AES) (e.g. Storey et al., 1988) and -Mass Spectrometry (ICP-MS) (Dussubieux, 2020) have been dominant in ceramic analyses for elemental chemical analyses (Glascock, 2016; Hunt, 2016; Pérez-Arantegui, 2018; Pollard et al., 2007). ICP-MS is the most frequently used, in which the sample must be first powdered and then solubilized for its analysis. Other destructive technique widely used is Neutron Activation Analysis (NAA), which is a very effective method and it does not need sample preparation, but it is less widely applied due to the requirement of accessing to a nuclear reactor (see for instance, the special issue on NAA by Speakman and Glascock (2007) and the works of García-Heras et al., 2001; Glascock, 1992, 2014; Iñañez et al., 2008; Neff, 2000). Other alternative techniques to those mentioned are based on X-Ray Fluorescence (XRF), which have a lower cost of sample preparation or do not need it. For the common XRF, for example, the sample needs to be prepared for its analysis. On the contrary, with other types of XRF, non-destructive analyses can be carried out. These are the cases of techniques such as ED-XRF (Energy Dispersive – X-Ray Fluorescence) screening methodology, optimized by Calparsoro et al. (2019a), or HH-ED-XRF (Hand-Held Energy Dispersive X-Ray Fluorescence Spectrometer) (Maguregui et al., 2018), or of portable XRF (pXRF) (Forster et al., 2011; Hunt, 2016; Hunt and Speakman, 2015; Kelloway et al., 2019; Liritzis et al., 2020; Millhauser et al., 2011; Speakman et al., 2011). However, the reliability of these instruments is not as high as the reliability of ICP-MS. Besides, the use of other alternative analytical approach of ICP, considered as non-destructive, is increasing, that is, the Laser Ablation-ICP-MS (LA-ICP-MS) (Dussubieux et al., 2016; Giussani et al., 2009; Neff, 2012; Resano et al., 2005). However, LA-ICP-MS or ED-XRF may require cutting the ceramic piece if it is bigger than the sample chamber. Whatever the case, although the cutting of the ceramics involves invasiveness of the technique, this step includes a very low-level of invasiveness compared to the powdering of the samples, since the cut fragments can be re-used to perform additional analyses or to be saved.

The fact that compositional analyses of archaeological ceramics have been carried out predominantly by destructive analytical techniques may become an important issue when dealing with cultural heritage and museum collections, since the conservation and preservation of our cultural heritage is one of our main concerns. Moreover, in some cases it is not possible to transport the sample to the laboratory, so the optimisation of methods for portable non-destructive instruments for the analyses of cultural heritage is crucial. In these lines, as an example, Maguregui et al. (2018) presented for the first time an in situ non-invasive methodology for HH-ED-XRF to characterise the composition of both metals/alloys and lacquers used to create a Japanese armour from the Edo period (1603–1869). The armour was in situ investigated, without the necessity of taking any sample, for its later conservation in the Restoration Service from the Provincial Council of Araba (Basque Country).

1.3.2. Post-depositional alteration processes in archaeological ceramics

Ancient ceramics recovered after a long burial period probably have undergone several alterations and contaminations. They introduce a chemical variability, affecting the natural variability, that is, the chemical and the mineralogical compositions of the ceramic paste after their deposition will not be the same as originally were (Buxeda i Garrigós, 1999). Therefore, it is important to know the alteration ways of buried ceramics. This section provides a general background about these type of alterations and it can be considered as the introduction to Chapter 5 of this Doctoral Thesis.

The main post-depositional alteration processes of archaeological ceramics are the result of the action of a set of extrinsic agents (those that define the burial context or the environment), intrinsic agents (those that are part of the object, such as the materials or the technology) and the result of the interaction between both of them (Fantuzzi, 2010 and references therein). Extrinsic agents include various natural site formation processes such as bioturbation and river transport, as well as some cultural processes (e.g. plowing, looting). In addition, abiotic agents, such as the abrasion produced by wind, are capable of producing various types of alterations on the ceramic. It is also important to study the sediments and soils to understand the burial conditions and post-depositional processes that occurred in the ceramics, since the behaviour of burial contexts is similar to that of soils (Cremaschi, 2000). A soil is the result of the complex interaction between a variety of physical, chemical and biological processes that act on rocks and sediments, and constitutes a dynamic system in which chemical movements and redistribution of its elements constantly take place (Holliday, 1992). Regarding the study of the material's preservation, the characteristics of soils affecting material's preservation are texture (granulometry, morphology, etc.), pH (acid, neutral or basic), redox potential (Eh) (reducing or oxidizing environment), humidity, salts and biologic agents (fauna and flora) (Guevara, 2001; Magaña et al., 2001). The granulometry influences the transport of air and water through the materials, thus influencing also the chemical processes of oxidation and hydrolysis. With respect to the pH of the soils, the ceramic materials are preserved better in basic soils, that is, rich in calcium, sodium and magnesium. The Eh is the capacity of a soil to give or take electrons depending on whether the environment is reducing or oxidizing, and it is related to the pH and the oxygen content of the environment. On the other hand, humidity acts as a catalyst in most reactions and it will depend on the climate and on edaphochemical factors such as permeability, expansion and contraction capacity and leaching, among others. Regarding flora and fauna, one of the main factors that can cause deterioration in ceramics is the action of the roots. Fauna of a certain size can also produce some physical alterations (e.g. fragmentation), not only in the case of digging animals but also due to other processes such as trampling. Beyond all these aspects of the burial context, it is important to note that climate is a crucial factor as it defines several of the mechanisms that take place within the soils where the materials are buried. For example, tropical climates are particularly harmful for the preservation of ceramics due to the presence of acid soils that favour the dissolution of especially calcareous components (Fantuzzi, 2010; Maritan, 2020).

Contrariwise, intrinsic agents include the characteristics of the ceramic material under study, which are the raw materials and the manufacturing and firing techniques used. They will determine the strength, durability and the degree of physical vulnerability of an object (Oakley and Jain, 2002). Therefore, it will be essential to know the different steps of the ceramic manufacturing (extraction and preparation of raw materials, manufacturing, drying, cooking and usage) to understand their influence in the transformation process of the ceramic (Buxeda i Garrigós and Madrid i Fernández, 2017). The characteristics that define

the material's preservation are the cohesion degree of the clay fraction acquired during firing, the grade of vitrification, the hardness of the ceramic and the porosity, which are interconnected (Berducou, 1990).

In addition, the material's preservation will also depend on the interaction between the ceramic and the environment. One of these interactions is, for example, the rehydration of the ceramics; during the firing, the clay particles lose the structural water, however, the ceramics can absorb it from the environment in the deposition context, producing an expansion in the material (Freestone, 2001; Rice, 1987). Another interaction is the salts crystallization; the solutions that circulate in the soil can penetrate into the ceramic through the pores by capillarity. Then, these solutions can evaporate as sodium, potassium, calcium and magnesium chlorides, sodium, potassium and magnesium sulphates, nitrates, bicarbonates, acetates and phosphates can crystallize on the surface and pores of the ceramics (Maritan, 2020; Paterakis, 1987). Furthermore, the interaction between the ceramic and the burial environment can result in the addition, elimination or ion exchange between both of them. The presence of anomalies in the concentration of some elements (in metals, such as K, Na, Mn, Mg, Ca, Fe and in non-metals, such as, F and P) can be linked to the contamination because of elements fixation (Buxeda et al., 2002a; Freestone et al., 1985, 2001; Lemoine and Picon, 1982; Maritan and Mazzoli, 2004; Maritan, 2020; Schwedt et al., 2004, 2006). This fixation phenomenon can be studied through a diffusion profile in the shape of a "U" along the walls of the ceramic; the surfaces will be more contaminated than the cores. Moreover, the circulation of water is the main factor in the alteration of ceramics, allowing cation exchange with the surrounding soil solution, and dependent on the ceramic's porosity. Other alterations, such as the abrasion of the surface, depend also on the hardness of the paste, porosity, distribution and orientation of the inclusions or tempering materials, etc. (Schiffer and Skibo, 1989; Skibo and Schiffer, 1987). The heterogeneity of the constituents of the coating and the paste of the ceramics is also another possible source of alteration. This heterogeneity can contribute to a different thermal behaviour of the ceramic, dilating and expanding it, which can cause ceramic fragmentation (Fantuzzi, 2010). However, the coating tends to prevent the penetration of soil solutions, inhibiting the corrosion (Freestone, 2001). Finally, another aspect that may affect their preservation is the functionality of the vessels; the vessels that were used for food storage can be altered by various types of acids (e.g. citric, malic, succinic and acetic) (De la Fuente, 2008; Skibo, 1992).

Regarding the state-of-the-art on studies about post-depositional alterations and contaminations, several authors have studied and evaluated these problems through the examination of real cases and by means of experimental approaches. On the one hand, among the works about the examination of real cases, for example, Amadori et al. (1998) studied the alteration forms occurred in majolica tiles from Italy. They documented wairakite and calcite as alteration products. In addition, Buxeda i Garrigós et al. (Buxeda i Garrigós, 1999; Buxeda i Garrigós and Cau, 1994; Buxeda i Garrigós et al., 2001, 2002a,b) studied the alterations and contaminations in archaeological ceramics. In these works, they documented the presence of secondary calcite (that is, the calcite appeared due to alteration processes; this issue was also studied by Cau et al. (2002) and Gilstrap et al. (2021)), the alterations of Na, K and Rb concentrations on pottery, related to analcime crystallization (these alteration forms are deeply explained in Chapter 5) as well as the crystallization of secondary pyrite in Roman Amphorae from the Iulia Felix Shipwreck (this alteration form is deeply explained in Chapter 6). Other studies related to alterations occurred in ceramics recovered in shipwrecks are one from Iñañez et al. (2020), in which pyrite was identified, from Renson and Glascock (2021), in which lead contamination was identified by lead isotope analysis and from Mise et al. (2021), in which the enrichment and depletion of some

elements were documented in amphoraes buried at marine environments. Moreover, Freestone (2001) studied the post-depositional changes in archaeological ceramics and glasses and Freestone et al. (1985) studied the retention of phosphate in buried ceramics. In these lines, Lemoine and Picon (1982) also studied the fixation of phosphorous in ceramics and Lemoine et al. (1981) studied alterations occurred in ceramics buried in marine environment and terrestrial environment. The alteration related to phosphorous is explained in Chapter 6. The work of Picon (1976) is another example of the study of alterations due to burial period. The author documented a fixation of magnesium from marine water. Besides, Pradell et al. (1996) and Secco et al. (2011) studied the alteration processes in ceramics buried in marine environments and lagoon-like environments, respectively, documenting the presence of pyrite and jarosite in the latter. Moreover, Schwedt et al. (2004, 2006) studied the alterations in pottery and the analcime crystallization, respectively, and Tschegg (2009) studied the post-depositional surface whitening of ceramic artifacts. Finally, Stoner and Shaulis (2021) and Golitko et al. (2021) performed, among other things, an elemental mapping of the pastes of several samples to identify potential leaching of mobile elements into or out of vessels. On the other hand, among the works about experimental approaches, Béarat et al. (1992) studied the physico-chemical alterations of the ceramics after their deposition in seawater. These authors carried out three groups of experiments, each experiment with a different type of clays, all of them fired at different temperatures. The ceramics of the first experiment were converted into powder and the authors submerged them in unrenewed seawater for 6 years. The ceramics of the second experiment were also converted into powder and submerged in seawater for 2 months. On the contrary, some ceramics from the third experiment were converted into powder while others where left as briquettes. They were submerged in renewed and unrenewed seawater for 3, 5, 6 and 10 months. Heimann and Maggetti (1981) also carried out experiments on simulated burial of ceramics in a humid climate. For that, the authors collected and fired clays from La Peniche and subjected them to solutions simulating natural conditions in Teflon-lined autoclaves. The authors introduced these autoclaves in a drying cabinet at 200 °C for 2 weeks to accelerate the reactions and simulate, in that way, a real burial period of the ceramics. In addition, Montana et al. (2014a) and Belfiore et al. (2014) carried out an experimental approach to study the alterations and contaminations of ceramics buried in seawater. These authors manufactured six different pastes with calcareous and low-calcareous clays and two different typologies of sand for tempering, all collected in Sicily. These pastes were used to make 150 ceramic briquettes and cylinders. These ceramics were placed in customized holders fixed into the open sea and in a confined system filled with seawater, which was constantly renewed. In addition, physico-chemical parameters such as temperature, pH, conductivity, salinity, total dissolved solids (TDS) and redox potential were monitored weekly. Finally, Franklin and Vitali (1985) studied the environmental stability of ceramics during burial at ambient temperatures. For this task, authors manufactured and fired calcareous ceramic briquettes of a known composition, and subjected them to a variety of aqueous solutions, which their pH and temperature (at 25 °C and 90 °C) were monitored.

Thanks to these studies (real cases and experimental approaches), it is known that alteration and contamination processes and the discrimination of some elements should be considered when studying the ceramics to avoid incorrect interpretations about their provenance, technology and the use of the artefact as well as its proper preservation (Buxeda, 1999; Buxeda et al., 2001; Calparsoro, 2019; Franklin and Vitali, 1985; Freestone, 2001; Maritan, 2020; Maritan and Mazzoli, 2004). Therefore, here is where attention must be paid when carrying out studies such as the provenance assessment.

CHAPTER 2: PRODUCTIONS FROM ZAMORA AND AVEIRO

In this Doctoral Thesis the productions that have been studied were those from Zamora region (Zamora city, Toro and Benavente villages, in Spain) and Aveiro (in Portugal). In this chapter, the two sites will be described regarding their pottery production.

2.1. Production of Zamora region

The city of Zamora lies in the northwestern area of the Iberian Peninsula in the Duero river basin, being the capital of the homonymous region in Spain (Figure 2.1.). The region has a long tradition in pottery and its Post-Medieval pottery keeps a strong tie with late Medieval Castilian ceramic tradition, specifically in relation to typologies. Thus, Zamoran pottery often shows open typologies, like plates and porringers, as well as closed ones, like jars and cooking pots (Larrén, 1991; Villanueva, 2011).

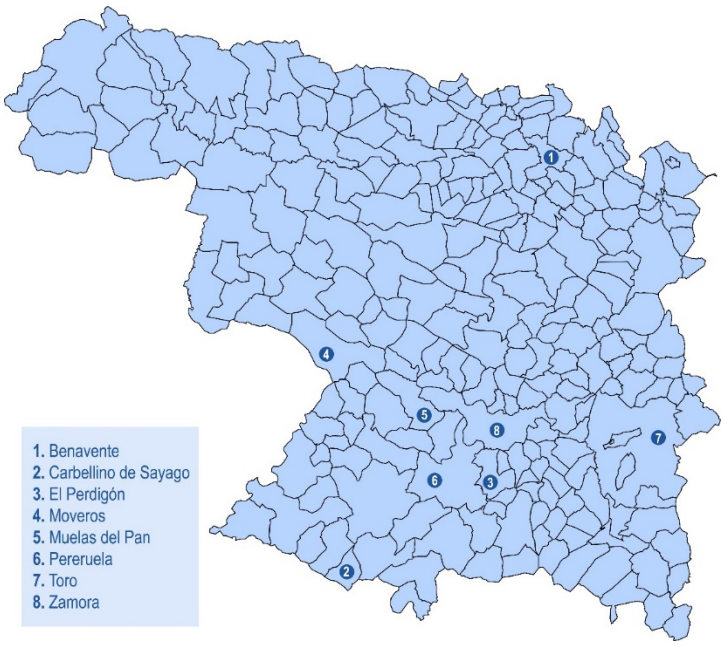

Figure 2.1. Map of Zamora province, where Zamora, Toro, Benavente, Pereruela, Muelas del Pan, Moveros, Carbellino de Sayago and El Perdigón are indicated

Almost all of the province of Zamora is located within the Duero River Basin. During the Alpine orogeny, a tectonic event developed, colliding the plaque of Africa and Europe, which led to the elevation of large mountain ranges such as the Cantabrian, Iberian system, Pyrenees, Betics or the Central system. The erosion of these alpine reliefs provided the materials that served to fill the basins that were formed during the Tertiary, such as the Duero. The sedimentation has continued with this pattern until today giving rise to quaternary deposits that are distributed throughout the territory, mainly located in the valleys of the current rivers, finally forming the current geological map of the province. In the province of Zamora two large geological regions or different rock complexes can be found, the basement that constitutes the Iberian Massif, which occupies the entire western border, and the sedimentary materials of the Duero Basin that emerge in the eastern half. Therefore, the hercinic basement is the base on which the whole province is based, rising

across the western border. In it several successions of sedimentary rocks of precambrian and paleozoic ages and abundant igneous rocks of variscan age can be found (Fadón, 2011).

In the province of Zamora two types of clays have been mainly exploited for pottery: red clays and white clays. On the one hand, the exploitation of the red clays is carried out mainly in the vicinity of the towns of Toro and Benavente, but for the ancient pottery production clays were also exploited in Pereruela, Moveros and Zamora, in smaller quarries. On the other hand, white clays include kaolinite (hydrated aluminium silicate) and kaolinite clays. Kaolinite has been (and still is) widely used in the manufacture of refractory materials (that is, materials resistant to high temperatures), because it is rich in impurities of thick grain size (granite). The exploitation of these clays has been carried out in Tamame de Sayago, Pereruela, Peñausende or Fresno (Fadón, 2011).

This geographical distribution of clays led to the specialization of the production of different ceramics in the different towns of Zamora. Thus, since the Middle Ages for example in Pereruela, Moveros and Muelas del Pan, kitchen ceramics were produced with kaolinite (and for that, potters often mixed kaolinite with red clays; Buxeda et al., 2003; Villanueva, 2011). The ceramics obtained from these clays are also called micaceous ceramics. The three towns mentioned, as well as Toro and Benavente (the latter two mainly produced non-micaceous red tableware), constituted the starting point for the manufacture of the ceramics of Zamora. Since then, other production centres were created and developed in Zamora region, such as in Zamora city, Carbellino de Sayago, Cibanal, Fornillos de Fermoselle, Junquera and Milla de Tera, El Perdigón and Venialbo. All of them formed a view of traditional ceramics in Zamora, until the beginning of the 20th century. At that time, most had to close their workshops in view of the advances of modernity, but others remain alive (Moratinos and Villanueva, 2006) (Figure 2.2.).

Figure 2.2. Paco, a ceramist working in his family's workshop called *Alfarería Pascual*, still alive, in Moveros, where also his wife and daughters participate actively in ceramic production. The picture was taken in 2019 by Sanchez-Garmendia

The history of Muelas del Pan (Figure 2.3.) begins with the oldest known reference, from 1547, in which one of its potters was in charge of producing the washbowls (*barreño*) that Queen Juana I of Castile needed for her palace in Tordesillas (Villanueva, 2011). This new is undoubtedly indicative of the existence of a previous, consolidated production of Muelas del Pan. In its workshops different types of micaceous tableware were made, among which the most popular were pots, jars, washbowls, jugs and crucibles. Besides, the pottery from Pereruela, characterized by being richer in intrusions of micas and quartz, starts from dates even older than that of Muelas del Pan, since it is already cited in the year 1410 (Figure 2.4.) (Moratinos and Villanueva, 2006; Villanueva, 2011).

Figure 2.3. A woman ceramist from Muelas del Pan (Source: Luis Cortés, Ethnographic Museum of Castilla y León, Zamora, retrieved from Moratinos and Villanueva (2006))

Figure 2.4. Micaceous ceramics kept in the workshop called *Alfarería de Pereruela*, of Víctor Redondo Tamame, a ceramist from Pereruela. The pictures were taken in 2019 by Sanchez-Garmendia

Moreover, in the city of Toro, there was also an important artisan sector dedicated to pottery. The archaeological excavations carried out at *Cuesta del Negrillo No. 11*, an area related to the traditional establishment of potters, recorded evidence of what could be a waster of defective pieces, among which were found vessels for cooking and tableware and storage (e.g. pots, cups, jars, bowls, jugs, plates) (Larrén 1991, 1992). In addition, the pottery activity in Benavente was also known in the transition from the Middle Ages to the Modern Era. In the middle of the 18th century, eleven potters appeared in the list of positions and trades. Among the production of Benavente, some jars stand out due to their peculiar typology, known as "jarritas carenadas". They could have served as tableware: the piece with a handle to pour liquids and the one without it, as a drinking glass. But also, and given their manufacture in three sizes, they could have another specific function, the function of measuring 300 ml, 200 ml or 100 ml (Villanueva, 2011).

The clays used by the potters from Toro and Benavente were ferruginous clays, not micaceous clays, also called red clays (known as *barro rojo o bermejo*) (Figure 2.5.) (De La Mata, 1989). The extraction was carried out by the potters themselves or by their assistants, obtaining the clays mainly in the areas of Los Toriles, Tagarabuena, Eras del Sepulcro, San Antón and Valle la Zarza, all of them near the villages. These clays had good physical characteristics for modeling due to their plasticity; although they were mixed with sand for the vessels destined to the fire (pans, pots...) (De La Mata, 1989; Larrén 1991).

Figure 2.5. Ceramics from Toro and Benavente (the first two are from Toro, and the last two from Benavente). Scale bar: 8 cm

In the city of Zamora, regarding the workshops of *Olivares*, they have been traditionally considered (since the high Middle Ages) as the places that supplied both the city and a large part of the region with the ceramics produced there (Villanueva, 2011). The first written evidence of the ceramic production in Zamora city dates back to 1279, mentioning the existence of a potter's quarter outside of the medieval walled city. Moreover, there are some further evidences of ceramic production activity in the 15th and 16th centuries according to the job names written down in the city old census. Later on the 18th century, the names of six potters appeared listed in the 1752 general cadastre (*Catastro de Marqués de la Ensenada*), and three of them had located their workshops in the quarter known as Olivares. Interestingly, just a few years later, in 1770, the number of potter masters working in Olivares had reached the number of ten, in addition to their officers and apprentices. Forward in 1807, potters established a guild to protect their collective interests and supplies, reaching the number of twelve workshops reported for that period (Moratinos and Villanueva, 2006). Besides, in the last decade of the 19th century, Pérez (1895) mentioned the existence of ten potters working in Olivares. However, this figure would decrease soon, remaining just two ceramists in 1930, and ceasing completely when the last of the potters, Benito Toranzo, passed away in 1944 (Moratinos and Villanueva, 2006). In Olivares the so-called "Olivares ceramics" were generally produced, which were a tableware with opaque white glaze (tin-lead glaze), decorated in blue, green, black and brown. The introduction of glazed pottery meant an important advance in the pottery technique. According to bibliographic documentation, in Olivares there was a need for a closed kiln to melt the glaze, and also the need for mills to grind this glaze, or for moulds to protect the pieces during firing. But also, among many other things, the glazing process required the use of special kilns to prepare the mixture of minerals (lead and tin minerals). These special kilns were known as "padillas" and tin minerals, lead minerals, sand and common salt were melted there to produce the frit. Then, the frit was reduced to a powder in the mills and diluted after in water for its final application on the biscuit ceramics. Potters used to buy lead by quintals (1 quintal = 100 kg) or arrobas (1 arroba = 25 pound), and tin by pounds (1 pound = 0.45 kg). Since the 18th century, the Spanish state, with its industrial development policy, proceeded to distribute these raw materials from state tobacco shops, generally located in cities or near production centers, to avoid their increase in price and possible shortage (Moratinos and Villanueva, 2006). On the other hand, according to bibliography, ceramics for kitchen use (micaceous, similar to those produced in the Muelas del Pan and Pereruela workshops), and red ceramics, similar to the red ceramics produced in Toro and Benavente, were also produced in Olivares (Moratinos and Villanueva, 2006) (Figure 2.6.).

Figure 2.6. Ceramics from Olivares workshops. Scale bar: 8 cm

The commercialization of Zamoran micaceous ceramics (e.g. from Muelas del Pan or Pereruela) surpassed the Zamora region. For example, in Valladolid, those were considered a basic necessity and, already in modern times, these productions arrived to the centre of Spain, to the Cantabrian Coast and even to Galicia in a later period. Additionally, it is possible that from Post-Medieval times they were glazed in the Olivares workshops in Zamora, as well as in the pottery production centres of the Basque Country (e.g. Elosu, Durango, Ametzaga, Zegama) (Ibabe, 1995; Solaun, 2005). The mule drivers carrying the pots arrived to the Basque and even French markets, to bring back all kinds of products and manufactures from those places, thus producing interesting commercial trading routes. There is documentation from 1612, referring that the residents of Muelas del Pan, Bartolomé Casquero and Alonso Miguel, brought a variety of goods from Vitoria-Gasteiz (Basque Country), mainly iron, after selling pots there. In the 20th century, and especially after the end of the Civil War, the uses of pottery gradually changed, decreasing street sales and increasing stable shops, or through fairs of popular pottery (from the 70s onwards) (Figure 2.7.) (Moratinos and Villanueva, 2006; Villanueva, 2011).

Figure 2.7. Poster of the 1974 Zamoran ceramic fair (retrieved from Moratinos and Villanueva (2006)

During the past two decades, several archaeological excavations have been conducted in the city of Zamora, alongside with the urban development regarding the expansion of the city and the construction of new public buildings. Among these rescue works, two archaeological excavations were carried out at the sites corresponding nowadays to the Provincial Historical Archive (Martín et al., 2002, 2003) and the Public Library of the State (Martín et al., 2003; Villanueva et al., 2000) (Figure 2.8.), another one at the Ethnographic Museum of Castilla y León (Misiego et al., 1997-1998) (Figure 2.9.) and the last one at the area known as Olivares (Piñel, 1993; Sanz et al., 2005) (Figure 2.10., 2.11., 2.12.).

Figure 2.8. The archaeological intervention carried out at the church of La Concepción (left photograph) and the church and the convent buildings nowadays, that is, the archive and the library (right photograph). Source: Martín et al. (2003) (left) and picture taken in 2019 by Sanchez-Garmendia (right)

Figure 2.9. The main portal of the Royal Prison (in the left), dated back to the end of the 16th century, where nowadays is the Ethnographic Museum (in the right). Source: Museo Etnográfico (2021)

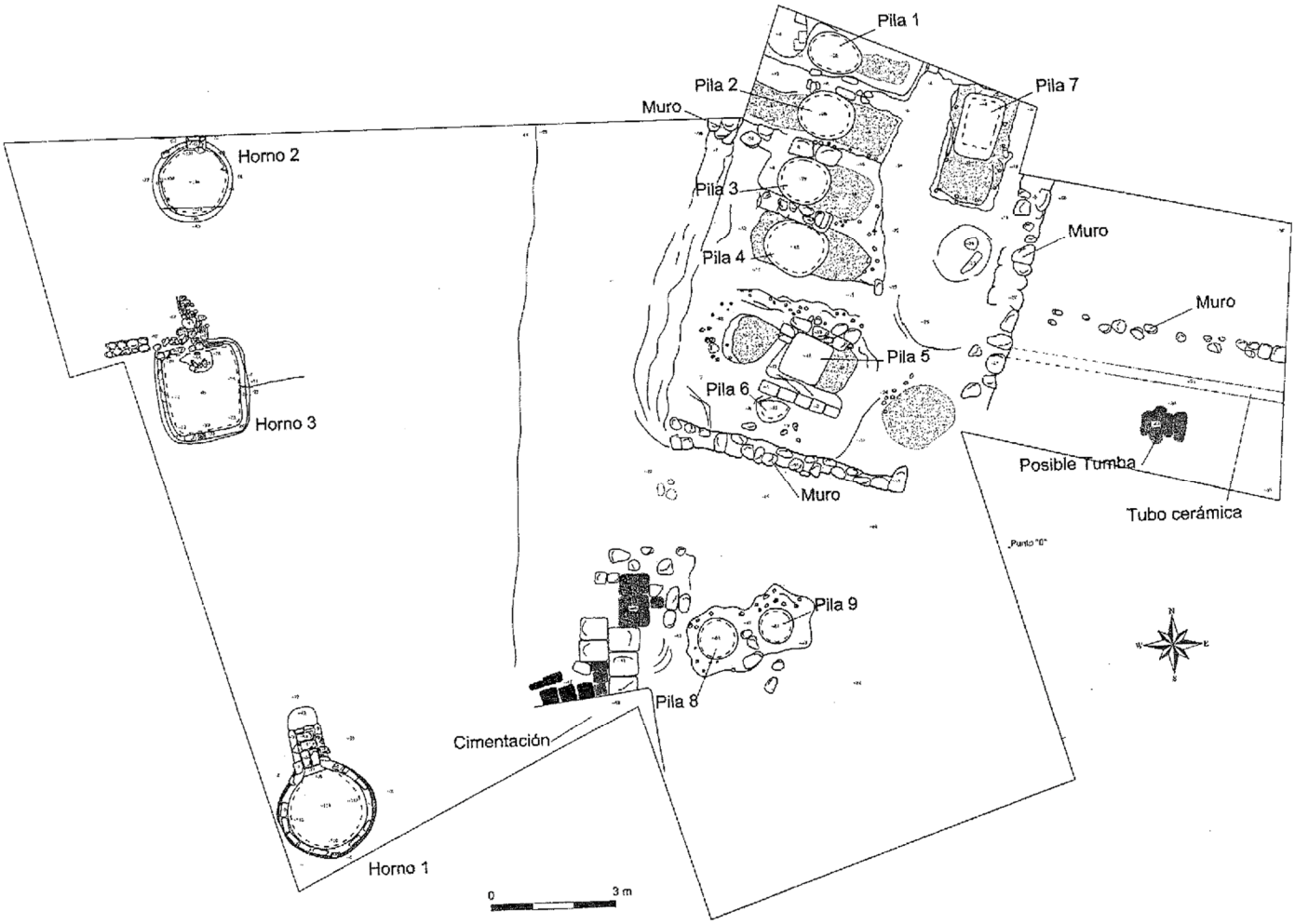

Figure 2.10. Map of the archaeological intervention area, where the different kilns of the workshops and the sinks of the tanneries located next to the ceramic workshops, stand out. *Horno = kiln; Pila = sink; Muro = wall; Cimentación = foundation; Posible tumba = possible tomb; Tubo cerámica = ceramic pipe*. (Source: Sanz et al. (2005))

Figure 2.11. Kilns in the surroundings of Santiago Viejo and San Claudio of Olivares. Source: Museo de Zamora (2018)

Figure 2.12. Map of part of the city of Zamora. Oilvares auzoa = Olivares quarter; Mengue etorbidea = Mengue Avenue; 1 = Ethnoraphic Museum; 2 = Public Library of the State; 3 = Provincial Historical Archive; 4 = San Claudio square

As regards the site where nowadays lies the Provincial Historical Archive, it was an old convent called *Convento de Nuestra Señora de La Concepción*, while in the adjacent plot, where the Public Library of the State was constructed, there was the church known as *Iglesia de Nuestra Señora de La Concepción*. Thanks to the archaeological interventions, the different phases of occupation that have undergone the old convent and church have been studied (Martín et al., 2002, 2003; Villanueva et al., 2000): in 1626, the religious community of the Conceptionists moved to the buildings known as "Casas de Gonzalo de Valencia" in the Claudio Moyano square, in the heart of the downtown area, which would be the Convent of La Concepción and their home for the next two centuries. Later on, the construction of the church started in 1672 and lasted until 1676 (Martín et al., 2003). In 1837, the Conceptionists were forced to leave because of a general confiscation ordered by the Spanish government, known as "Mendizabal's confiscation", and these two buildings passed to the property of the state (Martín et al., 2003). Moreover, archaeological works also shed light on the existence of evidences from earlier dates beneath the church. On the one hand, numerous holes stuffed with medieval hispanomuslim ceramics from the ages and dated before the 13th century were documented (Villanueva et al., 2000); and on the other hand, evidences of a goldsmithing workshop that was active between 13th and 16th centuries were also found (Martín et al., 2003) (Figure 2.8.).

Besides, in the Ethnographic Museum of Castilla y León, five occupation phases of the plot could be documented thanks to the rescue works (Figure 2.9.). The oldest evidence dates back to 1583, when a Royal Prison was built in this plot (1583-18th century) and the latest occupation of the plot took place at the end of the 19th century, hosting a storehouse of the Zamora Industrial S.A. company (Herrero, 2016; Martín et al., 1997; Misiego et al., 1997-1998).

Finally, the Olivares workshops were the remains of a potter complex, and the rescue works revealed the existence of three kilns that were used for pottery production in the San Claudio square, which is located in the SW outskirts of the city of Zamora, in the Duero's

riverfront (Sanz et al., 2005) (Figure 2.10.). The study of the materials and the stratigraphic evidences, have enabled the archaeologists to date the different kiln structures appeared to the late 19th century and up to early 20th century. This is the first time that kiln structures related to pottery activity have appeared in the city of Zamora, providing with an interesting milestone to study the long potting tradition of Zamora and its trade networks within the region and northern Iberian Peninsula context (Figure 2.11.). Furthermore, rests of tannery workshops (the sinks shown in Figure 2.10.) were also documented in this place (Sanz et al., 2005).

Besides, excavations in Benavente and Toro also shed light on the existence of pottery production centres. One of the emblematic buildings of the city of Benavente was demolished. It was the *Casa del Tinte*, which was part of the historical and artistic legacy of the city (De La Mata, 1989). Likewise, in Toro, interventions were carried out in Cuesta del Negrillo No. 11, *Patio del Siete* and *Cuesta del Matadero* sites

In the course of all these fieldworks, an important set of archaeological materials, including an important set of ceramics, was recovered (see the figures of the ceramics in Chapter 4, section 4.1.1.).

On the one hand, the ceramic vessels unearthed at La Concepción remains, specifically at the goldsmithing workshop strata (13th-16th centuries), can be subdivided in two groups: glazed and unglazed ceramics. Among the last ones, common and micaceous types, which constitute the majority amongst the unglazed pottery found, are distinguished (Villanueva et al., 2000). Additionally, among them, another typology of the pottery identified is the so-called "Duque de la Victoria" type. This name corresponds to the homonymous street in Valladolid where some pottery workshops were found and dated back to the late Medieval period as well. Six fragments of this type have been recovered in the goldsmithing workshop area. This typology comprises ceramics belonging to tableware, storage and transport and all have similar technical characteristics: they are wheel-made, as evidenced by the numerous parallel and circular grooves inside the pieces. The firing of these type of pieces was carried out in mainly oxidizing atmosphere, a system used throughout the Medieval Era, and the result are the pieces with orange tones (Fernández et al., 1991; Villanueva et al., 2000).

On the other hand, the set of ceramics unearthed at the site of the Ethnographic Museum contained different typologies: on the one hand, some ceramics are tableware, like plates, porringers or bowls; while on the other hand, cooking or storage typologies are also present in abundance, like jugs, pitchers, pots, pans, stoves, oil lamps (Herrero, 2016; Martín et al., 1997). In addition, those ceramic vessels can be subdivided into two groups according to their coatings: glazed tableware and unglazed ceramics for storage, transport, cooking and tableware. Among the unglazed ones (which constitute the majority of the pottery recovered), common and micaceous types are distinguished (Herrero, 2016; Martín et al., 1997; Misiego et al., 1997-1998).

Among the glazed pottery from the workshops of Olivares, white tin-lead glazed tableware has been rescued, sometimes decorated with blue or green motifs from vegetal to geometric ones, and showing forms related to food services like plates, bowls and jars (Larrén, 1991; Villanueva, 2011). Additionally, honey-coloured translucent lead glazed ceramics and micaceous ceramics have been also unearthed among the materials documented in the archaeological record (Sanz et al., 2005). While the white tin-lead glazed ceramics shows a cream-beige-pink colored tone (called *buff-coloured* along the text) (Turina, 1994), the honey-coloured translucent glazed ones show reddish paste bodies. This

is in agreement with the historical information provided by Ramos (1980), which reports the manufacturing of red paste unglazed and honey-coloured translucent glazed ceramics, at least during the last decades of activity of the workshops (early 20th century). In addition, micaceous ceramics, which are mainly cooking pots or big jars, have been also found during the archaeological works, although their origin is uncertain since there is a long tradition of micaceous production in other Zamoran villages, like Pereruela or Muelas del Pan. It should also be noted that a lot of pieces for waste were documented in different production stages, starting from biscuit unglazed fragments to glaze blobs in other pieces, etc. Trivets or auxiliary elements associated with the production of the pottery that would help to separate the ceramics from the kiln are also frequent. Some of them rescued at Olivares have splashes of glaze, thus confirming the production of glazes (Sanz et al., 2005). Furthermore, big jars were also unearthed at the site corresponding to the tanneries.

Additionally, the collection rescued in La Casa del Tinte in Benavente has around 1500 pieces. Among them, there are two well defined groups: 1) the set from the 17th-18th centuries, corresponding to ceramics for liquid storage (jugs, pitchers) and tableware (associated to a possible "wine cellar" of the Casa del Tinte). Some are similar to the ceramics identified in other productions of the province, specifically in Toro, and others are micaceous pastes fired in oxidant firing and buff-coloured ceramics with a white tin-lead glaze and different decorations (Arnau, 1997). 2) A set of jarritas carenadas, dated to the 15th century (Larrén, 1991, 1992, 1997-1998).

Finally, in Toro different forms were identified in the sets of Cuesta del Negrillo No. 11. Additionally, set of ceramics were also rescued in *Patio del Siete* and *Cuesta del Matadero* sites, however, these findings were not the result of archaeological excavations, but casual findings (Larren, 1992). All os these ceramics correspond to open forms, closed ones and construction elements. Besides, the finishing of the pieces is of two types: smoothing and glazing (finished in brown or red), limited to the inner surface and edges of the objects. In principle, according to the literature, it seems that this local pottery production center dedicates its activity to productions that were not luxury, while they seem to be associated with a rural environment. That is, they were basic and necessary forms in the development of daily life: pitchers and bowls for carrying and storing water, pots and pans, plates and cups for preparing and consuming food, chamber pots for personal hygiene and tubes to solve construction problems (Larrén, 1991).

Unfortunately, the current archaeometrical knowledge on the ceramic materials from Zamora and its region is fragmented and represented by a scattered collection of works. Among them, it has to be highlighted the ethnoarchaeometrical investigation about the cooking pot production of Pereruela, in which contemporary production and clay supply from a complex geological context was assessed (Buxeda et al., 2003). Other relevant study is the one carried out by Iñañez and collaborators (2018), in which the authors characterized the ceramics recovered in the old workshops of Olivares. Additionally, Calparsoro (2019) suggests a probable Zamoran provenance for some of the ceramics studied archaeometrically, recovered in Logroño and Nájera (La Rioja), as well as in Orduña, Elosu and Durango (Basque Country) (Calparsoro, 2019; Calparsoro et al., 2019b,c, 2021). Recently, Puig Barrachina (2016) suggested the provenance of Zamora (labelled as PB5 group) for different ceramics found in several early modern Basque sites (Durango, Munitibar, Getaria and Bilbo) after petrographic observations and chemical analyses.

2.2. Production of Aveiro region

Aveiro, a city located in the west of the Iberian Peninsula, in Portugal, lies next to a large lagoon area called “Ria de Aveiro” (Figure 2.13.). Separated from the Atlantic Ocean by a line of dunes more than 50 km long, the lagoon influenced the life of the inhabitants from Medieval times to the Early Modern age; and settlements, which were strongly related to maritime activities and trading, combined agriculture with salt production and fishing. As a consequence, it became an important maritime port. Moreover, these economic activities - often seasonal and complementary- marked the landscape of the lagoon (Alves et al., 2001; Amorim, 2011; Carvalho et al., 2014).

Figure 2.13. The location of Aveiro in the map of Portugal (the red circle that is in the little map in the left) and the location of *Ria de Aveiro A (RAVA)* and *Santo António* church in the principal map (red circles)

Nevertheless, Aveiro not only was famous because of its maritime activities and trading; the city was, and nowadays still is, a traditional ceramic production region, with high variety and availability of clay reserves. The chemical and mineralogical properties of these clays led to their use as a raw material for the ceramic manufacturing. Pottery production increased in the early 16th century, due to the growth of the city and the maritime trade, which demanded pottery to supply ships and commerce (Barbosa et al., 2009; Bettencourt and Carvalho, 2007-2008; Carvalho and Bettencourt, 2012).

Aveiro featured both red and black coarsewares, showing similar paste features. The red ware assemblage, fired in an oxidising environment, is composed of pieces of an orangey to red colours, with darker grey surfaces. Many exemplars have different shades and even black stains on the outer surfaces as a result of variations in the firing environment and kiln temperature. A small percentage of the assemblage is represented by black vessels, fired in a reductive environment, with pastes of grey and black tones, sometimes with a visible metallic shine. The macro-visual observation of red and black pastes revealed a very fine and hard paste, and the two groups show the same inclusions: quartz and mica, fine to medium grained, well distributed throughout the matrix. Mica is more abundant, being very visible on the exterior surfaces. Most of the vessels may have received some surface treatments that consisted mainly on smoothing the surfaces, in some cases after the

application of a slip of the same colour as the paste, but slightly darker (Bettencourt and Carvalho, 2007-2008; Carvalho and Bettencourt, 2012).

Those ceramics can be classified in different groups, such as for domestic use, like tableware (e.g. cups, bowls, jars), kitchenware (cooking pots) and personal hygiene (bacins); long-distance storage and transportation (e.g. olive jars); and sugar moulds (*formas de açúcar*) (Figure 2.14.).

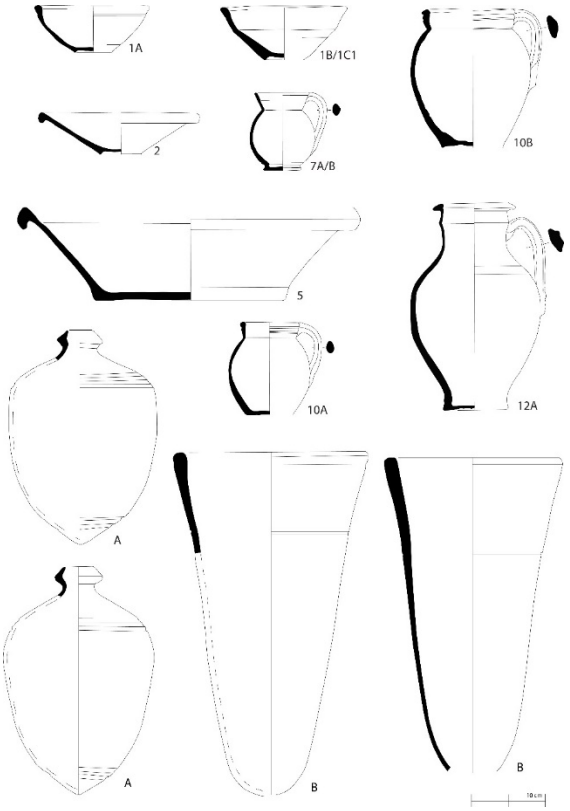

Figure 2.14. Main pottery forms: A – olive jars; B – sugar moulds; 1A/1B/1C – bowls; 2 – plate; 5 – basins; 7A/B – mugs; 10A/B – cooking pots; 12A – jar

Sugar moulds were essential for the sugar production process. They are conical moulds, with a hole in their top. Nowadays, it is common to find discarded pieces as a constituent element of the wall of the old buildings in the old town of the city (Bettencourt and Carvalho, 2007-2008; Morgado et al., 2012). In recent years, sugar moulds, as well as pottery with different typologies from Aveiro, have been identified in international locations. According to Silva (2018), Aveiro was, probably, since the 16th century, the main producer and supplier of sugar moulds in the sugar production areas of the Kingdom of Portugal, such as in Madeira, Azores and Cape Verde, and had a strong impact in other markets like Canaries. Ceramics from Aveiro were also found in England and Newfoundland. All these facts are evidence of the Atlantic and transatlantic trade flows during the Medieval and Modern Periods. Portugal was certainly a major consumer of English-caught Newfoundland cod (Bettencourt and Carvalho, 2007-2008; Carvalho and Bettencourt, 2012; Newstead, 2014; Silva, 2018).

On the other hand, the traditional salt production in the region is well known since the 10th century and the production was increased after the 13th century, due to the constant salinity levels of the lagoon water as well as the favourable landscape and environmental conditions. In fact, several maps show the salt production locations in the lagoon, such as the map made by the Dutch cartographer Lucas Janszoon Waghenaer in 1584 (Figure 2.15.). In this way, Aveiro also played an important role in the supply of salt since the Middle Ages, not only to North-western Europe (England, Finland and Sweden), but also to the north of Spain, in particular Galicia and Asturias, as well as to the Dutch market, during the 16th and 17th centuries (Amorim, 2019; Antunes, 2008a). Salt was used in manufacturing and preservation of food and hides. Fishing and other activities were heavily dependent on this by-product of the sea (Antunes, 2008b).

Figure 2.15. Sea map of Portugal made by the Dutch cartographer Lucas Janszoon Waghenaer in 1584. The salt production centres of Aveiro could be seen in the fourth river starting to the left. [Title: Gedaente en vodoeninge vant Landt van Portugal; from: Mariner's Mirror (T'eerste deel vande Spieghel der zeevaerdt, van de navigatie der Westersche zee, innehoudende alle de custen van Vranckrijck, Spaingen ende't principaelste deel van Engelandt, in diversche zee caerten begrepen", Leiden, Christoffel Plantijn, 1584). Source: University of Texas at Arlington Libraries]

The Atlantic distribution of the Aveiro ceramics is documented, in addition to the discovery of Aveiro wares in other localities, thanks to a diverse underwater archaeological record, with nearly a dozen archaeological sites (Carvalho et al., 2014). Some of the examples belong to the archaeological sites called "Ria de Aveiro A, B and C". In the two latter places, a large assemblage of Aveiro ceramics as well as several artefacts related to maritime activities were discovered, suggesting that Aveiro was connected to the routes with the North and the South of Europe since the Middle Ages (Bettencourt, 2009; Carvalho et al., 2014). Moreover, the former case corresponds to a shipwreck. *Ria de Aveiro A (RAVA)* (see the map of Figure 2.13.) was discovered in the Aveiro lagoon (Ílhavo) in 1992 (Figure 2.16.). The site preserved the aft end of a small wooden vessel, ca. 18-meter-long ship of Ibero-Atlantic tradition, which transported a coarseware cargo. The cargo was located in the hold of the ship, and the ceramics were protected by a dunnage "mattress" about 200 mm thick, made of interwoven sticks, undergrowth, straw and pine needles (Alves et al., 2001). Carbon-14 analysis conducted at an initial research stage, attributed the context to a chronology from mid-15th century (Alves et al., 2001), but the excavation and study of the ceramic cargo indicates a more recent date, from early modern period, 16th or beginning of the 17th

centuries (Carvalho and Bettencourt, 2012). RAVA was interpreted as containing a local ceramics cargo destined to be sold in markets outside the lagoon, but the final destination could not be defined. The size of the cargo and the archaeological context suggest, however, a port located in Portugal as the most probable destination (Bettencourt and Carvalho, 2007-2008).

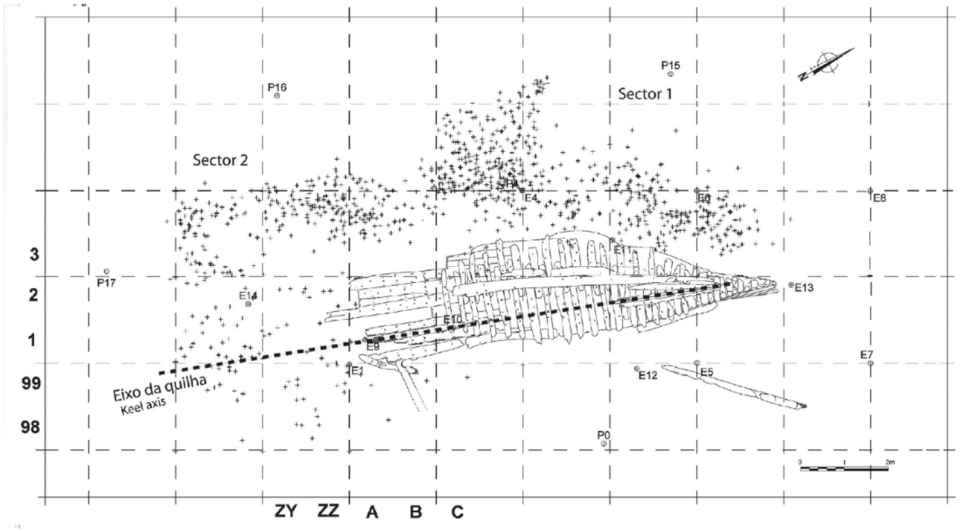

Figure 2.16. The RAVA archaeological site, in which the shipwreck and the distribution of materials that the ship was carrying are shown (the cross-marks). Source: Carvalho and Bettencourt (2012)

The large number of recovered ceramic pieces allowed the establishment of a typology with the shapes used in everyday life at that time. Some big ceramics, such as large pots, were carrying smaller pots inside them. Similar ceramics were found in Portugal, particularly in the North (Viana do Castelo, Porto, Coimbra), but also in the Atlantic, in places like Azores, Madeira, Newfoundland, in sites related to seasonal fishing settlement, or on England contexts (Alves et al., 2001; Bettencourt and Carvalho, 2007-2008; Carvalho and Bettencourt, 2012). It should also be noted that several pieces of evidence indicative of a fire on board were documented. These are visible in a set of ceramics, which are burnt, deformed and vitrified (Carvalho and Bettencourt, 2012) (these pieces are shown in Chapter 4, section 4.1.1.). Since the ceramics were located in the hold of the ship and they were wrapped, the firing environment produced around the ceramics could have been a reducing environment.

On the other hand, another archaeological works were carried out at the *Santo António* church in Aveiro (see the map of Figure 2.13.). In the filling of the upper choir dome, around 90 ceramics of different typologies were recovered (Figure 2.17.). The primitive Franciscan convent of Santo António, of which only the church and part of the cloister remains, was founded in 1524 and it was classified as a National Monument. The use of ceramics in the construction of domes is a peculiar technique of remote origin, probably Roman, which was developed in the Medieval Era. After cleaning the surface remains, it was discovered that the ceramics were methodically placed and surrounded by very fine and loose clay soil. The conditions and context of finding, allowed assigning this lot to a precise chronology (1524). As many of them had manufacturing defects, it is generally assumed that ceramics reused in these contexts were of local production. There was a predominance of red and unglazed earthenware, although some big black cooking pots were also recovered.

In addition to the assemblage of household ceramics and sugar moulds already well known in Aveiro, the finding of a group of several olive jars (called *botijas* in Spanish) was remarkable because they constituted the main part of the retrieved collection in the church. One of the most characteristic aspects of the olive jars is the distinctive exterior surface treatment by the white slip. This slip is not uniform and does not cover the entire pieces (Silva, 2018).

Figure 2.17. Upper choir dome of Santo António church (above) and Santo António church (below). Source: Silva (2018) (the upper photograph is of Andreia Lourenço (Silva, 2018))

Regarding the archaeometric analyses of the ceramic materials from Aveiro and surroundings, few studies have been carried out. Among them, the archaeometric investigation by Alves and collaborators (1998), concerning the ceramics recovered in the ship of Ria de Aveiro A, should be noted. In their research, Alves and colleagues catalogued those ceramics as local products after comparing them with the ceramics recovered in Bairro das Olarias (Aveiro) and Casa do Infante (Porto) by means of X-Ray Fluorescence (XRF). The authors additionally have identified, by XRD, the iron oxide as the common colouring agent, giving different colours (red, brown, grey and black) depending on the oxidation state of the iron. Other relevant study includes the one carried out by Sousa and collaborators (2005). Sousa and colleagues characterized sugar moulds exhumed in Machico (Madeira Island) concluding that these ceramics could have been produced in Aveiro. Additionally, Vieira and collaborators (2013) compared the spectroscopic data of Portuguese faience production from Mata da Machada (South of Lisbon) and tin-lead glazed shards found in a medieval house in Aveiro. The obtained results indicate a similarity in the spectrum in their glaze and clays

CHAPTER 3: OBJECTIVES

The general goals of this work are explained in the following points (1-3):

1. To optimize our analytical method for the chemical analyses of ceramics, improving the calibration curves and proposing a way to obtain reliable results. The explanation and results of this part are presented in Chapter 4.

2. To characterize the post-depositional alterations and contaminations that can happen in ceramics buried at water environments, through an aging laboratory experiment. The results of this part are presented in Chapter 5.

3. To develop relevant background of knowledge to facilitate the reconstruction and interpretation of the processes involved in the manufacture, use and trade of pottery from Zamora and Aveiro regions. The results are presented in Chapter 6 and include six case studies for Zamoran pottery and two case studies for pottery from Aveiro.

To reach these objectives, this Doctoral Thesis integrates both, the study of the archaeometric research problems and the application of a well-established archaeometric routine. Both aspects have contributed in a synergistic way during the course of the present investigation. On the one hand, the study of the archaeometric research problems allows the improvement of the archaeometric routine for the characterization of the ceramics, optimizing the analytical method (objective 1) and shedding more light on the ways of the post-depositional alterations and contaminations that occur in ceramics (objective 2). The optimization of the analytical method has been proposed in order to adequate it to the studied samples. Besides, the study of the alterations and contaminations ways occurred in ceramics due to their burial is proposed because they should be considered to avoid incorrect interpretations on different aspects related to ceramics. On the other hand, the application of a well-established archaeometric routine permits an archaeometric characterization of pottery production centres from Zamora and Aveiro (objective 3). In this way, the existing lack of information regarding the Medieval and Post-Medieval pottery production in Zamora and Aveiro will be filled and the provenance of local or regional origin of the ceramics will be assessed, shedding light on the regional or supraregional trade and local consumption patterns.

CHAPTER 4: METHODOLOGY

All aspects of the methodology related to the present work are handled in this chapter. First, the general sampling strategy and the selected samples of ceramics (section 4.1.), followed by the methodological process of the aging laboratory experiment carried out in the laboratory (section 4.2.), are explained. Then, all the techniques used in this work, in addition to the analytical methodology followed for the measurements are described (section 4.3.). Furthermore, analytical considerations taken into account (section 4.4.) and, finally, the statistical model used for treating the results of the chemical analyses are detailed (section 4.5.).

4.1. Sampling strategy for ceramics

It is convenient to think about some considerations prior to the ceramic sampling, in order to ensure the appropriateness of the sampling criteria. One of the considerations is whether the archaeological study of the territory and/or site and, especially, the morphological-stylistic analysis of the ceramic collection have been finished. Other consideration is the formulation of the archaeometric research questions and the last is the determination of the experimental procedure (Gliozzo, 2020a).

Regarding the appropriateness of the sampling criteria, it must be representative of the entire collection, functional and suitable. When it comes to the representativeness, individuals from different stratigraphic phases and periods should be sampled. In this way, it is possible to identify compositional differences between them. The second condition will ensure the functionality of the sampling strategy with respect to the overall research objectives. For example, if a research question regards the technological investigation of red and black pottery found at one specific distribution site, it will require first a collection representative of red and black types only. The last condition is the suitability between the types of samples taken and the analytical techniques used. Parameters such as whether the object is precious, or whether ceramic types were found in abundance, must be known when a material sample is taken to ensure that it is of the correct type and quantity (Gliozzo, 2020a).

4.1.1. Selected samples

Taking into account all explained above, the selected materials in each archaeological site are described in Table 4.1. and in the following lines.

Table 4.1. Samples, the region, village, archaeological site and the context where ceramics were rescued, in addition to their typology, colour decoration of the glazes, form and chronology. (n/d= non-documented)

Samples	Region	Village	Archaeological site	Context	Typology	Colour decoration	Form	Chronology
ZMR001	Zamora	Zamora city	Olivares	kiln 01	unglazed	-	bowl	late 19th-early 20th
ZMR002	Zamora	Zamora city	Olivares	kiln 01	tin-lead glazed	white and blue	plate	late 19th-early 20th
ZMR003	Zamora	Zamora city	Olivares	kiln 01	tin-lead glazed	white and green	plate	late 19th-early 20th
ZMR004	Zamora	Zamora city	Olivares	kiln 01	unglazed	-	plate	late 19th-early 20th
ZMR005	Zamora	Zamora city	Olivares	kiln 01	tin-lead glazed	white and blue	plate	late 19th-early 20th
ZMR006	Zamora	Zamora city	Olivares	kiln 01	tin-lead glazed	white and green	plate	late 19th-early 20th
ZMR007	Zamora	Zamora city	Olivares	kiln 01	unglazed	-	bowl	late 19th-early 20th
ZMR008	Zamora	Zamora city	Olivares	kiln 01	tin-lead glazed	white	porringer	late 19th-early 20th
ZMR009	Zamora	Zamora city	Olivares	kiln 01	unglazed	-	large jar	late 19th-early 20th
ZMR010	Zamora	Zamora city	Olivares	kiln 01	unglazed	-	cup	late 19th-early 20th

ZMR011	Zamora	Zamora city	Olivares	kiln 01	micaceous unglazed	-	large jar	late 19th-early 20th
ZMR012	Zamora	Zamora city	Olivares	kiln 01	micaceous translucent-glazed	beige (raw glaze)	large jar	late 19th-early 20th
ZMR013	Zamora	Zamora city	Olivares	kiln 01	micaceous unglazed	-	large jar	late 19th-early 20th
ZMR014	Zamora	Zamora city	Olivares	kiln 01	translucent-glazed	beige (raw glaze)	jar	late 19th-early 20th
ZMR015	Zamora	Zamora city	Olivares	kiln 01	micaceous translucent-glazed	beige (raw glaze)	jar	late 19th-early 20th
ZMR016	Zamora	Zamora city	Olivares	kiln 01	translucent-glazed	beige (raw glaze)	jar	late 19th-early 20th
ZMR017	Zamora	Zamora city	Olivares	kiln 01	unglazed	-	trivet (kiln tool)	late 19th-early 20th
ZMR018	Zamora	Zamora city	Olivares	kiln 01	unglazed	-	trivet (kiln tool)	late 19th-early 20th
ZMR019	Zamora	Zamora city	Olivares	kiln 01	translucent-glazed	beige (raw glaze)	plate	late 19th-early 20th
ZMR020	Zamora	Zamora city	Olivares	kiln 01	tin-lead glazed	white and green	plate	late 19th-early 20th
ZMR021	Zamora	Zamora city	Olivares	kiln 01	tin-lead glazed	white and blue	plate	late 19th-early 20th
ZMR022	Zamora	Zamora city	Olivares	kiln 02	translucent-glazed	brown	cooking pot	late 19th-early 20th

ZMR023	Zamora	Zamora city	Olivares	kiln 02	translucent-glazed	brown	cooking pot	late 19th-early 20th
ZMR024	Zamora	Zamora city	Olivares	kiln 02	translucent-glazed	green	cooking pot	late 19th-early 20th
ZMR025	Zamora	Zamora city	Olivares	kiln 02	translucent-glazed	brown	cooking pot	late 19th-early 20th
ZMR026	Zamora	Zamora city	Olivares	kiln 02	unglazed	-	trivet (kiln tool)	late 19th-early 20th
ZMR027	Zamora	Zamora city	Olivares	kiln 02	unglazed	-	bowl	late 19th-early 20th
ZMR028	Zamora	Zamora city	Olivares	kiln 02	micaceous translucent-glazed	brown	lid	late 19th-early 20th
ZMR029	Zamora	Zamora city	Olivares	kiln 03	translucent-glazed	beige (raw glaze)	small jar	late 19th-early 20th
ZMR030	Zamora	Zamora city	Olivares	kiln 03	translucent-glazed	black (burnt)	handle	late 19th-early 20th
ZMR031	Zamora	Zamora city	Olivares	kiln 03	unglazed	-	bowl	late 19th-early 20th
ZMR032	Zamora	Zamora city	Olivares	kiln 03	micaceous translucent-glazed	brown	large jar	late 19th-early 20th
ZMR033	Zamora	Zamora city	Olivares	kiln 03	micaceous translucent-glazed	white (burnt)	n/d	late 19th-early 20th
ZMR034	Zamora	Zamora city	Olivares	kiln 03	unglazed	-	trivet (kiln tool)	late 19th-early 20th

ZMR035	Zamora	Zamora city	Olivares	kiln 03	micaceous translucent-glazed	blackish (burnt)	handle	late 19th-early 20th
ZMR036	Zamora	Zamora city	Olivares	kiln 01	unglazed	-	cup	late 19th-early 20th
ZMR065	Zamora	Zamora city	Olivares	kiln 03	tin-lead glazed	black and white (burnt)	n/d	n/d
ZMR037	Zamora	Zamora city	La Concepción	goldsmithing workshop	micaceous unglazed	-	cooking pot	15th-16th
ZMR038	Zamora	Zamora city	La Concepción	goldsmithing workshop	micaceous unglazed	-	bowl	15th-16th
ZMR039	Zamora	Zamora city	La Concepción	goldsmithing workshop	micaceous unglazed	-	large jar	15th-16th
ZMR040	Zamora	Zamora city	La Concepción	goldsmithing workshop	tin-lead glazed	white	bowl	15th-16th
ZMR041	Zamora	Zamora city	La Concepción	goldsmithing workshop	tin-lead glazed	white	bowl	15th-16th
ZMR042	Zamora	Zamora city	La Concepción	goldsmithing workshop	micaceous unglazed	-	pitcher	15th-16th
ZMR043	Zamora	Zamora city	La Concepción	goldsmithing workshop	micaceous unglazed	-	cooking pot	15th-16th

ZMR044	Zamora	Zamora city	La Concepción	goldsmithing workshop	micaceous unglazed	-	pitcher	15th-16th
ZMR045	Zamora	Zamora city	La Concepción	goldsmithing workshop	tin-lead glazed	green, black and white	bowl	15th-16th
ZMR046	Zamora	Zamora city	La Concepción	goldsmithing workshop	tin-lead glazed	white and blue	bowl	15th-16th
ZMR047	Zamora	Zamora city	La Concepción	goldsmithing workshop	tin-lead glazed	white and blue	bowl	15th-16th
ZMR048	Zamora	Zamora city	La Concepción	goldsmithing workshop	tin-lead glazed	green, brown and white	plate	15th-16th
ZMR049	Zamora	Zamora city	La Concepción	goldsmithing workshop	tin-lead glazed	white	bowl	15th-16th
ZMR050	Zamora	Zamora city	La Concepción	goldsmithing workshop	unglazed - Duque de la Victoria type	-	n/d	15th-16th
ZMR051	Zamora	Zamora city	Ethnographic Museum	n/d	tin-lead glazed	white, green and black	bowl	17th-18th
ZMR052	Zamora	Zamora city	Ethnographic Museum	n/d	tin-lead glazed	white, green and black	bowl	16th
ZMR053	Zamora	Zamora city	Ethnographic Museum	n/d	tin-lead glazed	white and green	bowl	17th-18th

ZMR054	Zamora	Zamora city	Ethnographic Museum	n/d	tin-lead glazed	white and blue	porringer	17th-18th
ZMR055	Zamora	Zamora city	Ethnographic Museum	n/d	tin-lead glazed	white and blue	plate	17th-18th
ZMR056	Zamora	Zamora city	Ethnographic Museum	n/d	tin-lead glazed	white	plate	17th-18th
ZMR057	Zamora	Zamora city	Ethnographic Museum	n/d	tin-lead glazed	white	bowl	17th-18th
ZMR058	Zamora	Zamora city	Ethnographic Museum	n/d	tin-lead glazed	white	plate	17th-18th
ZMR059	Zamora	Zamora city	Ethnographic Museum	n/d	tin-lead glazed	white	plate	17th-18th
ZMR060	Zamora	Zamora city	Ethnographic Museum	n/d	tin-lead glazed	white	bowl	17th-18th
ZMR061	Zamora	Zamora city	Ethnographic Museum	n/d	tin-lead glazed	white	bowl	17th-18th
ZMR062	Zamora	Zamora city	Mengue Avenue	tannery	micaceous unglazed	-	large jar	n/d
ZMR063	Zamora	Zamora city	Mengue Avenue	tannery	micaceous unglazed	-	large jar	n/d
TOR001	Zamora	Toro	Cuesta del Negrillo No.11	dump	translucent-glazed	brown	mug	17th
TOR002	Zamora	Toro	Cuesta del Negrillo No.11	dump	translucent-glazed	brown	small jar	17th

TOR003	Zamora	Toro	Cuesta del Negrillo No.11	dump	unglazed	-	jar	17th
TOR004	Zamora	Toro	Cuesta del Negrillo No.11	dump	unglazed	-	chamber pot	17th
TOR005	Zamora	Toro	Cuesta del Negrillo No.11	dump	translucent-glazed	brown	small jar	17th
TOR006	Zamora	Toro	Patio del Siete	dump	unglazed	-	small jar	17th
TOR007	Zamora	Toro	Patio del Siete	dump	unglazed	-	jar	17th
TOR008	Zamora	Toro	Patio del Siete	dump	unglazed	-	large jar	17th
TOR009	Zamora	Toro	Cuesta del Matadero	kiln dump	unglazed	-	pitcher	17th
TOR010	Zamora	Toro	Cuesta del Matadero	kiln dump	translucent-glazed	brown	pitcher	17th
TOR011	Zamora	Toro	Cuesta del Matadero	kiln dump	translucent-glazed	brown	lid	17th
TOR012	Zamora	Toro	Cuesta del Matadero	kiln dump	translucent-glazed	brown	cup	17th
TOR013	Zamora	Toro	Cuesta del Matadero	kiln dump	unglazed	-	pipe	17th
TOR014	Zamora	Toro	Cuesta del Matadero	kiln dump	unglazed	-	pipe	17th
BNV001	Zamora	Benavente	Casa del Tinte	hospital	tin-lead glazed	white and blue	bowl	17th-18th
BNV002	Zamora	Benavente	Casa del Tinte	hospital	tin-lead glazed	white	plate	17th
BNV003	Zamora	Benavente	Casa del Tinte	hospital	tin-lead glazed	white	bowl	17th-18th
BNV004	Zamora	Benavente	Casa del Tinte	hospital	tin-lead glazed	white and green	chamber pot	17th-18th

BNV005	Zamora	Benavente	Casa del Tinte	dump (previous to the hospital)	unglazed	-	pitcher	16th-18th
BNV006	Zamora	Benavente	Casa del Tinte	dump (previous to the hospital)	unglazed	-	pitcher	16th-18th
BNV007	Zamora	Benavente	Casa del Tinte	dump (previous to the hospital)	unglazed	-	pitcher	16th-18th
BNV008	Zamora	Benavente	Casa del Tinte	dump (previous to the hospital)	unglazed	-	small jar	16th-18th
BNV009	Zamora	Benavente	Casa del Tinte	dump (previous to the hospital)	unglazed	-	small jar	16th-18th
BNV010	Zamora	Benavente	Casa del Tinte	dump (previous to the hospital)	unglazed	-	small jar	16th-18th
BNV011	Zamora	Benavente	Casa del Tinte	dump (previous to the hospital)	unglazed	-	small jar	16th-18th

BNV012	Zamora	Benavente	Casa del Tinte	dump (previous to the hospital)	unglazed	-	small jar	16th-18th
BNV013	Zamora	Benavente	Casa del Tinte	dump (previous to the hospital)	unglazed	-	jug	16th-18th
BNV014	Zamora	Benavente	Casa del Tinte	dump (previous to the hospital)	unglazed	-	jug	16th-18th
BNV015	Zamora	Benavente	Casa del Tinte	dump (previous to the hospital)	unglazed	-	jug	16th-18th
BNV016	Zamora	Benavente	Casa del Tinte	dump (previous to the hospital)	unglazed	-	jug	16th-18th
AVR001	Aveiro	Aveiro city	Ria de Aveiro A	RAVA	unglazed	-	basin	16th-17th
AVR002	Aveiro	Aveiro city	Ria de Aveiro A	RAVA	unglazed	-	basin	16th-17th
AVR003	Aveiro	Aveiro city	Ria de Aveiro A	RAVA	unglazed	-	plate	16th-17th
AVR004	Aveiro	Aveiro city	Ria de Aveiro A	RAVA	unglazed	-	mug	16th-17th

AVR005	Aveiro	Aveiro city	Ria de Aveiro A	RAVA	unglazed	-	storage jar	16th-17th
AVR006	Aveiro	Aveiro city	Ria de Aveiro A	RAVA	unglazed	-	bowl	16th-17th
AVR007	Aveiro	Aveiro city	Ria de Aveiro A	RAVA	unglazed	-	bowl	16th-17th
AVR008	Aveiro	Aveiro city	Ria de Aveiro A	RAVA	unglazed	-	basin	16th-17th
AVR009	Aveiro	Aveiro city	Ria de Aveiro A	RAVA	unglazed	-	bowl	16th-17th
AVR010	Aveiro	Aveiro city	Ria de Aveiro A	RAVA	unglazed	-	mug	16th-17th
AVR011	Aveiro	Aveiro city	Ria de Aveiro A	RAVA	unglazed	-	mug	16th-17th
AVR012	Aveiro	Aveiro city	Ria de Aveiro A	RAVA	unglazed	-	pitcher	16th-17th
AVR013	Aveiro	Aveiro city	Ria de Aveiro A	RAVA	unglazed	-	basin	16th-17th
AVR014	Aveiro	Aveiro city	Ria de Aveiro A	RAVA	unglazed	-	basin	16th-17th
AVR015	Aveiro	Aveiro city	Ria de Aveiro A	RAVA	unglazed	-	plate	16th-17th
AVR016	Aveiro	Aveiro city	Ria de Aveiro A	RAVA	unglazed	-	plate	16th-17th

AVR017	Aveiro	Aveiro city	Santo António church	upper choire dome	unglazed	-	olive jar (*anforeta/botija*)	16th
AVR018	Aveiro	Aveiro city	Santo António church	upper choire dome	unglazed	-	sugar mould (*forma de açúcar*)	16th
AVR019	Aveiro	Aveiro city	Santo António church	upper choire dome	unglazed	-	sugar mould (*forma de açúcar*)	16th
AVR020	Aveiro	Aveiro city	Santo António church	upper choire dome	unglazed	-	sugar mould (*forma de açúcar*)	16th
AVR021	Aveiro	Aveiro city	Santo António church	upper choire dome	unglazed	-	cooking pot	16th
AVR022	Aveiro	Aveiro city	Santo António church	upper choire dome	unglazed	-	cooking pot	16th
AVR023	Aveiro	Aveiro city	Santo António church	upper choire dome	unglazed	-	bowl	16th
AVR024	Aveiro	Aveiro city	Santo António church	upper choire dome	unglazed	-	pitcher	16th

AVR025	Aveiro	Aveiro city	Santo António church	upper choire dome	unglazed	-	pitcher	16th
AVR026	Aveiro	Aveiro city	Santo António church	upper choire dome	unglazed	-	mug	16th
AVR027	Aveiro	Aveiro city	wasters	dump	translucent-glazed	yellow	bowl	16th-17th
AVR028	Aveiro	Aveiro city	wasters	dump	tin-lead glazed	white and blue	plate	16th-17th

On the one hand, in Zamora city, 37 ceramic sherds (from the 19th-20th centuries) have been selected from the collection rescued in the Olivares workshops (Figure 4.1.). Among the selected 37, 22 were rescued in kiln 1, 7 in kiln 2 and 8 in kiln 3 and, among them, 4 are trivets (kiln furnitures). These last ones were selected to increase the chances of comparing unknown samples with local productions. Besides, 4 sherds over 37 sherds have evidences such as overfiring and glazing defects and 6 sherds have a raw glaze, that enable linking their production origin to the kilns of Olivares.

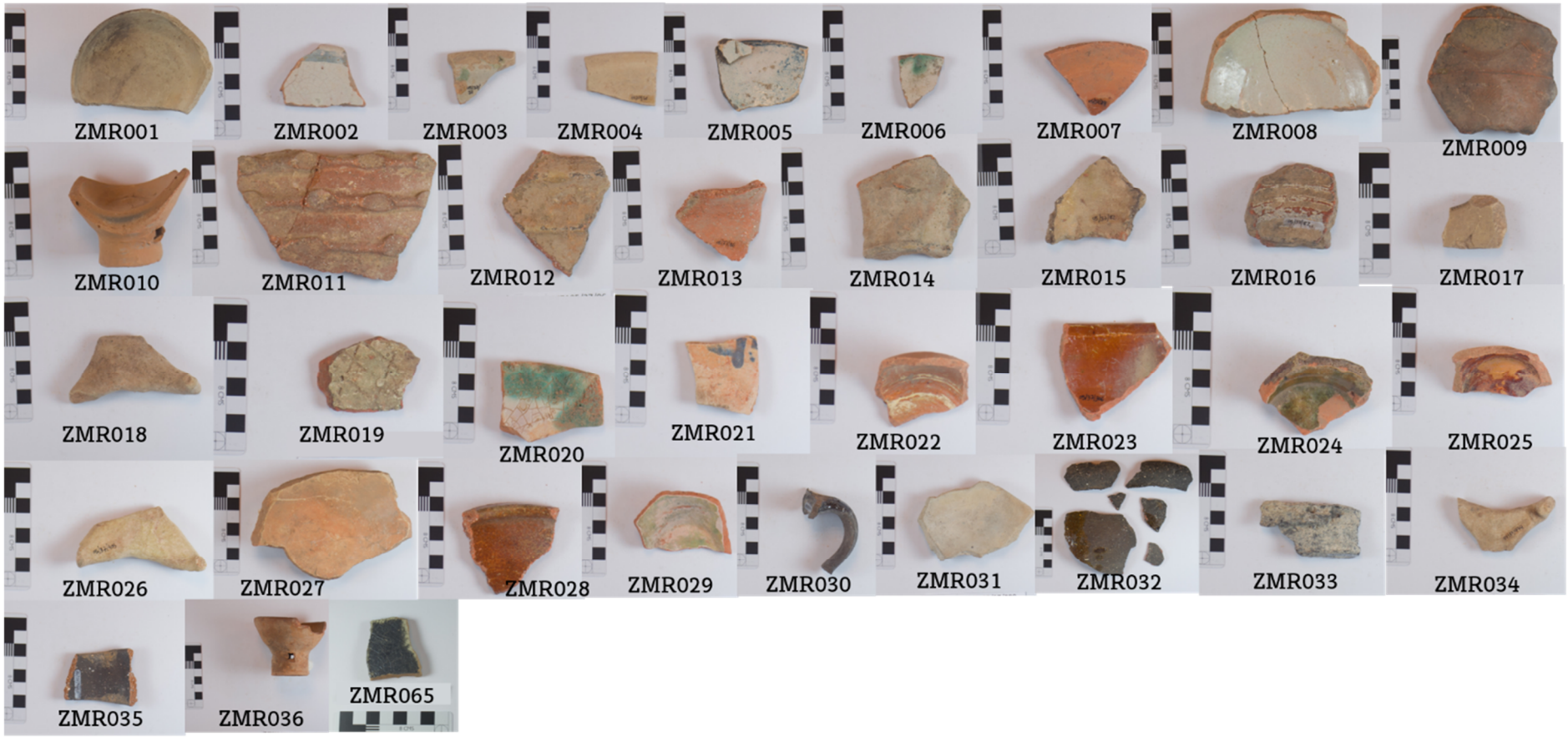

Figure 4.1. 37 ceramics rescued in the Olivares workshops, from left to right. Scale bar: 8 cm

Additionally, 14 sherds, dated back to the 15th-16th centuries, have been selected from La Concepción (Figure 4.2). They were rescued specifically in the strata corresponding to the goldsmithing workshop, which was active during the 13th-16th centuries. Among them, tableware, cooking and storage ceramics are present. There is also one ceramic of *Duque de la Victoria* type.

Figure 4.2. 14 ceramics rescued at La Concepción, scale-bar: 8 cm

Moreover, 11 tin-lead glazed tableware (from 16th-18th centuries) have been selected from the collection rescued at the Ethnographic Museum archaeological site (Figure 4.3.). That period agrees with the period when the Royal Prison was active (1583-18th century), so the ceramics would be related to the activity of the prison.

Figure 4.3. White opaque tin-lead glazed pieces unearthed at the site at the Ethnographic Museum of Zamora, scale-bar: 8 cm

In addition, two fragments of two large jars have been added. They were rescued in the tanneries located at the Mengue Avenue, next to the Olivares ceramic workshops (Figure 4.4.).

Figure 4.4. Micaceous large jars rescued in Mengue Avenue of Zamora, scale-bar: 8 cm

Besides, in Toro village, 5 fragments (from the 17th century) have been selected from the collection rescued at the dump of Cuesta del Negrillo No. 11 (a production site), whereas 3 (from 17th century) have been selected from the collection recovered in the dump of Patio del Siete. Finally, 6 sherds, whose chronology is from the 17th century, have been selected from the collection of the Cuesta del Matadero (Figure 4.5.). All of them are unglazed and translucent-glazed tableware and cooking ceramics, with the exception of two, which are pipe fragments.

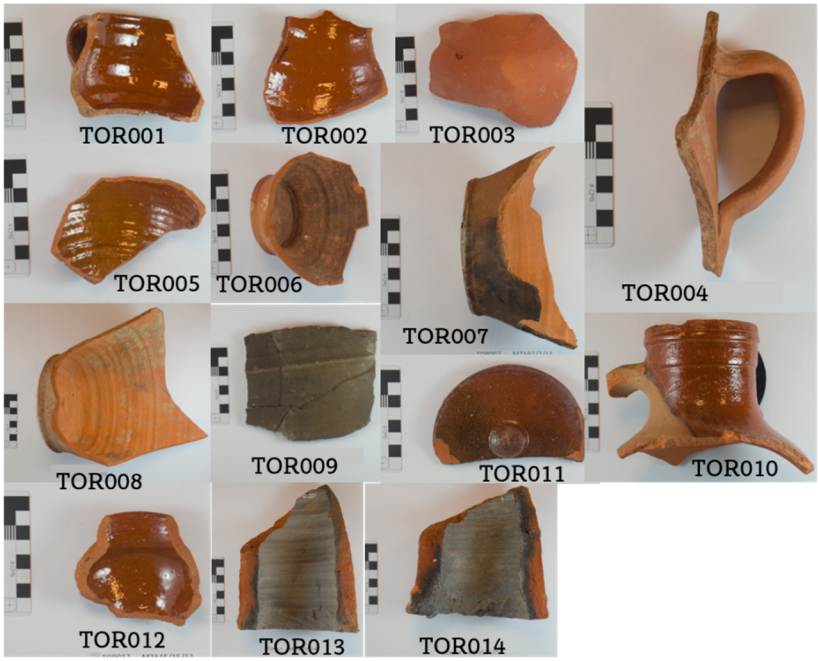

Figure 4.5. 14 red ceramics recovered in different sites of Toro (Cuesta del Negrillo No.11, Patio del Siete and Cuesta del Matadero), some translucent-glazed and others unglazed. Scale-bar: 8 cm

To finish, in Benavente city, 16 sherds have been selected. They were rescued in Casa del Tinte, and, among them, 4 tin-lead glazed ceramics (from the 17th-18th centuries) were rescued in the stratum corresponding to the hospital, whereas 12 unglazed ones (from the 16th-17th centuries) were rescued in a dump prior to the hospital (Figure 4.6.).

Figure 4.6. 16 ceramics (some tin-lead glazed and others unglazed) recovered in Casa del Tinte in Benavente. Scale-bar: 8 cm

On the other hand, in Aveiro city, 16 ceramics have been selected from the collection rescued at RAVA and 10 from the collection rescued at the upper choir dome of Santo António church, all from 16th-17th centuries. The group of household ceramics (AVR001, AVR002, AVR003, AVR004, AVR005, AVR006, AVR007, AVR008, AVR009, AVR010, AVR011, AVR012, AVR013, AVR014, AVR015, AVR016, AVR021, AVR022, AVR023, AVR024, AVR025 and AVR026) corresponds to unglazed with red and black pastes pottery production, and all ceramics are wheel-made evidenced by concentric marks and lines in their surfaces (Figure 4.7.). In addition, two lead-glazed ceramics (one translucent-glazed and the other tin-lead glazed), found in wasters of Aveiro, were added to the sample, summing up 28 ceramics rescued in Aveiro. Among the 28 ceramics, there is a predominance of red earthenware, with variations in the colour of the pastes between red-orange and beige. The pastes of this red earthenware are compact, medium hard and with laminar aspect, either purified or with the inclusion of small and medium non-plastic elements (essentially quartz and calcite) and mica, well distributed throughout the matrix. The black pastes are similar to the previous ones, distinguished only by the reducing cooking environment. Among these ceramics, AVR003 and AVR005 are the most uncommon ceramics. The former shows a two-coloured surface and a black paste, whereas the latter is composed by two ceramic shards stuck together (Figure 4.7.). Additionally, there are three pieces of sugar moulds (AVR018, AVR019 and AVR020) (Figure 4.7.). These are distinguished by compact pastes, a sandy texture, light orange colour and little purification, with poorly distributed abundant small-medium non-plastic elements (like quartz, dark-coloured ferruginous particles) and mica and their surfaces are black matte. Finally, the specific group of containers intended for long-distance storage and transportation is formed by an olive jar (AVR017) (Figure 4.7.). The orange, fine and purified paste differentiates the manufacture of the olive jars. Its surface is not glazed; however, it shows the distinctive exterior surface treatment by the white slip.

Figure 4.7. 28 ceramics rescued at RAVA, Santo António church and wasters in Aveiro, scale-bar: 8 cm

The finish of some black ceramics of this assemblage is also worthy of note: four ceramics show a black shiny metallic surface (AVR003, AVR005, AVR015 and AVR016), whereas nine show a black matte one (AVR001, AVR002, AVR012, AVR018, AVR019, AVR020, AVR021, AVR022 and AVR025) (Figure 4.7.). Regarding the evidence of the firing produced in the ship, AVR005 seems to be totally burnt, showing black pastes and vitrified surfaces. Another shard showing evidence of fire on its surfaces is AVR013. The information about pastes and surfaces is summarized in Table 4.2.

Table 4.2. Samples, archaeological site, form and the colour of the pastes and surfaces of the 28 ceramics rescued in Aveiro

Samples	Archaeological site	Form	Paste	Surface
AVR001	Ria de Aveiro A	basin	beige	black matte
AVR002	Ria de Aveiro A	basin	black	black matte
AVR003	Ria de Aveiro A	plate	black	shiny black and beige
AVR004	Ria de Aveiro A	mug	beige	beige
AVR005	Ria de Aveiro A	storage jar	black	shiny black
AVR006	Ria de Aveiro A	bowl	red	red
AVR007	Ria de Aveiro A	bowl	red	red
AVR008	Ria de Aveiro A	basin	beige	beige
AVR009	Ria de Aveiro A	bowl	beige	beige

AVR010	Ria de Aveiro A	mug	red	red
AVR011	Ria de Aveiro A	mug	red	red
AVR012	Ria de Aveiro A	pitcher	red	black matte
AVR013	Ria de Aveiro A	basin	red	red and black matte
AVR014	Ria de Aveiro A	basin	red	red
AVR015	Ria de Aveiro A	plate	black	shiny black
AVR016	Ria de Aveiro A	plate	dark red	shiny black
AVR017	Santo António church	olive jar (*anforeta/botija*)	red	white
AVR018	Santo António church	sugar mould (*forma de açúcar*)	red	black matte
AVR019	Santo António church	sugar mould (*forma de açúcar*)	red	black matte
AVR020	Santo António church	sugar mould (*forma de açúcar*)	red	black matte
AVR021	Santo António church	cooking pot	black	black matte
AVR022	Santo António church	cooking pot	red	black matte
AVR023	Santo António church	bowl	red	red
AVR024	Santo António church	pitcher	red	red
AVR025	Santo António church	pitcher	red	black matte
AVR026	Santo António church	mug	red	red
AVR027	Wasters	bowl	beige	translucent-glazed (yellow)
AVR028	Wasters	plate	beige	tin-lead glazed (white and blue)

4.2. Aging laboratory experiment for post-depositional alterations and contaminations assessment

The aging laboratory experiment was carried out in order to study the alterations and contaminations that occurred in 60 ceramic cylinders buried in two different underwater environments (tap and seawater). For that, sixty-nine cylinders were prepared using cylinder moulds of 30 mm diameter and 15 mm height. Sixty cylinders were submerged (test-pieces), but 9 were not (control-pieces), as the latter have been used as reference to compare them chemically and mineralogically with submerged pieces.

Three types of commercial clays were used to prepare the 69 pieces. The pieces were dried at room temperature and then at 100 °C in a laboratory electric kiln. After that, they were fired in a laboratory kiln at an oxidant environment at 850, 950 or 1100 °C, leaving them for an hour at the maximum temperature. In this way, 3 different pastes and 9 fabrics (3 fabrics for each paste) were produced out of commercial clays (Figure 4.8., Table 4.3.). It was important to produce several kinds of fabrics to see how the environment affected them. The repeatability of the experiment has also been calculated. For this, 3 pieces of each paste have been used, all fired at 850 °C and submerged in seawater because these conditions are supposed to be the most extreme. Hence, the repeatability calculated for these 9 ceramics is supposed to be representative of the whole experiment.

Figure 4.8. The manufacturing process of the test- and control-pieces before being fired: **(a)** the clay; **(b)** pieces before being fired; **(c)** test-pieces inside a seawater environment container; **(d)** the electric water bath containing the two containers with different environments (tap and seawater)

Table 4.3. The list of 9 manufactured fabrics, combining different clays and firing temperatures, and the number of test-pieces and control-pieces in addition to the pieces corresponding to each underwater environment. PF, PT and AP are the abbreviations used for each kind of clay. The pieces with a (*) are the pieces used for the calculation of the repeatability. The pieces are ordered by their deposition time (001, 006, 009, 012, 015 and 018 pieces were deposited for 3 months, 002, 007, 010, 013, 016 and 019 pieces for 10 months and 003, 004, 005, 008, 011, 014, 017 and 020 pieces for 18 months)

Fabrics	Clay	Firing Temperature (°C)	Test-Pieces	Seawater	Tap water	Control-Pieces
1	Low-calcareous (~5% CaO) (PF)	850	8	PF001-PF003*; PF004*; PF005*	PF006-PF008	1 (PF-01)
2	Low-calcareous (~5% CaO) (PF)	950	6	PF009-PF011	PF012-PF014	1 (PF-05)
3	Low-calcareous (~5% CaO) (PF)	1100	6	PF015-PF017	PF018-PF020	1 (PF-09)
4	High-calcareous (~14% CaO) (PT)	850	8	PT001-PT003*; PT004*; PT005*	PT006-PT008	1 (PT-01)
5	High-calcareous (~14% CaO) (PT)	950	6	PT009-PT011	PT012-PT014	1 (PT-05)
6	High-calcareous (~14% CaO) (PT)	1100	6	PT015-PT017	PT018-PT020	1 (PT-09)
7	Micaceous (~1% CaO) (AP)	850	8	AP001-AP003*; AP004*; AP005*	AP006-AP008	1 (AP-01)
8	Micaceous (~1% CaO) (AP)	950	6	AP009-AP011	AP012-AP014	1 (AP-05)
9	Micaceous (~1% CaO) (AP)	1100	6	AP015-AP017	AP018-AP020	1 (AP-09)

Then, test-pieces were submerged for 3 different time periods (3, 10 and 18 months), in two different water environments created in two containers of polypropylene of 4.7 L.

Thus, 3 pieces of each fabric were immersed in simulated seawater, which was prepared following the recipe of De Stefano et al. (1994), and other 3 pieces of each fabric in tap water (Figure 4.8.c). The periods of time were 3, 10 and 18 months, so two test-pieces of each fabric (one from seawater and the other from tap water) were taken in the 3rd month, other two in the 10th month and the other 4 (3 from marine water for repeatability and one from tap water) in the 18th month (see Table 4.3.). The two water environment containers were placed in an electric water bath at 50 °C (more than the double value of the seawater environment temperature), in order to simulate a real burial period, accelerating the alteration reactions (Figure 4.8.d). Additionally, different parameters of the experiment, such as pH, conductivity, TDS, salinity and temperature, were monitored, first, once every two weeks to see their variations and then on a monthly basis, as they were quite stable. Since the pH regulates many biological and chemical processes and reactions, it was important to measure this during the experiment (García-Castrillo et al., 2003). A change in the pH could be an indicator for an environmental attack to the ceramics (dissolution of minerals, for example) (Franklin and Vitali, 1985). Additionally, since conductivity is the capacity of a solution to conduct an electric current, it is related to the TDS (total dissolved solids) and salinity, providing an indication of the total number of ions. Moreover, salinity is the amount of solids dissolved in one kilogram of seawater, which may determine, among other factors, the oxidation-reduction capacity (García-Castrillo et al., 2003).

(The sections 4.3., 4.4. and 4.5. are in English in the pages 85-122 of the Doctoral Thesis).*

CHAPTER 5: Aging laboratory experiment for alterations and contaminations assessment

In this section, the results obtained in the aging laboratory experiment for alterations and contaminations assessment are explained. The details of the methodology of this experiment are in Chapter 4, section 4.2.

Once the pieces were taken out from the water environments, they were characterized by a multi-analytical approach. It should be noted that the pieces were not cleaned when they were taken out, nor before their analyses. On the one hand, ICP-MS and XRD were carried out for the chemical and mineralogical analyses of the test- and control-pieces. In addition, XRD analyses were also performed for the raw clays. ICP-MS is useful for identifying chemical changes, enrichment or leaching cases of the elements. Besides, XRD is useful for identifying and quantifying minerals present in the raw material (primary minerals). Furthermore, new minerals crystallized during firing and minerals formed due to burial alteration processes can be identified as well by XRD. On the other hand, microstructural characterization, assessment of the extent of vitrification and the presence of alterations and contaminations were also studied by SEM–EDS and Raman spectrometry (for general instrumental details, see Chapter 4, section 4.3.). In total, 69 test- and control-pieces and 3 raw clays were analysed (see Table 4.3. in Chapter 4). Finally, the 60 test-pieces were also analysed by a colorimeter before and after their immersion because colour changes may have been macroscopic indicators of the uses that the pottery had, as well as of post-depositional transformations (Maritan, 2020). This colorimeter is a PCE-CSM 5 PCE Instruments colorimeter (Meschede, Germany) and for the measures it used CIELAB colour space corresponding to an observer of 10°, illuminant D65 and an 8°/d geometry. In this way, L, a and b parameters were measured. L is the lightness parameter, which registers the values from 0 (black) to 100 (white), and a and b are Cartesian chromatic parameters. The former is from green to red, while the latter is from blue to yellow. The measurements were carried out on the same surface that had been in contact with the water environment.

5.1. Parameters of the water environments

Table 5.1. summarizes the average values of the measured parameters for each period in the two environments of water. The pH was quite stable in the two environments, with values ranging from a minimum of 8.02 to a maximum of 9.07 (in seawater) and from a minimum of 10.26 to a maximum of 10.71 (in tap water). Although the rest of the parameters were quite stable, a decrease was observed for the period of 18 months. However, there has not been identified any relation between these parameters and the chemical composition.

Table 5.1. Average values of the measured parameters (pH, conductivity, TDS, salinity and temperature) of the experiment

	pH		**Conductivity (ms/cm)**		**TDS (g/L)**		**Salinity**		**T(°C)**	
PERIOD (months)	seawater	tap water	seawater	tap water	seawater	tap water	seawater	tap water	seawater	tap water
3	8.02	10.26	43.60	1.49	25.24	0.66	28.15	0.61	49.97	49.39
10	8.68	10.71	43.86	1.06	25.16	0.56	27.94	0.5	49.7	49.55
18	9.07	10.71	40.87	0.97	23.49	0.51	25.83	0.48	43.48	43.54

5.2. Results of the colorimeter

The results of the colorimeter before and after the immersion are shown in Figure 5.1. They indicate that the colour of the samples fired at the maximum temperature (1100 °C) differed from the colour of the rest of the samples, before being immersed. The colours of the samples fired at the low (850 °C) and medium (950 °C) temperatures were more similar to each other before the immersion than after immersion. However, after the deposition in a water environment, it seems that the salt precipitated in the surface of the samples minimized the differences mentioned, but it makes the colour more heterogeneous. This fact reflects the importance of cleaning the samples before their analyses.

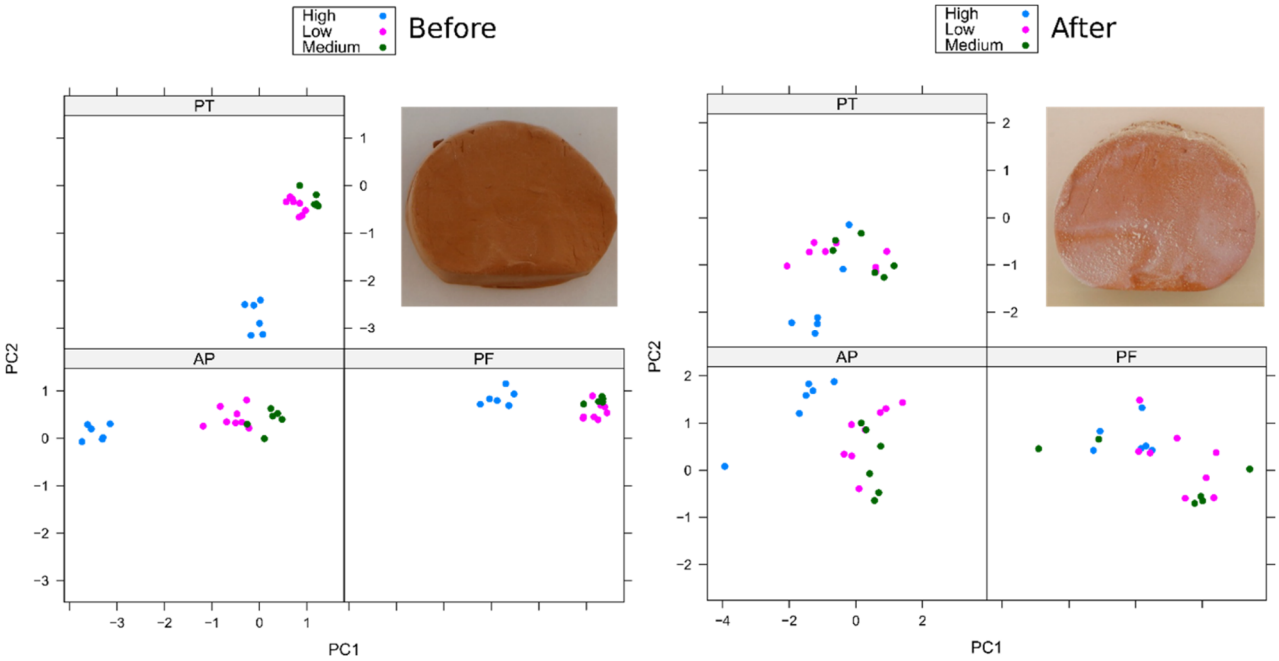

Figure 5.1. The results of the colorimeter for the samples of the three type of pastes, before and after their immersion in the corresponding water environment and the appearance of a piece from the PT group before and after its immersion for 18 months

5.3. ICP-MS results

The results of the elemental analyses and their relative average expanded uncertainties (U %) are shown in Table 5.2. Moreover, the repeatability (RSD %) for each type of paste (PT, PF, AP) is shown in Table 5.3. To calculate the uncertainty an approximation is made, because the type of calibration for the samples of the experiment was the same that for the whole set of Aveiro ceramics: thus, the uncertainties calculated for 25 ceramics of Aveiro are extrapolated to the ceramics of the experiment (see Chapter 6, section 6.2.). Besides, the repeatability was calculated using the next equation:

$$\text{RSD (\%)} = \frac{100s}{\bar{x}} \qquad Eq.\,5.1.$$

s is the standard deviation of the results of the three test-pieces (850 °C, seawater, 18 months) for each type of paste (PF, PT, AP) while x is their mean. In most of the cases, the repeatability was good (with values below 20 %). However, in some cases, the repeatability of a component was good for one type of paste but worse for another paste, e.g., CaO, Cu and Pb. The

components with a repeatability higher than 20 % were CaO (AP), Co (PF), Cu (PF, AP), Ni (PT, PF, AP), P_2O_5 (PT), Pb (PF) and Zn (PT, PF, AP). These facts could suggest that the post-depositional alterations that occurred in each ceramic depended on several factors, such as the position of the ceramic in the environment and the conditions of the environment. It also may suggest that the components with worse repeatability were more prone to varying in a deposition environment.

Table 5.1. Elemental composition of 69 samples. Samples; group= marine or tap water environment; Temperature= firing temperature; period= 3, 10, 18 months; piece= test- or control-piece; U (%)=relative average expanded uncertainties calculated following the GUM, with k=2 (see Chapter 4, section 4.4.3.)

Samples	Group	Temperature	Period	Piece	Al_2O_3	Ba	CaO	Ce	Co	Cr	Cs	Cu	Dy	Er	Eu	Fe_2O_3	Gd	Hf	Ho	K_2O	La	Lu
PT001	marine	850	3	Test-piece	15.4	3.79E+03	12.2	73.3	23.0	59.6	6.86	47.4	4.27	2.06	1.66	3.52	5.23	3.54	0.594	2.51	37.3	0.373
PT002	marine	850	10	Test-piece	15.2	3.46E+03	12.1	70.5	14.0	56.8	7.62	40.4	4.21	2.11	1.58	3.44	5.11	3.41	0.575	2.42	35.6	0.367
PT003	marine	850	18	Test-piece	14.9	3.29E+03	11.6	72.0	17.7	56.0	6.51	49.5	4.02	2.02	1.61	3.49	5.26	3.20	0.571	2.52	35.8	0.374
PT004	marine	850	18	Test-piece	15.2	3.51E+03	11.9	69.8	19.7	62.9	7.04	45.1	3.91	2.02	1.57	3.49	5.12	3.49	0.544	2.38	34.8	0.358
PT005	marine	850	18	Test-piece	15.3	3.32E+03	12.8	69.4	14.4	60.7	6.07	49.2	3.81	2.00	1.52	3.58	4.94	2.98	0.547	2.36	34.5	0.346
PT006	tap	850	3	Test-piece	14.3	2.99E+03	12.5	64.5	16.3	61.1	7.52	158	3.61	2.00	1.42	3.41	4.69	2.72	0.543	2.52	32.2	0.345
PT007	tap	850	10	Test-piece	15.0	3.30E+03	11.7	68.7	37.3	64.0	6.99	36.3	3.62	2.03	1.56	3.47	4.97	2.77	0.543	2.53	34.4	0.350
PT008	tap	850	18	Test-piece	15.0	3.24E+03	12.1	69.2	15.4	61.0	7.89	37.5	3.87	2.09	1.52	3.53	4.91	2.93	0.572	2.48	34.6	0.352
PT009	marine	950	3	Test-piece	14.9	3.36E+03	12.1	69.6	24.1	76.8	6.49	37.4	3.93	2.09	1.55	3.54	5.07	3.11	0.550	2.46	34.7	0.356
PT010	marine	950	10	Test-piece	15.0	3.46E+03	11.5	68.5	18.8	53.2	7.20	35.7	3.75	2.01	1.57	3.41	4.97	3.11	0.564	2.29	33.9	0.367
PT011	marine	950	18	Test-piece	14.9	3.47E+03	11.7	68.5	17.2	53.9	6.35	39.6	3.82	1.96	1.57	3.46	5.05	3.22	0.554	2.28	34.1	0.346
PT012	tap	950	3	Test-piece	14.9	3.57E+03	13.1	68.0	26.3	78.2	8.14	36.2	3.79	2.06	1.63	3.55	5.16	3.13	0.560	2.55	33.8	0.370
PT013	tap	950	10	Test-piece	15.0	3.44E+03	12.8	69.3	53.2	70.4	6.72	110	3.86	1.98	1.58	3.61	5.06	3.03	0.559	2.45	34.6	0.357
PT014	tap	950	18	Test-piece	15.0	3.63E+03	13.0	70.5	17.8	71.6	8.20	55.9	3.86	1.96	1.64	3.44	5.31	3.60	0.548	2.47	35.0	0.353
PT015	marine	1100	3	Test-piece	14.8	3.61E+03	12.0	68.7	26.4	60.2	7.92	28.1	3.75	1.93	1.57	3.47	5.05	3.02	0.521	2.37	34.0	0.350
PT016	marine	1100	10	Test-piece	15.0	3.63E+03	11.3	70.4	25.7	56.2	9.38	29.8	3.97	2.07	1.69	3.47	5.23	3.20	0.557	2.34	34.8	0.348

Samples	Group	Temperature	Period	Piece	Al_2O_3	Ba	CaO	Ce	Co	Cr	Cs	Cu	Dy	Er	Eu	Fe_2O_3	Gd	Hf	Ho	K_2O	La	Lu
PT017	marine	1100	18	Test-piece	14.6	3.63E+03	11.2	69.4	25.4	67.9	8.47	23.2	3.75	1.90	1.56	3.32	5.27	3.26	0.521	2.11	34.6	0.319
PT018	tap	1100	3	Test-piece	15.1	3.74E+03	14.0	70.7	24.2	58.9	9.76	21.2	3.95	1.99	1.66	3.43	5.44	3.37	0.538	2.75	35.1	0.349
PT019	tap	1100	10	Test-piece	15.2	3.95E+03	13.8	71.9	38.3	84.8	8.76	44.6	4.06	2.10	1.65	3.46	5.47	3.45	0.566	2.77	36.1	0.373
PT020	tap	1100	18	Test-piece	15.1	3.58E+03	12.2	69.9	33.1	79.9	9.63	24.5	3.92	1.98	1.61	3.48	5.23	3.11	0.551	2.61	34.7	0.365
PT-01	control	850	-	Control-piece	15.1	3.59E+03	12.6	68.5	19.5	61.7	7.88	19.7	4.08	2.06	1.56	3.48	4.97	2.24	0.599	2.59	33.6	0.335
PT-05	control	950	-	Control-piece	14.2	3.62E+03	13.2	67.0	29.8	60.3	7.97	39.3	3.98	2.12	1.52	3.40	4.97	2.27	0.581	2.57	33.1	0.335
PT-09	control	1100	-	Control-piece	15.8	3.92E+03	15.4	75.1	28.1	70.3	9.65	68.1	4.26	2.33	1.67	3.89	5.62	2.41	0.637	2.97	37.1	0.369
PF001	marine	850	3	Test-piece	16.6	9.06E+02	3.85	73.8	20.8	68.0	11.4	47.3	4.01	2.05	1.32	6.14	5.14	3.02	0.568	3.30	36.3	0.355
PF002	marine	850	10	Test-piece	17.8	9.66E+02	3.91	78.1	22.8	73.1	12.5	50.7	4.20	2.17	1.37	6.65	5.58	3.06	0.591	3.48	38.6	0.377
PF003	marine	850	18	Test-piece	16.9	9.22E+02	3.74	74.3	27.8	70.9	11.6	44.5	4.13	2.06	1.31	6.42	5.40	2.93	0.583	3.41	37.1	0.379
PF004	marine	850	18	Test-piece	17.3	9.33E+02	4.24	76.1	20.1	71.7	10.4	843	4.19	2.14	1.32	6.58	5.33	2.62	0.599	3.39	37.8	0.380
PF005	marine	850	18	Test-piece	17.3	9.20E+02	4.51	75.2	18.6	74.7	9.14	49.9	4.03	2.12	1.25	6.32	5.27	2.53	0.597	3.18	37.5	0.381
PF006	tap	850	3	Test-piece	17.6	9.50E+02	4.68	77.4	25.0	79.8	9.48	53.4	4.34	2.16	1.33	6.54	5.43	2.75	0.605	3.32	39.2	0.392
PF007	tap	850	10	Test-piece	17.6	9.43E+02	4.29	77.5	26.2	74.2	10.7	61.8	4.22	2.17	1.31	6.57	5.38	2.64	0.590	3.36	38.7	0.384
PF008	tap	850	18	Test-piece	17.6	9.59E+02	4.23	77.8	21.9	87.9	9.79	68.3	4.33	2.15	1.34	6.49	5.57	3.15	0.620	3.32	39.3	0.411
PF009	marine	950	3	Test-piece	17.7	9.32E+02	3.51	76.9	22.3	73.3	11.1	60.6	4.22	2.20	1.34	6.43	5.31	2.71	0.597	3.25	38.7	0.418
PF010	marine	950	10	Test-piece	16.0	8.71E+02	3.16	71.0	26.4	69.0	9.75	48.7	3.98	2.06	1.23	5.96	5.11	2.50	0.571	3.07	36.1	0.391

Samples	Group	Temperature	Period	Piece	Al_2O_3	Ba	CaO	Ce	Co	Cr	Cs	Cu	Dy	Er	Eu	Fe_2O_3	Gd	Hf	Ho	K_2O	La	Lu
PF011	marine	950	18	Test-piece	17.5	9.31E+02	3.83	77.0	22.6	70.4	11.8	55.9	4.20	2.23	1.34	6.47	5.39	2.47	0.589	3.28	38.9	0.414
PF012	tap	950	3	Test-piece	16.9	8.93E+02	3.50	73.7	34.4	71.2	9.66	39.7	4.06	2.23	1.30	6.41	5.30	2.59	0.579	3.20	36.7	0.389
PF013	tap	950	10	Test-piece	17.7	9.35E+02	3.70	76.2	29.6	89.9	12.1	49.9	4.16	2.26	1.40	6.55	5.44	2.97	0.597	3.44	38.3	0.377
PF014	tap	950	18	Test-piece	16.5	8.74E+02	3.66	69.5	21.1	71.1	10.4	57.5	4.00	2.08	1.27	6.12	5.07	2.91	0.547	3.32	34.7	0.369
PF015	marine	1100	3	Test-piece	17.3	9.02E+02	4.65	75.2	84.5	77.6	12.0	64.2	4.18	2.24	1.38	6.55	5.36	2.96	0.567	3.42	37.4	0.392
PF016	marine	1100	10	Test-piece	16.0	8.37E+02	4.15	68.3	47.4	68.5	10.7	53.7	3.84	2.06	1.21	6.14	5.01	2.85	0.549	3.31	33.4	0.342
PF017	marine	1100	18	Test-piece	15.6	8.52E+02	3.63	68.1	31.9	65.0	11.3	55.4	3.88	2.02	1.22	5.77	4.93	2.33	0.550	3.24	34.1	0.351
PF018	tap	1100	3	Test-piece	17.5	9.21E+02	4.80	76.1	42.7	83.4	11.6	55.0	4.27	2.25	1.40	6.99	5.60	2.96	0.601	3.67	37.9	0.406
PF019	tap	1100	10	Test-piece	17.4	9.25E+02	5.40	75.2	80.1	75.3	13.0	47.8	4.23	2.22	1.36	6.68	5.58	3.02	0.625	3.54	37.4	0.392
PF020	tap	1100	18	Test-piece	17.7	9.34E+02	4.84	76.0	35.9	74.9	13.1	52.1	4.27	2.26	1.39	6.61	5.62	2.95	0.639	3.51	38.1	0.394
PF-01	control	850	-	Control-piece	15.9	8.89E+02	4.45	71.1	25.1	72.1	13.0	66.2	4.07	2.05	1.22	6.16	5.21	2.21	0.588	3.49	35.0	0.346
PF-05	control	950	-	Control-piece	16.7	8.99E+02	4.64	73.5	25.7	74.7	12.1	57.9	4.12	2.05	1.32	6.12	5.38	2.35	0.597	3.33	36.0	0.351
PF-09	control	1100	-	Control-piece	15.7	8.52E+02	5.18	70.2	32.8	68.9	12.6	72.7	3.86	1.97	1.26	5.70	5.20	2.10	0.560	3.52	34.1	0.333
AP001	marine	850	3	Test-piece	22.3	1.70E+03	0.947	125	43.5	75.7	16.9	18.3	15.0	7.86	4.15	10.7	18.0	3.22	2.34	3.55	64.1	1.22
AP002	marine	850	10	Test-piece	22.0	1.72E+03	1.48	125	41.3	78.2	18.8	20.1	15.0	7.45	4.09	10.7	18.0	3.19	2.35	3.61	64.5	1.23
AP003	marine	850	18	Test-piece	21.1	1.63E+03	0.874	120	34.9	72.0	17.4	13.2	14.2	7.35	3.93	9.83	17.6	2.55	2.19	3.42	61.7	1.15
AP004	marine	850	18	Test-piece	19.6	1.55E+03	1.18	112	29.6	68.4	18.6	28.6	13.2	6.82	3.61	9.36	16.2	2.56	2.02	3.48	57.4	1.02

Samples	Group	Temperature	Period	Piece	Al_2O_3	Ba	CaO	Ce	Co	Cr	Cs	Cu	Dy	Er	Eu	Fe_2O_3	Gd	Hf	Ho	K_2O	La	Lu
AP005	marine	850	18	Test-piece	20.9	1.59E+03	1.40	119	29.5	77.8	17.6	13.6	14.0	7.20	3.87	9.55	16.9	2.55	2.12	3.38	61.0	1.06
AP006	tap	850	3	Test-piece	20.5	1.62E+03	1.69	115	29.3	102	19.9	17.3	13.7	6.91	3.69	9.55	16.8	2.45	2.03	3.54	59.5	1.00
AP007	tap	850	10	Test-piece	21.5	1.65E+03	1.44	120	30.5	89.8	18.8	13.7	13.9	7.20	3.77	9.75	17.5	2.55	2.08	3.49	61.2	1.02
AP008	tap	850	18	Test-piece	20.4	1.61E+03	1.56	115	28.4	73.9	20.3	12.7	13.6	6.99	3.64	9.65	16.6	2.32	2.00	3.58	59.5	0.971
AP009	marine	950	3	Test-piece	20.5	1.56E+03	0.612	115	49.1	89.0	15.8	18.2	13.7	6.92	3.65	9.41	16.6	2.07	1.98	3.19	59.2	0.989
AP010	marine	950	10	Test-piece	22.8	1.73E+03	1.30	127	55.8	86.8	15.2	9.71	15.0	7.75	4.19	10.6	18.1	2.47	2.20	3.25	65.4	1.09
AP011	marine	950	18	Test-piece	20.5	1.60E+03	1.48	116	37.5	87.8	13.0	15.7	13.7	7.03	3.84	9.80	16.8	2.25	2.05	3.16	59.9	1.04
AP012	tap	950	3	Test-piece	22.2	1.73E+03	1.23	125	43.6	83.2	15.9	20.3	14.9	7.61	4.20	10.3	17.8	2.42	2.19	3.39	64.3	1.15
AP013	tap	950	10	Test-piece	22.0	1.67E+03	2.53	123	46.6	81.8	13.9	23.3	14.5	7.46	4.09	10.1	17.7	2.46	2.13	3.28	62.4	1.14
AP014	tap	950	18	Test-piece	22.3	1.68E+03	1.17	124	36.1	77.7	16.3	12.2	14.6	7.53	4.35	10.2	17.8	2.49	2.22	3.33	63.3	1.24
AP015	marine	1100	3	Test-piece	20.6	1.64E+03	1.44	119	60.4	92.3	14.0	3.45	13.9	7.05	4.09	9.58	16.6	2.15	2.07	3.21	60.5	1.16
AP016	marine	1100	10	Test-piece	22.1	1.71E+03	1.07	128	79.5	90.5	17.1	18.6	14.8	7.66	4.29	10.4	17.8	2.56	2.30	3.44	64.6	1.19
AP017	marine	1100	18	Test-piece	20.5	1.59E+03	0.461	117	68.8	84.9	14.8	16.6	13.6	7.09	3.97	10.1	16.1	2.29	2.12	3.35	58.9	1.10
AP018	tap	1100	3	Test-piece	21.7	1.64E+03	2.19	124	57.1	83.2	16.8	19.0	14.5	7.72	4.25	10.5	17.1	2.70	2.25	3.44	62.0	1.14
AP019	tap	1100	10	Test-piece	21.9	1.66E+03	0.949	125	60.4	82.4	15.9	19.7	14.5	7.74	4.19	10.4	16.7	2.72	2.26	3.41	62.9	1.12
AP020	tap	1100	18	Test-piece	14.7	1.18E+03	0.460	85.0	33.8	52.2	15.5	0.264	10.1	5.35	2.88	7.17	11.8	1.92	1.57	2.96	42.7	0.745
AP-01	control	850	-	Control-piece	19.8	1.59E+03	1.01	116	41.2	77.8	16.6	26.0	13.4	6.83	3.74	9.64	16.4	2.10	1.97	3.44	57.8	0.991

Samples	Group	Temperature	Period	Piece	Al_2O_3	Ba	CaO	Ce	Co	Cr	Cs	Cu	Dy	Er	Eu	Fe_2O_3	Gd	Hf	Ho	K_2O	La	Lu
AP-05	control	950	-	Control-piece	19.0	1.48E+03	0.859	108	43.8	66.5	16.9	6.33	12.7	6.52	3.56	9.13	15.4	2.10	1.86	3.34	54.1	0.958
AP-09	control	1100	-	Control-piece	19.9	1.55E+03	0.972	115	66.2	76.1	15.8	15.8	13.5	6.96	3.71	9.83	16.6	2.19	1.97	3.39	57.6	0.993
U (%)					6	5	84	6	26	38	4	24	13	22	11	8	10	6	20	4	5	17

Table 5.2. ***(continues).*** Elemental composition of 69 samples. G = Group; T ºC= Temperature; S = Seawater; T = Tap water; L = Low (850 ºC); M = Medium (950 ºC); H = High (1100 ºC)

Samples	G	T ºC	MgO	MnO	Na_2O	Nb	Nd	Ni	P_2O_5	Pb	Pr	Rb	SiO_2	Sm	Sr	Ta	Tb	Th	TiO_2	Tm	U	V	Yb	Zn	Zr
PT001	S	L	2.08	0.0420	0.488	14.9	34.2	28.3	0.0913	20.0	8.97	121	46.4	6.45	242	1.52	0.767	11.6	0.667	0.365	3.95	96.9	2.09	15.8	165
PT002	S	L	2.11	0.0412	0.491	14.3	33.2	22.7	0.0857	29.9	8.73	119	46.6	6.44	230	1.46	0.775	11.7	0.661	0.394	3.82	96.6	2.19	14.0	151
PT003	S	L	2.49	0.0507	0.517	14.0	34.0	35.1	0.107	21.2	8.92	117	47.0	6.53	231	1.46	0.754	11.7	0.653	0.390	3.80	99.6	2.13	24.5	152
PT004	S	L	2.10	0.0422	0.552	12.1	33.5	105	0.0705	21.1	8.71	112	45.9	6.18	226	1.40	0.745	11.3	0.659	0.382	3.80	97.7	1.99	16.1	155
PT005	S	L	2.15	0.0439	0.521	14.2	33.4	26.6	0.0689	28.9	8.74	110	48.2	6.29	226	1.44	0.751	10.8	0.667	0.382	3.68	97.5	2.02	17.9	139
PT006	T	L	1.89	0.0422	0.366	13.4	31.0	207	0.0666	24.0	8.17	119	45.2	5.72	216	1.32	0.683	10.0	0.630	0.393	3.46	99.0	2.01	26.8	126
PT007	T	L	1.86	0.0422	0.249	12.9	31.9	29.1	0.0714	23.9	8.61	120	45.7	6.03	222	1.41	0.715	10.5	0.656	0.382	3.69	103	1.95	14.1	128
PT008	T	L	1.88	0.0423	0.317	12.7	32.3	26.0	0.0750	24.4	8.68	122	46.4	6.21	224	1.41	0.735	10.9	0.659	0.406	3.69	101	2.04	21.6	135
PT009	S	M	2.10	0.0421	0.494	10.6	32.5	29.1	0.0612	21.2	8.57	112	44.9	5.98	226	1.31	0.754	11.4	0.666	0.390	3.62	99.9	1.99	15.3	137
PT010	S	M	2.12	0.0403	0.514	11.2	31.9	24.7	0.0721	23.5	8.57	116	43.7	5.91	230	1.33	0.728	11.1	0.655	0.401	3.55	92.6	2.01	12.4	142
PT011	S	M	2.10	0.0401	0.482	10.5	32.3	25.1	0.0559	21.9	8.50	109	44.3	5.96	228	1.31	0.703	11.3	0.666	0.394	3.50	93.9	2.03	15.5	144
PT012	T	M	1.89	0.0451	0.241	10.3	31.8	23.8	0.0648	26.2	8.38	122	45.0	5.71	227	1.35	0.758	11.2	0.659	0.413	3.53	97.3	1.90	13.4	138
PT013	T	M	1.94	0.0433	0.338	10.4	32.5	28.2	0.0773	24.5	8.46	114	44.3	6.09	234	1.33	0.764	11.2	0.660	0.412	3.66	100	1.94	1.29E+03	144
PT014	T	M	1.92	0.0407	0.505	10.5	33.0	29.1	0.0799	88.7	8.75	123	44.1	6.17	244	1.38	0.742	11.5	0.662	0.425	3.63	97.4	1.91	30.2	156
PT015	S	H	2.49	0.0440	0.688	10.1	31.7	20.0	0.0754	32.0	8.48	123	43.8	6.09	223	1.30	0.724	11.3	0.656	0.399	3.53	91.0	1.94	3.10	144

Samples	G	T °C	MgO	MnO	Na_2O	Nb	Nd	Ni	P_2O_5	Pb	Pr	Rb	SiO_2	Sm	Sr	Ta	Tb	Th	TiO_2	Tm	U	V	Yb	Zn	Zr
PT016	S	H	2.93	0.0411	0.772	9.90	32.3	26.5	0.0765	23.0	8.76	133	42.8	6.58	231	1.38	0.793	11.7	0.644	0.429	3.71	93.3	2.06	2.87	151
PT017	S	H	2.73	0.0396	0.799	9.82	31.4	23.3	0.0823	23.1	8.39	127	41.6	6.35	229	1.33	0.758	11.6	0.630	0.406	3.63	92.5	1.98	4.41	148
PT018	T	H	1.87	0.0415	0.323	10.2	32.4	21.2	0.0964	24.8	8.54	152	42.6	6.53	246	1.39	0.812	12.0	0.643	0.410	3.80	80.6	2.02	3.12	155
PT019	T	H	1.95	0.0437	0.713	9.89	33.3	28.4	0.0948	88.9	8.88	154	41.4	6.90	265	1.35	0.836	11.9	0.662	0.425	3.89	86.8	2.14	36.1	155
PT020	T	H	1.94	0.0428	0.308	9.81	32.4	20.7	0.0652	23.0	8.52	161	44.3	6.47	235	1.35	0.763	11.6	0.665	0.417	3.63	89.6	2.07	1.38	147
PT-01	C	L	1.91	0.0418	0.261	8.32	31.5	22.6	0.0744	23.8	8.29	129	47.7	5.97	230	1.40	0.747	10.8	0.654	0.374	3.57	94.0	2.06	7.20	114
PT-05	C	M	1.82	0.0425	0.277	8.14	30.9	44.5	0.0563	22.7	8.02	125	45.8	5.99	218	1.39	0.734	10.8	0.622	0.391	3.46	90.1	2.12	4.87	111
PT-09	C	H	2.04	0.0456	0.295	8.87	34.1	42.6	0.0430	31.0	9.10	141	53.3	6.75	242	1.55	0.808	12.0	0.716	0.410	3.79	102	2.35	11.1	119
PF001	S	L	3.01	0.101	0.518	10.6	32.5	33.8	0.105	25.6	8.88	144	42.0	6.22	118	1.38	0.780	11.9	0.766	0.407	2.86	110	2.07	4.51	142
PF002	S	L	3.52	0.110	0.554	12.0	34.6	33.6	0.119	21.5	9.54	155	47.1	6.62	125	1.57	0.818	12.9	0.826	0.425	2.98	117	2.29	11.3	149
PF003	S	L	3.12	0.105	0.474	11.1	33.1	30.9	0.116	34.6	8.97	149	44.4	6.70	118	1.41	0.772	12.3	0.788	0.407	2.88	109	2.23	10.2	140
PF004	S	L	3.35	0.108	0.502	11.3	33.1	51.9	0.105	48.8	9.26	141	49.9	6.48	117	1.57	0.775	12.1	0.822	0.415	2.98	115	2.24	43.7	128
PF005	S	L	3.29	0.104	0.529	10.4	33.1	40.9	0.121	20.6	9.01	133	46.8	6.47	119	1.44	0.775	11.9	0.809	0.412	2.89	112	2.19	5.62	126
PF006	T	L	2.80	0.107	0.213	11.4	34.9	40.9	0.113	26.9	9.56	137	49.4	6.79	131	1.57	0.772	12.6	0.836	0.405	2.99	112	2.25	4.16	139
PF007	T	L	2.76	0.107	0.211	11.4	34.3	37.0	0.107	23.4	9.46	144	48.8	6.79	129	1.55	0.780	12.4	0.832	0.416	2.94	110	2.21	7.00	134
PF008	T	L	2.82	0.108	0.412	11.8	34.8	40.8	0.116	105	9.53	136	49.3	6.84	132	1.55	0.776	12.6	0.834	0.400	3.02	109	2.29	31.2	143
PF009	S	M	3.21	0.106	0.525	11.3	34.9	34.4	0.112	22.6	9.49	143	48.8	6.64	123	1.52	0.774	12.5	0.812	0.416	3.00	112	2.17	1.98	135
PF010	S	M	3.24	0.098	0.526	10.3	32.4	36.3	0.105	19.9	8.85	135	42.6	6.29	112	1.29	0.698	11.4	0.760	0.390	2.75	105	2.12	2.49	122
PF011	S	M	3.31	0.106	0.558	11.0	34.8	36.4	0.127	21.0	9.33	148	48.6	6.62	124	1.45	0.767	12.3	0.807	0.404	3.09	111	2.19	6.03	128
PF012	T	M	2.72	0.105	0.223	11.0	33.1	29.7	0.114	46.8	8.99	134	47.3	6.44	124	1.41	0.749	11.8	0.798	0.394	2.86	100	2.11	5.78	128
PF013	T	M	2.80	0.107	0.274	11.6	34.6	32.1	0.133	26.8	9.10	150	48.4	6.42	130	1.41	0.758	12.6	0.824	0.410	3.02	105	2.17	27.2	138
PF014	T	M	2.65	0.100	0.221	10.3	31.8	34.1	0.128	20.9	8.36	141	42.3	6.11	122	1.24	0.721	11.5	0.758	0.379	2.74	97.7	1.95	3.98	136
PF015	S	H	2.95	0.106	0.487	11.8	33.6	36.1	0.123	24.4	8.94	151	48.0	6.32	132	1.55	0.790	12.4	0.831	0.414	2.94	117	2.17	5.56	140
PF016	S	H	2.85	0.101	0.466	9.93	30.6	30.5	0.127	20.1	7.95	142	41.3	5.90	123	1.23	0.716	11.1	0.775	0.373	2.66	109	1.96	7.75	135
PF017	S	H	2.77	0.0988	0.464	8.14	30.3	33.2	0.129	22.0	8.06	145	38.0	5.79	120	1.16	0.718	10.6	0.754	0.366	2.66	104	1.98	5.85	116

Samples	G	T °C	MgO	MnO	Na_2O	Nb	Nd	Ni	P_2O_5	Pb	Pr	Rb	SiO_2	Sm	Sr	Ta	Tb	Th	TiO_2	Tm	U	V	Yb	Zn	Zr
PF018	T	H	3.01	0.114	0.298	10.5	34.3	36.9	0.110	26.9	8.91	148	49.7	6.65	126	1.44	0.808	12.8	0.899	0.418	2.97	121	2.21	15.0	141
PF019	T	H	2.75	0.107	0.256	10.8	32.9	32.2	0.123	22.7	8.72	157	47.3	6.22	130	1.58	0.807	12.7	0.850	0.427	3.00	111	2.31	3.81	145
PF020	T	H	2.76	0.107	0.278	10.7	34.5	32.6	0.123	21.3	9.04	159	47.7	6.65	131	1.52	0.790	13.1	0.831	0.422	2.98	112	2.26	3.21	145
PF-01	C	L	2.62	0.100	0.256	9.41	30.9	33.4	0.089	22.2	8.28	153	46.9	6.05	117	1.41	0.789	11.2	0.783	0.389	2.72	114	2.20	8.38	111
PF-05	C	M	2.63	0.100	0.221	9.90	31.9	28.9	0.119	20.5	8.62	151	46.7	6.07	121	1.51	0.733	11.7	0.772	0.408	2.85	110	2.18	7.05	118
PF-09	C	H	2.51	0.0956	0.269	9.54	30.1	30.3	0.107	31.4	8.12	153	44.4	6.06	120	1.42	0.719	10.7	0.741	0.389	2.65	105	2.06	9.34	108
AP001	S	L	1.17	0.0654	0.591	14.4	82.8	61.9	0.0548	36.6	18.5	232	45.2	19.1	68.8	2.66	2.80	14.2	0.827	1.44	4.24	117	7.00	6.30	158
AP002	S	L	1.23	0.0659	0.628	14.3	83.8	61.9	0.0327	25.4	18.4	234	45.2	19.1	68.8	2.75	2.82	14.2	0.824	1.40	4.22	116	6.93	5.43	150
AP003	S	L	1.13	0.0594	0.548	12.4	79.8	58.1	0.0409	22.2	17.7	228	41.8	18.3	64.7	2.52	2.67	13.2	0.785	1.34	4.03	111	6.56	6.69	131
AP004	S	L	1.05	0.0567	0.524	11.8	75.6	618	0.0485	20.9	16.5	229	38.8	17.5	59.2	2.29	2.47	12.1	0.721	1.25	3.78	101	6.12	3.66	123
AP005	S	L	1.09	0.0590	0.613	12.8	80.1	55.7	0.0411	24.2	17.6	229	40.2	18.2	65.3	2.51	2.59	13.0	0.745	1.32	4.06	107	6.38	13.3	130
AP006	T	L	0.992	0.0596	0.221	12.6	78.8	57.8	0.0379	46.1	17.0	234	41.1	17.8	74.5	2.42	2.53	12.4	0.763	1.25	3.99	102	6.19	11.5	121
AP007	T	L	1.02	0.0598	0.225	13.1	79.5	58.0	0.0422	22.0	17.6	226	42.8	18.4	79.0	2.59	2.60	12.7	0.789	1.31	4.05	100	6.55	11.4	127
AP008	T	L	0.99	0.0594	0.226	12.4	78.5	55.9	0.0321	23.2	17.0	225	41.6	17.9	69.7	2.50	2.43	12.0	0.752	1.23	3.92	94.2	6.12	7.91	115
AP009	S	M	1.18	0.0598	0.496	11.6	79.7	57.8	0.0295	31.0	16.9	217	41.2	17.4	66.3	2.44	2.50	11.7	0.752	1.25	3.90	111	6.15	8.89	111
AP010	S	M	1.42	0.0648	0.493	13.5	86.5	61.8	0.0495	22.7	18.8	220	46.6	19.4	72.1	2.79	2.72	13.2	0.826	1.39	4.36	121	6.92	15.4	123
AP011	S	M	1.35	0.0620	0.551	12.3	79.5	62.1	0.0582	27.5	17.0	206	42.5	17.6	71.5	2.41	2.49	11.8	0.764	1.27	3.91	111	6.33	29.5	116
AP012	T	M	1.08	0.0645	0.201	13.1	85.8	90.9	0.0362	23.2	18.4	223	46.7	18.1	74.5	2.69	2.70	12.9	0.835	1.37	4.22	116	6.84	14.1	122
AP013	T	M	1.06	0.0629	0.212	12.9	84.6	68.9	0.0487	20.7	17.8	213	45.2	17.9	77.8	2.58	2.63	12.7	0.809	1.35	4.28	113	6.58	18.2	125
AP014	T	M	1.04	0.0634	0.179	13.0	84.9	62.3	0.0489	24.9	18.1	227	45.1	17.7	74.0	2.54	2.68	12.5	0.802	1.34	4.22	109	6.85	6.50	125
AP015	S	H	1.04	0.0601	0.261	11.4	79.9	59.1	0.0360	25.6	17.3	212	42.7	17.3	68.2	2.53	2.52	12.0	0.780	1.27	4.01	117	6.44	7.21	109
AP016	S	H	1.14	0.0647	0.304	13.1	85.2	64.3	0.0386	23.9	18.7	231	46.5	18.5	73.4	2.69	2.70	13.1	0.835	1.38	4.23	131	7.00	10.7	126
AP017	S	H	1.11	0.0629	0.287	12.4	78.9	63.5	0.0262	21.8	17.2	214	44.9	17.0	66.8	2.46	2.55	12.0	0.792	1.22	3.93	124	6.36	8.39	115
AP018	T	H	1.07	0.0654	0.229	13.6	82.8	68.0	0.0401	27.6	18.1	229	46.6	18.6	75.3	2.62	2.73	13.0	0.818	1.30	4.15	127	6.79	44.2	127
AP019	T	H	1.02	0.0643	0.201	14.1	82.3	64.2	0.0432	26.5	18.4	229	44.7	18.8	74.1	2.55	2.74	13.2	0.785	1.34	4.12	119	7.01	27.3	130

Samples	G	T °C	MgO	MnO	Na_2O	Nb	Nd	Ni	P_2O_5	Pb	Pr	Rb	SiO_2	Sm	Sr	Ta	Tb	Th	TiO_2	Tm	U	V	Yb	Zn	Zr
AP020	T	H	0.728	0.0447	0.214	10.1	56.7	42.9	0.0349	16.4	12.5	202	29.6	13.5	50.5	1.57	1.87	8.8	0.544	0.876	2.73	83.3	4.70	3.31	89
AP-01	C	L	0.973	0.0588	0.219	12.3	74.1	62.1	0.0202	34.8	16.4	222	41.8	18.1	66.4	2.46	2.49	11.3	0.741	1.25	3.70	114	6.26	16.6	105
AP-05	C	M	0.898	0.0549	0.170	12.5	69.6	52.6	0.0415	20.8	15.4	222	38.9	16.6	63.9	2.34	2.33	10.7	0.686	1.18	3.50	103	5.84	4.07	104
AP-09	C	H	0.974	0.0594	0.189	13.2	73.7	59.7	0.0263	21.0	16.3	214	41.4	17.7	65.8	2.50	2.52	11.4	0.765	1.30	3.70	116	6.38	5.15	112
U (%)			18	28	34	4	6	82	-	63	5	3	5	6	19	8	8	13	9	22	17	16	19	-	6

Table 5.2. The repeatability (RSD %) of the components for each type of paste (PT, PF, AP)

Compounds	RSD (%)		
	PT	PF	AP
Al_2O_3	1.5	1.2	3.9
Ba	3.5	0.8	2.7
CaO	5.0	9.3	23
Ce	2.0	1.2	4.0
Co	15	22	10
Cr	5.9	2.8	6.6
Cs	7.4	12	3.7
Cu	5.2	147	47
Dy	2.8	1.9	3.8
Er	0.43	2.0	3.9
Eu	2.9	2.8	4.5
Fe_2O_3	1.5	2.0	2.5
Gd	3.1	1.2	4.1
Hf	7.9	7.7	0.18
Ho	2.7	1.5	4.0
K_2O	3.6	3.8	1.5
La	2.0	0.92	3.8
Lu	3.9	0.23	6.2
MgO	9.3	3.7	3.7
MnO	9.8	1.7	2.6
Na_2O	3.7	5.4	8.2
Nb	8.7	4.2	4.0
Nd	0.91	0.13	3.2
Ni	77	25	1.3
P_2O_5	26	7.3	10

Pb	19	41	7.5
Pr	1.3	1.7	3.6
Rb	3.2	5.8	0.25
SiO_2	2.5	6.0	3.8
Sm	2.9	1.9	2.4
Sr	1.2	0.77	5.3
Ta	2.0	5.8	5.5
Tb	0.59	0.21	4.0
Th	3.8	1.6	4.6
TiO_2	1.1	2.1	4.4
Tm	1.2	1.0	3.6
U	1.8	1.8	3.9
V	1.2	2.7	5.0
Yb	3.6	1.3	3.4
Zn	23	105	62
Zr	5.8	5.8	3.5

The interpretation of the chemical results obtained by ICP-MS followed the statistical procedure explained in Chapter 4, section 4.5. Besides, since the tungsten carbide cell used to mill the ceramics was a potential contaminator (see Chapter 4, section 4.4.2.), Co and Ta were removed from the statistical procedure. Furthermore, Sn, Ni, Cu and Zn were also removed, the first because it showed values under the quantification limit and the rest because they showed low repeatability, which could not have been related to any specific alteration, suggesting that an analytical error could have occurred.

In Figure 5.2., the compositional variation matrix of the 69 ceramics is shown, which provides an estimation of each component contribution to the total variation (see Chapter 4, section 4.5.). Figure 5.2.a shows that CaO was the component that introduced the highest variability to the 69 ceramics dataset, something that was expected because the clays were selected in the function of their CaO amount. In addition, the figure also shows that Sr, P_2O_5 and Ba introduce a high variability. Moreover, Figures 5.2.b,c present the Matrix of Compositional Variability (MCV) of 23 PT and PF samples (twenty test-pieces and three control-pieces), showing that the components that introduced the highest variability were Pb, Na_2O, P_2O_5 and Nb. Additionally, Figure 5.2.d presents the MCV of 23 AP samples, and in this case, Na_2O, CaO, P_2O_5 and Pb were the components introducing the highest variability. The variability of those components is explained below.

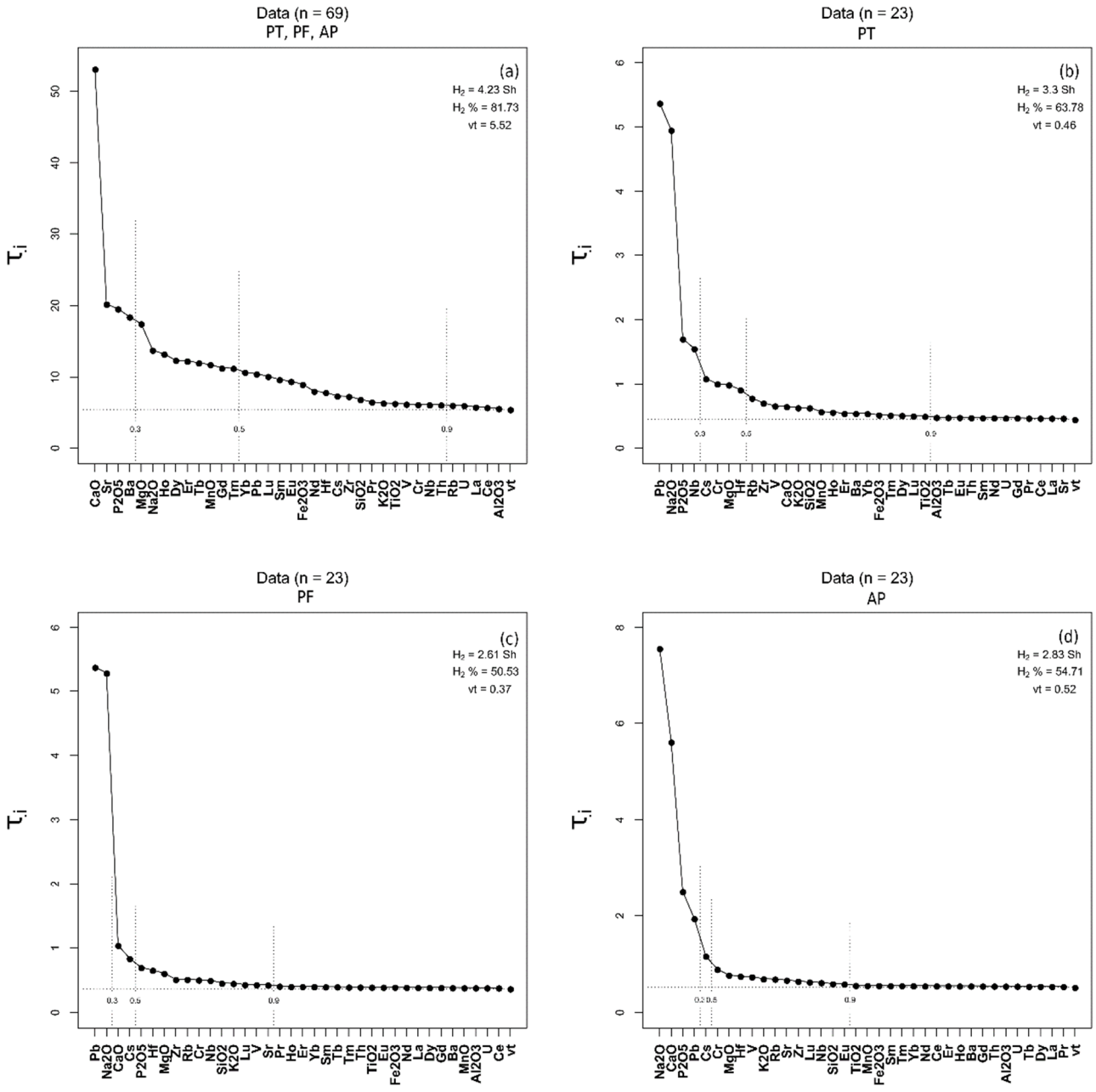

Figure 5.2. (a) Graphical representation of the evenness of the compositional variability of 69 analysed samples by ICP-MS; **(b)** Graphical representation of the evenness of the compositional variability of 23 PT samples; **(c)** Graphical representation of the evenness of the compositional variability of 23 PF samples; **(d)** Graphical representation of the evenness of the compositional variability of 23 AP samples. Co, Ta, Sn, Cu, Zn and Ni were omitted in all the graphs. (y-axis (τ.i) = the individual contribution of the variability from each element to the whole dataset, from the highest to the lowest; vt = Total variability; H_2 = information entropy; H_2% = percentage of information entropy over the maximum possible; n = number of specimens)

In addition, in Figure 5.3., four PCAs (Principal Component Analysis) are shown (see Chapter 4, section 4.5.), with samples labelled as L, M and H. L means that those samples were fired at low temperatures (850 °C), M at medium firing temperatures (950 °C) and H at high firing temperatures (1100 °C). Figure 5.3.a presents the PCA of 69 samples, in which a clear

differentiation of the three types of pastes can be seen. On the one hand, the control-pieces PT samples contained more CaO than the other samples (around 14 %, as is presented in Table 5.2.), so it was expected that PT samples would orient themselves that way. In addition, PT samples seemed to contain more Sr, Ba and Na_2O. Although these facts are mostly related to the nature of the raw materials, the burial also affects the elemental concentration of the ceramics. Thus, ceramics can be enriched in sodium because this element is present in both terrestrial and marine environments (Maritan, 2020), or due to the formation of analcime or precipitation of halite in the paste (Buxeda i Garrigós et al., 2002a; Secco et al., 2011). Besides, barium and strontium can also be absorbed in the surfaces, or barium can be precipitated as barite ($BaSO_4$) and strontium as carbonate, sulphate, borate, phosphate or halide (Maritan, 2020). Moreover, PF samples contained more MgO, MnO and P_2O_5 than the other samples, while AP samples contained more Cs, Rb, Fe_2O_3 and trace elements, related to their micaceous paste. It is common to detect an enrichment of magnesium in ceramics buried in marine environments (Lemoine et al., 1981; Maritan, 2020). Manganese also may accumulate on ceramics during burial, and it has the tendency to precipitate as oxides (Maritan, 2020). In addition, phosphorous and copper are commonly identified, adsorbed in ceramics buried in both terrestrial and marine environments, due to sediment, circulating waters and human activity affecting the surrounding soil (Buxeda i Garrigós, 1999; Buxeda i Garrigós and Kilikoglou, 2003; Freestone et al., 1985; Lemoine and Picon, 1982; Maritan and Mazzoli, 2004; Molera et al., 1993; Pradell et al., 1996). Besides, Figure 5.3.b shows the PCA of PT samples, for which Pb has been omitted because there was no specific reason for its high variability demonstrated in Figures 5.2.b,c. In the PCA of Figure 5.3.b, the three marine samples and one tap water sample fired at high temperatures (1100 °C) were the samples that contained the most Na_2O. Additionally, samples fired at the lowest temperature were those that contained more Nb, suggesting that this type of less vitrified samples absorb more Nb. Moreover, control-pieces are nearer to tap water samples than to marine samples, suggesting that more changes occurred in the marine samples. Regarding the Figures 5.3.c,d, they show the PCA of PF and AP samples (Pb has been omitted in 5.3.c). In both PCAs, the remarkable fact was that tap water samples seemed to contain more CaO, and, in the case of PF, those samples were fired at the highest temperature. A deeper discussion will be given when the XRD analyses and SEM–EDS analyses are explained (in the following lines).

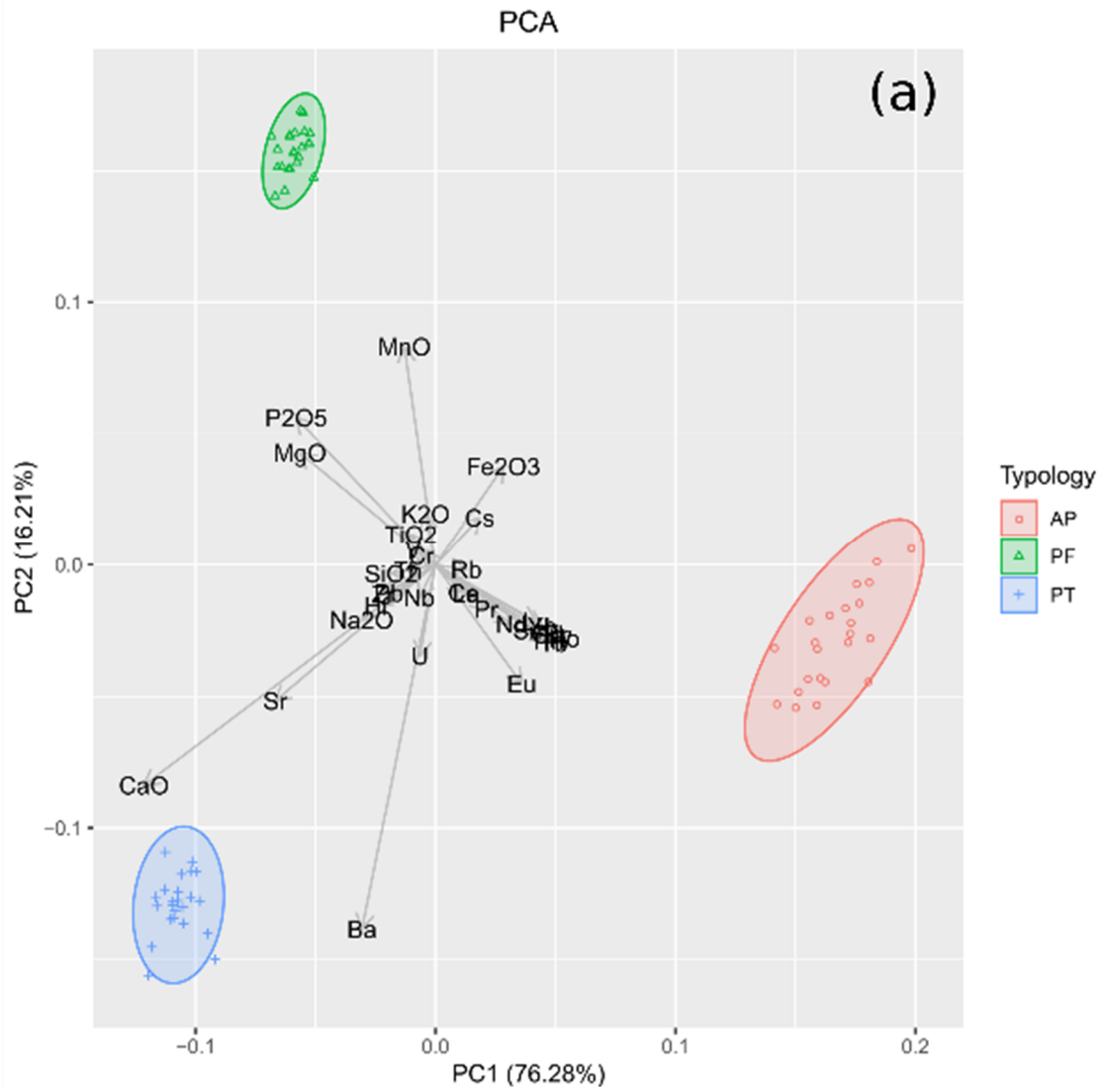
PCA
(a)
MnO
P2O5
MgO
Fe2O3
K2O
Cs
TiO2
Rb
Nb
Ce
Pr
Na2O
U
Eu
Sr
CaO
Ba
PC2 (16.21%)
PC1 (76.28%)
0.1
0.0
−0.1
−0.1
0.0
0.1
0.2
Typology
AP
PF
PT

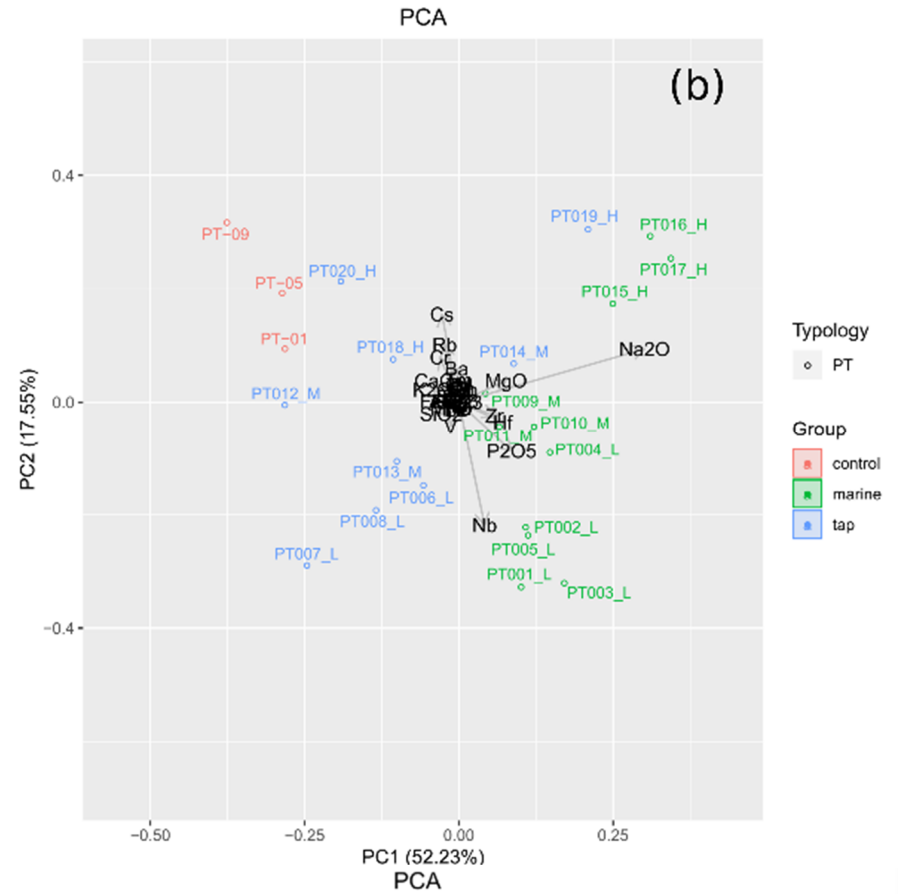
PCA
(b)
PT019_H
PT016_H
PT017_H
PT015_H
PT020_H
PT-05
PT-09
PT-01
PT018_H
PT014_M
Na2O
MgO
PT012_M
PT009_M
PT010_M
PT011_M
P2O5
PT004_L
PT013_M
PT006_L
PT008_L
Nb
PT002_L
PT005_L
PT007_L
PT001_L
PT003_L
Typology
PT
Group
control
marine
tap
PC2 (17.55%)
PC1 (52.23%)
0.4
0.0
−0.4
−0.50
−0.25
0.00
0.25

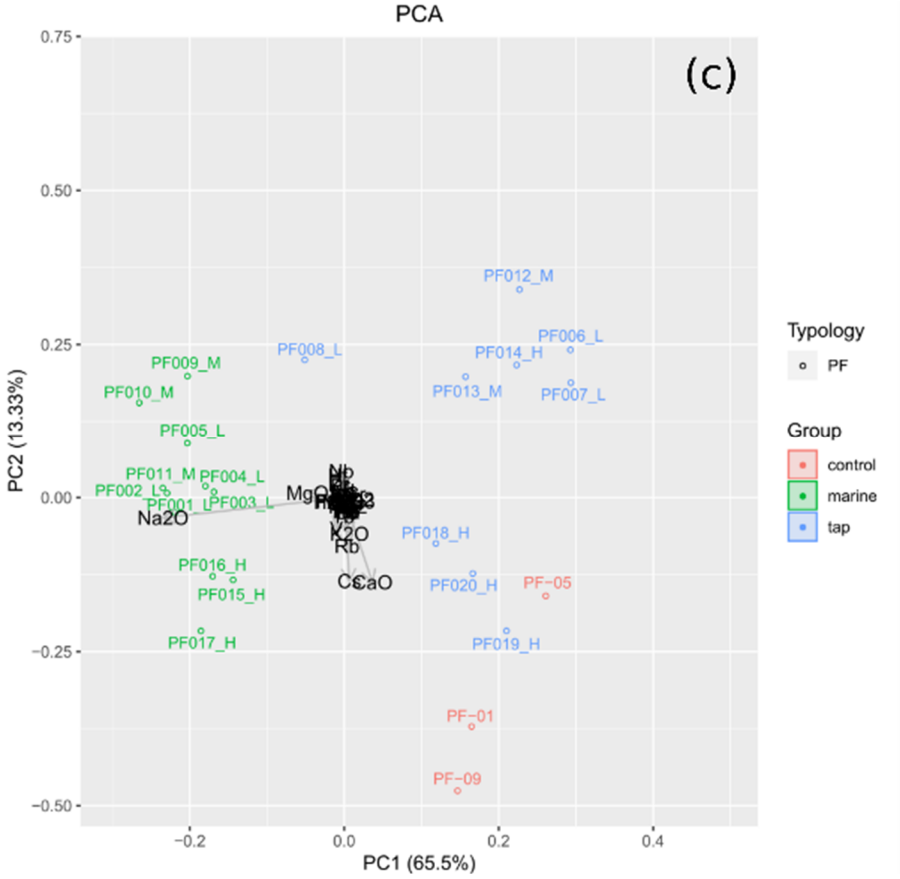
PCA
(c)
PF012_M
PF006_L
PF008_L
PF014_H
PF009_M
PF010_M
PF013_M
PF007_L
PF005_L
PF011_M
PF004_L
PF002_L
PF001_L
PF003_L
Na2O
MgO
K2O
Rb
CaO
PF018_H
PF016_H
PF015_H
PF020_H
PF-05
PF017_H
PF019_H
PF-01
PF-09
Typology
PF
Group
control
marine
tap
PC2 (13.33%)
PC1 (65.5%)
0.75
0.50
0.25
0.00
−0.25
−0.50
−0.2
0.0
0.2
0.4

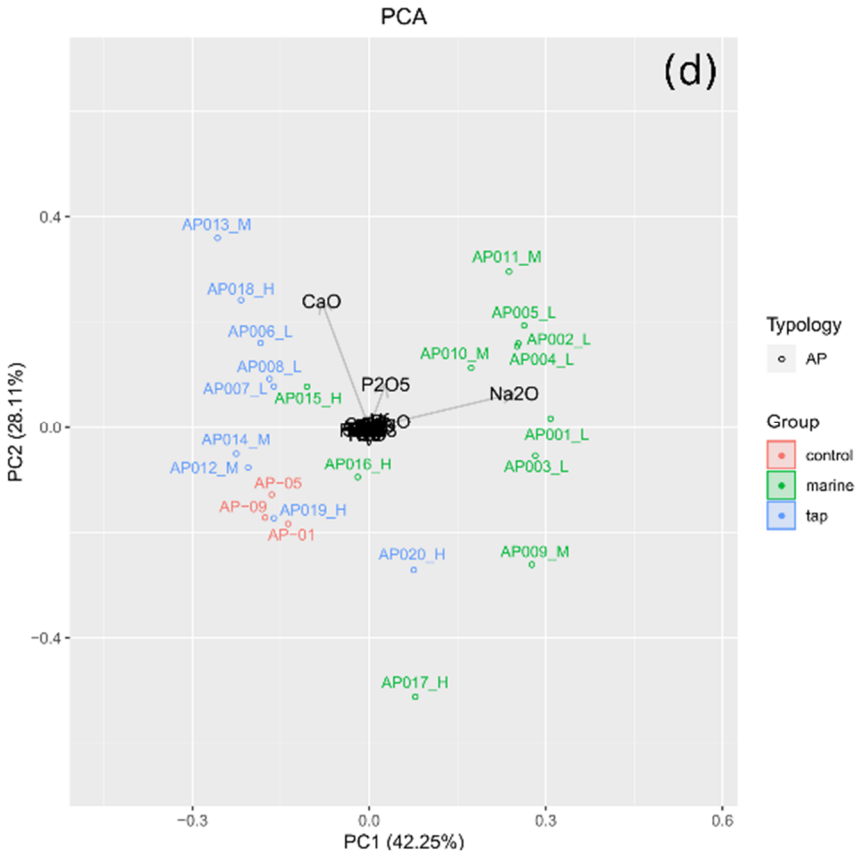

Figure 5.3. (a) Principal component analysis of 69 samples; **(b)** Principal component analysis of 23 PT samples; **(c)** Principal component analysis of 23 PF samples; **(d)** Principal component analysis of 23 AP samples. The four PCAs were calculated on the sub-composition of Al_2O_3, Ba, CaO, Ce, Cr, Cs, Dy, Er, Eu, Fe_2O_3, Gd, Hf, Ho, K_2O, La, Lu, MgO, MnO, Na_2O, Nb, Nd, P_2O_5, Pb, Pr, Rb, SiO_2, Sm, Sn, Sr, Tb, Th, TiO_2, Tm, U, V, Yb and Zr, but in (b) and (c), Pb was also omitted

After the chemical analyses and colour measurements, 69 pieces were analysed by XRD and SEM–EDS techniques. For SEM–EDS, 69 freshly fractured surface ceramics were prepared. The results were interpreted through the comparison between the test- and control-pieces for each paste type. On the one hand, the XRD results show the mineralogical composition of the ceramics, which have been studied in relation with the SEM–EDS results. On the other hand, the SEM examination provides information about the internal morphology developed during the original firing, the extent of vitrification and pore structure (see Chapter 4, section 4.3.3.). This also enables the study of the appearance of any concretion or alteration due to the post-depositional period. Besides, through the EDS analyses, the elemental microanalysis can be carried out.

5.4. XRD results

In this section post-depositional changes and transformations due to the firing will be described according to their chemical reaction paths.

First, raw clays were analysed by XRD for comparison purposes (Table 5.4.). The difference between them is mostly the presence or absence of calcite, dolomite and hematite, facts directly related to the colour of raw materials (buff-colour for PT and red

colour for PF and AP). Moreover, since they were not fired, the presence of phyllosilicates was evident.

Table 5.3. Summary of the mineralogical phases of the clays used for manufacturing the ceramic pastes. Qz = quartz; Cal = calcite; Dol = dolomite; Hem = hematite; Kfs = potassium feldspar; X = the presence of each mineral in the raw material, abbreviations according to Whitney and Evans (2010)

Raw Material	Mineralogy					
	Qz	Cal	Dol	Hem	Kfs	Phyllosilicates
High-calcareous clay (≈14 % CaO) (PT)	X	X			X	X
Low-calcareous clay (≈5 % CaO) (PF)	X	X	X	X	X	X
Micaceous clay (≈1 % CaO) (AP)	X			X		X

In the following lines, the mineralogical compositions of PT (Table 5.5.), PF (Table 5.6.) and AP (Table 5.7.) control- and test- pieces will be shown, and detailed ways of firing and post-depositional alterations are given.

As it is shown in Table 5.5., there are some mineralogical differences between the PT control-pieces, which were due to the firing alteration processes, as they were fired at different temperatures. The first clear difference is the disappearance of illite (clay mineral) with the increase of the firing temperature. This phenomenon occurs because the clay minerals lose the water they contain, so their lattice structure collapses and the clay minerals start to break down, forming new silicates (Rice, 1987). In addition, although kaolins were not present in the ceramic, they probably were present in the raw material. The dihydroxylation of kaolinite occurs at 400–500 °C and metakaolinite is formed. Then, at around 900 °C, alumina-rich spinel ($MgAl_2O_4$) starts to form from this metakaolinite and at 1000–1100 °C it crystallizes into mullite ($3Al_2O_3{\cdot}2SiO_2$). Mullite exists in needles or rod-like crystals, reinforcing and strengthening the fired piece (Abubakar et al., 2020; Aras, 2004; Rice, 1987). The presence of mullite is interesting in this context because, in general, when small amounts of carbonates are present (< 10 %) in high-calcareous clays, the mullite formation is inhibited and Ca-silicates are formed. However, depending on the concentration of Al_2O_3 in the samples, and if the amount of carbonates is higher than 10 %, mullite can be formed. El Ouahabi et al. (2015) identified mullite in a high-calcareous ceramic, whose Al_2O_3 concentration was around 15 %. The PT ceramics had around 14–16 % Al_2O_3 content, which justifies the presence of mullite in these ceramics. The diffractogram of PT-09 control-piece, in which mullite was present, is shown in Figure 5.4.

Table 5.5. Summary of the mineralogical phases of the control, marine and tap PT pieces. Qz = quartz; Cal = calcite; Gh = gehlenite; Hem = hematite; Kfs = potassium feldspar; Pl = plagioclase; Di = diopside; Ilt = illite; Gp = gypsum; Anl = analcime; Mul = mullite, abbreviations according to Whitney and Evans (2010)

		Mineralogy											
		Qz	Cal	Gh	Hem	Kfs	Pl	Di	Ilt	Mul	Gp	Anl	Wo
	PT-01 (850 °C)	X	X	X	X	X			X				
	PT-05 (950 °C)	X		X	X	X	X	X	X				
	PT-09 (1100 °C)	X		X	X	X	X	X		X			
Marine	PT001 (850 °C, 3 months)	X	X	X	X	X			X				
Marine	PT002 (850 °C, 10 months)	X	X	X	X	X			X		X		
Marine	PT003 (850 °C, 18 months)	X	X	X	X	X			X		X		
Marine	PT009 (950 °C, 3 months)	X	X	X	X	X	X	X	X				
Marine	PT010 (950 °C, 10 months)	X		X	X	X	X	X	X				
Marine	PT011 (950 °C, 18 months)	X		X	X	X	X	X	X				
Marine	PT015 (1100 °C, 3 months)	X		X	X	X	X	X		X		X	
Marine	PT016 (1100 °C, 10 months)	X		X	X	X	X	X		X		X	
Marine	PT017 (1100 °C, 18 months)	X		X	X	X	X	X				X	
Tap	PT006 (850 °C, 3 months)	X	X	X	X	X			X				
Tap	PT007 (850 °C, 10 months)	X	X	X	X	X			X				
Tap	PT008 (850 °C, 18 months)	X	X	X	X	X			X				
Tap	PT012 (950 °C, 3 months)	X		X	X	X	X	X	X				
Tap	PT013 (950 °C, 10 months)	X		X	X	X	X	X	X				
Tap	PT014 (950 °C, 18 months)	X		X	X	X	X	X	X				
Tap	PT018 (1100 °C, 3 months)	X		X	X	X	X	X		X			
Tap	PT019 (1100 °C, 10 months)	X		X	X	X	X	X		X			X
Tap	PT020 (1100 °C, 18 months)	X		X	X	X	X	X		X			

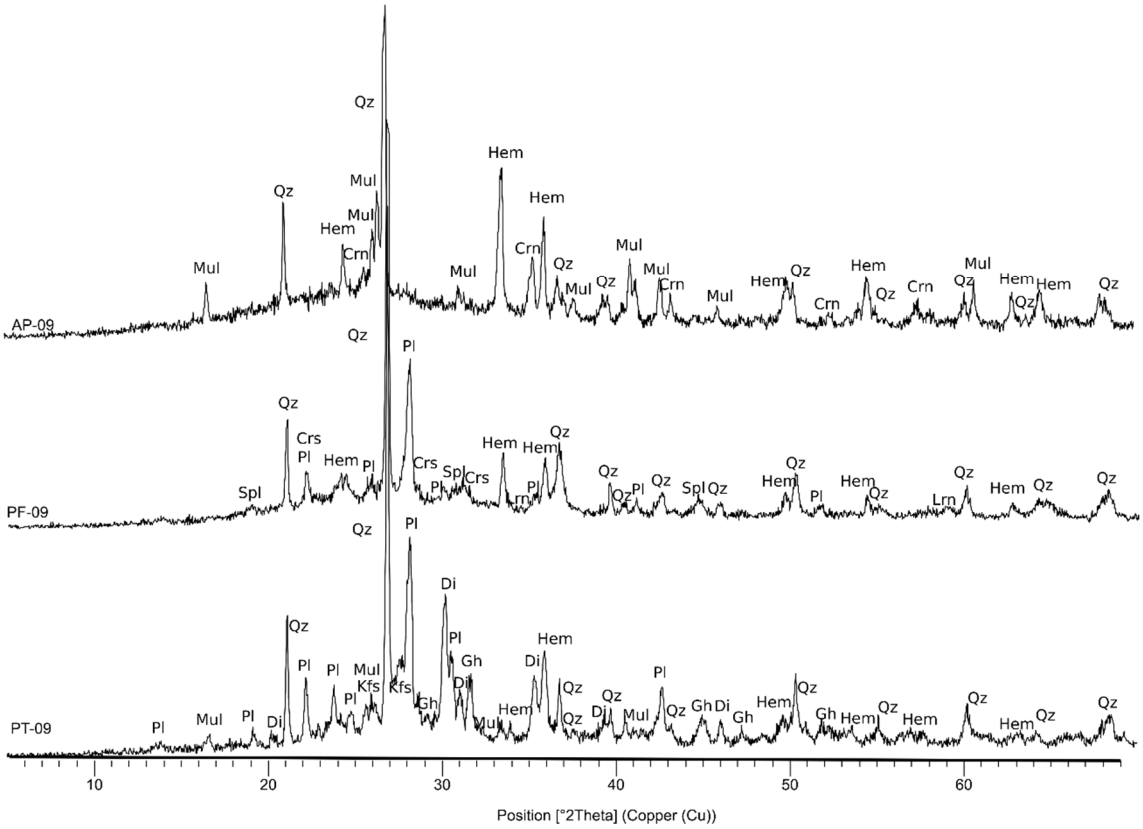

Figure 5.4. The diffractograms of AP-09, PF-09 and PT-09 control-pieces. Qz = quartz; Cal = calcite; Gh = gehlenite; Hem = hematite; Kfs = potassium feldspar; Pl = plagioclase; Di = diopside; Ilt = illite; Gp = gypsum; Anl = analcime; Mul = mullite; Crs = Cristobalite; Spl = spinel; Lrn = larnite, Crn = corundum, abbreviations according to Whitney and Evans (2010)

Additionally, calcite is present in the sample fired at lower temperature, but it is not present in the other samples, while gehlenite ($Ca_2Al_2SiO_7$) and diopside ($Ca(Mg,Fe)Si_2O_6$) appeared. The decrease in calcite is due to its decomposition at approximately 600–900 °C, forming lime (CaO) and carbon dioxide gas (CO_2), according to the following reaction (Buxeda i Garrigós and Cau, 1994; Cau et al., 2002; Fabbri et al., 2014; Rice, 1987):

$$CaCO_3 \xrightarrow{650-900\ ^\circ C} CaO + CO_2 \uparrow \quad \text{Eq. 5.2.}$$

Then, the CaO reacts, depending on the firing temperature, the duration of the firing, the granulometry of the carbonate fragments or their crystalline structure, with the clay minerals present in the body. In this way, Ca-silicates and aluminosilicates such as gehlenite, anorthite ($CaAl_2Si_2O_8$, which increased with the firing temperature in the control-pieces) and diopside (Cau et al., 2002) are formed. That is the reason why diopside, plagioclase (e.g., anorthite, albite) and gehlenite appeared in the control-pieces fired at higher temperatures.

In addition, Heimann and Maggetti (1981) described the reactions for the alterations of gehlenite to form anorthite at temperatures close to and above 1000 °C.

$$Al_2SiO_7 + 2\ SiO_2 \rightarrow CaAl_2Si_2O_8 + CaSiO_3 \quad \text{Eq. 5.3.}$$

$$Ca_2Al_2SiO_7 + 3\ SiO_2 + Al_2O_3 \rightarrow 2\ CaAl_2Si_2O_8 \quad \text{Eq. 5.4.}$$

These reaction paths can explain the increment of anorthite and the decrease for gehlenite in PT-09 (fired at 1100 °C). Additionally, the amount of hematite also increased with

temperature. The reason for this could be that hematite may crystallize due to the decomposition of calcite in the presence of quartz and Fe-bearing clay minerals (Nodari et al., 2007). The carbonates decompose to produce calcium silicates reacting with the amorphous phase. Thus, hematite can nucleate and grow.

When it comes to the XRD results of marine PT test-pieces (Table 5.5.), from the samples fired at 850 °C (PT001, PT002, PT003), PT001 had a greater amount of calcite and gehlenite (3 months of burial). The decomposition reaction paths of calcite and gehlenite due to the post-depositional period could support the findings of their lower amounts in the pieces with longer deposition periods (Buxeda i Garrigós and Cau, 1994; Fabbri et al., 2014; Heimann and Maggetti, 1981). The amounts of Qz, Pl, Kfs and Ilt were similar in all the samples, but the presence of gypsum ($CaSO_4{\cdot}2H_2O$) in PT002 and PT003 marked the most important difference between these samples. The presence of gypsum is associated with the pyrite formation in reductive marine environments or to the dissolution of calcite and reaction with sulphate, in an acid environment (Secco et al., 2011); however, these were not the case because the marine environment of the experiment was oxidizing and both environments were basic. The presence of gypsum might be associated with the raw material but in the control-pieces it has not been identified. Thus, the most probable source was the precipitation of sulfate from the seawater. Additionally, from samples fired at 950 °C (PT009, PT010, PT011), calcite appeared in PT009, and the amount of Qz, Pl, Gh, Hem, Kfs and Ilt were similar in all the samples. Calcite should not appear in PT009 because it was not present in the control-piece PT-05. However, the CaO that did not react could have recarbonated to $CaCO_3$ (Buxeda i Garrigós and Cau, 1994; Fabbri et al., 2014; Freestone, 2001; Freeth, 1967) and at a basic pH (higher than 7–8) it precipitated (Maritan, 2020). First, it reacts with the water to give calcium hydroxide ($Ca(OH)_2$, portlandite) and, then, portlandite reacts with CO_2 leading to the formation of calcite, according to the next reaction path (Fabbri et al., 2014).

$$CaO + H_2O \rightarrow Ca(OH)_2 \quad \text{Eq. 5.5.}$$

$$Ca(OH)_2 + CO_2 \rightarrow CaCO_3 + H_2O\uparrow \quad \text{Eq. 5.6.}$$

Gehlenite appeared in a smaller amount than in the corresponding control-piece (PT-09), probably due to the alteration of gehlenite to form anorthite. In addition, mullite was not present in PT017, possibly making visible the fact that factors such as the firing of ceramics in the kiln were subjected to variations. It could be that the amount of carbonates in this particular sample was lower than in the rest of the samples due to the mentioned variations, so mullite was not formed (El Ouahabi et al., 2015).

Finally, in samples fired at 1100 °C (PT015–017), analcime ($NaAlSi_2O_6{\cdot}H_2O$) appeared in all of them. Buxeda i Garrigós et al. (2002a) recorded in calcareous ceramics fired at temperatures above 1000 °C, an increase in the concentration of Na and sometimes of Mg and Sr, and a decrease in the concentration of K and Rb, under certain burial conditions. Several studies (Buxeda i Garrigós, 1999; Buxeda i Garrigós et al., 2001, 2002a; Heimann and Maggetti, 1981; Schwedt et al., 2006) have documented the formation of analcime mineral, also known as analcite, as the reason for these facts. Buxeda i Garrigós et al. (2002a) explain from the observations of Picon (1976) that, depending on the firing temperature, a glassy phase is formed in the ceramics. This glassy phase contains a large part of the overall K of the shard, which is leached with Rb from the ware during the burial because of the instability of the glassy phase under certain weathering conditions. Then, analcime crystallizes from the remaining silicate material by the fixation of Na from the burial environment. This fact can be seen in the ceramics immersed in marine water, with high concentration of Na, which explains why analcime is found in those ceramics but not in the similar ceramics immersed

in tap water. Moreover, this fact is in accordance with the PCA shown in Figure 5.3.b, in which those marine samples fired at 1100 °C were the samples that contained the most Na_2O.

Regarding the XRD results of tap water PT test-pieces (Table 5.5.), no change was identified in the phases of the samples of different burial periods, probably because tap water is not as aggressive as marine water. Wollastonite was the new phase that appeared in PT pieces, specifically in PT019. This mineral is a high-temperature secondary phase, which crystallizes from Ca-rich clays (Gliozzo, 2020b).

Besides, as it is shown in Table 5.6., the mineralogical changes occurred in PF samples were very similar to the changes occurred in PT control-pieces. The differences were the appearance of mullite in PT samples but not in PF samples as well as the presence of cristobalite, spinel and larnite in PF samples (unlike in PT samples). The alteration paths for the calcite, gehlenite, hematite, plagioclase and diopside mineral phases are the same as those explained in the PT control-pieces section. Moreover, cristobalite, a polymorph of quartz, appears in PF-09 (1100 °C), due to the inversions that occur in quartz at high temperatures. In addition, larnite, a calcium silicate (Ca_2SiO_4), and alumina-rich spinel ($MgAl_2O_4$), appeared due to high-temperature alterations of clay minerals (Rice, 1987). The diffractogram of PF-09 control-piece, in which larnite, cristobalite and spinel are present, is shown in Figure 5.4.

Table 5.6. Summary of the mineralogical phases of the marine and tap PF test-pieces and control-pieces. Qz = quartz; Cal = calcite; Gh = gehlenite; Hem = hematite; Kfs = potassium feldspar; Pl = plagioclase; Di = diopside; Ilt = illite; Crs = Cristobalite; Spl = spinel; Lrn = larnite, abbreviations according to Whitney and Evans (2010)

		Mineralogy									
		Qz	**Cal**	**Gh**	**Hem**	**Kfs**	**Pl**	**Di**	**Ilt**	**Crs**	**Spl**	**Lrn**
	PF-01 (850 °C)	X	X	X	X	X	X		X			
	PF-05 (950 °C)	X		X	X	X	X		X			
	PF-09 (1100 °C)	X			X		X	X		X	X	X
Marine	**PF001 (850 °C, 3 months)**	X	X	X	X	X	X		X			
	PF002 (850 °C, 10 months)	X	X	X	X	X	X		X			
	PF003 (850 °C, 18 months)	X	X	X	X	X	X		X			
	PF009 (950 °C, 3 months)	X	X	X	X	X	X		X			
	PF010 (950 °C, 10 months)	X	X	X	X	X	X		X			
	PF011 (950 °C, 18 months)	X		X	X	X	X		X			
	PF015 (1100 °C, 3 months)	X			X		X	X			X	X
	PF016 (1100 °C, 10 months)	X			X		X	X			X	

		Qz	Cal	Gh	Hem	Kfs	Pl	Di	Ilt	Crs	Spl	Lrn
	PF017 (1100 °C, 18 months)	X			X		X	X			X	X
Tap	**PF006 (850 °C, 3 months)**	X	X	X	X	X	X		X			
	PF007 (850 °C, 10 months)	X	X	X	X	X	X		X			
	PF008 (850 °C, 18 months)	X	X	X	X	X	X		X			
	PF012 (950 °C, 3 months)	X	X	X	X	X	X		X			
	PF013 (950 °C, 10 months)	X	X	X	X	X	X		X			
	PF014 (950 °C, 18 months)	X	X	X	X	X	X		X			
	PF018 (1100 °C, 3 months)	X			X		X	X			X	
	PF019 (1100 °C, 10 months)	X			X		X	X			X	X
	PF020 (1100 °C, 18 months)	X			X		X	X			X	

When it comes to the XRD results of the marine PF test-pieces (Table 5.6.) fired at 850 °C (PF001–003), the amount of calcite and gehlenite was greater in PF001 (3 months of immersion) due to the same reasons explained in PT section. Additionally, in samples fired at 950 °C (PF009–011), calcite appeared in PF009 due to the recarbonation of CaO, as in the PT009 sample, and the amounts of Qz, Pl, Gh, Hem, Di, Kfs and Ilt were similar in all the samples. Finally, for samples fired at 1100 °C, plagioclase and hematite were higher in PF017 (18 months of burial). The reason for the greater amount of plagioclase could be, as has been afore mentioned, the alteration of gehlenite to form anorthite. Qz, Spl and Di were in similar amount to the rest of the samples and Ilt disappeared. Crs was not detected in these samples as it may have not developed during firing, and larnite appeared in PF015 and PF017 but not in PF016.

In addition, results of the PF test-pieces immersed in tap water were almost the same as those of the PT test-pieces, thus, very few changes were identified in the phases of the samples of different burial periods (Table 5.6.).

Besides, regarding the micaceous (AP) test- and control-pieces, Table 5.7. shows that there were some mineralogical differences between the AP control-pieces due to the firing alteration processes. The first clear difference was the presence of mullite in high-fired ceramics, as in the PT pieces. In addition, the amount of hematite increased with temperature. This phenomenon also occurred with PT and PF samples. Similarly, corundum (Al_2O_3) appeared in AP-09, due to high firing temperatures.

Table 5.4. Summary of the mineralogical phases of the AP control-pieces. Qz = quartz; Ilt = illite; Mul = mullite; Hem = hematite; Kfs = potassium feldspar; Crn = corundum, abbreviations according to Whitney and Evans (2010)

	Mineralogy					
	Qz	**Illt**	**Mul**	**Hem**	**Kfs**	**Crn**
AP-01 (850 °C)	X	X		X	X	
AP-05 (950 °C)	X	X	X	X	X	
AP-09 (1100 °C)	X		X	X		X

When it comes to the XRD results of marine and tap water AP test-pieces, it is noted that there were no significant differences either in the phases (that is, all the samples had the same phases as their corresponding control-pieces) or between samples with different immersion periods. The existing differences between the samples were those that corresponded to the firing temperatures, shown in Table 5.7.

5.5. SEM-EDS results

Regarding the SEM–EDS analyses for the control-pieces of the three types of samples, first, the control-pieces fired at 850 °C (PT-01, PF-01 and AP-01) showed an early initial vitrification in accordance with their firing temperature, due to the appearance of isolated smooth-surfaced areas (Figure 5.5.a–c). Additionally, PT-05, PF-05 and AP-05 (fired at 950 °C) showed a medium vitrification (Figure 5.5.d–f) and those fired at 1100 °C (PT-09, PF-09 and AP-09) showed a continuous vitrification (Figure 5.5.g–i) due to the formation of a continuous smooth vitrified layer over the whole fractured surface (Maniatis and Tite, 1978). In PF, mineral phases of different sizes were identified. By EDS analyses it was known that these mineral phases were mainly composed of Si, O, Ca, Fe, Mg, Al, K and, sometimes, Ti, suggesting, according to XRD results, the presence of quartz, potassium feldspar, illite, calcite, hematite, gehlenite, plagioclase, cristobalite and diopside, among others. Furthermore, the EDS analyses of the PT control-pieces revealed the high presence of calcium and magnesium in the three control samples. These elements can appear in the form of carbonates, oxides and silicates, among others. Additionally, S and Cl were present in PT-05, demonstrating that those elements had their origin in the raw material. In this case, S may be associated with gypsum, supporting the presence of gypsum in the XRD analyses of PT002 and PT003 test-pieces. Finally, it was observed that AP pieces contained long and plane mineral phases, which formed a laminar structure within the ceramic paste, likely from the mica group. The pieces fired at 850 °C kept this laminar structure, while the samples fired at 1100 °C did not so much because they showed a continuous, smooth vitrified layer. EDS analyses showed that these mineral phases were mainly composed of Si, O, Fe, K, Al, Mg, Ca, and, sometimes, Ti, suggesting, in agreement with XRD results, the presence of quartz, potassium feldspar, illite, and hematite, among others. It was also noted that the presence of Ca and Mg seemed to be related. Additionally, the EDS analyses of AP-05 showed, as in AP-01, mineral phases composed of Fe, Ca, K, Mg, C, Al, Ca, O, Si, Ti and, in some cases, S and Mn, in agreement with the presence of quartz, potassium feldspar, illite and mullite, according to XRD analyses. Although calcium carbonates and silicates were not identified by XRD,

probably due to their lower amount, some aggregates were recognized by SEM–EDS, but in lower amounts than in PT and PF samples.

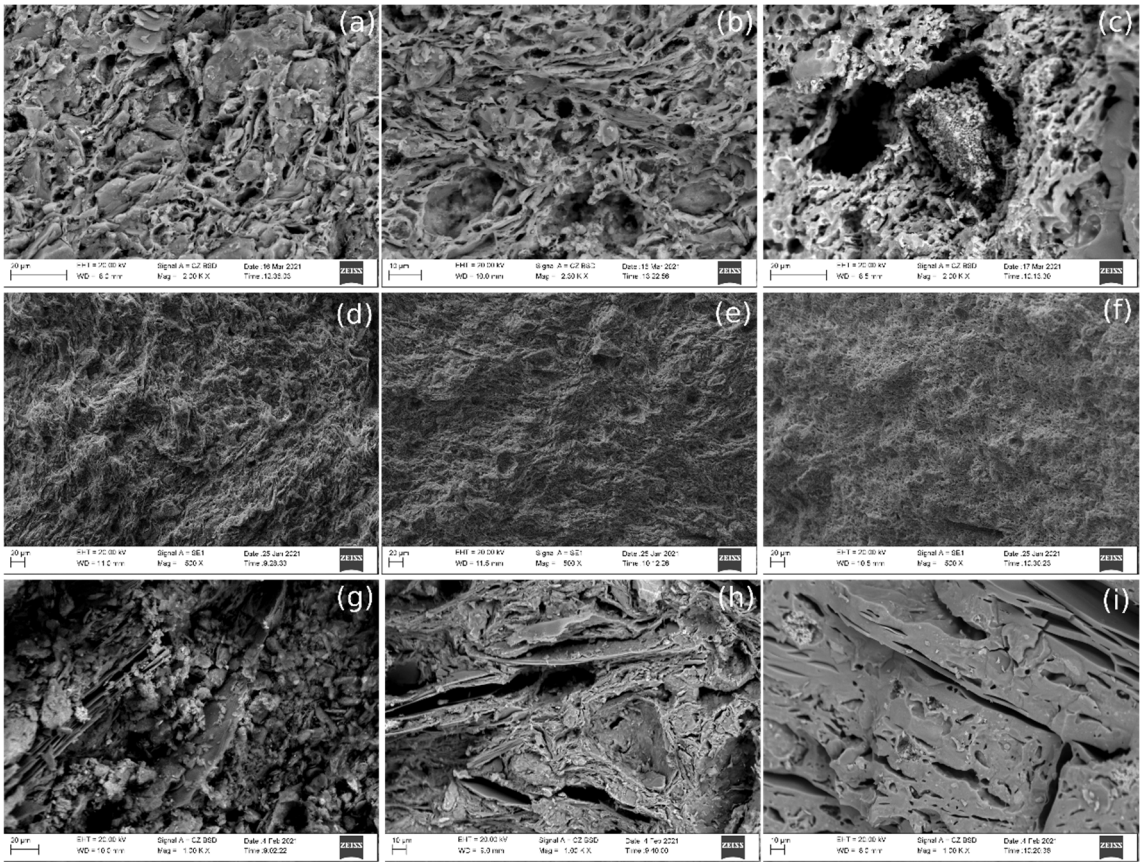

Figure 5.5. SEM-BSD (a,b,c,g,h,i) and SEM-SED (d,e,f) images of the fractured surfaces of PT, PF and AP control-pieces: **(a–c)** PT-01, PT-05, PT-09; **(d–f)** PF-01, PF-05, PF-09; **(g–i)** AP-01, AP-05, AP-09

Additionally, the SEM and EDS results of test-pieces were very diverse and mineral forms such as needles, flakes, sponges and long and short prisms, were found, mostly in PT and PF samples. Regarding the SEM–EDS analyses of AP marine and tap water test-pieces, it was noted that, in comparison to PT and PF pieces, AP pieces showed much fewer aggregates inside their pastes. Contrary to what would be expected, in AP, more secondary phases were identified in samples fired at high temperatures than in those at low temperatures, even though the pastes fired at low temperatures were more porous. Perhaps the reason for this is that the laminar structure that the pastes contain makes it difficult for solutions from the environment to access, and therefore, may block the formation of the secondary phases. On the contrary, it is likely that the vitrification of AP samples fired at high temperatures helps to form canals through which solutions from the environment can access.

Marine samples of the three pastes showed some crystallizations containing Na, Cl and S (Figure 5.6.). These crystallizations could correspond to NaCl (halite) and calcium sulphate, both in most of the cases precipitated from seawater. However, there is a possibility that gypsum in some PT and AP samples was coming from the raw material because S was identified by EDS analyses in control-pieces. While in PT and PF samples, it seems that the mentioned aggregates were formed in cavities, in AP they seemed to rest on top of large mineral phases, suggesting that the movement of the water could have been of

laminar flux instead of percolation, due to the structure of AP. However, as an exception, marine AP samples fired at 1100 °C showed NaCl aggregates in the cavities formed in the vitrified pastes. Besides, AP samples submerged in tap water and fired at 850 °C and 950 °C did not show any newly formed aggregate.

Additionally, Figure 5.7. shows one of the crystallizations identified in both PF and PT samples submerged in marine and tap water environments. These crystallizations mostly appeared in PF tap water samples but were also present in marine and tap PT samples. They were similar to sponges and were composed mainly of Ca and F, appearing principally in cavities. In addition, Mn was identified in the extremities of this aggregate, as well as elements such as Ca, O, C, Al and Si (probably related to calcium silicates) around these cavities.

According to Thomas et al. (1977), fluorine is an element that can be present in raw clays. García-Ten et al. (2006) explain that, during the ceramics firing, the fluorine ion replaces OH^- groups present in the crystalline structure of mica and other clay minerals (such as illite or montmorillonite). This reaction leads to the formation of hydrofluoric acid (HF) and silicon tetrafluoride (SiF_4), among others. These compounds are released during firing between 500–700 °C. However, in high-calcareous ceramics, HF can react with calcite to form fluorite (CaF_2). Additionally, De Bonis et al. (2014) reported newly formed cuspidine [$Ca_4Si_2O_7(F,OH)_2$] at the edges of silicates (such as feldspars and quartz) in contact with fluorite-based carbonates, in ceramics fired from 850 °C to 1100 °C. The authors proposed the next reaction path for cuspidine formation.

$$3CaO + 2SiO_2 + CaF_2 \rightarrow Ca_4Si_2O_7F_2 \quad \text{Eq. 5.7.}$$

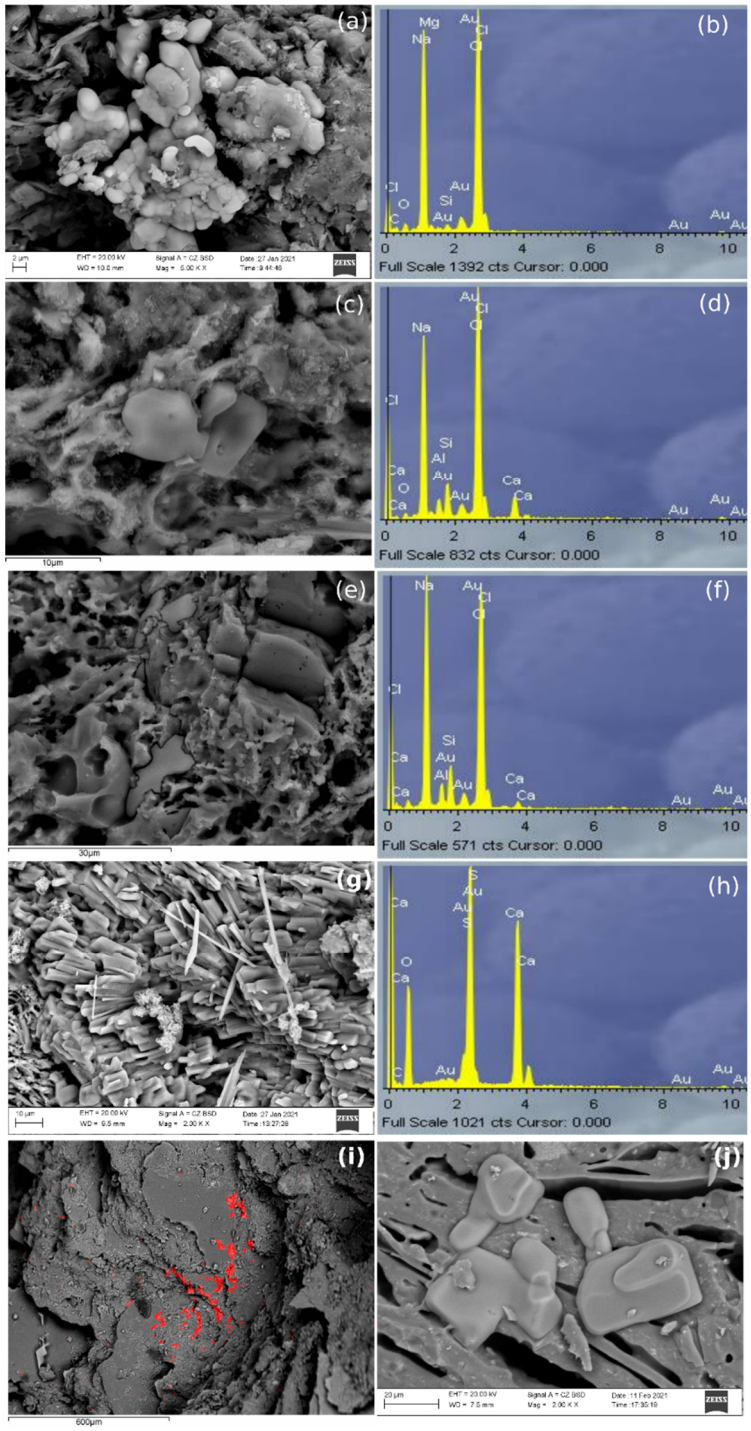

Figure 5.6. SEM-BSD images of the fractured surfaces of PT and PF marine samples and their elemental analyses by EDS; **(a–f)** aggregates composed of Na and Cl, suggested to be NaCl. They appear in different forms; **(g,h)** aciculate crystals composed of Ca, S, O, suggested to be a calcium sulphate; **(i)** NaCl (marked in red) in top of big mineral phases of AP002; **(j)** NaCl in the cavities of AP015

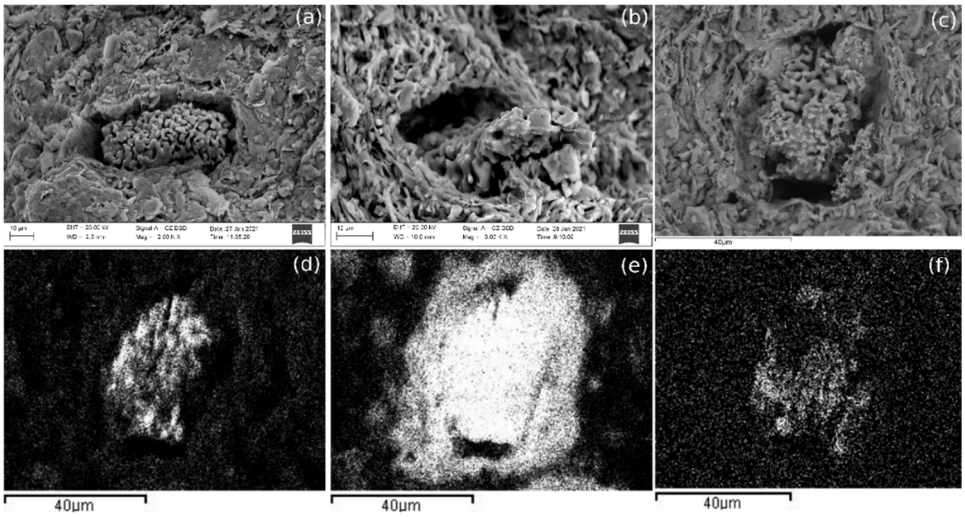

Figure 5.7. SEM-BSD images of the common crystallization identified in PT and PF samples; **(a)** Ca-F aggregate in a cavity of PF008, a sample immersed in tap water; **(b)** Ca-F aggregate in a cavity of PF012, a sample immersed in tap water; **(c)** Ca-F aggregate in a cavity of PF013, a sample immersed in tap water; **(d)** elemental mapping: the distribution of F in the Ca-F aggregate of (c); **(e)** elemental mapping: the distribution of Ca in in the Ca-F aggregate of (c); **(f)** elemental mapping: the distribution of Mn in the Ca-F aggregate of (c)

Therefore, the sponge-like structures of these samples may be cuspidine. The presence of Mn in the extremities of the Ca-F aggregate could suggest that, in these cases, the newly formed mineral might be a mineral from the cuspidine group containing Mn, such as normandite [NaCa(Mn,Fe)(Ti,Nb,Zr)(Si_2O_7)OF]. These newly formed structures may have their origin in calcite. Calcite decomposed to CaO leaving cavities, so cuspidine or normandite may have formed in these cavities. Moreover, it has been noted that it seems that there were more cavities in tap water samples than in seawater samples. The reason could be that there is more fluorine in tap water environment, so more calcite reacted with fluorine to form CaF_2. Additionally, in some cases, these aggregates did not show the same structure; the reason could be their different grade of crystallization. Finally, although AP test-pieces contained F in their EDS analyses, the sponge-like structures were not present. In comparison with what I saw using qualitative SEM–EDS analyses for AP, PT and PF samples, PF and PT samples had much more calcium-containing minerals, so the changes in the pastes were notable. In the case of AP pieces, as they did not contain much calcium, most probably the fluorine of the raw material or of the water solution was unable to react with the calcite.

Moreover, aggregates of calcium carbonate with salts such as NaCl and $MgCl_2$ (present in the environment) and barium sulphate (probably barite, as commented in Figure 5.3.a), were also identified in PT010 sample (Figure 5.8.) as well as a structure that seemed to be formed by Mg and calcium hydroxide or carbonate, in PT016. In addition, calcium-containing phases may have existed in AP samples but in such little amounts that was difficult to see them. The exceptions appeared in AP011 and AP014, in which calcium silicate and calcium related to Mg were identified, probably with their origin in calcite and phyllosilicates. Finally, AP samples submerged in the marine environment and fired at 1100 °C showed calcium carbonate or silicate aggregates. Figure 5.9. shows an alteration in the paste of one of the AP samples fired at 1100 °C; Mg and O were homogeneously distributed and in the same place, there were also some parts composed of NaCl (coming from seawater). This aggregate was surrounded by Ca (which suggests it had its origin in dolomite

or in calcite). AP samples submerged in tap water and fired at 1100 °C also showed the same type of aggregates of calcium carbonate or silicates.

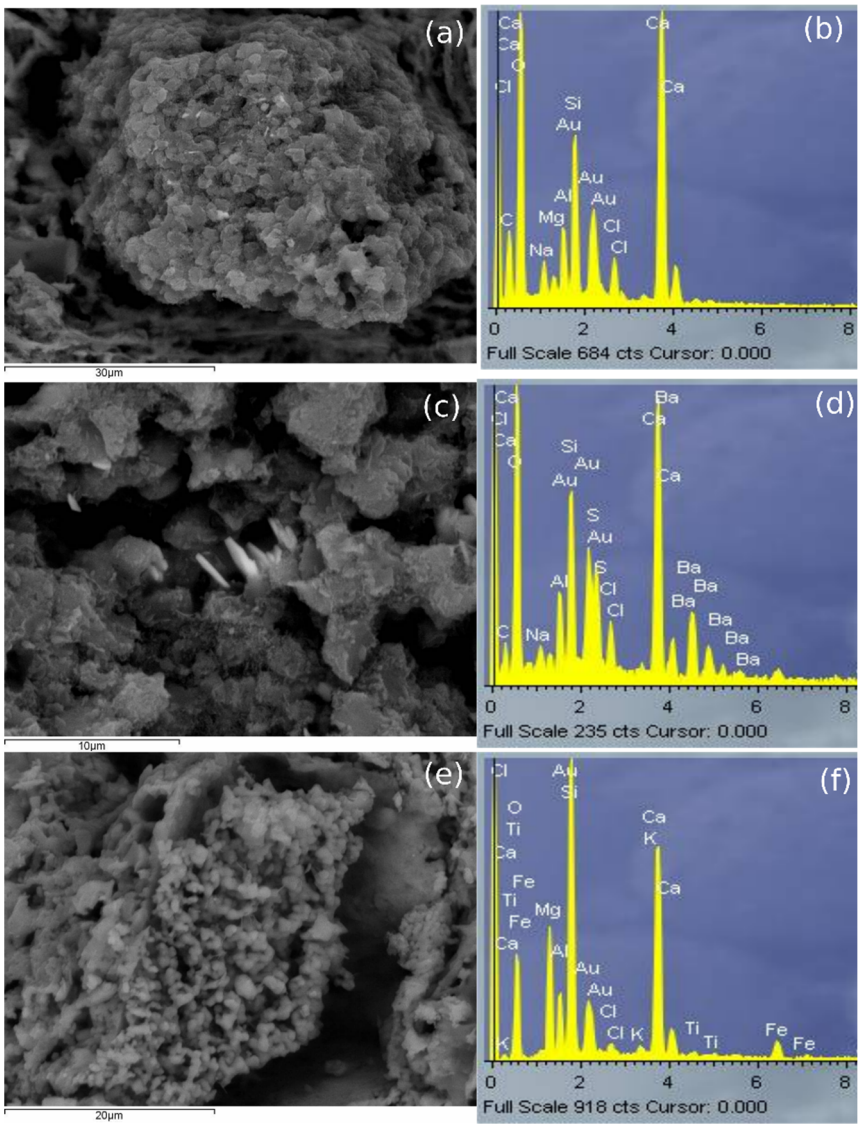

Figure 5.8. (a,b) SEM-BSD images and EDS analyses of an aggregate of PT010 composed mainly of Ca, Mg, O, C, Na and Cl, probably a calcium carbonate and salts; **(c,d)** SEM-BSD image and EDS analysis of an aggregate of PT010, probably barite; **(e,f)** SEM-BSD image and EDS analysis of an aggregate of PT016, probably magnesium and calcium hydroxide or carbonate

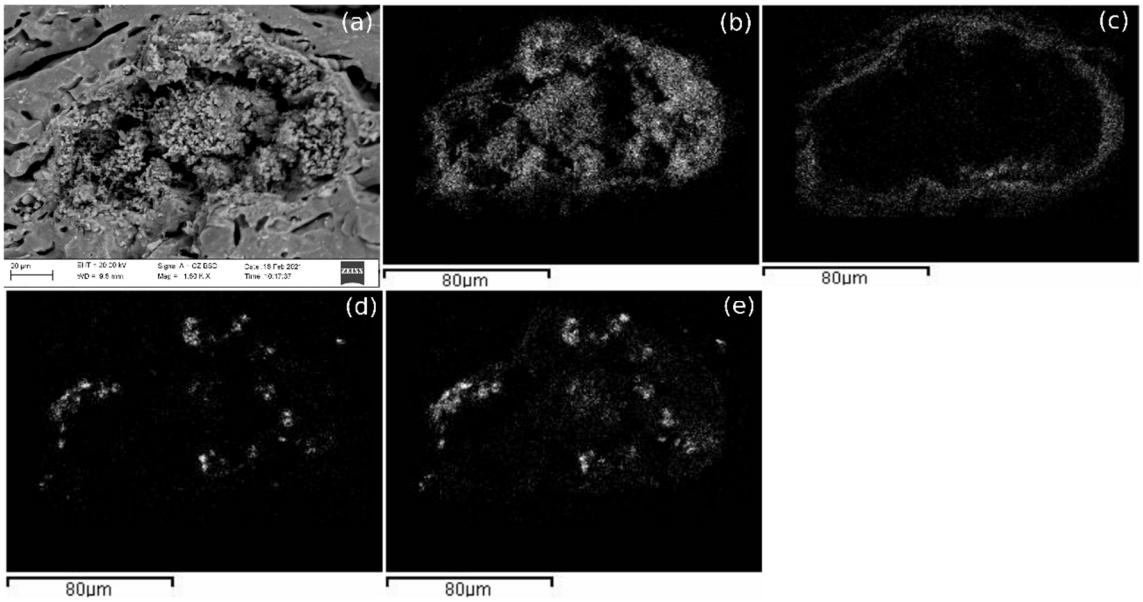

Figure 5.9. (a) SEM-BSD image of an aggregate present in AP016; **(b)** elemental mapping: the distribution of Mg in the aggregate of (a); **(c)** elemental mapping: the distribution of Ca in the aggregate of (a); **(d)** elemental mapping: the distribution of Na in the aggregate of (a); **(e)** elemental mapping: the distribution of Cl in the aggregate of (a)

Apart from the paste analyses, the surfaces of PF010 and PF014 samples were analysed by Raman spectroscopy (Figure 5.10.). The results demonstrated that NaCl and different forms of calcium sulphate were salts that precipitated from the seawater and they rested on the surface of the ceramic. It has been concluded that the aciculate crystals of different forms were calcium sulphate; the former (a) corresponded to anhydrite ($CaSO_4$), while (c) corresponded to calcium sulphate hemihydrate (bassanite) [$CaSO_4 \cdot \frac{1}{2}(H_2O)$]. Probably, there was a mixture of different phases of $CaSO_4$-H_2O system, as Prieto-Taboada et al. (2014) explained. Additionally, calcite was identified in the paste of PF014 by Raman (e), supporting the hypothesis of the recarbonation of calcite samples fired at 950 °C and 1100 °C.

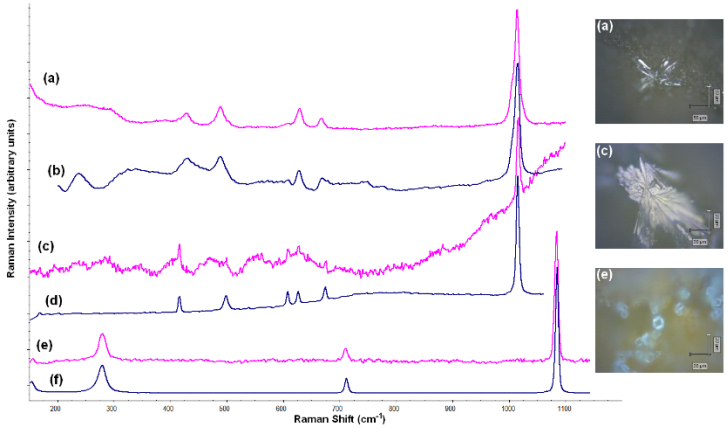

Figure 5.10. Raman analyses in the PF010 surface and PF014 paste: **(a)** spectrum of anhydrite ($CaSO_4$) in PF010 surface; **(b)** spectrum of anhydrite in the database; **(c)** spectrum of bassanite [$CaSO_4 \cdot \frac{1}{2}(H_2O)$] in PF010 surface; **(d)** spectrum of bassanite in the database; **(e)** spectrum of calcite ($CaCO_3$) in PF014 paste; **(f)** spectrum of calcite ($CaCO_3$) in the database

CHAPTER 6: CASE STUDIES

The results and discussion of the analysed ceramics introduced in Chapter 4, section 4.1.1. are presented in two parts; Zamora and Aveiro. On the one hand, the results of ceramics from the archaeological sites of Olivares, La Concepción, Ethnographic Museum, Benavente and Toro are presented in Zamora section (Chapter 6, section 6.1.), whereas results of ceramics from RAVA, Santo António church, wasters and Angra D (a shipwreck, which will be introduced later) are presented in Aveiro section (Chapter 6, section 6.2.). Finally, the lead isotopic case study carried out in Zamoran glazes is described in depth in Chapter 6, section 6.3.

6.1. Zamora

The concentrations of each component and their relative average expanded uncertainties (U %) for the 94 ceramics analysed by ICP-MS, are presented in Table 6.1. The expanded uncertainty of the results has been calculated for 11 ceramics of the Ethnographic Museum, following the Guide to the Expression of Uncertainty in Measurement (GUM) with k = 2, which is equivalent to a 95 % confidence level, considering the whole analytical procedure (see Chapter 4, section 4.4.3.). Figure 4.13. from Chapter 4 shows that the uncertainty of the calibration and the uncertainty of the first reference concentration (which is also related to the calibration) are the major contributors to the uncertainty in the specific case of Fe_2O_3 concentration in AVR001, being negligible the contribution of the ceramic material. Therefore, since the type of calibration was the same for the whole set of Zamoran ceramics, an approximation has been made: the uncertainties calculated for the 11 ceramics of the Ethnographic Museum are extrapolated to the rest of ceramics (see Table 6.1.). However, it should be highlighted that the uncertainties of Tb and U could not be calculated because their concentrations for the Ethnographic Museum ceramics were below the quantification limit.

Table 6.5. Elemental concentrations and their relative average expanded uncertainties (U %) for the 94 ceramics analysed by ICP-MS. The line refers to values below the quantification limit. The uncertainties of Tb and U could not be calculated because their concentrations for the Ethnographic Museum ceramics were below the quantification limit. The concentrations of the elements are expressed in ng/g and of the oxides in wt %. The calcareous or high-calcareous ceramics are marked in bold (those with CaO ≥ 6 %)

Samples	Al_2O_3	Ba	CaO	Ce	Co	Cr	Cs	Cu	Dy	Er	Eu	Fe_2O_3	Gd	Hf	Ho	K_2O	La	Lu	MgO	MnO	Na_2O
ZMR001	12.5	423	**10.1**	66.9	17.0	49.2	6.46	-	4.58	2.52	1.16	3.94	5.36	5.39	0.783	3.88	32.4	0.363	2.42	0.0639	1.27
ZMR002	11.7	417	**9.56**	63.8	29.6	45.4	5.83	-	4.51	2.45	1.05	4.01	5.17	5.78	0.761	3.94	30.5	0.339	2.32	0.0661	1.37
ZMR003	13.4	458	**9.19**	72.7	37.7	44.6	6.12	-	5.07	2.66	1.19	3.84	5.97	6.44	0.823	3.76	34.8	0.392	1.91	0.0617	1.35
ZMR004	13.3	458	**10.4**	71.4	27.0	52.8	6.83	-	4.70	2.50	1.25	4.27	5.66	5.61	0.816	4.01	34.4	0.362	2.45	0.0703	1.31
ZMR005	12.1	419	**12.1**	61.5	23.3	55.1	5.74	-	4.25	2.27	1.10	4.62	5.08	4.85	0.752	3.57	29.9	0.310	2.67	0.0715	1.31
ZMR006	11.6	403	**10.5**	59.3	50.3	55.9	6.69	-	4.22	2.42	1.02	4.50	4.89	5.17	0.763	3.75	28.8	0.362	2.50	0.0710	1.36
ZMR007	12.6	289	1.03	76.4	20.9	63.2	9.67	-	4.81	2.58	1.16	4.30	5.56	7.68	0.816	1.70	39.4	0.418	0.483	0.0195	0.739
ZMR008	11.2	390	**9.81**	59.9	12.6	44.0	6.30	-	4.15	2.36	1.08	3.93	4.82	4.80	0.737	3.37	29.0	0.324	2.60	0.0604	1.17
ZMR009	12.7	266	1.13	66.5	10.8	62.5	9.51	-	5.00	2.76	1.18	4.02	5.49	7.91	0.823	1.67	33.2	0.425	0.462	0.0224	0.723
ZMR010	17.9	538	**6.67**	90.9	19.0	84.3	8.73	-	5.46	2.82	1.66	6.47	6.94	4.56	0.876	4.22	44.6	0.410	1.84	0.104	1.05
ZMR011	19.1	392	1.09	50.3	14.8	56.6	11.3	-	3.61	1.86	1.31	5.21	4.91	2.65	0.641	3.14	23.6	0.202	1.00	0.0298	0.899
ZMR012	17.9	416	1.49	74.8	19.2	48.8	11.6	-	4.35	2.08	1.54	4.04	6.48	3.40	0.714	3.15	33.8	0.224	0.730	0.0233	0.922
ZMR013	18.8	400	1.28	97.9	11.3	45.8	7.63	-	3.60	1.72	1.55	3.61	6.56	3.35	0.610	2.57	43.8	0.185	0.570	0.0193	0.856
ZMR014	12.8	295	1.40	69.5	24.0	65.3	10.7	-	4.60	2.64	1.05	4.21	5.24	6.83	0.803	1.89	35.3	0.368	0.482	0.0205	0.744
ZMR015	16.0	379	1.14	65.1	37.5	46.2	13.1	-	5.60	2.58	1.71	4.70	7.41	3.02	0.867	2.64	33.7	0.288	0.711	0.0262	0.786
ZMR016	12.2	290	0.332	67.9	39.5	66.1	7.71	-	4.79	2.85	1.13	5.14	5.38	8.15	0.861	1.79	35.0	0.408	0.466	0.0391	0.818
ZMR017	12.7	433	**10.6**	66.7	34.3	47.7	6.10	-	4.45	2.56	1.21	4.02	5.38	4.92	0.777	2.98	32.5	0.328	2.36	0.0606	1.18
ZMR018	11.9	409	**12.1**	66.4	26.3	53.2	6.00	-	4.39	2.43	1.10	4.34	5.15	5.02	0.766	3.79	32.3	0.322	2.51	0.0729	1.33
ZMR019	12.8	292	0.869	73.1	31.3	63.4	9.63	-	5.07	2.86	1.26	4.01	5.89	7.62	0.870	1.80	37.3	0.433	0.421	0.0290	0.784

	Al_2O_3	Ba	CaO	Ce	Co	Cr	Cs	Cu	Dy	Er	Eu	Fe_2O_3	Gd	Hf	Ho	K_2O	La	Lu	MgO	MnO	Na_2O
ZMR020	13.0	442	**11.2**	67.7	25.0	45.2	7.73	-	4.69	2.65	1.16	3.86	5.41	5.39	0.818	3.18	33.4	0.405	2.20	0.0630	1.26
ZMR021	12.9	433	**11.4**	68.8	36.6	53.2	6.29	-	4.70	2.61	1.15	4.12	5.38	5.55	0.800	3.22	33.6	0.374	2.32	0.0642	1.34
ZMR022	13.2	297	1.01	80.8	20.4	56.2	7.82	-	4.71	2.57	1.13	3.34	5.39	7.36	0.795	1.58	41.2	0.364	0.450	0.0171	0.731
ZMR023	14.3	317	1.51	74.7	24.9	61.2	11.1	-	4.79	2.76	1.13	4.43	5.63	7.41	0.831	1.69	38.3	0.415	0.483	0.0177	0.759
ZMR024	11.5	298	0.398	72.9	30.8	58.0	6.99	-	4.45	2.56	1.16	4.18	5.29	7.50	0.786	1.37	37.6	0.377	0.422	0.0345	0.730
ZMR025	13.2	285	0.561	66.1	36.1	54.5	11.2	-	5.23	2.92	1.08	4.15	5.29	7.98	0.866	1.54	33.9	0.443	0.429	0.0150	0.720
ZMR026	12.4	424	**9.88**	66.8	30.7	45.5	6.07	-	4.56	2.49	1.15	3.75	5.37	5.56	0.776	3.12	32.4	0.339	2.24	0.0589	1.34
ZMR027	11.7	409	**13.0**	63.8	21.4	50.9	5.64	-	4.54	2.46	1.13	4.22	5.05	5.25	0.755	3.54	31.1	0.341	2.31	0.0684	1.37
ZMR028	20.1	351	3.75	70.9	20.3	36.0	9.38	-	4.10	1.96	1.51	3.21	6.19	3.07	0.650	2.18	34.7	0.200	0.558	0.0164	0.809
ZMR029	16.0	357	1.18	105	29.0	85.6	13.0	-	4.83	2.69	1.41	5.20	6.45	8.41	0.818	2.92	50.6	0.379	0.559	0.0215	0.947
ZMR030	12.2	277	1.46	72.3	60.2	61.9	7.25	-	5.09	2.80	1.16	4.47	5.54	8.87	0.820	1.48	36.3	0.433	0.468	0.0290	0.699
ZMR031	12.4	409	**11.1**	63.7	21.0	48.8	4.48	-	4.16	2.27	1.18	4.00	4.96	4.57	0.715	3.30	31.1	0.326	2.66	0.0608	1.16
ZMR032	21.5	482	1.75	111	27.6	57.7	15.8	-	5.20	2.33	2.05	4.86	8.03	3.78	0.784	2.26	56.0	0.279	0.720	0.0194	0.808
ZMR033	19.4	389	0.733	76.0	53.4	42.9	11.3	-	7.07	3.18	2.30	3.60	9.05	3.35	1.00	3.14	36.5	0.395	0.552	0.0204	0.837
ZMR034	13.8	461	**10.4**	68.1	27.2	58.0	6.20	-	4.56	2.50	1.32	4.49	5.39	4.59	0.815	3.54	33.2	0.350	2.91	0.0703	1.22
ZMR035	21.3	418	0.455	64.7	30.7	51.8	17.5	-	6.59	2.92	1.99	4.93	7.95	3.78	0.961	3.92	32.5	0.399	0.734	0.0231	0.894
ZMR036	17.4	506	**7.48**	89.2	20.2	79.2	7.92	-	5.29	2.77	1.67	5.95	6.65	4.46	0.878	3.65	43.7	0.415	1.88	0.0919	0.963
ZMR037	22.5	291	0.473	92.4	20.1	14.3	10.8	1.74	4.14	1.81	1.95	2.12	7.46	2.85	0.592	2.12	39.7	0.128	0.769	0.0101	0.348
ZMR038	26.5	334	3.80	44.3	27.9	20.9	33.4	15.6	6.76	3.52	1.13	2.58	6.54	5.19	1.12	3.35	21.2	0.499	0.949	0.0383	0.670
ZMR039	23.2	459	2.63	82.2	7.44	29.9	10.9	6.33	4.99	2.10	1.93	2.85	8.01	3.19	0.718	2.80	35.4	0.137	0.746	0.00933	0.484
ZMR040	11.9	377	**18.5**	67.1	22.6	50.4	2.58	14.1	4.59	2.57	1.35	3.81	5.79	5.91	0.768	2.85	33.6	0.322	1.94	0.0711	0.711
ZMR041	8.7	276	**15.1**	50.3	9.40	32.9	3.34	4.71	3.37	1.99	0.924	2.95	4.35	4.87	0.614	2.52	24.9	0.227	1.54	0.0489	0.651
ZMR042	21.7	277	2.34	54.6	15.6	22.7	25.3	4.65	5.29	2.77	0.969	2.30	5.76	4.54	0.845	2.97	27.1	0.311	0.758	0.0367	0.566
ZMR043	25.6	314	4.02	45.4	10.5	21.1	29.5	1.67	5.43	2.98	0.876	2.52	5.43	4.80	0.871	3.84	21.5	0.336	1.02	0.0437	0.583
ZMR044	24.9	294	4.03	46.3	9.38	22.5	34.4	2.39	5.24	3.00	0.787	2.51	4.98	4.92	0.890	3.73	21.1	0.355	0.853	0.0422	0.653

	Al_2O_3	Ba	CaO	Ce	Co	Cr	Cs	Cu	Dy	Er	Eu	Fe_2O_3	Gd	Hf	Ho	K_2O	La	Lu	MgO	MnO	Na_2O
ZMR045	13.6	385	**7.09**	72.0	16.9	64.3	5.62	18.4	4.56	2.56	1.42	4.54	5.98	4.58	0.759	3.36	36.4	0.336	1.86	0.0591	0.597
ZMR046	16.2	425	**19.2**	79.2	29.3	73.7	7.32	49.3	5.27	2.93	1.47	5.30	6.78	4.95	0.875	3.84	42.2	0.425	3.02	0.0803	0.523
ZMR047	10.6	307	**13.8**	55.4	14.2	44.0	5.87	74.4	3.74	2.11	1.06	3.31	4.89	3.42	0.671	2.73	28.5	0.233	1.97	0.0347	0.462
ZMR048	17.0	469	**9.09**	90.2	18.1	74.5	7.61	64.1	5.70	3.02	1.74	5.82	7.59	5.33	0.931	3.51	45.9	0.416	2.44	0.0929	0.606
ZMR049	11.3	376	**19.3**	67.5	12.7	43.1	3.21	115	4.44	2.60	1.22	3.70	5.69	5.55	0.742	2.89	33.5	0.290	2.15	0.0560	0.764
ZMR050	22.3	606	5.04	94.8	17.4	93.0	9.87	74.0	5.89	3.28	1.91	7.47	7.80	4.46	0.972	5.38	47.8	0.380	2.40	0.0488	0.624
ZMR051	11.8	408	**10.3**	70.7	11.4	40.7	5.46	75.3	5.06	2.85	1.39	3.62	6.20	5.94	0.833	3.01	35.4	0.346	1.77	0.0554	0.693
ZMR052	13.6	427	**16.5**	75.1	12.6	44.7	6.42	58.4	5.15	2.79	1.42	4.21	6.39	5.52	0.826	3.40	37.4	0.363	2.17	0.0645	0.669
ZMR053	9.1	337	**12.0**	59.7	12.5	29.3	4.05	105	4.11	2.32	1.12	2.95	5.17	5.15	0.697	2.51	29.4	0.298	1.59	0.0424	0.553
ZMR054	10.7	392	**18.6**	63.9	10.7	41.5	4.14	50.8	4.49	2.36	1.24	3.57	5.48	5.72	0.729	2.45	31.7	0.269	1.74	0.0484	0.473
ZMR055	10.1	304	**16.7**	59.8	9.58	38.4	2.85	107	4.19	2.31	1.08	3.34	5.14	5.68	0.697	2.52	29.4	0.305	1.94	0.0439	0.578
ZMR056	12.1	437	**20.7**	67.7	11.7	44.9	3.11	45.8	4.61	2.53	1.28	3.92	5.51	5.48	0.778	2.83	33.6	0.310	2.07	0.0620	0.773
ZMR057	11.2	415	**15.8**	69.0	23.2	40.7	4.69	18.9	4.95	2.63	1.36	3.59	5.86	5.72	0.772	2.89	34.7	0.353	2.16	0.0591	0.611
ZMR058	12.8	421	**17.1**	74.3	33.1	49.1	5.50	18.7	5.47	2.77	1.44	3.86	6.45	6.00	0.839	3.33	37.3	0.425	2.46	0.0559	0.645
ZMR059	9.3	316	**13.8**	53.4	12.0	33.6	2.91	10.6	3.48	1.98	1.05	3.24	4.54	4.78	0.657	2.43	26.8	0.242	1.86	0.0451	0.498
ZMR060	9.6	341	**13.6**	58.3	9.69	33.0	4.93	7.64	4.24	2.32	1.09	3.00	5.16	4.54	0.718	2.58	29.4	0.293	2.15	0.0480	0.550
ZMR061	10.4	376	**14.8**	63.7	11.7	42.6	4.55	6.69	4.29	2.52	1.27	3.44	5.62	5.37	0.769	2.98	31.9	0.337	2.35	0.0524	0.724
ZMR062	18.0	246	4.10	71.7	4.59	13.5	6.36	-	2.94	1.50	1.08	1.70	5.35	2.71	0.499	2.35	33.3	0.048	0.584	0.00476	0.546
ZMR063	22.7	343	**8.30**	89.8	7.29	18.9	7.58	-	3.56	1.70	1.54	2.10	6.59	3.00	0.563	2.24	43.3	0.092	0.538	0.00564	0.484
ZMR065	13.6	458	**10.5**	69.4	35.0	50.4	5.83	-	4.74	2.62	1.24	3.96	5.50	5.16	0.796	2.99	33.5	0.359	2.29	0.0640	1.18
BNV001	13.5	457	**14.3**	73.7	20.8	64.4	3.98	38.2	4.63	2.47	1.35	5.18	5.84	5.66	0.759	3.14	37.6	0.383	1.81	0.0561	0.565
BNV002	8.5	282	**11.9**	50.7	12.2	41.2	3.07	33.0	3.23	1.85	0.955	3.55	4.24	3.98	0.585	1.95	25.2	0.216	1.73	0.0493	0.507
BNV003	14.7	413	**13.5**	78.8	13.4	72.7	4.92	84.7	5.00	2.66	1.59	5.69	6.56	5.38	0.808	3.74	39.4	0.410	1.55	0.0610	0.518
BNV004	10.2	337	**9.31**	55.4	23.2	50.0	3.57	59.7	3.54	2.02	1.09	4.28	4.80	3.41	0.613	2.54	27.3	0.257	1.66	0.0424	0.506
BNV005	21.7	616	1.90	95.6	34.0	109	7.88	43.4	6.31	3.13	2.10	8.03	8.09	5.56	0.939	3.36	47.3	0.567	1.21	0.0487	0.634

	Al_2O_3	Ba	CaO	Ce	Co	Cr	Cs	Cu	Dy	Er	Eu	Fe_2O_3	Gd	Hf	Ho	K_2O	La	Lu	MgO	MnO	Na_2O
BNV006	20.3	655	0.599	80.1	24.2	96.4	7.03	55.7	5.22	2.70	1.82	6.88	6.92	4.43	0.809	3.23	40.7	0.458	1.10	0.0342	0.591
BNV007	24.7	657	1.54	84.5	30.8	122	8.84	54.6	5.51	2.80	1.90	8.73	7.16	4.64	0.806	3.72	43.4	0.457	1.38	0.0444	0.587
BNV008	21.2	583	1.18	72.3	20.3	109	7.44	48.4	4.60	2.38	1.64	7.09	6.18	4.04	0.737	3.33	36.9	0.398	1.24	0.0320	0.566
BNV009	22.9	668	1.73	89.9	35.4	122	8.71	27.8	6.00	3.18	2.06	8.31	8.01	5.24	0.943	3.73	45.2	0.527	1.33	0.0438	0.633
BNV010	22.1	576	1.79	85.3	35.9	120	7.21	15.2	5.42	2.78	1.91	7.92	7.06	5.29	0.820	3.36	43.7	0.429	1.30	0.0384	0.628
BNV011	23.8	673	1.44	85.7	31.5	122	9.05	12.8	5.43	2.90	1.91	8.00	7.24	4.94	0.870	3.59	44.3	0.481	1.31	0.0360	0.612
BNV012	25.9	713	1.90	86.0	29.5	141	8.41	10.1	5.60	2.98	2.01	9.53	7.50	4.66	0.853	3.99	44.6	0.458	1.59	0.0529	0.621
BNV013	25.1	696	1.90	89.8	25.6	135	8.94	6.40	6.13	3.10	2.09	8.93	7.92	4.51	0.927	4.05	46.1	0.496	1.59	0.0515	0.628
BNV014	25.0	672	1.82	84.5	21.6	131	8.01	5.72	5.54	2.93	1.86	8.49	7.27	5.32	0.874	3.91	44.4	0.440	1.54	0.0420	0.637
BNV015	26.0	679	4.29	90.5	27.5	134	9.12	5.69	5.82	3.07	1.89	8.89	7.73	4.96	0.892	4.00	47.0	0.443	1.49	0.0426	0.615
BNV016	25.0	731	1.91	92.5	31.2	132	8.36	5.81	5.89	3.00	1.94	9.41	7.87	5.38	0.899	3.89	47.9	0.475	1.45	0.0577	0.612
TOR001	21.0	596	2.16	103	25.5	89.7	8.23	16.7	6.32	3.35	2.21	6.71	8.56	5.41	0.982	3.83	52.7	0.535	1.17	0.0251	0.501
TOR002	14.9	464	0.689	74.0	16.9	68.3	8.26	19.4	4.66	2.43	1.47	4.84	6.23	4.03	0.729	3.32	37.6	0.338	0.859	0.0192	0.449
TOR003	21.3	623	1.86	101	16.2	91.5	8.66	71.2	6.80	3.36	2.14	6.50	8.31	4.92	0.977	3.77	51.3	0.498	1.16	0.0251	0.485
TOR004	15.0	458	0.872	71.1	10.8	61.8	7.50	105	4.63	2.43	1.53	4.62	6.03	3.75	0.751	3.40	35.2	0.343	0.863	0.0160	0.455
TOR005	20.4	583	1.68	99.1	19.4	85.7	10.5	24.6	6.32	3.29	1.95	6.08	7.97	5.01	0.982	3.77	51.2	0.492	1.04	0.0234	0.507
TOR006	16.1	547	0.871	82.9	16.5	69.9	8.47	7.72	5.62	2.87	1.61	5.48	6.78	4.84	0.814	3.46	42.2	0.439	1.11	0.0404	0.453
TOR007	21.7	613	1.26	96.9	17.2	94.0	11.0	8.87	6.19	3.02	2.04	6.43	7.63	4.94	0.886	4.04	49.8	0.480	1.11	0.0234	0.475
TOR008	22.7	657	1.82	105	20.7	110	9.95	7.04	7.00	3.28	2.13	7.21	8.36	5.19	0.960	4.33	53.3	0.511	1.34	0.0316	0.524
TOR009	15.4	397	1.43	84.4	13.4	47.6	10.7	3.74	5.12	2.56	1.19	4.34	6.65	6.03	0.768	3.70	40.7	0.335	1.55	0.0512	1.07
TOR010	20.0	638	1.76	105	25.9	92.2	8.81	4.84	6.53	3.35	2.11	7.05	8.43	6.42	0.969	3.85	52.8	0.515	1.19	0.0648	0.518
TOR011	20.9	664	1.56	104	20.1	96.9	10.1	4.27	7.00	3.47	2.16	6.92	8.33	6.17	1.01	4.16	53.0	0.557	1.45	0.0503	0.521
TOR012	19.9	630	2.08	101	25.2	85.3	8.63	6.16	6.60	3.25	2.21	6.35	8.23	6.23	0.981	3.73	51.5	0.533	1.18	0.0451	0.459
TOR013	13.3	475	0.211	69.4	24.4	57.9	7.92	4.40	4.62	2.33	1.35	4.49	5.76	4.14	0.754	3.10	35.0	0.296	0.927	0.0403	0.401
TOR014	20.3	624	0.786	102	32.2	86.9	8.67	10.6	6.69	3.28	2.10	6.32	8.46	6.26	0.951	3.61	51.6	0.554	1.17	0.0535	0.428

	Al_2O_3	Ba	CaO	Ce	Co	Cr	Cs	Cu	Dy	Er	Eu	Fe_2O_3	Gd	Hf	Ho	K_2O	La	Lu	MgO	MnO	Na_2O
U (%)	53	6	12	31	19	30	28	26	30	15	10	32	16	22	21	30	31	57	14	53	172

(continues)

Samples	Nb	Nd	Ni	P_2O_5	Pb	Pr	Rb	SiO_2	Sm	Sn	Sr	Ta	Tb	Th	TiO_2	Tm	U	V	Yb	Zn	Zr
ZMR001	13.0	33.2	-	-	9.50E+02	8.04	126	63.7	6.23	15.5	186	1.26	0.807	12.4	0.645	0.380	2.87	58.3	2.50	-	238
ZMR002	12.4	31.7	-	-	8.99E+02	7.64	121	74.3	6.13	15.6	184	1.27	0.773	12.5	0.661	0.365	2.77	59.7	2.32	-	248
ZMR003	14.1	36.1	-	-	6.82E+02	8.73	131	67.4	6.76	46.3	189	1.45	0.860	14.5	0.640	0.397	3.22	55.7	2.69	-	270
ZMR004	13.5	35.2	-	-	7.98E+02	8.53	129	73.4	6.67	28.7	194	1.36	0.843	14.1	0.679	0.382	3.09	57.2	2.47	-	243
ZMR005	12.6	30.5	-	-	2.74E+03	7.41	116	70.3	5.64	27.4	206	1.14	0.741	11.8	0.728	0.330	2.95	72.0	2.23	-	194
ZMR006	11.9	29.2	-	-	2.06E+03	7.12	120	75.4	5.87	8.67	188	1.25	0.729	11.7	0.730	0.343	2.84	67.0	2.35	-	214
ZMR007	17.1	35.7	-	-	4.40E+02	8.68	96.1	82.8	6.58	8.09	103	1.97	0.833	14.7	0.972	0.386	3.01	58.4	2.68	-	359
ZMR008	11.8	29.4	-	-	5.99E+02	7.27	118	64.2	5.64	17.6	191	1.16	0.724	11.6	0.626	0.334	2.67	55.0	2.27	-	198
ZMR009	17.8	32.4	-	-	6.68E+02	7.74	94.1	83.8	6.52	7.99	69.7	2.00	0.854	14.6	1.01	0.427	3.24	54.5	2.88	-	361
ZMR010	17.1	45.2	-	-	1.52E+02	10.9	148	63.2	7.97	7.90	203	1.72	1.04	15.9	0.946	0.436	3.67	116	2.85	-	181
ZMR011	12.5	31.1	-	-	4.44E+01	7.15	136	72.6	6.61	16.9	163	2.08	0.708	7.46	0.495	0.235	2.87	68.0	1.71	-	93.8
ZMR012	12.0	42.1	-	-	1.15E+04	10.0	135	67.3	8.18	20.9	197	1.88	0.902	9.88	0.493	0.249	2.80	57.2	1.93	-	126
ZMR013	12.2	49.1	-	-	3.23E+01	12.0	105	79.3	8.90	19.0	109	2.04	0.807	9.76	0.419	0.210	2.02	48.4	1.55	-	129
ZMR014	16.9	32.2	-	-	4.47E+02	7.97	107	81.7	6.32	8.48	77.2	1.91	0.826	14.2	0.998	0.375	3.15	66.1	2.63	-	318
ZMR015	11.2	41.6	-	-	5.01E+04	9.44	126	58.8	8.55	16.5	92.8	1.57	1.11	9.08	0.441	0.342	2.26	59.6	2.29	-	103
ZMR016	15.9	32.8	-	-	4.86E+02	7.73	91.9	81.5	6.45	7.58	66.5	1.78	0.809	13.8	0.945	0.422	3.54	59.7	2.85	-	394
ZMR017	12.9	33.1	-	-	4.10E+03	8.02	119	54.4	6.56	60.1	226	1.28	0.789	12.5	0.595	0.352	3.14	60.5	2.40	-	205
ZMR018	12.5	33.2	-	-	4.32E+03	8.04	117	73.8	6.39	49.4	200	1.26	0.787	12.5	0.702	0.356	3.06	68.9	2.38	-	219
ZMR019	15.6	36.6	-	-	1.05E+03	8.58	99.6	70.1	7.40	7.88	77.1	1.81	0.925	14.4	0.946	0.410	3.31	55.1	2.81	-	348
ZMR020	13.1	34.1	-	-	1.97E+03	8.09	135	60.5	6.69	70.0	225	1.28	0.849	13.1	0.604	0.400	3.25	56.4	2.57	-	228
ZMR021	13.1	34.3	-	-	4.44E+03	8.29	118	66.2	6.79	69.2	220	1.26	0.822	13.0	0.651	0.371	3.30	71.3	2.52	-	243

	Nb	Nd	Ni	P_2O_5	Pb	Pr	Rb	SiO_2	Sm	Sn	Sr	Ta	Tb	Th	TiO_2	Tm	U	V	Yb	Zn	Zr
ZMR022	16.1	37.0	-	-	7.44E+02	9.00	96.6	74.9	7.02	7.75	94.8	1.74	0.825	14.6	0.832	0.412	3.13	55.1	2.67	-	356
ZMR023	17.5	34.5	-	-	5.27E+02	8.31	112	70.9	6.74	9.92	95.7	1.97	0.861	15.6	0.890	0.408	3.27	58.5	2.81	-	356
ZMR024	14.7	35.5	-	-	3.07E+02	8.41	81.2	67.8	6.95	6.93	109	1.73	0.828	13.5	0.819	0.380	3.28	45.0	2.62	-	359
ZMR025	19.4	30.2	-	-	9.43E+02	7.39	95.5	76.1	6.07	9.73	71.1	2.23	0.910	14.9	0.941	0.462	3.34	52.0	2.95	-	384
ZMR026	12.9	33.4	-	-	6.05E+03	8.01	123	61.5	6.50	95.6	195	1.31	0.813	12.9	0.623	0.377	3.15	58.5	2.48	-	240
ZMR027	12.6	32.5	-	-	4.05E+03	7.59	115	71.3	5.96	53.4	201	1.20	0.797	12.1	0.680	0.395	3.07	64.8	2.43	-	219
ZMR028	12.9	39.7	-	-	1.46E+03	9.31	127	67.2	8.10	25.2	241	2.63	0.862	8.58	0.355	0.260	2.80	43.8	1.66	-	109
ZMR029	18.0	46.4	-	-	7.79E+02	11.4	124	74.2	7.98	10.3	95.4	1.94	0.921	15.5	0.930	0.422	3.93	81.9	2.77	-	375
ZMR030	15.3	35.1	-	-	1.57E+02	8.31	88.7	86.8	6.67	7.27	78.7	1.82	0.894	13.5	0.896	0.483	3.51	69.8	2.91	-	430
ZMR031	12.5	31.5	-	-	6.78E+02	7.56	105	50.2	5.83	11.0	261	1.15	0.752	11.9	0.554	0.394	3.12	64.7	2.34	-	195
ZMR032	14.0	60.7	-	-	6.06E+02	14.8	128	67.0	10.3	19.1	193	2.05	1.03	11.7	0.472	0.336	3.05	68.7	2.17	-	146
ZMR033	11.9	51.9	-	-	1.63E+04	11.1	148	60.6	10.9	24.7	129	2.13	1.39	11.2	0.435	0.474	2.47	54.7	2.73	-	130
ZMR034	13.7	33.5	-	-	8.57E+03	7.97	123	55.7	6.33	79.6	229	1.53	0.822	12.9	0.665	0.398	3.15	74.9	2.50	-	185
ZMR035	14.2	42.4	-	-	1.21E+02	9.49	185	69.5	9.17	25.2	112	2.86	1.26	10.4	0.469	0.447	2.88	59.4	2.77	-	141
ZMR036	17.4	43.8	-	-	1.87E+02	10.5	140	59.6	7.85	6.61	207	1.52	0.965	15.6	0.833	0.448	3.66	105	2.74	-	175
ZMR037	14.5	51.7	6.62	0.1	5.28E+01	12.4	147	76.7	9.61	16.3	248	3.56	0.421	7.79	0.218	0.250	-	22.1	1.65	13.4	96
ZMR038	26.1	21.5	12.1	1.1	4.38E+01	5.44	478	71.3	5.15	35.4	126	8.30	0.460	7.83	0.275	0.597	-	25.9	3.51	90.7	209
ZMR039	15.3	46.2	9.80	1.3	8.88E+01	11.1	155	77.0	9.29	46.8	275	3.56	0.435	9.00	0.337	0.278	-	30.5	1.76	66.2	117
ZMR040	13.9	31.4	30.5	2.2	9.22E+03	8.04	91.8	58.6	6.28	31.9	328	1.43	0.424	12.5	0.556	0.427	-	46.7	2.40	54.6	337
ZMR041	10.0	23.4	14.8	0.6	3.85E+03	6.05	89.1	47.7	4.57	22.6	233	0.88	0.402	9.58	0.417	0.329	-	38.3	1.98	25.3	264
ZMR042	22.7	26.6	11.4	0.4	9.87E+01	6.67	375	57.9	5.44	32.3	141	6.90	0.444	8.59	0.272	0.438	-	25.1	2.60	39.2	196
ZMR043	25.5	21.5	9.40	0.2	4.68E+01	5.40	451	69.9	5.12	32.7	102	7.95	0.426	8.65	0.276	0.478	-	22.5	2.78	46.4	212
ZMR044	24.1	19.4	6.75	0.1	5.47E+01	5.16	455	71.5	4.57	34.8	57.9	7.73	0.452	8.57	0.312	0.498	-	23.3	2.97	75.3	227
ZMR045	14.7	33.1	25.6	0.5	2.86E+03	8.60	121	55.9	6.47	67.5	217	1.40	0.402	12.4	0.584	0.417	-	70.3	2.70	57.8	254
ZMR046	17.4	39.2	35.6	0.9	8.35E+03	9.84	149	54.6	7.19	22.5	314	1.92	0.434	14.4	0.655	0.460	-	71.1	2.95	49.6	257

	Nb	Nd	Ni	P_2O_5	Pb	Pr	Rb	SiO_2	Sm	Sn	Sr	Ta	Tb	Th	TiO_2	Tm	U	V	Yb	Zn	Zr
ZMR047	12.1	26.0	20.3	0.9	1.11E+04	6.60	111	37.0	5.07	13.5	224	1.28	0.414	9.78	0.471	0.329	-	48.2	2.16	62.1	160
ZMR048	18.7	43.0	31.9	0.6	2.19E+03	10.9	148	66.9	7.91	34.5	258	1.85	0.437	15.8	0.747	0.480	-	74.0	3.00	70.3	292
ZMR049	12.9	32.0	18.0	0.4	3.76E+03	8.05	101	61.7	5.80	10.2	346	1.33	0.414	12.4	0.548	0.375	-	46.2	2.59	45.6	318
ZMR050	21.6	45.3	40.7	0.4	6.39E+01	11.5	205	63.0	8.36	5.51	241	2.37	0.478	18.0	0.818	0.516	-	99.1	3.22	98.1	212
ZMR051	14.5	33.2	16.4	1.3	1.01E+03	8.45	129	56.6	6.43	7.55	235	1.50	0.418	13.4	0.567	0.455	-	42.4	2.85	58.5	338
ZMR052	15.3	35.4	21.9	3.6	9.69E+02	8.84	141	58.5	6.58	6.22	327	1.59	0.420	14.2	0.577	0.450	-	51.3	2.75	100	293
ZMR053	12.0	28.1	14.7	3.9	1.47E+03	7.21	105	44.4	5.50	4.26	243	1.21	0.421	11.6	0.448	0.386	-	34.2	2.42	77.1	281
ZMR054	13.2	29.1	24.5	1.7	2.92E+03	7.59	104	59.7	5.67	6.99	282	1.20	0.431	11.5	0.493	0.405	-	35.9	2.40	47.7	308
ZMR055	11.9	26.9	17.3	1.2	5.01E+03	7.09	94.0	51.0	5.32	16.2	279	1.14	0.412	11.0	0.445	0.395	-	35.7	2.37	32.8	319
ZMR056	13.3	31.1	21.1	1.3	1.36E+04	8.05	97.9	58.4	6.19	12.6	388	1.35	0.448	12.4	0.496	0.388	-	46.9	2.59	34.0	307
ZMR057	13.9	32.7	17.1	3.3	9.01E+02	8.31	115	53.8	6.40	5.02	278	1.51	0.417	12.8	0.537	0.419	-	41.5	2.67	65.7	310
ZMR058	14.9	35.5	19.6	2.4	1.07E+03	8.84	131	57.3	6.98	7.10	300	1.54	0.415	14.4	0.577	0.467	-	50.9	2.82	65.8	337
ZMR059	10.8	25.4	8.42	3.6	5.22E+03	6.22	90.0	49.3	4.90	5.62	326	1.06	0.404	9.55	0.432	0.311	-	38.4	2.02	35.9	252
ZMR060	12.0	27.6	11.1	2.0	3.48E+03	6.87	114	41.8	5.54	5.95	261	1.11	0.421	10.7	0.460	0.358	-	37.0	2.37	29.9	230
ZMR061	13.1	29.7	11.2	1.6	1.53E+03	7.65	113	54.1	6.16	6.33	273	1.30	0.450	11.8	0.562	0.401	-	44.0	2.61	56.7	295
ZMR062	12.2	32.9	0.431	0.1	5.12E+01	8.49	102	52.2	6.14	11.2	375	2.67	0.426	6.61	0.215	0.190	-	19.8	1.34	4.04	93.9
ZMR063	15.0	44.2	3.13	0.1	8.31E+01	11.2	119	70.1	8.47	14.4	1.02E+03	3.32	0.463	9.21	0.261	0.230	-	23.9	1.56	18.9	104
ZMR065	13.8	34.2	-	-	1.07E+03	8.22	124	60.5	6.35	72.6	232	1.38	0.850	12.9	0.612	0.411	3.28	65.1	2.59	-	217
BNV001	14.3	34.0	27.8	0.9	4.94E+04	8.78	103	63.6	6.31	551	422	1.34	0.410	12.7	0.565	0.432	-	81.8	2.67	34.4	310
BNV002	9.7	23.0	14.6	0.3	6.48E+03	5.97	82.6	39.3	4.32	8.14	370	0.76	0.400	8.47	0.390	0.307	-	47.9	1.88	13.1	200
BNV003	15.2	35.4	30.3	1.0	1.49E+04	9.28	122	61.8	6.68	7.35	454	1.44	0.456	13.6	0.568	0.444	-	83.0	2.74	33.9	293
BNV004	10.2	24.8	18.7	0.5	7.97E+03	6.43	89.8	47.6	5.02	11.5	321	0.77	0.413	9.43	0.382	0.335	-	57.5	2.03	23.4	154
BNV005	19.7	45.4	35.8	0.2	8.07E+01	11.3	164	68.9	8.10	3.01	120	1.89	0.429	18.9	0.835	0.553	-	107	3.37	49.2	320
BNV006	18.5	37.5	28.9	0.1	9.43E+01	9.49	159	53.0	6.90	3.09	109	1.68	0.418	16.2	0.744	0.451	-	102	2.77	55.5	237
BNV007	20.4	40.1	32.0	0.1	8.11E+01	10.1	182	64.7	7.36	3.27	132	1.92	0.409	18.9	0.828	0.491	-	122	2.84	54.7	246

	Nb	Nd	Ni	P_2O_5	Pb	Pr	Rb	SiO_2	Sm	Sn	Sr	Ta	Tb	Th	TiO_2	Tm	U	V	Yb	Zn	Zr
BNV008	18.0	34.2	26.8	0.1	5.62E+01	8.67	158	54.6	6.23	3.24	116	1.55	0.410	15.5	0.745	0.434	-	110	2.60	54.8	207
BNV009	20.8	41.7	30.7	0.2	2.80E+01	10.7	180	64.5	8.10	3.11	122	2.06	0.482	18.5	0.844	0.547	-	111	3.27	71.4	278
BNV010	19.3	40.4	32.9	0.1	4.14E+01	10.3	153	71.9	7.32	2.88	117	1.89	0.412	17.5	0.853	0.470	-	118	2.93	43.4	297
BNV011	20.4	40.9	33.7	0.1	4.63E+01	10.2	180	66.6	7.65	3.00	124	1.90	0.430	18.6	0.817	0.495	-	123	2.92	60.8	269
BNV012	20.9	41.2	43.7	0.1	7.97E+01	10.4	181	68.8	7.86	3.31	140	2.00	0.421	19.1	0.843	0.489	-	121	3.00	59.1	234
BNV013	21.4	43.6	42.9	0.1	3.97E+01	10.7	186	67.3	8.13	3.57	137	1.93	0.429	18.6	0.822	0.525	-	121	3.13	48.9	237
BNV014	22.1	40.7	39.4	0.1	4.59E+01	10.1	173	69.1	7.46	3.15	137	1.93	0.400	19.0	0.913	0.490	-	118	3.07	42.6	286
BNV015	21.4	43.1	45.7	0.1	5.01E+01	10.8	187	68.3	8.23	3.49	141	1.99	0.430	20.0	0.815	0.513	-	123	3.21	55.7	253
BNV016	21.5	44.5	44.8	0.1	8.53E+01	10.9	175	72.0	8.03	3.95	134	1.92	0.427	20.0	0.840	0.497	-	123	3.11	75.9	293
TOR001	19.4	49.5	32.4	0.1	4.35E+02	12.3	175	72.2	8.73	4.12	202	2.04	0.445	19.0	0.752	0.568	-	104	3.29	44.3	288
TOR002	14.0	34.9	21.7	0.0	1.80E+03	8.77	155	46.6	6.51	3.46	149	1.41	0.414	13.6	0.588	0.407	-	76.6	2.59	52.2	199
TOR003	19.5	49.3	35.7	0.1	8.68E+02	12.3	178	69.4	8.74	4.06	211	2.07	0.413	19.0	0.766	0.552	-	88.0	3.51	50.4	272
TOR004	13.9	32.5	20.2	0.0	1.09E+03	8.51	142	44.5	6.06	3.26	142	1.30	0.412	13.5	0.519	0.422	-	75.9	2.47	43.6	189
TOR005	18.8	48.5	28.5	0.1	7.05E+03	12.0	186	66.0	8.56	4.31	185	1.99	0.462	18.6	0.731	0.540	-	88.8	3.39	52.7	281
TOR006	16.2	38.9	26.3	0.1	1.94E+02	10.0	155	57.8	7.19	3.61	153	1.66	0.431	15.4	0.630	0.495	-	86.2	2.94	51.2	257
TOR007	19.0	47.0	35.2	0.1	5.92E+01	11.9	194	62.8	8.28	4.34	190	1.86	0.387	18.9	0.734	0.517	-	87.6	3.09	67.3	259
TOR008	20.4	50.0	42.1	0.2	6.19E+02	12.7	193	70.7	9.09	8.17	219	2.12	0.448	20.2	0.834	0.535	-	105	3.40	64.4	270
TOR009	15.7	40.8	15.1	0.1	4.18E+01	10.5	181	54.9	7.71	5.28	78.1	2.00	0.418	19.2	0.572	0.398	-	51.3	2.61	46.6	332
TOR010	19.8	48.6	43.7	0.2	4.29E+02	12.6	167	73.1	9.13	4.32	181	2.00	0.445	20.0	0.788	0.551	-	104	3.47	54.9	340
TOR011	19.9	48.6	43.5	0.1	2.34E+02	12.8	183	75.7	9.00	4.24	194	2.01	0.451	19.6	0.821	0.565	-	107	3.55	60.1	327
TOR012	19.1	48.8	33.5	0.2	3.05E+02	12.3	170	70.4	8.73	4.14	176	1.99	0.432	18.8	0.744	0.555	-	92.9	3.33	40.8	328
TOR013	13.0	31.5	25.4	0.0	1.69E+02	8.37	140	44.7	5.80	2.55	126	1.23	0.405	13.1	0.522	0.383	-	76.0	2.48	50.4	199
TOR014	19.3	49.2	38.0	0.2	1.10E+02	12.5	169	72.5	8.97	3.62	181	2.05	0.398	19.4	0.716	0.560	-	101	3.50	48.6	349
U (%)	4	18	27	16	44	2	21	39	19	149	21	4	-	11	1	25	63	-	27	33	623

The interpretation of the chemical results obtained by ICP-MS with a view to identifying the compositional groups has followed the statistical procedure explained in Chapter 4, section 4.5. In this statistical procedure, the analytical variance should be minimized in such a way that is originated by natural sources and not because of experimental errors and/or alterations arising from post-depositional processes. For this reason, several components have been omitted for the statistical analyses (see Chapter 4, section 4.4.2.). On the one hand, the potential contamination by the tungsten carbide cell used to mill the ceramics has been regarded: as Co is a known binder of tungsten alloys and usually occurs along with Ta traces (Boulanger et al., 2013), they have been removed from the statistical analyses. On the other hand, as Pb is the major component of the glaze composition and Sn is also for tin-lead glazed wares, they are not used in the statistical treatment in order to avoid contamination from the glaze components migrating into the paste (Molera et al., 2001). In addition, components with values below the quantification limit, need to be omitted too. These components are Cu, Ni, P_2O_5 and Zn for ceramics recovered in Olivares; Cu and U for ZMR062 and ZMR065; and U for the rest. Moreover, P_2O_5 and Cu are normally discarded in statistical routines due to they are present in underground and underwater environments (Buxeda i Garrigós, 1999; Buxeda i Garrigós and Kilikoglou, 2003; Freestone et al.,1985; Lemoine and Picon, 1982; Maritan and Mazzoli, 2004; Molera et al., 1993; Pradell et al., 1996). Besides, some notes about the uncertainty of the samples should be given. In fact, since the uncertainty of some components for Zamoran ceramics is high (53 % for Al_2O_3, 57 % for Lu, 53 % for MnO, 172 % for Na_2O, 63 % for U and 623 % for Zr), the possibility of removing them was considered. However, on the one hand, in this case some of the compounds that have a high uncertainty have relevance when studying the technology of ceramics (e.g. Al_2O_3 and Na_2O can provide information about the type of tempers and raw materials). On the other hand, when compounds are removed, the whole view of the variability of the sample is omitted. It is true that compounds related to post-depositional (e.g. Cu, P_2O_5), sample preparation (e.g. Co, Ta) and sample nature (e.g. Pb, Sn) alterations have been removed, and that this fact also omits the whole variability of the sample, but in this case, their contribution to the variability has a known source. On the contrary, the source of the variability of the compounds with high uncertainty is not known, but it is probably related to the material nature (see for example Figure 6.1., which shows that MnO and Zr contribute to the variability of the set of 64 ceramics). Therefore, taking into account all that has been explained, it has been decided to keep these compounds for the statistical treatment.

As described in Chapter 4, the 94 analysed ceramics correspond to production and consumption centres. In the next lines, the study of the 94 ceramics in order to define the reference groups and the PCRUs, will be done in three parts: first, 64 ceramics corresponding to Zamora city will be studied (section 6.1.1.). Then, 16 ceramics corresponding to Benavente (section 6.1.2.), and, finally, 14 ceramics corresponding to Toro (section 6.1.3.). Once the reference groups and the PCRUs are defined, they will be described in section 6.1.4.

6.1.1. Ceramics recovered in Zamora city

In this case, the heterogeneous set (referring to the typology) of 64 ceramics from Zamora city (ZMR001-ZMR036 and ZMR065 from Olivares; ZMR037-ZMR050 La Concepción; ZMR051-ZMR061 Ethnographic Museum and ZMR062-ZMR063 Mengue Avenue) (see Table 4.1. from Chapter 4) shows a high vt (8.46). This vt reveals the high contribution of specially Pb, CaO and Sn (Figure 6.1.a), and suggests that the dataset is polygenic, that is, the presence of several compositional groups is probable (Buxeda i Garrigós and Kilikoglou, 2003). On the one hand, the contribution of Pb and Sn was expected, since they are the major components

of the glaze composition for tin–lead glazed wares, and as commented, they can migrate from the glaze into the paste, contributing to the overall Pb and Sn concentration of the pastes. The 64 ceramics are of several typologies, such as tin-lead glazed, translucent-glazed and micaceous ceramics, and this is one of the reasons for the high variability of those elements. On the other hand, the reason for the high variability of CaO might be that some ceramics are calcareous (≥ 6 %), whereas others are low-calcareous or micaceous ceramics (see Table 6.1.) and this fact is probably related to the different provenance of the raw materials. Moreover, when Pb, Sn and components related to alterations (Co and Ta) are omitted from the statistical routine, the vt decreases to 4.4, still a high value, supporting the hypothesis of a polygenic set (Figure 6.1.b).

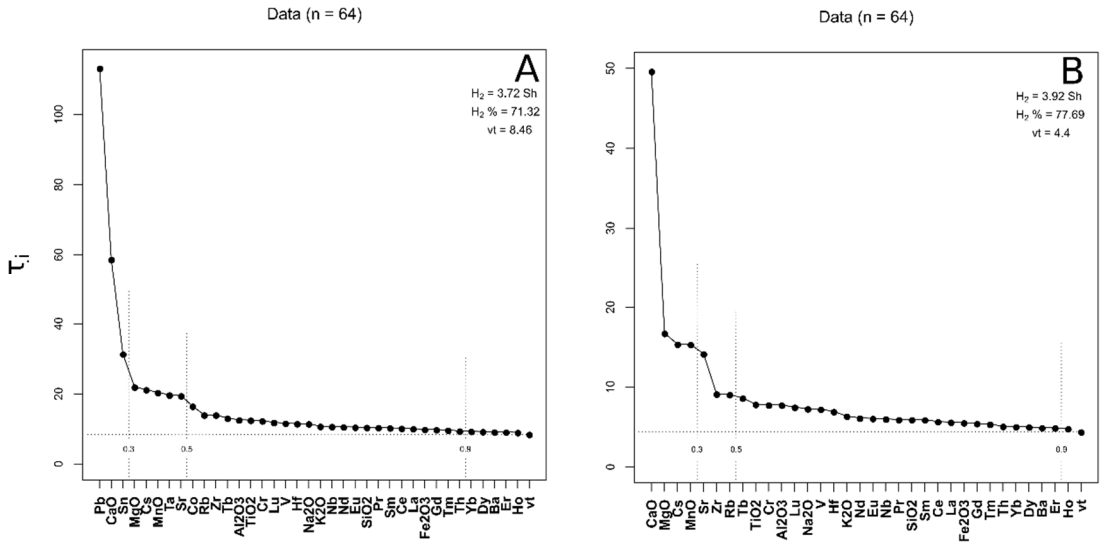

Figure 6.1. Graphical representations of the evenness of the compositional variability of 64 analysed ceramics, recovered in Zamora, by ICP-MS: **(a)** Ni, Cu, P_2O_5, U and Zn were omitted because their values are below the quantification limit; **(b)** Co, Pb, Sn and Ta were omitted due to their potential effect for alterations, in addition to Cu, Ni, P_2O_5, U and Zn. (y-axis (τ.i) = the individual contribution of the variability from each element to the whole dataset, from the highest to the lowest; vt = Total variability; H_2 = information entropy; H_2% = percentage of information entropy over the maximum possible; n = number of specimens)

Additionally, since Olivares was a production centre, first, the 37 ceramics recovered in Olivares have been evaluated performing a Hierarchical Cluster Analysis (HCA), in order to identify the potential reference groups (RG) for this production centre (Figure 6.2.). The dendrogram of Figure 6.2. demonstrates that there are ceramics corresponding to 3 meaningful ceramic groups (PCRUs), called Z-1, Z-2 and Z-3 (Table 6.2.). The identification of these PCRUs is an important progress in the study of the ceramic production from Zamora region because these groups can be considered as reference groups, since failure ceramics and kiln furniture have been rescued and analysed among the set. However, kiln furniture belongs to Z-3 calcareous group (see Table 6.3.), whereas the failure glazed ceramics belong to Z-1 (redware) and Z-2 (micaceous) groups. According to the literature, lead glazing of micaceous cooking pots produced in Pereruela and Muelas del Pan (villages from Zamora province) were not carried out in their own workshops but elsewhere (Escribano, 2014). Thus, Olivares might be an important workshop in relation to such activity, where glazing of exogenous productions occurred as suggested in the literature (Villanueva, 2011). Therefore,

the possibility of Z-2 being a production group for glazing the exogenous micaceous ceramics only should be taken into account, whereas Z-1 and Z-3 are reference production groups: the first one for reddish low-calcareous unglazed ceramics and for translucent-glazed ceramics, and the second one for calcareous unglazed pastes and tin-lead glazed ceramics.

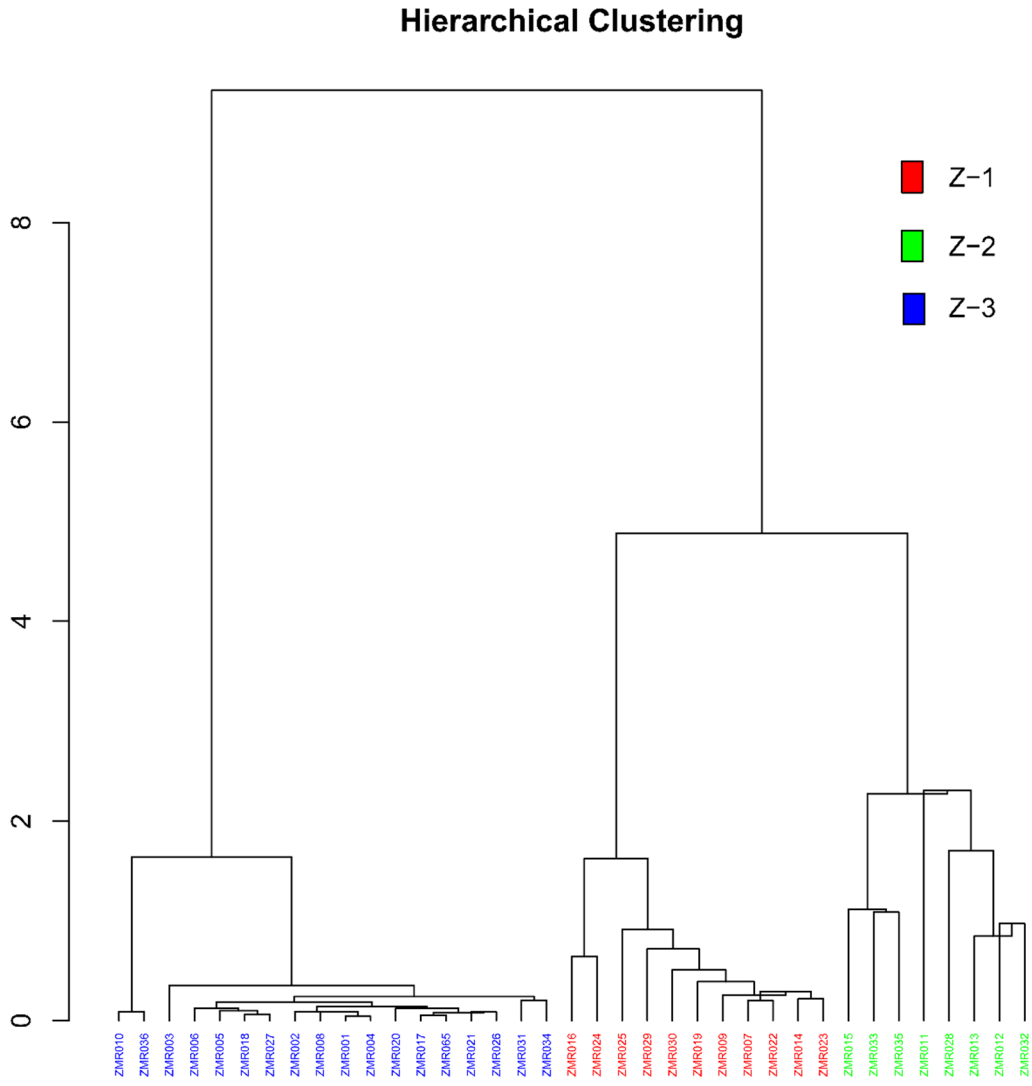

Figure 6.2. Dendrogram of Euclidean squared distances using centroid algorithm of 37 individuals from Olivares (Zamora) on the sub-composition of all the measured components (42) (with the exception of Co, Cu, Ni, P_2O_5, Pb, Ta, Sn and Zn) divided by the geometric mean. Z-1, Z-2 and Z-3= reference groups of Olivares productions

Table 6.2. Samples, the archaeological site and the context where ceramics were rescued, in addition to their typology, colour decoration of the glazes, form, chronology, the reference group or PCRU they belong to and their paste colour. The table is ordered by groups. ZMR = ceramics recovered in Zamora city; BNV = ceramics recovered in Benavente; TOR = ceramics recovered in Toro; unk = ceramics with unkown PCRU nor reference group. "Buff-coloured" refers to a beige-cream-pink colour and "reddish" to a paler red tone

Samples	Archaeological site	Context	Typology	Colour decoration	Form	Chronology	Group	Paste colour
ZMR007	Olivares	kiln 01	unglazed	-	bowl	late 19th-early 20th	z-1	red
ZMR009	Olivares	kiln 01	unglazed	-	large jar	late 19th-early 20th	z-1	red
ZMR014	Olivares	kiln 01	translucent-glazed	beige (raw glaze)	jar	late 19th-early 20th	z-1	red
ZMR016	Olivares	kiln 01	translucent-glazed	beige (raw glaze)	jar	late 19th-early 20th	z-1	red
ZMR019	Olivares	kiln 01	translucent-glazed	beige (raw glaze)	plate	late 19th-early 20th	z-1	red
ZMR022	Olivares	kiln 02	translucent-glazed	brown	cooking pot	late 19th-early 20th	z-1	red
ZMR023	Olivares	kiln 02	translucent-glazed	brown	cooking pot	late 19th-early 20th	z-1	red
ZMR024	Olivares	kiln 02	translucent-glazed	green	cooking pot	late 19th-early 20th	z-1	red
ZMR025	Olivares	kiln 02	translucent-glazed	brown	cooking pot	late 19th-early 20th	z-1	red
ZMR029	Olivares	kiln 03	translucent-glazed	beige (raw glaze)	small jar	late 19th-early 20th	z-1	red
ZMR030	Olivares	kiln 03	translucent-glazed	black (burnt)	handle	late 19th-early 20th	z-1	black
ZMR011	Olivares	kiln 01	micaceous unglazed	-	large jar	late 19th-early 20th	z-2	red
ZMR012	Olivares	kiln 01	micaceous translucent-glazed	beige (raw glaze)	large jar	late 19th-early 20th	z-2	red
ZMR013	Olivares	kiln 01	micaceous unglazed	-	large jar	late 19th-early 20th	z-2	red and grey
ZMR015	Olivares	kiln 01	micaceous translucent-glazed	beige (raw glaze)	jar	late 19th-early 20th	z-2	red
ZMR028	Olivares	kiln 02	micaceous translucent-glazed	brown	lid	late 19th-early 20th	z-2	red
ZMR032	Olivares	kiln 03	micaceous translucent-glazed	brown	large jar	late 19th-early 20th	z-2	red
ZMR033	Olivares	kiln 03	micaceous translucent-glazed	white (burnt)	n/d	late 19th-early 20th	z-2	black
ZMR035	Olivares	kiln 03	micaceous translucent-glazed	blackish (burnt)	handle	late 19th-early 20th	z-2	red
ZMR001	Olivares	kiln 01	unglazed	-	bowl	late 19th-early 20th	z-3	beige

ZMR002	Olivares	kiln 01	tin-lead glazed	white and blue	plate	late 19th-early 20th	z-3	buff-coloured
ZMR003	Olivares	kiln 01	tin-lead glazed	white and green	plate	late 19th-early 20th	z-3	buff-coloured
ZMR004	Olivares	kiln 01	unglazed	-	plate	late 19th-early 20th	z-3	buff-coloured
ZMR005	Olivares	kiln 01	tin-lead glazed	white and blue	plate	late 19th-early 20th	z-3	buff-coloured
ZMR006	Olivares	kiln 01	tin-lead glazed	white and green	plate	late 19th-early 20th	z-3	buff-coloured
ZMR008	Olivares	kiln 01	tin-lead glazed	white	porringer	late 19th-early 20th	z-3	buff-coloured
ZMR010	Olivares	kiln 01	unglazed	-	cup	late 19th-early 20th	z-3	reddish and grey
ZMR017	Olivares	kiln 01	unglazed	-	trivet (kiln tool)	late 19th-early 20th	z-3	buff-coloured
ZMR018	Olivares	kiln 01	unglazed	-	trivet (kiln tool)	late 19th-early 20th	z-3	buff-coloured
ZMR020	Olivares	kiln 01	tin-lead glazed	white and green	plate	late 19th-early 20th	z-3	buff-coloured
ZMR021	Olivares	kiln 01	tin-lead glazed	white and blue	plate	late 19th-early 20th	z-3	buff-coloured
ZMR026	Olivares	kiln 02	unglazed	-	trivet (kiln tool)	late 19th-early 20th	z-3	buff-coloured
ZMR027	Olivares	kiln 02	unglazed	-	bowl	late 19th-early 20th	z-3	buff-coloured
ZMR031	Olivares	kiln 03	unglazed	-	bowl	late 19th-early 20th	z-3	beige
ZMR034	Olivares	kiln 03	unglazed	-	trivet (kiln tool)	late 19th-early 20th	z-3	beige
ZMR036	Olivares	kiln 01	unglazed	-	cup	late 19th-early 20th	z-3	reddish and grey
ZMR040	La Concepción	goldsmithing workshop	tin-lead glazed	white	bowl	15th-16th	z-3	buff-coloured
ZMR041	La Concepción	goldsmithing workshop	tin-lead glazed	white	bowl	15th-16th	z-3	buff-coloured
ZMR045	La Concepción	goldsmithing workshop	tin-lead glazed	green and black on white	bowl	15th-16th	z-3	reddish
ZMR046	La Concepción	goldsmithing workshop	tin-lead glazed	white and blue	bowl	15th-16th	z-3	buff-coloured
ZMR047	La Concepción	goldsmithing workshop	tin-lead glazed	white and blue	bowl	15th-16th	z-3	buff-coloured
ZMR048	La Concepción	goldsmithing workshop	tin-lead glazed	green and brown on white	plate	15th-16th	z-3	reddish
ZMR049	La Concepción	goldsmithing workshop	tin-lead glazed	white	bowl	15th-16th	z-3	buff-coloured

ZMR051	Ethnographic Museum	n/d	tin-lead glazed	white, green and black	bowl	17th-18th	z-3	buff-coloured
ZMR052	Ethnographic Museum	n/d	tin-lead glazed	white, green and black	bowl	16th	z-3	buff-coloured
ZMR053	Ethnographic Museum	n/d	tin-lead glazed	white and green	bowl	17th-18th	z-3	buff-coloured
ZMR054	Ethnographic Museum	n/d	tin-lead glazed	white and blue	porringer	17th-18th	z-3	buff-coloured
ZMR055	Ethnographic Museum	n/d	tin-lead glazed	white and blue	plate	17th-18th	z-3	buff-coloured
ZMR056	Ethnographic Museum	n/d	tin-lead glazed	white	plate	17th-18th	z-3	buff-coloured
ZMR057	Ethnographic Museum	n/d	tin-lead glazed	white	bowl	17th-18th	z-3	buff-coloured
ZMR058	Ethnographic Museum	n/d	tin-lead glazed	white	plate	17th-18th	z-3	buff-coloured
ZMR059	Ethnographic Museum	n/d	tin-lead glazed	white	plate	17th-18th	z-3	buff-coloured
ZMR065	Olivares	kiln 03	tin-lead glazed	black and white (burnt)	n/d	n/d	z-3	beige
ZMR060	Ethnographic Museum	n/d	tin-lead glazed	white	bowl	17th-18th	z-3	beige
ZMR061	Ethnographic Museum	n/d	tin-lead glazed	white	bowl	17th-18th	z-3	buff-coloured
BNV001	Casa del Tinte	hospital	tin-lead glazed	white and blue	bowl	17th-18th	z-3	reddish
BNV002	Casa del Tinte	hospital	tin-lead glazed	white	plate	17th	z-3	beige
BNV003	Casa del Tinte	hospital	tin-lead glazed	white	bowl	17th-18th	z-3	reddish
BNV004	Casa del Tinte	hospital	tin-lead glazed	white and green	chamber pot	17th-18th	z-3	buff-coloured
ZMR038	La Concepción	goldsmithing workshop	micaceous unglazed	-	bowl	15th-16th	z-4	beige
ZMR042	La Concepción	goldsmithing workshop	micaceous unglazed	-	pitcher	15th-16th	z-4	grey and beige
ZMR043	La Concepción	goldsmithing workshop	micaceous unglazed	-	cooking pot	15th-16th	z-4	grey and beige
ZMR044	La Concepción	goldsmithing workshop	micaceous unglazed	-	pitcher	15th-16th	z-4	grey and beige
BNV005	Casa del Tinte	dump (previous to the hospital)	unglazed	-	pitcher	16th-18th	b-1	red
BNV006	Casa del Tinte	dump (previous to the hospital)	unglazed	-	pitcher	16th-18th	b-1	reddish
BNV007	Casa del Tinte	dump (previous to the hospital)	unglazed	-	pitcher	16th-18th	b-1	red
BNV008	Casa del Tinte	dump (previous to the hospital)	unglazed	-	small jar	16th-18th	b-1	red

BNV009	Casa del Tinte	dump (previous to the hospital)	unglazed	-	small jar	16th-18th	b-1	red
BNV010	Casa del Tinte	dump (previous to the hospital)	unglazed	-	small jar	16th-18th	b-1	red
BNV011	Casa del Tinte	dump (previous to the hospital)	unglazed	-	small jar	16th-18th	b-1	red
BNV012	Casa del Tinte	dump (previous to the hospital)	unglazed	-	small jar	16th-18th	b-1	red
BNV013	Casa del Tinte	dump (previous to the hospital)	unglazed	-	jug	16th-18th	b-1	red
BNV014	Casa del Tinte	dump (previous to the hospital)	unglazed	-	jug	16th-18th	b-1	red
BNV015	Casa del Tinte	dump (previous to the hospital)	unglazed	-	jug	16th-18th	b-1	red
BNV016	Casa del Tinte	dump (previous to the hospital)	unglazed	-	jug	16th-18th	b-1	red
TOR001	Cuesta del Negrillo No.11	dump	translucent-glazed	brown	mug	17th	t-1	red
TOR002	Cuesta del Negrillo No.11	dump	translucent-glazed	brown	small jar	17th	t-1	red
TOR003	Cuesta del Negrillo No.11	dump	unglazed	-	jar	17th	t-1	red
TOR004	Cuesta del Negrillo No.11	dump	unglazed	-	chamber pot	17th	t-1	red
TOR005	Cuesta del Negrillo No.11	dump	translucent-glazed	brown	small jar	17th	t-1	red
TOR006	Patio del Siete	dump	unglazed	-	small jar	17th	t-1	red
TOR007	Patio del Siete	dump	unglazed	-	jar	17th	t-1	red
TOR008	Patio del Siete	dump	unglazed	-	large jar	17th	t-1	red
TOR010	Cuesta del Matadero	kiln dump	translucent-glazed	brown	pitcher	17th	t-1	red
TOR011	Cuesta del Matadero	kiln dump	translucent-glazed	brown	lid	17th	t-1	red
TOR012	Cuesta del Matadero	kiln dump	translucent-glazed	brown	cup	17th	t-1	red
TOR014	Cuesta del Matadero	kiln dump	unglazed	-	pipe	17th	t-1	red
ZMR037	La Concepción	goldsmithing workshop	micaceous unglazed	-	cooking pot	15th-16th	unk	beige
ZMR039	La Concepción	goldsmithing workshop	micaceous unglazed	-	large jar	15th-16th	unk	beige

ZMR050	La Concepción	goldsmithing workshop	unglazed - Duque de la Victoria type	-	n/d	15th-16th	unk	red
ZMR062	Mengue Avenue	tannery	micaceous unglazed	-	large jar	n/d	unk	white
ZMR063	Mengue Avenue	tannery	micaceous unglazed	-	large jar	n/d	unk	white
TOR009	Cuesta del Matadero	kiln dump	unglazed	-	pitcher	17th	unk	black
TOR013	Cuesta del Matadero	kiln dump	unglazed	-	pipe	17th	unk	red

After that, a Hierarchical Cluster Analysis (HCA) was performed to evaluate the aggrupations of 64 Zamoran ceramics, having as a reference the Z-1, Z-2 and Z-3 reference groups (Figure 6.3.). Examination of the resulting dendrogram shows a clear 4-group structure that corresponds to the different productions identified in La Concepción, the Ethnographic Museum and the Olivares productions already established. Most of the groups show clear and defined cuts from the rest. Moreover, most of the samples belonging to a given cluster also exhibit a certain degree of homogeneity within their chemical composition, as can be observed by their fusion links, pointing to a similar composition. Interestingly, all of the tin-lead glazed ceramics unearthed at La Concepción and the Ethnographic Museum show a chemical fingerprint compatible with the already identified Z-3 group from Olivares workshops. The fact that ceramics from the Ethnographic Museum correspond to Z-3 group is in accordance with the article published by Martín et al. (1997), in which the authors suggest that the type of ceramic collected in that archaeological site corresponds to the same type of ceramics produced in Olivares at these periods. Furthermore, another set of ceramics has been identified into a new PCRU called Z-4 (ZMR038, ZMR042, ZMR043 and ZMR044), all from La Concepción, unglazed micaceous ceramics and, basically, cooking pots and serving vessels. Upon further examination, Figure 6.3. also reveals the existence of five ceramics (ZMR037, ZMR039 and ZMR050 recovered in La Concepción and ZMR062 and ZMR063 recovered in Mengue Avenue) that do not match any of the paste reference groups identified in the workshop of Olivares, nor La Concepción. On the one hand, ZMR037 and ZMR039 are of micaceous paste but, surprisingly at first sight, do not cluster together with Z-2 nor Z-4 groups, which are also micaceous. This fact is evidenced by the the lower content on CaO and, at the same time, higher amounts of Sr of the outlier ceramics (Table 6.1.). On the other hand, ZMR062 and ZMR063 micaceous large jars neither cluster together with any group. This fact might be related to their high amount on Sr and Al_2O_3. Likely, all these micaceous ceramics belong to ceramic productions from the renowned vicinity potting villages in the region, like Moveros, Pereruela or Muelas del Pan. In these lines, it is important to give some information that the craftman Víctor Redondo, from Pereruela, provided (2019, pers. comm.). He commented that the potters in Pereruela mixed two different raw materials (50:50 %) for kitchen micaceous ceramics. These materials were red clays from Pereruela and kaolins from Pereruela or surroundings (in his case, he nowadays uses kaolin from Tamame, a village located 12 km south from Pereruela). This information is in accordance with the ethnoarchaeometrical study on ceramics from Pereruela carried out by Buxeda et al. (2003). In this work, the authors concluded that the micaceous ceramics produced in Pereruela by different potters, even by the same technology and using local clays, showed a high variability. Moreover, a high chemical variability was also identified in different samples of the same pot. The authors related this variability principally to the mixture of different raw materials and the presence

of monazite inclusions in red clays, a phosphate mineral containing Rare Earth Elements (REEs). Therefore, the authors stated that these facts can lead to classify productions from Pereruela (or similar productions), or even one ceramic, with a different provenance, even though this is not the case. In detailed, authors identified that the contribution of variability for some ceramics was given by mostly Th and Y. Furthermore, they analized different samples from the same pot, documenting a high variability contributed by REEs such as Sm, Lu, Yb, La, Ce, Th, Eu and Y. Taking all of this into account, and as monazite is present in small amounts in granitic igneous rocks from Pereruela and surroundings related to the red clays (Buxeda et al., 2003), it is important to make a comparison between Z-2, Z-4 and ZMR037, ZMR039, ZMR062 and ZMR063 micaceous ceramics, removing the mentioned REEs, to confirm the groupings. It is important to note that this would make sense if these micaceous ceramics were produced mixing red clays with kaolin, like in the case of Pereruela. Thus, Figure 6.3.a shows a high vt (4.5) when REEs are taken into account, and it still shows a high vt when REEs are removed (3.75) (Figure 6.3.b), because in this case, the REEs do not make an important contribution to the variability. These numbers suggest that the nature of these ceramics is polygenic.

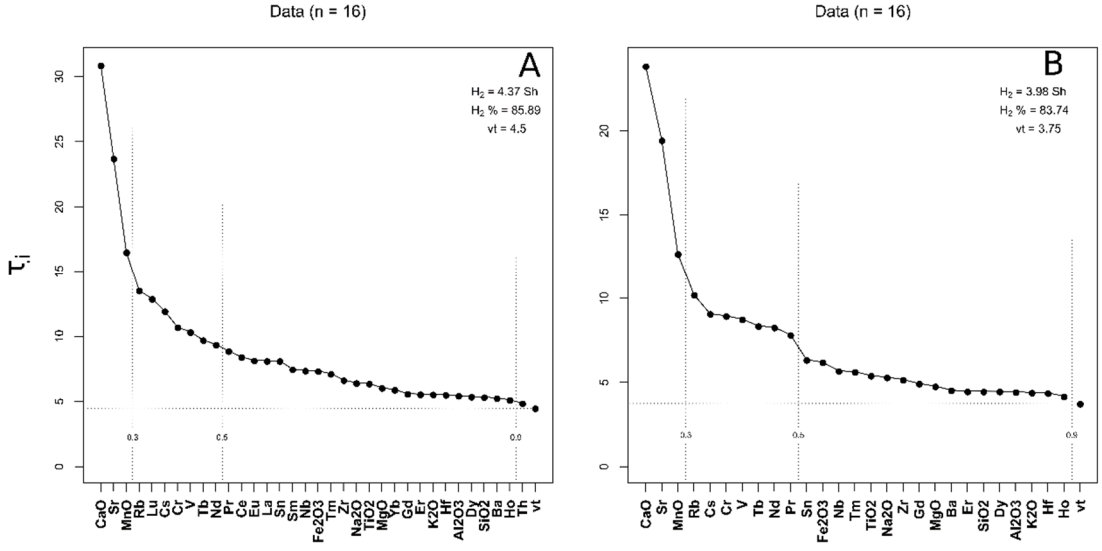

Figure 6.3. Graphical representations of the evenness of the compositional variability of 16 analysed micaceous ceramics from Z-2, Z-4 and unkown groups: **(a)** Co, Cu, Ni, P_2O_5, Pb, Ta, and U were omitted because their values are below the quantification limit; **(b)** Co, Cu, Ni, P_2O_5, Pb, Ta and U were omitted due to their potential effect for alterations, in addition to Sm, Lu, Yb, La, Ce, Th and Eu (y-axis (τ.i) = the individual contribution of the variability from each element to the whole dataset, from the highest to the lowest; vt = Total variability; H_2 = information entropy; H_2% = percentage of information entropy over the maximum possible; n = number of specimens)

In addition, Figure 6.4.a shows that ZMR037 and ZMR039 are more similar to Z-2 ceramics when REEs are taken into account, and that they might be considered from the same group when REEs are removed (Figure 6.4.b). But still this group and individual ceramics seem to have a different provenance. Buxeda et al. (2003) demonstrated that, the ceramics from Pereruela are prone to be treated as ceramic with different provenance due to their high variability. Therefore, the case of Z-2, Z-4, ZMR037, ZMR039, ZMR062 and ZMR063 can be the same case, but since I do not have more information about the production of these ceramics (e.g. if they were produced mixing red clays and kaolin) and the

high variability is not specially related to REEs in this case, I will treat them like ceramics with different and unknown provenance, with some exceptions: one is Z-2, for which I have explained that a) they could have been produced in Olivares or b) in Pereruela or Muelas del Pan and be exported to Olivares for their glazing. Moreover, ZMR062 and ZMR063 probably have the same but unknown provenance, but they will be not be treated as a PCRU because it is not very clear yet, and I do not have more ceramics for comparison. Finally, ZMR037 and ZMR039 might have a different provenance, because their fusion link is high (see Figure 6.5.).

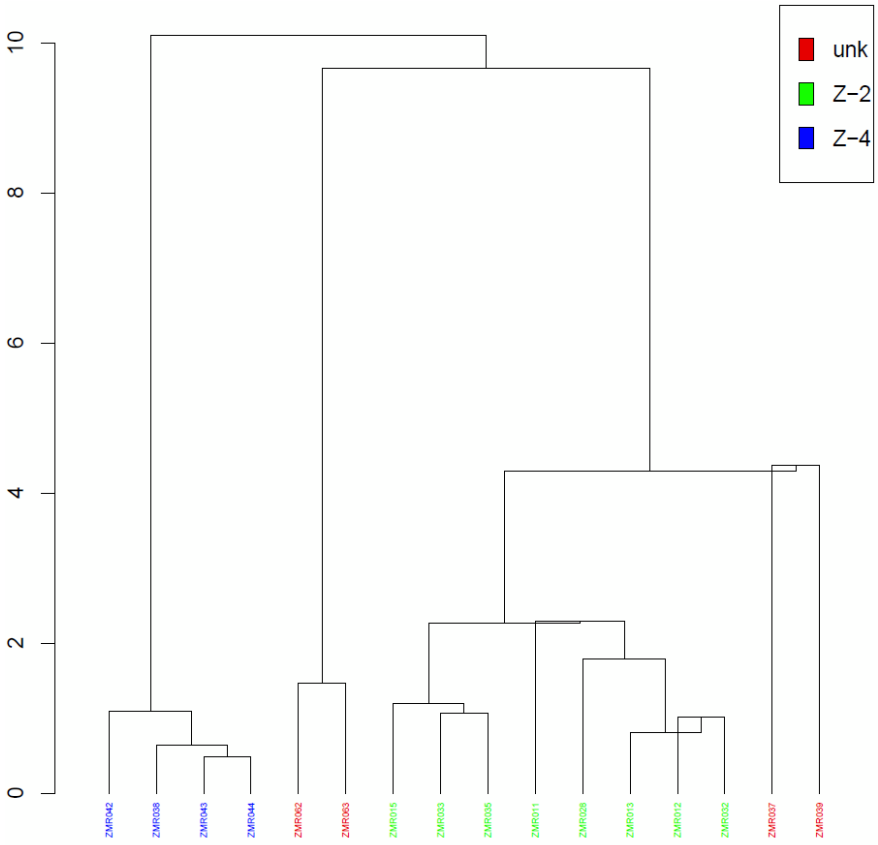

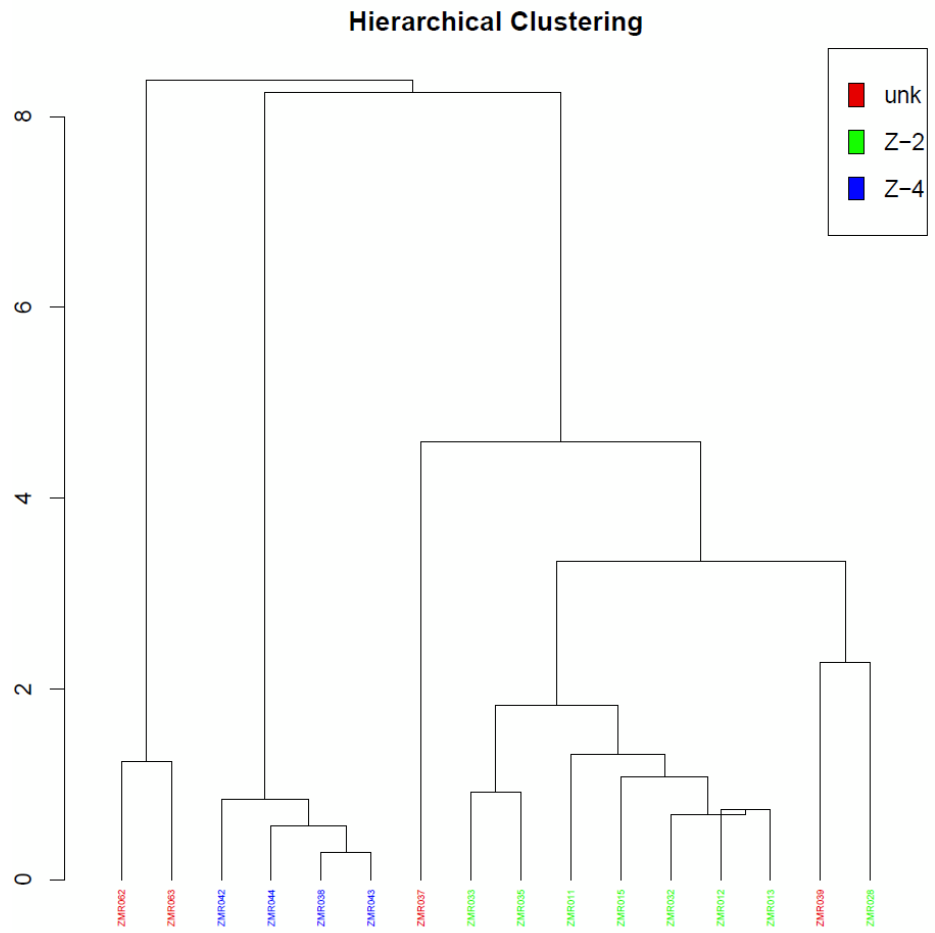

Figure 6.4. Dendrograms of Euclidean squared distances using centroid algorithm of 16 micaceous individuals from Z-2, Z-4 and unggrouped ceramics; **(a, up)** dendrogram on the sub-composition of all the measured components (42) (with the exception of Co, Cu, Ni, P_2O_5, Pb, Ta, and U) divided by the geometric mean; **(b, below)** dendrogram on the sub-composition of all the measured components (42) (with the exception of Co, Cu, Ni, P_2O_5, Pb, Ta, U, Sm, Lu, Yb, La, Ce, Th and Eu) divided by the geometric mean

Finally, although in Figure 6.5. it seems that ZMR050 is part of Z-3, caution should be kept with this ceramic. Its fusion link with Z-3 is relatively high in comparison with the rest of ceramics from Z-3. Furthermore, Figure 6.6. demonstrates that ZMR050 does not belong to Z-3. Probably, this ceramic belongs to a production from Valladolid, because, as commented in Chapter 2, this name corresponds to the homonymous street in Valladolid where some pottery workshops dated back to the late Medieval period were found (Fernández et al., 1991; Villanueva et al., 2000). All the information about the groupings is summarized in Table 6.2.

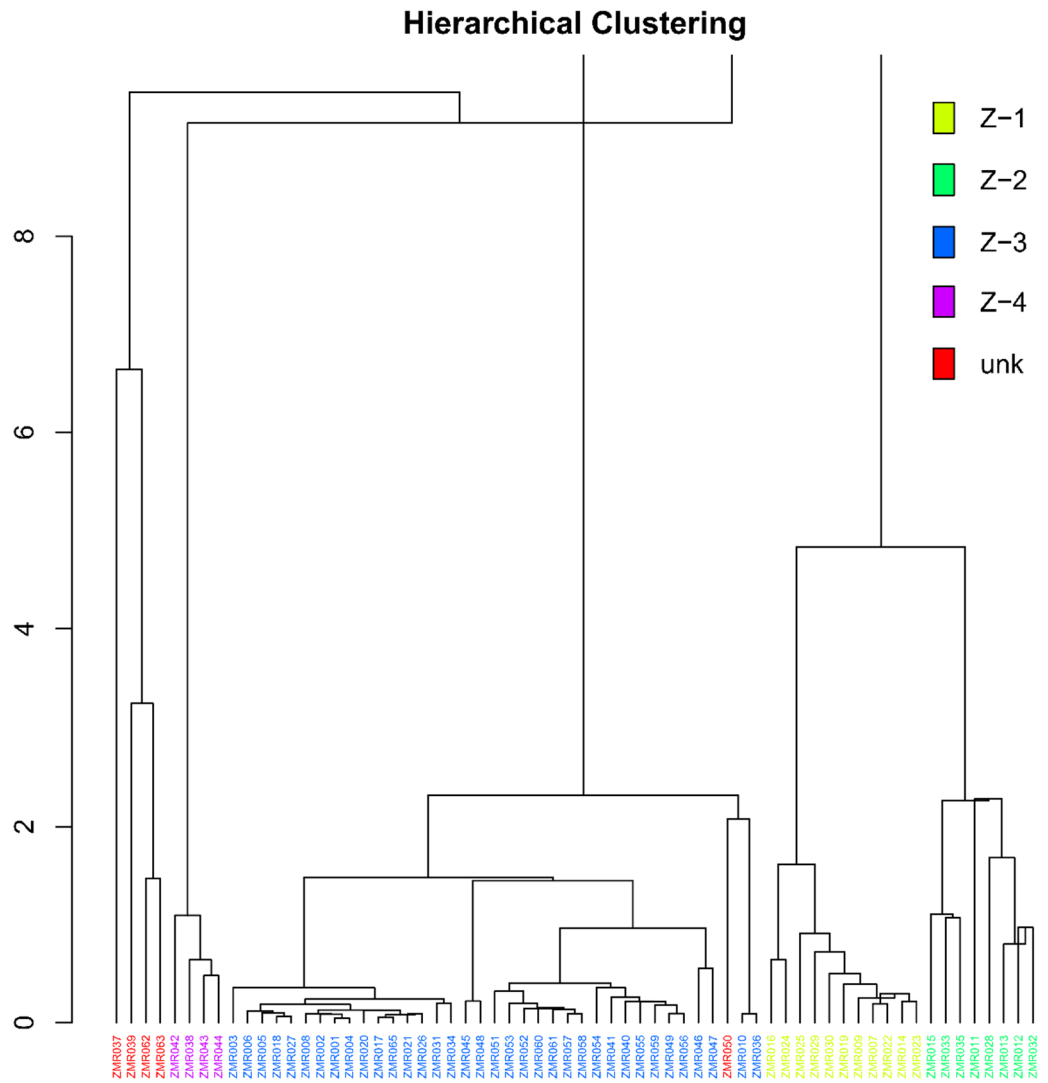

Figure 6.5. Dendrogram of Euclidean squared distances using centroid algorithm of 64 individuals from different sites of Zamora (Olivares, Ethnographic Museum, La Concepción and Mengue Avenue) indicated by the PCRUs and reference groups they correspond to, on the sub-composition of all the measured components (42) (with the exception of Co, Cu, Ni, P_2O_5, Pb, Sn, Ta, U and Zn) divided by the geometric mean. Z-1, Z-2 and Z-3= reference groups of Olivares productions; Z-4= PCRU of regional origin; unk= ceramics with unknown provenance

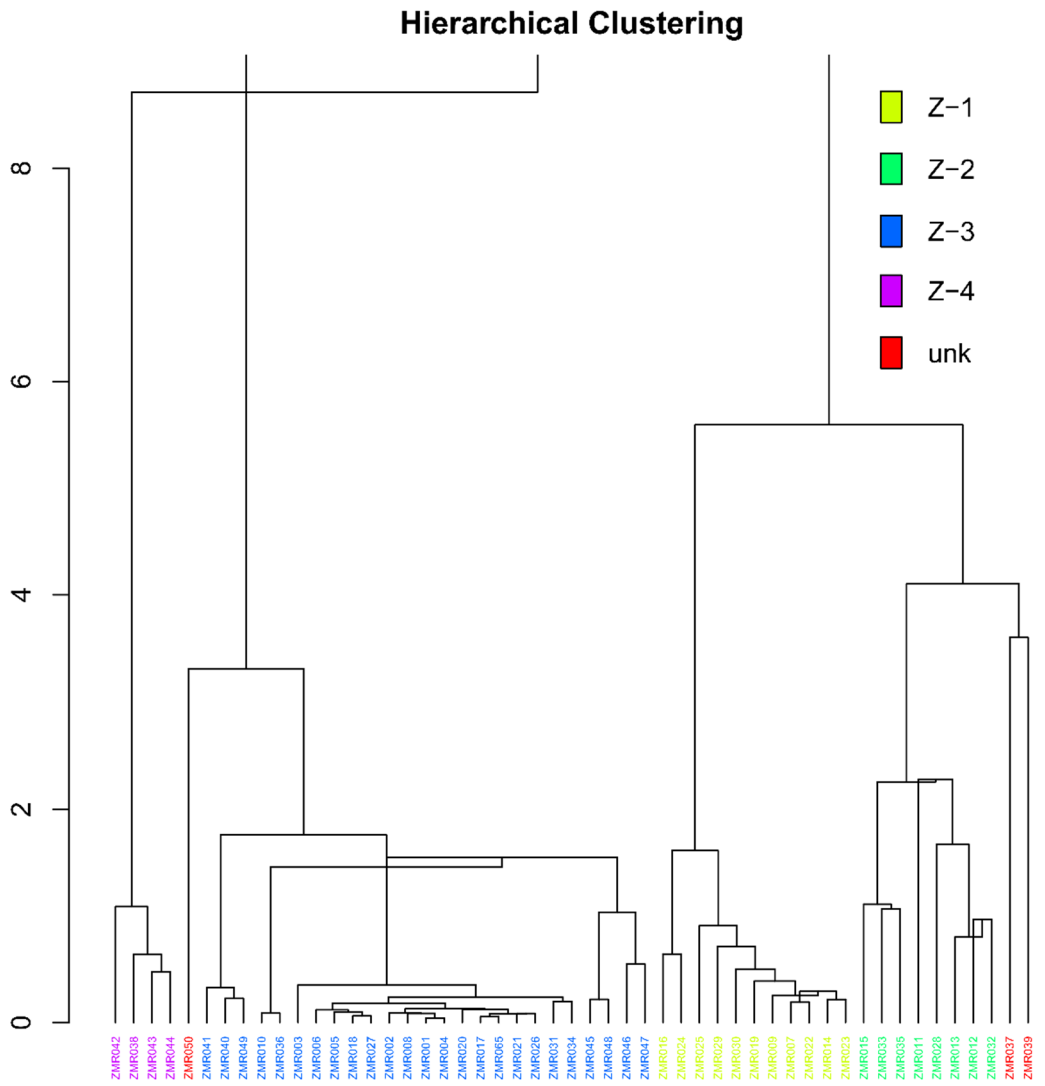

Figure 6.6. Dendrogram of Euclidean squared distances using centroid algorithm of 51 individuals from different sites of Zamora (Olivares and La Concepción) indicated by the PCRUs and reference groups they correspond to, on the sub-composition of all the measured components (42) (with the exception of Co, Cu, Ni, P_2O_5, Pb, Sn, Ta, U and Zn) divided by the geometric mean. Z-1, Z-2 and Z-3= reference groups of Olivares productions; Z-4= PCRU of regional origin; unk= ceramics with unknown provenance. Z-1, Z-2 and Z-3= reference groups of Olivares productions; Z-4= PCRU of regional origin; unk= ceramics with unknown provenance

6.1.2. Ceramics recovered in Benavente

As commented in Chapter 2, Benavente village was a production centre active from the Middle Ages to the Modern Era, in which non-micaceous red pottery was mainly produced (De La Mata, 1989).

In this case, the heterogeneous set (referring to the typology) of 16 ceramics from Benavente (Casa del Tinte) (BNV001-BNV016) shows a high vt (12.31), which reveals the high contribution of specially Pb, CaO and Sn (Figure 6.7.a). Since some ceramics are tin-lead glazed high-calcareous ceramics, and the rest are low-calcareous without any glaze, the high variability of Pb, CaO, Sn and Cu was something expected. Moreover, the vt of this set of

ceramics drops down to 2.15 when omitting Co, Cu, P_2O_5, Pb, Sn and Ta components, which still suggests a possible polygenic nature of the set (Figure 6.7.a).

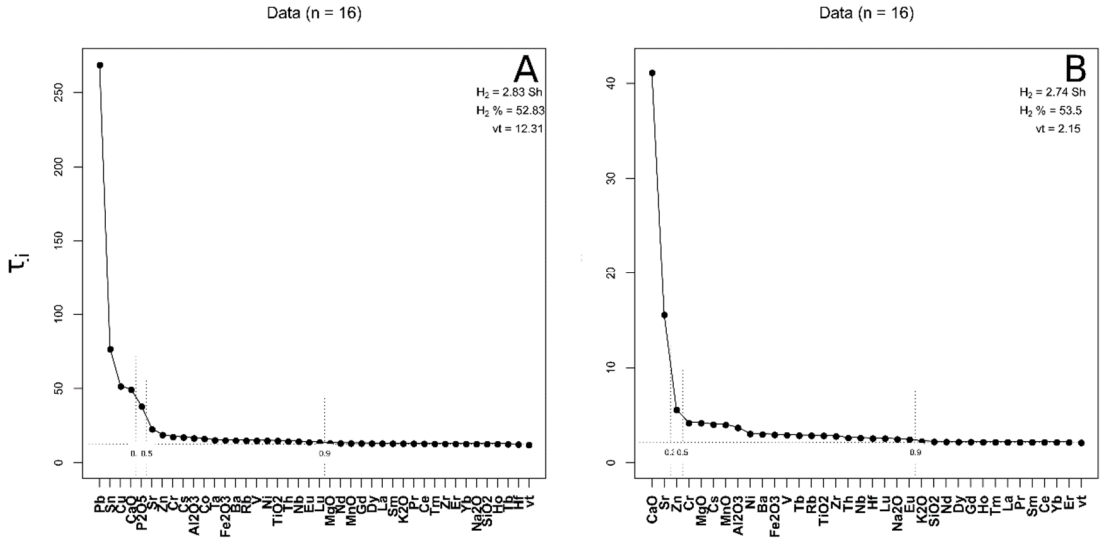

Figure 6.7. Graphical representation of the evenness of the compositional variability of 16 analysed ceramics, recovered in Benavente, by ICP-MS; **(a)** U was omitted because its values are below to the quantification limit; **(b)** Co, Cu, P_2O_5, Pb, Sn and Ta were omitted due to their potential effect for alterations, in addition to U. (y-axis (τ.i) = the individual contribution of the variability from each element to the whole dataset, from the highest to the lowest; vt = Total variability; H_2 = information entropy; H_2% = percentage of information entropy over the maximum possible; n = number of specimens)

In addition, the dendrogram of Figure 6.8. shows that the set of 16 ceramics collected in Benavente forms two PCRUs. Moreover, the dendrogram of Figure 6.9. demonstrates that four calcareous tin-lead glazed ceramics (BNV001-BNV004) correspond to Z-3 Olivares production group, whereas the rest form a new reference group of the Benavente redware production, called B-1.

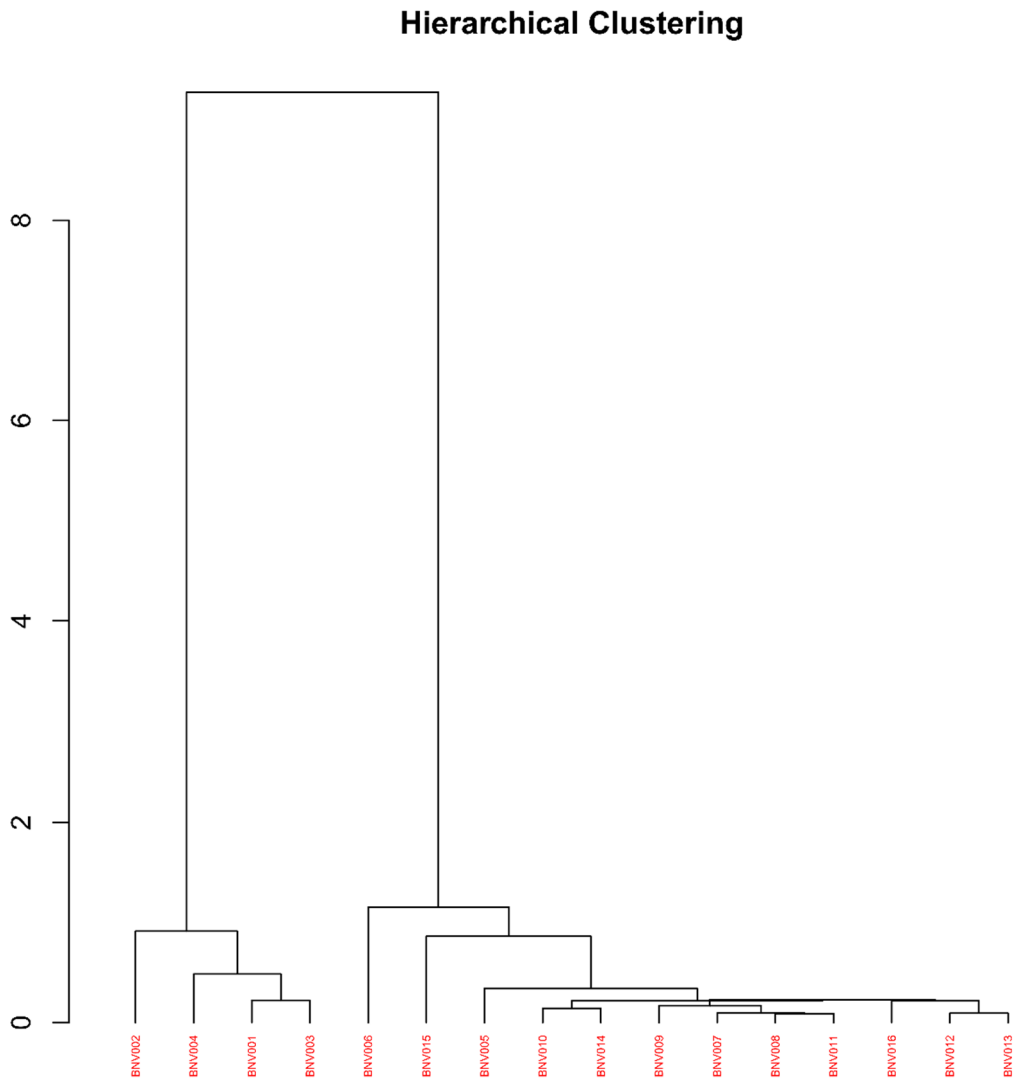

Figure 6.8. Dendrogram of Euclidean squared distances using centroid algorithm of 16 individuals from Benavente on the sub-composition of all the measured components (42) (with the exception of Co, Cu, P_2O_5, Pb, Ta, Sn and U) divided by the geometric mean

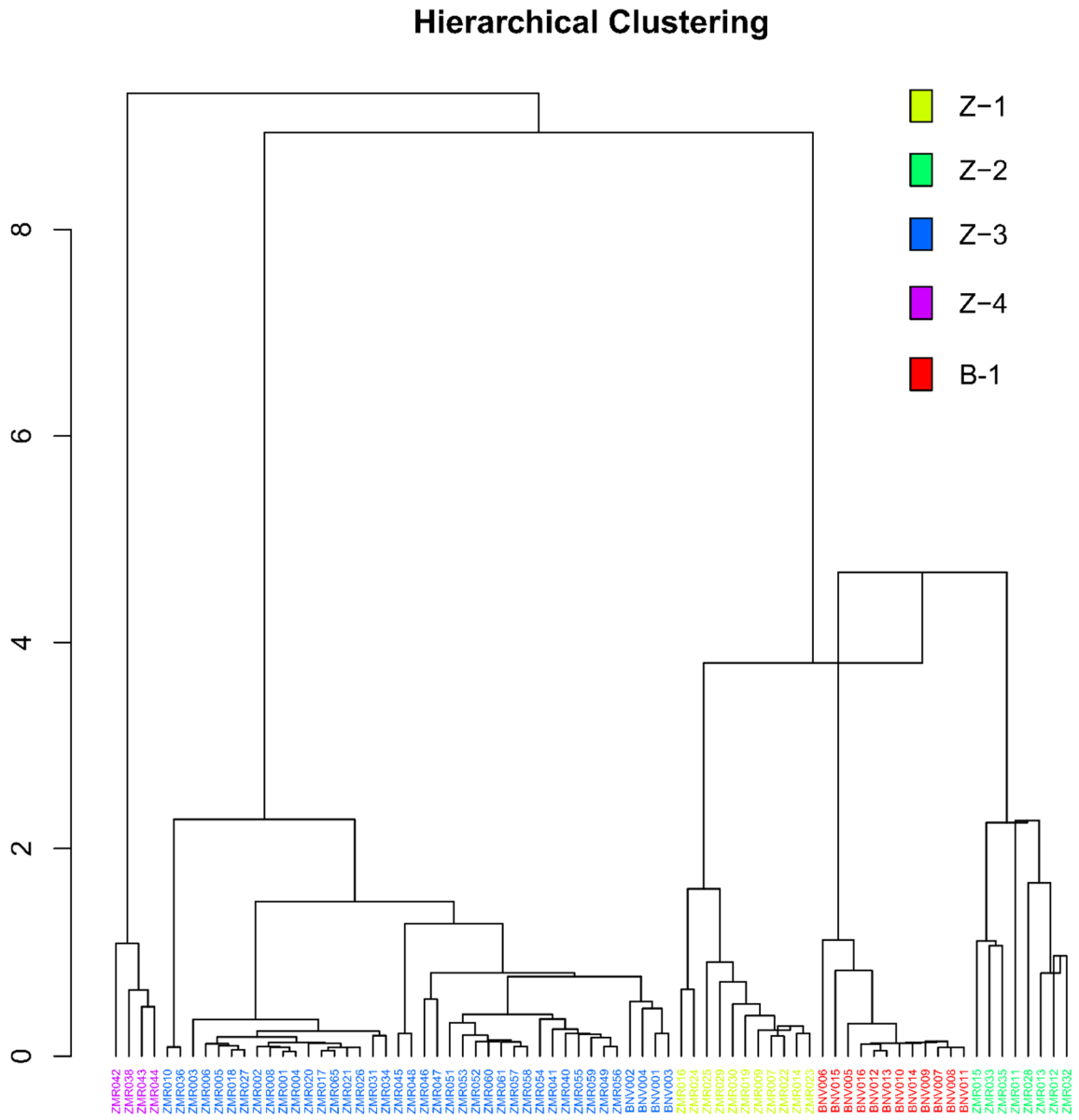

Figure 6.9. Dendrogram of Euclidean squared distances using centroid algorithm of 75 individuals from different sites of Zamora (Olivares, Ethnographic Museum and La Concepción) and Benavente, indicated by the compositional groups they correspond to, on the sub-composition of all the measured components (42) (with the exception of Co, Cu, Ni, P_2O_5, Pb, Sn, Ta, U and Zn) divided by the geometric mean. Z-1, Z-2 and Z-3= reference groups of Olivares productions; B-1= reference group of Benavente production; Z-4= PCRU of regional origin

6.1.3. Ceramics recovered in Toro

Like Benavente, Toro also was a production centre active from the Middle Ages to the Modern Era, in which non-micaceous red pottery was mainly produced (see Chapter 2).

In this case, the set of 14 ceramics from Toro (TOR001-TOR005 from Cuesta del Negrillo; TOR006-TOR008 from Patio del Siete and TOR009-TOR014 from Cuesta del Matadero) shows a relatively high vt (3.97), which reveals the high contribution of some components (specially Pb, Cu, CaO, MnO and P_2O_5) (Figure 6.10.a). The lead is very variable because some of these ceramics are translucent lead-glazed, and others do not have any glaze. In addition, Cu and P_2O_5 are components normally subjected to post-depositional

contaminations due to sediment, circulating waters and human activity affecting the surrounding soil (Buxeda i Garrigós, 1999; Buxeda i Garrigós and Kilikoglou, 2003; Freestone et al., 1985; Lemoine and Picon, 1982; Maritan and Mazzoli, 2004; Molera et al., 1993; Pradell et al., 1996). If Pb, Co, Ta, Cu and P_2O_5 are omitted, the vt decreases to 0.85, suggesting a possible monogenic nature of the dataset (Figure 6.10.b).

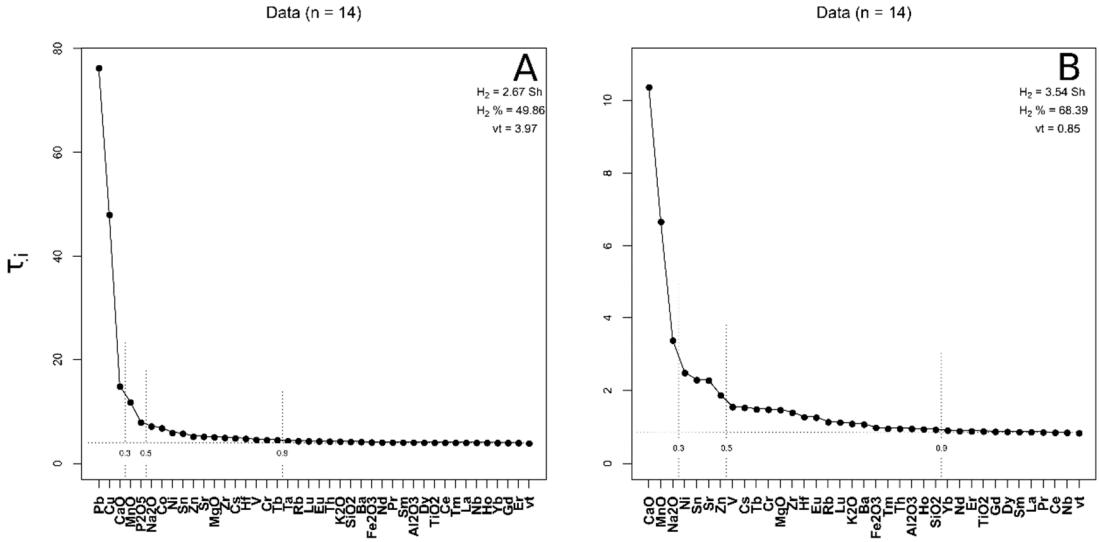

Figure 6.10. Graphical representation of the evenness of the compositional variability of 14 analysed ceramics, recovered in Toro, by ICP-MS; **(a)** U was omitted because its values are below to the quantification limit; **(b)** Co, Cu, P_2O_5, Pb and Ta were omitted due to their potential effect for alterations, in addition to U. (y-axis (τ.i) = the individual contribution of the variability from each element to the whole dataset, from the highest to the lowest; vt = Total variability; H_2 = information entropy; H_2% = percentage of information entropy over the maximum possible; n = number of specimens)

Moreover, Figure 6.11. shows that 12 out of the 14 ceramics collected in Toro (the exceptions are TOR009 and TOR013) form the reference group of the production of redware from Toro. In addition, Figure 6.12. shows that TOR009 nor TOR013 correspond to any reference group or the ceramics with an unknown provenance from Zamora, thus, their provenance remains unknown.

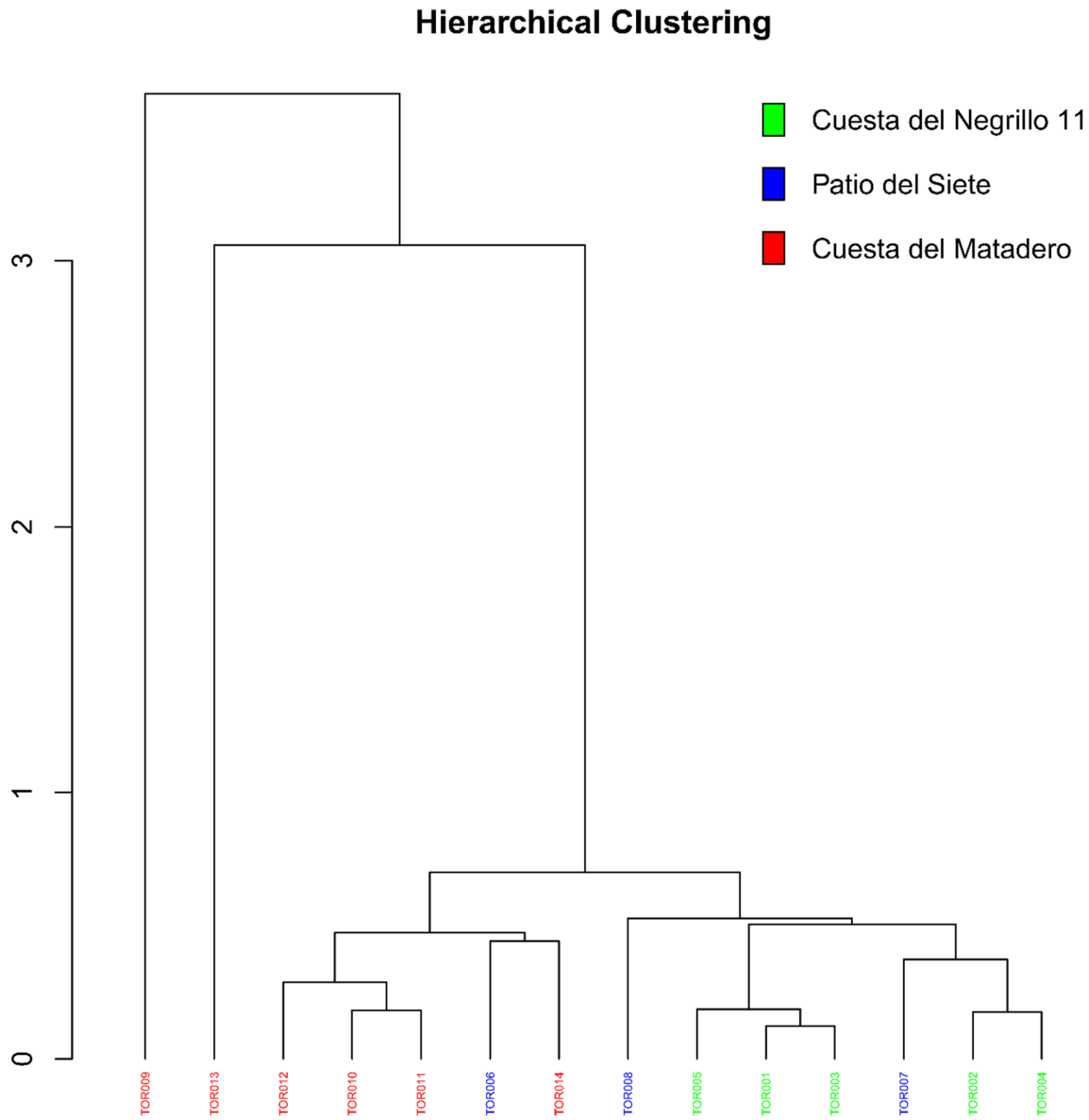

Figure 6.11. Dendrogram of Euclidean squared distances using centroid algorithm of 14 individuals from different sites of Toro (Cuesta del Negrillo, Patio del Siete and Cuesta del Matadero) on the sub-composition of all the measured components (42) (with the exception of Co, Cu, P_2O_5, Pb, Ta and U) divided by the geometric mean

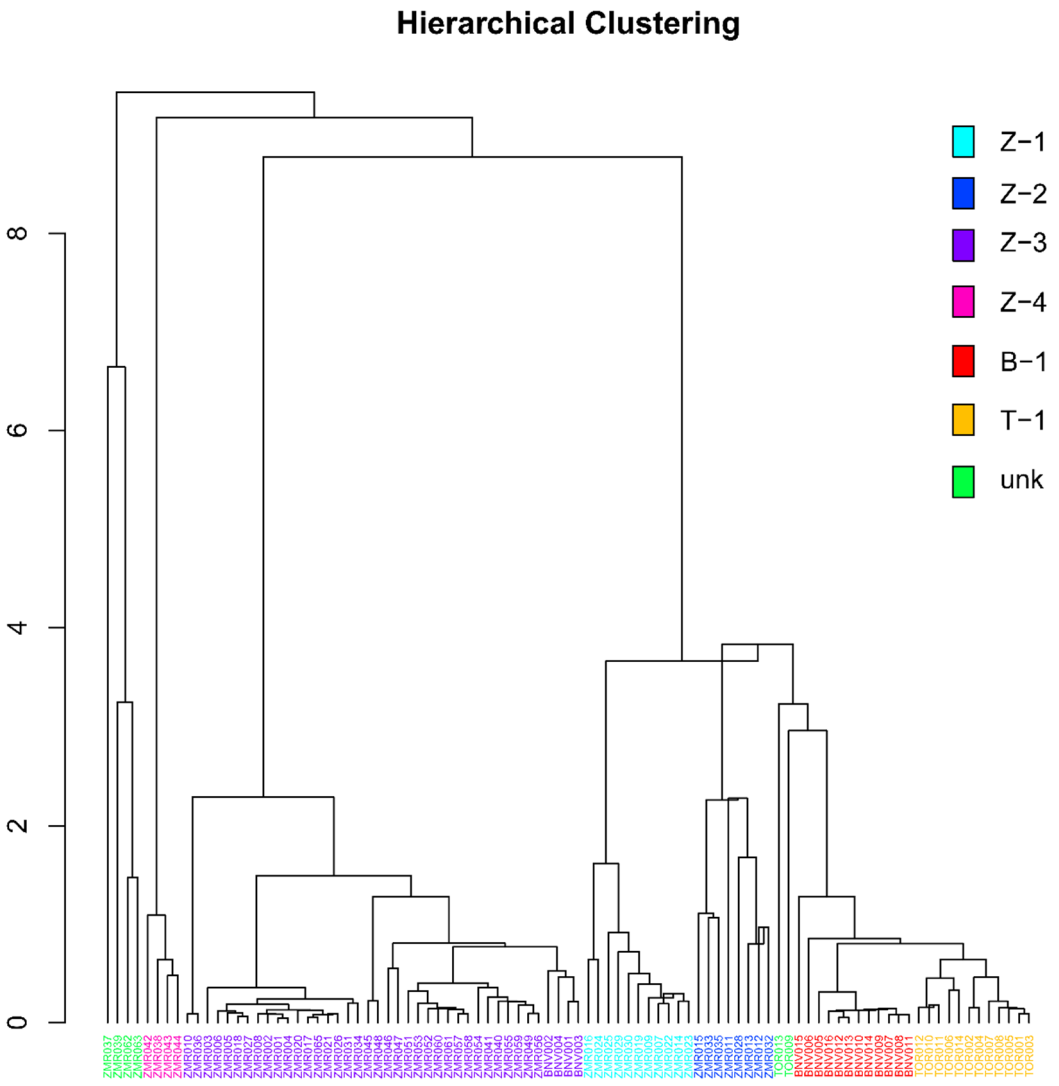

Figure 6.12. Dendrogram of Euclidean squared distances using centroid algorithm of 93 individuals from different sites of Toro, Zamora and Benavente, indicated by the compositional groups they correspond to, on the sub-composition of all the measured components (42) (with the exception of Co, Cu, Ni, P_2O_5, Pb, Sn, Ta, U and Zn) divided by the geometric mean. Z-1, Z-2 and Z-3= reference groups of Olivares productions; B-1= reference group of Benavente production; T-1= reference group of Toro production; Z-4= PCRU of regional origin

6.1.4. Characterisation of the reference groups and PCRUs

After identifying the reference groups and the PCRUs, the mineral phases and different production fabrics were identified, by means of XRD analyses. The Equivalent Firing Temperature (EFT) in which the fabrics were fired was also evaluated according to Heimann (2010 and references therein) observations. As commented in Chapter 1, a fabric is the final result that reaches the paste, after completing the technological process of the fabrication of the ceramics (Buxeda i Garrigós and Cau, 1995; Buxeda i Garrigós and Madrid i Fernández, 2017), which can be observed by the array of mineralogical composition and paste textures.

Besides, SEM-EDS and Raman analyses were carried out in some of the ceramics, in order to characterize more deeply Z-1, Z-2, Z-3, T-1 and B-1 reference groups, deepening more into the understanding of their clay microstructure as well as into their glaze composition.

Z-1 reference group

Z-1 is mainly composed by 2 unglazed and 9 translucent-glazed ceramics with red pastes, with the exception of one black, which is burnt (Table 6.3.). The forms include plates, cooking pots and jars, and among them, 5 are failure ceramics (with raw and burnt glazes). Chronologically, the ceramics of this group correspond to the late 19th-early 20th centuries (see Table 6.2.). These ceramics are low-calcareous, CaO concentration averaging to 1 wt % (see Table 6.3.). In addition, Z-1 ceramics also show higher amounts, than the rest of Olivares (Z-2, Z-3) productions, of SiO_2 and Zr contents, in relation to a possible higher sandy phase.

Table 6.3. The chemical composition of each reference group and PCRU, in addition to the ceramics belonging to each group, their typology and paste colour. The concentrations of the elements are expressed in ng/g and of the oxides in wt %

Samples	Group	Typology	Paste colour	Al_2O_3	Ba	CaO	Ce	Co	Cr	Cs	Cu	Dy	Er	Eu	Fe_2O_3	Gd
ZMR007; ZMR009; ZMR014; ZMR016; ZMR019; ZMR022-ZMR025; ZMR029-ZMR030	Z-1	unglazed (2), translucent-glazed (9)	red (10), black (1)	13.1	297	0.989	75.0	29.8	63.4	9.50	-	4.85	2.73	1.17	4.31	5.56
ZMR011-ZMR013; ZMR015; ZMR028; ZMR032-ZMR033; ZMR035	Z-2	micaceous unglazed (2), micaceous translucent-glazed (6)	red (6), red and grey (1), black (1)	19.2	403	1.46	76.4	26.9	48.2	12.2	-	5.01	2.33	1.74	4.27	7.07
ZMR001-ZMR006; ZMR008; ZMR010; ZMR017-ZMR018; ZMR020-ZMR021; ZMR026-ZMR027; ZMR031; ZMR034; ZMR036; ZMR040-ZMR041; ZMR045-ZMR049; ZMR051-ZMR061; ZMR065; BNV001-BNV004;	Z-3	unglazed (10), tin-lead glazed (30)	beige (6), buff-coloured (28), reddish and grey (2), reddish (4)	12.3	404	12.7	67.3	21.1	50.3	5.37	48.2	4.53	2.49	1.24	4.13	5.55
ZMR038; ZMR042-ZMR044	Z-4	micaceous unglazed (4)	beige (1), grey and beige (3)	24.7	305	3.55	47.7	15.9	21.8	30.7	6.09	5.68	3.07	0.940	2.48	5.68
BNV005-BNV016	B-1	unglazed (12)	red (11), reddish (1)	23.7	660	1.83	86.4	29.0	123	8.25	24.3	5.62	2.91	1.93	8.35	7.41
TOR001-TOR008; TOR010-TOR012; TOR014	T-1	unglazed (6), translucent-glazed (6)	red (12)	19.5	591	1.45	95.5	20.6	86.0	9.07	23.9	6.20	3.12	1.97	6.21	7.78

(continues)

Samples	Group	Typology	Paste colour	Hf	Ho	K_2O	La	Lu	MgO	MnO	Na_2O	Nb	Nd	Ni	P_2O_5	Pb	Pr	Rb	SiO_2	Sm
ZMR007; ZMR009; ZMR014; ZMR016; ZMR019; ZMR022-ZMR025; ZMR029-ZMR030	Z-1	unglazed (2), translucent-glazed (9)	red (10), black (1)	7.79	0.826	1.77	38.0	0.406	0.466	0.0241	0.763	16.7	35.3	-	-	595	8.50	98.8	77.3	6.79
ZMR011-ZMR013; ZMR015; ZMR028; ZMR032-ZMR033; ZMR035	Z-2	micaceous unglazed (2), micaceous translucent-glazed (6)	red (6), red and grey (1), black (1)	3.30	0.779	2.88	36.8	0.272	0.697	0.0222	0.851	12.6	44.8	-	-	1.00E+04	10.4	136	67.8	8.84
ZMR001-ZMR006; ZMR008; ZMR010; ZMR017-ZMR018; ZMR020-ZMR021; ZMR026-ZMR027; ZMR031; ZMR034; ZMR036; ZMR040-ZMR041; ZMR045-ZMR049; ZMR051-ZMR061;	Z-3	unglazed (10), tin-lead glazed (30)	beige (6), buff-coloured (28), reddish and grey (2), reddish (4)	5.15	0.766	3.19	33.3	0.337	2.16	0.0618	0.892	13.4	32.4	20.5	1.57	5.04E+03	8.04	117	58.6	6.19

ZMR065; BNV001-BNV004;																			
Samples	**Group**	**Typology**	**Paste colour**	**Hf**	**Ho**	**K_2O**	**La**	**Lu**	**MgO**	**MnO**	**Na_2O**	**Nb**	**Nd**	**Ni**	**P_2O_5**	**Pb**	**Pr**	**Rb**	**SiO_2**	**Sm**
ZMR038; ZMR042-ZMR044	Z-4	micaceous unglazed (4)	beige (1), grey and beige (3)	4.86	0.932	3.48	22.7	0.375	0.895	0.0402	0.618	24.6	22.2	9.92	0.460	61.0	5.67	440	67.6	5.07
BNV005-BNV016	B-1	unglazed (12)	red (11), reddish (1)	4.91	0.864	3.68	44.3	0.469	1.38	0.0437	0.614	20.4	41.1	36.4	0.101	60.7	10.3	173	65.8	7.61
TOR001-TOR008; TOR010-TOR012; TOR014	T-1	unglazed (6), translucent-glazed (6)	red (12)	5.26	0.916	3.77	48.5	0.483	1.14	0.0348	0.481	18.3	45.5	33.4	0.125	1.10E+03	11.6	172	65.1	8.25

(continues)

Samples	**Group**	**Typology**	**Paste colour**	**Sn**	**Sr**	**Ta**	**Tb**	**Th**	**TiO_2**	**Tm**	**U**	**V**	**Yb**	**Zn**	**Zr**
ZMR007; ZMR009; ZMR014; ZMR016; ZMR019; ZMR022-ZMR025; ZMR029-ZMR030	Z-1	unglazed (2), translucent-glazed (9)	red (10), black (1)	8.35	85.3	1.90	0.862	14.5	0.926	0.417	3.34	59.7	2.78	-	367
ZMR011-ZMR013; ZMR015; ZMR028; ZMR032-ZMR033; ZMR035	Z-2	micaceous unglazed (2), micaceous translucent-glazed (6)	red (6), red and grey (1), black (1)	20.9	154	2.15	1.01	9.77	0.447	0.319	2.64	57.5	2.10	-	122

Samples	Group	Typology	Paste colour	Sn	Sr	Ta	Tb	Th	TiO_2	Tm	U	V	Yb	Zn	Zr
ZMR001-ZMR006; ZMR008; ZMR010; ZMR017-ZMR018; ZMR020-ZMR021; ZMR026-ZMR027; ZMR031; ZMR034; ZMR036; ZMR040-ZMR041; ZMR045-ZMR049; ZMR051-ZMR061; ZMR065; BNV001-BNV004;	Z-3	unglazed (10), tin-lead glazed (30)	beige (6), buff-coloured (28), reddish and grey (2), reddish (4)	40.0	260	1.32	0.601	12.5	0.591	0.391	3.1	58.9	2.49	48.8	251
ZMR038; ZMR042-ZMR044	Z-4	micaceous unglazed (4)	beige (1), grey and beige (3)	33.8	107	7.72	0.446	8.41	0.284	0.503	-	24.2	2.96	62.9	211
BNV005-BNV016	B-1	unglazed (12)	red (11), reddish (1)	3.26	127	1.89	0.425	18.4	0.825	0.496	-	116	3.02	56.0	263
TOR001-TOR008; TOR010-TOR012; TOR014	T-1	unglazed (6), translucent-glazed (6)	red (12)	4.30	182	1.88	0.428	18.0	0.719	0.522	-	93.0	3.21	52.5	280

Technological assessment by XRD

Besides, by the mineralogical analyses, five mineralogical fabrics have been identified in this reference group, F-I, F-II_a, F-II_b, F-III, F-IV and F-V, respectively (Table 6.4.). The five fabrics have hematite included in their pastes, which is the phase related to the red colour of the paste (Heimann, 2010; Molera et al., 1998, 2015). Then, illite (a phase indicating a low firing temperature) is present in F-I and F-II, suggesting an Equivalent Firing Temperature (EFT) around 800 °C for F-I and F-II ceramics. Moreover, the appearance of potassium feldspar in F-II may suggest a higher temperature range (800-850 °C) for ceramics of F-II. Besides, F-II_a differs from F-II_b due to the appearance of calcite in the latter. Given that calcite decomposes above 650 °C, it is likely that this calcite is related to re-carbonation processes and/or secondary precipitation processes that could take place during the post-depositional period (Buxeda and Cau, 1995) (see Chapter 5, section 5.4.). On the other hand, F-III is made by only one ceramic (ZMR007), which already shows the decomposition of illite, along with the presence of potassium feldspars and hematite. Thus, an EFT in the range of 850-900 °C has been suggested for this fabric. Finally, F-IV evidences the crystallization of plagioclase as a firing phase and F-IV and F-V show the presence of mullite. Therefore, such mineralogical array permits establishing an EFT above 1000 °C, likely a lower temperature range for F-IV (1000-1050 °C) and a higher temperature range for F-V (at least 1050-1100 °C) (Table 6.4. and Figure 6.13.).

Table 6.4. The mineralogical composition and the Equivalent Firing Temperature (EFT) corresponding to each fabric, in addition to the ceramics belonging to each group, their typology and paste colour. Qz= quartz; Kfs= potassium feldspar; Pl= plagioclase; Cal= calcite; Ak-Gh= akermanite-gehlenite; Di= diopside; Ilt= illite; Hem= hematite; Mul= mullite; Crs= cristobalite, abbreviations according to Whitney and Evans (2010)

Group	Typology	Paste colour	Samples	Fabric	Qz	Kfs	Pl	Cal	Ak-Gh	Di	Ilt	Hem	Mul	Crs	EFT (° C)
Z-1	unglazed (1), translucent -glazed (1)	red (2)	ZMR009; ZMR019	F-I	x						x	x			800
	translucent -glazed (3)	red (3)	ZMR022-ZMR023; ZMR025	F-II_a	x	x					x	x			800-850
	translucent -glazed (1)	red (1)	ZMR029	F-II_b	x	x		x			x	x			800-850
	unglazed (1)	red (1)	ZMR007	F-III	x	x						x			850-900
	translucent -glazed (1)	black (1)	ZMR030	F-IV	x	x	x					x	x		1000 - 1050
	translucent -glazed (3)	red (3)	ZMR014; ZMR016; ZMR024	F-V	x	x						x	x		1050
Group	**Typology**	**Paste colour**	**Samples**	**Fabric**	**Qz**	**Kfs**	**Pl**	**Cal**	**Ak-Gh**	**Di**	**Ilt**	**Hem**	**Mul**	**Crs**	**EFT (° C)**
Z-2	micaceous unglazed (1), micaceous translucent -glazed (2)	red (3)	ZMR011-ZMR012; ZMR035	F-I_a	x	x					x	x			800-850

	micaceous unglazed (1)	red and grey (1)	ZMR013	F-I_b	x	x					x				800-850
	micaceous translucent-glazed (1)	red (1)	ZMR028	F-I_c	x	x		x			x	x			800-850
	micaceous translucent-glazed (1)	black (1)	ZMR033	F-II	x	x						x	x		1050
	micaceous translucent-glazed (1)	red (1)	ZMR015	F-III	x	x				x		x	x	x	1050-1100
	micaceous translucent-glazed (1)	red (1)	ZMR032	F-IV	x							x	x	x	1100
Group	**Typology**	**Paste colour**	**Samples**	**Fabric**	**Qz**	**Kfs**	**Pl**	**Cal**	**Ak-Gh**	**Di**	**Ilt**	**Hem**	**Mul**	**Crs**	**EFT (° C)**
Z-3	unglazed (2), tin-lead glazed (2)	reddish and grey (2), reddish (2)	ZMR010; ZMR036; BNV001; BNV003	F-I	x	x	x	x			x				850
	unglazed (3), tin-lead glazed (13)	beige (2), buff-coloured (12), reddish (2)	ZMR001-ZMR006; ZMR008; ZMR020; ZMR027; ZMR045; ZMR048; ZMR051-ZMR052; ZMR058; ZMR061; ZMR065	F-II_a	x	x	x	x	x	x	x				850-900
	unglazed (1)	beige (1)	ZMR031	F-II_b	x	x	x		x	x	x				850-900
	unglazed (2), tin-lead glazed (1)	buff-coloured (2), beige (1)	ZMR017; ZMR021; ZMR034	F-III	x	x	x			x	x				900
	tin-lead glazed (6)	buff-coloured (6)	ZMR040-ZMR041; ZMR049; ZMR054-ZMR056	F-IV_a	x	x		x	x	x					900-950
	tin-lead glazed (4)	buff-coloured (3), beige (1)	ZMR053; ZMR057; ZMR059-ZMR060	F-IV_b	x	x	x	x	x	x					900-950
	tin-lead glazed (4)	buff-coloured (3), beige (1)	ZMR046-ZMR047; BNV002; BNV004	F-V	x	x	x		x	x					950
	unglazed (2)	buff-coloured (2)	ZMR018; ZMR26	F-VI	x	x	x	x	x	x					950-1000

Group	Typology	Paste colour	Samples	Fabric	Qz	Kfs	Pl	Cal	Ak-Gh	Di	Ilt	Hem	Mul	Crs	EFT (° C)
Z-4	micaceous unglazed (4)	beige (1), grey and beige (3)	ZMR038; ZMR042-ZMR044	F-I	x	x	x	x			x				850-900
Group	**Typology**	**Paste colour**	**Samples**	**Fabric**	**Qz**	**Kfs**	**Pl**	**Cal**	**Ak-Gh**	**Di**	**Ilt**	**Hem**	**Mul**	**Crs**	**EFT (° C)**
B-1	unglazed (5)	red (4), reddish (1)	BNV006; BNV009; BNV012-BNV014	F-I	x	x		x			x	x			800-850
	unglazed (3)	red (3)	BNV005; BNV010; BNV015	F-II	x	x						x			850-900
	unglazed (4)	red (4)	BNV007-BNV008; BNV011; BNV016	F-III	x	x						x	x		1050
Group	**Typology**	**Paste colour**	**Samples**	**Fabric**	**Qz**	**Kfs**	**Pl**	**Cal**	**Ak-Gh**	**Di**	**Ilt**	**Hem**	**Mul**	**Crs**	**EFT (° C)**
T-1	unglazed (5), translucent-glazed (3)	red (8)	TOR002-TOR004; TOR005-TOR008; TOR012	F-I	x	x		x			x	x			800-850
	unglazed (1), translucent-glazed (3)	red (4)	TOR001; TOR010-TOR011; TOR014	F-II	x	x					x	x			850-900

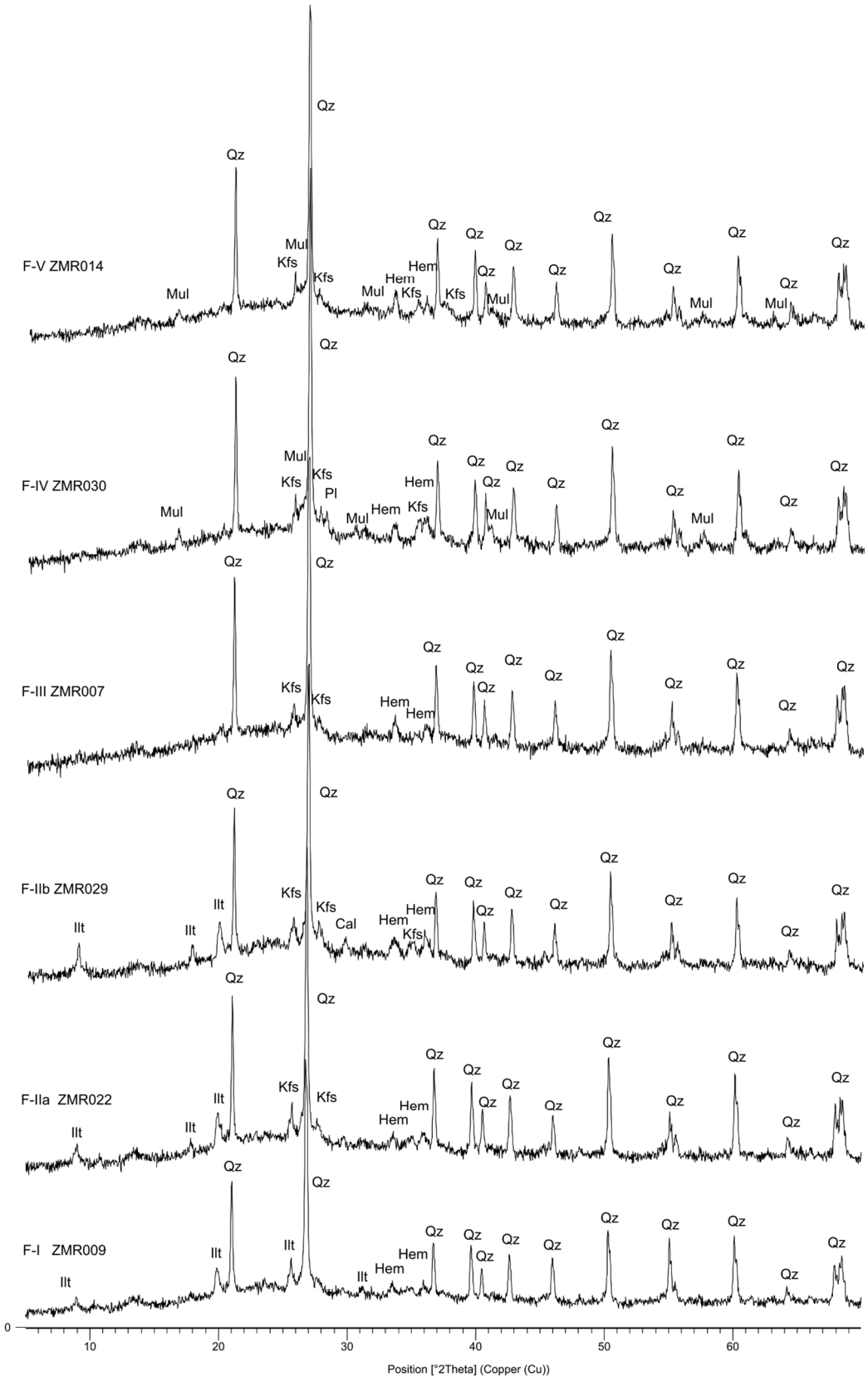

Figure 6.13. Reference diffractograms of the fabrics from Z-1 reference group. Qz = quartz; Ilt = illite; Kfs = potassium feldspar; Pl = plagioclase; Hem = hematite; Cal = calcite; Mul = mullite, abbreviations according to Whitney and Evans (2010)

SEM-EDS assessment

3 ceramics were selected for SEM-EDS analyses: ZMR009 unglazed (F-I), ZMR025 (translucent-glazed, F-II_a) and ZMR014 (translucent-glazed, F-V) (Figure 6.14.). First, ZMR009 shows an early-initial vitrificated clay structure, due to the appearance of isolated smooth-surfaced areas, corresponding to F-I (Maniatis and Tite, 1978). Then, ZMR014 represents the higher temperature range reached for ceramics of Z-1 chemical group, evidencing a highly continuous vitrification. Furthermore, ZMR025 and ZMR014 show microstructural chemical evidence of the nature of glazing for these ceramics. Hence, Z-1 ceramics were glazed using a mixture of Pb and Si, probably using a frit before, according to the literature (Iñañez, 2007). The brown (honey) colour of the translucent-glaze coating was provided by the presence of Fe ions in the glaze mixture and the oxidizing firing conditions purportedly mainly used by Zamoran potters, indicating that Fe is the responsible for such coloration, in agreement with literature (Molera et al., 2015).

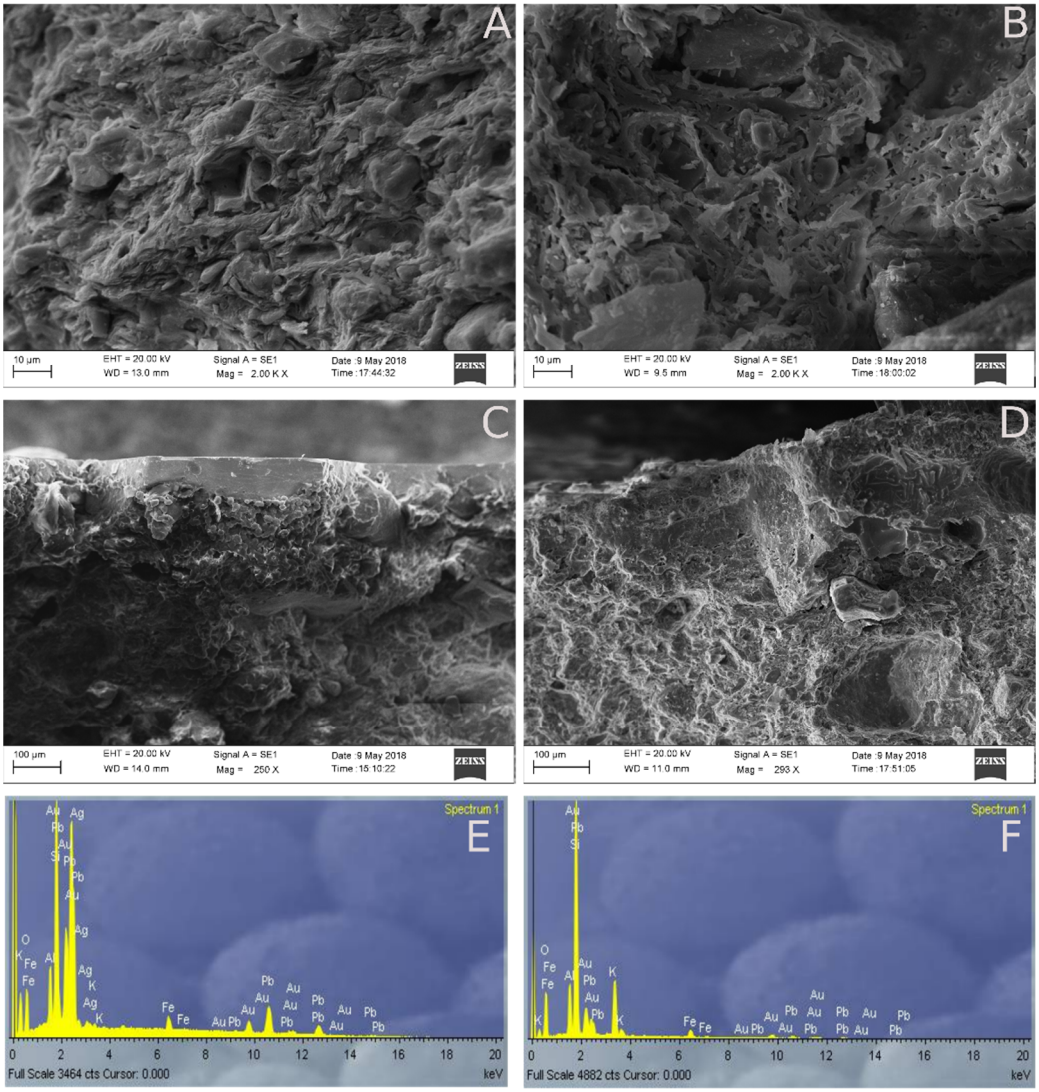

Figure 6.14. SEM-SED microphotographs and SEM-EDS microanalyses of Z-1 chemical group ceramics (from upper left to bottom right: **(a)** ZMR009 paste; **(b)** ZMR014 paste; **(c)** ZMR025 glaze; **(d)** ZMR014 glaze; **(e)** ZMR025 glaze EDS spectrum; **(f)** ZMR014 glaze EDS spectrum

Z-2 reference group

Z-2 group is composed by 8 micaceous ceramics. Among them, 6 are translucent-glazed (from which 4 are failure ceramics). Chronologically, the ceramics of this group correspond to the late 19th-early 20th centuries (see Table 6.2.). These micaceous ceramics are high aluminium and low-calcareous ceramics, averaging to 19 wt % in Al_2O_3 and 1 wt % in CaO contents (see Table 6.3.). The visual appearance and the high aluminium content is linked to the high quantity of phyllosilicates (e.g. mica) present in the clay paste, which provide these ceramics with optimal technical properties for thermal shock resistance. The extraction of the raw material may be in relation to the Cambrian squist and quarcite formations existing in the vicinity of the city, which may provide with illitic clays and mica (Corrochano, 1980; Corrochano et al., 1976).

Technological assessment by XRD

Besides, four different fabrics have been identified in this group, F-I_a, F-I_b, F-I_c, F-II, F-III and F-IV, respectively. F-I, with three subgroups with minor differences, evidences the presence of illite peaks, suggesting a low firing temperature, likely around 800-850 °C. Additionally, unlike F-I_b, F-I_a and F-I_c both show hematite on their diffractograms, and secondary calcite is also present in F-I_c (Table 6.4.). The fact that F-I_b does not show peaks of hematite does not mean that hematite is not present. Furthermore, the concentration of Fe_2O_3 for F-I_b is around 4 %, so hematite can be present but not well crystallised or in such a low concentration that the XRD does not identify it (the 4 % of Fe_2O_3 also refers to iron silicates and minerals). However, its low concentration is enough to give the red colour to the paste (Pollard et al., 2007). Furthermore, F-II contains mullite, suggesting an EFT around 1050 °C. Besides, F-III shows diopside, mullite and cristobalite. The last, a polymorph of quartz, appears due to the inversions that occur in quartz at high temperatures, providing an EFT in the range of 1050-1100 °C. Finally, F-IV, unlike the others, does not contain potassium feldspars. Furthermore, it contains phases of high temperature, such as quartz,

hematite, mullite and cristobalite, providing an EFT around 1100 °C (Table 6.4. and Figure 6.15.).

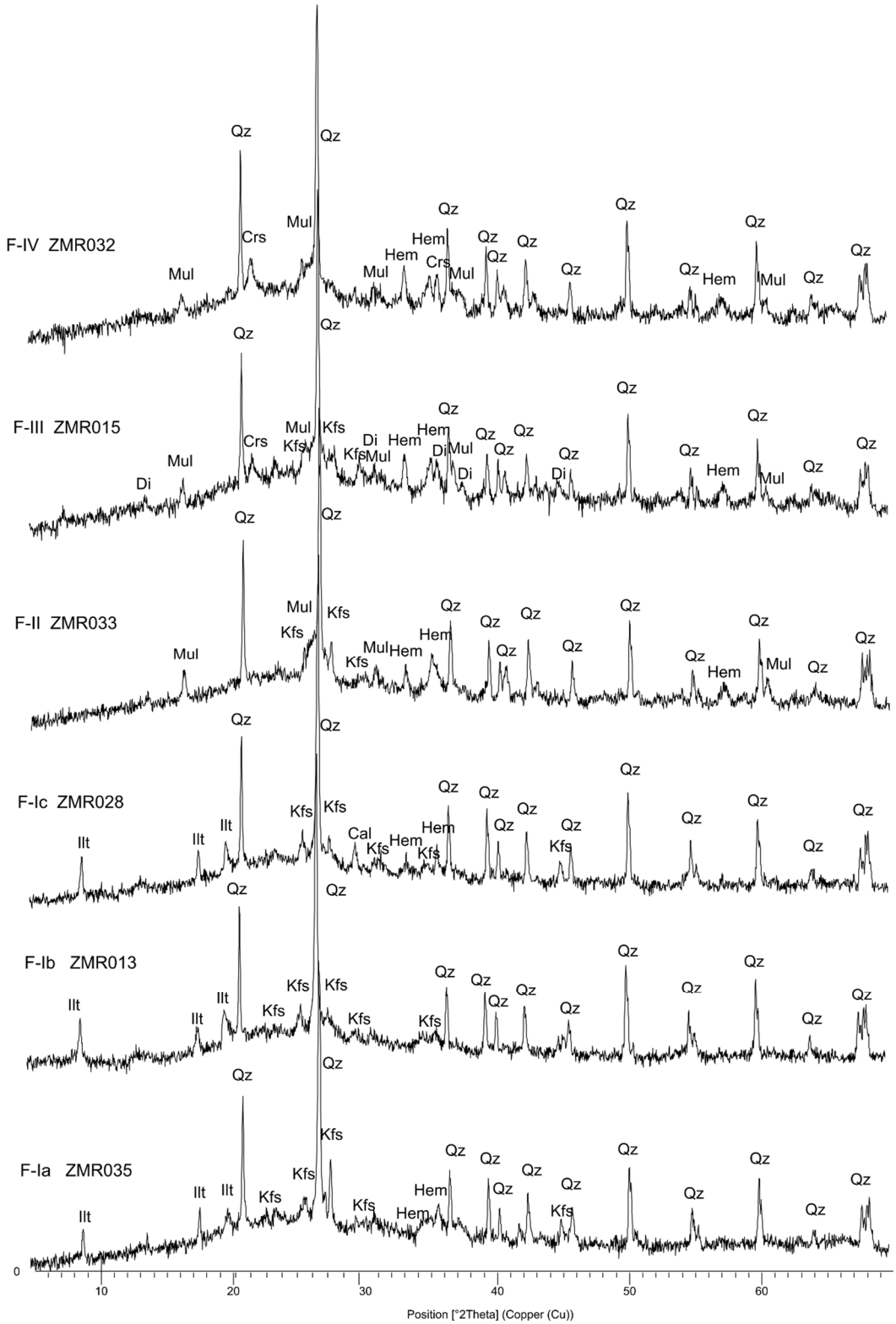

Figure 6.15. Reference diffractograms of the fabrics from Z-2 reference group. Qz = quartz; Ilt = illite; Kfs = potassium feldspar; Hem = hematite; Cal = calcite; Mul = mullite; Di = diopside; Crs = cristobalite, abbreviations according to Whitney and Evans (2010)

SEM-EDS assessment

Furthermore, 3 ceramics from Z-2 were analysed by SEM-EDS. Figure 6.16. permits visualizing the early-initial vitrification of ZMR013 (F-I_b) and the continuous vitrification of ZMR015 (F-III), in agreement with high and sustained firing temperatures. Moreover, glaze coatings and their EDS spectrums of ZMR015 and ZMR033 ceramics are also visible in Figure 6.16. They show that these glazes (like the rest of the glazes of the group), were glazed with a translucent honey-glaze, like their counterparts from Z-1 group.

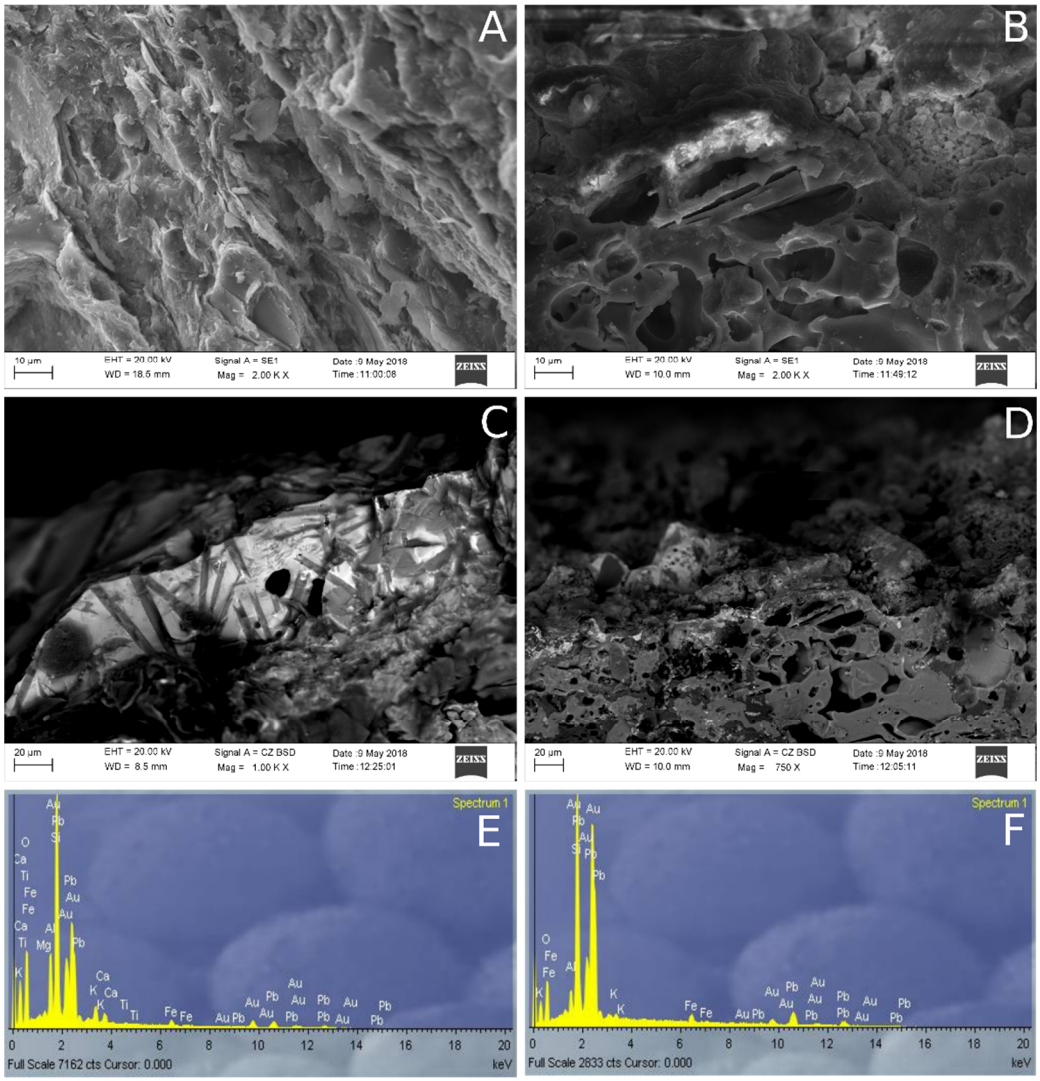

Figure 6.16. SEM-SED (a,b), SEM-BSD (c,d) microphotographs and SEM-EDS microanalyses of Z-2 chemical group ceramics: **(a)** ZMR013 paste; **(b)** ZMR015 paste; **(c)** ZMR033 glaze; **(d)** ZMR015 glaze; **(e)** ZMR033 glaze EDS spectrum; **(f)** ZMR015 glaze EDS spectrum

(The sections 6.1. (last part), 6.2. and 6.3. are in English in the pages 208-294, and the Chapter 7 in the pages 295-308 of the Doctoral Thesis).*

eman ta zabal zazu

Universidad del País Vasco
Euskal Herriko Unibertsitatea